

INTERNATIONAL COUNCIL FOR BUILDING RESEARCH STUDIES AND DOCUMENTATION

WORKING COMMISSION W18A - TIMBER STRUCTURES

CIB - W18 A

VOLUME II

MEETING TWENTY - TWO

BERLIN

GERMAN DEMOCRATIC REPUBLIC

SEPTEMBER 1989

CONTENTS

CIB-W18A Papers 22-8-1 up to 22-102-3

INTERNATIONAL COUNCIL FOR BUILDING RESEARCH STUDIES AND DOCUMENTATION

WORKING COMMISSION W18A - TIMBER STRUCTURES

RELIABILITY ANALYSIS OF VISCOELASTIC FLOORS

by

F Rouger

Centre Technique du Bois et de l'Ameublement

Paris, France

and

J D Barrett

R O Foschi

University of British Columbia

Vancouver, B.C. Canada

MEETING TWENTY - TWO

BERLIN

GERMAN DEMOCRATIC REPUBLIC

SEPTEMBER 1989

Reliability Analysis of Viscoelastic Floors

by

Dr Frederic Rouger Dr John David Barrett Dr Ricardo Foschi

1. Introduction.

This paper summarizes results of a project activity undertaken at the University of British Columbia (Vancouver CANADA) in cooperation with the Centre Technique du Bois et de l'Ameublement (Paris FRANCE) The objective of this study is to analyze the effect of joist and panel viscoelastic behavior on reliability of wood structural systems. Since previous work has not considered the influence of creep on structural performance, this study was initiated with the objective of undertaking initial studies of the influence of creep behavior on systems performance.

Recent studies by Foschi et al. have shown that wood structural systems designed according to present codes have a somewhat lower average safety level that might have been anticipated considering the performance record. Load sharing factors are incorporated into wood structural design codes to account to the additional safety developed by the structural interaction of parallel members in systems such as floors, roofs and trusses. The additional safety develops in part due to the redistribution of framing member stresses, due to the interaction between framing members and the panels (or cover) material and the between member variation in modulus of elasticity. Studies of the elastic behavior of redundant member wood structures have shown that the correlation between strength and modulus of elasticity of wood members contributes to a redistribution of stresses in which the weaker member will be subjected to lower stresses and the stronger members will have higher than average stresses.

Foschi et al. investigated the longterm behavior of wood roof systems subjected to cyclic snow loads. System time-to-failure was calculated using damage accumulation models. Damage accumulation under simulated snow loads was evaluated using member stresses derived from an elastic stress analysis. The time-to-failure distributions derived from the analysis formed the basis for system reliability studies using First Order Reliability Methods.

The creep of system framing members and panels product will affect the member and panel stresses. The purpose of this paper is describe a series of analysis undertaken to assess the impact of viscoelastic behavior on roof joist and sheathing stresses for a roof system subjected to constant and cyclic snow loads.

2. Theory of viscoelastic behavior and applications to finite elements analysis.

2.1 Viscoelastic behavior.

A viscoelastic material is usually characterized by two types of experiments :

- **Creep** : Strain response (evolution with time) to a constant stress history
- **Relaxation** : Stress response (evolution with time) to a constant strain history.

The viscoelastic behavior is linear if the response \mathbf{R} to a linear combination of histories (S_1, S_2) is the linear combination of the individual responses R_1 and R_2 . In a more general case, we say that the response \mathbf{R} (stress or strain) at a time t is a function of \mathbf{S} , the applied strain or stress. Constitutive relationship between \mathbf{R} and \mathbf{S} is an integral-derivative equation .

$$R_i(t_r) = \int_0^{t_r} A_{ij}(t_r - u) \dot{S}_j(u) du \dots\dots\dots(1)$$

where

\mathbf{R} and \mathbf{S} are 6 terms vectors.

\mathbf{A} is a 36 terms matrix (9 terms = 0 in the case of an orthotropic material).

2.2 Time Discretization.

The integration of equation (1) can be achieved by dividing time interval $[0;t_r]$ into $(r-1)$ intervals $[t_{k-1};t_k]$ ($k \in (2,r)$)

The first step is a finite difference approximation for time derivative :

$$\dot{S}(u) = \frac{S(t_k) - S(t_{k-1})}{t_k - t_{k-1}} = \frac{\Delta S(t_k)}{\Delta t_k} \dots\dots\dots(2)$$

The second step is a numerical integration for each time interval $[t_{k-1};t_k]$ by the trapezoid method :

$$\int_{t_{k-1}}^{t_k} f(t) dt = \frac{t_k - t_{k-1}}{2} [f(t_{k-1}) + f(t_k)] \dots\dots\dots(3)$$

Finally, equation (1) becomes :

$$R_i(t_r) = \left\{ \frac{A_{ij}(0) + A_{ij}(t_r - t_{r-1})}{2} \right\} S_j(t_r) + \sum_{k=2}^{r-1} \left\{ \frac{A_{ij}(t_r - t_k) + A_{ij}(t_r - t_{k-1})}{2} \right\} \Delta S_j(t_k) - \left\{ \frac{A_{ij}(0) + A_{ij}(t_r - t_{r-1})}{2} \right\} S_j(t_{r-1}) \dots\dots(4)$$

2.3 Finite Element Model.

The finite element method is based on the following equations :

(1) Minimum of total potential energy for an elastic body (Volume=V) :

$$\int_V \langle \delta \epsilon \rangle \langle \sigma \rangle dV = \int_{S_f} \langle \delta u \rangle \langle T \rangle dS \dots \dots \dots (5)$$

where

u, σ, ϵ are displacements, stresses and strains respectively.

$\delta u, \delta \epsilon$ are small variations of u and ϵ respectively.

T are external loads.

(2) Discretization applied in volume V to u and ϵ :

$$\langle u \rangle = [N] \langle U_n \rangle \quad \langle \epsilon \rangle = \langle U_n \rangle [B]^T \dots \dots \dots (6)$$

where

$[N]$ are the shape functions.

$[B]$ is the derivative operator.

$\langle U_n \rangle$ is the vector of nodal displacements.

(3) Constitutive Equations

$$\langle \sigma \rangle = [D] \langle \epsilon \rangle \dots \dots \dots (7)$$

where $[D]$ is the stiffness matrix of the material.

Finally, Equation (5) can be rewritten using equations (6) & (7) :

$$\sum_{\text{elts}} \int_{V_e} [B]^T [D] [B] \langle U_n \rangle dV_e = \sum_{\text{elts}} \int_{S_{f_e}} [N]^T \langle T \rangle dS \dots \dots \dots (8)$$

In the case of a viscoelastic material, we use its constitutive equation (4) which can be expressed as :

$$\sigma_i(t_r) = D_{ij}(t_r) \cdot \epsilon_j(t_r) + \sigma_{j_0}(t_r) \dots \dots \dots (9)$$

Equation (8) becomes :

$$\sum_{\text{elts}} \int_{V_e} [B]^T [D(t_r)] [B] \langle U_n(t_r) \rangle dV_e = \sum_{\text{elts}} \left(\langle F_e(t_r) \rangle - \int_{V_e} [B]^T \langle \sigma_0(t_r) \rangle dV_e \right) \dots \dots \dots (10)$$

This expression gives the system to solve at each time step t_r . The $\sigma_0(t_r)$ vector requires the storage of $U_n(t_k)$ ($\forall k < r$). This is the major reason for which viscoelastic calculations are expensive. If the constitutive equation of the material is expressed in terms of exponentials, recurrent relations may be established ([1]).

3. Implementation of viscoelastic behavior in a Floor Analysis Program.

3.1 The original FAP program.

The FAP program was originally developed by R.O. Foschi ([3]). It is used to modelize the behavior of wood floors constituted by several joists and a cover (see Figure 1). Connections between the joists and the cover may be taken into account. The floor must be at least simply supported for $x=0$ and $x=L$. The analysis is carried out using a finite element approximation in (Y,Z) plane and a Fourier series expansion in X direction.

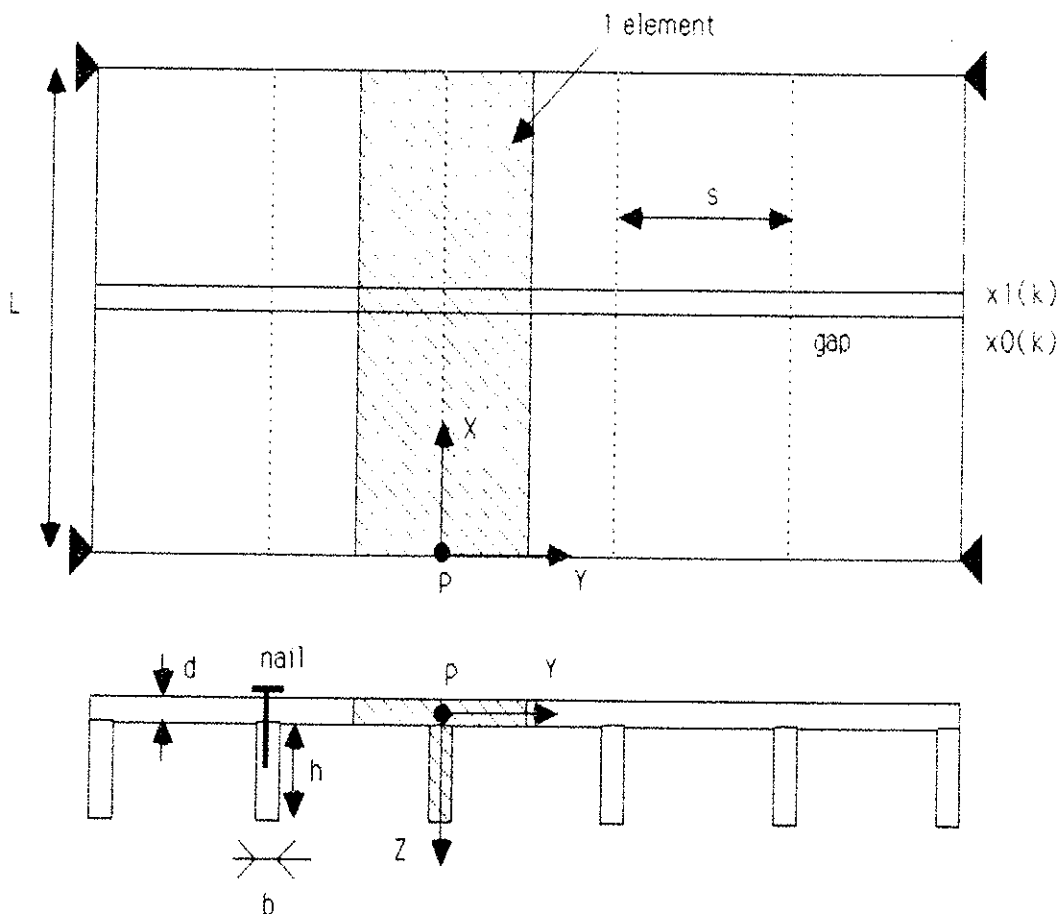


Figure 1 : Floor Geometry

An element and its degrees of freedom (u, v, w are displacements in X, Y, Z directions respectively) is described in Figure 2

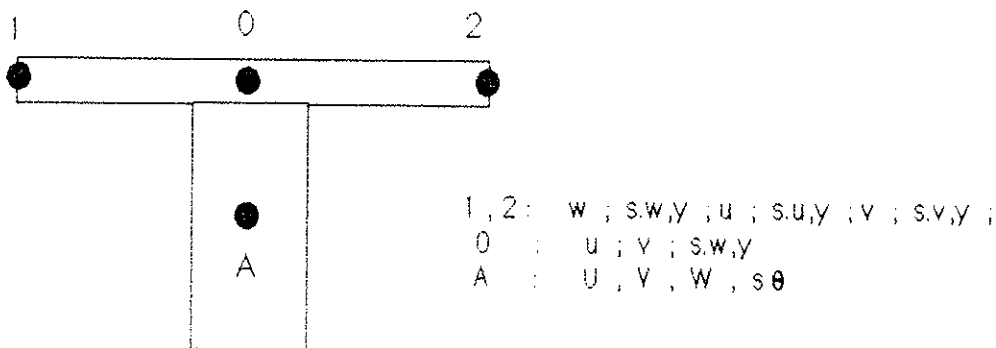


Figure 2 : Degrees of freedom for an element.

The finite element model is obtained by the minimum of total potential energy :

$$\delta \left[\sum_{i=1}^{NJT} (U_c + U_j + U_N - U_L) \right] = 0 \dots \dots \dots (11)$$

where

- NJT : number of joists
- U_L : potential energy of external loads
- U_c : strain energy of the cover (theory of orthotropic plates).
- U_j : strain energy of the joists (theory of beams).
- U_N : strain energy of the connections (considered as springs).

3.2 Viscoelastic version : FAPVEL.

To obtain the viscoelastic version FAPVEL, we need to write each of the stress-strain relationships for both joists and cover. The elastic equations are as follows :

Joists

$$\begin{aligned} \epsilon_{xx} &= U_{,x} - y V_{,xx} - z W_{,xx} & \sigma_{xx} &= E \epsilon_{xx} \\ \gamma_{xy} &= r \theta_{,x} & \tau_{xy} &= G \gamma_{xy} \dots \dots \dots (12) \end{aligned}$$

Cover

$$\begin{aligned} \epsilon_{xx} &= U_{,x} - z W_{,xx} & \sigma_{xx} &= \frac{E_x}{1 - \nu_{xy} \nu_{yx}} [\epsilon_{xx} + \nu_{xy} \epsilon_{yy}] \\ \epsilon_{yy} &= V_{,y} - z W_{,yy} & \sigma_{yy} &= \frac{E_y}{1 - \nu_{xy} \nu_{yx}} [\epsilon_{yy} + \nu_{yx} \epsilon_{xx}] \\ \gamma_{xy} &= u_{,y} + v_{,x} - 2z W_{,xy} & \tau_{xy} &= G \gamma_{xy} \dots \dots \dots (13) \end{aligned}$$

Equations (12) & (13) are rewritten in the way of equation (9) Then, the strain energy of each constituent (joists and cover) is modified using equation (10) The global system to solve at each time step would be too difficult to describe in this paper but details are reported in [6].

A reliability analysis was performed to understand the effect of viscoelasticity on the behavior of floors. Many results and curves are reported in chapter 4. In order to understand the behavior of viscoelastic floors, a simple example is reported below

If a floor is subjected to a constant load, how do stresses and strains vary with time if the cover is viscoelastic and the joists are elastic ?

** If the load is constant and the cover is viscoelastic, then the strains increase in the cover (creep).*

** If the strains increase in the cover, then the strains increase in the joists (because cover and joists are connected via the nails).*

** If the strains increase in the joists, then the stresses increase in the joists (because they are elastic).*

** If the stresses increase in the joists and the load is constant, then the stresses decrease in the joists.*

Therefore, the stresses increase in the joists and decrease in the cover. In a more general manner, that means that stresses migrate from the "more viscoelastic" component to the "less viscoelastic" component. That would be the case in wood floors in which cover is made of particleboard or plywood.

3.3 Damage Accumulation Model.

As explained in previous chapters, if a wood floor is subjected to a constant load, the stresses increase in the joists. Therefore, failure mechanisms should be involved rather in the joists. For this reason, we implemented in FAPVEL program the capability to predict damage accumulation in the joists.

In [9], a model was developed to determine the relationship between time-to-failure and stress history. The damage is a state variable α which has the following characteristics :

$$\begin{cases} 0 < \alpha < 1 \\ \alpha = 0 \text{ for "virgin" material} \\ \alpha = 1 \text{ at failure} \end{cases} \dots \dots \dots (14)$$

At every time t , α can be evaluated by solving the differential equation :

$$\frac{d\alpha}{dt} = a (\tau(t) - \sigma_0 \tau_s)^b + c (\tau(t) - \sigma_0 \tau_s)^n \alpha \dots \dots \dots (15)$$

where :

$\tau(t)$ = applied stress history

τ_s = short term strength

σ_0 = threshold stress ratio and

a, b, c, n are model parameters

Because τ_s is determined by a ramp load test conducted at a specified rate K_s , the parameter a is related to the other parameters, according to :

$$a = \frac{K_s (b+1)}{(\tau_s - \sigma_0 \tau_s)^{b+1}} \dots \dots \dots (16)$$

To solve this equation, we can use a direct integration method, assuming that the load is constant during every time step Δt :

$$\alpha_{i+1} = \alpha_i K_0(i+1) + K_1(i+1) \dots \dots \dots (17)$$

with :

$$\begin{cases} K_0(i) = \exp \left\{ c (\tau(t_i) - \sigma_0 \tau_s)^a \Delta t \right\} \\ K_1(i) = \frac{a}{c} (\tau(t_i) - \sigma_0 \tau_s)^{b-n} (K_0(i) - 1) \end{cases} \dots \dots \dots (18)$$

Time-to-failure is the time for which damage α is equal to 1.

4. Reliability Analysis of Viscoelastic Floors.

As explained in previous chapters, viscoelastic calculations are quite "CPU consuming". To compare the performance of viscoelastic and elastic floors, it would have been interesting to perform a first order analysis. But some estimations led to a global CPU time of more than 100 days. Therefore, we preferred to use Monte-Carlo simulations with a small number of replications (200 for each load case), which is enough to get a first idea.

In the same context, we decided to study only 3 joists floors (simply supported at $X=0$ and $X=L$). The limit state system is a series system: if failure of one joist occurs, it implies failure of the floor. For each joist, the failure function is :

$$G = 1 - \alpha$$

where α is the damage parameter of equation (15).

- $G > 0$ the joist is safe.
- $G = 0$ limit state.
- $G < 0$ failure of the joist.

4.1 Materials behavior.

4.1.1 Joists

Joists are Douglas-Fir Lumber (1650f-1.5E).

* Viscoelastic Behavior.

An experimental study on viscoelastic behavior for this lumber was carried out in [2]. These results are fitted to a power model whose creep function is given by :

$$f(t) = J_0 \left[1 + \left(\frac{t}{\tau} \right)^k \right] \dots \dots \dots (19)$$

Nielsen [4] explains how to obtain the relaxation function, complex compliance and complex modulus for the power model using different transformation methods. When k is less than 0.3, the relaxation function can be approximated by:

$$r(t) \approx \frac{1}{J_0 \left[1 + \left(\frac{t}{\tau} \right)^k \right]} \dots \dots \dots (20)$$

Overall best-fit solution was obtained using a non-linear minimization procedure [5]. The distributions for J_0 , τ , k are reported in Table 1.

* Damage Accumulation Model.

The short term strength was investigated in [2].

The other parameters b, c, n, σ_0 are derived from [9] in which Western Hemlock was studied. The distributions are reported in Table 1.

4.1.2 Panels.

At this date, very few studies have been conducted to evaluate viscoelastic behavior of structured panels. We took some data from a comprehensive report published by University of Alberta [8]. In this study, bending creep tests were done for OSB panels (Oriented Strandboard).

We picked up elastic distributions of E_{parallel} and $E_{\text{perpendicular}}$.

To get viscoelastic parameters, we fitted in the same way than for lumber a power model. Distributions of the viscoelastic parameters are reported in Table 1.

4.1.3 Random and Deterministic Variables.

* Each of the random variables used in the simulation is reported below.

Variable	Model	Mean	Standard Deviation
<i>Joists (Douglas-Fir 1650f-1.5E)</i>			
E (psi)	Lognormal	1.58e6	2.2e5
τ (hours)	Lognormal	5.83e4	1.66e4
k	Lognormal	0.264	0.0587
σ (psi)	Lognormal	6800	2047
<i>Panels (OSB)</i>			
E_{parallel} (psi)	Lognormal	1.08e6	7.72e4
$E_{\text{perpendicular}}$ (psi)	Lognormal	0.458e6	3.03e4
τ (hours)	Lognormal	1320	770
k	Lognormal	0.262	0.081
<i>Damage Model</i>			
b	Lognormal	35.2	6.59
c	Lognormal	0.156e-6	0.96e-7
n	Lognormal	1.43	0.14
σ_0	Lognormal	0.58	0.163

Table 1 : Random Variables for Monte-Carlo Simulations.

* Deterministic variables are given below :

- * Joist Cross Section : 1.5 in. x 7.25 in.
- * Joist Spacing : 16 in.
- * Thickness of the Sheathing : 0.625 in.
- * Span = 240 in.

The span was calculated to produce a preselected number of failures under a design load in order that a comparison could be made between elastic and viscoelastic floors.

Nails Properties

- * Nails Spacing = 8"
- * $k_x = 10^5$ psi
- * $k_y = 10^5$ psi
- * $k_\theta = 10^6$ psi

4.2 Load Models.

4.2.1 Constant Loads

Five different constant load levels were used for simulation studies :

- 43.44 psf (Design Snow Load of Ottawa) and
- 45, 50, 70 and 90 psf.

These values were chosen to give a probability of failure ranging from 4% to 90% in order to get good estimates of the relationship between the load level and the probability of failure.

For each load level 200 elastic input files and 200 viscoelastic input files were evaluated.

The duration of load is 10 years.

For each simulation, the following information was recorded :

- maximum bending stress in the joists (over 3 joists within 10 years)
- maximum deflection in the joists (over 3 joists within 10 years)
- maximum bending stress in the cover (within 10 years).
- time-to-failure if the floor fails (before 10 years).

4.2.2 Cyclic Loads

The load model combines a fixed dead load component (D) and an annual live load component of intensity (Q_i) and duration (L_i).

For one simulation, the dead load is assumed to be constant over 10 years.

The length L_i of the i th winter segment is a Lognormal random variable with

- mean = 45.4 days and
- standard deviation = 34 days

The total load P_i of the i th segment can be expressed as :

$$P_i = D + Q_i \dots\dots\dots (21)$$

$$\text{with } \begin{cases} Q_i = 0 & \text{if summer} \\ Q_i \neq 0 & \text{if winter} \end{cases}$$

$$\begin{aligned} P_i &= D + Q_i \\ &= Q_n \left(\frac{D}{D_n} \frac{D_n}{Q_n} + \frac{Q_i}{Q_n} \right) \\ &= Q_n (d \gamma + q_i) \dots\dots\dots (22) \end{aligned}$$

where

- $\gamma = 0.25$
- $q_i = r_i \cdot g_i$
- $Q_n = \text{Design Live Load of Ottawa} = 43.44 \text{ psf}$

The distribution assumption and model parameters chosen for d , r_i , g_i are summarized as follows :

Parameter	Distribution	Model Parameters
d	Normal	Mean = 1.0 Standard Deviation = 0.1
r_i	Lognormal	Mean = 0.6 Standard Deviation = 0.27
g_i	Gumbell	$A^* = 5.644$ $B^* = 0.4$

As a summary, the table below shows the complete set of simulations which have been performed :

Load Case (1)	Elastic Analysis (2)	Visco-Elastic Analysis (3)
Cyclic Loads	200	200
Constant Load - 43.44 psf	200	200
- 45 psf	200	200
- 50 psf	200	200
- 70 psf	200	200
- 90 psf	200	200
Total	1200	1200
	2400	

4.3 Results.

4.3.1 Failures

The numbers of failures observed for cyclic and constant load simulations are summarized in Table 2.

Under cyclic loads, the same number of failures was observed for both the elastic and viscoelastic floors. This result is explained by the fact that the failures occur under a high live load at the time the live load is applied. The viscoelastic behavior does not have any significant effect on damage accumulation rates.

Under constant loads, there is a small difference between elastic and viscoelastic case. Of course, this difference decreases as the load increases. (Under very high loads, the number of failures will tend to 200 in both elastic and viscoelastic cases.)

The distributions of times-to-failure (for the floors that failed only) are reported in Table 3.

For cyclic load cases, 5 (of the 6) failures occurred exactly at the same time in elastic and viscoelastic cases. This time was always the beginning of a winter segment. For constant loads, we can say that the average time-to-failure decreases as the load level increases (except 43 44 psf for elastic case where only 2 failures occurred).

To analyze the reduction of time-to-failure due to viscoelastic effects, we tried different predictors

$$R = (\text{Average Time-to-failure Elastic}) / (\text{Average Time-to-failure viscoelastic})$$

(Table 3, Column 5)

Usually, this ratio is less than 1. But the distributions are so skewed that we did not trust this estimator.

* In Table 4, Columns 2 & 3, we reported the distributions of ratios of Times-to-failure. This ratio is evaluated for each simulation that failed both under elastic and viscoelastic assumptions.

For low load levels, these distributions have a mean of 0.5-0.7.

But for high loads, the distributions are slightly different.

* In Table 4, Column 4, we reported the median of these distributions. This median is always less than 1 (0.5-0.8).

* In Table 4, Column 5, we reported the probability of getting a ratio less than 1. We see that for high loads, we have 15% of chances to get a ratio over than 1. This can happen if the joist that fails creeps more than the others.

4.3.2 Stresses in Lumber and Panels.

* Cyclic Loads.

Examples of stress evolutions for viscoelastic systems are given in figures 6 and 7.

Usually, the stress due to the dead load decreases in the cover. During the live load segments, the viscoelastic behavior does not have time enough to affect the stresses.

During the dead load segments, the stress evolution in the joists is affected by a combination of two factors: 1) increasing stresses due to the transfer of stress from the cover to joists and 2) decreasing stresses due to the recovery of live load segments. Therefore, the stress tends to be essentially constant. During the live load segments, the response is nearly elastic since stresses do not vary significantly with time.

* Constant Loads.

As expected, the general trend for stresses is to increase in the joists (figure 3) and decrease in the cover (figure 4). For constant load studies, the stress levels changed less than 5% due to time-dependent effects.

In spite of a general trend of decreasing stresses in the cover, some local redistributions occur which may affect the maximum stress of the cover (figure 4, first 5000 hours).

In Tables 5 and 6, we reported the maximum bending stresses for the joists and the cover.

Maximum stresses for the viscoelastic analysis are less than 5% (Columns 5) greater than maximum elastic stresses.

The constant load equivalent to cyclic loads is between 45 and 50 psf.

4.3.3 Deflections.

* Cyclic Loads.

A typical creep and recovery curve for a cyclic load case is given in Figure 5. The deflection can be regarded as a superposition of two curves: 1) an average creep curve due to the dead load and 2) superimposed segments of short term creep curves due to the live loads. The short term creep curves have much higher creep rates. Segments of dead load creep may be modified by some recovery from the live loads.

* Constant Loads.

The typical constant load creep curve (Figure 5) has the deflection pattern of a traditional creep curve.

Maximum values of deflections are summarized in Table 7. The viscoelastic effect, i.e. the additional deflection due to creep, ranges from 50% to 100% of the initial elastic response.

As for the stresses, we see that the ratio of maximum deflections for high loads tends to the cyclic loads case. The reason is that the maximum deflections in cyclic loads cases occur during live loads, which are high.

For the cyclic loads, the ratio is low because live loads segments are short.

For the constant loads, this is rather explained by a large proportion of failures which limit the creep.

Conclusion :

Considering linear viscoelastic behavior in floor calculations leads to some remarks

- probabilities of failure are not affected
- times-to-failure might be reduced of 10-20%
- bending stresses are not affected.
- deflection amplification factors are large and even larger than predicted by the codes. This should be taken into account in further calibrations

The calculation required data for both lumber and panels which had to be adapted from many different sources to generate the required input files. If viscoelastic studies should be pursued, it means that much more effort must be directed to obtaining the viscoelastic material property data for wood products.

The Monte-Carlo simulation was limited to a small number of replications (200), the number of joists is small (3), the duration of load is short (10 years). All these limitations restrict the interpretation of the results. Additional studies would need to be completed to establish the general applicability of the conclusions derived herein.

Even with these limitations we must remember that a few years ago this study could not have been performed. The evolution of computers is so fast that in near future, more extensive studies will be possible and work should be continue to develop analytical tools and material property data required for viscoelastic behavior studies.

References :

- [1] ANDERSON D L
Viscoelasticity and Plasticity
Graduate Course University of British Columbia Dept of Civil Engineering
- [2] CRAIG B 1986
Comparison of Creep Duration of Load Performance in bending for Parallam Parallel Strand Lumber to Machine Stress Rated Lumber
Masters Thesis University of British Columbia Faculty of Forestry 223 pages
- [3] FOSCHI R O July 1982
Structural Analysis of Wood Floor Systems (Journal of The Structural Division Proceedings of The American Society of Civil Engineers ASCE Vol 108 N ST⁷ July 1982 p 1557-1574)
- [4] NIELSEN L F 1984
Power law creep as related to relaxation elasticity damping rheological spectra and creep recovery with special reference to wood
Paper prepared for the International Union of Forestry Research Organizations Timber Engineering Group Meeting Dec 10-15 1984 Xalapa Mexico
- [5] ROUGER F 1988
Application des Methodes Numeriques aux Problemes d'Identification des Lois de Comportement du Materiau Bois
These de doctorat de l'Universite de Technologie de Compiègne 135 pages
- [6] ROUGER F 1988
Structural Analysis of Wood Systems considering viscoelastic behavior
Part I Theoretical Development
Univ of British Columbia Reliability of Wood Structures Series 43 pages
- [7] ROUGER F BARRETT J D FOSCHI R O 1988
Structural Analysis of Wood Systems considering viscoelastic behavior
Part II Reliability Analysis of Viscoelastic Floors
Univ of British Columbia Reliability of Wood Structures Series 63 pages
- [8] WONG P C K BACH L CHENG J J 1988
The Flexural Creep Behavior of OSB stressed skin Panels
Univ of Alberta Dept of Civil Engineering Struct Eng Report 158 155 pages
- [9] YAO Z C Apr 1984
Reliability of Structures with load history dependent strength and an application to wood members
Masters Thesis Univ of British Columbia Dept of Civil Engineering 104 pages

Loading Case (1)	Elastic (2)	Visco-Elastic (3)	Ratio (4)
Cyclic Loads	6	6	1
Constant Load = 43.44 psf	2	5	2.5
- 45 psf	5	6	1.2
- 50 psf	10	13	1.3
- 70 psf	80	87	1.09
- 90 psf	164	172	1.05

Table 2 : Number of Failures

Loading Case (1)	Elastic		Visco-Elastic		Ratio (6)
	Mean (2)	STD ^a (3)	Mean (4)	STD ^a (5)	
Cyclic Loads	6.32e4	2.3e4	5.4e4	3.1e4	0.86
Const. Load = 43.44 psf	2.3e4	1.9e4	4.9e4	2.8e4	2.15
- 45 psf	5.3e4	3.3e4	4.4e4	2.7e4	0.83
- 50 psf	3.9e4	3e4	3.5e4	2.5e4	0.91
- 70 psf	2.7e4	3.05e4	2.1e4	2.5e4	0.78
- 90 psf	1.5e4	2.35e4	1.1e4	2.03e4	0.76

Note: 1 lb = 4.45 N, 1 in = 25.4 mm, 1 psi = 6.9E-03 MPa
^a STD - Standard Deviation

Table 3 : Times to Failure (hours)

Loading Case (1)	Mean (2)	STD ^a (3)	Ratio @ p=0.5 (4)	p @ Ratio=1 (5)
Cyclic Loads	0.85	0.32	xxx	xxx
Const. Load - 43.44 psf	0.61	0.22	0.6	1.00
- 45 psf	0.62	0.14	0.7	1.00
- 50 psf	0.72	0.38	0.63	0.85
- 70 psf	3.3	22.5	0.73	0.83
- 90 psf	1.3	3.35	0.76	0.83

^a STD Standard Deviation

Table 4 : Ratios of Times-to-Failure

Loading Case (1)	Elastic		Visco-Elastic		Ratio (6)
	Mean (2)	STD ^a (3)	Mean (4)	STD ^a (5)	
Cyclic Loads	2375	696	2454	712	1.03
Const. Load - 43.44 psf	2156	108	2286	127	1.06
- 45 psf	2233	112	2368	131	1.06
- 50 psf	2482	125	2630	145.6	1.06
- 70 psf	3474	175	3650	203	1.05
- 90 psf	4467	225	4602	254	1.03

Note: 1 lb = 4.45 N, 1 in = 25.4 mm, 1 psi = 6.9 E-03 MPa
^a STD Standard Deviation

Table 5 : Maximum Stresses (psi) in Joists

Loading Case (1)	Elastic		Visco-Elastic		Ratio (6)
	Mean (2)	STD ^a (3)	Mean (4)	STD ^a (5)	
Cyclic Loads	142	49.8	142	51	1.00
Const. Load - 43.44 psf	128.5	24.1	132	26.5	1.03
- 45 psf	133.1	25	136.8	27.5	1.03
- 50 psf	147.9	27.7	152	30.5	1.03
- 70 psf	207	39	212	42.6	1.02
- 90 psf	266	50	270	52	1.015

Note: 1 lb = 4.45 N, 1 in. = 25.4 mm, 1 psi = 6.9E-03 MPa
^a STD - Standard Deviation

Table 6 : Maximum Stresses (psi) in Cover

Loading Case (1)	Elastic		Visco-Elastic		Ratio (6)
	Mean (2)	STD ^a (3)	Mean (4)	STD ^a (5)	
Cyclic Loads	2.19	0.652	3.42	0.87	1.56
Const. Load - 43.44 psf	2	0.136	4.41	0.4	2.21
- 45 psf	2.075	0.14	4.56	0.42	2.20
- 50 psf	2.3	0.156	5.04	0.49	2.19
- 70 psf	3.23	0.22	6.29	1.38	1.95
- 90 psf	4.15	0.28	6.28	1.97	1.51
<i>Joists acting alone at P = 43.44 psf</i>	<i>2.824</i>	<i>0.41</i>	<i>6</i>	<i>0.91</i>	<i>2.125</i>

Note: 1 lb = 4.45 N, 1 in. = 25.4 mm, 1 psi = 6.9E-03 MPa
^a STD - Standard Deviation

Table 7 : Maximum Deflections (inches) in Joists

Constant Loading (50 psf)

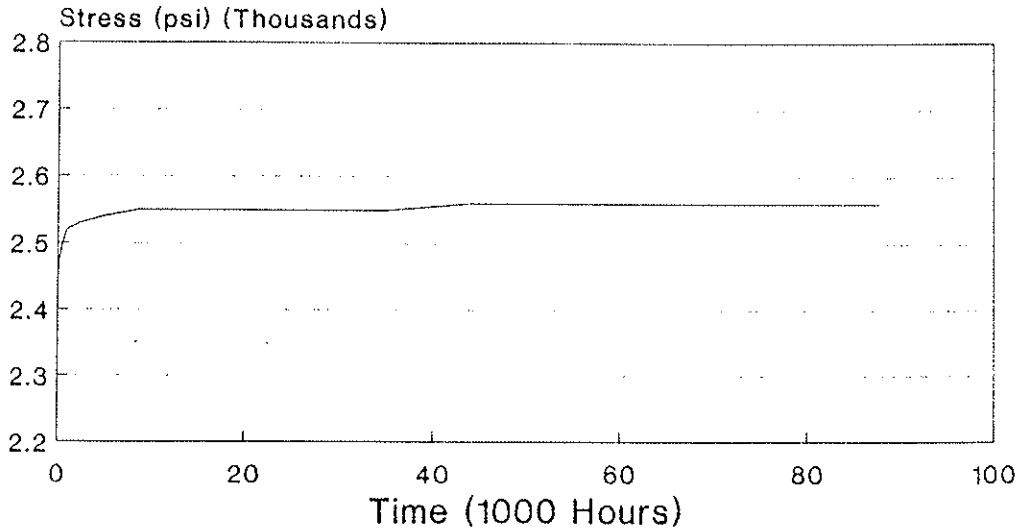


Figure 3 : Bending Stress in the joists

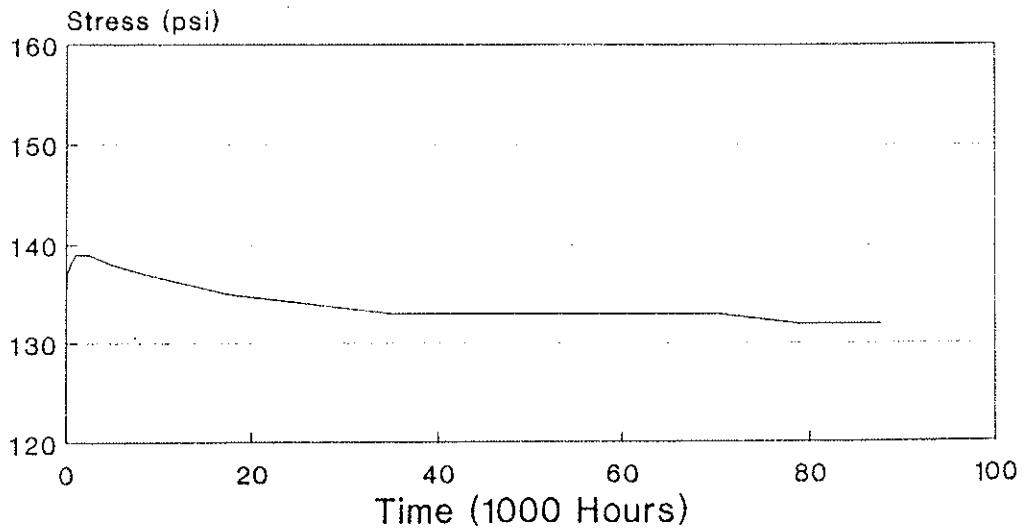


Figure 4 : Bending Stress in the cover

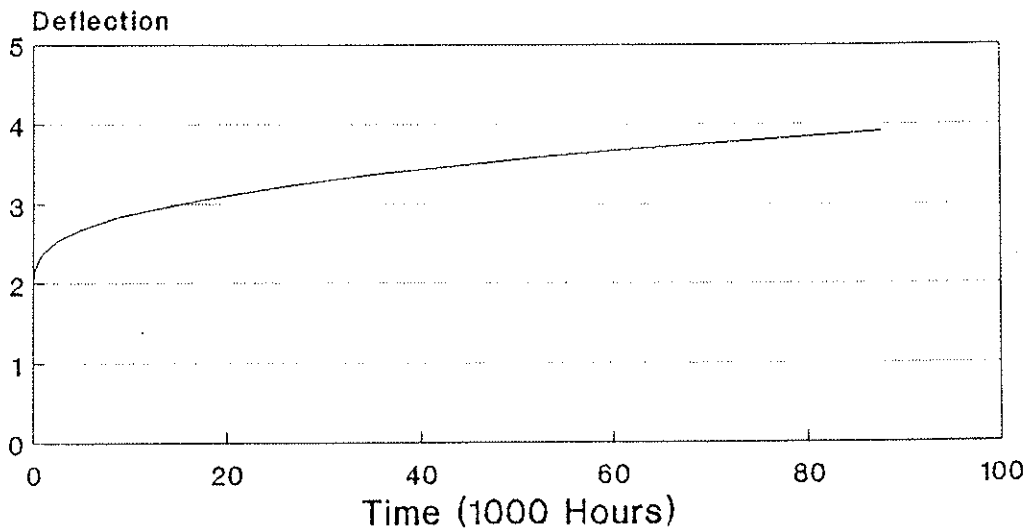


Figure 5 : Deflection.

Cyclic Loadings

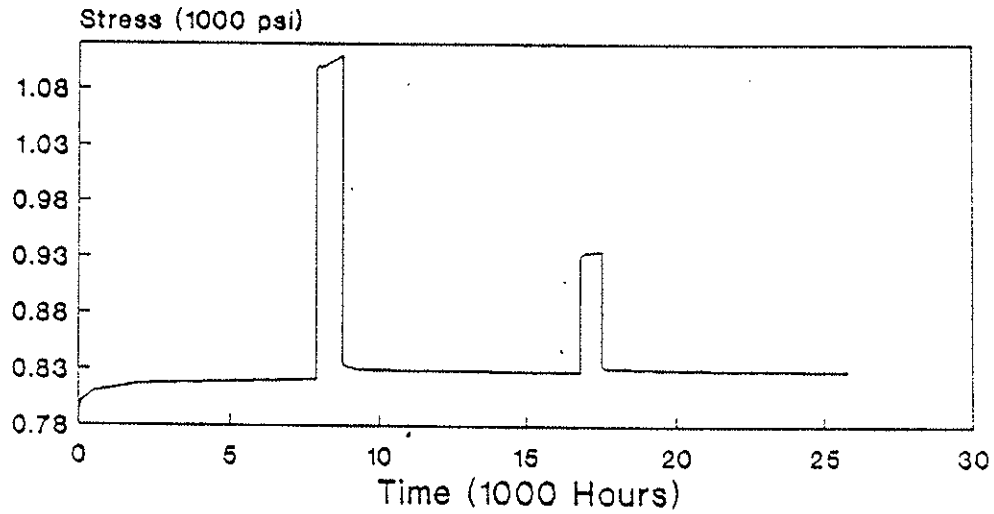


Figure 6 : Bending Stress in the joists

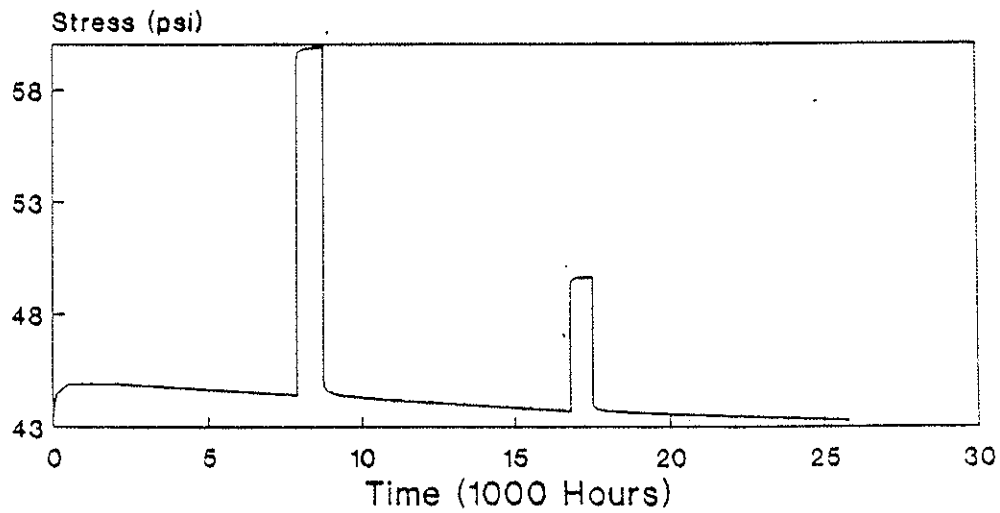


Figure 7 : Bending Stress in the cover

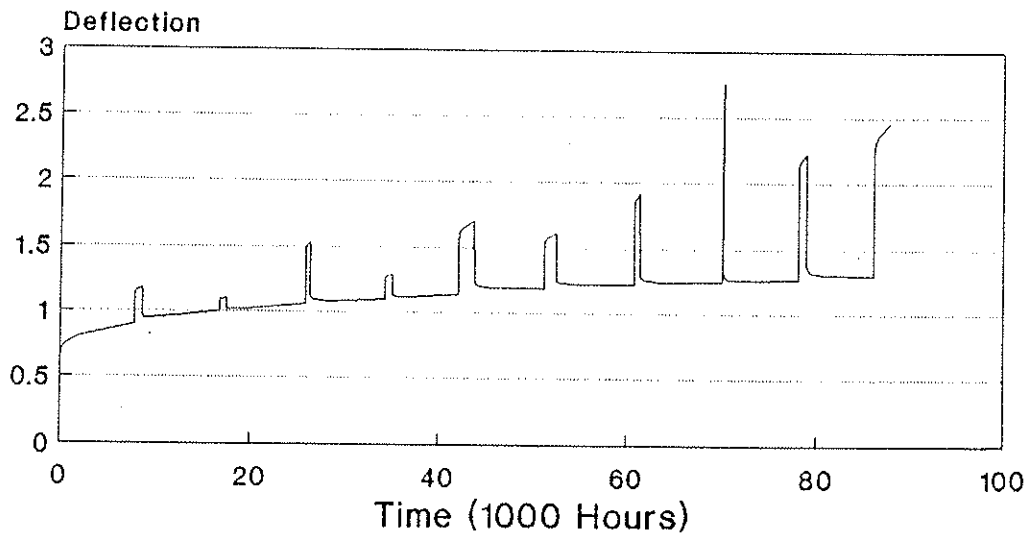


Figure 8 : Deflection.

INTERNATIONAL COUNCIL FOR BUILDING RESEARCH STUDIES AND DOCUMENTATION

WORKING COMMISSION W18A - TIMBER STRUCTURES

LONG-TERM TESTS WITH GLUED LAMINATED TIMBER GIRDERS

by

M Badstube and W Rug
Academy of Building of the GDR
Institute for Industrial Buildings
German Democratic Republic

and

W Schone
Institute for Building Units
and Fibre Building Materials
German Democratic Republic

MEETING TWENTY - TWO

BERLIN

GERMAN DEMOCRATIC REPUBLIC

SEPTEMBER 1989

1. Introduction

The present report is dealing with the preparation and implementation of long-term investigations and tests with glued laminated timber girders subjected to bending. The layers of the "BSH M3"-type glued laminated timber have been sorted mechanically to obtain strength grades. The tests are being carried out under an outdoor roofed storage facility and will be continued for a minimum period of 10 years. In this connection, the girders are being exposed to a variable long-term loading.

The objective of the tests and investigations is the measurement of time-dependent deformations and the determination of the residual loadbearing capacity after a loading period of at least ten years.

From the results and findings, the creep factor K_{creep} and the modification factor as to "load action period" $K_{\text{mod},1}$ will be obtained.

They are being compared with those factors indicated in the Eurocode 5 /1/ and will possibly be applied in the new TGL 33 135/04 GDR Industrial Code Specification /2/.

2. Determination of the variable long-term stressing

In addition and as a supplement to the factors

- creep factor K_{creep} , and
- "load action period" modification factor $K_{\text{mod},1}$

as used in the specifications mentioned under /1/and /2/, long-term tests with a loading being variable in terms of the time are required which shall be accomplished with a climate (environment) of "outdoors under a roof".

Timber is an elastoplastic material creeping until failure when subjected to a constant long-term load, with the strength decreasing with an increasing period of loading.

Similar properties are being found in the glue (adhesive) with glued laminated timber. Therefore, the tests and investigations are being performed by means of glued laminated timber girders.

The evaluation of publications as included in /3/ shows that mainly the individual influence of constant long-term loads with different periods of loading on the long-term strength of structural timber has been investigated.

However, it is necessary indeed to study and investigate the complex influence of variable long-term loads together with the action and effect of the air temperature, relative air humidity and timber moisture on structural timber and glued laminated timber.

The load combination of "dead load + snow" is being allocated to the variable long-term load.

Based on /4/, a timber roof frame (truss) is being selected the loading of which includes a large portion of dead load with a small portion of snow load. Thus, an insignificant rebound is occurring when relieving from "dead load + snow" to "dead load". The loading of the selected roof frame being supported by steel members D 24.5 (see /4/, page 34) is as follows:

dead load of roof:	0.27 kN/m ²
dead load of floor:	0.45 kN/m ²
dead load of installation:	0.29 kN/m ²

total dead load: s_K	=	1.01 kN/m ²
snow load: s_K	=	0.5 kN/m ²

dead load portion:

$$\frac{s_K}{s_K + s_K} = \frac{1.01}{1.01 + 0.5} = 0.67$$

The long-term tests are being accomplished by using glued laminated timber girders of the grade BSH M3 (see Figure 1).

Short-term tests carried out by means of BSH M3 specimens demonstrated that the flexural strength $f_{m,K}$ and the modulus of

elasticity $E_{o,mean}$ of grade BSH M3 timber are almost coinciding with strength grade C 5 as indicated in the Eurocode 5, 10/87 (see /1/, page 109). The characteristic value of the flexural strength is as follows:

$$f_{m,K} = 24 \text{ N/mm}^2.$$

The "load action period" modification factor being selected according to /1/, page 42, due to the large portion of dead load for the "long/medium" load action period grade and the moisture grade 1 or 2 amounts to

$$K_{mod,1} = 0.85.$$

The material factor being selected according to /1/, page 31, for glued laminated timber with regard to the adoption of a neutral foreign supervision in the manufacture of glued laminated timber (in German, abbreviated: BSH) amounts to

$$\gamma_M = 1.3.$$

This results in a design value of the flexural strength amounting to:

$$f_{m,d} = \frac{f_{m,K} \cdot K_{mod,1}}{\gamma_M} = \frac{24 \cdot 0.85}{1.3} = 15.7 \text{ N/mm}^2.$$

The design value is for the

- top stress:

$$\sigma_{m,1,d} = f_{m,d} = 15.7 \text{ N/mm}^2$$

- bottom stress:

$$\sigma_{m,2,d} = \frac{s_K}{s_K + s_K} \cdot \sigma_{m,1,d} = 0.67 \cdot 15.7 = 10.5 \text{ N/mm}^2.$$

The action periods for snow loads per annum are indicated as follows:

- 1 week to 6 months according to /1/, page 40
- 1.8 months according to /5/, page 217
- 2 months according to /6/, page 70
- 2.5 months according to /7/.

With regard to possible locations at a higher altitude above sea level, the action period being selected for the snow load is 2.5 months.

Now, this results in a variable long-term stressing (see Figure 2) amounting to:

$$\begin{aligned}\bar{\sigma}_{m,1,d} &= 15.7 \text{ N/mm}^2, \text{ action period of 75 d (days)} \\ \bar{\sigma}_{m,2,d} &= 10.5 \text{ N/mm}^2, \text{ action period of 285 d.}\end{aligned}$$

3. Description of the test specimens

12 test specimens consisting of BSH M3 grade glued laminated timber (see Figure 1) are being used for the long-term tests.

The specimens are girders subjected to bending with a width of $b = 97 \text{ mm}$, a height (depth) of $h = 192 \text{ mm}$, an effective span of $l_1 = 2880 \text{ mm}$ and a length of $l = 3080 \text{ mm}$.

The layers of boards of the glued laminated timber girders are consisting of sawn coniferous timber (pine) and are being sorted mechanically into strength grades according to the flexural modulus of elasticity and to the knottiness as follows:

- The 1st and 6th layer (see Figure 1) are belonging to the F II strength grade
($E \geq 9500 \text{ N/mm}^2$, individual knots according to Figure 3, accumulations of knots according to Figure 4, /8/)
- The 2nd to 5th layers (see Figure 1) are belonging to the F III strength grade
($E \geq 7000 \text{ N/mm}^2$, individual knots acc. to Fig, 3, accumulations of knots acc. to Fig. 4, /8/).

Decisive for the allocation to a strength grade is the unfavourable value of one sorting parameter.

The glueing (bonding) of the layers of boards with one another as well as of the key-dovetail connections is being performed by using a "Plastasol L47 N"-type phenolic resin bonding adhesive.

As a general principle, a key-dovetail connection is being arranged in layer 1 (being the lowest layer - tension layer -; see Figure 1) within the test zone (see Figure 5). In our instance, the key-dovetailing length amounts to 50 mm.

The distance of the key-dovetail connections (key-dovetail staggering; in German abbreviated as KZV) between the 1st and 2nd layer is being guaranteed with an amount of $KZV \geq 250$ mm.

The equilibrium moisture of the layers of boards after the manufacture amounts to $\omega \approx 12$ %.

4. Test arrangement

With a view to achieving a zone being free from transverse forces, a four-point loading is being selected for the test arrangement of the glued laminated timber girders (see Figure 5).

The results and findings from studies and investigations performed by using structural timber /9/ are showing that - in order to avoid shear failures - the ratio of the flexural stress $\sigma_{m,d}$ to the shear stress τ_d shall be 22 whereas for a shear influence of about 6 % the ratio of the effective span l_1 to the specimen height h shall be 15. With these prerequisites prevailing, the length of the test zone l_2 is being designed as $l_2 = 4 h$ /9/ (see Figure 5).

The values of the variable long-term load resulting from the long-term stresses are as follows:

- for dead load + snow:	$F_{1,d}$	=	17.74 kN;	t	=	75 d
- for dead load:	$F_{2,d}$	=	11.89 kN;	t	=	285 d

The force $F_{1,d}$ (see Figure 5) is being introduced by means of a mass piece (weight) M through a lifting rack-type facility.

The hinge G is vertically movable in order to ensure a horizontal position of the load lever also with an increasing deflection U_z .

The long-term tests are being accomplished under the cover of a roofed-over outdoor facility. With such a climatic test condition, the test specimens are freely exposed to the air temperature, air humidity and air motion of the external climate. However, the specimens are protected from precipitations and sunshine.

The maximum equilibrium moisture to be expected amounts to $\omega \leq 18\%$ according to /10/ and corresponds to the moisture grade 2 in compliance with /1/.

5. Measurements

The measurements to be performed during the long-term tests with regard to the time are as follows:

(a) Girder deflection U_z

It is being determined at the central position of the effective span (see Figure 5) by means of a dial gauge with a reading accuracy of 0.1 mm and in addition - for control purposes - by means of a gauge stick (measuring rod) and a level with a reading accuracy of 0.5 mm.

(b) Strains ϵ_x

Within the layers of boards 1 and 6 (see Figure 1), respectively, at the central position of the effective span the strains of the timber $\epsilon_{x,1}$ and $\epsilon_{x,6}$ are being measured by means of a mechanical strain gauge (stress-probing extensometer; manufacturer: Messrs. Holle, Magdeburg/GDR).

(c) Timber moisture ω

It is being determined through a pair of electrodes being permanently inserted into the girder - with a depth of penetration of about 20 mm - by means of measuring the electrical resistance (type of unit: "Hydromette H 65"; manufacturer: Messrs. Gann, Stuttgart/FRG).

(d) Air temperature T and relative air humidity φ

They are being recorded continuously by means of thermo-hygrographs (type 406; manufacturer: VEB Feingerätebau Drebach/GDR).

6. Initial results and findings

The long-term tests and investigations with the 12 girders have been started for test-engineering reasons only on April 15, 1988, instead of January 1, 1988, with the load stage $F_{1,d}$. The load stage $F_{2,d}$ was effective from June 29 until December 31, 1988. On January 1, 1989, the load stage $F_{1,d}$ of the 2nd year of loading has been applied.

The values and data of the measurements accomplished concerning T, φ , ω , ϵ_x and U_z are plotted and shown in the Figures 6 to 10 for the period from April 15 until December 31, 1988. /11/

The graphical representations of the measured quantities X are comprising X_{mean} , X_{max} and X_{min} .

With a view to increasing and improving the lucidity, the graphical representations are being drawn up on semilogarithmic paper.

Due to the fact that the time ranges immediately after the loading or relief, respectively, are of a particular interest, the time scales (units) of minutes (min) and days (d) are being used in the graphical representations (Figures 6 to 10).

The most significant measured quantities are the girder deflections U_z and the creep deformations occurring in the course of time.

The mean deflections $U_{z,\text{mean}}$ amount to

$$- U_{z,\text{mean},0} = 12.5 \text{ mm}$$

with $t = 0$ for $F_{1,d}$ according to Figure 6;

$$- U_{z,\text{mean},75 \text{ d}} = 18.5 \text{ mm}$$

with $t = 75 \text{ d}$ for $F_{1,d}$ according to Figure 7;

the creep factor corresponding to this is as follows:

$$K_{\text{creep},1} = \frac{U_{z,\text{mean},75 \text{ d}}}{U_{z,\text{mean},0}} = \frac{18.5}{12.5} = 1.5$$

$$- U_{z,\text{mean},186 \text{ d}} = 14.1$$

with $t = 186 \text{ d}$ for $F_{2,d}$ according to Figure 10;

the creep factor corresponding to this is as follows:

$$K_{\text{creep},2} = \frac{U_{z,\text{mean},186 \text{ d}}}{U_{z,\text{mean},0}} = \frac{14.1}{12.5} = 1.1$$

The measured deflections provide for an initial comparison with the data included in the Eurocode 5 /1/.

The mean values of the measured relative air humidity φ_{mean} and timber moisture ω_{mean} (see the Figures 7, 9 and 10) are within the ranges of

$$\varphi_{\text{mean}} = 65 \text{ to } 95 \% ; \quad \omega_{\text{mean}} = 12 \text{ to } 18 \%$$

Thus, according to /1/, para 2.5.4., the moisture grade 2 is prevailing.

As for the load portions being applied during the tests -"dead load"

$$\frac{\varepsilon_K}{\varepsilon_K + s_K} = 0.67 ; \quad \text{"snow"} \quad \frac{s_K}{\varepsilon_K + s_K} = 0.33 \text{ -}, \text{ the creep}$$

factor $K_{\text{creep},1}$ resulting according to /1/, table 4.1, for moisture grade 2 and $F_{1,d}$ "dead load + snow" amounts to $K_{\text{creep},1} = 0.67 \cdot 1.8 + 0.33 \cdot 1.3 = 1.64$.

This value is exceeding that of $K_{\text{creep},1} = 1.5$ as determined during the test for $F_{1,d}$ at $t = 75 \text{ d}$.

According to /1/, table 4.1, the creep factor $K_{\text{creep},2}$ resulting for moisture grade 2 and $F_{2,d}$ "dead load" amounts to $K_{\text{creep},2} = 1.8$.

This value is exceeding that of $K_{\text{creep},2} = 1.1$ as determined during the test for $F_{2,d}$ at $t = 75 + 186 = 261 \text{ d}$.

However, a final statement concerning the creep factors can be provided only after a period of about 10 years upon the completion of the long-term tests and investigations.

In compliance with /1/, page 48, the deflection in the final state shall not exceed $\frac{l_1}{250}$.

In the hitherto accomplished tests and investigations, the largest mean deflection for $F_{1,d}$ "dead load + snow" at $t = 75$ d is as follows:

$$U_{z,mean,75 d} = 18.5 \text{ mm} > \frac{l_1}{250} = \frac{2680}{250} = 11.5 \text{ mm.}$$

The exceeding in the limit state of the usability does not mean that the loading $F_{1,d}$ as selected was too high.

This finds its expression by fixing $K_{mod,1}$ and γ_{II} for the determination of $\sigma_{m,1,d} = f_{m,d}$ in chapter 2 as follows:

$$\begin{aligned} K_{mod,1} &= 0.85 \quad \text{instead of } 0.9 \quad \text{according to /1/, page 42;} \\ \gamma_{II} &= 1.3 \quad \text{instead of } 1.25 \quad \text{according to /1/, page 31.} \end{aligned}$$

A consideration of the values of $K_{mod,1}$ and γ_{II} as indicated in /1/ would result in even higher loads and thus even larger deflections.

The development (curve) of the mean timber moisture ω_{mean} is following that of the mean relative air humidity φ_{mean} (see the Figures 7 and 9).

One can see that in the case of autumn weather lasting for a longer period with a high relative air humidity of $\varphi_{mean} \approx 93\%$ the timber moisture will reach the value of $\omega_{mean} = 18\%$ (see Figure 9).

However, connections between timber moisture changes and deflection changes cannot be discerned (see the Figures 9 and 10).

Similar observations apply to the strain change as well.

The developments (curves) of $U_{z,mean}$ within the load range of $F_{1,d}$ (see the Figures 6 and 7) are showing that immediately after the load application a very large increase in deflection ΔU_z can be observed (amounting to 2.2 mm/d on an average) which, however, is increasingly decaying with an amount of 0.1 mm/d.

Considerably less distinct are the creep deformations after the partial load relief to $F_{2,d}$ (see the Figures 8 and 10). Initially the decrease in deformation is only 0.1 mm/d on an average. The

backcreep processes can be regarded as decayed already after a period of 5 days.

7. Regression equations

The mathematical description of the time-dependent deflections is possible by means of simple regression equations.

The influence factor is the time t whereas the objective (target) factor is the mean deflection $U_{z,mean}$ of 12 test specimens.

The regression analysis is being performed by means of both exponential functions ($y = a \cdot \exp(bx)$) and logarithmic functions ($y = a + b \cdot \ln x$).

The regression equations with the highest correlation coefficients r are indicated in Figure 11.

8. Summary

Long-term tests and investigations are being carried out using glued laminated timber girders subjected to bending with the action of a variable long-term load at a climate (environment) of "outdoors under a roof".

Initial results and findings of the measurements are providing information on the magnitude of the creep factors to be expected.

Final values concerning the creep factors K_{creep} and the "load action period" modification factor $K_{mod,1}$ for the moisture grade 2 will be available after a period of about 10 years.

9. References (Publications)

- /1/ Eurocode 5 "Holzbauwerke" - Deutsche Entwurfsfassung;
Oktober 1987
(Eurocode 5 "Timber Structures" - German draft wording;
October 1987)
- /2/ DDR-Fachbereichsstandard TGL 33 135/04 E 89
"Holzbau, Tragwerke, Berechnung, Bauliche Durchbildung"
(Industrial GDR Code Specification TGL ...:
"Timber construction; Loadbearing structures; Calcula-
tion; Structural design")
Draft, September 1989
- /3/ Forschungsbericht G 2: "Langzeituntersuchungen an maschi-
nell sortiertem Brettschichtholz unter Biegebeanspruchung"
(Research Report G 2: "Long-term investigations with me-
chanically sorted glued laminated timber subjected to bending")
Academy of Building of the GDR, Institute for Industrial
Buildings; Berlin, December 1988
- /4/ "Dach- und Hallenkonstruktionen in Holzbauweise"
Informationen und Systemübersichten 1986
("Roof and hall structures built by adopting the
timber construction method" - Information and system
abstracts of 1986)
"Baufa" Research Institute, Leipzig
- /5/ Spaethe, G.:
"Die Sicherheit tragender Baukonstruktionen"
("The safety of loadbearing building constructions")
Published by: VEB Verlag für Bauwesen; Berlin 1987
- /6/ Steck, G.:
"Die Zuverlässigkeit des Vollholzbalkens unter reiner
Biegung"
("The reliability of the solid timber beam subjected to
pure bending")
Fridericiana University, Karlsruhe 1982
- /7/ Glos, P.:
"Was darf der Holzbau von dem neuen probabilistischen
Sicherheitskonzept erwarten?"
("What may timber construction expect of the new proba-
bilistic safety concept?")
Published in: Bauen mit Holz (1983) 1, pp. 26 - 31

References:(continued)

- /8/ DDR-Fachbereichsstandard TGL 33 135/03 E 88
"Holzbau, Tragwerke, Gütebedingungen, Bauschnittholz"
(Industrial GDR Code Specification TGL ...:
"Timber construction; Loadbearing systems; Quality specifications; Sawn structural timber")
Draft; March 1988
- /9/ Apitz, R.:
"Ermittlung von Festigkeitskennwerten für Vollholz bei der Beanspruchung Biegung durch Versuche"
("Determination of strength characteristics for solid timber subjected to bending by tests")
Wismar Engineering College; Progress Report dated 1982-11-27
- /10/ DDR-Fachbereichsstandard TGL 33 135/01
"Holzbau, Tragwerke, Berechnung, Bauliche Durchbildung"
(Industrial GDR Code Specification TGL ...:
"Timber construction; Loadbearing systems; Calculation; Structural design")
1st Modification dated 1986-06-24
- /11/ Prüfbericht Nr. 329 4005/88
"Langzeituntersuchung an festigkeitssortiertem Brett-schichtholz"
(Test Report No.: "Long-term investigation with strength-sorted glued laminated timber")
Researcher: W. Schöne; VEB Kombinat Bauelemente und Faserbaustoffe, Forschungsinstitut (Trust for Building Units and Fibre Building Materials; Research Institute)
Leipzig, 1988-11-14

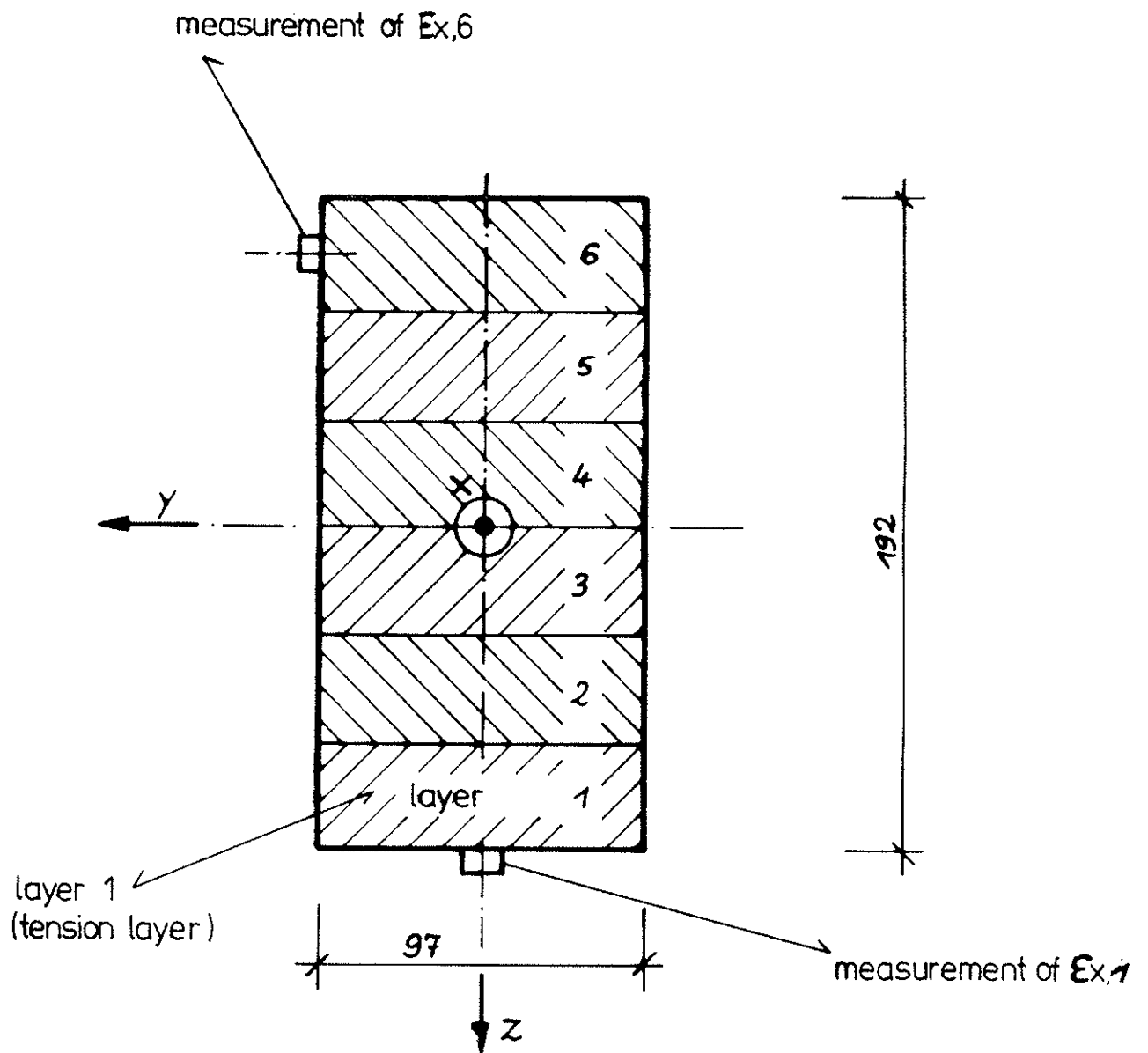


Figure 1: Girder cross section

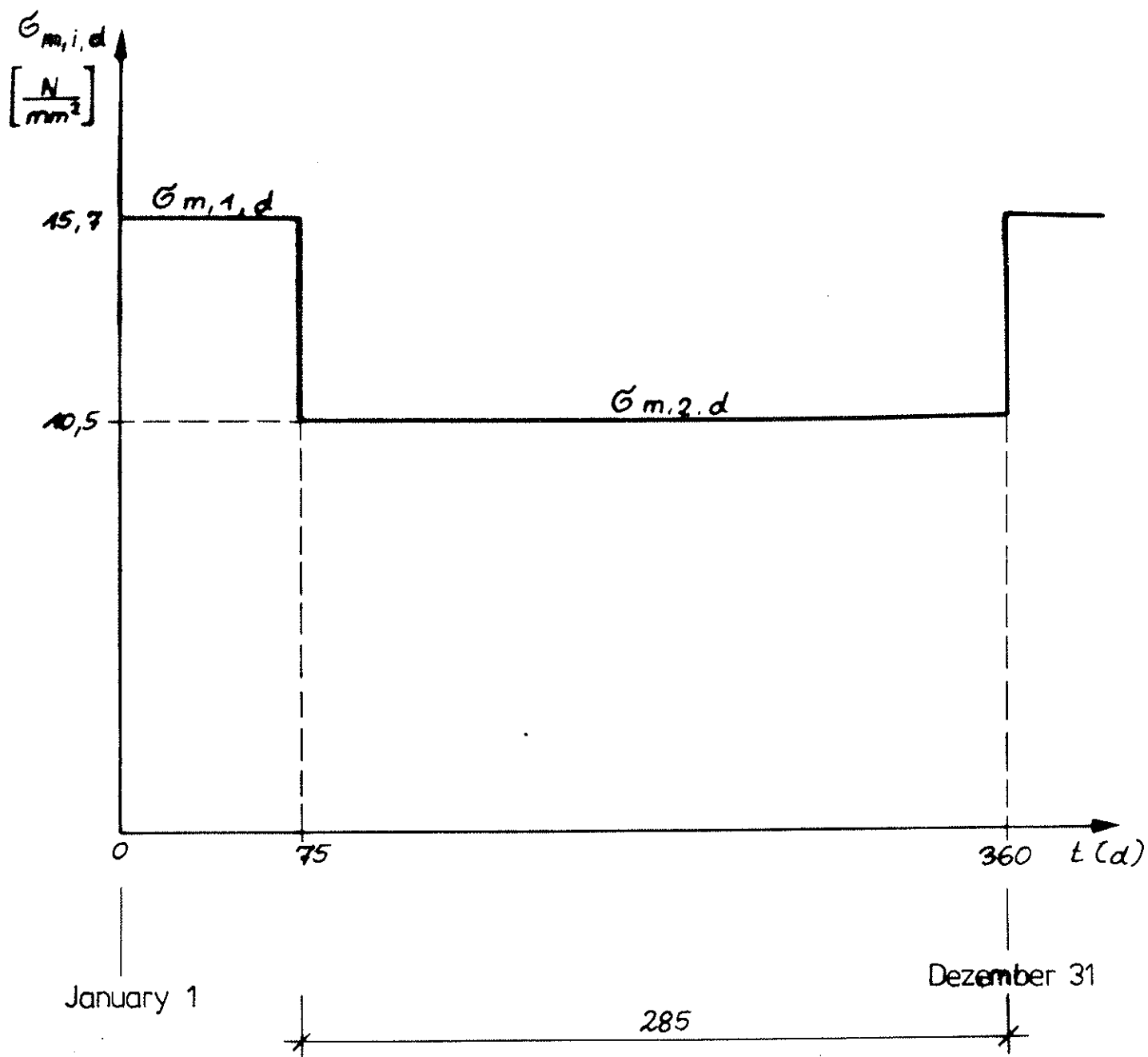
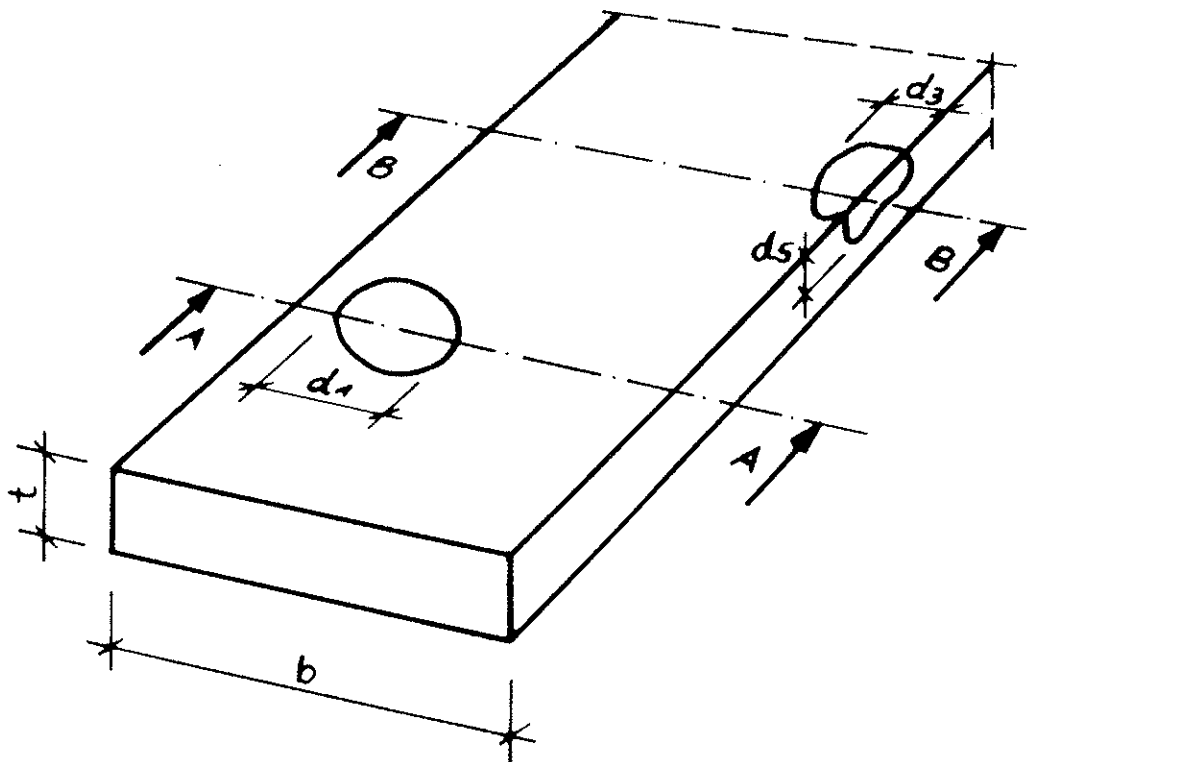
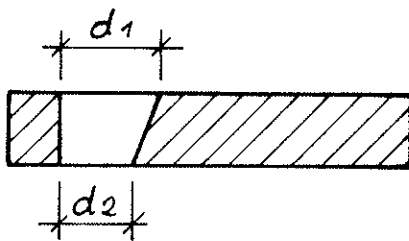


Figure 2: Variable long-term stressing

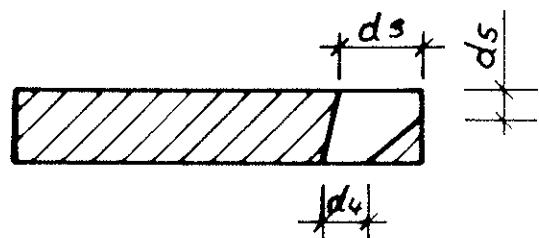


section AA



$$k = \frac{d_1 + d_2}{2b}$$

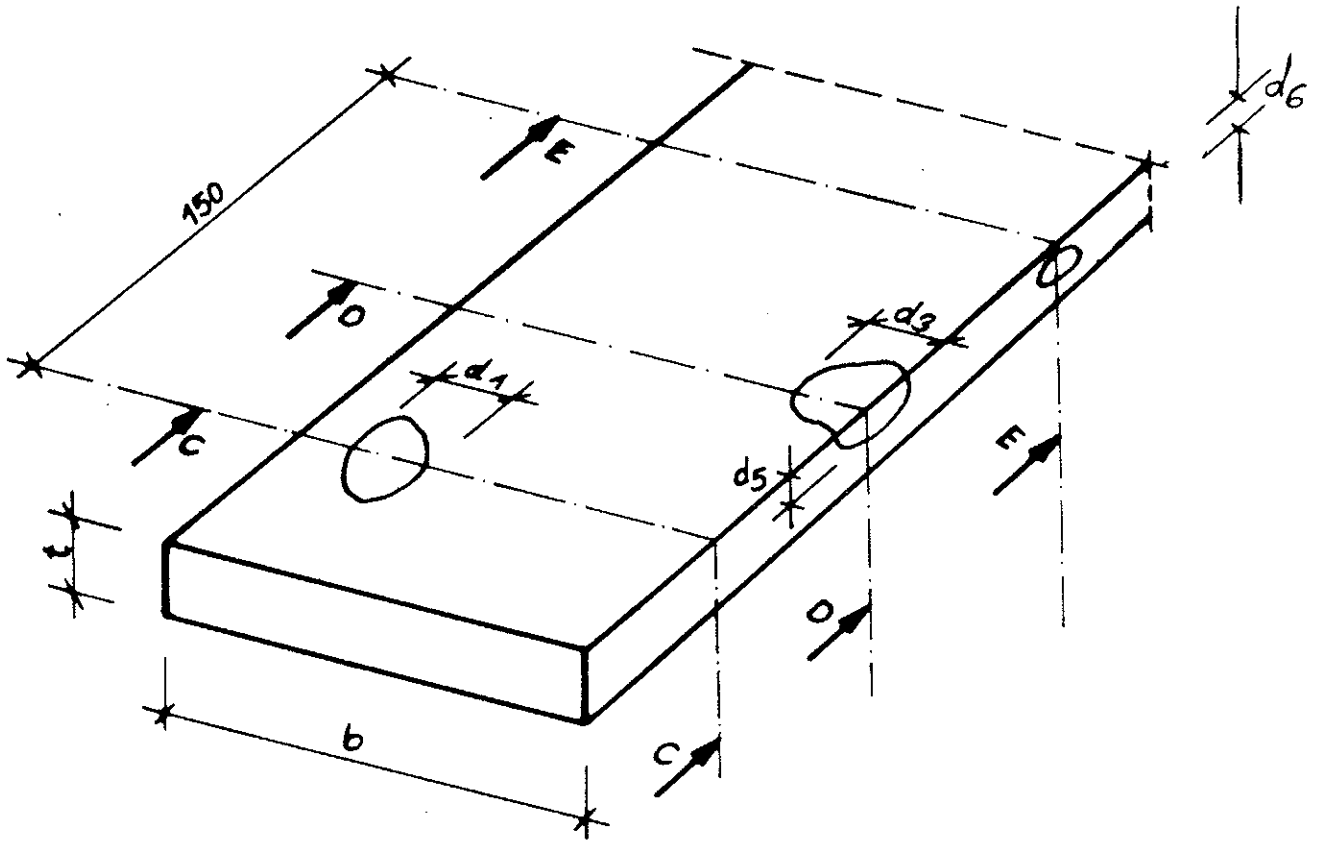
section BB



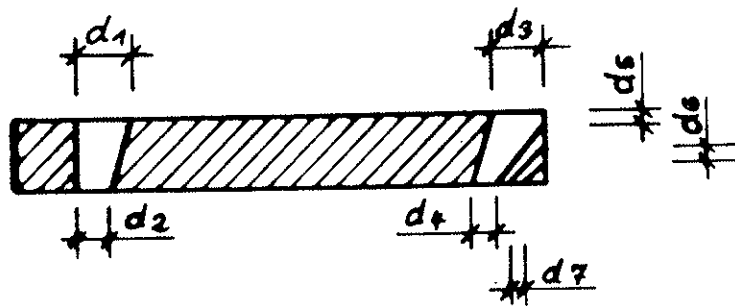
$$\frac{d_3 + d_4 + d_5}{2b}$$

k	strength grade
$\leq \frac{1}{3}$	F II
$\leq \frac{1}{2}$	F III

Figure 3: Sorting by individual knots



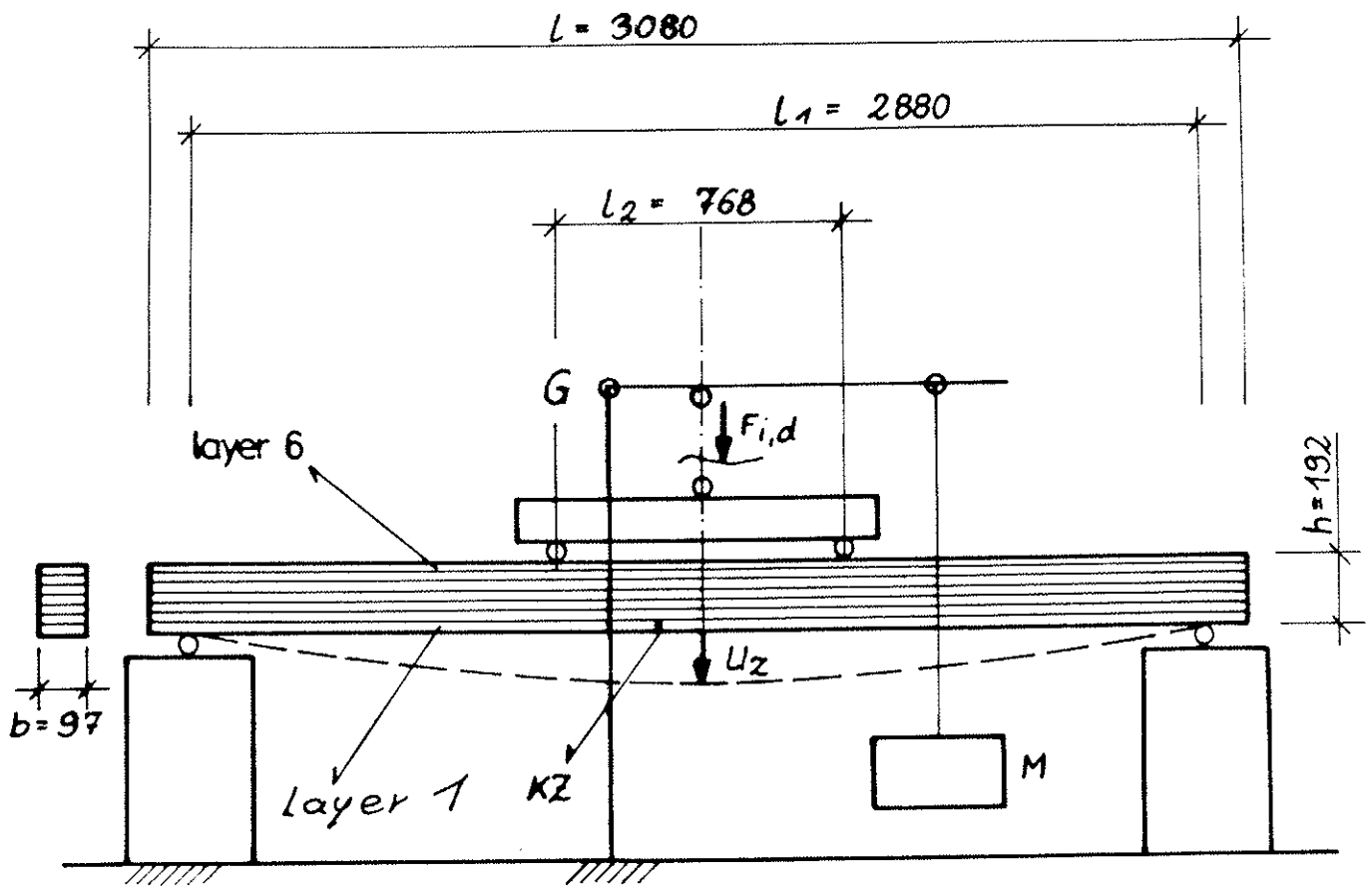
sections CC, DD, EE shown in one sectional drawing



$$K = \frac{d_1 + d_2 + d_3 + d_4 + d_5 + d_6 + d_7}{2b}$$

K	strength grade
$\leq \frac{1}{2}$	F II
$\leq \frac{2}{3}$	F I

Figure 4: Sorting by accumulations of knots



designations:

- a) F -with $i=1,2$ - variable long-term load
- b) U -maximum deflection
- c) h -test specimen height
- d) l -test specimen length
- e) l_1 -effective span $l_1 = 15h$
- f) l_2 -test zone length $l_2 = 4h$
- g) G -vertically adjustable hinge
- h) M -mass piece (weight)
- i) KZ -key-dovetail connection, always located within the test zone l , layer 1

Figure 5: Test arrangement

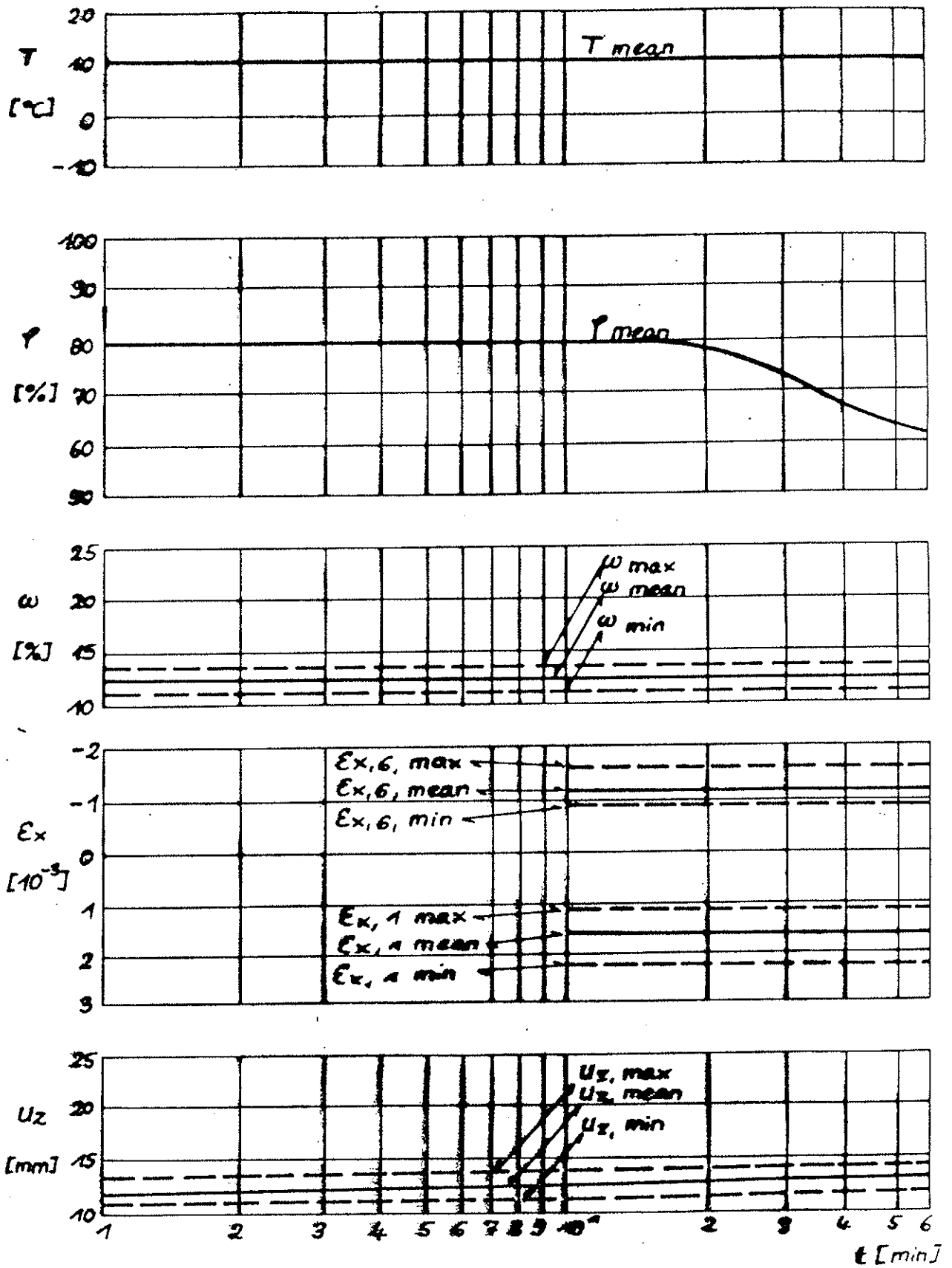


Figure 6: Measurements within the load range $F_{1,1}$, $t=1$ to 60 minutes, 1st year of loading, from April 15 until June 29 1988

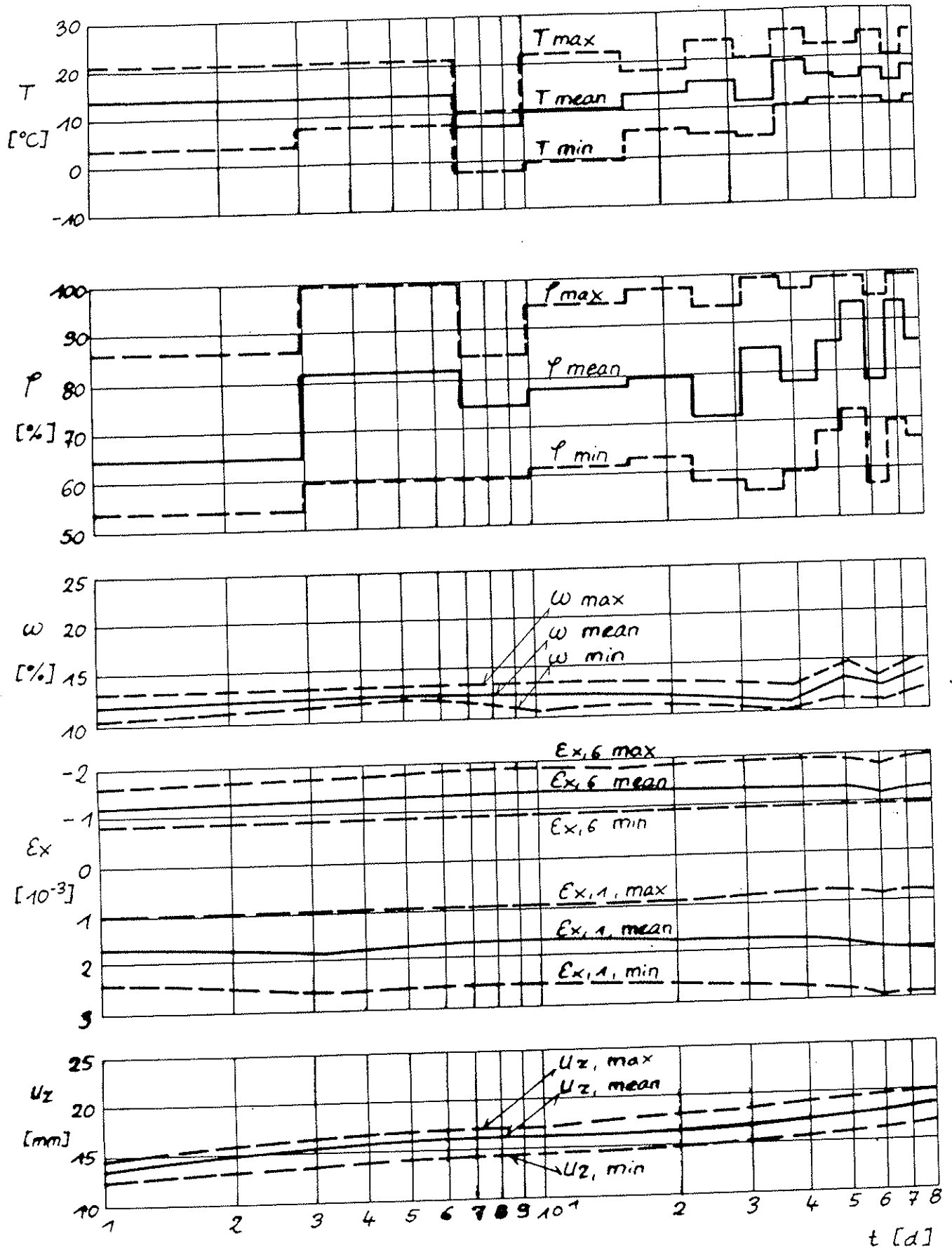


Figure 7: Measurements within the load range $F_{1,d}$; $t=1$ to 75 days; 1st year of loading; from April 15 until June 29, 1988

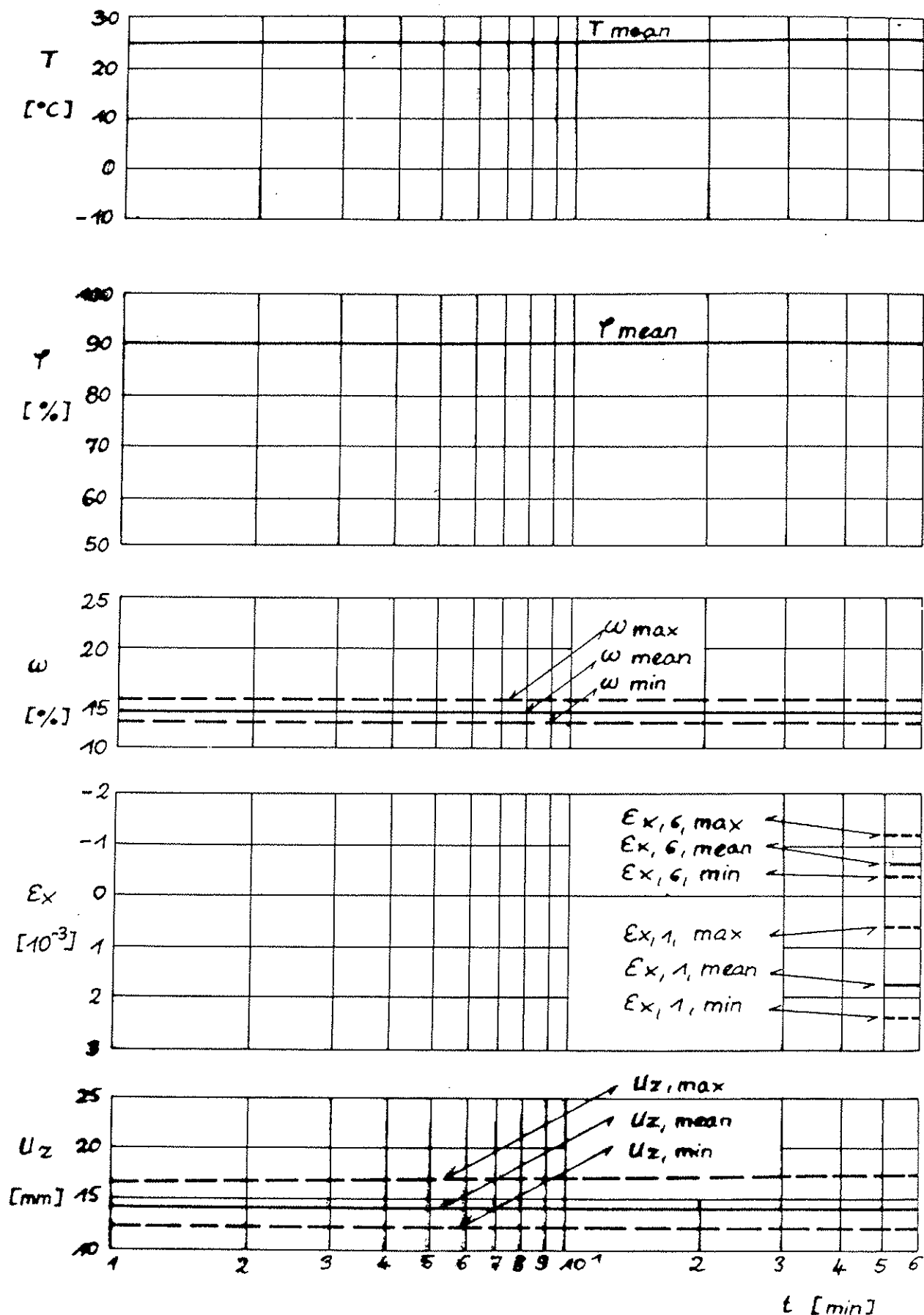


Figure 8: Measurements within the load range $F_{2,d}$; $t=1$ to 60 minutes; 1st year of loading, from June 29 until December 31, 1988

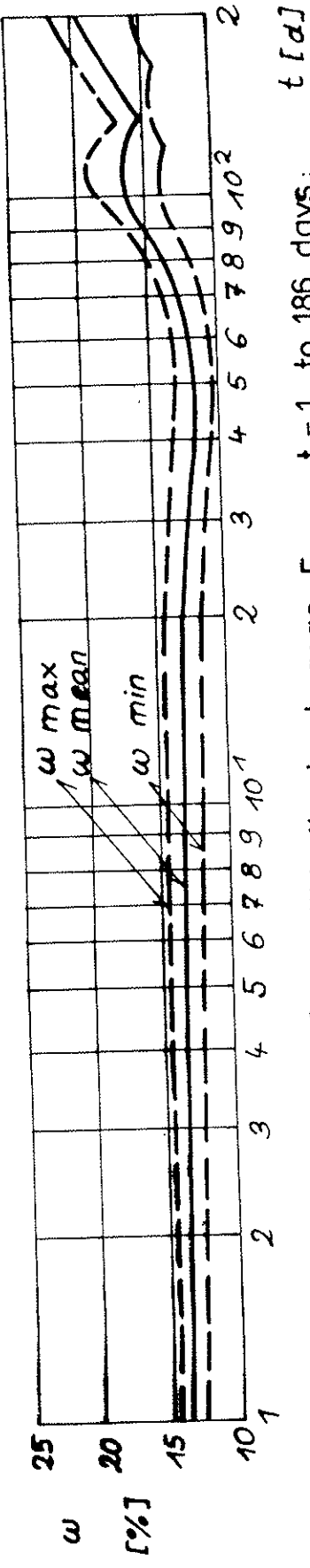
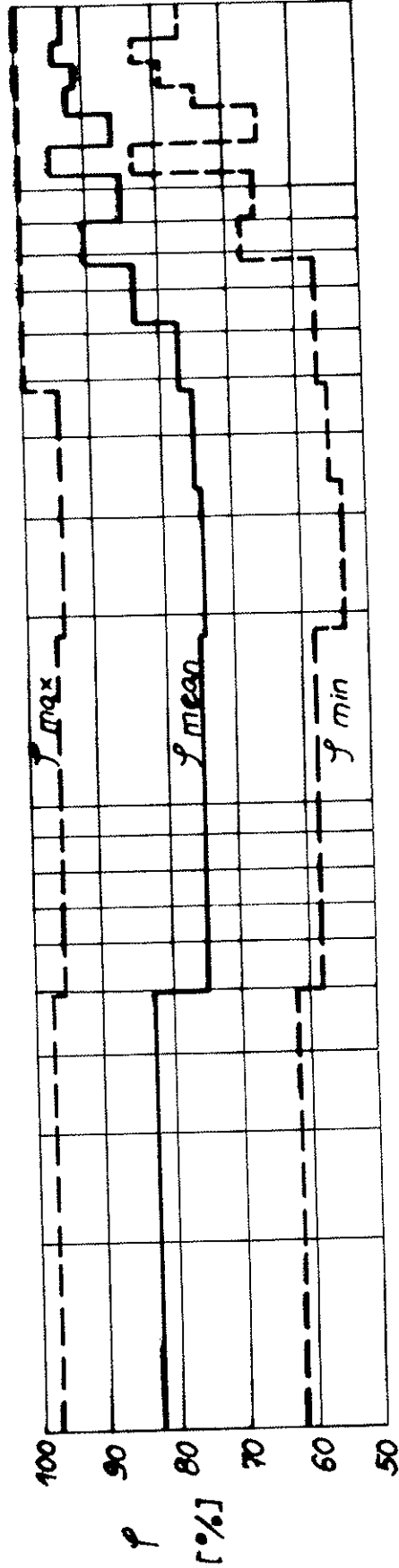
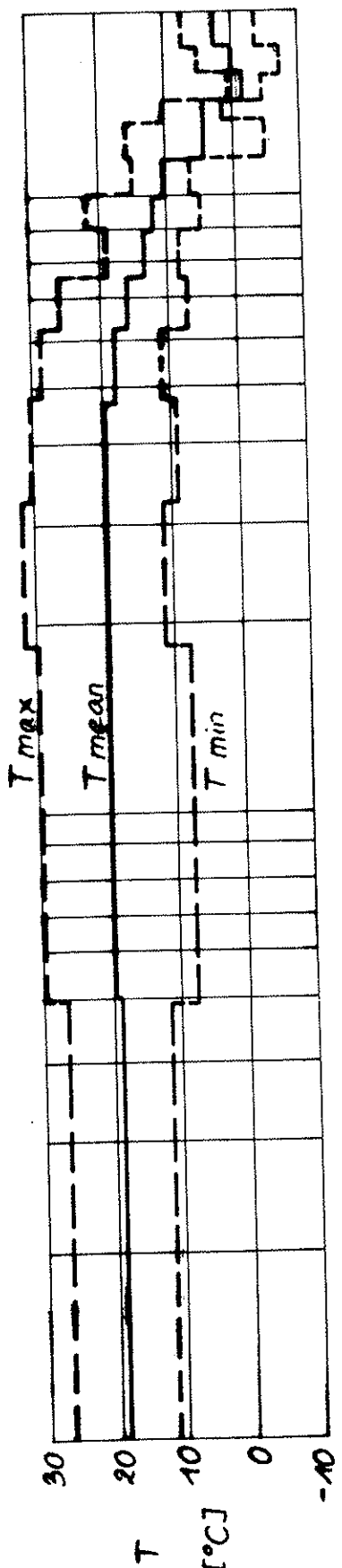


Figure 9: Measurement of T , φ , ω , within the load range $F_{2,d}$; $t = 1$ to 186 days; 1st year of loading; from June 29 until December 31, 1988

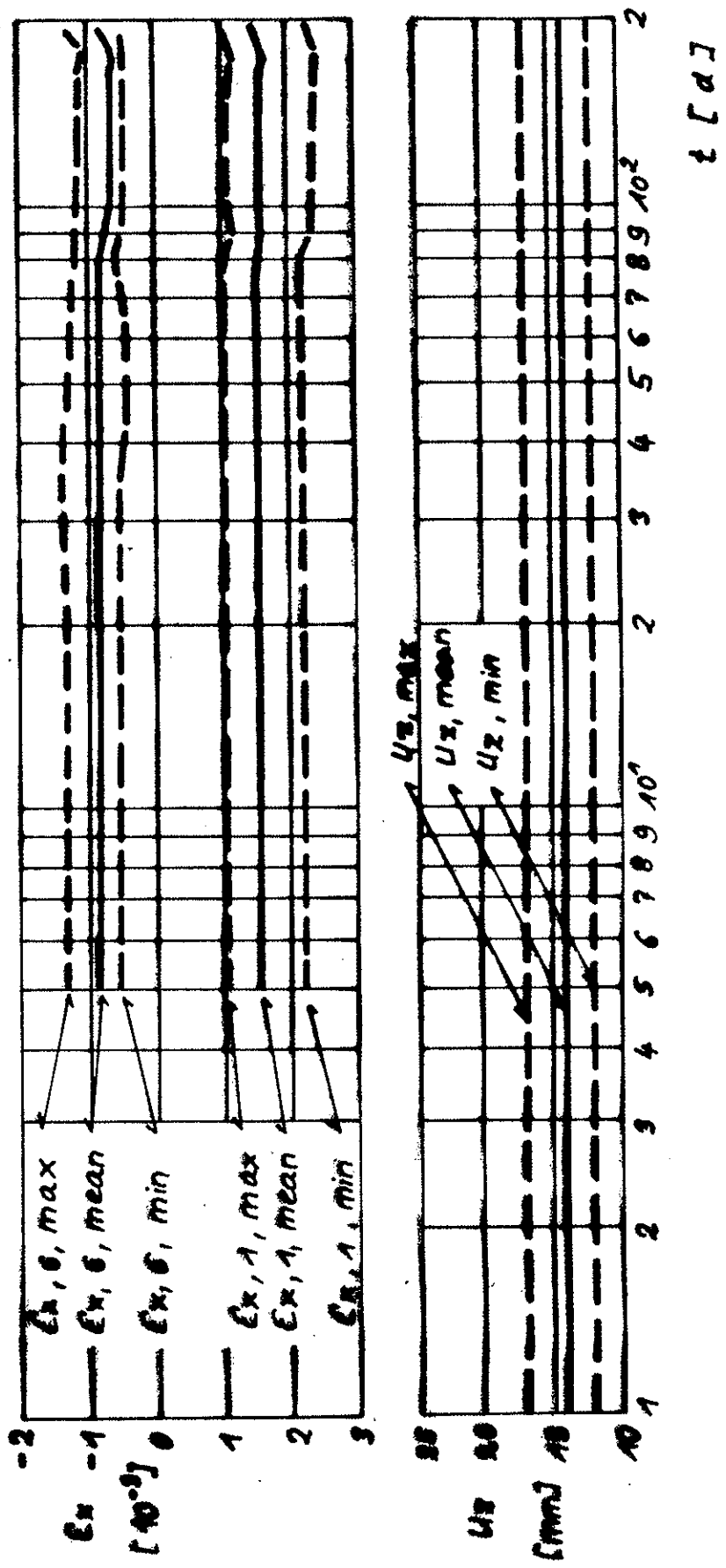


Figure 10: Measurement of ϵ_x, U_z within the load range $F_{2,d}$; $t = 1$ to 186 days; 1st year of loading; from June 29 until December 31, 1988

Load range	time range	$U_{z, \text{mean}}^{*})$ [mm]	r [-]
$F_{1,d}$	0,1 - 60 min	$12,51 + 0,135 \text{ } \ln t$	0,92
	0,1 - 108 000 min (75 d)	$12,13 + 0,488 \text{ } \ln t$	0,94
$F_{2,d}$	0 - 60 min	$14,4 \exp(-1,37 \cdot 10^4 t)$	0,9
	0,1 - 267 840 min (186 d)	$14,38 - 0,0475 \text{ } \ln t$	0,95

* t in minutes is to be entered

Figure 11: Regression equations of the mean deflections $U_{z, \text{mean}}$ according to /11/

INTERNATIONAL COUNCIL FOR BUILDING RESEARCH STUDIES AND DOCUMENTATION
WORKING COMMISSION W18A - TIMBER STRUCTURES

**STRENGTH OF ONE-LAYER SOLID AND LENGTHWAYS GLUED ELEMENTS
OF WOOD STRUCTURES AND ITS ALTERATION FROM SUSTAINED LOAD**

by

L M Kovaltchuk, I N Boitemirova and G B Uspenskaya
ZNIISK Moscow
USSR

MEETING TWENTY - TWO
BERLIN
GERMAN DEMOCRATIC REPUBLIC
SEPTEMBER 1989

Strength of one-layer solid and lengthways
glued elements of wood structures and its
alteration from sustained load

Nowadays, lengthways glued elements find wide application in wood structures, side by side with solid wood elements. As dimensional and species wood structure becomes worse and because of the necessity of its most full and rational use, the volume of lengthways glueing by means of tooth joints will increase.

Therefore, there appears the necessity of strength commensurability of lengthways glued elements and solid wood elements at the level of short-term values as well as the necessity of strength decrease estimation of these elements, depending on time and on operation actions.

Comparison of solid elements strength and lengthways glued elements strength was realized during the most widespread kind of stressed state, that is edge bending.

Test plans of solid and lengthways glued specimens are analogous: loading by means of concentrated forces in span thirds. Cross section of specimens $\sim 50 \times 150$ mm, span ~ 1900 mm, respectively. Test results of 3 samples of solid specimens from different regions, Arkhangelsky (samples 1a, b), Permsky (samples 2a, b) and Novovyatsky (samples 3a, b), as well as of 12 samples of lengthways glued specimens from 4 enterprises (EPZ "Krasny Octyabr", Yureskaya SPMK, Volokolamsky EZSK, Vologodsky DOK), with different types of tooth joints and different adhe-

sive sorts, are presented in Table 1. It was tested all together about 800 glued specimens and more than 300 solid specimens.

Average strength values of solid elements of group K24 vary from 33,7 MPa to 40,9 MPa, and norm values - from 26,09 to 26,5 MPa, for strength group K16 the values mentioned make up from 33,2 to 27,7 MPa and from 19,9 to 17,25 MPa, respectively.

Table 1

Initial strength of solid and glued
wood elements

Sam- ple No.	Sample characteristic	Quan- tity, pcs	Average strength value, MPa	Coeffi- cient of vari- ation,%	Norm strength value, MPa
1	2	3	4	5	6
Solid wood specimens of visual strength groups sorting					
1a	K 24	87	40,9	21,96	26,08
1b	K 16	56	33,2	32,50	17,13
2a	K 24	70	37,3	18,2	26,09
2b	K 16	34	29,6	19,9	19,90
3a	K 24	37	33,7	13,0	26,5
3b	K 16	24	27,7	18,9	19,1
Glued specimens					
4a	Type Z.S.II-20, adhe- sive FRF-50	20	39,38	16,20	28,85
4b	Type Z.S. I-50, adhe- sive FRF-50	20	43,51	15,79	32,14
4c	Type Z.S. I-50, adhe- sive FRF-50	20	42,12	15,00	31,65
4d	Type Z.S. I-32, adhe- sive FRF-50	29	44,55	14,99	33,51

1	2	3	4	5	6
4e	Type Z.S. I-32, adhesive FRF-50	60	39,25	20,40	27,35
5a	Type Z.S.II-20, adhesive FRF-50	24	33,9	15,96	24,23
5b	Type Z.S.II-20, adhesive FRF-50	26	36,64	23,20	22,62
6a	Type Z.S. I-32, adhesive KF-G	12	33,27	18,47	23,13
6b	Type Z.S. I-32, adhesive DFK-14R	30	40,16	16,80	29,03
7a	Type Z.S. I-38, adhesive FRF-50	93	40,14	27,33	25,57
7b	Type Z.S. I-32, adhesive FRF-50	50	43,68	34,77	24,04
7c	Type Z.S.II-20, adhesive FRF-50	421	39,24	17,30	28,10

Strength indices of glued elements are different at individual factories and even at one and the same enterprise but in different periods of time. Glued elements of EPZ "Krasny Octyabr" (samples 4a-4e) and Volokolamsky EZSK (sample 6b) show the highest average strength values of edge bending (about 40 MPa) and norm values (about 30 MPa). These samples have minimum strength indices changeability, up to 17%. Specimens of Vologodsky DOK have high strength at average values level (samples 7a-7b), but in view of high changeability of samples 7a and 7b, their coefficient of variation being about 30%, norm strength values make up 24-25 MPa. Mass factory tests were held at this enterprise (sample 7c) and presented good results, the tests having low spread in strength indices (17,3%).

As for glued elements of enterprises mentioned, strength of lengthways glued specimens of Yureskaya SPMK is somewhat lower (samples 5a and 5b). It is also characteristic of Volokolamsky EZSK elements (sample 6a) on adhesive KF-G (medium water resistance).

As appears from Table 1, glued elements strength of all the samples by edge bending at the level of average values is higher than that of samples of solid elements, group K 24 (and the more so group K 16).

The most part of glued elements samples have higher norm strength than solid wood elements strength, group K 24, and only 2 samples are higher - those of group K 16.

One can draw the conclusion that under conditions of practicable production technology the short-term (initial) strength of glued elements is ensured higher than that of solid wood elements of corresponding strength groups.

Therefore, it is not necessary to introduce any limitations against use of tooth joints when realizing required production and control level.

For estimation of time strength decrease, samples of specimens were prepared from sample lot 1a, b (by short-term tests) and 3 samples of lengthways glued elements from sample lot 4a, 5a, 6a.

Element cross section and test plan are analogous to short-term tests.

Specimens tests were held with step-increase load according to two regimes, imitating co-action of permanent and

short-term wind load (given time $10^3 \div 10^4$ sec.) and co-action of permanent and snow load (given time $\sim 10^6$ ^{sec}) under normal temperature and humidity conditions ($T_{\text{air}} = 20 \pm 2^\circ\text{C}$; $W_{\text{of air}} = 65\%$); as well as short-term tests.

In Table 2 test results are presented, from comparison of strength decrease of solid elements of visual sorting and of lengthways glued elements. It is obvious that for specimens, samples 4a and 6a, strength decrease according to first regime of loading is insignificant and nears solid elements at the level of average strength values and the difference almost disappears at the level of norm strength values. Thus, on time basis of the first regime of loading, imitating co-action of permanent load and short-term wind load, there are no differences in strength decrease of solid and glued elements.

Time basis of the second regime of loading, imitating co-action of permanent load and snow load is the foundation for forming of calculation wood resistance (not considering its quality).

Tests according to the second regime of loading show the following regularities:

- at the level of norm strength values of this regime, time strength decrease of glued elements of lot 4a in comparison with solid elements of group K 24 makes up 12,1%;

- time strength decrease coefficient of glued elements of lot 5a is by 9,8% lower than strength decrease coefficient of solid elements, group K 24;

- in comparison with solid wood elements of group K 24,

strength decrease coefficient of glued elements, sample 6a, decreased by 8,8%.

Table 2

Specimens strength by long-term
load action

Load- ing re- gime	Sam- ple No.	Sample characteris- tic	Spe- ci- qua- lity, pcs	Ave- rage stre- ngth value, MPa	Coe- ffi- ci- ent of va- ria- tion	Norm stre- ngth value MPa	Strength decrea- se in comparison with short-term	
							at the level of ave- rage values	at the level of norm values
I regime (given time 10^3-10^4 sec.)	1a	Solid K 24	28	34,93	15,74	25,29	0,854	0,970
	1b	wood K 16	14	31,97	19,01	21,94	0,942	1,281
	4a	elements -	18	38,5	12,05	32,32	0,978	0,954
	6a	of strength groups	12	29,09	10,72	24,11	0,880	1,042
II regime (given time $\sim 10^6$ sec.)	1a	Solid K 24	21	29,65	18,33	20,47	0,725	0,785
	1b	wood K 16	14	25,90	19,86	17,41	0,717	0,717
	4a	elements -	18	28,98	23,98	19,84	0,736	0,688
	5a	of strength -	12	25,77	17,25	18,43	0,761	0,712
	6a	groups -	12	25,09	20,35	16,67	0,754	0,721

Thus, on time basis of the second loading regime, imitating co-action of permanent and snow load, greater ($\sim 15\%$) strength decrease of lengthways glued elements was established in comparison with solid wood ones.

It is experimentally established that for time ensuring of equal strength of solid and lengthways glued elements of wood structures it is necessary at the manufacture stage to ensure short-term strength of lengthways glued elements by 15% higher

than norm resistance of corresponding sort of solid wood elements. The researches, presented above in Table 1, confirm the possibility of ensuring of corresponding strength of glued joints under the conditions of modern production technology.

INTERNATIONAL COUNCIL FOR BUILDING RESEARCH STUDIES AND DOCUMENTATION

WORKING COMMISSION W18A - TIMBER STRUCTURES

DESIGN OF ENDNOTCHED BEAMS

by

H J Larsen

Danish Building Research Institute

Denmark

and

P J Gustafsson

Lund Institute of Technology

Sweden

MEETING TWENTY - TWO

BERLIN

GERMAN DEMOCRATIC REPUBLIC

SEPTEMBER 1989

Introduction

The general design rules for notched beams in clause 5.1.7 of [Eurocode 5, 1988] have been criticized for not taking into account the effect of the depth of the beam, a factor which has been demonstrated by tests to have a significant influence on the strength.

Further the special rules for glued laminated beams, clause 5.1.7.2, is criticized for mixing global design considerations (total beam volume, load distribution etc), and problems related to small local areas.

A consistent design method based on a simplified fracture analysis was presented in [Gustafsson, 1988a] and [Gustafsson, 1988b]. The former paper was discussed at the CIB W18 meeting in September 1988, and it was agreed that it should be used as basis for future versions of the CIB Structural Timber Design Code.

In the following is indicated how the code text could be formulated. The proposal only concerns the requirements for the notched part of the beams additional to the general requirements for the shear design of un-notched beams, and is thus independent of the method which might eventually be codified for beams in general (i.e. for instance whether the effect of volume and load distribution will be taken into account).

Further a draft for a test method for determination of the determining factor – the fracture energy – is given.

Design formulae

The structure treated is shown in figure 1. It is a sharp bottom notch at the end of a rectangular beam. The notch is characterized by α – the depth of the end section (h_e) relative to the depth of the beam (h) – and (β) – the length of the notch, measured from the center of the support and relative to the depth.

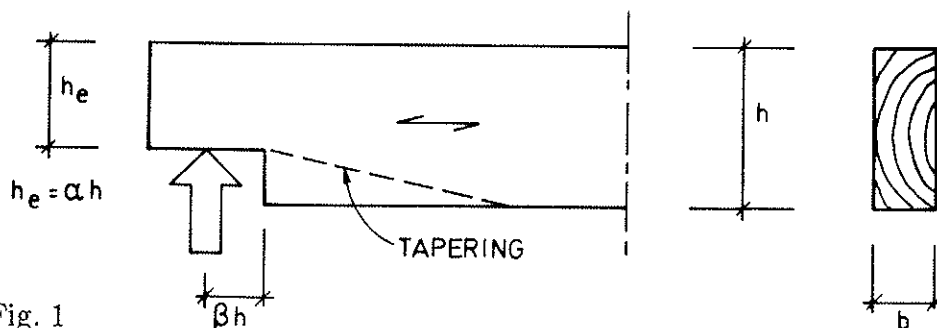


Fig. 1

The shear force (the reaction is V), and the shear stress is assumed to be calculated as

$$\tau = \frac{1.5V}{(bh_e)} = \frac{1.5V}{(\alpha bh)} \quad (1)$$

where b is the width of the beam.

The simplest design requirement given in [Gustafsson, 1988a] (formula 17) is

$$\tau \leq \frac{1.5\sqrt{G_c/h}}{\sqrt{0.6\alpha(1-\alpha)/G} + \beta\sqrt{6(1/\alpha-\alpha^2)/E_0}} \quad (2)$$

where

- G_c is the fracture energy for splitting along the grain
- E_0 is the modulus of elasticity parallel to the grain, and
- G is the normal beam shear modulus

This expression is derived from assuming that the length of the fracture region is negligible. It leads for small values of β to results that are slightly illogical (the stress at failure is the same for a beam with effective depth αh and $(1-\alpha)h$).

The length l_z of the fracture zone can be taken into account by replacing β in the denominator of (2) by $(\beta+l_z/h)$ and this is done in the proposal. The length of the fracture region depends on the material parameters, but can for practical purposes be taken as a constant, about 10 mm.

In [Gustafsson, 1988a] an alternative expression of the requirements is given, based on normalization of τ with respect to the tensile strength perpendicular to the grain, $f_{t,0}$, but it leads to problems in the code context: In the code $f_{t,0}$ is related to a uniformly stressed volume of 0.02 m³, while Gustafsson's value is related to a smaller volume, giving a much higher tensile strength (a factor of 5–10).

To reduce the effect of the notch, beams are often tapered at the end, see figure 1. For a sufficiently flat taper the notch will have no effect, the shear strength will correspond to that of an un-notched beam with depth h_e . There exist, however, no test results indicating the necessary slope or how to interpolate for steeper taperings. It has, however, normally been assumed in codes that a taper of 1:3 should be sufficient, and this is accepted in the following. No interpolation rules for steeper tapering are proposed; the rules for a sharp notch is assumed to apply.

Safety design

In accordance with the general safety format it is necessary to use design values for all strength determining properties, in this case the modulus of elasticity, the shear modulus and the fracture energy (i.e. characteristic values (5-percentiles) reduced by material factors). In the proposal it is assumed that the same material factor apply to all properties and the design value can then be found by reducing the strength calculated with characteristic values by the factor $1/\gamma_m$.

Fracture energy

In the design, knowledge of the fracture energy is needed. There exists only few test data for this material property, and it is recommended to do more test to determine it and its dependence on species, density, etc.

The fracture energy found depends also on the test method. The test specimen and testing procedure used in [Gustafsson, 1988b] is shown in Figure 2a–c. Since it was found that the fracture energy thus determined could be used directly in the design formulae, this test method is recommended.

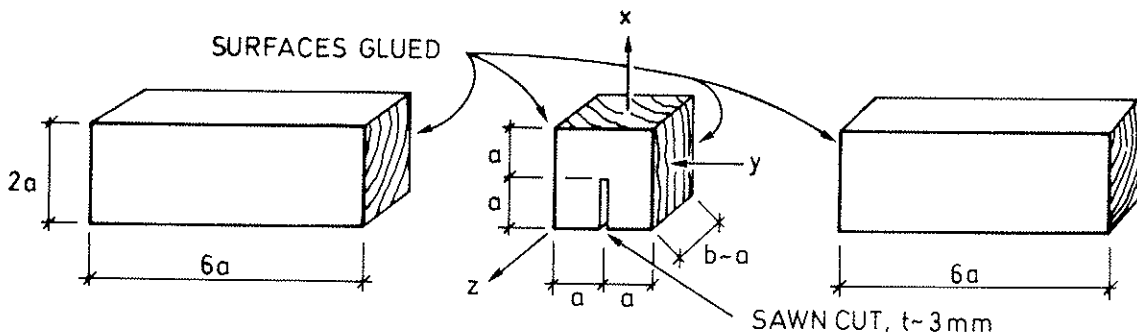


Fig. 2a The test specimen is composed of three pieces of wood glued together to form a beam with approximately square cross-section ($a \cdot b$) and a length of about $13a$.

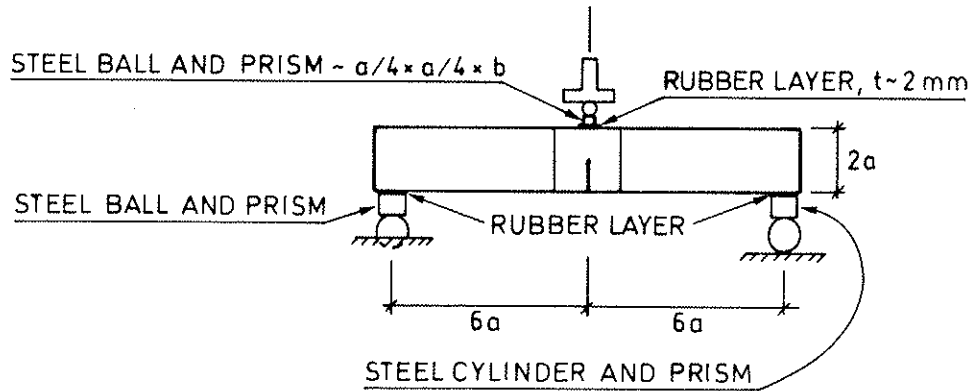


Fig. 2b The beam is loaded in three-point bending with a constant rate of movement of the cross-head of the testing machine u , so that collapse is obtained in about 3 minutes. To get the same time to failure, the rate of u must be greater for large beams than for small beams.

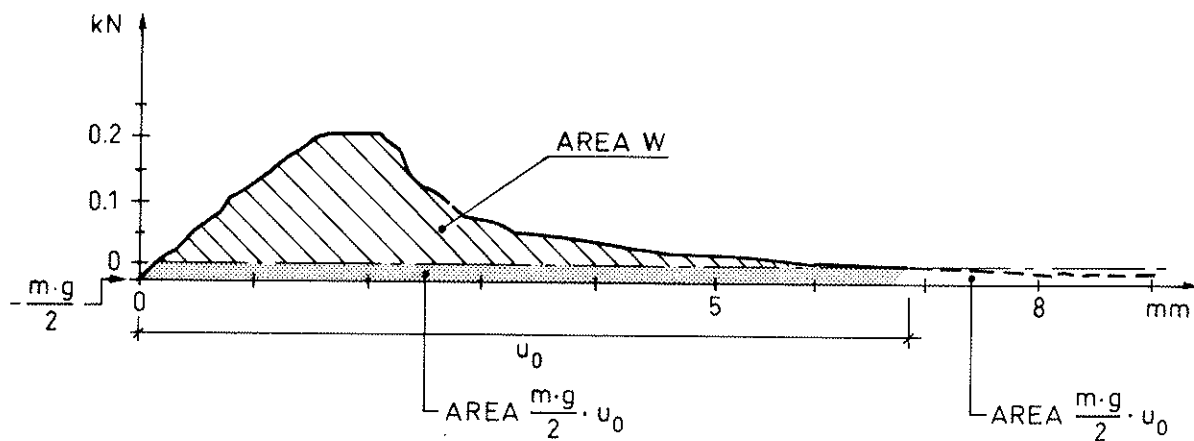


Fig. 2c From the complete and stable load deflection curve the external work is calculated as $W + mgu_0$, where W is the work done by the midpoint force, m is the mass of the beam, g is the gravity acceleration and u_0 is the deflection at failure. (The work from the mass of the beam before u_0 is $mgu_0/2$, and it is assumed that the failure energy after u_0 is of the same magnitude). The fracture energy is then determined by $G_c = (W + mgu_0)/ab$.

CODE PROPOSAL

Shear

For all beams the following condition shall be satisfied.

$$\tau_d \leq f_{v,d} \quad (a)$$

where

τ_d is the design shear stress, and
 $f_{v,d}$ is the design shear strength

(may be modified to take into account the effect of size, load distribution etc).

For beams notched at the ends, see figure 1, the shear stress shall be calculated on the effective (reduced) depth h_e and for beams notched at the bottom (the loaded side) and with a taper steeper than 1:3 it should be shown that

$$\tau_d \leq \frac{1}{\gamma_m} \frac{1.5 \sqrt{E_{o,k} G_{c,k}} / h}{\sqrt{0.6 \alpha (1-\alpha) E_{o,k} / G_k} + (\beta + l_z / h) \sqrt{6(1/\alpha - \alpha^2)}} \quad (b)$$

where

$E_{o,k}$ is the characteristic (5-percentile) value of the modulus of elasticity parallel to the grain

G_k is the characteristic (5-percentile) value of the shear modulus

$G_{c,k}$ is the characteristic (5-percentile) value of the fracture energy for splitting along the grain

l_z is the length of the failure region.

For softwoods the following values may be assumed:

$$G_{c,k} = 200 \text{ N/m}$$

$$E_{0,k}/G_k = 16$$

$$l_z = 10 \text{ mm}$$

Examples

In the following the effect of end notches are shown for different beam depths and different lengths of the notch. The strength of the notched beam is V_{notch} and is determined according to (2), taking into account the non-zero length of the fracture region by $l_z = 10 \text{ mm}$. As reference is taken the strength V_o of an unnotched beam with the depth h_e :

$$V_o = \frac{2}{3} b h_e f_{v,k}$$

The following material parameters are assumed (corresponding to strength class G4 of [Eurocode 5, 1987]):

$$E_{0,k} = 10000 \text{ MPa}$$

$$G_k = E_{0,k}/16$$

$$f_{v,k} = 2.1 \text{ MPa}$$

$$G_{c,k} = 0.2 \text{ N/mm}$$

The results are shown in figure 3. Values of V_{notch}/V_o greater than unity means that the notch will not cause the failure, it will take place as a normal shear failure in the section with reduced depth.

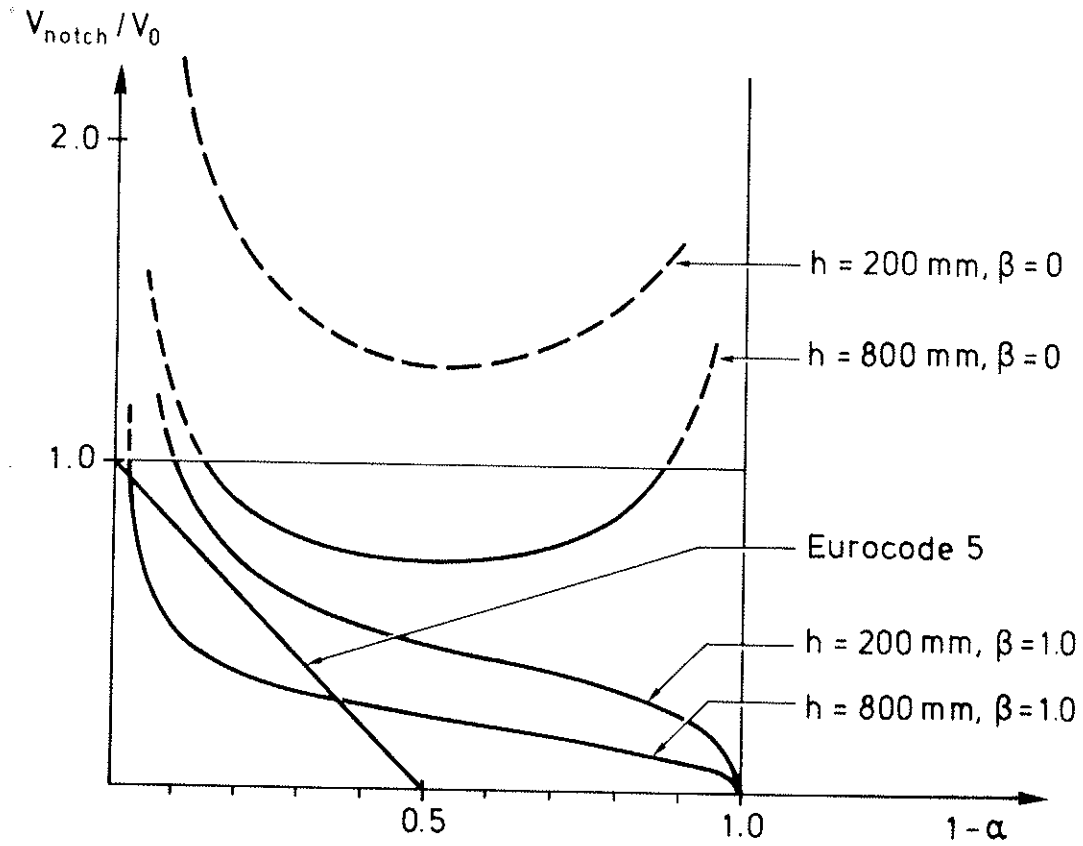


Fig. 3 The ratio between the strength of a notched beam and the shear strength of an unnotched beam with depth $h_e = \alpha h$. [Eurocode 5, 1987] in all cases gives the straight line.

References

Eurocode 5; Common Unified Rules for Timber Structures. Commission of the European Communities, Report EUR 9887. 1987.

Gustafsson, Per Johan: A Study of Strength of Notched Beams. CIB-W18 Paper 21-10-1, Parksville, Canada. 1988a.

Gustafsson, Per Johan: Träbalks Hållfasthet vid Rätvinklig Urtagning. Lund Institute of Technology, Division of Structural Mechanics, Report TVSM-7042, 1988b.

INTERNATIONAL COUNCIL FOR BUILDING RESEARCH STUDIES AND DOCUMENTATION
WORKING COMMISSION W18A - TIMBER STRUCTURES

DIMENSIONS OF WOODEN FLEXURAL MEMBERS UNDER CONSTANT LOADS

by

A Pozgai
Technical College Zvolen
Czechoslovakia

MEETING TWENTY - TWO
BERLIN
GERMAN DEMOCRATIC REPUBLIC
SEPTEMBER 1989

DIMENSIONS OF WOODEN FLEXURAL MEMBERS UNDER CONSTANT LOADS

1. Introduction

The determination of the deflection of flexural members during constant loads requires first of all the knowledge of the deformation properties of wood. During load most of the timber structures are exposed to different states of relative air humidity and temperature. On its surface wood reaches different states of moisture content equilibrium. In fact, this requires the investigation of wood deflection in the interaction with mechanical and sorption stress in the structure of wood.

In the calculation of the deflections an important constant of the material is the E-modulus. We issue from the idea that the knowledge of the E-modulus under different conditions of the moisture content of wood in arbitrary time of load gives the most optimal possibilities for the calculation of the deflection. This paper is a contribution to the solution of this idea.

2. Experimental work

Experiments were carried out under the conditions of two different climates, under the protected outside climate and under the inner one at the relative air humidity $\varphi = 65 \pm 5\%$ and temperature $t = 20 \pm 1^\circ\text{C}$.

In both cases faultless specimens were used with the dimensions 20 x 20 x 500 mm /Table 1/.

In the sampling of testing material we took into consideration that each specimen should represent one stem of spruce wood - *Picea abies* L. This tree species is used most frequently for structural purposes in Czechoslovakia.

Constant load varied within the span 7 - 16 % of the breaking strength under the conditions of both climates.

The deflection was measured in 24 hour intervals with the accuracy 0,01 mm under load. Simultaneously the air humidity and temperature were measured. The moisture content of specimens was measured on control specimens by weight method. The cross

section was measured in the middle under load with the accuracy 0,01 mm.

The whole experiment under the conditions of the outer climate lasted from 17 to 21 000 hours, under the inner one 2 400 hours.

In the investigation of creep in bending under the outer climate we did not load all the specimens at once, but only two of them gradually in one month's intervals. Before starting the experiments the specimens were placed in the given environment for about one week. After finishing the experiment we determined the density according to the Czechoslovak Standards on the additional parts of the specimens.

The magnitude of the modulus of elasticity for our case of load was calculated according to the relation

$$E = \frac{F \cdot l_0^3}{4 b h^3 \cdot y_t} \quad [1]$$

where F is the constant load in N,

l_0 - span, in mm,

b - beam width, in mm,

h - height, in mm,

y_t - deflection in time "t", in mm.

3. Results of experimental measurements

The obtained experimental results are given in Fig.1,2,3, 4 and in Tables 1,2,3,4. It is possible to state univocally that a much more expressive change of the E-modulus in bending takes place under the conditions of the outer climate in comparison with the constant /Fig. 1,2,3,4/.

The absolute magnitude of the E-modulus decrease under the constant climate is several times smaller, a stabilization taking place in comparison with the outer climate.

4. Modelling of the relation $E = f/t$

In the description of the change of the E-modulus of elasticity during constant-load we have started from the Poynting-Thompson's body /Fig.5/.

The total stress in Kelvin's model is expressed by

$$\sigma_0 = \sigma_H + \sigma_N = \epsilon_1 \cdot E_1 + \lambda_1 \frac{d\epsilon_1}{dt} \quad [2]$$

The total deformation of Poynting-Thomson's body will be calculated by

$$\epsilon_t = \epsilon_0 + \epsilon_1 \quad [3]$$

at which

$$\epsilon_0 = \frac{\sigma_0}{E_0} \quad [4]$$

By solving the linear differential equation [2] and under the assumption when $t = 0$ and $\epsilon_0 = 0$ and $\sigma_0 = \text{constant}$, we get the expression

$$\epsilon_1 = \frac{\sigma_0}{E_1} \left(1 - e^{-\frac{E_1 \cdot t}{\lambda_1}} \right) \quad [5]$$

where λ_1 is the coefficient of viscosity and "t" the time of load. By substituting the formulae [4] and [5] into the relation [3] we get the expression

$$\epsilon_t = \frac{\sigma_0}{E_0} + \frac{\sigma_0}{E_1} \left(1 - e^{-\frac{E_1 \cdot t}{\lambda_1}} \right) \quad [6]$$

Let us seek for the function $E = f/t/$

In time $t = 0$

$$E_0 = \frac{\sigma_0}{\epsilon_0} \quad [4']$$

and in a certain time "t"

$$E_t = \frac{\sigma_0}{\epsilon_t} \quad [7]$$

By substituting the relation [7] and by modification of the relation [6] we get the calculation of the E-modulus of elasticity in time "t".

$$E_t = \frac{E_0 \cdot E_1}{E_1 + E_0 \left(1 - e^{-\frac{E_1 \cdot t}{\lambda_1}} \right)} \quad [8]$$

The relation [8] is defined for $t \in /0, \infty/$. When $t = 0$, then $E_t = E_0$, which is the instantaneous E-modulus. When $t \rightarrow \infty$

$$E_t = \frac{E_0 \cdot E_1}{E_1 + E_0} = E_{tr} \quad [8']$$

which is in fact the long-term E-modulus.

The constants E_0, E_1 in the formula [8] have been calculated according to the relation [1], at which in E_0 we have considered the deflection y_0 and in E_1 the difference $y_1 = y_{max} - y_0$. The coefficient of viscosity $\lambda_1 = \frac{E_1}{C}$. The constant "C" has been determined in such a way to make the relation [8] express the lower limit values of the E-modulus during the load "t".

5. Use of the model in the calculation of beam deflection

As an example we have taken a wooden beam with a rectangular cross section, with a uniformly distributed load and placed on two supports

$$y = \frac{5 \cdot q \cdot l_0^4}{384 \cdot E \cdot I} \quad [9]$$

The change of the modulus of elasticity in dependence on time has been expressed by the relation [8].

When considering the load :

- a/ long-term q_1 with the relevant modulus E_{tr} /relation 8/
- b/ medium-term q_2 with E_{t_2} , in time t_2 ;
- c/ short-term q_3 with E_{t_3} , in time t_3 ;
- d/ instantaneous q_4 with E_0 in time $t_4 = 0$;

The relation [9] will obtain the form

$$y_t = \frac{5.l_o^4}{384.I} \left[\frac{q_1}{E_{tr}} + \frac{q_2}{E_{t2}} + \frac{q_3}{E_{t3}} + \frac{q_4}{E_o} \right] \quad [10]$$

By substituting the relations [8] and [8'] into the relation [10] and by modification we get the formula for the calculation of the deflection

$$y_t = \frac{5.l_o^4}{384.I} \left[\frac{E_1/q_1 + q_2 + q_3 + q_4 / + E_o}{E_o \cdot E_1} \left[q_1 + q_2 \left(1 - e^{-\frac{E_1 \cdot t_2}{\lambda_1}} \right) + q_3 \left(1 - e^{-\frac{E_1 \cdot t_3}{\lambda_1}} \right) \right] \right] \quad [11]$$

In the case of the action of the constant load only q_1 and $q_2 = q_3 = q_4 = 0$ and by using the relation [8'], the equation [11] will obtain the form

$$y_t = \frac{5.q_1 \cdot l_o^4}{384.I \cdot E_{tr}} \quad [11']$$

If only the instantaneous load q_4 acts, then the relation [11] has the form

$$y_o = \frac{5.l_o^4 \cdot q_4}{384.I \cdot E_o} \quad [11'']$$

6. Discussion

As mentioned above, experiments were carried out on spruce wood - *Picea abies* L. We have chosen two climates, the protected outside one and the one with constant relative air humidity $\varphi = 65 \pm 5\%$ and temperature $20 \pm 1^\circ\text{C}$.

By comparison of the E-modulus of elasticity under the conditions of both climates we can observe a univocally more expressive decrease in the outer climate. Such an expression of creep only confirms the obtained results given by Armstrong-Kingston /1962/, Grossman /1976/, etc. Further we can see that in constant load under the outer climate the whole course is irregular, especially with specimens with a higher density.

This irregularity of the changes of the E-modulus are caused by different states of equilibrium moisture content of wood changing with the relative air humidity and temperature.

The desorption process with a casual temperature increase causes the increase of deflection and thus also the decrease of the E-modulus of elasticity, the adsorption process acting in the opposite way. In specimens with a higher density the change of the E-modulus due to the sorption phenomena is more expressive. We assume that this is due to larger shrinkage and swelling in comparison with specimens with a lower density. The intensity of the change of the E-modulus is dependent on wood density.

The whole decrease of the E-modulus of elasticity under the conditions of the outer climate, up till stabilization, may be characterized in the initial stages of load by a rapid decrease, gradually disappearing, but also with simultaneous changes / increase-decrease/ as a result of the adsorption and desorption phenomena in wood structure.

The courses of the E-moduli changes /Fig. 1,2,3,4/ confirm univocally that approximately to 8 - 10 000 hours of load the deformation caused by mechanical forces discontinues, the further changes being caused only by sorption stresses. Under the constant climate /Fig. 1,2,3,4/ we do not observe such expressive changes. The stabilization of the E-modulus rather takes place in comparison with the outer climate. In our case the smaller dispersion of points on graphs is caused by the variation of the relative air humidity within the inaccuracy of the maintained relative air humidity $\pm 5\%$.

Comparison of the creep factors with Eurocode 85.

a/ Long-term

The change of the E-moduli of elasticity under the conditions of the outer climate has been described by the relation [8]. The model does not intercept changes due to different moisture content of specimens during their load, but it intercepts the lowest magnitudes of the E-moduli during the load /Fig. 1,2, 3,4/. These values must be taken into consideration in the dimensioning of limiting deflections.

The average creep factor for the investigated specimens under the conditions of both climates is given in Table 4. For the outer climate we have calculated the creep factor 3,27. It is higher than that given by Eurocode 85 for the moisture class 3.

The conditions of our outer climate during the experiments may be characterized by the average moisture content of wood 13,5 %. The relative air humidity above 80 % lasted 49 days per year. The temperature of the environment varied from - 23°C to 35°C. According to the categorization of the moisture classes of Eurocode 85 these conditions are rather closer to the moisture class 2 than 3. Our creep factor, if compared with the given standard, is substantially higher for both moisture classes 2 and 3. For moisture class 1 it is contrary.

According to our opinion, the calculation of the deflections of beams made of spruce wood for our protected outer climate does not correspond with the conversion by means of creep factors of the second and third moisture class given in the Eurocode. Maybe, only in the cases with maximum density. According to our measurements we should work with the coefficient 3,27. The most accurate conversions could be reached if we could obtain the coefficients of structural elements.

b/ Medium-term

In the first moisture class our coefficients correspond with the Eurocode 85. The coefficients of moisture classes 2 and 3 in comparison with our outer protected climate are substantially lower /Table 4/.

We suppose that the creep of spruce wood under the conditions of outer climate and under our conditions differs from the Eurocode 85.

c/ Short-term

For this case of load our creep factor under the conditions of constant climate corresponds with the moisture class 2. The creep factor under the conditions of outer climate is lower in comparison with moisture class 3 of the Eurocode.

Although the experiments were carried out on a smaller amount of observations, we do not think that the obtained results are not reliable. The selection was carried out in such a way that one specimen represented one stem and we have recorded almost the complete scale of density /0,342-0,494 g.cm³/.

With the exception of the comparison of creep factors we also give a scholl-example of the calculation of the distance of the spans /Table 3/ for the given beam. Conversions were carried out according to the proposed relation [11] and the procedure given in Eurocode 85. From the individual examples it follows that the conversions according to relation [11] are more strict if compared with the method for the Eurocode moisture classes 2 and 3. With the moisture class 1 it is contrary. By the proposed relation [11] we have tried to express more sensitively the deflection in constant-load.

We calculate the limiting factor by taking into consideration the time of load by different kinds of stress. We also consider the mutual relation between sorption and mechanical stresses originating in the wood structure during the changes of relative air humidity and temperature of the environment. This is expressed especially in the last two examples given in Table 3. In the first case we count with snow 1 N/mm and time of load $t = 3 \text{ 264 hours}$ which corresponds in our country with a mountainous area. In the second case we consider the area which is not pretentious to load by snow $q_1 = 0,5 \text{ N/mm}$ and $t_2 = 1 \text{ 248 hours}$. Even such a difference brings a change in the dimensions of a structure.

7. Conclusion

The presented paper points out the possibility of the calculation of limiting deflections of wooden flexural members under the presumption that wood is a linear viscoelastic material.

The lower limit change of the E-modulus of elasticity in constant-load under the conditions of the boath climate is described by the rheological model /Fig.5, relation [8] which we have used in the calculations of limiting deflections of beams.

By relation [11] we have tried to take into consideration more sensitively the action of outer forces during simultaneous stresses which had originated in the structure of wood due to sorption in the calculation of limiting deflections of timber structures.

REFERENCES

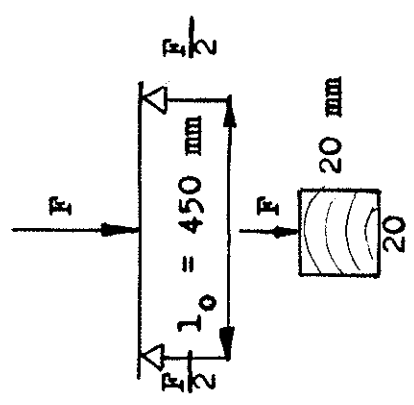
1. Armstrong, L.D.-Kingston, R.S.T.: The Effect of Moisture Content Changes on the Deformation of Wood Under Stress. Austr. J. Appl. Sci. 1962, Vol. 13, p. 257-276.
2. Grossmann, A.V.O.: Requirements for Model, that Exhibits Mechano-Sorptive Behaviour. Wood Science and Technology, Vol. 10. 1976, No. 1976, p. 163-168.
3. Sobotka, Z.: Rheology of Materials and Structures. Academia Praha 1981, p. 499.
4. Crubilé, P.-Ehlbeck, J.-Brüninghoff, H.-Larsen, J.H.-Sunley, J.: Eurocode 5. Timber Structures. Oktober 1985 European Communities.

A. P o ž g a j

Department of Wood Science and Mechanical Technology,
University of Forestry and Wood Technology,
Marxova 24, 960 53 Z v o l e n, Czechoslovakia

TABL.1 Rheological constants of spruce wood under a long-term duration of load in bending /Roofed outside climate/

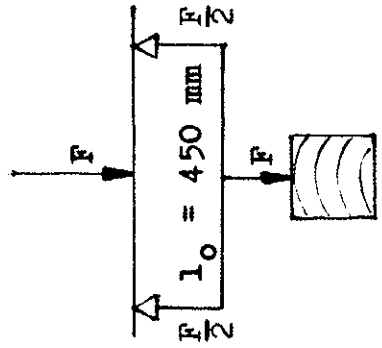
SPECI-MENS	INSTANTA NECUS E-MODULUS E_0 (MPa)	CREEP E-MODULUS E_1 (MPa)	LONG-TERM E-MODULUS E_{tr} (MPa)	COEFFICIENT OF VISCOSITY $\lambda_1 \cdot 10^6$ (MPa.h)	DENSITY ρ_0 (g.cm ⁻³)	$\frac{E_0}{E_{tr}}$
1	13 656	6 120	4 226	20,40	0,364	3,23
2	8 556	3 883	2 671	12,13	0,352	3,20
3	11 201	4 858	3 388	16,19	0,359	3,30
4	15 711	9 071	5 750	25,92	0,484	2,73
5	10 003	3 735	2 719	9,31	0,348	3,67
6	13 606	5 564	3 953	11,12	0,385	3,44
7	9 128	4 358	2 950	7,26	0,354	3,09
8	12 668	6 679	4 373	8,74	0,368	2,89
9	12 279	4 372	3 224	7,29	0,382	3,80
10	12 872	4 617	3 398	9,23	0,391	3,78
11	13 028	6 970	4 540	8,71	0,422	2,86
AVERAGE \bar{x}	12 064	5 475	3 744	12,39	0,382	3,27
v /%/ *	16,97	28,17	23,71	46,29	9,96	10,80



Time of the load-duration :
17 000 - 21 000 h.
Moisture min. 8 %
content: aver. 13,3 %
max. 21 %
Relative humidity
exceeding 0,80 : 49
days per year
* Coefficient of
variation

TABLE.2 Rheological constants of spruce wood under a long-term duration of load in bending
 /climate $\varphi = /65 \pm 5\%$, $t = /20 \pm 1/^\circ\text{C}$

SPECI-MENS	INSTANTANEOUS E_0 E-MODULUS /MPa/	CREEP E_1 E-MODULUS /MPa/	LONG-TERM E-MODULUS E_{tr} /MPa/	COEFFICIENT OF VISOOSITY $\lambda_{1.10}$ /MPa.h/	DENSITY ρ_0 /g.cm ⁻³ /	$\frac{E_0}{E_{tr}}$
1	8 734	30 080	6 361	7,52	0,342	1,37
2	8 401	43 088	7 030	2,87	0,356	1,19
3	8 344	26 772	6 361	1,78	0,364	1,31
4	9 044	41 420	7 423	2,76	0,367	1,21
5	10 805	56 667	9 074	5,66	0,406	1,19
6	11 739	44 481	9 287	22,24	0,407	1,26
7	10 780	42 841	8 612	14,28	0,432	1,25
8	9 354	34 016	7 336	8,5	0,435	1,27
9	13 342	36 831	9 794	14,73	0,448	1,36
10	14 402	60 597	11 636	30,3	0,450	1,23
11	12 146	51 083	9 812	14,56	0,459	1,24
12	13 056	53 656	10 500	15,33	0,470	1,24
13	15 756	66 388	12 733	16,59	0,486	1,23
14	14 221	71 108	11 850	17,8	0,494	1,20
AVERAGE \bar{x}	11 437	47 073	9 129	12,49	0,422	1,24
v /%/*	20,07	27,42	21,83	62,29	11,36	5,50



Moisture content : $\approx 12\%$
 * coefficient of variation

TABLE 3. Calculation of the length of the span "l_o" according to Eurocode and our experiments

Parameters of flexural members $y = \frac{l_o}{300}$; $I = 14197 \cdot 10^4$	Calculated length of the span "l _o " /mm/ According to Eurocode 1985	Calculated length of the span "l _o " /mm/ According to our experiments
$\rho_o = 0,352 \text{ g.cm}^{-3}$ $E_o = 8556 \text{ MPa}$ $E_1 = 3883 \text{ MPa}$ $E_{tr} = 2671 \text{ MPa}$ $q_1 = 2 \text{ N/mm}$	Moisture class (3) $l_o = 3728 >$ Moisture class (2) $l_o = 4420 >$	Roofed outside climate $l_o = 3647$
$\rho_o = 0,356 \text{ g.cm}^{-3}$ $E_o = 8401 \text{ MPa}$ $E_1 = 43088 \text{ MPa}$ $E_{tr} = 7030 \text{ MPa}$ $q_1 = 2 \text{ N/mm}$	Moisture class (1) $l_o = 4668 <$	Relative humidity $/65 \pm 5\%$ Temperature $/20 \pm 1/^\circ\text{C}$ $l_o = 5036$
$\rho_o = 0,391 \text{ g.cm}^{-3}$ $E_o = 12872 \text{ MPa}$ $E_1 = 4617 \text{ MPa}$ $E_{tr} = 3398 \text{ MPa}$ $q_1 = 2 \text{ N/mm}$	Moisture class (3) $l_o = 4272 >$ Moisture class (2) $l_o = 5065 >$	Roofed outside climate $l_o = 3952$
$\rho_o = 0,406 \text{ g.cm}^{-3}$ $E_o = 10805 \text{ MPa}$ $E_1 = 56667 \text{ MPa}$ $E_{tr} = 9074 \text{ MPa}$ $q_1 = 2 \text{ N/mm}$	Moisture class (1) $l_o = 5077 <$	$\psi = /65 \pm 5\%$ $T = /20 \pm 1/^\circ\text{C}$ $l_o = 5483$
$\rho_o = 0,484 \text{ g.cm}^{-3}$ $E_o = 15711 \text{ MPa}$ $E_1 = 9071 \text{ MPa}$ $E_{tr} = 5760 \text{ MPa}$ $q_1 = 2 \text{ N/mm}$	Moisture class (3) $l_o = 4565 <$ Moisture class (2) $l_o = 5413 \underline{=}$	Roofed outside climate $l_o = 5483$
$\rho_o = 0,486 \text{ g.cm}^{-3}$ $E_o = 15756 \text{ MPa}$ $E_1 = 66388 \text{ MPa}$ $E_{tr} = 12733 \text{ MPa}$ $q_1 = 2 \text{ N/mm}$	Moisture class (1) $l_o = 5757 <$	$\psi = /65 \pm 5\%$ $T = /20 \pm 1/^\circ\text{C}$ $l_o = 6139$

$\rho_0 = 0,352 \text{ g.cm}^{-3}$ $E_0 = 8556 \text{ MPa}$ $E_1 = 3883 \text{ MPa}$ $\lambda_1 = 12,13 \cdot 10^6 \text{ MPa.h}$ $t_2 = 4320 \text{ h}$ $t_3 = 168 \text{ h}$ $q_1 = 2 \text{ N/mm}$ $q_2 = 1 \text{ N/mm}$ $q_3 = 0,5 \text{ N/mm}$	Moisture class (3) $l_0 = 3287 >$ Moisture class (2) $l_0 = 3849 >$	Roofed outside climate $l_0 = 3186$
$\rho_0 = 0,356 \text{ g.cm}^{-3}$ $E_0 = 8401 \text{ MPa}$ $E_1 = 43088 \text{ MPa}$ $\lambda_1 = 2,87 \cdot 10^6 \text{ MPa.h}$ $t_2 = 4320 \text{ h}$ $t_3 = 168 \text{ h}$ $q_1 = 2 \text{ N/mm}$ $q_2 = 1 \text{ N/mm}$ $q_3 = 0,5 \text{ N/mm}$	Moisture class (1) $l_0 = 4019 <$	$\psi = /65 \pm 5/\%$ $T = /20 \pm 1/^{\circ}\text{C}$ $l_0 = 4182$
$\rho_0 = 0,391 \text{ g.cm}^{-3}$ $E_0 = 12872 \text{ MPa}$ $E_1 = 4617 \text{ MPa}$ $\lambda_1 = 9,23 \cdot 10^6 \text{ MPa.h}$ $t_2 = 4320 \text{ h}$ $t_3 = 168 \text{ h}$ $q_1 = 2 \text{ N/mm}$ $q_2 = 1 \text{ N/mm}$ $q_3 = 0,5 \text{ N/mm}$	Moisture class (3) $l_0 = 3767 >$ Moisture class (2) $l_0 = 4411 >$	Roofed outside climate $l_0 = 3423$
$\rho_0 = 0,381 \text{ g.cm}^{-3}$ $E_0 = 12055 \text{ MPa}$ $E_1 = 135126 \text{ MPa}$ $\lambda_1 = 9,00 \cdot 10^6 \text{ MPa.h}$ $t_2 = 4320 \text{ h}$ $t_3 = 168 \text{ h}$ $q_1 = 2 \text{ N/mm}$ $q_2 = 1 \text{ N/mm}$ $q_3 = 0,5 \text{ N/mm}$	Moisture class (1) $l_0 = 4534 <$	$\psi = /65 \pm 5/\%$ $T = /20 \pm 1/^{\circ}\text{C}$ $l_0 = 4836$

$\rho_0 = 0,484 \text{ g.cm}^{-3}$ $E_0 = 15711 \text{ MPa}$ $E_1 = 9071 \text{ MPa}$ $\lambda_1 = 25,92 \cdot 10^6 \text{ MPa.h}$ $t_2 = 4320 \text{ h}$ $t_3 = 168 \text{ h}$ $q_1 = 2 \text{ N/mm}$ $q_2 = 1 \text{ N/mm}$ $q_3 = 0,5 \text{ N/mm}$ $q_4 = 0$	Moisture class ③ $l_0 = 4026 \equiv$ Moisture class ② $l_0 = 4714 >$	Roofed outside climate $l_0 = 4087$
$\rho_0 = 0,486 \text{ g.cm}^{-3}$ $E_0 = 15756 \text{ MPa}$ $E_1 = 66388 \text{ MPa}$ $\lambda_1 = 16,59 \cdot 10^6 \text{ MPa.h}$ $t_2 = 4320 \text{ h}$ $t_3 = 168 \text{ h}$ $q_1 = 2 \text{ N/mm}$ $q_2 = 1 \text{ N/mm}$ $q_3 = 0,5 \text{ N/mm}$ $q_4 = 0$	Moisture class ① $l_0 = 4957 <$	$\psi = /65 \pm 5/\%$ $T = /20 \pm 1/^\circ\text{C}$ $l_0 = 5118$
$\rho_0 = 0,391 \text{ g.cm}^{-3}$ $E_0 = 12872 \text{ MPa}$ $E_1 = 4617 \text{ MPa}$ $\lambda_1 = 9,23 \cdot 10^6 \text{ MPa.h}$ $t_2 = 3264 \text{ h}$ $t_3 = 0$ $q_1 = 2 \text{ N/mm}$ $q_2 = 1 \text{ N/mm}$ $q_3, q_4 = 0$	Moisture class ③ $l_0 = 3881 >$ Moisture class ② $l_0 = 4570 >$	Roofed outside climate $l_0 = 3509$
$\rho_0 = 0,391 \text{ g.cm}^{-3}$ $E_1 = 4617 \text{ MPa}$ $E_0 = 12872 \text{ MPa}$ $\lambda_1 = 9,23 \cdot 10^6 \text{ MPa.h}$ $t_2 = 1248 \text{ h}$ $t_3 = 0$ $q_1 = 2 \text{ N/mm}$ $q_2 = 0,5 \text{ N/mm}$	Moisture class ③ $l_0 = 4058 >$ Moisture class ② $l_0 = 4792 >$	Roofed outside climate $l_0 = 3771$

TABL.4 Creep factor " k_{cr} " according to our experiments for Picea abies L.

Load-duration class	Moisture class	
	Constant climate $\varphi=(65 \pm 5)\%$; $t=(20 \pm 1)^\circ\text{C}$	Roofed outside climate
Long - term	1,24 ¹ /1,5/ [*]	3,27 ³ /3,0/ [*]
Medium - term	1,21 ¹ /1,2/ [*]	2,87 ³ /2,00/ [*]
Short - term	1,11 ¹ /1,00/ [*]	1,16 ³ /1,5/ [*]

¹
* according to Eurocode 85

*3

INTERNATIONAL COUNCIL FOR BUILDING RESEARCH STUDIES AND DOCUMENTATION
WORKING COMMISSION W18A - TIMBER STRUCTURES

THIN-WALLED WOOD-BASED FLANGES IN COMPOSITE BEAMS

by

J König
Swedish Institute for Wood Technology Research
Sweden

MEETING TWENTY - TWO
BERLIN
GERMAN DEMOCRATIC REPUBLIC
SEPTEMBER 1989

SUMMARY

The loadbearing capacity of thin-walled wood-based flanges in composite beams can be reduced due to shear lag, buckling and flange curling. However, flanges in compression have considerable loadbearing capacity even after the flange has buckled. The effective width concept which is well established in the field of sheet metal construction can also be used in designing wood-based board material with respect to buckling. This is shown by an evaluation of tests carried out at Delft. Design formulae for the effect of flange curling are derived, and design criteria are proposed.

1. INTRODUCTION

In the field of timber construction, structural elements comprising thin-walled components of wood-based board material have been used for some time. These structural elements are characteristic for lightweight construction, and it is expected that they will be used more extensively in the future.

Typical examples are composite sections comprising webs of solid wood and flanges of board material. The webs may also be made up of components of board material and solid wood, see figure 1. However, owing to the small thickness of the board material, there are a number of properties which demand more accurate analysis if the material is to be utilised in the optimum manner. The flange often has the duty of distributing load in the transverse direction. In floors, consideration must also be given to the stiffness requirement which determines the thickness of the flange. In these structures it is generally only the shear lag in the board material which limits the loadbearing capacity of the flange when the flanges are very wide in proportion to the span of the beam. In other structures, for instance in roof cassettes, the load distribution task may be of subordinate importance and certain deformations may be tolerated. Finally,

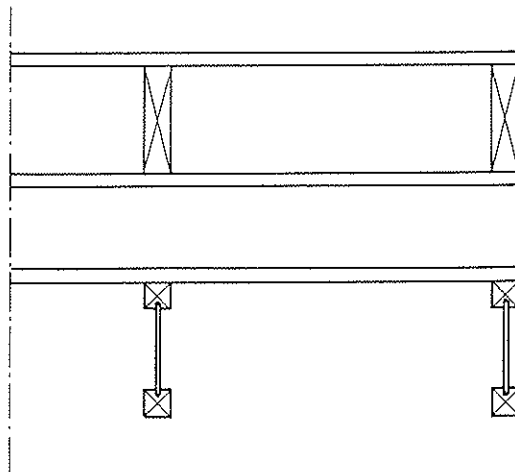


Figure 1. Examples of composite sections with thin walled components.

direct application of load on the flange can often be avoided, for instance by application of the load over the web of the composite section or on the bottom flange of the section. Flanges in compression may also be subject to buckling. When the beam is curved, or becomes curved owing to the external load, the flanges are deformed inwards towards the neutral axis of the cross section (flange curling), and the contribution of the flanges to the loadbearing capacity and stiffness of the box section is therefore reduced.

It is well known that thin-walled plates in compression have considerable postcritical loadbearing capacity, i.e. the load can be further increased after the critical buckling stress of the plate has been reached. This favourable behaviour has been utilised for a long time, first in aeroplane construction and since the end of the 1940s also in building construction, mainly in thin-walled structural elements of steel and aluminium sheeting. In the field of timber construction also the postcritical loadbearing capacity of buckled plate elements has been known. In order that this phenomenon may be utilised to some extent, the coefficient of safety is slightly reduced in the structural regulations for timber in most countries.

In accordance with the CIB Structural Timber Code /1/, it is permissible to utilise the postcritical loadbearing capacity. The code lays down some values regarding the effective width of the flange, but these values are undifferentiated since neither the critical buckling load of the flange nor its compressive strength is taken into consideration. As far as the author is aware, the effect of these is reflected only in the Swiss timber code SIA 164 (1981) /5/. It is however not known whether the rules in the code had been verified for wood-based board materials when the code was written. In /6/, which gives the background to the Swiss code, no reference is made to this.

The research reports which deal with the buckling of wood-based boards or thin-walled components in structural elements mainly confine them-selves to determination of the critical buckling load, see e.g. /2/, /3/ and /4/. While most structural regulations for timber structures take account of the fact that the loadbearing capacity of thin-walled flanges is limited due to shear lag in the board material, there is no requirement, as far as the author is aware, that the effect of flange curling on the loadbearing capacity of the composite section should be checked.

It is shown below that the effective width concept in utilising the postcritical region can also be applied to wood-based thin-walled flanges. Design rules are also given which take the effect of flange curling into consideration. The effect of shear lag in wood-based board materials is already well documented and requires no further elucidation.

2. POSTCRITICAL LOADBEARING CAPACITY AFTER BUCKLING OF A FLANGE IN COMPRESSION

2.1 Definition of the effective width

The effective width concept is well established in the field of sheet metal construction. The effective width b_{ef} is defined so that the following relationship holds (see figure 2):

$$\int_0^b \sigma_x(y) dy = b_{ef} \sigma_e$$

The formula which is most widely used at present for determination of the effective width is that determined empirically by Winter /7/ and later somewhat modified in the AISI Code (1968) /8/:

$$\frac{b_{ef}}{b} = \sqrt{\frac{\sigma_{cr}}{\sigma_e}} \left(1 - 0,22 \sqrt{\frac{\sigma_{cr}}{\sigma_e}}\right) \quad (2)$$

where σ_{cr} is the critical buckling stress

σ_e is the compressive edge stress in the buckled state, see figure 1.

Expression (1) is a development of the formula according to von Karman:

$$\frac{b_{ef}}{b} = \sqrt{\frac{\sigma_{cr}}{\sigma_e}} \quad (3)$$

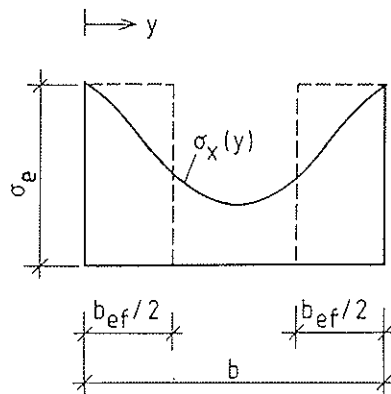


Figure 2. Definition of the effective width b_{ef} . The condition

$$\int_0^b \sigma_x(y) dy = b_{ef} \sigma_e \text{ must be satisfied.}$$

According to this formula, the loadbearing capacity of a plate in compression is not reduced until the critical buckling stress is reached, while Winters formula takes account of imperfections which reduce the loadbearing capacity at compressive stresses which are lower than the critical buckling stress.

2.2 Evaluation of tests carried out at Delft

Dekker et al (1978) /9/ carried out a test series on 100 sheets of plywood loaded in compression. The object of this test series was to investigate whether the linear buckling theory could be applied to plywood also. In the following, only the data and results which are important with regard to evaluation with respect to the postcritical loadbearing capacity are given.

The material in the tests was Canadian Oregon Pipe Plywood, Select Sheathing, Ext. 1". Two different widths, 600 and 400 mm, and two different nominal thicknesses, 8 and 13 mm, were used. The aspect ratio a/b varied between 0,5 and 4,5. One half of the test specimens were simply supported on four sides, while the unloaded edges of the other half were subjected to some restraint. Since there are no data regarding the degree of restraint, these specimens are not included in this evaluation.

The test report sets out the measured thickness t of the test specimens and their stiffnesses N_x , N_y and N_{xy} which are defined as follows:

$$N_x = \frac{E_x t^3}{12(1-\nu_x \nu_y)}$$

$$N_y = \frac{E_y t^3}{12(1-\nu_x \nu_y)}$$

$$N_{xy} = \frac{Gt^3}{6} + \frac{1}{2} (\nu_x N_x + \nu_y N_y)$$

The theoretical critical buckling stress can then be calculated as

$$\sigma_{cr} = k \frac{4\pi^2}{b^2 t} \sqrt{N_x N_y} \quad (4)$$

with the buckling coefficient

$$k = \frac{m^2}{4\alpha_v} + \frac{n}{2} + \frac{\alpha_v}{4m^2} \quad (5)$$

where m is the number of half wavelengths in the longitudinal direction in the buckled state. It is assumed that in the transverse direction there is only one half wave. We further have

$$\alpha_v = \frac{a}{b} \sqrt{\frac{4N_y}{N_x}} \quad (6)$$

$$\eta = \frac{N_{xy}}{\sqrt{N_x N_y}} \quad (7)$$

The critical buckling load N_{cr} was determined for each test specimen in accordance with Equation (4) using the experimental stiffness values. The experimental critical buckling stress was also determined by means of the relationship between the load and the perpendicular displacement of the plate. The critical load was defined by the point of intersection of the load axis and the extension of the practically straight portion of the curve in the postcritical region.

The ultimate load N_u was also recorded for each test specimen, but the compressive strengths $f_{c,0}$ and $f_{c,90}$ of the sheets of plywood were not recorded. In spite of this omission in the investigation, it is possible to study the properties of the specimens in the postcritical region as shown below.

In the evaluation, only the specimens whose modified aspect ratios α_v according to Equation (6) are larger than 1 were used. The experimental effective width of the test specimens in the ultimate state was determined as

$$\frac{b_{ef}}{b} = \frac{\sigma_u}{f_c}$$

where $\sigma_u = \frac{N}{bt}$

In calculating the slenderness ratio $\alpha = \sqrt{\sigma_e/\sigma_{cr}}$, the extreme fibre stress σ_e was put equal to the compressive strength $f_{c,0}$ or $f_{c,90}$. The compressive strength here is an effective value, i.e. plywood is considered to be homogeneous. In view of the uncertainty in determining the experimental critical buckling stress $\sigma_{cr,test}$, the values $\sigma_{cr,calc}$ calculated using the experimental stiffness values N_x , N_y and N_{xy} in accordance with Equation (4) were used instead. When $\sigma_{cr,calc}$ and $\sigma_{cr,test}$ are compared in Table 1, it is seen that the latter exhibit a considerably larger scatter. In order to simplify calculations, the mean values of each test series, set out in Table 1, were used. The slenderness ratio α thus contains a small error which is however negligible.

Since the compressive strength of the plywood material had not been determined, both b_{ef} and α were calculated for several assumed values of f_c , see Table 2. The results are set out in figure 3. Curves in accordance with Equations (2) and (3) are also plotted in this figure.

An estimate of the compressive strength of the plywood material can be made on the basis of the characteristic compressive strengths of similar materials which it is understood /9/ will be included in the Canadian code for timber structures to be published in 1990. The coefficient of variation of the strength values is approximately 0,13. This means that the mean values are ca 25% greater than the characteristic values, which approximately corresponds to the 5th percentile. Table 2 also sets out the effective widths and slenderness ratios for the mean values of the compressive strength determined in this way.

It can be seen that the experimental results are in good agreement with the curves and that the results are not particularly sensitive to the choice of the correct compressive strength. Most of the values lie above the curve in accordance with Equation (3) by von Karman. It is only for slenderness ratios greater than 3,6 that there are values noticeably below the curve. One reason for this may be that the value $\sigma_{cr,calc}$ used is somewhat too large owing to some errors in determining the stiffness values of the plywood sheets. In test series 600/8 in which load was applied parallel and perpendicular to the direction of the grain, considerably smaller critical buckling stresses $\sigma_{cr,test}$ were measured. The corresponding slenderness ratio α is then much higher, so that even the lowest values of b_{ef}/b will be very near the curve (3).

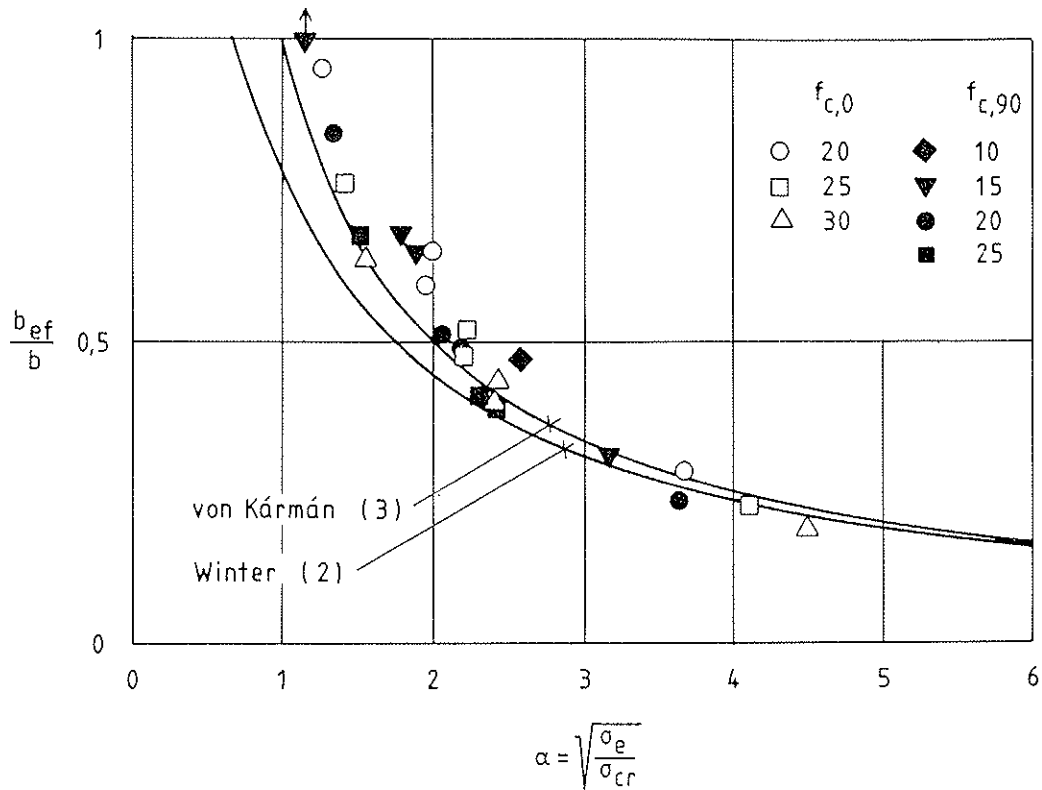


Figure 3. Effective widths determined using test results by Dekker et al (1978) /8/.

In the other test series $\sigma_{cr,calc}$ is a little smaller than $\sigma_{cr,test}$. In these cases the value of the slenderness ratio is reduced to some extent, i.e. the plots in the diagram are moved to the left by a small distance. The difference is however small and has no significance.

2.3 Proposed design regulations

For large values of the slenderness ratio, there is very little difference between the formulae according to Winter and von Kármán. However, for slenderness ratios near 1 and below, the difference is large. In the test series under consideration there are no test specimens with slenderness ratios as low as this, and it is therefore not possible to verify Winter's formula in this region.

With reference to the procedure at present applied for sheet metal structures, it is proposed that in conjunction with design in the ultimate limit state the effective width of thin-walled wood-based flanges supported on two webs should be calculated as

$$b_{ef} = b \quad \text{for } \alpha \leq 0,67$$

$$b_{ef} = b \sqrt{\frac{\sigma_{cr}}{\sigma_e}} (1 - 0,22 \sqrt{\frac{\sigma_{cr}}{\sigma_e}}) \quad \text{for } \alpha \geq 0,67 \quad (8)$$

where $\alpha = \sqrt{\sigma_e / \sigma_{cr}}$

TABLE 1. Mean values, standard deviations and coefficients of variation for the test data. Only test specimens with $\alpha_U > 1$ are included.

b/t_{nom}	Direction of load	No of specimens with $\alpha_U > 1$		$\sigma_{cr, calc}$ N/mm ²	$\sigma_{cr, test}$ N/mm ²	σ_U N/mm ²	t mm
400/8		7	\bar{x}	5,02	5,20	13,00	8,01
			s	0,545	1,34	2,91	0,113
			δ	0,109	0,258	0,224	0,014
400/13		7	\bar{x}	12,11	12,26	19,03	11,97
			s	0,876	1,82	1,05	0,111
			δ	0,072	0,148	0,052	0,093
600/8		3	\bar{x}	1,47	1,13	5,65	7,55
			s	0,176	0,234	0,522	0,035
			δ	0,120	0,207	0,092	0,005
600/13		4	\bar{x}	5,14	5,21	11,88	12,2
			s	0,16	1,06	1,66	0
			δ	0,032	0,203	0,140	0
400/8	⊥	5	\bar{x}	4,15	4,44	9,74	7,78
			s	0,488	0,937	0,466	0,129
			δ	0,117	0,211	0,048	0,017
400/13	⊥	5	\bar{x}	10,82	12,76	16,86	12,24
			s	0,576	1,36	1,39	0,152
			δ	0,053	0,107	0,083	0,012
600/8	⊥	3	\bar{x}	1,51	1,073	4,72	7,85
			s	0,097	0,158	0,544	0,551
			δ	0,064	0,147	0,115	0,070
600/13	⊥	3	\bar{x}	4,66	5,26	10,23	12,37
			s	0,099	0,108	1,069	0,058
			δ	0,021	0,020	0,104	0,005

TABLE 2. Experimental effective width b_{ef} and slenderness ratio α for different values of the compressive strength f_{cb} .

b/t_{nom}	Direction of load	f_c N/mm ²	$\frac{b_{ef}}{b}$	α
400/8		20	0,650	1,996
		25	0,520	2,232
		30	0,433	2,445
		21,7 a)	0,600	2,079
400/13		20	0,952	1,285
		25	0,761	1,437
		30	0,634	1,574
		17,0 a)	1,119	1,185
600/8		20	0,282	3,685
		25	0,226	4,120
		30	0,188	4,513
		21,7 a)	0,260	3,842
600/13		20	0,594	1,974
		25	0,475	2,207
		30	0,396	2,417
		17,0 a)	0,699	1,819
400/8	⊥	15	0,649	1,901
		20	0,487	2,195
		25	0,390	2,454
		6,7 a)	1,454	1,271
400/13	⊥	15	1,177	1,121
		20	0,843	1,360
		25	0,675	1,520
		7,9 a)	2,130	0,855
600/8	⊥	10	0,472	2,576
		15	0,315	3,155
		20	0,236	3,643
		25	0,189	4,073
600/13	⊥	6,7 a)	0,705	2,106
		15	0,682	1,794
		20	0,512	2,071
		25	0,409	2,316
		7,9 a)	1,295	1,302

a) Estimated mean strength according to /9/.

When there is a glue joint between the flange and the webs, b is put equal to b_f , i.e. the clear distance between the webs. For nailed or screwed connections, $b = b_f + t_w$ where t_w is the thickness of the web.

In a composite section according to figure 1, the strengths of the flange and web materials are normally different. When the compressive strength of the flange material is lower than that of the web material, σ_c in the above formula is put equal to the compressive strength f_c of the flange material. When, on the other hand, ultimate stress in the web is reached before this occurs in the flange, σ_c is put equal to the compressive edge stress which obtains in the flange. Investigations on sheet metal structures have shown that the formula according to Winter yields good accuracy in the ultimate limit state while it is conservative for lower loads, see e.g. /11/, /12/ and /13/. Pending the availability of test results for wood-based boards, it is proposed however that the above formula should also be used for stresses which are lower than the compressive strength.

Thin-walled flanges which are supported along one edge and have a free edge also have postcritical loadbearing capacity. For wood-based flanges no test results are available at present. It is proposed therefore that the postcritical loadbearing capacity should not be utilised in such cases.

The compressive strength of plywood is normally quoted as loadbearing capacity per unit width (e.g. N/mm). The value of f_c can be obtained by dividing this value by the thickness of the plywood.

It is proposed that in determining the critical buckling stress σ_{cr} , simply supported conditions should be assumed unless a more accurated investigation is carried out. Full fixity is very difficult to achieve in sheet metal structures. However, restraint has a favourable effect in the postcritical region also. This was shown in /11/ for hinged supports. When thin-walled flanges are bonded to solid wood webs, restraint is likely to be very effective. It is therefore proposed that some restraint should be permitted in determining σ_{cr} if the degree of restraint can be ascertained.

In conjunction with design for the serviceability limit state, it is proposed that f_c in the above expression should be replaced by the actual compressive stress in the flange. Imperfections which can give rise to visible buckling already in the subcritical region can be allowed for in this way.

3. FLANGE CURLING

In a curved beam, or beam which becomes curved owing to the external load, components of force which are directed towards the neutral layer arise in the axially loaded flanges (figure 4). These forces cause both the flange in compression and the flange in tension to curl inwards towards the centre of the section (figure 5). When this deformation of the flange becomes excessive, the loadbearing capacity of the composite section as a whole is affected. The Swedish Code for Light Gauge Metal Structures, StBK-N5 /14/ specifies that deflection shall not exceed 5% of the depth of the cross section in order that flange curling may be ignored in calculating the loadbearing capacity.

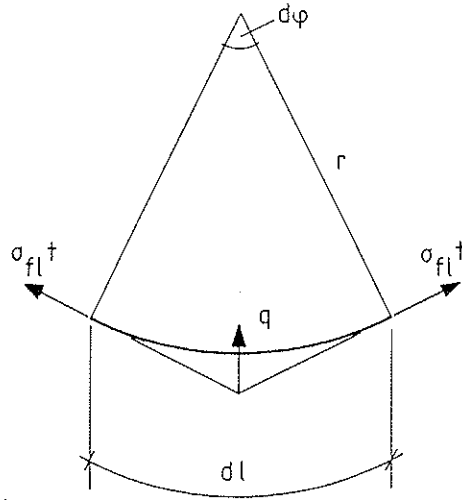


Figure 4. Forces in the flange of a curved beam.

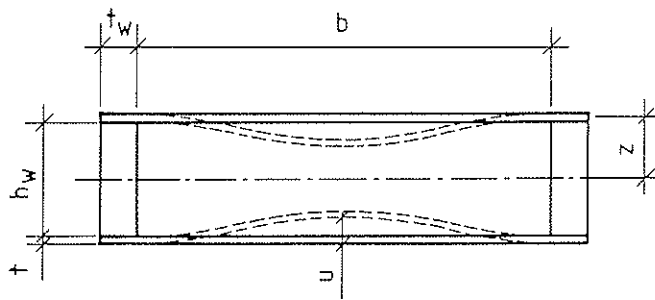


Figure 5. Curling of thin walled flanges.

The inward force component may be determined as (figure 4)

$$q = \frac{\sigma_f t d\phi}{dl}$$

With $dl = r d\phi$ and $\frac{1}{r} = \frac{M}{E_b I_b}$, we have

$$q = \frac{\sigma_f t}{r} = \frac{\sigma_f t M}{E_b I_b}$$

and with $\sigma_f = \frac{M}{I_b} z$ we finally have

$$q = \frac{\sigma_f^2 t}{E_b z} \quad (9)$$

where z is the distance between the neutral layer and the midplane of the flange (figure 5). The moduli of elasticity of the web and flange in a composite section are usually different. Conventionally, this is taken into consideration by e.g. putting the modulus of elasticity of the web equal to E_b and using a modified flange area in calculating the second moment of area I_b of the composite section.

This load causes the flange to deflect, and under simply supported conditions the value of this at the midpoint of the flange is

$$u = \frac{5}{384} \frac{qb^4}{(EI)_f}$$

where $(EI)_f$ is the flexural rigidity of the flange in the transverse direction of the beam.

Substitution of (9) yields

$$u = \frac{5}{384} \frac{\sigma_f^2 t b^4}{E_b (EI)_f z} \quad (10)$$

In the same way, when the web is fully restrained, we have

$$u = \frac{1}{384} \frac{\sigma_f^2 t b^4}{E_b (EI)_f z} \quad (11)$$

In box sections with solid webs and glue joints between webs and flanges, full fixity can probably be assumed. When the webs and flanges are joined by mechanical fasteners, the degree of restraint is very uncertain, and Equation (9) for the simply supported case should be used.

For open sections, i.e. where the section comprises only a compression or tension flange which is bonded to the web, the degree of restraint depends on the torsional rigidity of the web. It should be possible to make use of some fixity by taking the mean value of Equations (10) and (11).

In the same way as in StEK-N5, the following is proposed as the limiting value of the maximum flange displacement where this must be taken into consideration:

$$u_{\max} = 0,05 h$$

where $h = h_w + t$ for a box section

and

$$h = h_w + \frac{t}{2}$$

When the maximum displacement of the flange exceeds u_{\max} , this must be allowed for in calculating the second moment of area of the composite section. Approximately, the effective distance between the flange and the neutral layer of the cross section is

$$z_{fl} = z \frac{2}{3} u$$

See figure 6.

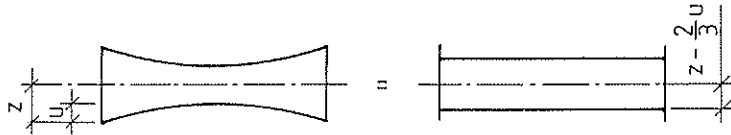


Figure 6. Effective cross section when flange curling is taken into consideration.

When the loadbearing capacity of the flange is reduced due to buckling or the effect of shear deformations, the displacement u of the flange for the mean stress in the flange is determined as

$$\sigma_f = f_c \frac{b_{ef}}{b}$$

When the flange is in the ultimate limit state, the compressive edge stress in the flange, σ_e , is put equal to the compressive strength f_c .

REFERENCES

- /1/ CIB Structural Timber Code. CIB Report, Publication 66, 1983.
- /2/ Buckling of Flat Plywood Plates in Compression, Shear, or Combined Compression and Shear. USDA, Forest Products Laboratory, Madison, Report No. 1316 with Supplements 1316A-1316J.
- /3/ Foschi, R.O. 1969. Buckling of the compressed skin of a plywood stressed-skin panel with longitudinal stiffeners. Canadian Forestry Service, Publ. No. 1265.
- /4/ Halasz, R. von & Cziesielski, E.: Berechnung und Konstruktion geleimter Träger mit Stegen aus Furnierplatten. Berichte aus der Bauforschung, Heft 47.
- /5/ SIA 164, 1981, Swiss Timber Code, Schweizerischer Ingenieur- und Architekten-Verein, Zürich.
- /6/ Einführung in die Norm SIA 164 (1981), Holzbau, Publikation Nr 21-1, Baustatik und Stahlbau, Eidg. Techn. Hochschule, Zürich.
- /7/ Winter, G. 1947. Strength of Thin Steel Compression Flanges. Trans. ASCE, Vol. 112, 1947.
- /8/ AISI. 1968. Specification for the Design of Cold-formed Steel Structural Members. 1968 Edition. Americal Iron and Steel Institute, Washington.
- /9/ Dekker, J., Kuipers, J. & Ploos van Amstel, H. (1978). Buckling strength of plywood, Stevin-Laboratorium, Delft.
- /10/ Foschi, R., private communication.
- /11/ König, J. 1978. Transversally loaded thin walled C shaped panels with intermediate stiffeners. Swedish Council for Building Research, Stockholm. Document D7:1978.
- /12/ Graves-Smith, T.R. 1971. A variational method for large deflection elasto-plastic theory in its application to arbitrary flat plates. Proc. Int. Conf. on Structures, Solid Mechanics and Engineering Design, Southampton University 1969, John Wiley, London (1971), pp 1249-1256.
- /13/ Thomasson, P-O. 1978. Thin walled C-shaped panels in axial compression. Swedish Council for Building Research, Stockholm. Document D1:1978.
- /14/ StBK-N5, Swedish Code for Light Gauge Metal Structures, Stockholm, 1980.

INTERNATIONAL COUNCIL FOR BUILDING RESEARCH STUDIES AND DOCUMENTATION
WORKING COMMISSION W18A - TIMBER STRUCTURES

THE CALCULATION OF WOODEN BARS WITH FLEXIBLE JOINTS
IN ACCORDANCE WITH THE POLISH STANDART CODE
AND STRICT THEORETICAL METHODS

by

Z Mielczarek
Szczecin Technical University
Poland

MEETING TWENTY - TWO
BERLIN
GERMAN DEMOCRATIC REPUBLIC
SEPTEMBER 1989

Prof. Zbigniew Mielczarek, D. Eng.

Szczecin, Technical University, Poland,

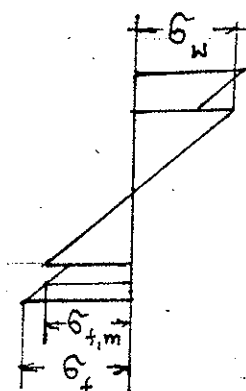
The calculation of wooden bars with flexible joints in accordance of the Polish Standard code and strict theoretical methods.

1. Introduction.

Limited commercial dimensions of timber bring about necessity of connecting elements both lengthwise and crosswise when designing and making constructions of more considerable spans. To this purpose serve mechanical joints of various kinds, such as nails, bolts, screws, rings and shear plates etc., and applied in modern technologies—glued joints. Mechanical joints are characterized by greater or lesser flexibility, which has a basic effect on the bearing of compound bars under load. The rigidity and load carrying capacity of bars connected with such joints is reduced in relation to bars uniform of similar dimensions, and moreover there occurs quite different character of distribution of normal and shear stresses.

2. Polish Standards formulae for calculation of normal stresses in elements of bend compound beams with flexible joints.

The Polish Standards PN-81/b-03150 gives the following formulae to calculate normal stresses in compound beams of symmetrical cross-sections:



In which

$$|\sigma_w| = \frac{M}{J_{red}} \cdot \frac{h_w}{2} \leq R_{dm} \cdot m$$

$$|\sigma_{f,m}| = \frac{M}{J_{red}} \cdot \gamma \cdot \frac{h_w + h_f}{2} \leq R_{dt} \cdot m$$

$$|\sigma_f| = |\sigma_{f,m}| + \frac{M}{J_{red}} \cdot \frac{h_f}{2} \leq R_{dm} \cdot m$$

$$\gamma = \frac{1}{1 + \frac{\pi^2 A_f \cdot E_m}{l^2 \cdot K} e_1}$$

$\sigma_{f,m}$ - normal stresses in the lower flange/element/central line, MPa

σ_w - normal stresses at the web edge, MPa

σ_f - normal stresses in extreme fibres of the flange, MPa

$h_t = \frac{h_w}{2} + \gamma \left(\frac{h_w}{2} - a \right)$ - height of the tension zone

h_w - height of the web, mm

h_f - thickness/height/ of the flange, mm

l - span of the beam, mm

J_{gr} - gross moment of inertia of total cross-section, mm⁴

- area of the flange cross-section, mm²

J_i - moments of inertia of components of the cross-section in relation to the flange cross-section, mm⁴

k - modulus of joints flexibility according to PN-81/B-C3150

E_m - modulus of elasticity, MPa

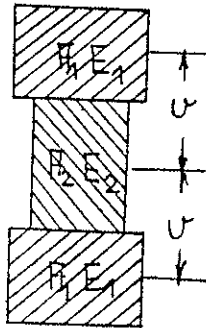
e_1 - distance between connectors brought to one series, mm

3. Theoretical analysis of effect of joints flexibility on distribution of normal stresses and deflections of bent compound bars.

a/Initial equation.

The subject to research is a bar of an I cross-section, compound from three elements, symmetric in relation to its longitudinal axis/fig.1/, but this research can as well refer to a bar of a rectangular cross-section, as a particular case of an I-section. From the point of view of statistics, the bar is a free-ends beam. The bar has joints evenly distributed on its whole length.

As a basis to consideration the method of A.R.Rzanicyn has been applied/1/.



According to this method it is possible to determinate values of shear forces T occurring in junction planes of a compound beam, by aid of the following system of differential equations

$$\begin{aligned} \frac{T_1''}{E_1} &= \Delta_{11}T_1 + \Delta_{12}T_2 + \dots + \Delta_{1n}T_n + \Delta_{10} \\ \frac{T_2''}{E_2} &= \Delta_{21}T_1 + \Delta_{22}T_2 + \dots + \Delta_{2n}T_n + \Delta_{20} \\ \frac{T_n''}{E_n} &= \Delta_{n1}T_1 + \Delta_{n2}T_2 + \dots + \Delta_{nn}T_n + \Delta_{n0} \end{aligned} \quad [1]$$

in a general case particular equations, e.g. for k- of this joint having the form

$$\frac{T_k''}{E_k} = \Delta_{k,k-1}T_{k-1} + \Delta_{kk}T_k + \dots + \Delta_{k,k+n}T_{k+n} + \Delta_{k0}$$

in which:

$$T_k = \int_0^x \tau_k dx \quad - \text{total shear force in k-th joint acting leftward from the section x-x}$$

$$\Delta_{kk} = \frac{1}{A_k E_k} + \frac{1}{A_{k+1} E_{k+1}} + \frac{U_k^2}{\sum E J}$$

$$\Delta_{k,k-1} = \frac{1}{A_k E_k} + \frac{U_k U_{k-1}}{\sum E J}$$

$$\Delta_{k,k+1} = -\frac{1}{A_{k+1} E_{k+1}} + \frac{U_k U_{k+1}}{\sum E J} \quad [2]$$

$$\Delta_{k0} = -\frac{N_k^0}{A_k E_k} - \frac{N_{k+1}^0}{A_{k+1} E_{k+1}} - \frac{M_k^0 U_k}{\sum E J}$$

N_k^0, M_k^0 -external load in form of axial forces and bending moments in the most general case

ε -coefficient of rigidity of joints subject to shear of N/mm^2 dimension

On Fig.2 there is shown a section of the bar under examination with marked shear forces T , substituting action of rejected joints, the system of equations/1/ will resolve itself to two following differential equations.

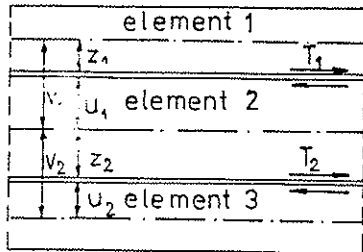


Fig.2. The section of the bar.

$$T_1'' = \varepsilon (\Delta_{11} T_1 + \Delta_{12} T_2 + \Delta_{10})$$

$$T_2'' = \varepsilon (\Delta_{21} T_1 + \Delta_{22} T_2 + \Delta_{20})$$

[3]

where

$$\Delta_{11} = \Delta_{22} = \frac{1}{A_1 E_1} + \frac{1}{A_2 E_2} + \frac{U^2}{\Sigma E J}$$

$$\Delta_{12} = \Delta_{21} = -\frac{1}{A_2 E_2} + \frac{U^2}{\Sigma E J}$$

Taking advantage of symmetry conditions, the equation/3/ can be resolved to one differential equation in the form:

$$T'' = \varepsilon \gamma T + \varepsilon \Delta Q$$

[4]

in which:

$$\gamma = \Delta_{11} + \Delta_{21} = \frac{1}{A_1 E} + \frac{2U^2}{\Sigma E J}$$

$$\Delta = -\frac{M^0 U}{\Sigma E J}$$

A_1 - cross-section of the flange

For the symmetrical cross-section

$$U_1 = U_2 = U$$

In the basic system in place of rejected joints there were taken forces T , so calculating stresses they can be determined like for the basic system/of multiple beam without joints/ plus stresses caused by forces T . Let us assume that the total contracting force T , equal to one in the section where is the point "A", arcses in this point the stress σ_T so the total stress in the point "A" will be:

$$\sigma = \sigma_w + T \sigma_T$$

and since in a monolithic beam $T=T_M$

so
$$\sigma = \sigma_w + T \sigma_T$$

hence
$$\sigma_T = \frac{\sigma_M - \sigma_w}{T_M}$$

and substituting it to /5/

$$\sigma = \sigma_w + (\sigma_M + \sigma_w) \frac{T}{T_M}$$

and introducing marking

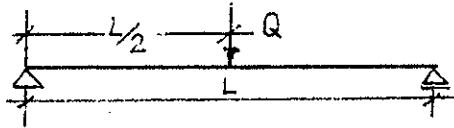
$$\frac{T}{T_M} = \psi$$

we will receive finally

$$\sigma = \sigma_w (1 - \psi) + \sigma_M \psi$$

4. Determining value of coefficients designating the degree of collaboration of elements of compound beams, for more important patterns of loads.

a/Beam loaded with a force concentrated in the middle of span.



Solving the equation/4/ because of the unknown T / total shearing force/ and making use of boundary conditions/ for $x=0$ $T=0$.

and $x=L/2$ $T=0$ / we receive:

$$\psi = \frac{2x}{L} - 2 \frac{\text{sh} \lambda x \text{sh} \lambda L/2}{\frac{\lambda L}{2} \text{sh} \lambda L}$$

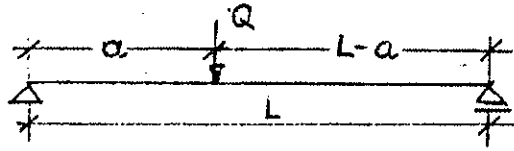
when $x=L/2$

$$\psi = \frac{1}{2} - 2 \frac{(\text{sh} \frac{\lambda L}{2})^2}{\frac{\lambda L}{2} \text{sh} \lambda L}$$

where

$$\lambda = \sqrt{\epsilon \cdot \gamma}$$

b/Beam loaded with a force concentrated, applied in any distance from supports.



Proceeding similarly as previously we can determine values of coefficients designating degree of collaboration of elements, which in the given case will have the form:

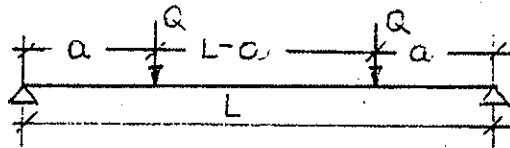
For the left-side section of the beam / $x \leq a$ /

$$\psi = 1 - \frac{L \operatorname{sh} \lambda (L-a) \operatorname{sh} \lambda x}{(L-a) \lambda x [\operatorname{sh} \lambda (L-a) \operatorname{ch} \lambda a + \operatorname{sh} \lambda a \operatorname{ch} \lambda (L-a)]}$$

For the right-hand side of the beam / $a < x < L$ /

$$\psi = 1 - \frac{L \operatorname{sh} \lambda a \operatorname{sh} \lambda (L-x)}{\lambda a (L-x) [\operatorname{sh} \lambda (L-a) \operatorname{ch} \lambda a + \operatorname{sh} \lambda a \operatorname{ch} \lambda (L-a)]}$$

c/Beam loaded with two forces concentrated applied symmetrically



Coefficients designating the degree of collaboration of elements will have in this case the form:

For the segment between the support and concentrated force / $x < a$ /

$$\psi_1 = 1 - \frac{\operatorname{ch} \lambda (L/2 - a) \operatorname{sh} \lambda x}{\operatorname{sh} \lambda a [\operatorname{ch} \lambda (L/2 - a) \operatorname{ctg} h \lambda a + \operatorname{sh} \lambda (L/2 - a)] \lambda x}$$

For the segment between concentrated forces / $a < x < L-a$ /

$$\psi_2 = 1 - \frac{\operatorname{ch} \lambda (L/2 - x)}{\lambda a [\operatorname{ch} \lambda (L/2 - a) \operatorname{ctg} h \lambda a + \operatorname{sh} \lambda (L/2 - a)]}$$

d/Beam with uniformly distributed load on its whole length.

Coefficient designating the degree of collaboration of elements has the form

$$\psi = \frac{1}{x(L-x)} \frac{2}{\lambda^2} \left(\frac{e^{-\frac{\lambda L}{2}} \operatorname{sh} \lambda x}{\operatorname{ch} \frac{\lambda L}{2}} + e^{-\lambda x} - 1 \right) + 1$$

when $x = L/2$

$$\psi = \frac{8}{(\lambda L)^2} \left[e^{-\frac{\lambda L}{2}} \left(\operatorname{th} \frac{\lambda L}{2} + 1 \right) - 1 \right] + 1$$

5. Analysis of changeability of the coefficient ψ lengthwise of beams and results of experimental verifying tests:

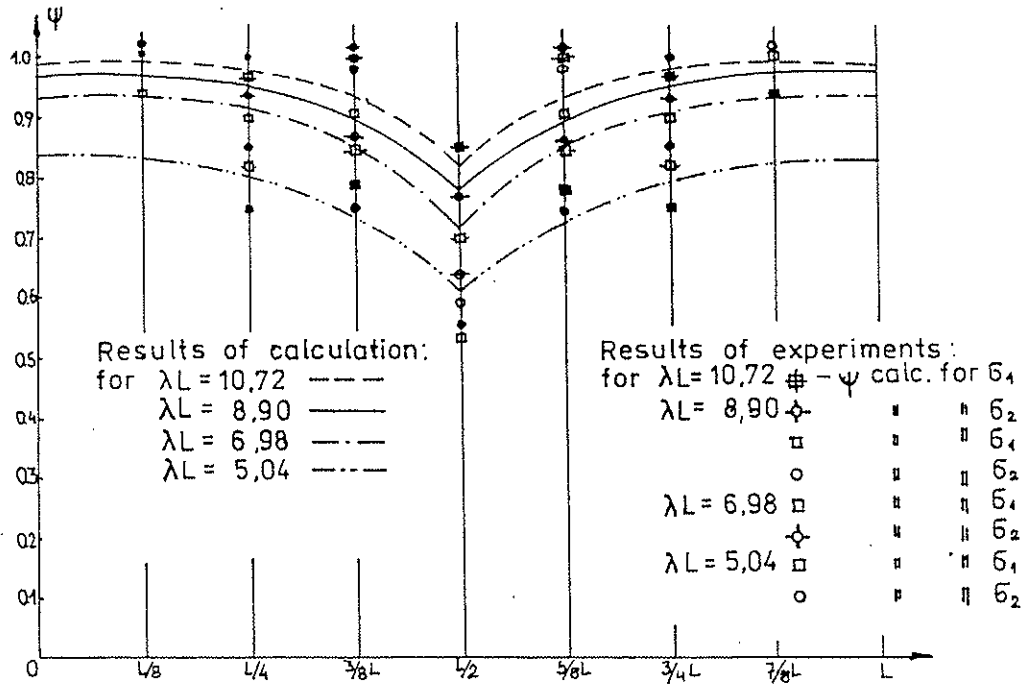


Fig.3. Graphs of changeability of the coefficient ψ for beams loaded with forces concentrated in the middle of the span.

On the fig.3 there are shown graphs presenting values of coefficients ψ , designating the degree of collaboration of elements in cross-sections placed lengthwise beams, loaded with concentrated forces in the middle of the span.

The graphs have been made for beams of different parameters λL . The parameter λ takes into account the number and elasticity of used joints and configuration of the cross-section.

On the fig.4 there are shown similar graphs for beams loaded with force concentrated in any distance a from the support, and on the fig.5 with two symmetrically applied forces also in any distance a from the supports.

Verification experimental tests have been executed for the case of these forces being situated in the distance $a \approx 1/4$

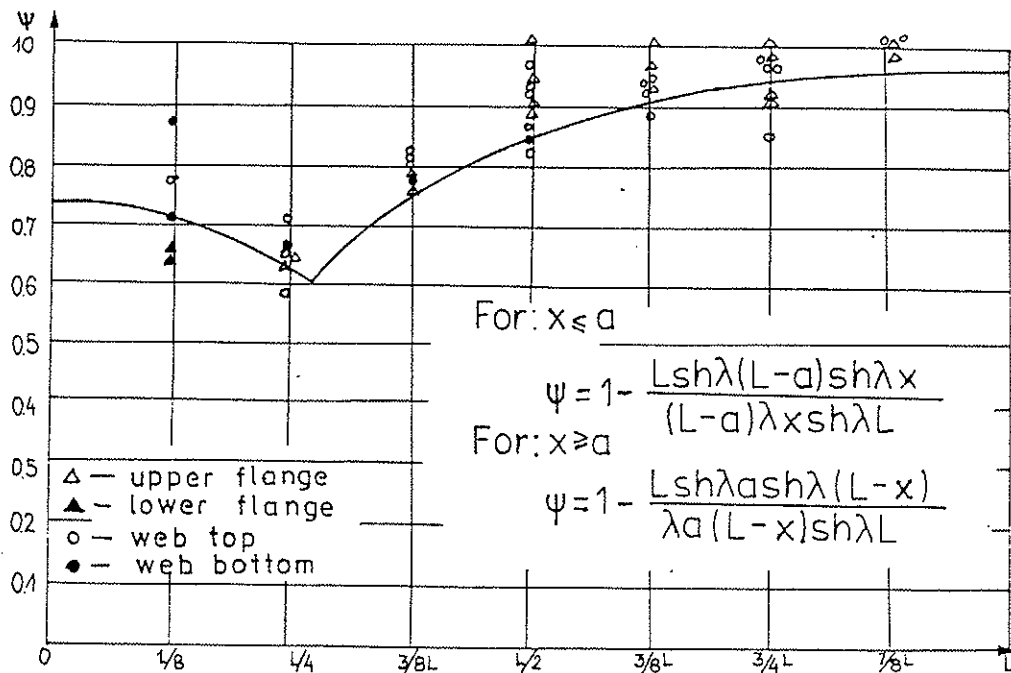


Fig.4. Graph of changeability of the coefficient ψ for a beam with force concentrated in the distance $1/4$ from the support.

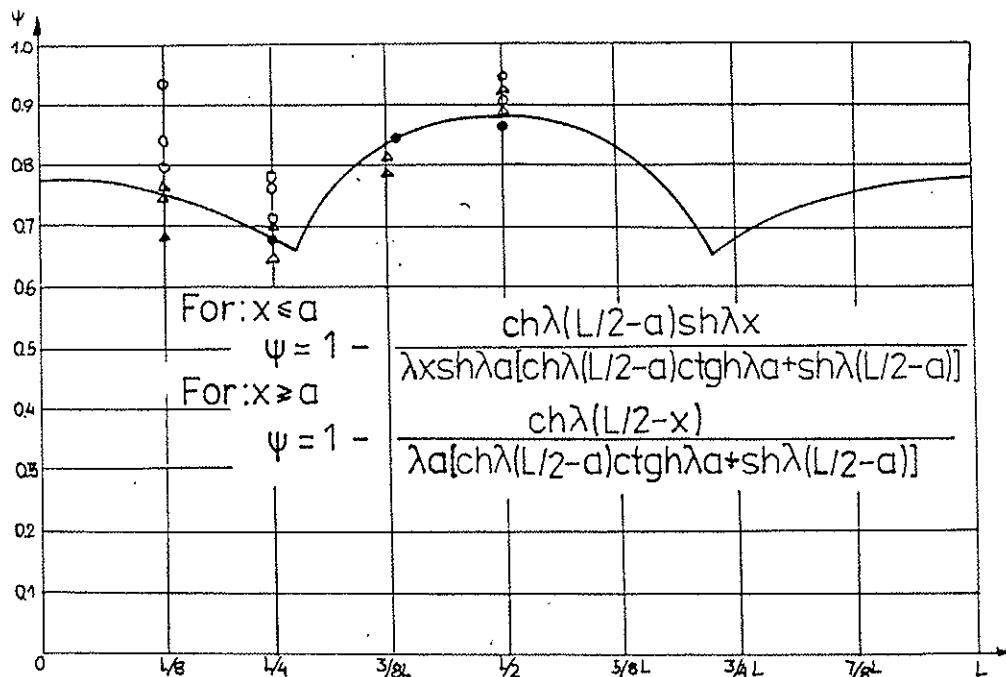


Fig.5. Graph of changeability of the coefficient ψ for a beam loaded symmetrically with two concentrated forces.

6. Results of calculations taking into account an effect of various parameters on the degree of collaboration of elements ψ

On the fig.6 there are shown graphs illustrating changeability of coefficient ψ on the length of beams with different ratio l/h for beams with uniformly distributed load, where: h -height of total cross-section

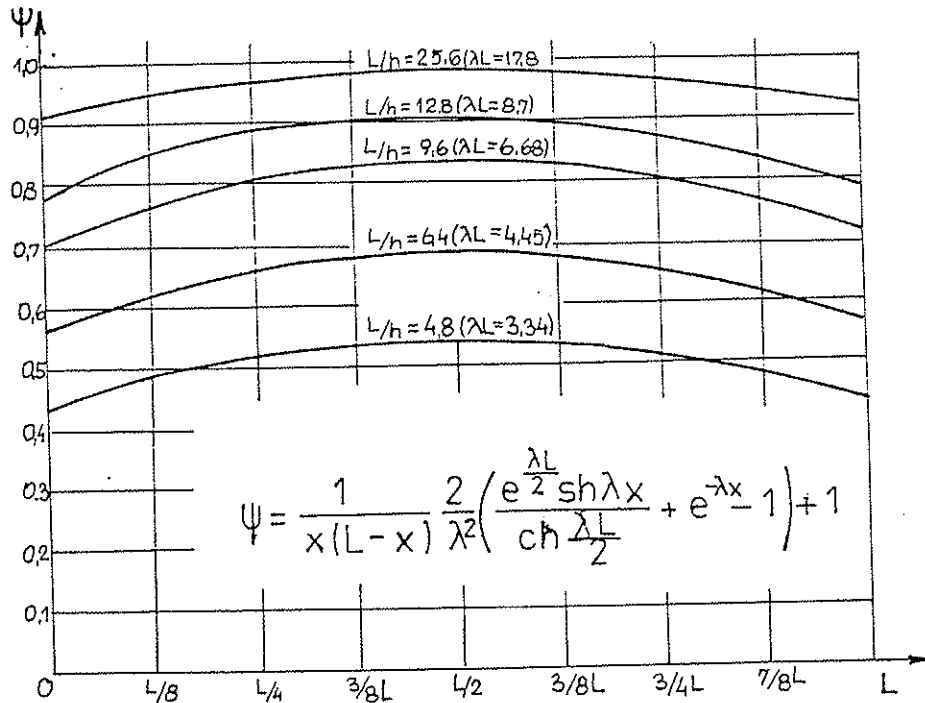


Fig.6. Graphs of changeability of the coefficient ψ for a beam with uniformly distributed load.

On the fig.7 there have been graphs illustrating changeability of the coefficient ψ on the length of beams of different flexibility of joints. The graphs have been made basing on calculation regarding beams of a constant cross-section and length and with the same pattern of load- with force concentrated in the middle of the span.

The graphs given in the Fig.8 illustrate the effect of the place of application of a concentrated force on the character of changeability of the coefficient ψ in beams loaded with a force concentrated in distances $a = 1/8, 1/4, 1/3$ and $1/2$

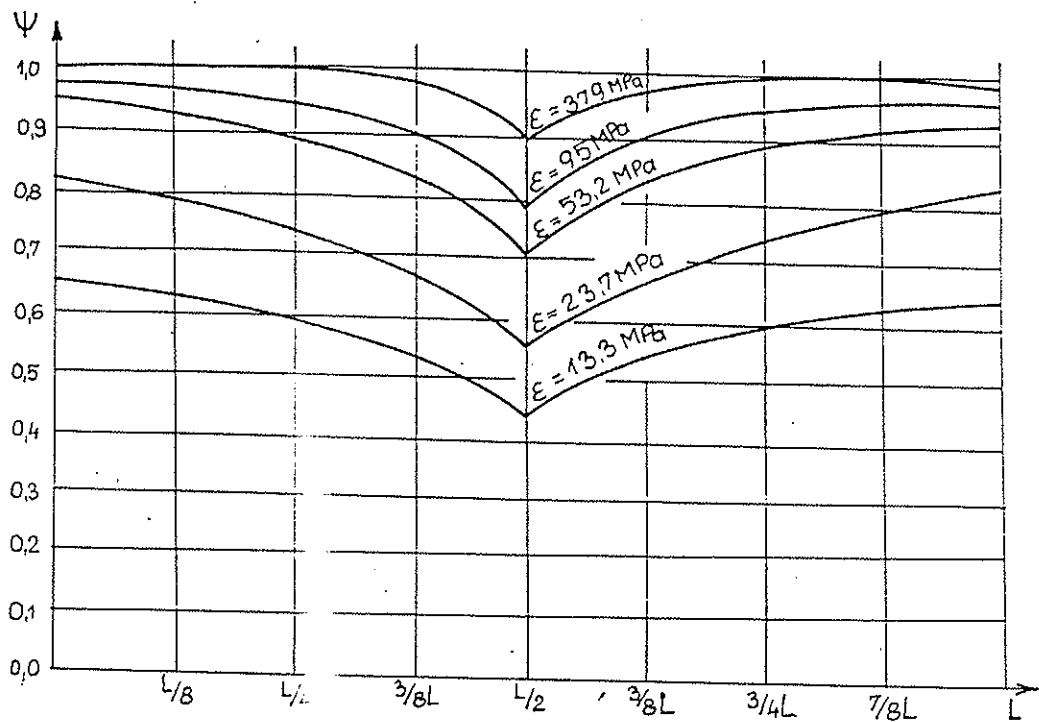


Fig.7. Graphs of changeability of the coefficient Ψ , for beams of different elasticity of joints.

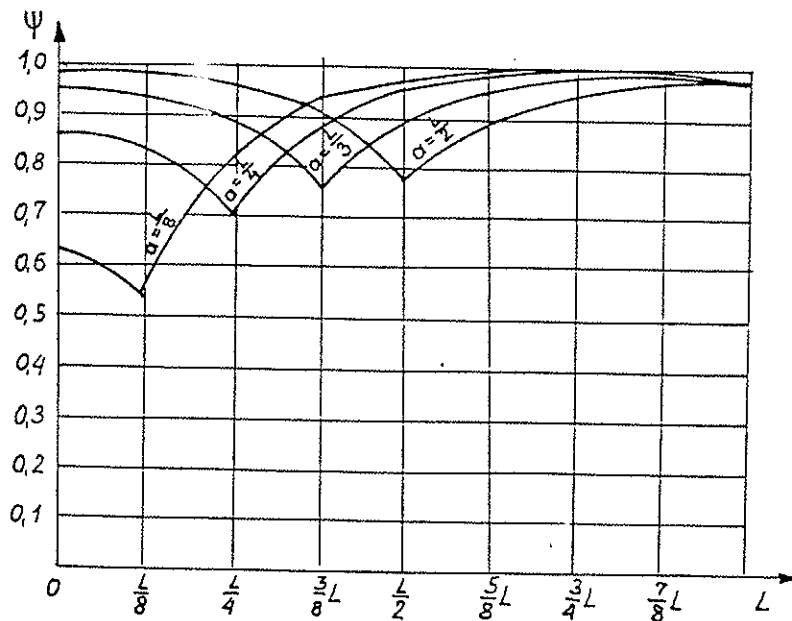


Fig.8. Effect of the place of application of a concentrated force on the value of the coefficient Ψ

TABLE 1

Comparison of values of normal stresses in the midspan of beams with elastic joints, computed by aid of standard formulae to those obtained using theoretical formulae

Cross-section	Beam Length /mm/	Spacing of joints in terms of one series /mm/	Computation load /KN/m/	Kind of stresses /MPa/	Normal stresses		
					Calculate using Polish Standard Formulae	Computed by formulae for Load evenly distributed lengthwise the beam	Force concentrated in the beam midspan
1. B = 130 b = 76 h _s = 240 h _p = 35	6000	35	3,52		10,03	9,88	11,71
					6,75	6,84	5,76
					8,21	8,28	7,47
2. -/-	5000	51	3,52		8,33	8,28	9,55
					3,86	3,90	3,18
					5,08	5,11	4,57
3. -/-	4000	121	3,52		7,34	7,35	7,77
					1,29	1,29	1,05
					2,36	2,36	2,18

7. Conclusion.

Basing on performed experimental research and theoretical analyses, one can state that the degree of collaboration of elements in compound beams with elastic joints, determined by the coefficient ψ depends first of all on the following parameters:

- length of rods
- kind and number of joints determined by the coefficient ϵ
- pattern of the cross-section
- character of load

The greater rigidity of used joints, the more similar in its work under load is the beam to a monolithic one.

Comparative calculations have proved that:

- formulae PN-81/B-03150 reflect correctly distributions of normal stresses in cross-section situated in the midspan of beams bent with evenly distributed load,
- in case of loading with force concentrated in the midspan, normal stresses computed theoretically surpass by about 17% these computed by aid of norm formulae,
- graphs of the index variability lengthwise the beams/Figures...../ show, that still greater divergences are to be expected in case where concentrated forces will be applied near supports.

REFERENCES

1. A. R. Rżanicyn, Teoria sostawnych stróitielnych konstrukcji. Strojizdat /1948/
2. A. A. Pikowskij, Statika stierżniewych sistiem so szatymi elementami. Fizmatgiz, Moskwa/1961/
3. P. F. Pleszkow, Teoria rasczeta dieriewiannyh sostawnych stierżniej. Gosizdat, Leningrad/1952"

4. H. Granholm, Om samansatta balkar och pelare med särskild hänsyn till apikade trakonstruktionen. Göteborg 1949, Sweden.
5. A. Hoischen, Beitrag zur Berechnung Zusammengesetzter Vollwandträger mit elastischen Verbindungsmitteln. Technische Hochschule Karlsruhe 1952.
6. Möhler, Versuche mit dem Holzbau, 1964, Fortschritte Forschungen.
7. W. Schelling, Biegung nachgiebig verbundener, zusammengesetzter Biegeträger in Ingenieurholzbau. Karlsruhe 1968. Tech. Hochschule.
8. Z. Mielczarek, Określenie stopnia współpracy elementów w ściankachozginanych drewnianych prętach złożonych połączonych na gwoździe. Archives of Civil Engng. Polish Academy of Science. Vol. XI, IV, 1975.
9. Lombardi, Giovanni, Der zusammengesetzte Druckstabe. Schweizerische Bauzeitung 1951, Heft 22.

INTERNATIONAL COUNCIL FOR BUILDING RESEARCH STUDIES AND DOCUMENTATION
WORKING COMMISSION W18A - TIMBER STRUCTURES

CORROSION AND ADAPTATION FACTORS FOR CHEMICALLY AGGRESSIVE MEDIA
WITH TIMBER STRUCTURES

by

K Erler

Wismar College of Technology
German Democratic Republic

MEETING TWENTY - TWO
BERLIN
GERMAN DEMOCRATIC REPUBLIC
SEPTEMBER 1989

CORROSION AND ADAPTATION FACTORS FOR CHEMICALLY AGGRESSIVE MEDIA WITH TIMBER STRUCTURES

By Dr. sc. techn. Klaus Erler, lecturer
Wismar College of Technology, Wismar (GDR)

1. Objective

The calculation of the loadbearing capacity of new timber structures or the check of that of old timber structures will be accomplished a few years hence in all European countries by adopting the limit states method. In this connection, the most important outside influences are being taken into consideration by applying adaptation factors, e.g. the kind and duration of the stress and strain (loading or action), the moisture of timber as well as adaptation factors for chemically aggressive media. The last-mentioned influence is included hitherto only in a few regulations (specifications) like - for instance - in the Polish Timber Construction Code /1/. Also the draft of a CMEA Code /2/ is indicating some media and their degrees of aggressiveness to timber; however, only a limited number of media is being mentioned and no adaptation factors are being referred to.

The aim of the studies and investigations described hereinafter is to clarify corrosion processes and rates with timber components for the relevant aggressive media. Conclusions may be drawn therefrom concerning reductions for the design (dimensioning). It is particularly important from the national-economic point of view to determine and check with which influences an insignificant corrosion is occurring.

The determination of the influence of chemically aggressive media on the loadbearing capacity of timber structures with long service-life periods and different conditions of utilization shall be supported by documentary evidence.

The objectives consist in

- . enabling a statical check of old structures with regard to

- the corresponding degree of damage done to them, and
- . taking into consideration in the case of new planning and design activities (projects) the reduction of the load-bearing capacity by means of scientifically ensured adaptation factors.

In this connection, relevant influences such as air humidity, kind of the acting medium and cross-sectional dimensions of the timber components concerned must be considered and applied when determining the adaptation factors.

2. Corrosion with timber

Timber is a corrosion-inert building material which is one of the reasons why building constructions (structures) made of timber have a longer service life with corrosion-promoting influences such as high air humidity or/and aggressive media than structural components and members made of steel or concrete.

For instance, such conditions are prevailing in the chemical industry, in agriculture and in fertilizer storage halls. There, the use of timber provides a significant national-economic effect. Since also timber is corroding though - even if very slowly -, it is of some technical and economic interest to determine the corrosion processes, conditions and rates.

Definition:

The term "corrosion" in connection with timber has not much been used hitherto. It is only of recent years that this term is starting to prevail even with timber for damages and failures due to chemical substances. - The definition being recommended is as follows:

"Timber corrosion is the damage or destruction of the timber starting from the surface due to the chemical and/or chemophysical reaction in an interaction with its environment". The fact that the term "timber corrosion" is commencing to prevail also within the scope of the standardization of the

CMEA countries is demonstrated by the draft of the code as mentioned under /2/. A distinction being important in the case of timber must be drawn with regard to damages caused by detrimental organisms, the so-called "biological or biotic corrosion". In concrete construction, "biogenic corrosion" is being defined - e.g. under /3/ - as "damage done to building materials by chemical conversions starting from the surface with the participation of microorganisms".

This implies that also there - like with the other types of corrosion - formulations reading "starting from the surface" and "with the participation of chemical reactions" are decisive in the definition. Therefore, the inclusion of timber damages caused by detrimental organisms (wood insects, wood fungi) in the term "timber corrosion" is being rejected by the author since on the one hand the destruction is not in general starting from the surface and proceeding to the inside and on the other hand no chemical reactions are participating in the timber component with damages due to insects' biting. Thus, the terms of "biotic damages", "attacks by fungi or insects" or "dry-rot" used hitherto for this purpose are relevant and should be adhered to.

Corrosion complex with timber

Timber is in a state of an almost perfect chemical equilibrium with its natural environment. This is the reason why its service life with a normal air humidity is very long. Timber is offering a high resistance even to major chemical attacks. It becomes a suitable construction engineering material - also for an employment in the chemical industry and in agriculture - owing to its resistance to acid fumes, to cold and hot solutions of neutral and acid salts as well as to diluted acids and bases. However, over long periods of time and with a strong chemical action (attack) also with timber a corrosion is occurring. This destructive action is starting from the surface and is proceeding only slowly towards the inside.

The factors playing a decisive or determinant part with the corrosion of timber and the types of corrosion are summarized as a block diagram in Figure 1.

Concerning the types of corrosion, the explanations are as follows:

- Chemical degradation (decomposition) of wood constituents

The hemicelluloses and subsequently the lignin are being degraded by the majority of agents earlier and more extensively than the cellulose. This knowledge is being exploited on a large scale in the production of paper and cellulose. Due to the structure and the composition of the wood, heart-wood is being degraded much slower than the sap-wood, and in general the rate of destruction is decreasing with an increasing depth (as from the surface). Softwood is being destroyed slower than hardwood by the majority of chemical agents, in particular by lyes, though.

- Mechanical destruction

Due to the sorption property of wood, from the environment in the form of high air humidity, of gases and solutions and also of dissolved salts an uptake of water is taking place which results in a swelling or - with a moisture decrease - in a volume reduction of the cell substance. With a frequent alternation of such processes or with an incorporation of highly hygroscopic matters, the destructive action (effect) is increasing and physical changes in the cell substance are the result. The considerable swellings and penetrated crystals are destroying the cell bond or cell walls. Thus, for instance, also the strip-shaped detachment of timber in salt storage halls must be attributed mainly to the above-mentioned action.

- Leaching

This is a process of the extraction of substances - e.g. of minor constituents such as minerals, resins, alcohols, starch and the like - by water, in particular at high temperatures. There, chemical and physical processes are involved. In practice, this is taking place in chemical works, e.g. with containers (tanks), floor coverings and the like. With building constructions (structures), the leaching phenomenon is appearing seldom and only with a corresponding production technology.

The aggressive action on timber is mainly subject - according to the state of aggregation of the medium concerned - to the following:

- . with gaseous media - kind, concentration, air humidity;
- . with liquid media - pH value, concentration degree of dissociation;
- . with solid media - kind, solubility in water, hygroscopicity, pH value in solution, air humidity.

So, the influence of chemically aggressive media on timber components is a multifarious one and can be determined and recorded only with some difficulties since

- . the media may occur in the different states of aggregation (solid, liquid, gaseous),
- . the number of kinds of the media is large,
- . the degree of damage is considerably dependent on the kind of timber, the moisture of timber and the chemical protective measures.

The corrosion phenomena are somewhat similar with the majority of agents acting in an aggressive way on timber; they are as follows:

- . brown or dark-yellow colouration advancing from the boundary zones (cases) into the interior of the cross sections;
- . increased percentage of timber moisture in the boundary (case) areas or regions;
- . incorporation of salt crystals or residual acid ions;
- . separation into fibres up to powdery decomposition of the wood substance near the surface;
- . detachment of wood strips along the boundaries of the annual rings under certain conditions;
- . reduced strengths in the boundary zones (cases).

3. New studies and investigations

Studies and investigations concerning the influence of aggressive media on timber are being accomplished somewhat more frequently only of late; mostly they have been carried out under laboratory conditions by means of faultless (sound) small test specimens and for selected individual parameters. Selected papers to be mentioned in this context are the references /4/ and /5/ with regard to the influence of gaseous media as well as /6/ and /7/ with regard to liquid media.

In addition to the tests and experiments performed by means of small timber specimens and with the concentrated action of aggressive media in the laboratory, of recent years the chemical and mechanical changes have been determined by studying and testing timber components sampled from buildings or structures which are exposed to a high aggressive stress and strain (loading). Such studies and investigations are included in the references mentioned under /7/, /8/ and /9/.

The types of destruction (decomposition) of the cell substance have been analysed to a great extent. The depths of penetration of the media, the rate of destruction and consequently the decrease in loadbearing capacity with component cross sections shall be described hereinafter.

4. Selected results and findings of studies and investigations

The corrosion of timber under the influence of different chemically aggressive media is being dealt with in /7/. Both laboratory tests with a storage in various solutions and investigations using timber specimens sampled from loadbearing systems of buildings and structures in the chemical industry and the potash industry as well as from fertilizer storage halls have been carried out.

Hereinafter, relevant results, findings and information will be presented.

4.1. Depths of penetration of the acting media

Timber structures in industrial works or in agriculture are frequently being subjected to a change of the chemical composition by the penetration of agents such as salts, acids or bases. The pH-value is a significant characteristic index for evaluating the depth of penetration of such agents, their basicity and thus also their destructive action as to timber. The determination of different pH-values in timber cross sections by areal moistening is too inaccurate since thus no distinct boundary (limit) lines and no exact pH-values can be determined. The atomizing application (spraying-on) of a universal indicator solution by means of an atomizer renders it possible to determine different pH-values and - as colour boundary lines - the depths of penetration of agents into the timber. Due to the discolourations (stainings) taking place, the pH-value of the penetration ranges can be defined with an adequate accuracy through a comparison with a colour scale or chart. Checks and verifications being chemically tuned or synchronized to definite agents can be accomplished by means of special indicating reagents which are also being sprayed on. They are an extension and - in particular in such cases where the agent has a similar pH-value like the natural wood - an exact possibility of detection (verification). For instance, this becomes obvious in the detection with regard to the fertilizer of ammonium sulphate.

Examples for depths of penetration of acids, bases and salt solutions subject to the storage period can be found in the paper indicated under /6/.

The cross sections of timber components from buildings which have been exposed to a chemical influence for many years are in general showing a discolouration of the boundary regions (cases). Said discolouration or staining is with the majority of media dark-yellow to brown but anyway darker than the inside cross-sectional areas. It was to be clarified whether and to what extent the widths of the discoloured or stained boundary areas can be used to draw conclusions concerning the strength or to estimate the loadbearing capacity. For this purpose, removed square timber components - mainly from build-

ings and structures of the potash industry - have been studied and tested with regard to the following:

- . measurement of the widths of the zones of discolouration;
- . determination of the depths of penetration and quantities of incorporations of the agents, with the latter being performed by means of a spectral analysis using a flame photometer;
- . determination of the flexural strengths through the cross-sectional width by separation (parting-off) and testing of thin disks or slices in the Dynstat-type machine.

Figure 2 is illustrating one example with zones of discolouration, measured depths of penetration and salt content percentages.

- Figure 2 -

For instance, with this cross section the salts penetrated into the timber on all sides to a depth of 32 mm on an average. The limit of discolouration can be found at 23 mm. A great number of square timber disks and of test cores sampled by drilling in situ has been investigated in this way.

The results and findings of the evaluation (interpretation) can be described as follows:

- (1) The zones of discolouration caused by the penetration and incorporation of chemical agents - in particular of salts - are an indication or symptom of the incorporation. The width of discolouration is dependent on the air humidity, kind of medium and duration of action.
- (2) The zones of discolouration can be found at the whole perimeter (circumference); they are similarly wide at the lateral edges as well as at the top and bottom side.
- (3) For instance, the limit of discolouration is forming with a percentage of the incorporation of salts amounting - on an average - to
0.85 % with KCl,
1.30 % with NaCl.

- (4) The widths of the zones of discolouration amount to 20 mm on an average with a period of occupation of the building concerned totalling about 60 years. However, the scattering is fairly considerable subject to the place of installation, the quantity of deposition and the air humidity.
- (5) The depths of penetration with pine sapwood timber are considerably larger than with spruce timber!
- (6) Strength tests are clearly demonstrating that the limit of discolouration is no limit or threshold of a considerably strength-reduced boundary region; however, the decrease in strength is commencing as from this limit.

4.2. Changes in strength of the timber

Also with a view to determining the change in strength - using to this end almost exclusively the flexural strength of small and large test specimens -, both timber rods after their storage in aggressive solutions and timber specimens sampled from building constructions which have been exposed to an aggressive loading (stress and strain) for several decades have been tested. Tests of such a type - where it is possible to cut out small slices from cross-sectional disks of removed timber components, to test them by means of the Dynstat-type machine as to their flexural strength and subsequently to provide information and data concerning the strength distribution within a timber component - have been performed for the first time to a larger extent. In particular, this approach has been extended also to test cores and thus an exact statement (information) concerning the strength distribution was achieved with a fairly small expenditure by adopting a low-destructive method.

Figure 3 is illustrating one example by showing the strength distribution of the test specimen S 1.

- Figure 3 -

Conformities with natural law (theoretical interrelationships and principles) have been deduced from more than on thousand

measured values. Thus, regression functions could be laid down for the strength developments from the cross-sectional boundary into the cross-sectional interior. A good adaptation to the measured values was achieved by means of logarithmic functions as follows:

$$\sigma_b = A + B \cdot t + C \cdot \ln(t)$$

where σ_b is the bending failure stress, in N/mm^2 , and

t is the distance from the cross-sectional boundary, in mm.

Figure 4 is illustrating one example of measurements performed with test core slices sampled from structures of the potash industry.

- Figure 4 -

The parameters identified as significant for the change of the flexural strengths are the duration of the action or influence - that is the period of occupation of the buildings concerned - and the air humidity prevailing in the buildings, and accordingly evaluations (interpretations) have been accomplished. Thus, the regression curves as shown in Figure 5 for the flexural strength with different ages (i.e. periods of occupation) of the buildings and different air humidities have been determined from several factories of the potash industry /7/.

- Figure 5 -

With all conditions, a considerable strength reduction can be detected in fairly narrow boundary zones (cases) whereas already at a depth of 10 to 15 mm almost the values of undamaged timber are being obtained.

Based on comparison calculations, the following theoretical principles and interrelationships have been realized:

Subject to the duration of action (period of occupation of the building concerned) and to the prevailing air humidity, a largely damaged and considerably strength-reduced boundary zone (case) is occurring.

The interior regions are nearly corresponding to undamaged timber. With considerations in terms of the loadbearing capacity of corrosion-damaged timber components, the assumption

of a corroded boundary layer with the width d being unable to support load any longer can be taken as a basis. The determination of the corrosion product layer thickness d is resulting from the point of intersection of the mean-value straight line of the 0.75-fold flexural strengths in the interior, undamaged region with the mean-value line of the flexural strengths in the boundary region. The derivation can be found in /7/.

5. Determination of the corrosion product layer thickness d by means of a diagram

Such strength developments have been determined and evaluated by using more than 100 cross sections, namely with beam disks or slices and test cores. Inasmuch as the air humidity and thus the conveyance of the salts and of other aggressive ions into the timber cross sections is decisive for the corrosion rate, three air humidity ranges with corresponding corrosion rates and thus different corrosion product layer widths d are being defined as follows:

Humidity range (Fb)	Air humidity φ (%)	Occupation of the building
Fb 1	< 65	
Fb 2	65 to 85	Industry with dissolution and impregnation processes; stable facilities
Fb 3	> 85	Wet rooms, industry with a high production of steam or vapour, open crude salt storage facilities (warehouses)

Figure 6 is showing a summary result of the tests and investigations performed with specimens from the salt industry.

- Figure 6 -

Here, the increase of the corrosion product layer thickness d over the increasing period of occupation of the building concerned (corrosion rate) with different air humidity ranges is

plotted. This graphic representation (diagram) is providing the following information:

- (1) The development of the corrosion rate is not a linear one but shows small values during the first 15 years, is then increasing to a greater extent - among other things due to the hygroscopicity of the salts already stored or incorporated -, and is after that - as from a period of occupation of about 40 years - diminishing again. This means that the corrosion rate is decreasing as from a duration of action of about 40 years.
- (2) By using this diagram (graph), the corrosion product layer thickness d can be determined when evaluating the loadbearing capacity of timber structures for definite periods of occupation and air humidity ranges. The timber cross section must then be reduced circumferentially by the width d , and thus the checks of the loadbearing capacity are to be accomplished.

In Figure 6, as an example of a building with a service life (period of occupation) of 60 years and the air humidity range Fb 2 ($\varphi = 65$ to 85 %) - taking into account the shredded, woolly surface - a boundary layer (case) having a thickness of $d \approx 6$ mm and being no more able to support load can be found on the ordinate.

Concerning this, design (dimensioning) aids are available with the author for selected cross sections.

6. Adaptation factors for covering the influence of chemically aggressive media

Hitherto, the corrosion and thus the reduction of the loadbearing capacity of timber structures has hardly been taken into consideration. An exception to this is the code mentioned under /1/. When preparing expert opinions concerning the residual loadbearing capacity - e.g. of halls or sheds in the potash industry -, only lump (i.e. flat-rate) reduction factors at a subjective discretion were being chosen. Based on the paper mentioned under /7/, an algorithm and adap-

tation factors for covering the influence of chemically aggressive media on timber components are being proposed. The algorithm (see Figure 7) is covering the necessary characteristic values as to the occupation of the building concerned as well as the approach to the determination of the adaptation factor.

- Figure 7 -

The aggressiveness of the media has been determined on the basis of the tests and investigations - in particular of the reduced cross sections - as conditioned by the corroded boundary zone (case) not being able to support load. In this connection, ranges (grades) of aggressivity have been defined. With regard to solutions, Figure 8 is showing some significant media.

- Figure 8 -

With gases, vapours and granular materials to be stored, the air humidity is playing an important part. Therefore, selected gases and solid media are being assigned - with the air humidity ranges as mentioned hereinbefore - to stress degrees (BG).

The determination of the adaptation factor γ_{m4} is being accomplished by means of the stress degrees (BG) to be drawn from the tables following hereinafter and subsequent to this by means of the table concerning the cross-sectional areas of the timber components.

Stress degree (BG)	Explanation
BG I	not or slightly aggressive
BG II	moderately aggressive
BG III	heavily aggressive

The assignment (grouping) of the stress degrees BG according to the corrosive action for gaseous, liquid and solid media is as follows:

- Gaseous media

T a b l e 1

Medium	Concentration	Stress degrees BG with moisture grades (FK)		
		FK 1	FK 2	FK 3
formaldehyde		I	I	I
ammonia		I	I	I
sulphur dioxide	0.2 to 10 mg/m ³	I	I	I
	10 " 200 "	I	II	II
nitrogen oxide	0.1 " 5 "	I	I	I
	5 " 25 "	I	II	II
	>25 "	II	II	II
hydrogen chloride	0.05 " 1 "	I	I	I
	1 " 10 "	I	II	II
	>10 "	II	II	II
chlorine	0.02 " 1 "	I	I	I
	1 " 5 "	I	II	II
	>5 "	II	II	II

- Solutions

The permanent contact of aggressive solutions (acids, bases, salt solutions) with structural components is occurring seldom.

Salt solutions: BG II

Strong acids and bases: BG III

Expert opinion is required in the individual case concerned.

- Solids

T a b l e 2

Medium	Stress degree BG with			Examples Function of the building/structure
	FK 1	FK 2	FK 3	
potash fertilizer	I	II	II	BG I: • production in the potash industry finished product storage facilities
urea	I	II	II	
superphosphate, } sodium chloride }	I	I	II	BG II: • crude salt storage facilities with FK 2 • fertilizer storage halls with FK 2
ammonium sulphate	I	I	I	

The stress degrees BG together with the groups for the dimensions of the timber cross sections are resulting in the required adaptation factors for the influence of aggressive media (see Table 3 following hereinafter).

- Adaptation factor γ_{m4}

T a b l e 3

Stress degree (BG)	Cross-sectional dimension of the timber components	Factor γ_{m4}
BG I		1.0
BG II	< 90 cm ²	0.75
	< 300 cm ²	0.85
	IV 300 cm ²	0.95
BG III	< 90 cm ²	0.65
	< 300 cm ²	0.75
	IV 300 cm ²	0.85

With the stress degrees BG II and BG III, the minimum dimension of the timber components should be 40 mm.

Timber cross sections of glued laminated timber are showing an even more resistant behaviour than solid timber with the majority of media.

7. Summary

The corrosion of timber components when exposed to a chemically aggressive influence is being described with the evaluation of new results and findings of studies, tests and investigations. In general, timber as building material is more resistant to the majority of chemical agents than steel and concrete. The significant parameters for the intensity of the corrosion with timber are being indicated. The destroyed boundary zone (case) of the width d which is assumed to be no longer able to support load is being determined subject to

the duration of action (period of occupation of the buildings concerned), to the kind of medium and to the air humidity.

Based on the description, the depths of penetration of the agents and the reduced strengths can be determined. Subsequent to the testing of specimens sampled from the timber structure concerned - e.g. test cores -, it is possible to exactly determine the boundary zone (case) being no more able to support load or to draw an approximate value for same from a graph (diagram). The residual loadbearing capacity of existing structures or components can be checked and verified by means of the timber cross sections reduced by d.

In the draft of the new GDR Code "Timber Construction - Load-bearing Systems" adopting the method of limit states, for timber the most significant agents have been assigned to ranges (grades) of aggressivity, and stress degrees have been defined accordingly. Subject to the stress degree and to the cross-sectional dimension of the timber component concerned, adaptation factors for the influence of aggressive media have been fixed.

References

- /1/ Polnischer Standard PN-73/B-03150 - Holzkonstruktionen - Statische Berechnungen und Projektierung (Polish Code... Timber structures - Static calculations and planning & design) - Edition dated Dec. 30, 1973.
- /2/ RGW-Standard 22.700.12-84
 "Korrosionsschutz im Bauwesen - Holzkonstruktionen - Klassifizierung der Aggressivität von Medien" (CMEA Code ... "Corrosion protection in the building industry - Timber structures - Classification of the aggressiveness of media") - Draft: Moscow, April 1985.
- /3/ TGL 33408 Bl. 01 und Bl. 02 (DDR-Standard)
 Betonbau - Korrosion und Korrosionsschutz
 Bl. 01: Beanspruchungsgrade; Ausgabe Nov. 1980
 Bl. 02: Aktive Schutzmaßnahmen für Beton und Leichtbeton; Ausgabe Nov. 1980
 (TGL...sheet 01 and sheet 02 (GDR Code): Concrete construction - Corrosion and corrosion protection
 Sheet 01: Stress degrees / Edition of Nov. 1980
 Sheet 02: Active protection measures for concrete and lightweight concrete / Edition of Nov. 1980).

References (cont'd.)

- /4/ Gos, B.
Physikalische und chemische Veränderungen in Kiefernholz und Phenol-Resorzin-Harz infolge des Einwirkens konzentrierter aggressiver Gase. (Physical and chemical changes in pine timber and phenolic resorcinol formaldehyde resin due to the action of concentrated aggressive gases). - Published in: Holztechnologie - Leipzig 27 (1986) 1, pp. 20-24.
- /5/ Bosold, C.; Fengel, D.
Systematische Untersuchungen der Wirkung aggressiver Gase auf Fichtenholz (Systematic investigations into the action of aggressive gases on spruce timber). - Published in: Holz als Roh- und Werkstoff. - Berlin (West), 41 (1983), pp. 227-232, 265-269, 333-337, 509-513.
- /6/ Erler, K.
Wirkungen aggressiver Lösungen auf Kiefernholz (Actions of aggressive solutions on pine timber). - Published in: Holztechnologie. - Leipzig 25 (1984) 5, pp. 249-252.
- /7/ Erler, K.
Bauzustandsanalyse und Beurteilung der Tragfähigkeit von Holzkonstruktionen unter besonderer Berücksichtigung der Korrosion des Holzes (Analysis of the structural state of repair and evaluation of the loadbearing capacity of timber structures with particular consideration of the corrosion of timber). - Thesis, type B; Wismar College of Technology, 1988. - 149 pages and 11 annexes.
- /8/ Kerner, G.; Ritter, H.
Grundlagenuntersuchungen zur Beständigkeit von Nadelsschnittholz gegen Mineraldünger (Fundamental investigations into the resistance of sawn coniferous timber to mineral fertilizers). - Published in: Holztechnologie. - Leipzig 25 (1984) 5, pp. 233-237.
- /9/ Parameswaran, N.
Zur Mikromorphologie von Fichtenholz nach längerem Einsatz in einer Kali-Lagerhalle (On the micromorphology of spruce timber after a longer use in a potash storage hall). - Published in: Holz als Roh- und Werkstoff. - Berlin (West), 39 (1981) 4, pp. 149-156.

82

C a p t i o n s

- Figure 1 Corrosion complex in timber with the action of chemical media
- Figure 2 Squared timber sized 150/218 mm from a finished product storage facility; Sollstedt potash factory; period of occupation = 55 years:
Measured values of the widths of discolouration and salt incorporations, in per cent (KCl and NaCl)
- Figure 3 Timber test specimen S 1, squared timber sized 100/120 mm from a crude salt storage facility; Sondershausen potash factory; period of occupation = 70 years:
Distribution of the flexural strengths σ_b , in mm, over the cross section
- Figure 4 Flexural strength development from the cross-sectional boundary towards the cross-sectional centre, with regression function; specimens from the Sollstedt potash factory; period of occupation = 55 years
- Figure 5 Development of the bending failure stresses from the cross-sectional boundary towards the cross-sectional interior, in the form of regression curves for timber components damaged by salts subject to the air humidity and period of occupation
- Figure 6 Increase of the corrosion product layer thickness d over the period of occupation of the buildings (corrosion rate), with different air humidities and with salt attack
- Figure 7 Algorithm for the determination of the adaptation factor as to the influence of chemically aggressive media

Captions (cont'd.)

Figure 8 Decrease of the loadbearing capacity in bending
of pine timber rods with cross sections of 40 x 40
mm after 2 and 3 months of storage in selected so-
lutions

Zu Bild 6:

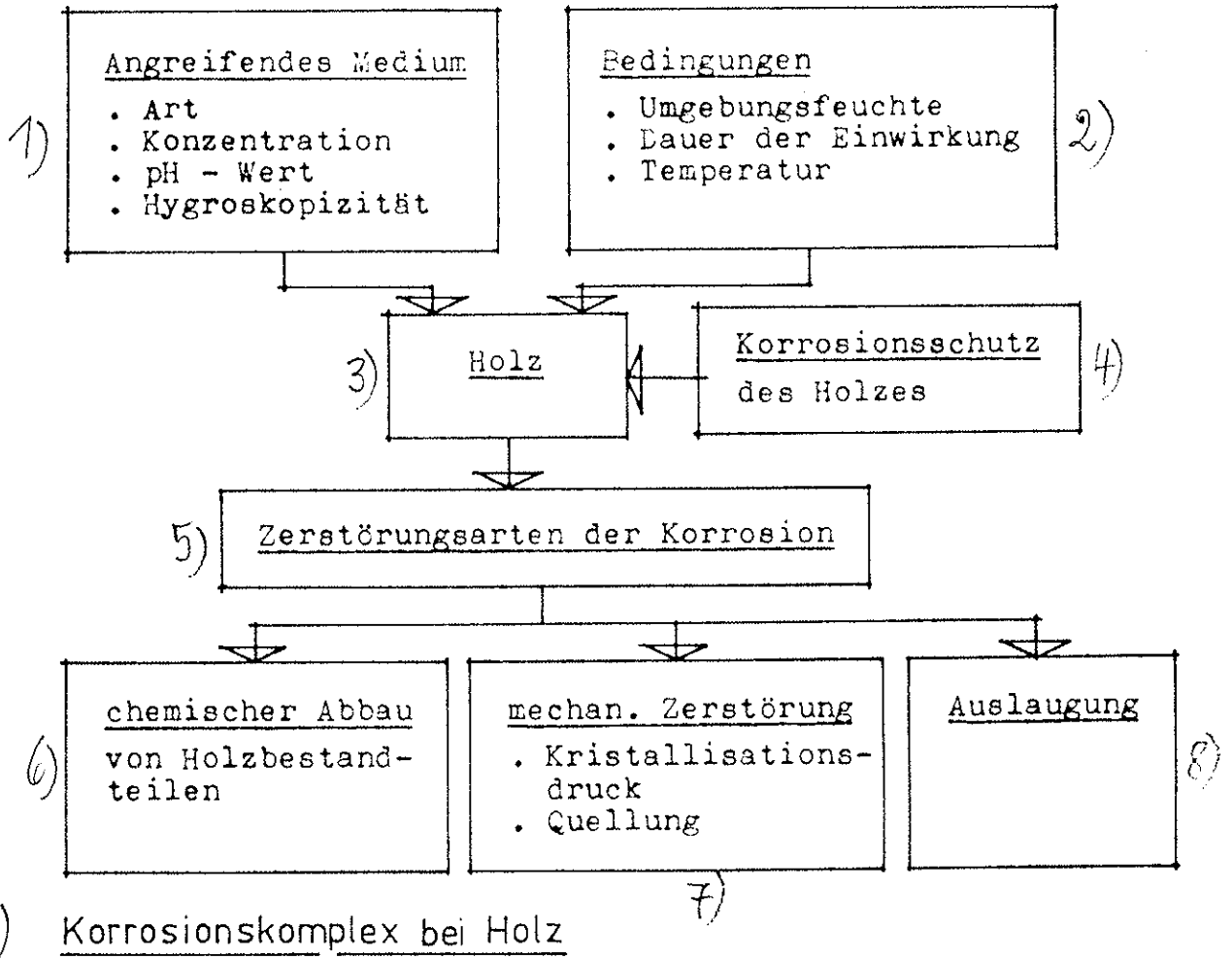
- 1) period of occupation (years)
- 2) with woolly surface layer
- 3) without woolly surface layer
- 4) Figure 6: Corrosion product layer thickness d with salt action

Zu Bild 7:

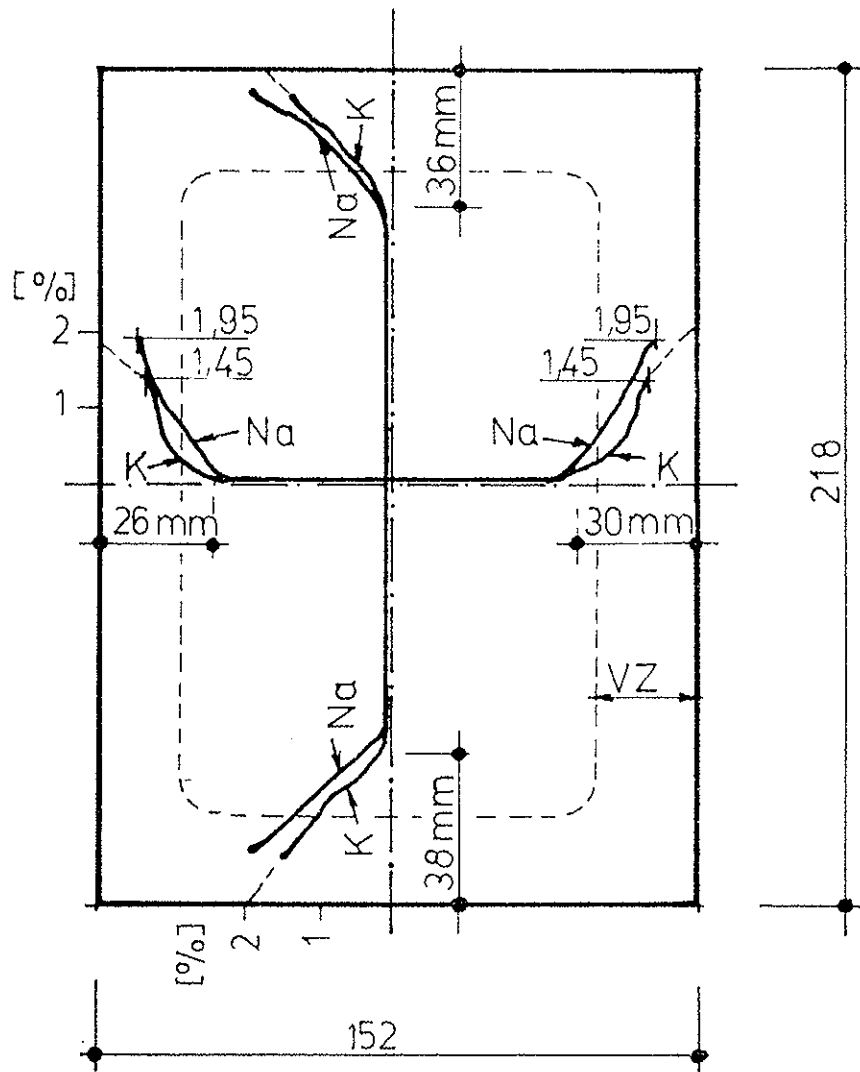
- A) Algorithm for the determination of the adaptation factor γ_{m4} "Influence of aggressive media on timber"
1. Kind of medium a) gases b) solids c) solutions
 2. Relevant criteria a) concentration b) solubility
 c) concentration hygroscopicity
 pH-value
 3. Moisture grade FK 1 FK 2 FK 3
 4. Stress degree a) aggressiveness
 b) no/slight c) moderate d) heavy
 BG 1 BG 2 BG 3
 5. Timber cross section
 6. Adaptation factor
- B) Figure 7

Zu Bild 8:

- a) existing flexural strength b) test specimens not stored
 - c) ... after a storage period of 2 months
 - d) ... after a storage period of 3 months
- | | | |
|---------------------|-----------------------------|---------------------|
| 1 hydrochloric acid | 3 urea | 8 ammonium sulphate |
| 2 nitric acid | 4 sodium hydroxide solution | 9 hydrogen peroxide |
| | 5 superphosphate | |
| | 6 potassium chloride | |
| | 7 sulphuric acid | |
- e) Figure 8

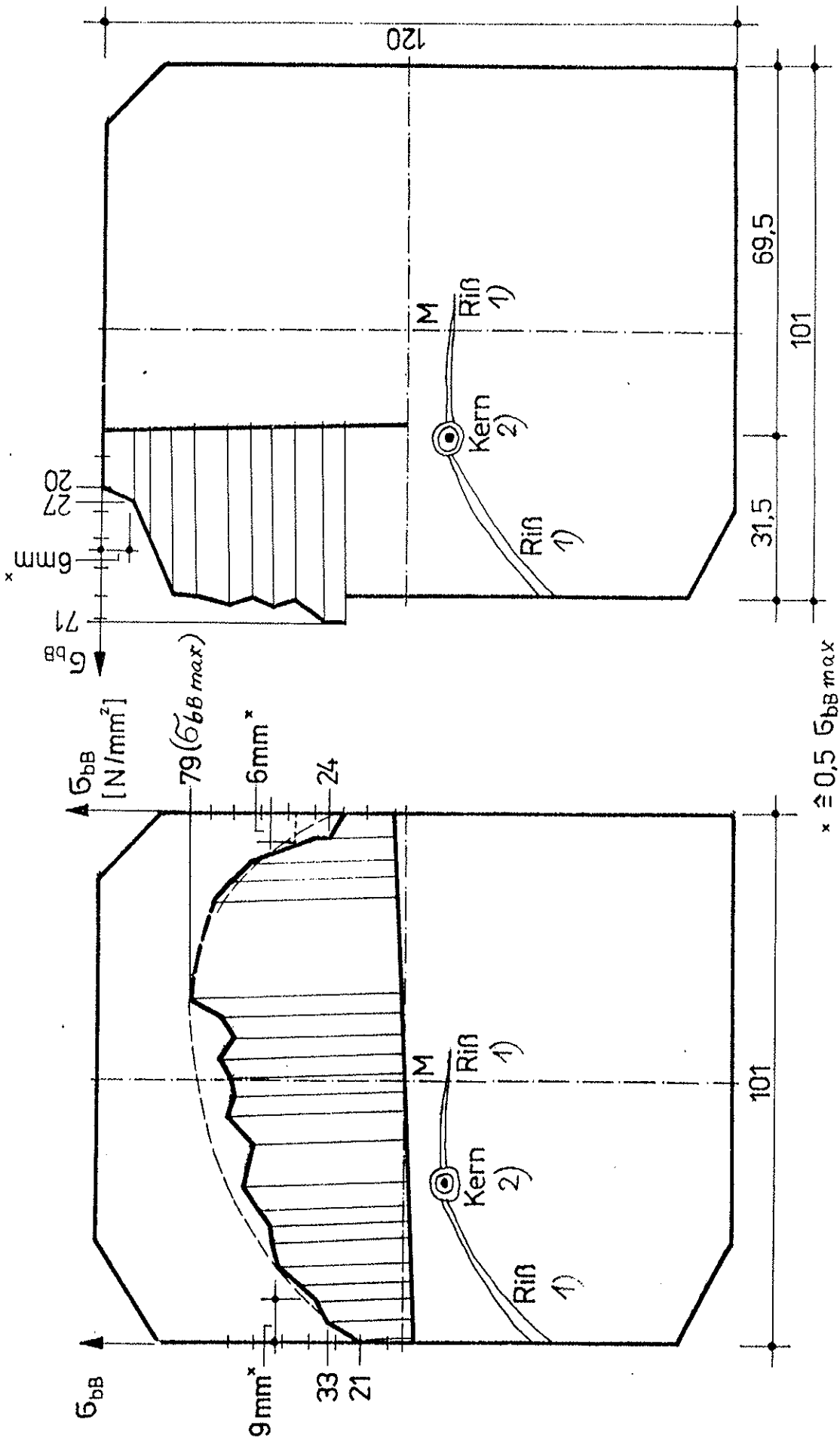


10) Bild 1



- 1) VZ verfärbte Zone
- 2) Na Natrium (Salze)
- 3) K Kalium (Salze)

4) *Bild 2*



x ≥ 0,5 σ_{bb max}

3) Bild 3

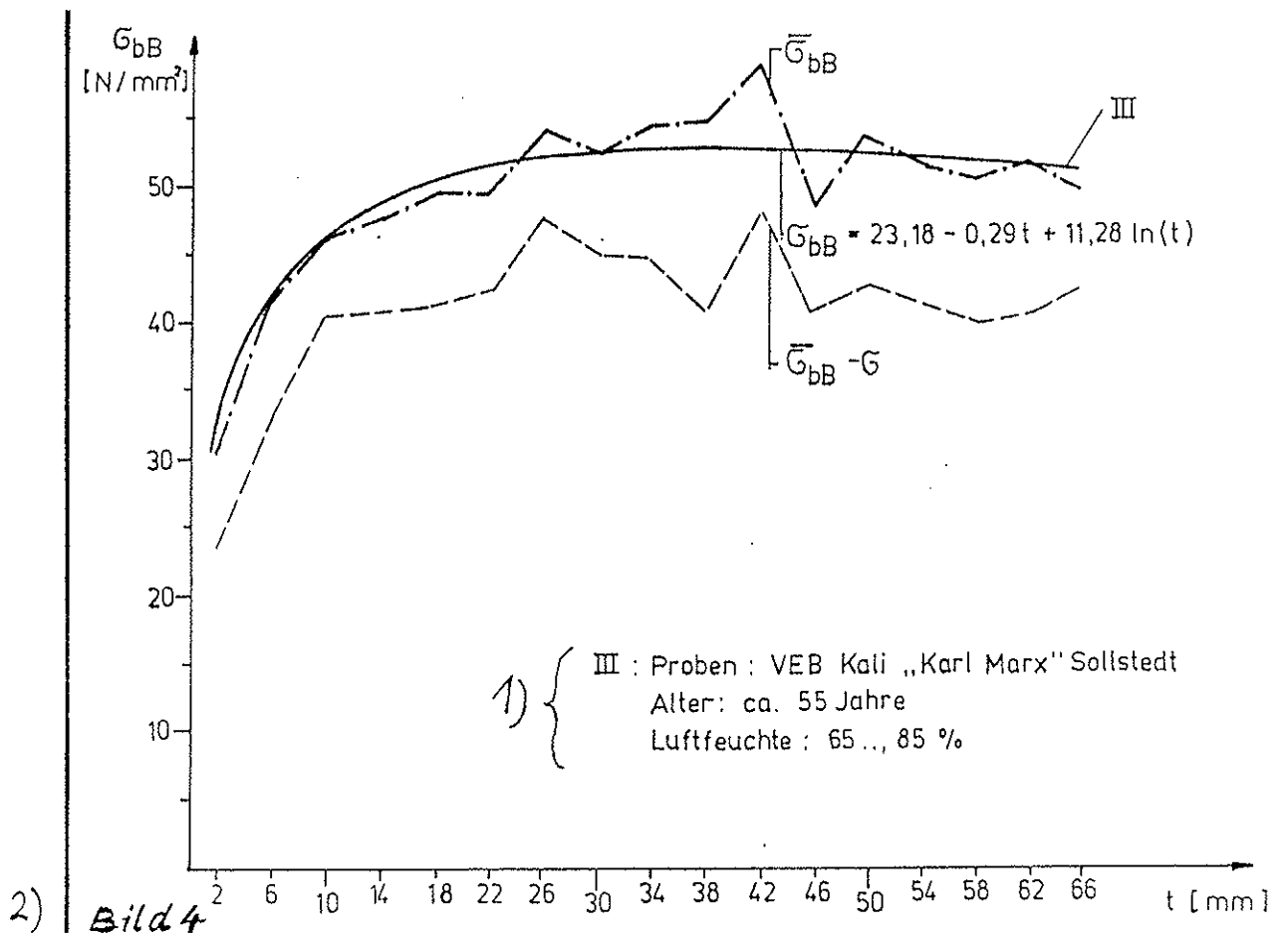
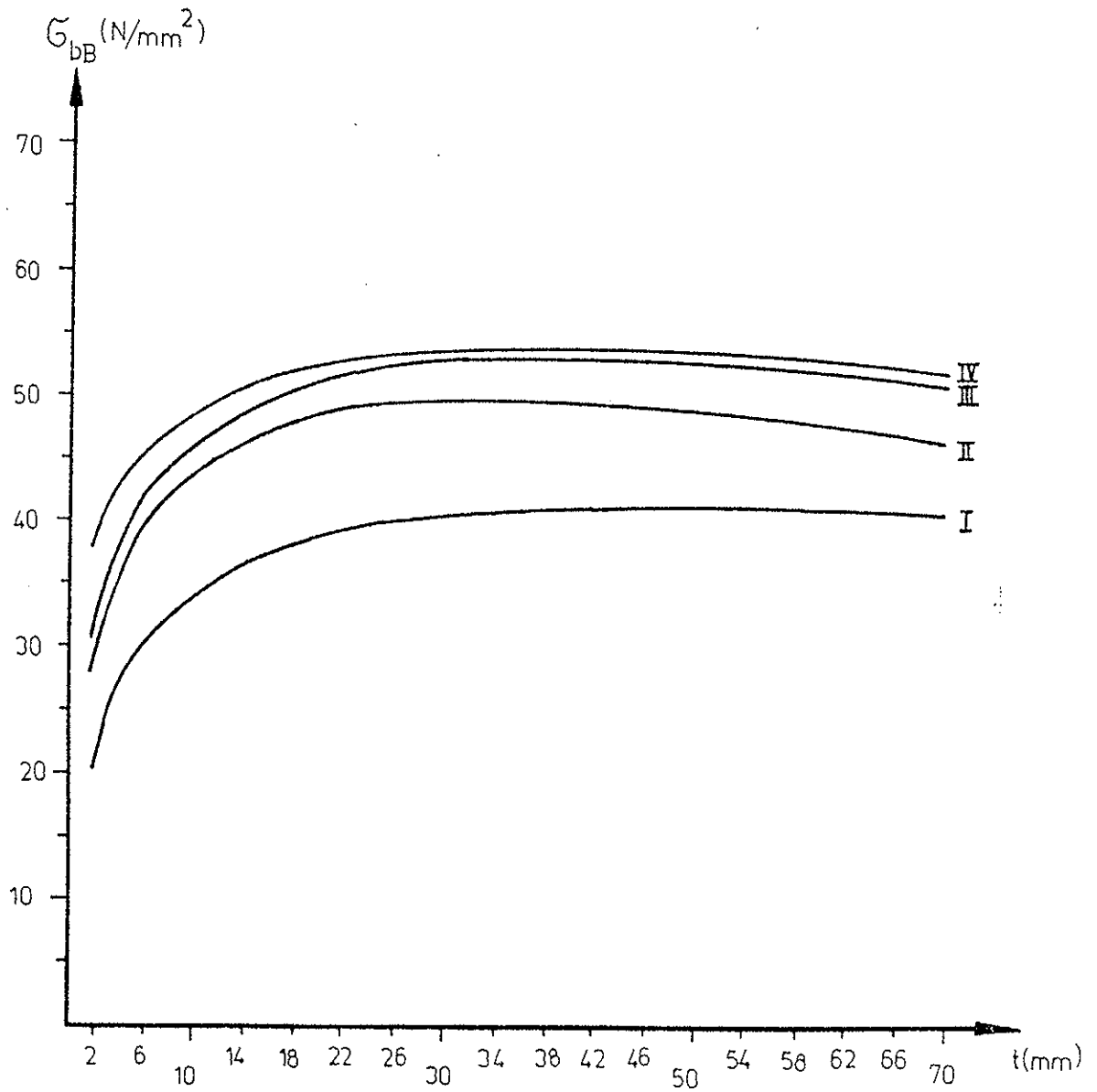


Bild 5: Verlauf der Biegebruchspannungen in Abhängigkeit

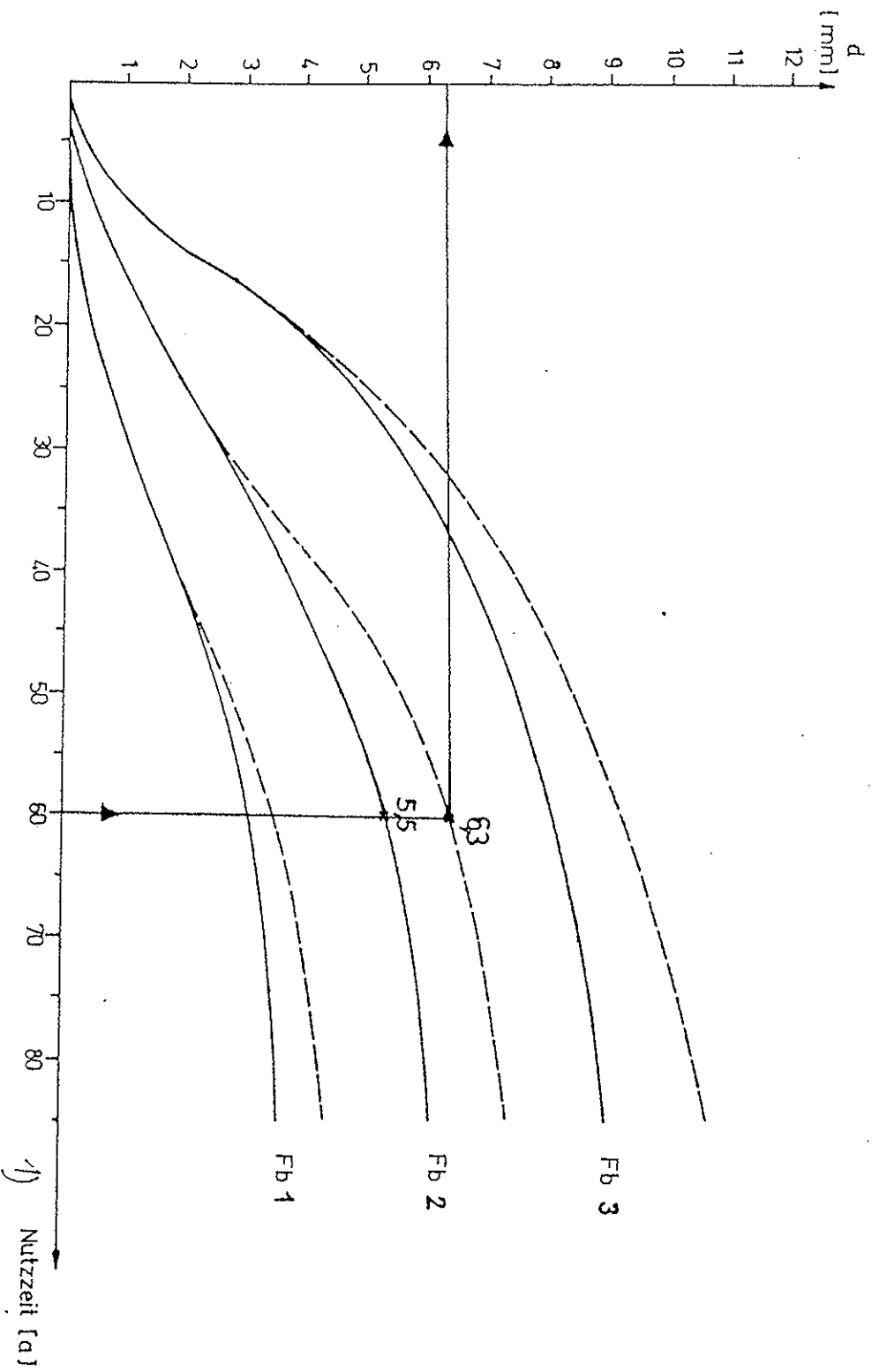
1) vom Querschnittsrandabstand bei durch Kalisatz geschädigten Holzbauteilen, beschrieben durch Regressionsfunktionen

2)

Nr.	Ort	Alter	Luftfeuchte
I	Kalibetrieb Merkers	70 a	> 85 %
3) II	Kalibetrieb Merkers	60 a	65... 85 %
III	Kalibetrieb Sollstedt	55 a	65... 85 %
IV	Kalibetrieb Merkers	50 a	65... 85 %



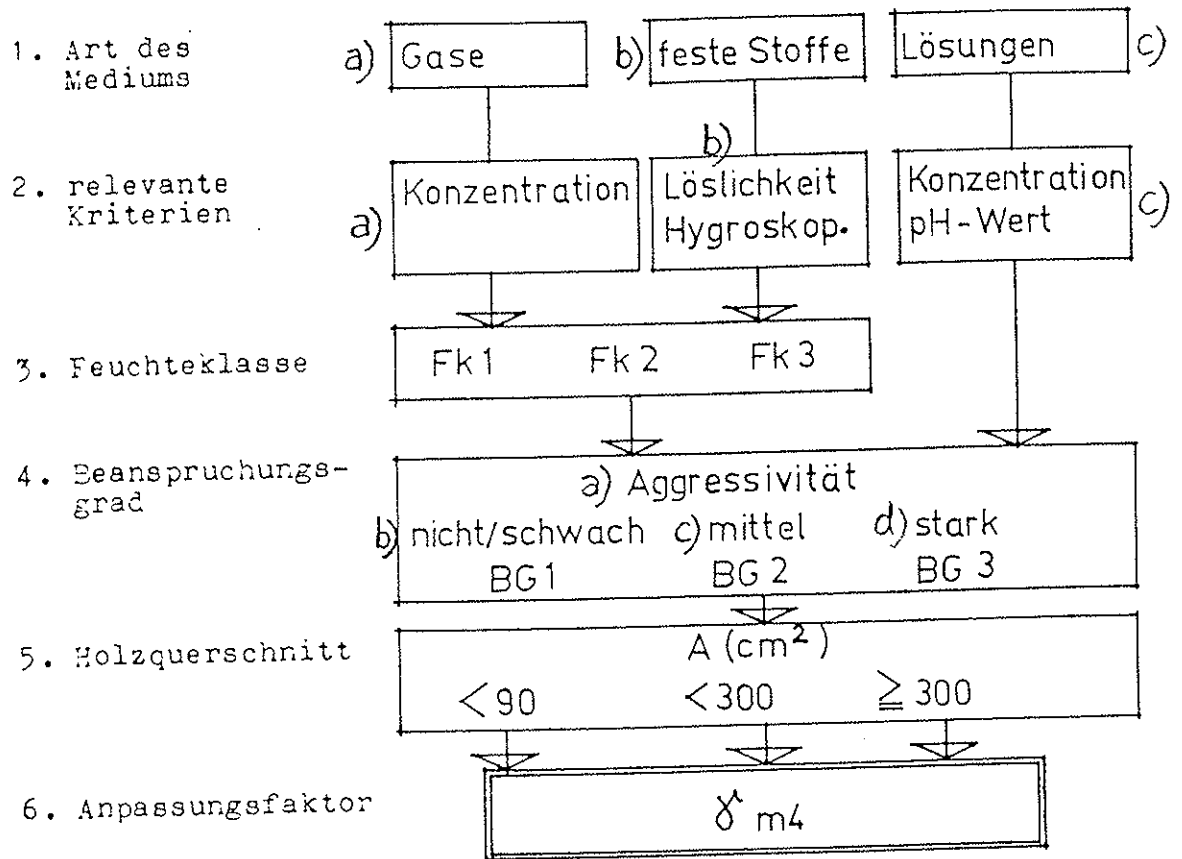
4) Bild 5



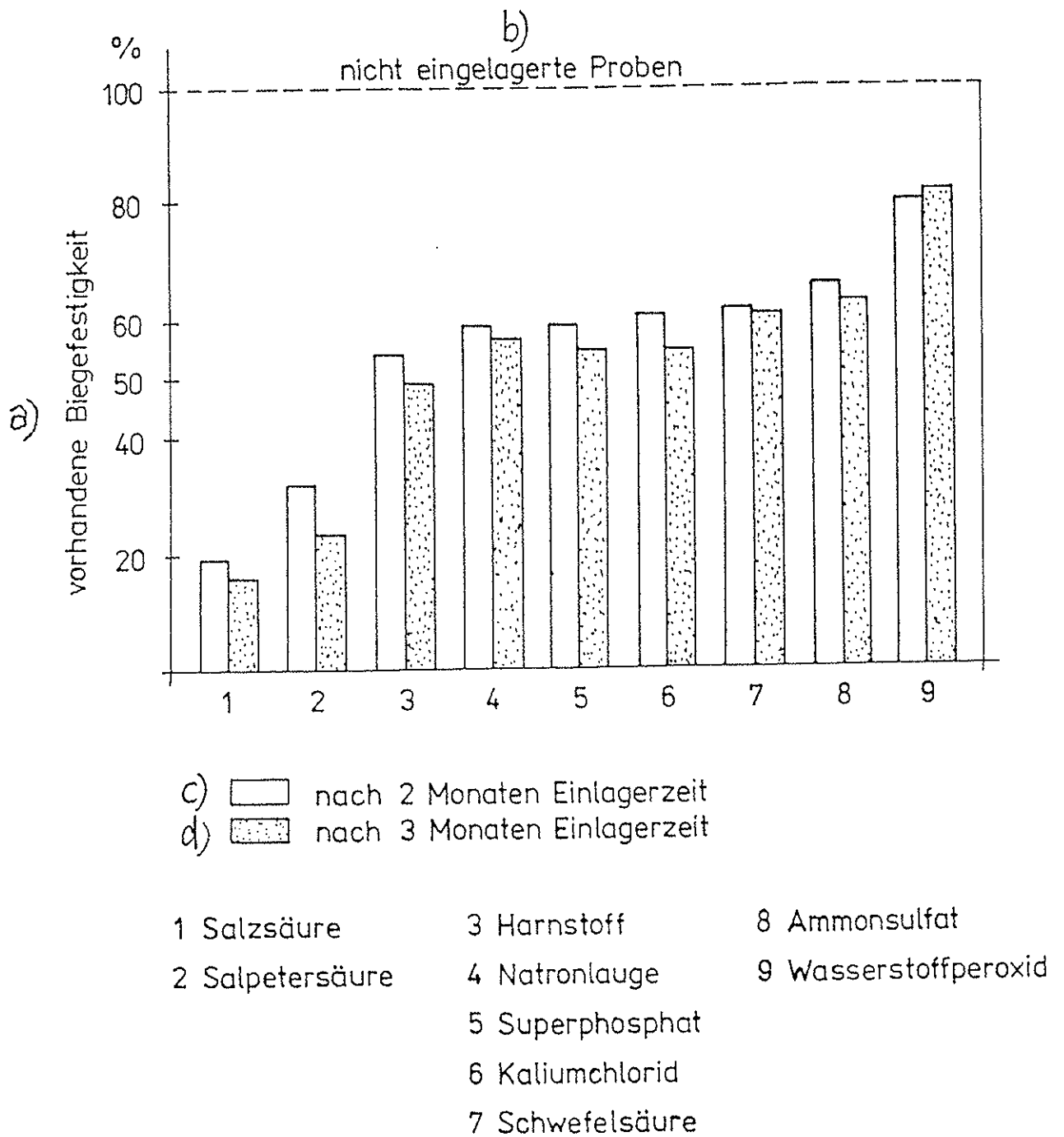
4) Bild 6

- - - mit welliger Oberflächenschicht 2)
 ——— ohne wellige Oberflächenschicht 3)
 Korrosionsschichtdicke d bei Salzeinwirkung

A) { Algorithmus zur Ermittlung des Anpassungsfaktors γ_{m4}
"Einfluß aggressiver Medien auf Holz"



B) Bild 7



e) Bild 8

INTERNATIONAL COUNCIL FOR BUILDING RESEARCH STUDIES AND DOCUMENTATION

WORKING COMMISSION W18A - TIMBER STRUCTURES

**THE DEPENDENCE OF THE BENDING STRENGTH
ON THE GLUED LAMINATED TIMBER GIRDER DEPTH**

by

M Badstube and W Rug
Academy of Building of the GDR
Institute for Industrial Buildings
German Democratic Republic

and

W Schone
Institute for Building Units and Fibre Building Materials
German Democratic Republic

MEETING TWENTY - TWO

BERLIN

GERMAN DEMOCRATIC REPUBLIC

SEPTEMBER 1989

1. Introduction

With a view to determining the influence of the girder depth on the bending strength of glued laminated timber, experimental investigations and tests are being carried out. It is the objective of these tests and investigations to find out data and information concerning the application of the "depth dependence" modification factor k_h (depth factor) for glued laminated timber (abbreviated hereinafter referred to as: BSH in German or GLT in English, respectively).

2. Objective of the experimental investigations

Due to the interrelation or connection between the girder depth and the bending strength of GLT girders which is yet obscure, experimental investigations are required. Publications by Ehlbeck and Colling (see the bibliographical references /1/ and /2/) are verifying that in the case of GLT girders with which the failure was to be attributed to a key-dovetail connection or "finger joint" (abbreviated hereinafter referred to as: KDC in English or KZ in German, respectively) no dependence of the bending strength on the girder depth could be determined. The bending strength of the GLT girders was within the order of magnitude of the tensile strength of the KDC.

Thus, according to this the introduction and application of a so-called "depth factor" seems not to be justified.

The bending strength of GLT girders is being influenced by two independent factors, i.e. the timber strength and the KDC strength.

A stricter visual sorting is not influencing the KDC (or "finger joint") strength.

Only a mechanical sorting based on the bulk density or the modulus of elasticity of the boards is likely to provide increased KDC strengths as well.

Below the girder depth of 500 mm, the bending strength of the GLT girders being free from KDCs in the zone of maximum flexural

tension is decreasing (see /1/ and /2/).

Above the girder depth of 500 mm, there is no considerable decrease in bending strength.

With GLT girders the KDCs of which are failing, no interrelation between bending strength and girder depth is being determined. Tests showed that GLT girders the KDCs ("finger joints") of which were failing had about the same bending strength with a girder depth of 330 mm as girders with a girder depth of 1,000 mm.

Schöne /3/ has investigated and tested the following two types of GLT girders:

- (A) girders being provided with a KDC within the zone of maximum flexural tension;
- (B) girders with which the zone of maximum flexural tension is free from KDC.

With the type (A) girders, the failure of the structural component was always occurring within the KDC area. The mean bending strength of the GLT girders is approximately equal to the mean tensile strength of the KDC. Consequently, a strength-increasing overlapping effect to be expected due to the KDC staggering can therefore not be verified /3/.

Since in the manufacture of GLT girders at the glued wood construction enterprises the location or position of the KDC ("finger joint") is a random event and the average length of the machined boards is hardly amounting to more than 2 metres, already with girders having a length as from about 6 metres the type (A) pattern is the normal case.

However, also with shorter girders the probability is very large that KDCs ("finger joints") are located within the heavily stressed zone.

Therefore, from the aspect of the real production of GLT girders, the application of the "depth factor" is rejected and the tensile strength of the KDCs is being regarded as the decisive feature.

Taking into account the data and information indicated in the publications concerned with regard to the dependence of the bending strength of GLT girders on their depth, specific experimental

studies and investigations are being accomplished. In this connection, the following two grades of glued laminated timber are being considered (see Figure 1):

"BSH O"-type GLT

- the layers of boards are being sorted visually;
- the position of the key-dovetail connection (KDC) is random.

"BSH M 3"-type GLT

- the layers of boards are being sorted mechanically;
- the KDC ("finger joint") is located within the zone of maximum flexural tension.

3. Description of the test specimens

3.1. GLT girders of the "BSH O"-type grade

For the short-term tests, the "BSH O"-type girders as shown and described in the Figures 1, 4 and 5 are being used.

The layers of boards of the "BSH O"-type glued laminated timber girders consist of sawn coniferous timber (pine) and are being sorted visually according to the knottiness into the quality class GK II as follows:

- individual knots according to Figure 2;
- accumulations of knots according to Figure 3.

The glueing (bonding) of the layers of boards with one another as well as of the KDCs ("finger joints") is being performed by using a "Plastasol L 47 N"-type phenolic resin bonding adhesive.

The position (place) of the KDC is at random. The key-dovetail ("finger joint") length is 20 mm. The distance of the KDCs (dovetail staggering; in German being abbreviated as KZV) between the 1st and 2nd layer of boards (see Figure 4) is being guaranteed with an amount of KZV = 250 mm.

The equilibrium moisture of the layers of boards after the manufacture amounts to $\omega \approx 12\%$.

3.2. GLT girders of the "BSH M 3"-type grade

For the short-term tests, the "BSH M 3"-type girders as shown and described in the Figures 1, 4 and 6 are being used.

The layers of boards of the "BSH M 3"-type glued laminated timber girders consist of sawn coniferous timber (pine) and are being sorted mechanically according to the modulus of elasticity in bending and to the knottiness into strength classes as follows:

- external layers (see Figure 1) are falling under the strength class F II
($E \geq 9,500 \text{ N/mm}^2$; individual knots according to Figure 2, accumulations of knots according to Figure 3; see /4/);
- internal layers (see Figure 1) are falling under the strength class F III
($E \geq 7,000 \text{ N/mm}^2$; individual knots according to Figure 2, accumulations of knots according to Figure 3; see /4/).

Decisive for the allocation to a strength class is the unfavourable value of one sorting parameter.

The glueing (bonding) of the layers of boards with one another as well as of the KDCs ("finger joints") is being performed by using a "Plastasol L 47 N"-type phenolic resin bonding adhesive.

As a general principle, a KDC ("finger joint") is being arranged in layer 1 (being the lowest girder layer - the tension layer -; see Figure 1) within the test zone (see Figure 4).

The key-dovetail ("finger") length amounts to 50 mm. The distance of the KDCs (dovetail staggering; in German: KZV) between the 1st and 2nd layer is being guaranteed with an amount of $KZV \geq 250 \text{ mm}$.

The equilibrium moisture of the layers of boards after the manufacture amounts to $\omega \approx 12 \%$.

4. Test procedure

With a view to achieving a zone being free from transverse forces, a four-point loading is being selected for the test arrangement of the GLT girders (see Figure 4).

The results and findings from studies and investigations performed by using structural timber (see /5/) are showing that - in order to avoid shear failures - the ratio of the flexural stress $\sigma_{m,d}$ to the shear stress τ_d shall be 22 whereas for a shear influence of about 6 % the ratio of the effective span l_1 to the specimen height h shall be 15.

With these prerequisites prevailing, the length of the test zone l_2 is being designed as $l_2 = 4 h$ /5/ (see Figure 4).

The load is being applied by increments in such a way that the failure will occur after a loading period of 3 to 5 minutes.

The tests are being carried out at an air temperature of $T = 20$ °C, a relative air humidity of $\varphi = 65$ % and a timber moisture of $\omega = 12$ %.

The girder deflection U_z is being measured at the central position of the effective span by means of a dial gauge.

5. Test evaluation

5.1. Bending tests by using "BSH 0"-type GLT girders

The test results are indicated in Figure 5.

The following two types of failure are distinguished:

- A) tensile failure in the KDC ("finger joint") within the test zone l_2 , layer 1 (see Figure 4);
- B) tensile failure in the knot or timber within the test zone l_2 , layer 1 (see Figure 4).

For the failure type A, the mean values of the bending strength $f_{m,mean}$ are not showing any dependence on the girder depth (see Figure 5).

For the failure type B, the reduction of $f_{m,mean}$ is occurring up to $h = 608$ mm but no longer beyond this depth.

The characteristic value of the bending strength (5%-quantile) $f_{m,k}$ was obtained from the Gauss normal distribution by conversion from small to large random sample numbers /6/.

With the characteristic values of the bending strength $f_{m,k}$, a reduction is occurring for the failure type A up to $h = 608$ mm and no more beyond that (see Figure 5).

As for the failure type B, the reduction is also occurring up to $h = 608$ mm and no more beyond that.

5.2. Bending tests by using "BSH M 3"-type GLT girders

The test results are indicated in Figure 6.

With the mean values of the bending strength $f_{m,mean}$, no reduction is occurring up to $h = 608$ mm in the case of the failure type A whereas a reduction can be perceived in the case of the failure type B.

Similar findings are being obtained with regard to the characteristic values of the bending strength $f_{m,k}$ as well.

5.3. Evaluation of the results and findings

The insignificant number of random samples as well as the interaction of different influences are only admitting of a limited statement.

Nevertheless, from the data and particulars included in the bibliography and based on our specific tests and investigations the following tendency becomes apparent:

With the characteristic values of the bending strength $f_{m,k}$, a reduction is occurring for the failure type A with "BSH 0"-type glued laminated timber up to $h = 608$ mm and no more beyond that.

An explanation concerning this may be as follows:

According to Ehlbeck /2/, with a KDC (i.e. key-dovetail connection or "finger joint") the tensile strength amounts to 80 % of the bending strength:

$$f_{t,o,k;fi} \sim 0.8 f_{m,k;fj}$$

In the case of one dovetailed layer of boards pure flexural stressing with the corresponding bending strength $f_{m,k}$ is prevailing whereas in the KDC ("finger joint") with an increasing

depth of girder also tensile stressing in addition to the bending stress and strain is occurring.

With a layer thickness of 32 mm, the KDC is quasi being stressed only just by tension as from a girder depth of 608 mm (see Figure 7).

This would be an explanation of the phenomenon why the dovetail ("finger") tensile strength becomes decisive and the "depth factor" is being eliminated beyond $h = 608$ mm.

Addition tests and investigations for the failure type A within the range of $h = 608$ mm are still required in order to provide for a final statement. The available small number of random samples does not yet permit to come to a conclusion.

6. "Depth dependence" modification factor k_h for glued laminated timber ("depth factor")

With a view to determining the modification factor k_h , the mean values of the bending strength $f_{m,mean}$ of "BSH 0"-type glued laminated timber are being applied (see Figure 8).

The experimental depth factor is being calculated according to Figure 9 (equation (1)) for the failure types A and B subject to the volume ratio V / V_1 and the depth ratio h / h_1 and is being entered for the failure type B into the Figures 11 and 12. In this connection, the volume amounts to $V = b \cdot h \cdot l_1$ (with l_1 being the effective span).

The regression analysis results in very small correlation coefficients r (see Figure 10) for the failure type A.

This means that there doesn't exist any depth dependence for the failure type A.

As for failure type B, significant correlation coefficients are existing (see Figure 10, equations (8) to (11)).

They are verifying the depth dependence of the bending strength for the heavily stressed zone being free from KDC ("finger joints") (failure type B).

The obtained regression equations with the highest correlation coefficients r from (8) and (9) are being entered into the Figures 11 and 12.

Furthermore, the theoretical depth factor $k_{h,theor.}$ is being calculated according to Colling /7/ for the failure type B subject to the volume ratio according to Figure 9 (2) and (3) and is being entered into Figure 11. One can see that the theoretical depth factor curve is developing below the k_h depth factor curve being determined as a result of the test values.

A comparison of the depth factor determined from the test values with the k_h -value according to the Eurocode 5 /8/, Annex 2, page 110

$$k_h = \left(\frac{200}{h} \right)^{0.2} = \frac{1}{\left(\frac{h}{200} \right)^{0.2}} \quad (12)$$

results - with equal depth ratios h / h_1 - almost in a conformity (see Figure 12).

7. Summary

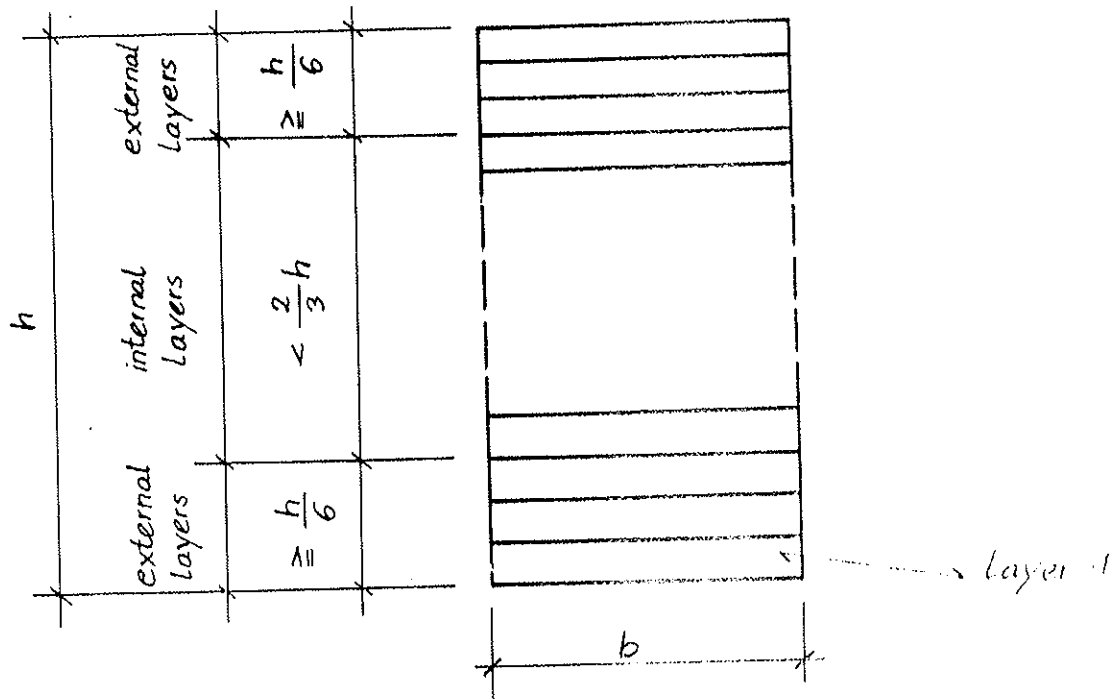
The evaluation of the bibliography (publications) and our own specific tests and investigations performed by means of glued laminated timber girders are demonstrating that for the failure type A (KDC ("finger joint") failure within the stressed zone) there doesn't exist any interrelation between the girder depth and bending strength.

As for the failure type B (knot or timber failure within the heavily stressed zone), a statistically covered and verified interrelation between the stressed volume or girder depth and the bending strength can be determined.

The tests are verifying the depth factor as indicated in the Eurocode 5 for the failure type B.

8. Bibliographical references

- /1/ J. Ehlbeck, F. Colling:
 "Die Biegefestigkeit von Brettschichtholzträgern in Abhängigkeit von den Eigenschaften der Brettlamellen"
 (The bending strength of glued laminated timber girders subject to the properties of the board lamellae)
 Published in: Bauen mit Holz, No. 10/87, pp. 646 - 655.
- /2/ J. Ehlbeck, F. Colling:
 "The strength of glued laminated timber (GLULAM) - Influence of lamination qualities and strength of timber joints"
 CIB W 18, 2 1-12-3; Canada, September 1988.
- /3/ W. Schöne:
 "Der Einfluß der Trägerhöhe auf die Biegefestigkeit von Brettschichtholz"
 (The influence of the girder depth on the bending strength of glued laminated timber)
 Submitted for being published in: Bauplanung - Bautechnik, 1989.
- /4/ GDR Industrial Code Specification TGL 33 135/03 E 88:
 "Holzbau - Tragwerke; Gütebedingungen für Bauschnittholz"
 (Timber construction - Loadbearing structures; Quality specifications for sawn structural timber)
 Draft, March 1988.
- /5/ R. Apitz:
 "Ermittlung von Festigkeitskennwerten für Vollholz bei der Beanspruchung Biegung durch Versuche"
 (Determination of strength characteristics for solid timber subjected to bending stress by tests)
 Wismar Engineering College; Progress report dated 1982-11-27.
- /6/ B. John:
 "Statistische Verfahren für technische Meßreihen"
 (Statistical methods for technical series of measurements)
 Published by: Carl Hauser Verlag, Munich/Vienna, 1979.
- /7/ F. Colling:
 "Einfluß des Volumens und der Spannungsverteilung auf die Festigkeit eines Rechteckträgers"
 (Influence of the volume and of the stress distribution on the strength of a rectangular girder)
 Published in: Holz als Roh- und Werkstoff, No. 44 (1986) 4, pp. 121 - 125; and No. 44 (1986) 5, pp. 179 - 183.
- /8/ Eurocode 5:
 "Holzbauwerke" (Timber Structures)
 Deutsche Entwurfsfassung (German draft wording)
 October 1987

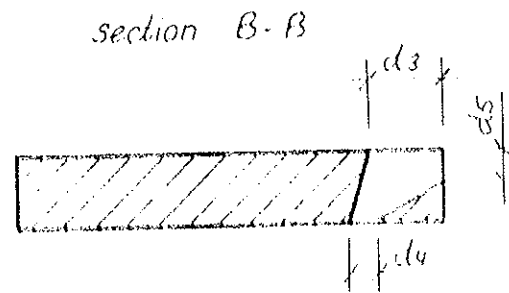
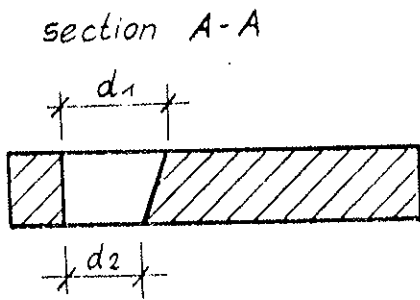
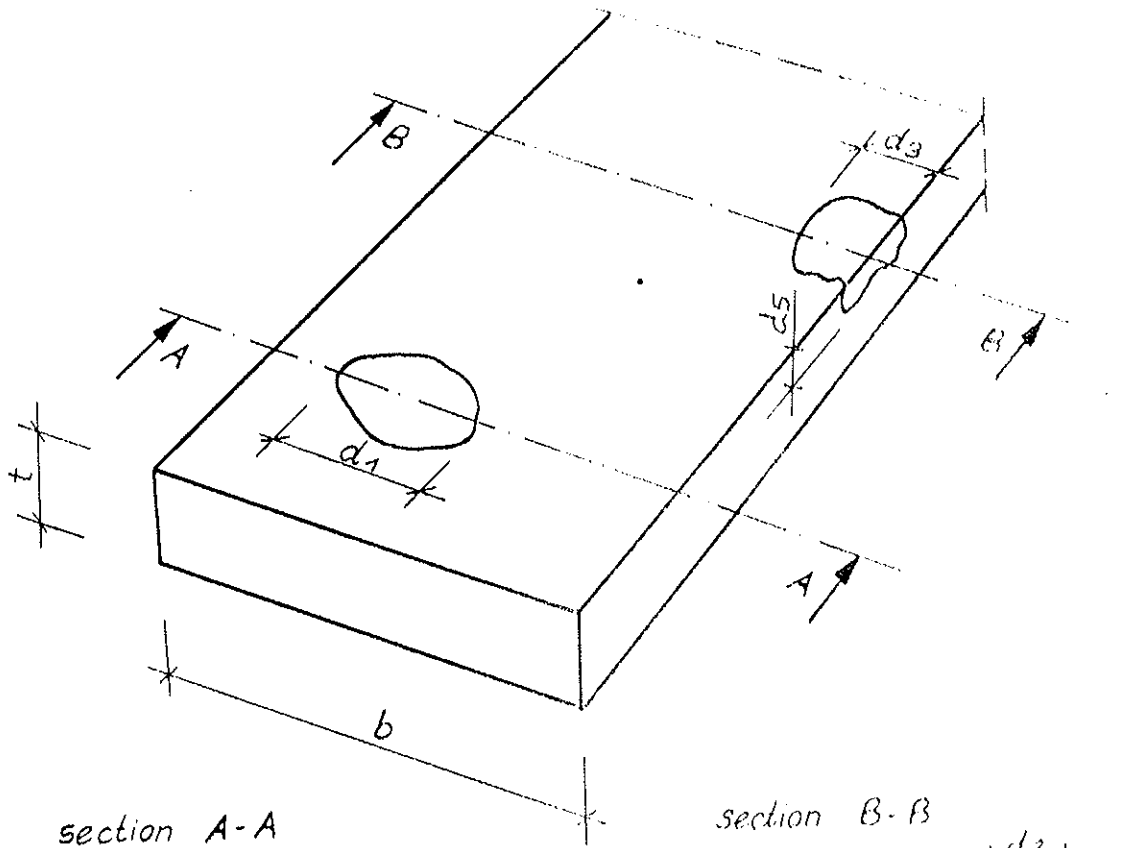


grade		BSH 0	BSH M3
sorting of the layers		visually	mechanically
external layers	kind of timber	NSH GK II	NSH F III
	KZV (mm)	≥ 250	≥ 250
internal layers	kind of timber	NSH GK II	NSH I III
	KZV (mm)	≥ 0	≥ 0

Meanings:

- BSH = glued laminated timber
- NSH = sawn coniferous timber
- KZV = Key-dovetail connection ("finger joint") staggering
- GK = quality class
- F = strength class

Figure 1: Grades of glued laminated timber

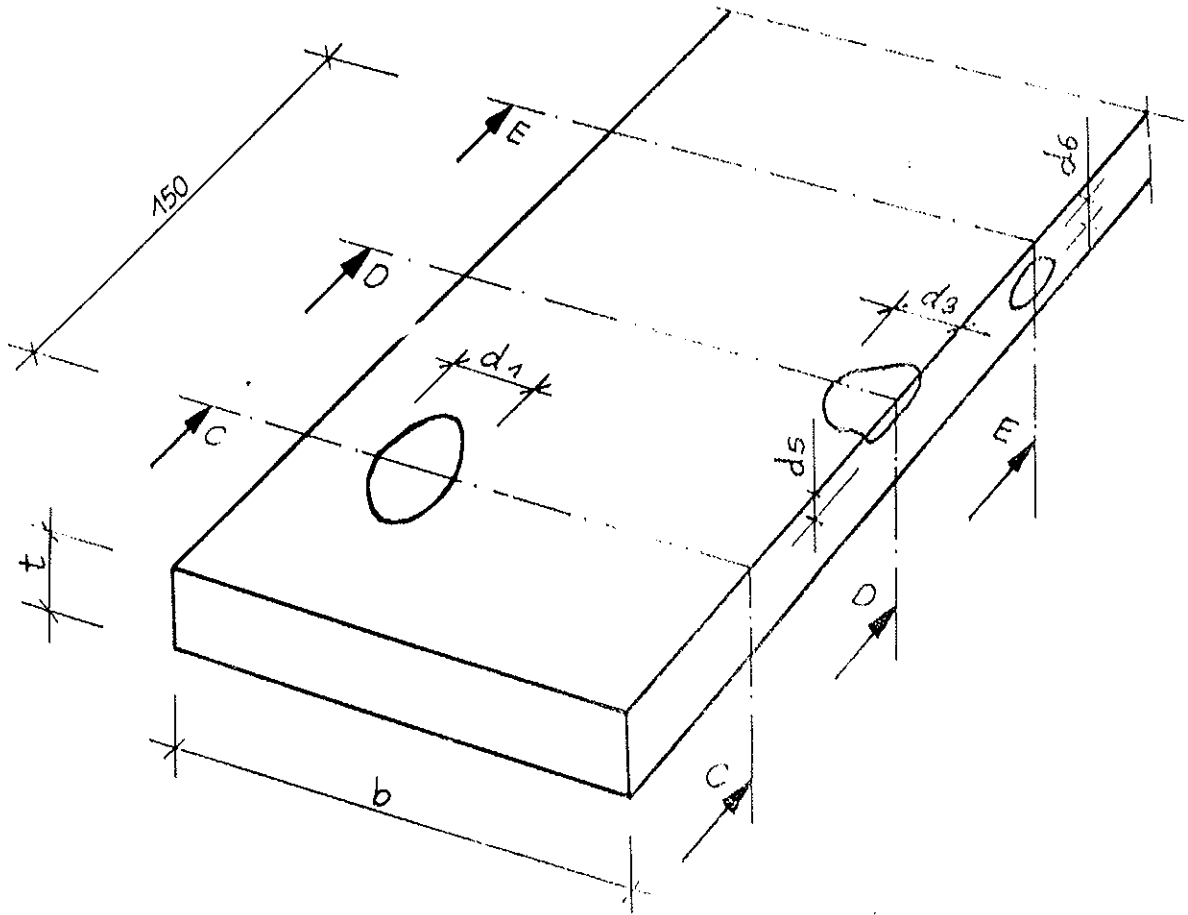


$$k = \frac{d_1 + d_2}{2b}$$

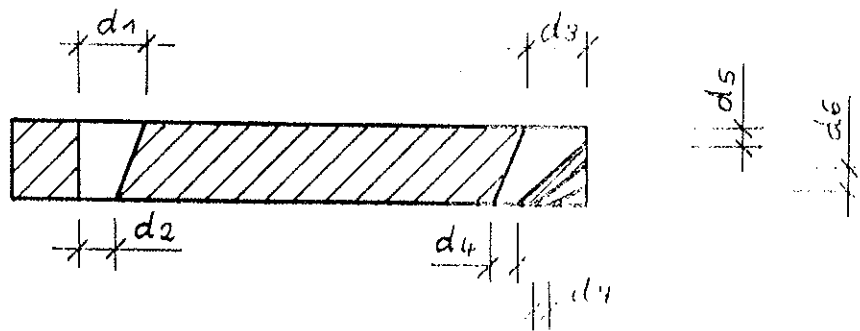
$$\frac{d_3 + d_4 + d_5}{2b}$$

	quality class	strength class
$\leq \frac{1}{3}$	GK II	F II
$\leq \frac{1}{2}$	GK III	F III

Figure 2: Sorting by individual knots



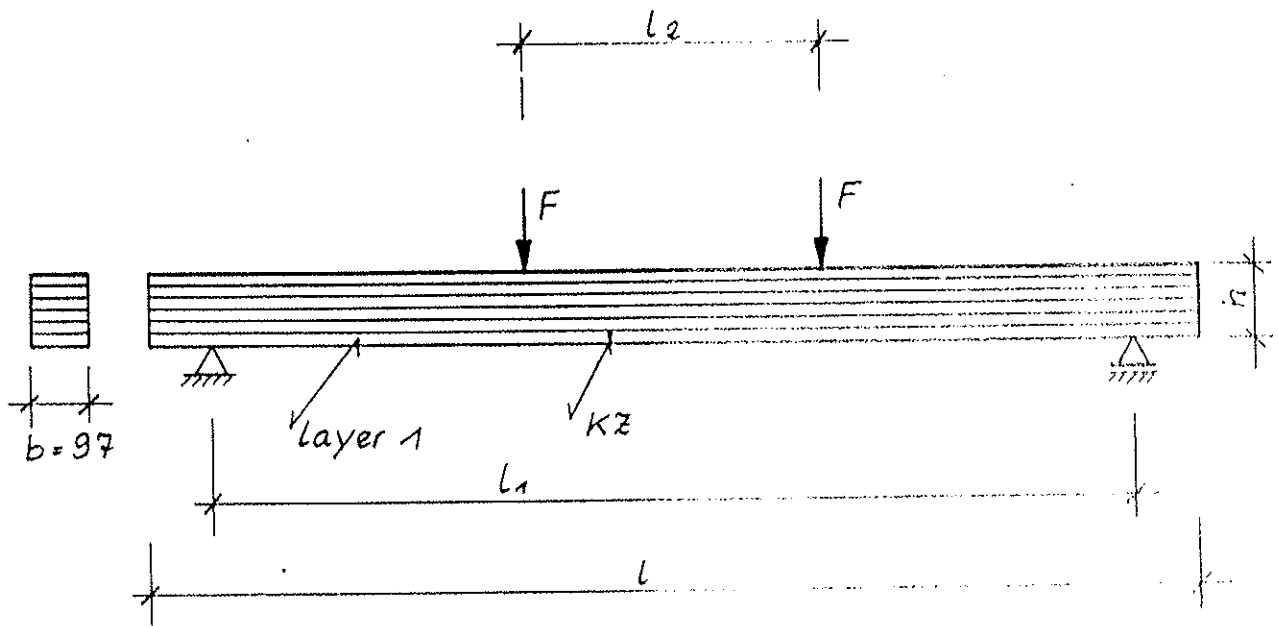
sections C-C, D-D, E-E in one sectional drawing



$$K = \frac{d_1 + d_2 + d_3 + d_4 + d_5 + d_6 + d_7}{2b}$$

K	quality class	strength class
$\leq \frac{1}{2}$	GK II	F II
$\leq \frac{2}{3}$	GK III	F III

Figure 3: Sorting by accumulations of knots



Meanings:

h = test specimen height

l = test specimen length

l_1 = effective span, $l_1 = 1.5h$

l_2 = test zone length, $l_2 = 4h$

KZ = Key - dovetailing ("finger joint"),
always located within the test zone l_2 ,
layer 1

Figure 4: Test arrangement

Test No.	h mm	L ₀ mm	L ₂ mm	n	E _{m, mean} $\frac{N}{mm^2}$	f _{m, mean} $\frac{N}{mm^2}$	S $\frac{N}{mm^2}$	K	f _{m, K} $\frac{N}{mm^2}$	tensile failure within the test zone L ₂ , failure type:
1	288	4320	1152	5	11830	38,0	1,93	2,26	33,6	KDC ("finger joint")
2				28	11214	45,0	5,73	1,645	35,6	Knot or timber
3	608	9120	2432	F	12014	36,0	4,12	2,13	27,2	KDC ("finger joint")
4				5	11200	36,6	4,51	2,26	26,4	Knot or timber
5	800	12000	3200	8	13663	37,4	6,26	2,09	24,3	KDC ("finger joint")
6				3	13267	38,7	3,06	2,61	30,7	Knot or timber
7	992	14880	3968	5	13700	39,1	5,35	2,26	27,0	KDC ("finger joint")
8				5	12960	36,9	4,75	2,26	26,2	Knot or timber

b = 97 mm

Meanings:

n = number of test specimens

E_{m, mean} = mean value of the modulus of elasticity in bending

f_{m, mean} = mean value of the bending strength

S = standard deviation

K = factor of conversion from small to large random sample numbers

f_{m, K} = characteristic value of the bending strength (5% - quantile)

Figure 5: Test results of "Bsh 0" - type glued laminated timber girders subjected to bending

test No.	h mm	l ₁ mm	l ₂ mm	n	E_m, mean $\frac{N}{\text{mm}^2}$	f_m, mean $\frac{N}{\text{mm}^2}$	s $\frac{N}{\text{mm}^2}$	K	$f_{m,k}$ $\frac{N}{\text{mm}^2}$	tensile failure within the test zone l ₂ , failure type :
1	192	2880	768	12	10 909	33,3	5,27	1,99	22,8	KDC ("finger joint")
2	*			12	11 683	42,3	10,8	1,99	20,8	Knot or timber
3	288	4320	1152	7	12 447	37,1	5,52	2,13	25,3	KDC ("finger joint")
4				5	12 070	37,4	8,06	2,26	19,2	Knot or timber
5	608	9120	2432	10	12 851	35,8	5,59	2,03	24,5	KDC ("finger joint")
6				-	-	-	-	-	-	Knot or timber

b = 97 mm

h = test specimen height

l₁ = effective span

l₂ = test zone length

n = number of test specimens

E_m, mean = mean value of the modulus of elasticity in bending

f_m, mean = mean value of the bending strength

s = standard deviation

K = factor of conversion from small to large random sample numbers

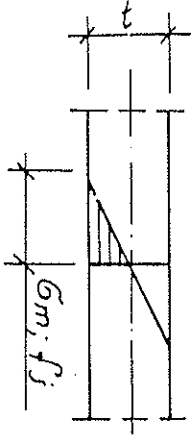
$f_{m,k}$ = characteristic value of the bending strength (5% - quantile)

Figure 6 : Test results of "BSH M 3" - type glued laminated timber girders subjected to bending

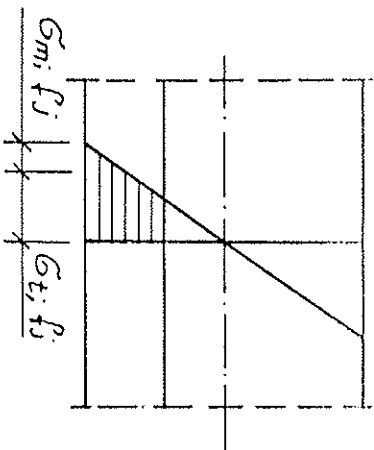
c) quasi-tension within the KDC

a) pure bending within the KDC ("finger joint")

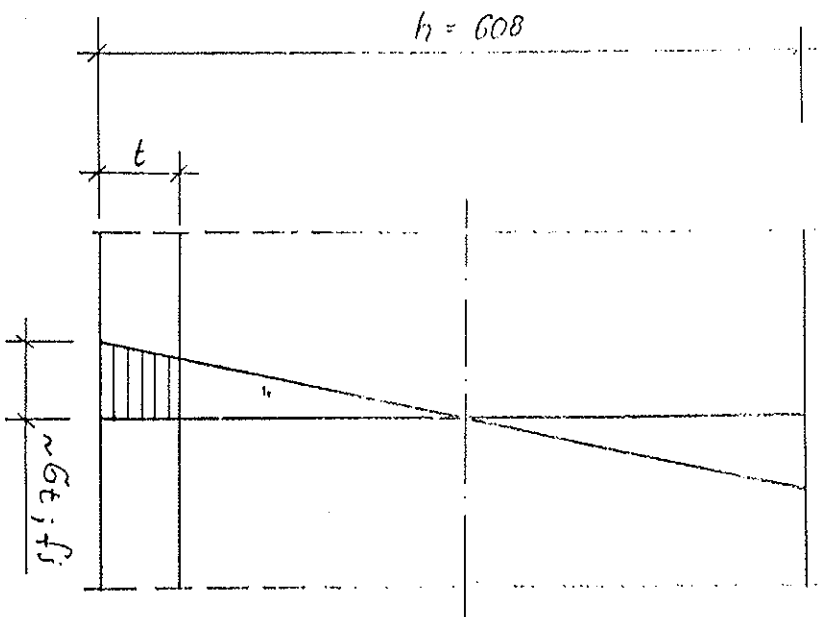
b) bending and tension within the KDC



$$\sigma_m; f_s = f_{mk}; f_s$$



$$f_{t,0,k}; f_s < \sigma_m; f_s + \sigma_t; f_s < f_{mk}; f_s$$



$$\sigma_t; f_s = f_{t,0,k}; f_s$$

Meanings:

$\sigma_m; f_s$ = stress within the KDC
 $f_k; f_s$ = characteristic strength of the KDC (5% - quantile)
 KDC = key-dovetail connection ("finger joint")

Figure 7: Stressing of the key-dovetail connection ("finger joint") with increasing depth of a quasi-laminated timber girder

i	h	l_1	l_2	$V_i = b \cdot h \cdot l_1$	n	$f_{m,mean}$	$K_h, exp.$	failure type	λ_L	$\frac{\lambda_{L,1}}{\lambda_{L,i}}$	$\frac{V_i}{V_1}$	$\frac{h_i}{h_1}$	$K_h, theor.$
	mm	mm	mm	m^3	-	$\frac{N}{mm^2}$	-		-	-	-	-	(3)
1	288	4320	1152	0,121	5 28	38,0 45,0	1 1	A B	- 2,38	- 1	1	1	- 1
2	608	6080	2432	0,359	1 4	40 44,1	1,053 0,98	A B	- 2,61	- 0,912	2,97	2,11	- 0,796
3	608	9120	2432	0,538	3 3	33,2 34,0	0,874 0,756	A B	- 2,61	- 0,912	4,45	2,11	- 0,757
4	608	12160	2432	0,717	4 2	38,1 40,5	1,003 0,9	A B	- 2,61	- 0,912	5,93	2,11	- 0,730
5	800	8000	3200	0,621	6	37,5 -	0,987 -	A B	- 2,70	- 0,881	5,19	2,78	- 0,718
6	800	12000	3200	0,931	4 1	33,8 36	0,889 0,8	A B	- 2,70	- 0,881	7,69	2,78	- 0,683
7	800	16000	3200	1,242	4 2	41,0 40,0	1,079 0,889	A B	- 2,70	- 0,881	10,26	2,78	- 0,659
8	929	9290	3716	0,837	6	36,0 -	0,947 -	A B	- 2,75	- 0,865	6,92	3,23	- 0,679
9	992	14880	3968	1,432	3 3	40,2 38,7	1,058 0,86	A B	- 2,78	- 0,856	11,83	3,44	- 0,629
10	992	19840	3968	1,909	3 2	35,8 34,3	0,942 0,762	A B	- 2,78	- 0,856	15,78	3,44	- 0,606

$b = 97 \text{ mm}$

Figure 8: Mean value of the bending strength $f_{m,mean}$ and modification factor K_h of "BSH 0"-type glued laminated timber

$$K_{h,exp} = \frac{f_{m,mean,i}}{f_{m,mean,1}} \quad (1)$$

According to /7/, the result is

$$\lambda_L = \left[\frac{1}{m+1} \cdot (1 + L_2 m) \right]^{\frac{1}{m}}$$

m Weibull's exponent, depending on the variation coefficient of the corresponding type of stressing, $m = 8$

$$\lambda_L = \left[\frac{1}{9} \cdot (1 + 8 L_2) \right]^{0,125} \quad (2)$$

λ_L = solidity ratio in the direction of L_1

According to /7/, the result is

$$K_{h,theor.} = \frac{\lambda_{L,1}}{\lambda_{L,i}} \cdot \frac{\lambda_{h,1}}{\lambda_{h,i}} \left(\frac{V_1}{V_i} \right)^{\frac{1}{m}}$$

$$\lambda_h = \left(\frac{1}{m+1} \right)^{\frac{1}{m}}$$

λ_h solidity ratio in the direction of h

The result for an equal m is $\lambda_{h,i} = \lambda_{h,1}$

and thus

$$K_{h,theor.} = \frac{\lambda_{L,1}}{\lambda_{L,i}} \cdot \left(\frac{V_i}{V_1} \right)^{-\frac{1}{m}}$$

With $m = 8$, the result is

$$K_{h,theor.} = \frac{\lambda_{L,1}}{\lambda_{L,i}} \left(\frac{V_i}{V_1} \right)^{-0,125} \quad (3)$$

Figure 9: Calculation of $K_{h,exp}$ and $K_{h,theor.}$

failure type A

$$K_h = 0,9863 \cdot \left(\frac{V}{0,121} \right)^{-0,0031} ; V \text{ in } m^3 \quad (4)$$

$$r = 0,034$$

$$K_h = 0,9899 \left(\frac{h}{288} \right)^{-0,0033} ; h \text{ in mm} \quad (5)$$

$$r = 0,048$$

$$K_h = 0,9764 e^{0,00065} \left(\frac{V}{0,121} \right) \quad (6)$$

$$r = 0,040$$

$$K_h = 0,9868 e^{-0,0023} \left(\frac{h}{288} \right) \quad (7)$$

$$r = 0,024$$

failure type B

$$K_h = 0,993 \cdot \left(\frac{V}{0,121} \right)^{-0,0796} ; V \text{ in } m^3 \quad (8)$$

$$r = 0,664$$

$$K_h = 0,996 \left(\frac{h}{288} \right)^{-0,1677} ; h \text{ in mm} \quad (9)$$

$$r = 0,628$$

$$K_h = 0,9512 e^{-0,0128} \left(\frac{V}{0,121} \right) \quad (10)$$

$$r = 0,593$$

$$K_h = 1,052 \cdot e^{-0,0796} \left(\frac{h}{288} \right) \quad (11)$$

$$r = 0,608$$

Figure 10: Regression analysis for "BSH 0" - type glued laminated timber

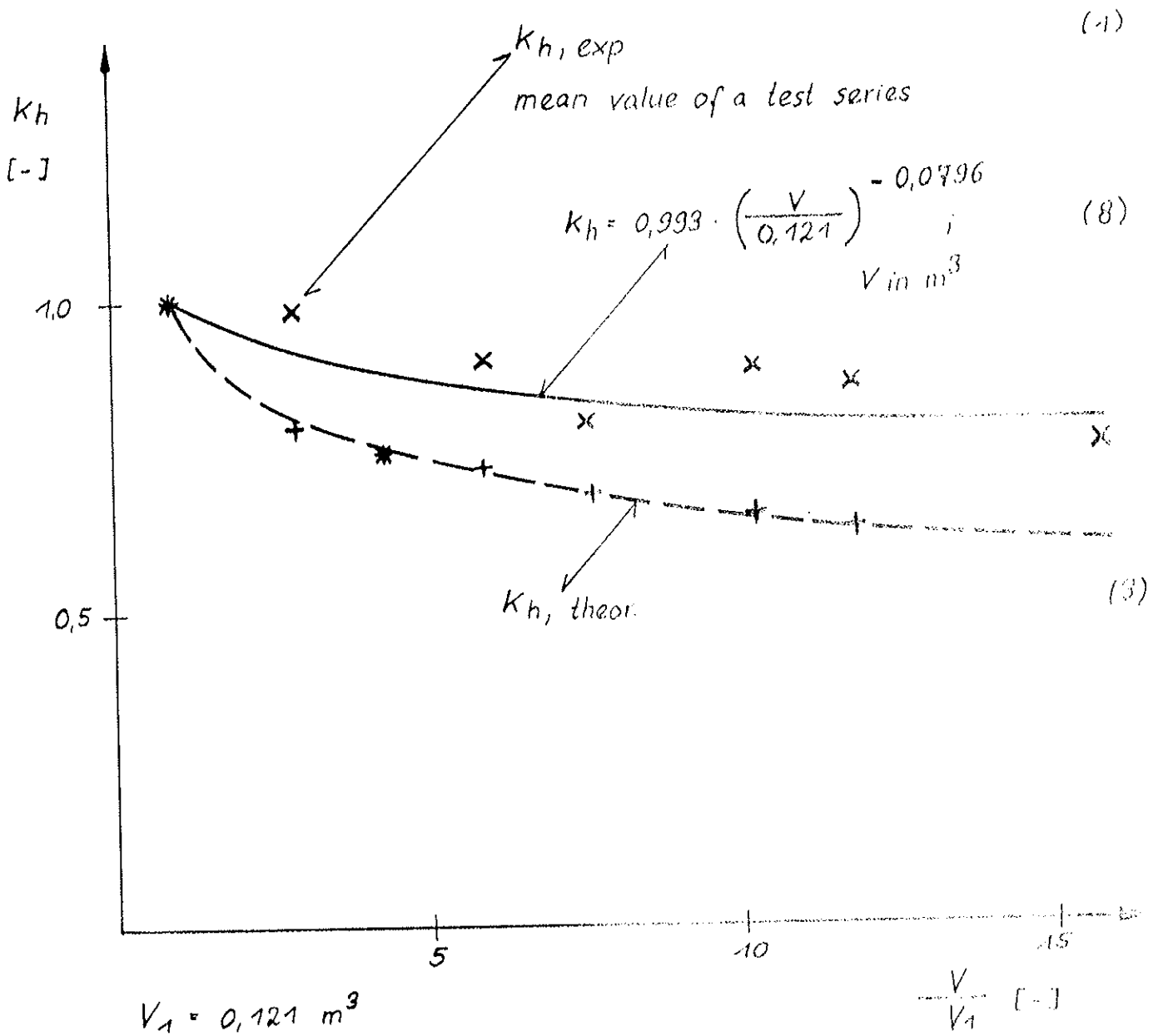
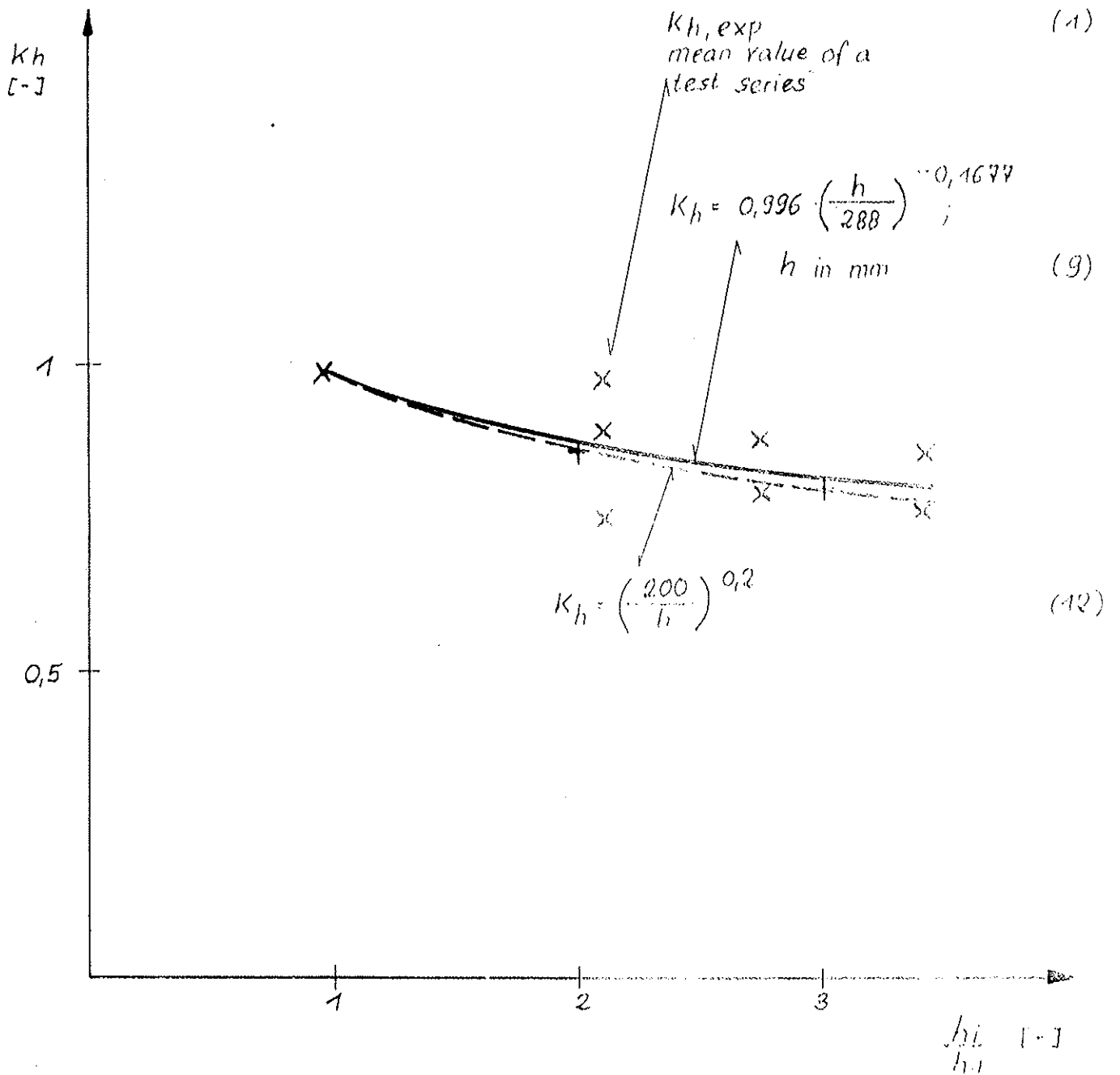


Figure 11: Modification factor K_h , subject to the volume ratio for failure type B (BSH 0)



$h_1 = 288$ mm with (1) and (9)

$h_1 = 200$ mm with (12)

Figure 12: Modification factor k_h subject to the cross-sectional height for failure type B3 (BSH 0)

INTERNATIONAL COUNCIL FOR BUILDING RESEARCH STUDIES AND DOCUMENTATION
WORKING COMMISSION W18A - TIMBER STRUCTURES

ACID DETERIORATION OF GLULAM BEAMS IN BUILDINGS
FROM THE EARLY HALF OF THE 1960s

Preliminary summary of the research project
Overhead pictures

by

B A Hedlund
Swedish National Testing Institute
Sweden

MEETING TWENTY - TWO
BERLIN
GERMAN DEMOCRATIC REPUBLIC
SEPTEMBER 1989

SUMMARY

The collapse of a gymnasium built with steel reinforced glulam beams with cold setting phenol-formaldehyde resin in 1988 raised the question of the safety of other buildings with phenol resin beams. A project was initiated to locate such buildings and determine their present and future safety.

The work was performed at Building Technology at the Swedish National Testing Institute, in cooperation with the Swedish Institute for Wood Technology Research in Stockholm and Luleå Technical University.

The project was financed by The National Testing Institute and the Swedish Council for Building Research.

This paper summarizes the preliminary results of the project. The final results will be published in the form of a technical report from the Swedish National Testing Institute.

During the project a total of 33 buildings have either been inspected or samples been analysed in order to determine the condition of the beams.

Laboratory tests on resin of the same formula as the resin used in the suspected buildings were used to study the damage process. Samples from inspected buildings were used to determine the type and amount of acid hardener in the beams.

The result of the project indicates that a majority of the buildings in Sweden that are built with phenol resin beams have extensive damage in the gullelines.

The results indicate that the damage is caused by fibre damage on the wood close to the gulleline. In several cases the fibre damage was made worse by a poor original gulleline quality, possibly in combination with a higher acid content in the resin than recommended.

A fast method of detecting phenol resin in glulam beams with energy dispersive X-ray analysis was developed.

The project has not given sufficient data to make it possible to determine the life expectancy of phenol resin beams.

BACKGROUND

Cold setting phenol-formaldehyde resin was introduced in Sweden after the second world war, but it was not until the end of the 1950s that the resin was used for wood structure purposes to any larger extent. In 1965 two buildings with cold setting phenol-formaldehyde resin in steel reinforced glulam beams collapsed. After these collapses and after the risk of fibre damage from the acid hardener of the glue had been realized, the use of the resin type in glulam was stopped.

The investigations into the two collapsed buildings indicated that the reason for the collapses was very poor craftsmanship in the part of the manufacturer, possibly in combination with fibre damage from the acid hardener of the resin.

This resulted in an investigation, in 1966, of buildings delivered by the manufacturer, revealing poor glulam beams in 25 out of 42 inspected buildings. The manufacturer went into liquidation. After 1966 no major cases of damaged glulam beams of this kind were reported until the late 1980s.

Due to the sudden collapse of a school gymnasium in February 1988 attention was again drawn to buildings with cold setting phenol-formaldehyde resin in glulam beams.

A project to investigate the problems concerning buildings with cold setting phenol-formaldehyde resin in glulam beams was initiated by the Swedish National Testing Institute (SP) and the National Board of Physical Planning and Building. The project was financed by SP and The Swedish Council for Building Research.

AIM AND SCOPE

The project had two main aims; to find the buildings with cold setting phenol-formaldehyde resin and to establish methods to determine the present and future safety of these buildings. This included:

- localizing the suspected buildings
- determining the present condition of the buildings
- determining whether the beams contain phenol resin or not
- determining whether the damage is caused by acid attack or by some other factor
- finding out the circumstances under which damage occur and the factors that influence the process
- establishing whether the glue contained the right amount and type of acid when the beams were produced
- establishing a method to determine the life expectancy of the buildings.

THEORETICAL BACKGROUND

Fibre damage

Fibre damage in wood glued with cold setting phenol-formaldehyde resin is caused by a hydrolyzation of the cellulose molecule. The hydrolysis breaks up the molecules into short segments, which greatly reduces the strength of the wood fibres close to the resin. The glueline strength is greatly reduced and the glueline can be broken up either by external load on the beam or by internal stresses caused by shrinking and swelling.

Fibre damage will in the following mean the loss of strength of the glueline rather than the actual hydrolyzation of the cellulose molecule.

Effect of the acid hardener

Cold setting phenol-resin is hardened at a low pH-value. The acid hardener is used to lower the pH-value of the resin in order to start the reaction, but it is not consumed in the chemical process. When the resin has hardened, the acid is still more or less free in the resin [1]. The free acid in the resin acts as a catalyst for the hydrolyzation of the wood close to the glueline.

Factors influencing the damage process

The acid content of the resin influences both the initial quality of the glueline and the hydrolyzation process. A higher acid content lowers the pH-value of the resin. A lower pH-value makes the hardening more rapid and can lead to a higher degree of cure. Rapid hardening makes the risk of prehardening higher. A higher degree of cure makes the glue more brittle. A higher acid content makes the concentration of acid in contact with the wood higher, and thus the hydrolyzation process is accelerated.

The glueline thickness affects both the initial glueline strength and the damage process. Shrinking of the resin during hardening can lead to stresses within the joint. Higher concentrations of acid enhances the danger of fibre damages [2].

The hydrolyzation of the wood consumes water and thus the damage process is influenced by the moisture content of the wood. Water might also have an effect in the transport of acid out of the glue [1]. Changes in moisture content in the wood cause internal stresses due to shrinking and swelling, which can break up weakened gluelines.

Like all chemical processes, the hydrolyzation of the wood is accelerated by higher temperatures.

LOCALIZATION AND INSPECTION

Inventory

An inventory made during the inspections in 1966 revealed 128 objects with beams sold by one (now liquidated) manufacturer [3]. The 1966 inventory list was used as the basis for an inquiry from the National Board of Physical Planning and Building to the local housing committees of the municipalities about buildings suspected to have phenol resin beams.

As a result of the inquiry, and through the aid of current manufacturers of glulam beams in Sweden, the 1966 inventory was updated.

One building containing phenol resin beams in the study was investigated as a result of damage observed in 1987.

Inspections and sample collection

Inspections have been carried out on 17 objects with a total of 27 buildings.

In addition to the inspection of buildings, samples have been collected from an additional 6 objects with 6 buildings by other organisations for analysis at SP.

Method of inspection

The beams were inspected visually. Visual flaws such as cracks in the gluelines, traces of water damage and biological attack were recorded. Special care was taken to localize repairs of earlier damage or attempts to hide improper fabrication of the beams.

The dimensions of the beams, lamellae and lamellae-joints were measured. Measured values were compared with data from constructional drawings, when available.

The depth of cracks in the gluelines was measured with a 0.1 mm feeler gauge. The length of the cracks were measured with measuring tape where possible. The end of a crack was defined as where it was no longer wide enough for the gauge or where it was too shallow to make the gauge hang by itself when stuck into the crack. The lengths of cracks which were out of reach were estimated visually.

Possible existence and position of steel reinforcement bars was determined with a metal detector. Moisture content was measured with an electric moisture meter. Sagging of the beams was measured with a tensioned string.

A cross mouthed chisel was used to take samples from the gluelines for analysis at the laboratory of SP.

The glulam beams of one of the buildings inspected had been investigated in 1966, during which a map of open gluelines had been made. When the building was inspected again in 1988 a new map was made. The two mappings made it possible to study the growth of glueline damage during the period 1966-1988.

Determining the condition of the buildings

The present condition of the buildings was judged from the result of the inspection and from laboratory analyses of samples from the beams. The judgement was based on the following factors:

- size and location of cracks in the gluelines
- results from laboratory analyses of glueline samples
- location and estimated quality of lamellae joints
- calculation of stresses in the beams according to modern practice.

Results of inspections and sample analysis

General condition of the buildings

Of the 27 buildings inspected, 20 had visual damage in phenol resin gluelines, 2 had seemingly intact phenol gluelines and 5 did not contain phenol resin in the beams.

The samples that were sent in to SP by other organisations from 6 buildings revealed damaged phenol resin gluelines in one building, while the other 5 did not contained phenol resin. The results of the inspections and the analysis of the samples are summarized in table 1.

Table 1. Results of inspections and sample analysis.

	Beams with visual damage in gluelines	Beams without visual damage in gluelines
Phenol-formaldehyde resin	21 buildings	2 buildings
Other resins	1 building	9 buildings

Of the 21 buildings with damaged phenol resin gluelines, two were being rebuilt, two had permanent bracings and 15 were judged to be in need of repair.

14 of the 15 buildings in need of repair were judged to be in danger of collapsing if snowloads reach the code values.

Old and new damage

The damage in the gluelines could in four cases be shown to be of different age. Some gluelines had been open when the beams were delivered from the factory while others were of a later date.

Plastic wood in the gluelines showed that some gluelines had been open when the beams were delivered from the factory. Traces of water running across wide cracks, cracked paint and repairs of known date showed that the damage had occurred after the erection of the building.

Comparison of the maps of cracks in one building revealed a dramatic increase in damage between 1966 and 1988, see Figures 1 and 2.

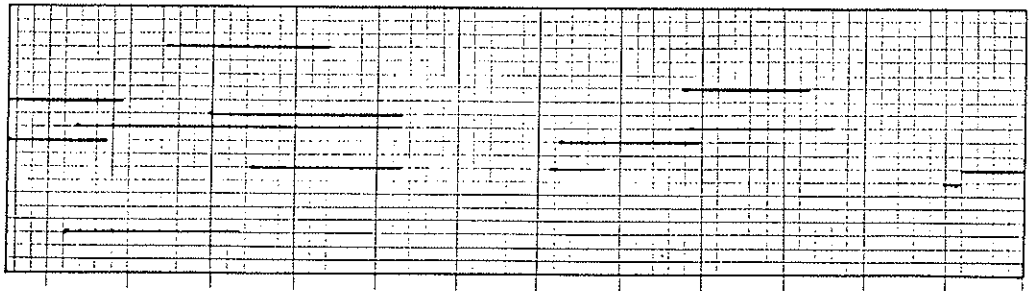


Figure 1. Cracks in gluelines, mapped 1966.

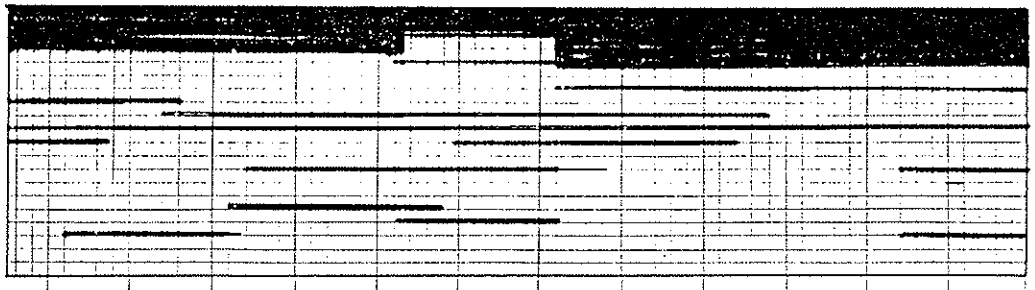


Figure 2. Cracks in gluelines, mapped 1988. The top of the beam has been covered with insulation.

Climatic influence

It could be expected that the location of visible damage would be influenced by climatic factors. Information exists on the climatic conditions around the beams for 13 objects with phenol resin:

- 8 objects had serious damage and had been exposed to running water or high relative humidity.
- 2 objects had serious damage without having been exposed to water. Both of these had been exposed to high temperatures during long periods.
- 3 objects did not show serious damage. None of these had been exposed to water or heat.

The results confirm that the climate has a strong influence on the damage process.

Fibre damage test

Fibre damage tests according to the principles of DIN 68 141 were conducted on spruce (*picea abies*) testpieces glued with cold setting phenol-formaldehyde resin and resorcinol-phenol resin.

Resin mixtures

The cold setting phenol-formaldehyde resin was of the same formulae as the glue that had been used by the manufacturers in Sweden when the damaged beams were produced. The resin was produced specially for this project by Casco-Nobel AB. Test assemblies were glued with varying amounts of hardener, see Table 1. A cold setting resorcinol-phenol resin was used to glue reference assemblies.

Table 1. Mixing ratios of phenol resin.

phenol-formaldehyde resin (parts by weight)	60 % para-toluene sulphonic acid (parts by weight)
100	12
100	10
100	9
100	8
100	7
100	6.2
100	5

Four test assemblies were bonded for each glue mixture, two with thin gluelines and two with thick gluelines. The thin gluelines were bonded with a gluespread of 300 g/m². The thick gluelines were bonded with 0.6 mm veneer spacers. Six testpieces were made for each test assembly and each massive piece of board.

Aging of test pieces

The test pieces were divided into three groups. Each group consisted of five testpieces from each board, two with thin glueline, two with thick glueline and one solid test piece.

One of the groups of test pieces was stored in 20°C 65% RH and the other two were aged through a cyclic treatment in a climate chamber, 4 cycles and 8 cycles respectively. Each 48 h cycle consisted of 3 periods, see Table 2.

Table 2. Cyclic treatment of test pieces.

Period	Duration (hours)	Temperature (°C)	Relative humidity (%)
A	24	50	100
B	8	10	100
C	16	50	20

Tensile testing

The tensile strength perpendicularly to the glueline was determined at a crosshead speed of 2 mm per minute. See Figure 3. Maximum tension force was determined and tensile stress calculated.

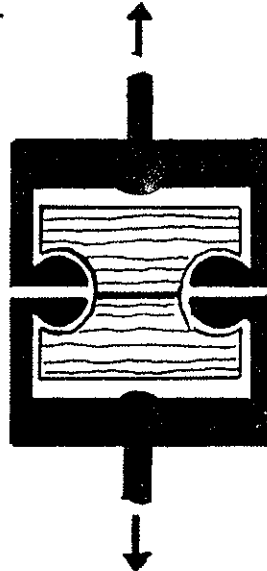


Figure 3. Tensile strength test according to ASTM D 143.

Correction for density

The density was calculated for each test piece. The tensile strength values were compensated for density by means of multiplication with a density factor: C_{density} .

$$(1) \quad C_{\text{density}} = \frac{\text{Average density of all bonded test pieces}}{\text{Density of test piece}}$$

$$(2) \quad \sigma_{\text{korr}} = C_{\text{density}} \times \sigma_{\text{test piece}}$$

Elimination of defective testpieces

Values from testpieces with knots, ring shake, missing glue and similar defects were sorted out.

Results of the fibre damage test

The fibre damage test on thin gluelines showed no particular reduction of the tensile strength after cyclic treatment.

The thick gluelines showed a reduction of tensile strength after cyclic treatment in relation to the uncycled testpieces for all concentrations of hardener. The loss of strength increased rapidly as the amount of hardener increased over the recommended amount of 6 parts hardener to 100 parts resin. Figure 4 show the tensile strength after 4 and 8 aging cycles compared to the tensile strength of uncycled testpieces.

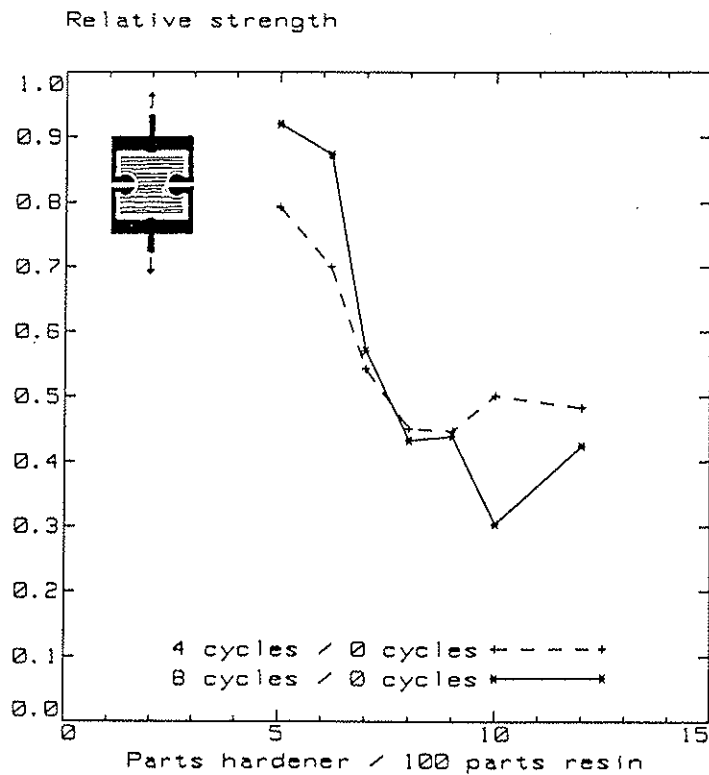


Figure 4. Relative tensile strength for thick phenol-formaldehyde resin gluelines after cycling. Average strength of cycled testpieces divided by average strength of uncycled pieces.

The resorcinol-phenol glue showed no loss of tensile strength after aging, see Figur 5.

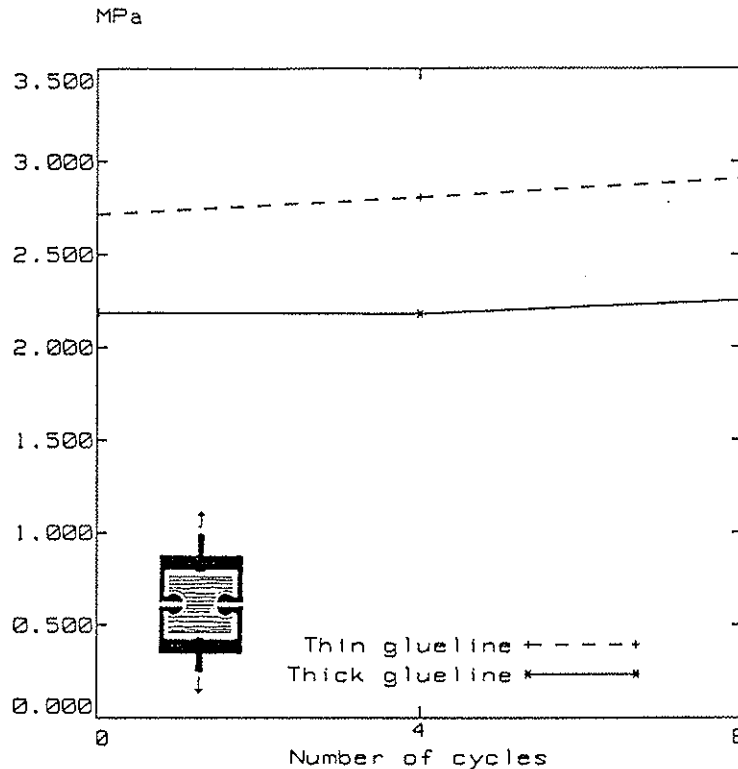


Figure 5. Average tensile strength of resorcinol-phenol gluelines, uncycled and cycled.

IR-analysis

Information from interviews stated that the manufacturer of the majority of the damaged beams might have used other acids than the recommended to harden the resin. Use of other types of acid could greatly affect the damage.

Analyses with infrared spectrophotometer were conducted on material extracted from samples of 3 objects to establish what kind of acid had been used as hardener. Two of the objects had beams with unknown acid hardeners while the third was known to have para-toluene sulphonic acid (PTSS) in the gluelines. The analysis showed that the samples had been hardened with para-toluene sulphonic acids.

XRF-analysis

The presence of large amounts of sulphur atoms in the gluelines was used to determine if the glue contained acid. The sulphur was detected by means of energy dispersive X-ray analysis (XRF).

Samples of gluelines were split and an XRF-analyser was used to determine the spectras of the glueline surface and the back surface of the sample. If the comparison of the two spectras showed high levels of sulphur in the glueline in comparison with the pure wood, then the glue contained acid. Figure 6 show the energy-spectras of a glueline with cold setting phenol resin. The method can be used on rough surfaces of varying shapes, and thus avoiding expensive preparation of the samples.

Split glue line - Test glue - Test wood

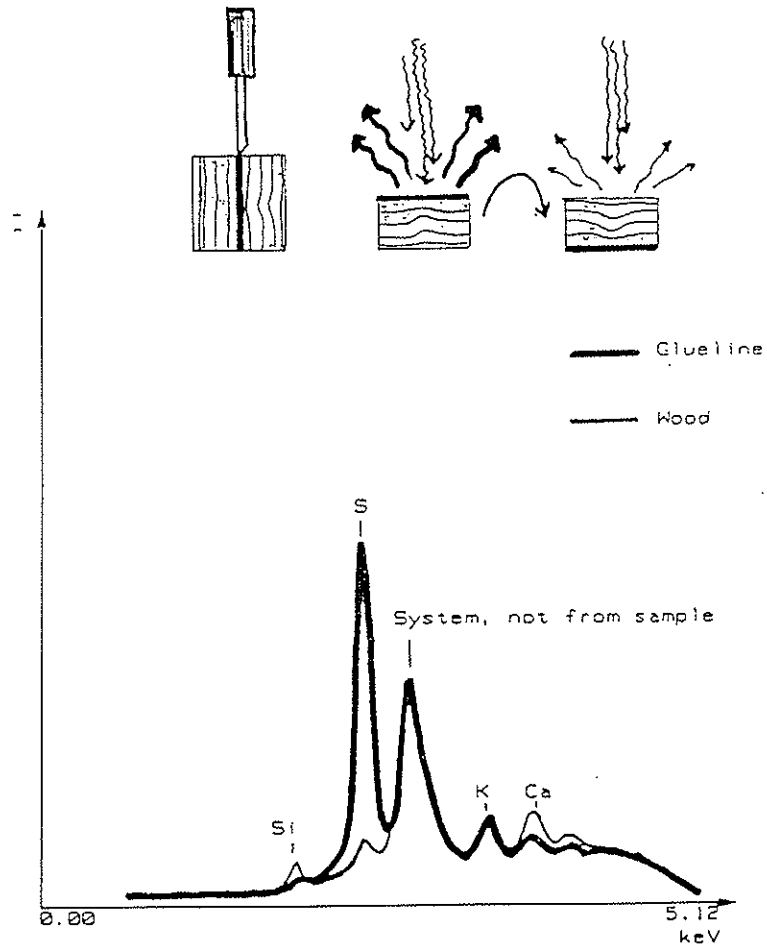


Figure 6. XRF-spectra of glue line with phenol resin.

SEM/EPMA-analysis

The distribution of acid across the glue lines was determined from the sulphur atoms with a scanning electron microscope equipped with a frequency dispersive X-ray spectrometer (SEM/EPMA). The analysis was carried out on samples from the fibre damage test and on samples from inspected buildings.

The results show a spread of sulphur out from the glue line during the cycling of the test pieces. Several testsamples show a relatively constant concentration of sulphur for a distance from the glue line and out rather than a rapid decline. This would indicate that the acid spreads into the wood faster than it is extracted from the resin. See Figure 7.

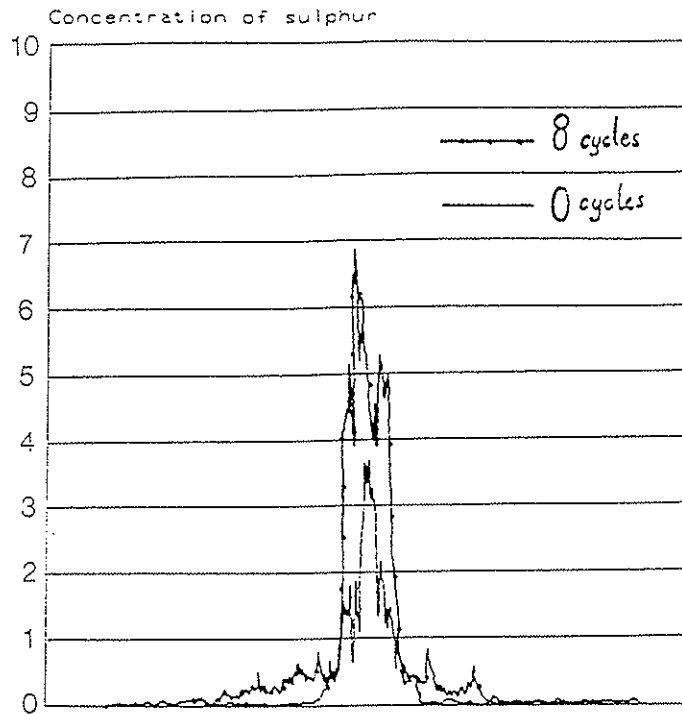


Figure 7. Acid distribution across a glueline before and after cyclic treatment. Acid content: 12 parts hardener to 100 parts resin. Thin glueline.

Analysis of field samples seems to indicate a connection between the amount of acid in the glueline and fibre damage. Samples from objects with severe damage tend to have a higher acid content than samples from objects with less damage, with some exceptions. See Figure 8.

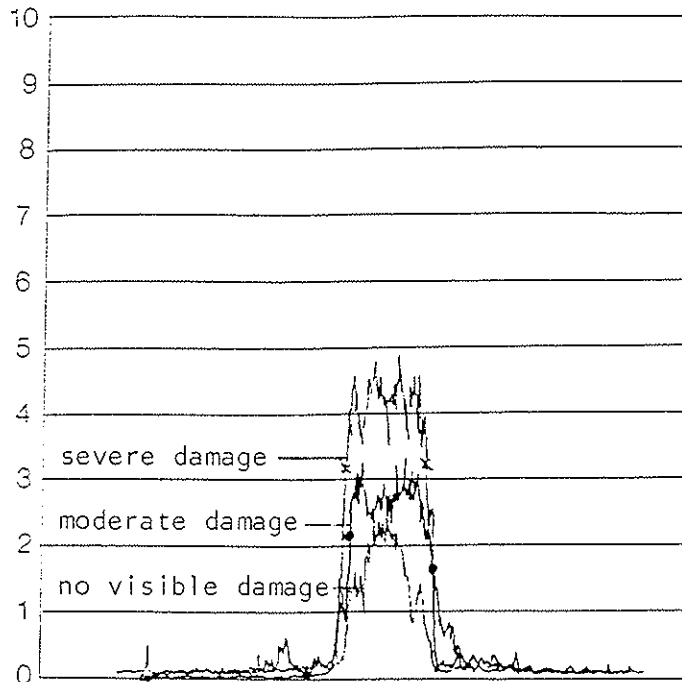


Figure 8. Acid distribution across gluelines of field samples. Samples from buildings with severe damage tend to have high acid content in the gluelines.

The scanning of gluelines gives a qualitative picture of the distribution of acid across the glueline, but it cannot give a quantitative measure of the amount of acid in the glueline. However, a rough estimate of the amount of acid in the field samples can be made by means of comparing the field samples with the laboratory samples with a known amount of acid. The comparison indicate that the amount of hardener has in several cases been higher than recommended.

CONCLUSIONS

The results indicate that the damage in the beams is caused by fibre damage from the acid hardener. In some cases the effect of the acid attack has been aggravated by a poor original quality of the gluelines.

Climate has a strong influence upon the damage process, and the process is accelerated by high moisture and temperature.

Gluelines with high acid concentration show greater damage, but damage also occurs in gluelines with low concentration of acid.

Cold setting phenolic glue can be detected by means of energy dispersive X-ray analysis.

More research is needed in order to establish a method of judging the life expectancy of phenol resin gluelines.

LITTERATURE

- [1] RAKNES, Eirik. Trälimning. Stockholm : Swedish Institute for Wood Research, 1988. p 45-47.
ISBN 91-970513-7-3
- [2] KOLLMAN, Franz, KUENZI, Edward, STAMM, Alfred. Principles of Wood Science and Technology. II: Wood Based Materials. Berlin : Springer-Verlag, 1975.
p. 57-66.
- [3] National Board of Physical Planning and Building. Circular. 1966, nr T 184 / 66. Stockolm.

INTERNATIONAL COUNCIL FOR BUILDING RESEARCH STUDIES AND DOCUMENTATION
WORKING COMMISSION W18A - TIMBER STRUCTURES

EXPERIMENTAL INVESTIGATION OF NORMAL STRESS DISTRIBUTION
IN GLUE LAMINATED WOODEN ARCHES

by

Z Mielczarek and W Chanaj
Szczecin Technical University
Poland

MEETING TWENTY - TWO
BERLIN
GERMAN DEMOCRATIC REPUBLIC
SEPTEMBER 1989

Prof. Zbigniew Mielosarek, D.Eng.

Wiesław Chanaj, D.Eng.

Szczecin Technical University

Experimental investigation of normal stress
distribution in glue laminated wooden arches.

1. Introduction

1.1. General informations

In Poland, during the period of the Second World War, there was great devastation of woods, forests and decreasing of standing timber as the result of war activities as well as too intensive exploitation of timber. That fact in turn had its influence on building trade profile in the period of after war restoration, what was based first of all on cement. Timber as a scarce material was regulated in distribution by state and it could be used only in constructions of small, rather temporary buildings, for example in elements of builder's yards. The result was that, during the several after war years, wooden constructions were used in the very limited range in our country.

Only about 20 years ago, Ministry of Building Industry started to act in the direction of enlarging the range of the usage of wood and wood derived materials in building trade. As the result of the activity a number of research works in this field was carried on and a factory of great size glued constructions as well as some number of houses factories were arranged.

1.2. Purpose of the paper

According to Polish building law new constructions introduced in building trade should be first tested and they should have certificates issued by proper Research Institutes.

Through the glued wooden construction are very popular abroad but in Poland we started the task from testing and manufacturing the stright shaped elements.

The research works were aimed not only on designating the limitary archs load capacity but recognition of their bearing under different loads especially regarding the character and distribution of normal stresses as well as the kind and size of strains or eventual distartions.

To eliminate the influence of the research work "scale" it was planned to carry on the research works in natural conditions.

1.3. The research works programme.

For carrying on the researches, 4 arch with span 18.0m and constant section 120 x 496 mm, consisting of 16 layers - 31 mm boards, were prepared. The archs used for carrying on the research works were manufactured by The State Enterprise for Great Size Wooden Construction Production at Cierpice near Toruń.

For gluing the board layers, they used resorcinol glue.
Each arch was tested in five following load cycles:

cycle First /I/ 0-0.5 p^d - 0
where p^d = admissible standard load of the arch = 21 KN

Cycle Second /II/ included the three subcycles.

II A	0 - p^d - 0	in each subcycle measurements of
II B	0 - p^d - 0	linear strains and stresses every 0.25
II C	0 - p^d - 0	p^d were done.

Cycle Third /III/ 0- 0.5 p^d - 0

Cycle Four /IV/ included the three subcycles

IV A	0 - p^d - 0	in each subcycle measurements of
IV B	0 - p^d - 0	linear strains and stresses every
IV C	0 - p^d - 0	0.25 p^d were done

Cycle Fifth /V/ was the destructive cycle and in it the arch was given the characteristic load p^d and stayed under that load for 24 hours. Next the arch was loaded until it was damaged, during that time the measurements were done every 0.25 p^d . The arch Nos 1, 2, 3 were damaged under non-symmetrical load and arch No 4 under symmetrical load.

2. Experimental testing

2.1. Method of testing

The arch loading was made by means of the ropes system going through rolls and timbles as well as jacks used for the ropes tensioning. Scheme of the above mentioned installation is shown on Figure No.1

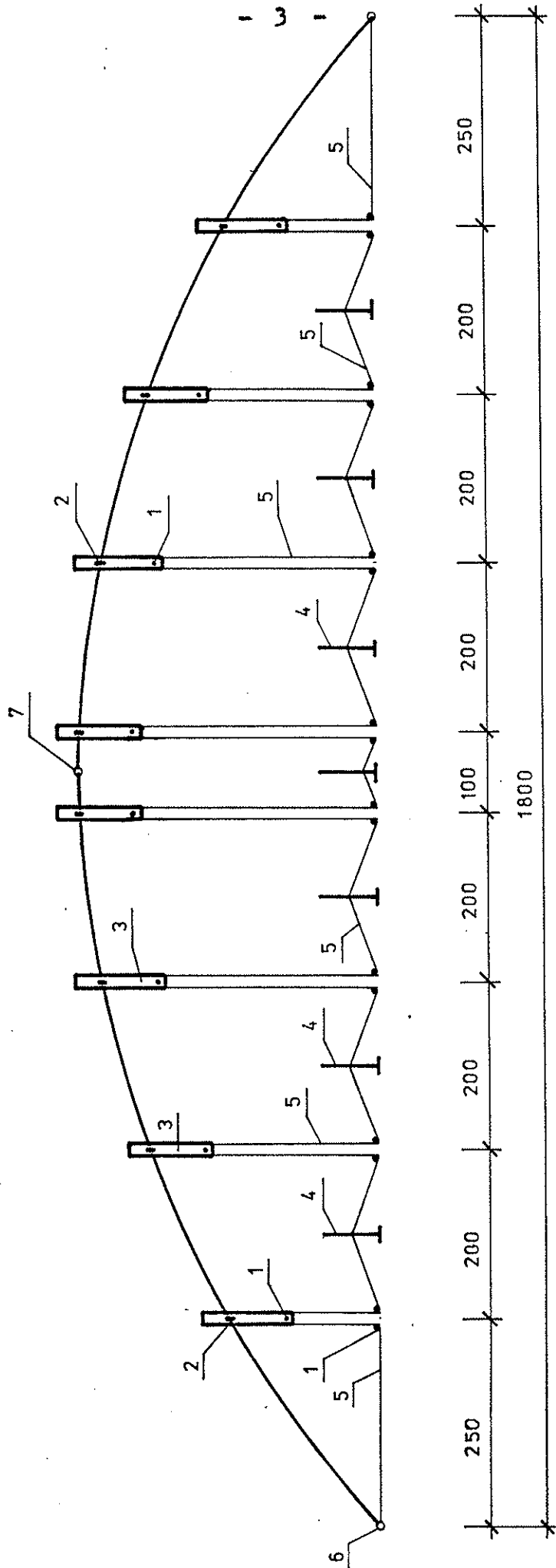


Fig.1. Scheme of installation for testing the arch load.

- 1 - rolls,
- 2 - dynamometer,
- 3 - thimble,
- 4 - jack,
- 5 - steel rope,
- 6 - support joint,
- 7 - ridge joint,

For measuring the value of load transferred on the archs we used electric resistance dynamometers which were designed and tested in our Institute. For measuring unitary linear extensions the strain gauge bridge TT4 as well as electric resistance sensors type RL 285/75 /k=2.15/ were used. Localization of sections, in which measurements were carried on is shown on Figure No.2

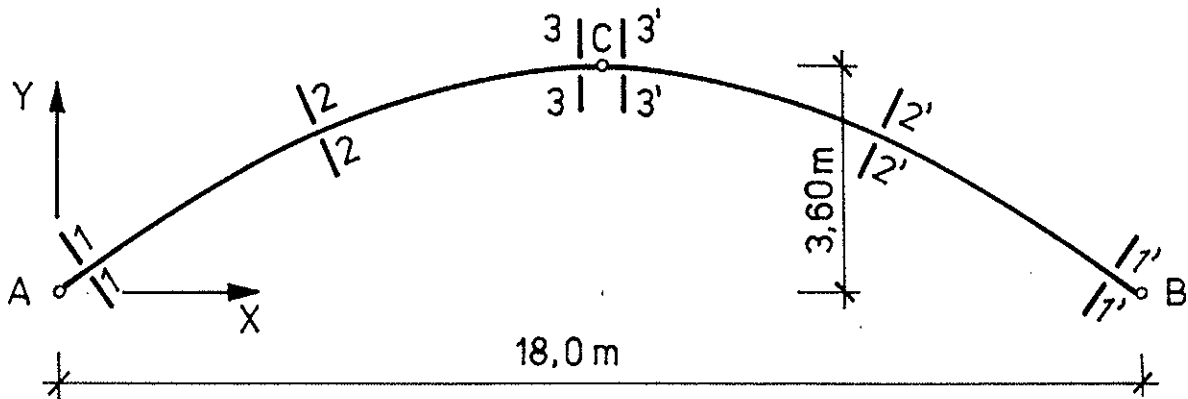


Fig.2. Scheme of section arrangement on the arch, where the unit linear strain were measured.

1-1	x = 0,425m	y = 0,332m
2-2	x = 4,285m	y = 2,610m
3-3	x = 8,660m	y = 3,595m
3'-3'	x = 9,340m	y = 3,595m
2'-2'	x = 13,715m	y = 2,610m
1'-1'	x = 17,575m	y = 0,332m

Arrangement of sensors in those section in the Arch No.1 is shown on Figure No.3 and the Arches No.2,3,4 are shown on Fig.4.

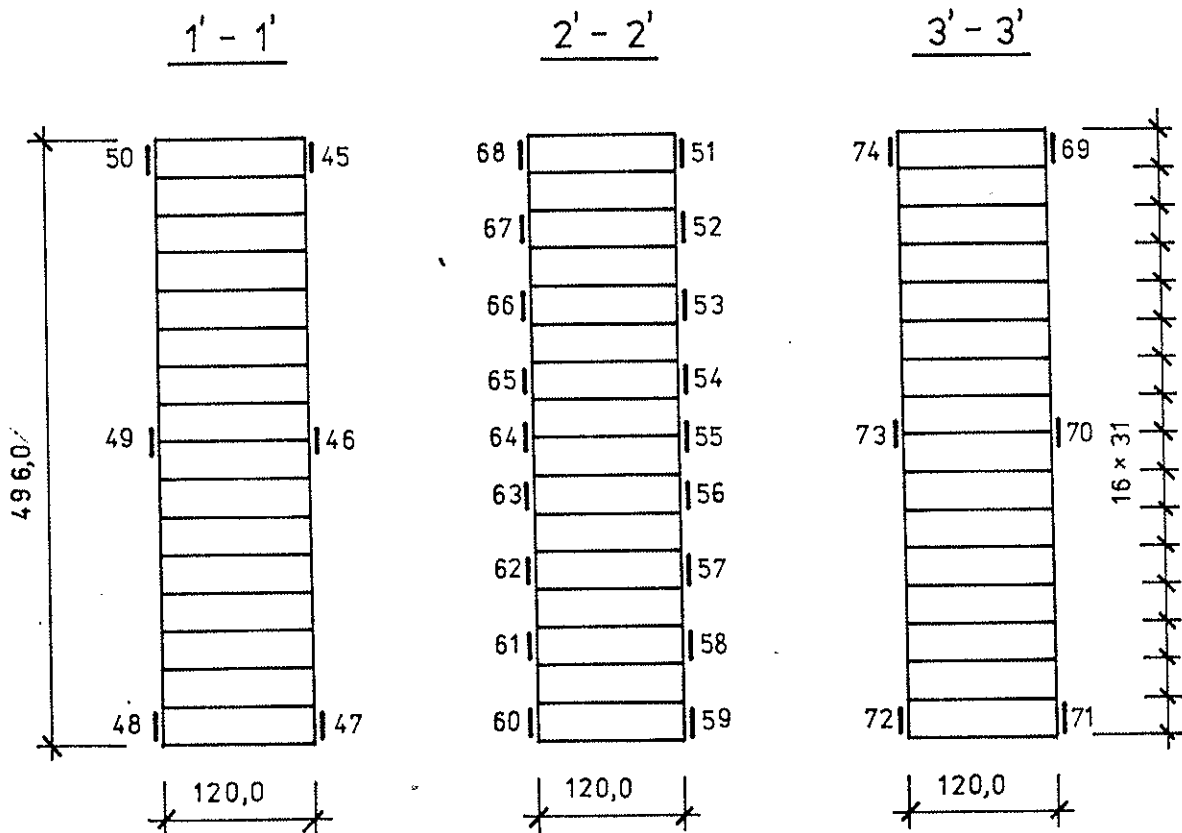
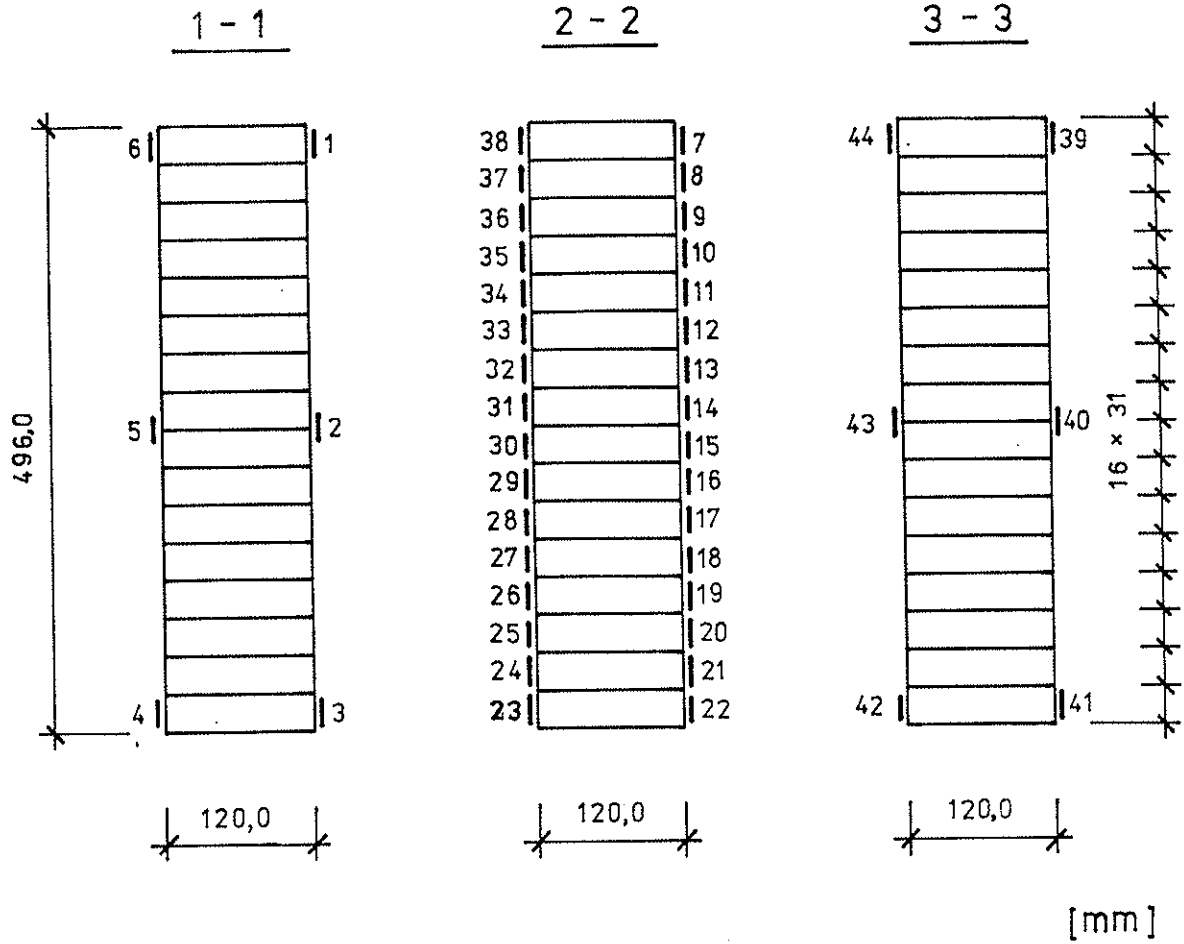
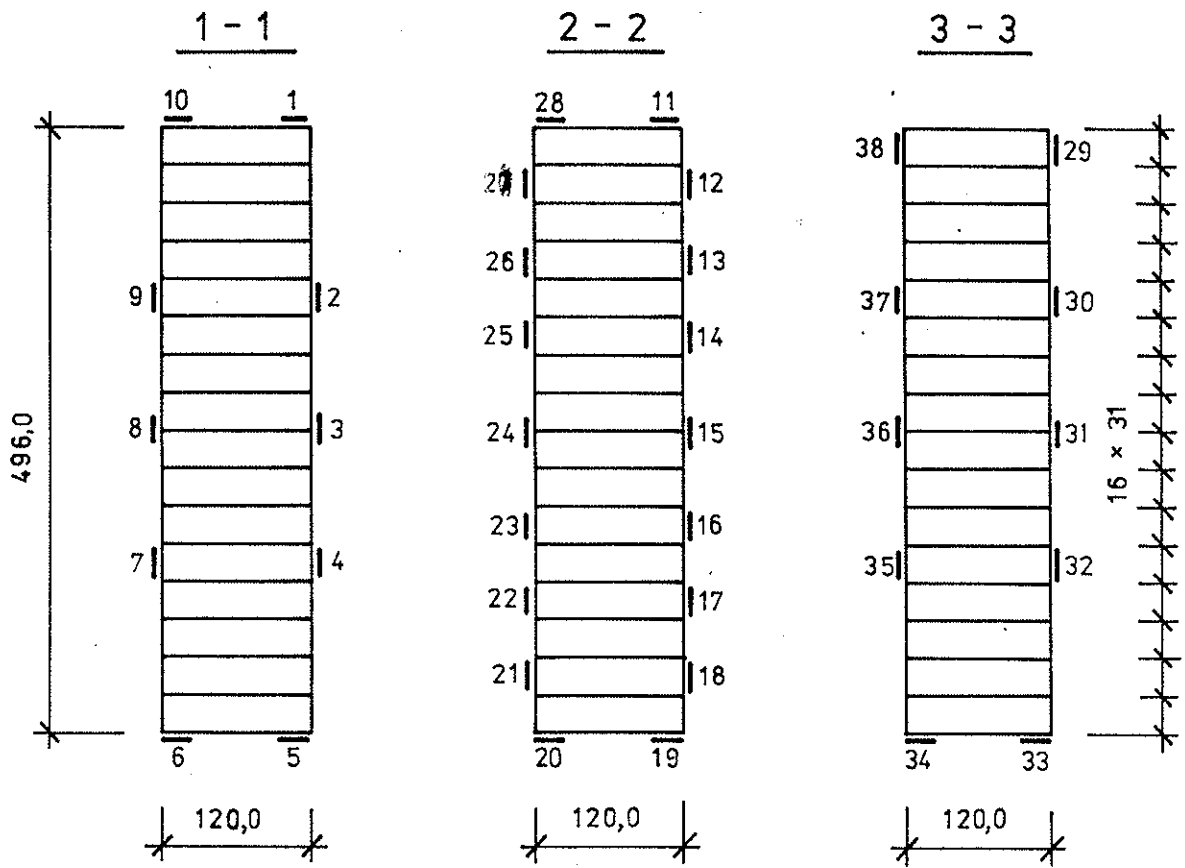


Fig.3. Arrangement of strain gauges in separate cross-sections of the arch No.1.



[mm]

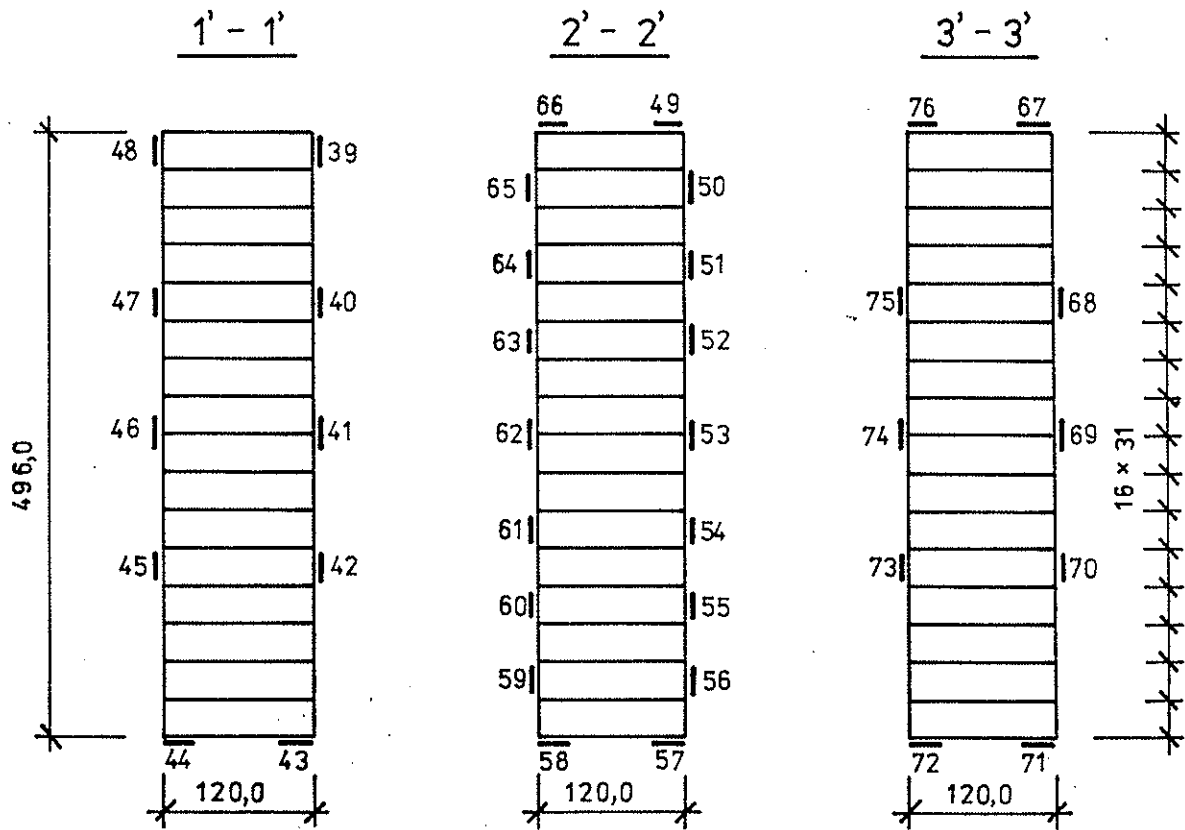


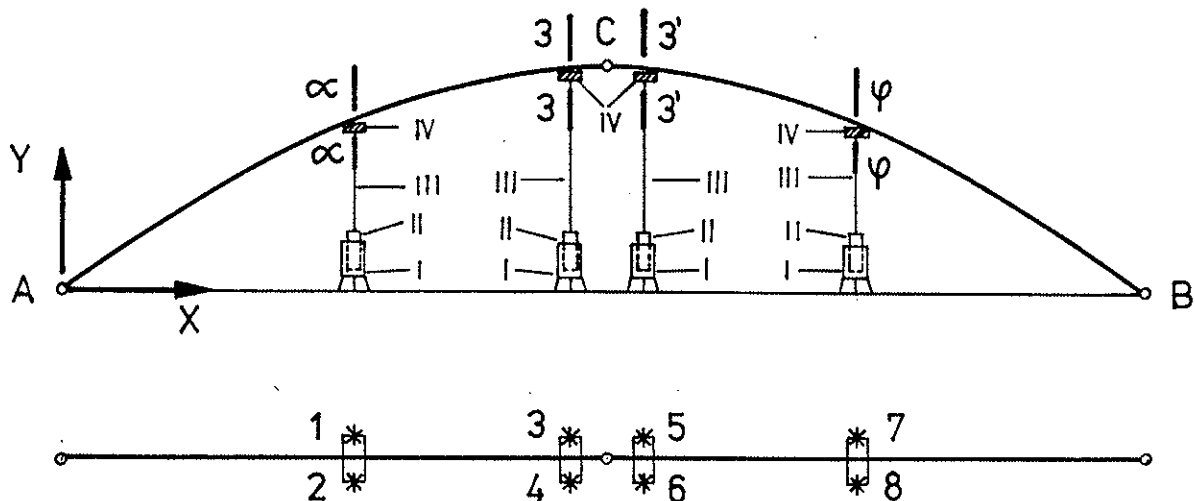
Fig.4. Arrangement of strain gauges in separate cross-sections of the archs Nos 2,3 and 4.

For deflections measuring the special device consisting of four parts was made. Each part of the device included:

- steel sleeve located on the testing stand plate
- steel cylinder put inside the sleeve
- steel wire on which the cylinder was hanged on a crosspiece fixed to the arch.

The arch distortion caused movement of the cylinder inside the sleeve. Value of the cylinder movement was measured with dial indicators with the read accuracy - 0.01 mm.

Scheme of the archs deflection measuring device is shown on Figure No.5



$\alpha-\alpha$ $x = 470\text{cm}$ $y = 277,8\text{cm}$

3-3 $x = 850\text{cm}$ $y = 358,9\text{cm}$

3'-3' $x = 950\text{cm}$ $y = 358,9\text{cm}$

$\varphi-\varphi$ $x = 1330\text{cm}$ $y = 277,8\text{cm}$

I - steel sleeve

II - steel cylinder

III - steel wire

IV - crosspiece

Fig.5. Scheme of installation for the arch deflection measuring as well as arrangement of measuring points.

2.2. Results of the testing

a/ Normal stress distribution in the L/4 arch.

The stresses were tested in different load cycles as well as in discharging conditions.

Graphs for the average measurements values obtained during the second /II/ load cycle are shown below:

$$\left/ \frac{\text{II A} + \text{II B} + \text{II C}}{2} \right/ \quad \text{in } 2' - 2' \text{ section /Fig.2/}$$

The stresses values in this cycle were caused by characteristic standard load. Figures Nos 6,7, 8 and 9 refers to the respective archs Nos 1,2,3 and 4. On these graphs, results of theoretical calculations are marked with continuous line and the measuring point /showing results of measurements/ are joined with dashed line.

b/ ^{tr}Independences between load and stresses.

On figures Nos. 10,11,12 and 13 there are Graphs showing dependences between load values "P" and normal stress values which appear in lower fibres of 2 - 2 and 2' - 2' sections during the second cycle of loads. The Graphs on figures Nos. 10,11,12 and 13 refers to the respective archs Nos. 1,2,3 and 4.

c/ Interdependences between load and deflections.

On figures Nos. 14,15,16 and 17 there are graphs showing dependences between load values and deflection values. The graphis on above mentioned figures are made for 3 - 3 and 3' - 3' sections during the second cycle of archs Nos 1,2,3 and 4 loads.

d/ ^{tr}Independences between load values "P" from one side and stress values as well as deflections from the other side, during the fifth cycle of loads.

The fifth cycle of loads was carried on until the arch No.4 destruction. On figure No. 18 there is a graph showing interdependences between loads and stresses in the outer lower fibres of 2 - 2 and 2' - 2' sections. Fig. 19 shows the graphs of interdependences between loads and stresses of 3 - 3 and 3' - 3' sections.

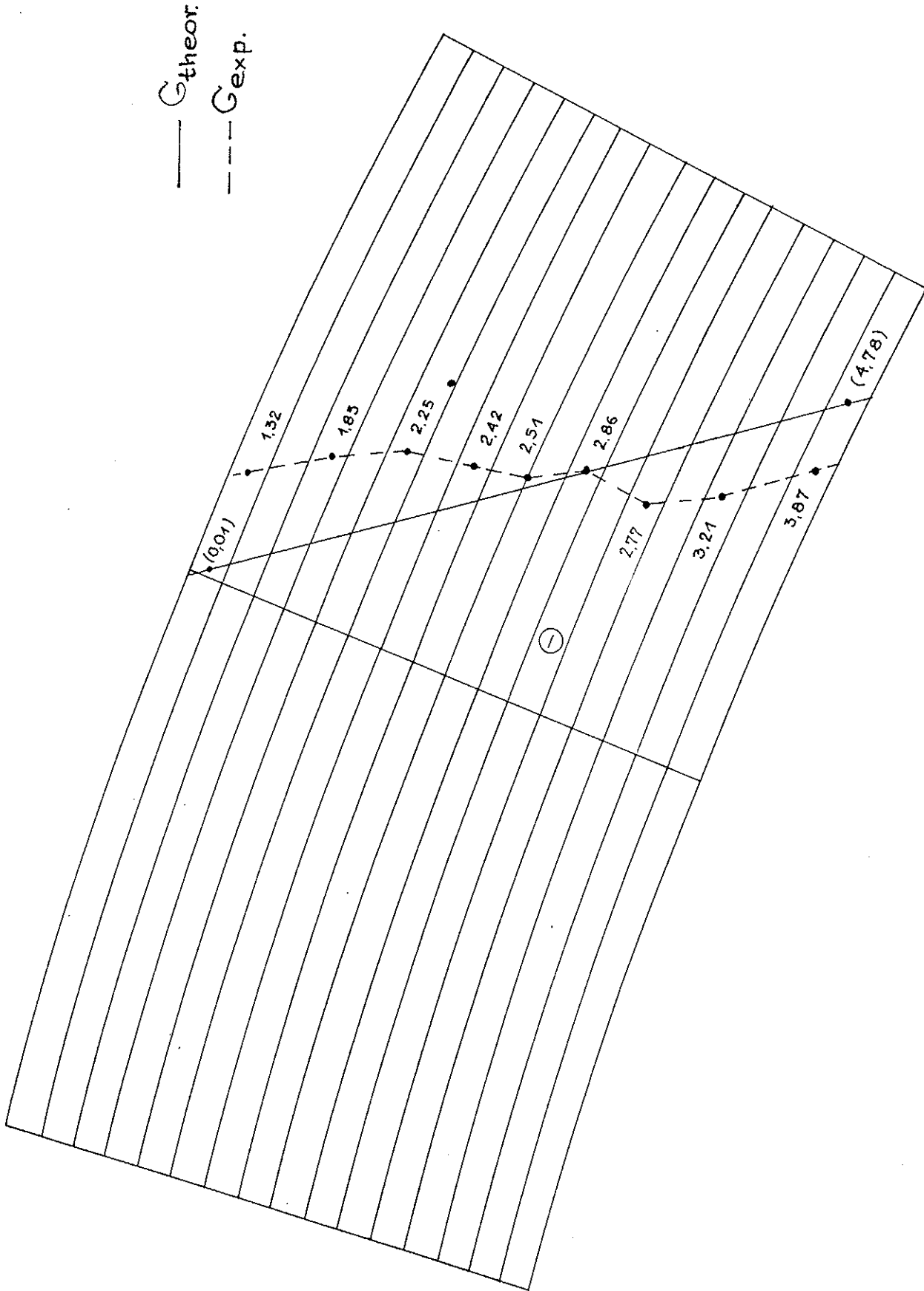


Fig.6. Distribution of normal stresses in 2'-2' section of the arch No.1.

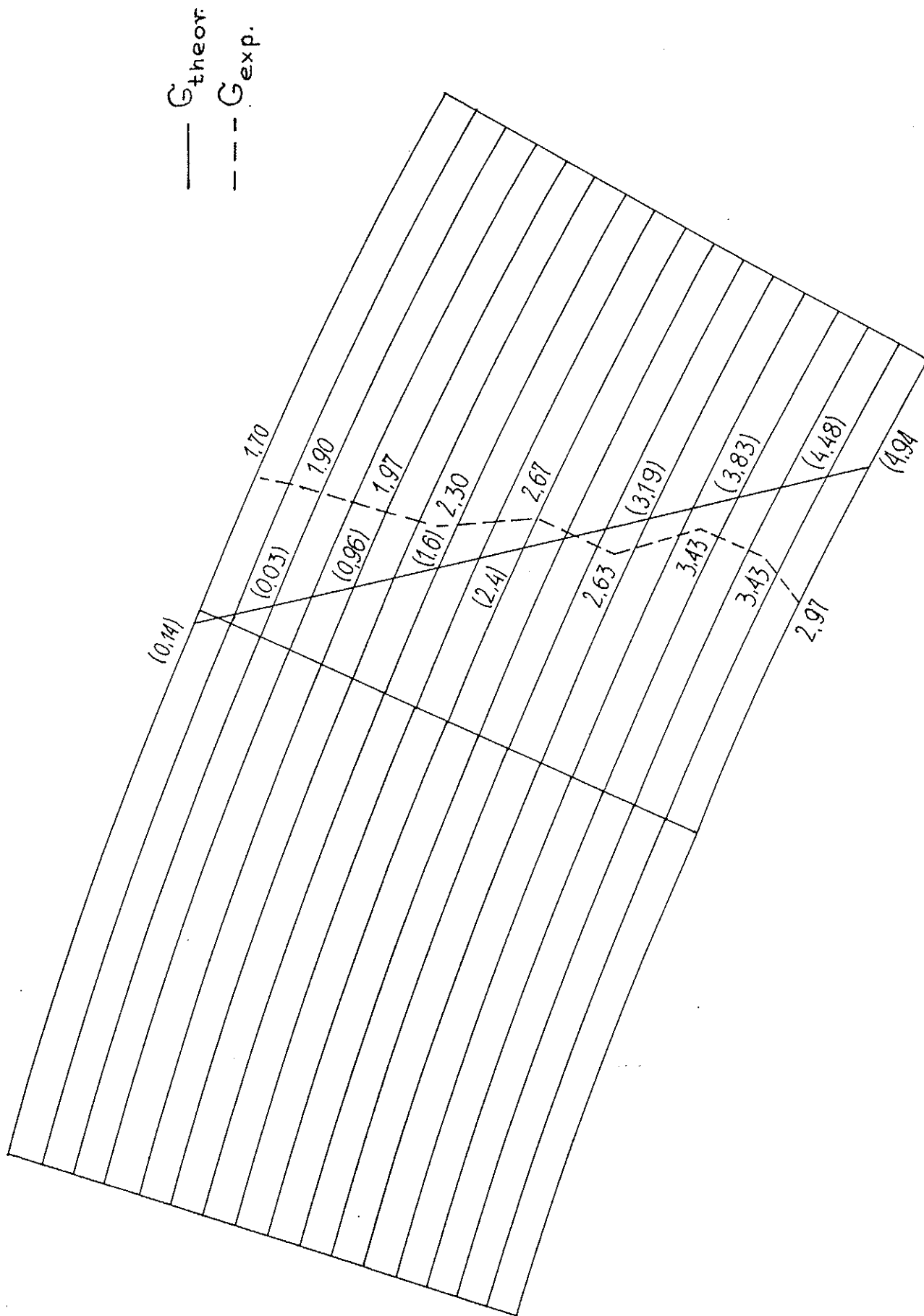


Fig. 7. Distribution of normal stresses in 2' - 2' section of the arch No.2.

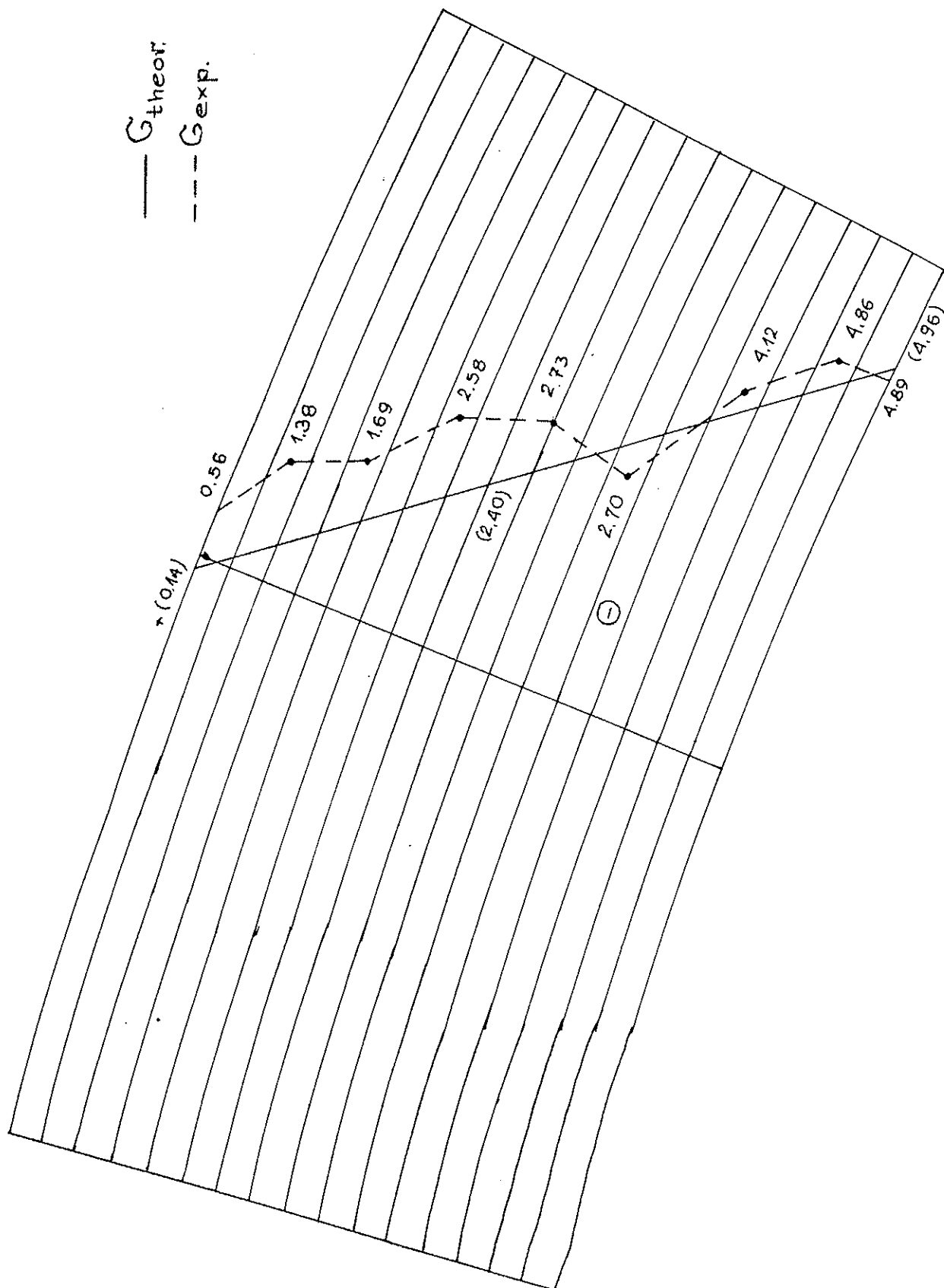


Fig. 8. Distribution of normal stresses in 2'-2' section of the arch No. 3.

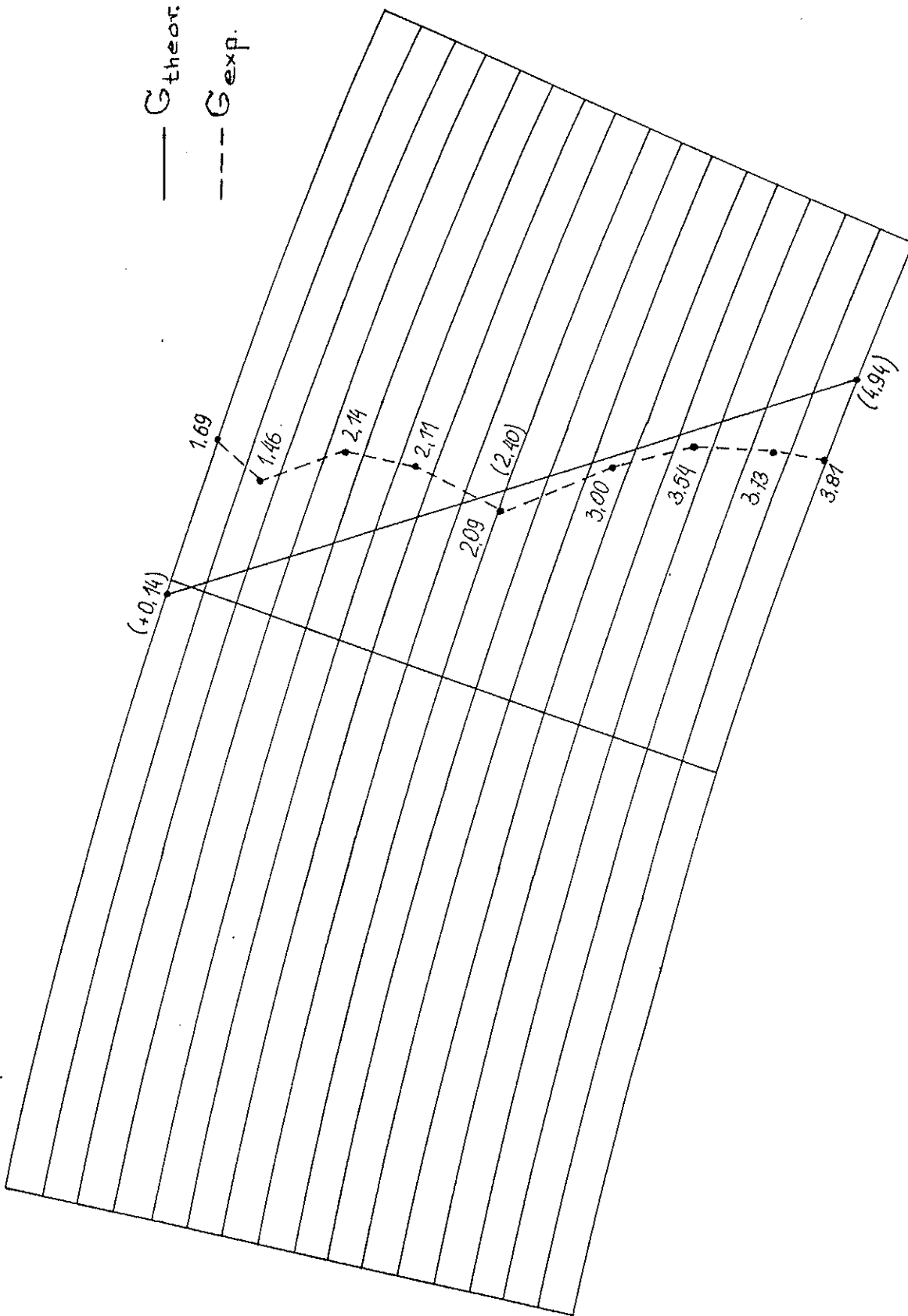


Fig.9. Distribution of normal stresses in 2' - 2' section of the arch No.4.

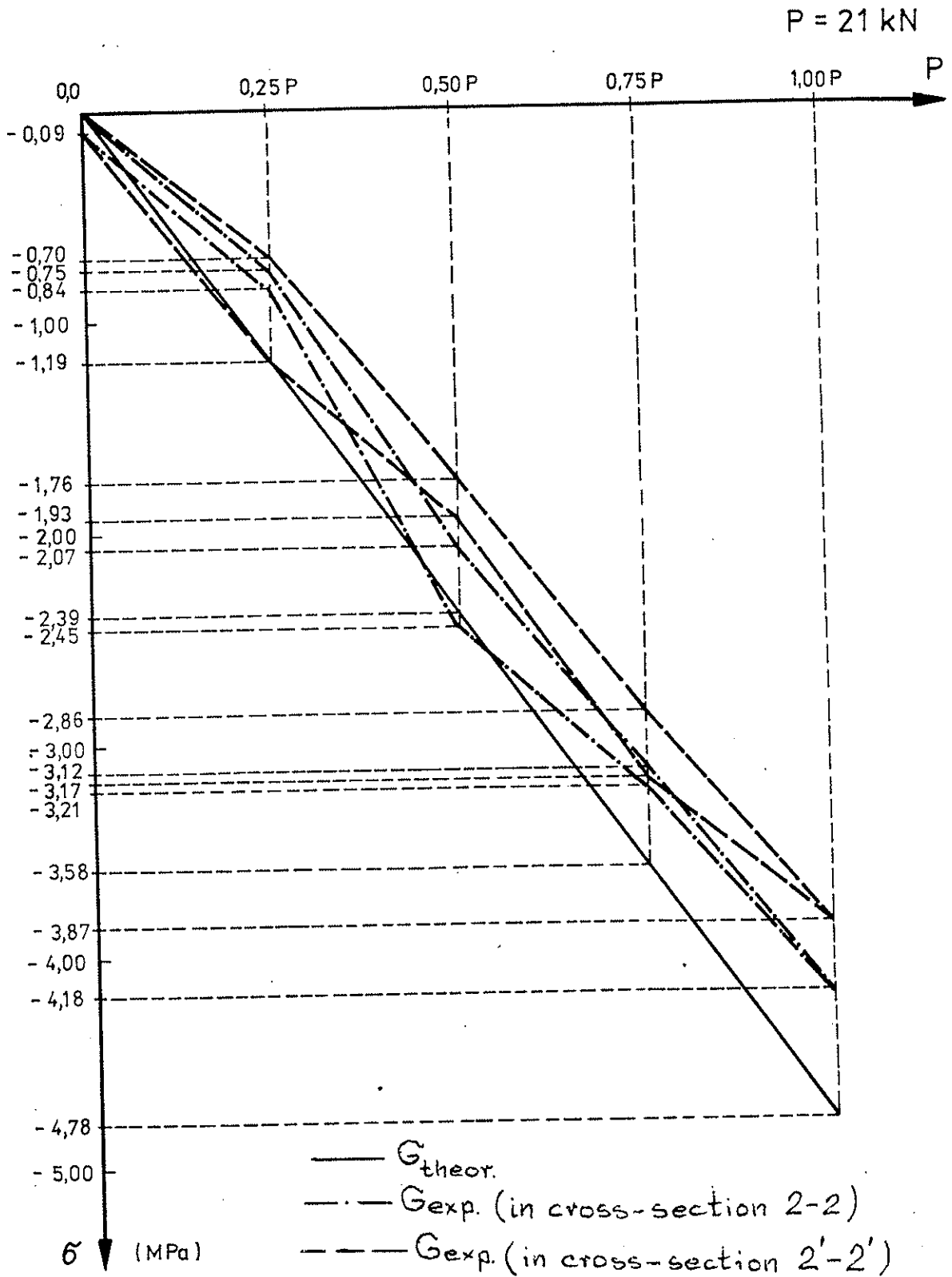


Fig.10. Graphs of relation between load "P" and stresses " σ " in lower fibres of 2 - 2 and 2' - 2' sections during the second cycle of the arch No.1 loads .

P = 21 kN

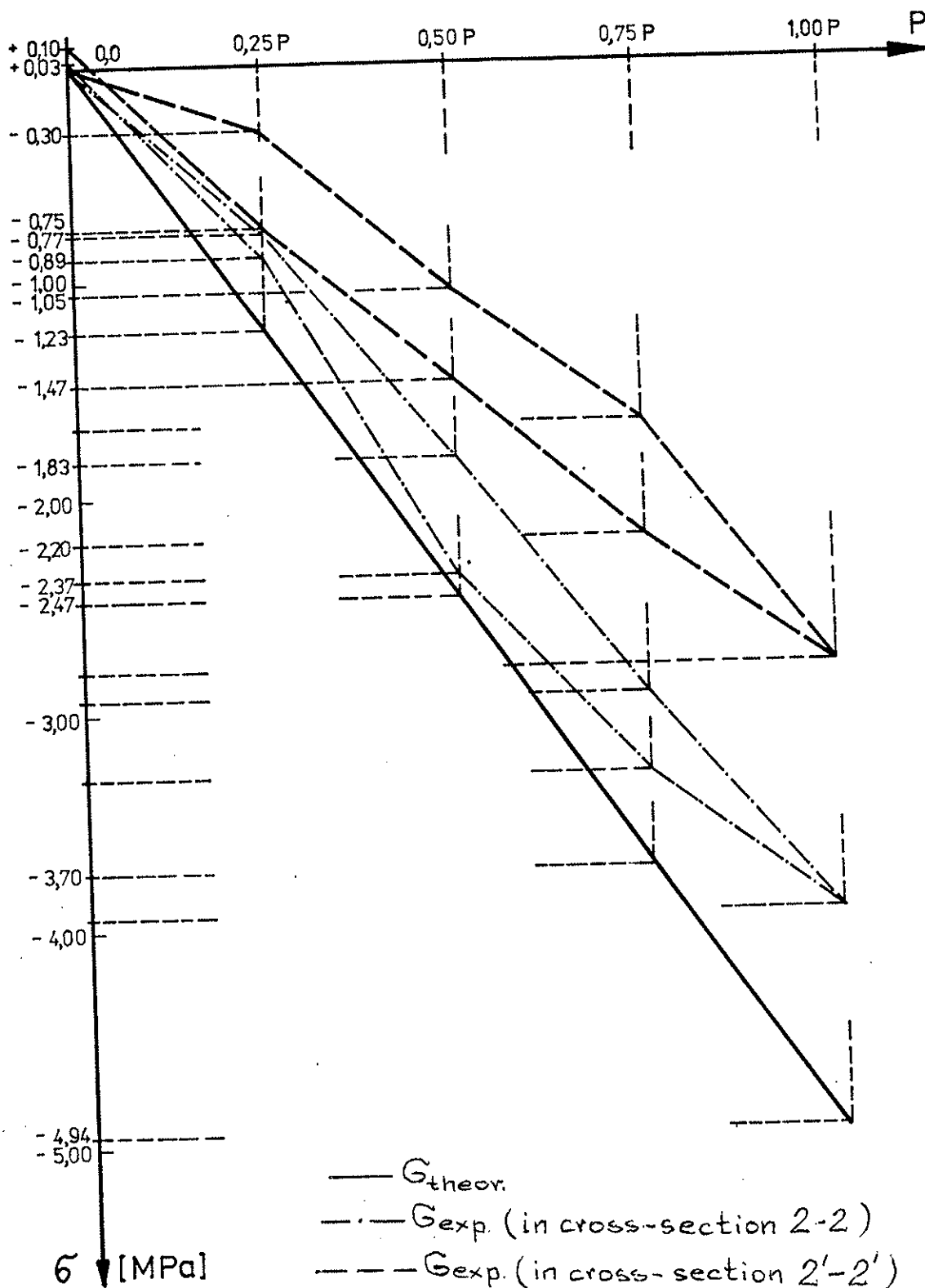


Fig.11. Graphs of relation between load "P" and stresses " σ " in lower fibres of 2 - 2 and 2' - 2' sections during the second cycle of the arch No.2 loads.

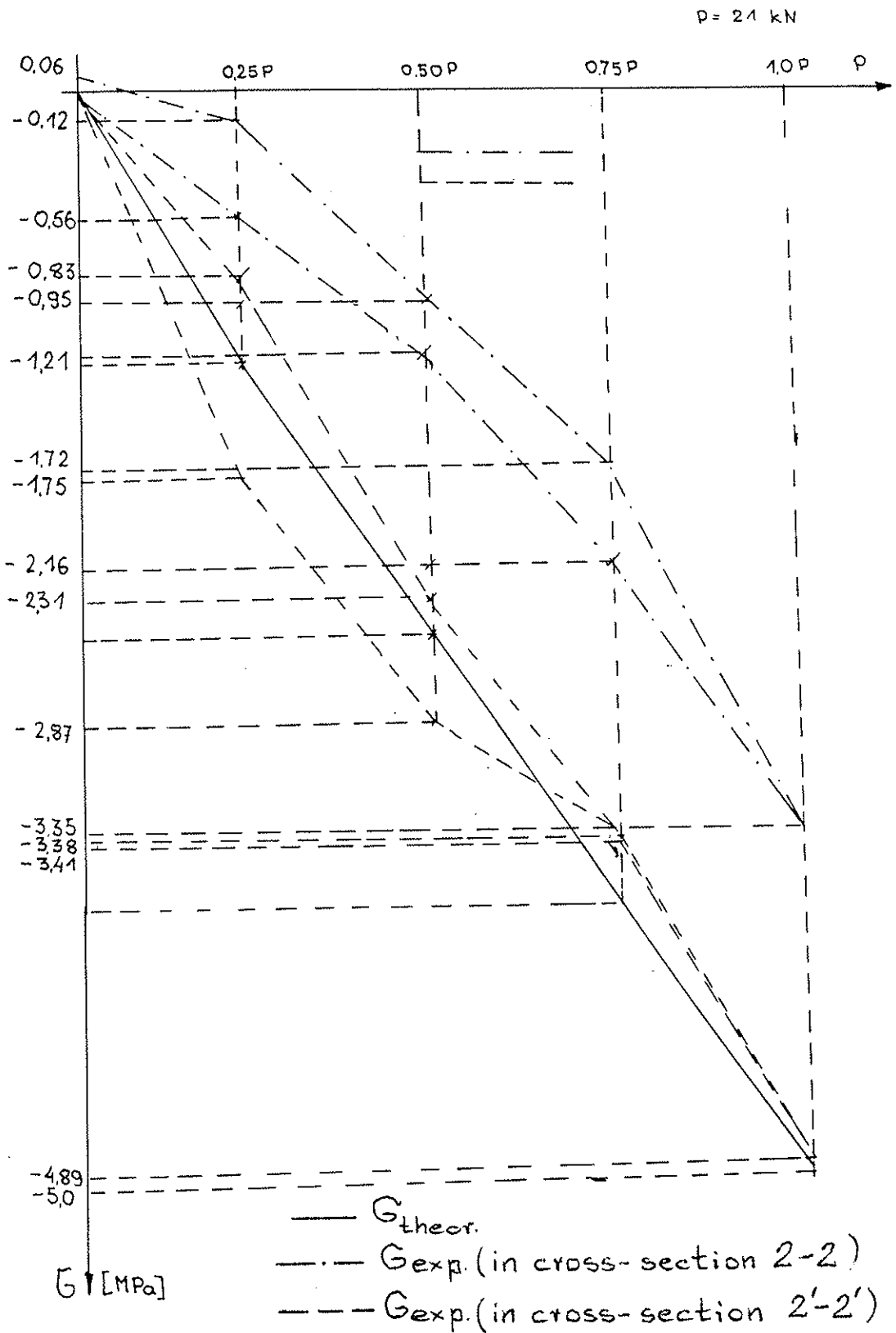


Fig.12. Graphs of interdependence between load "P" and stresses "G" in lower fibres of 2 - 2 and 2' - 2' sections during the second cycle of the arch No. 3 loads .

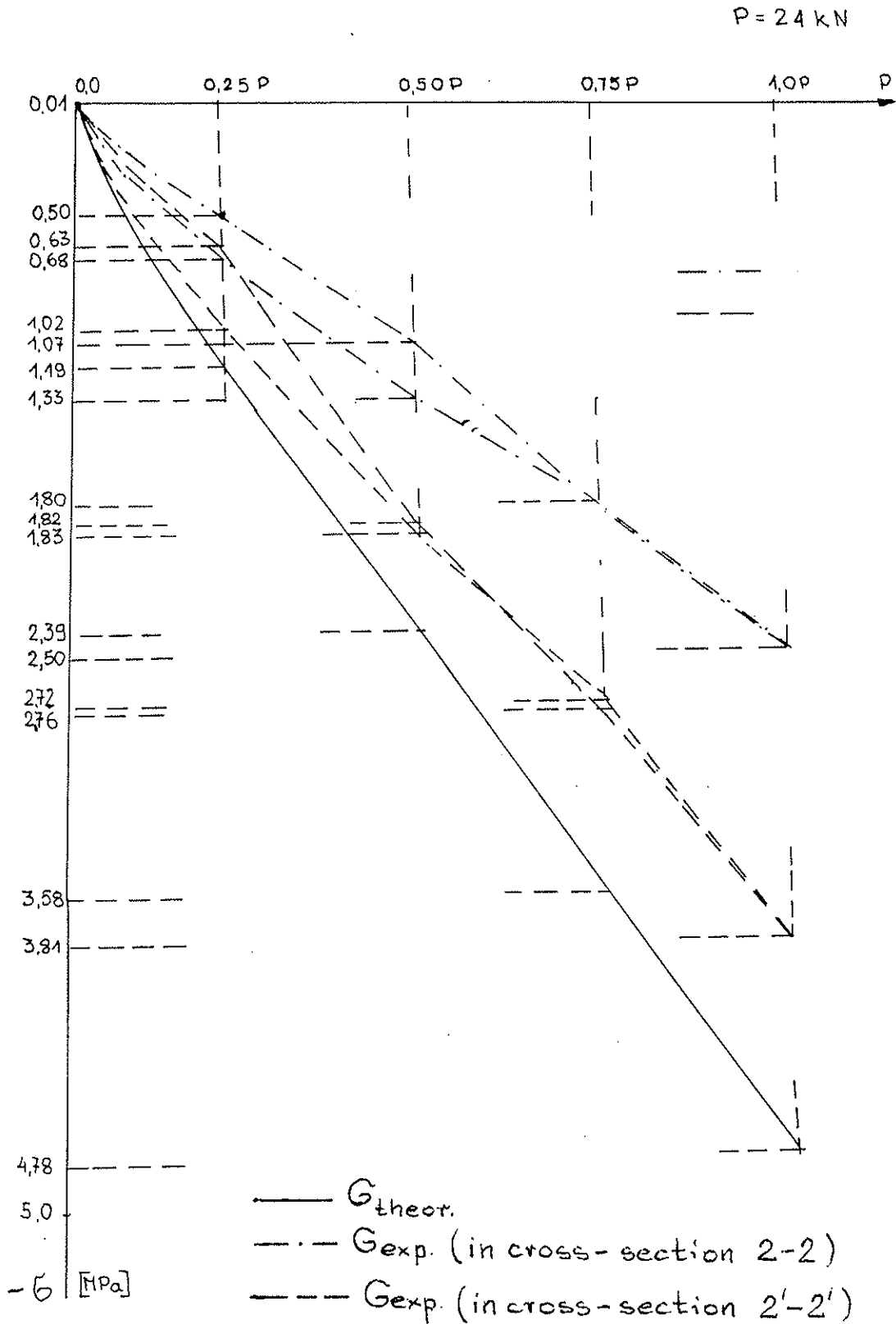


Fig.13. Graphs of interdependence between load "P" and stresses "σ" in lower fibres of 2 - 2 and 2' - 2' sections during the second cycle of the arch No.4 loads.

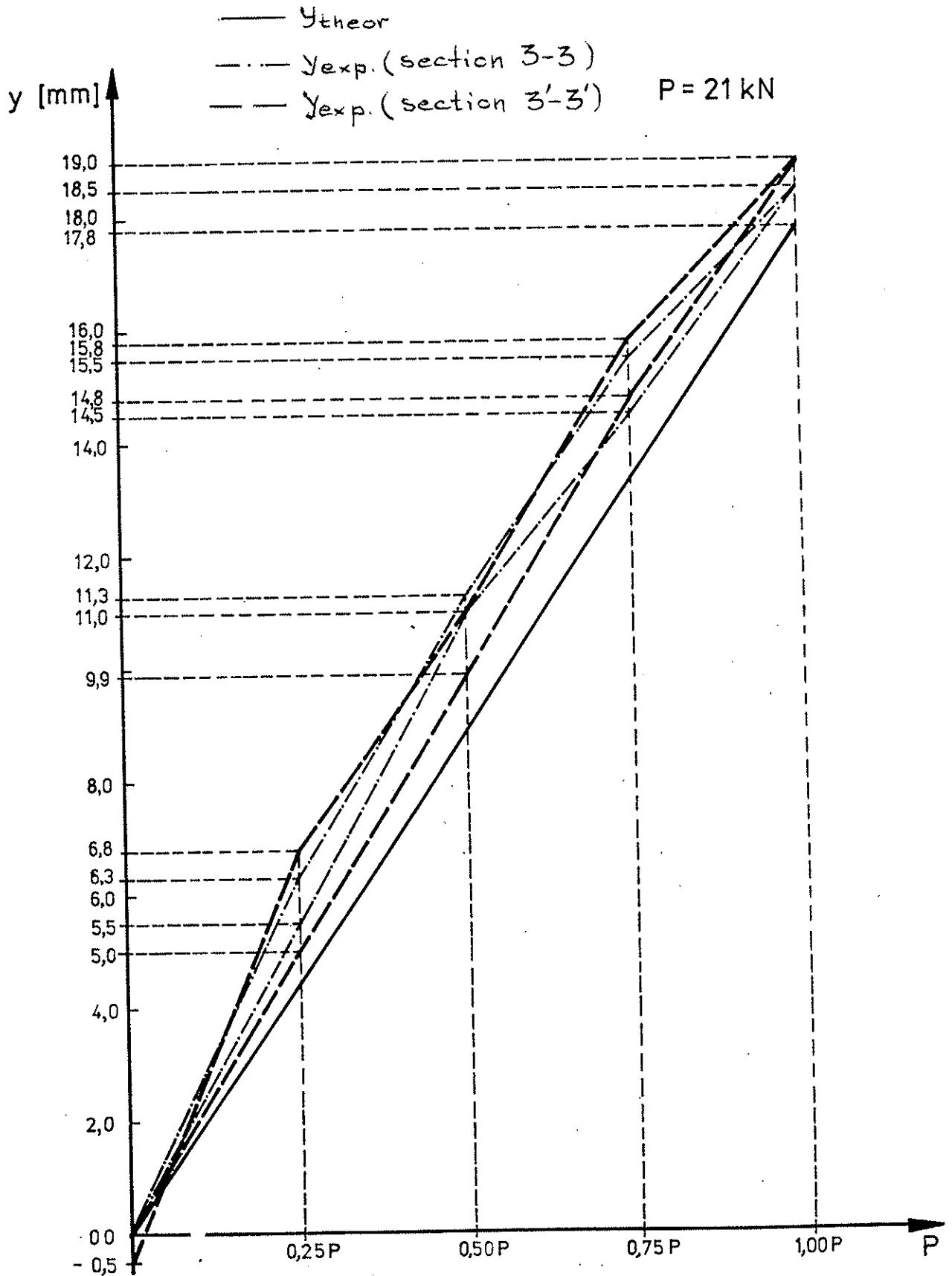


Fig.14. Graphs of interdependence between load "P" and deflection "y" in 3 - 3 and 3' - 3' sections during the second cycle of the arch No.1 loads.

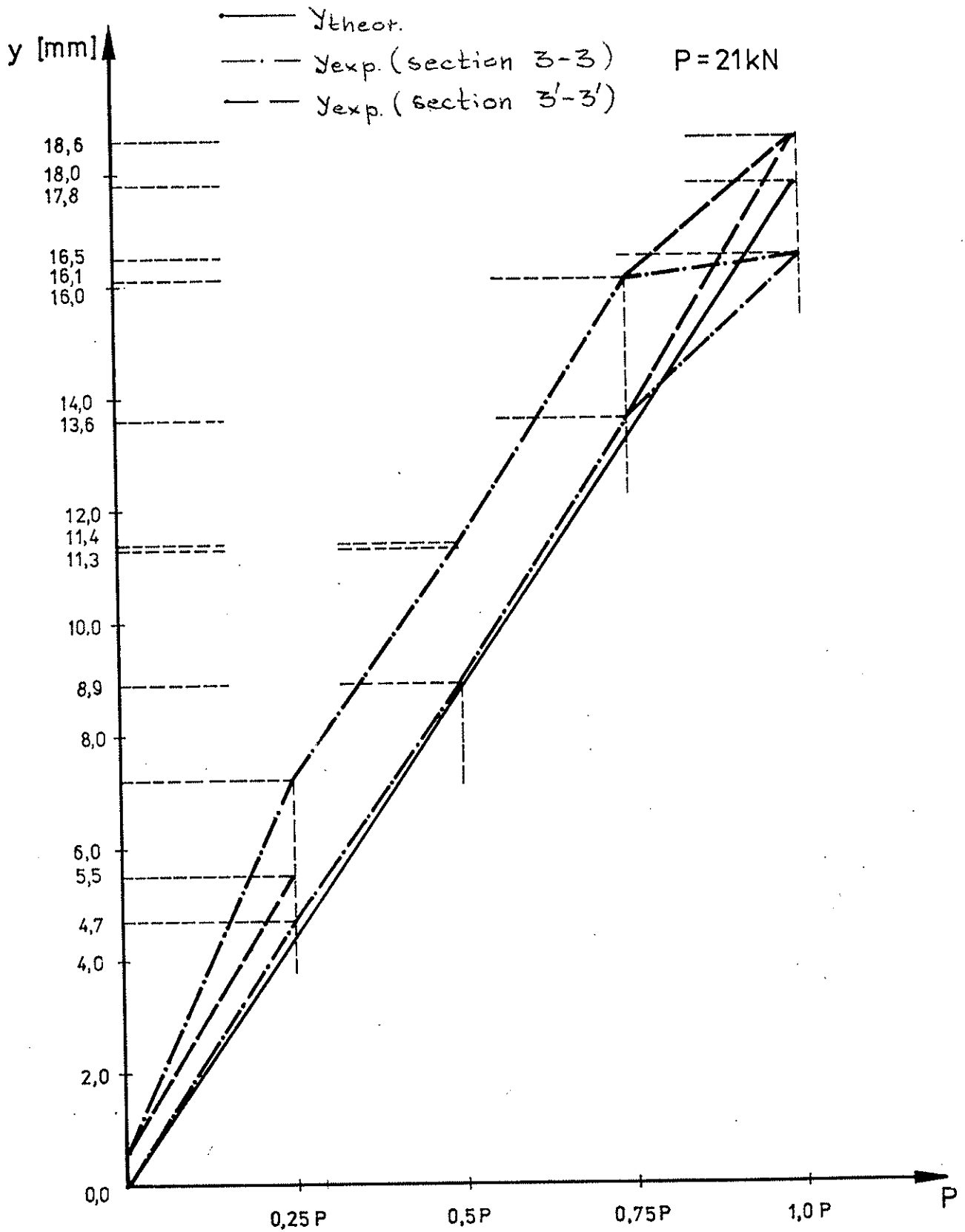


Fig.15. Graphs of interdependence between load "P" and deflection "y" in 3 - 3 and 3' - 3' sections during the second cycle of the arch No.2 loads.

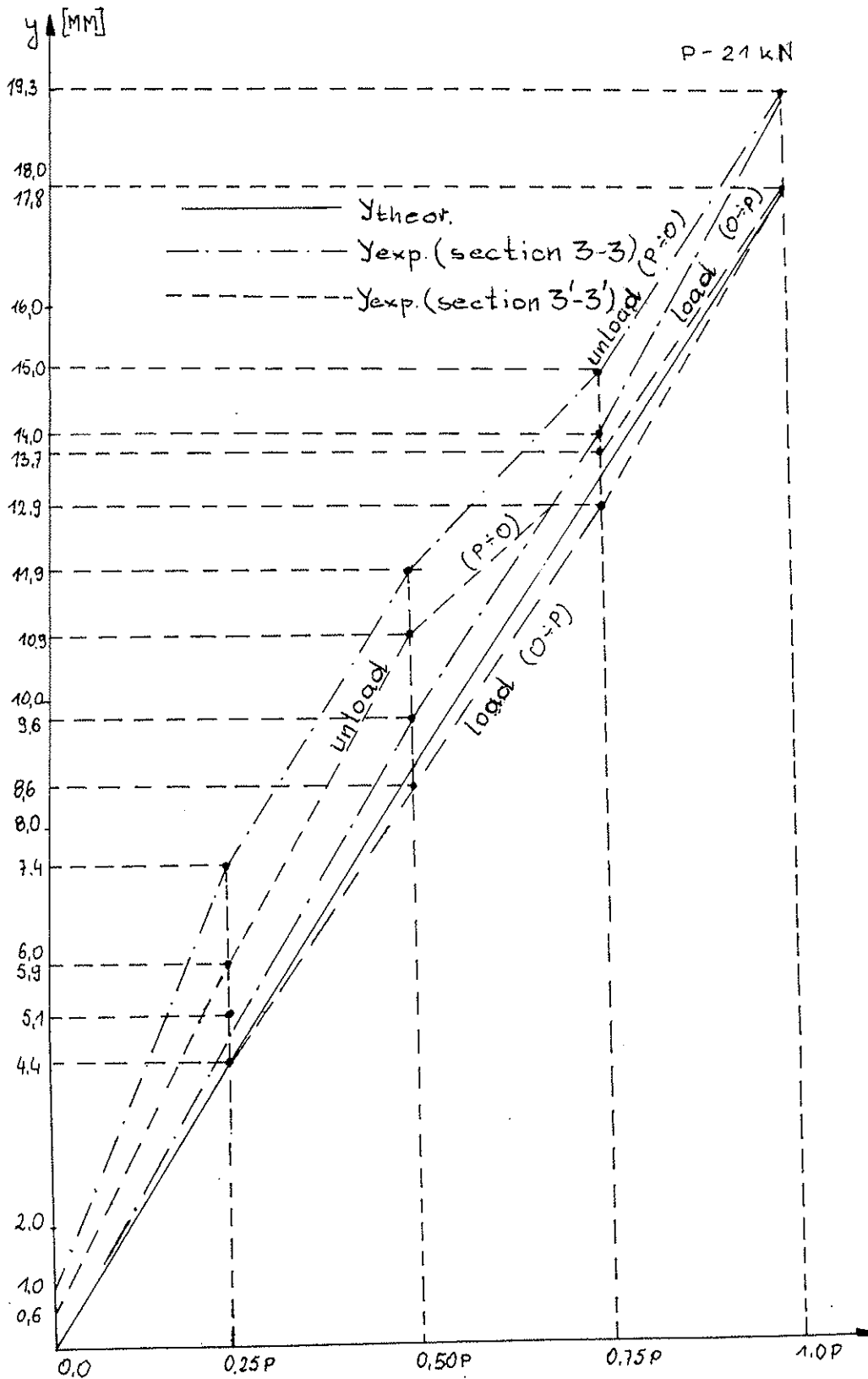


Fig.16. Graphs of interdependence between load "P" and deflection "y" in 3 - 3 and 3' - 3' sections during the second cycle of the arch No.3 loads.

P = 21 kN

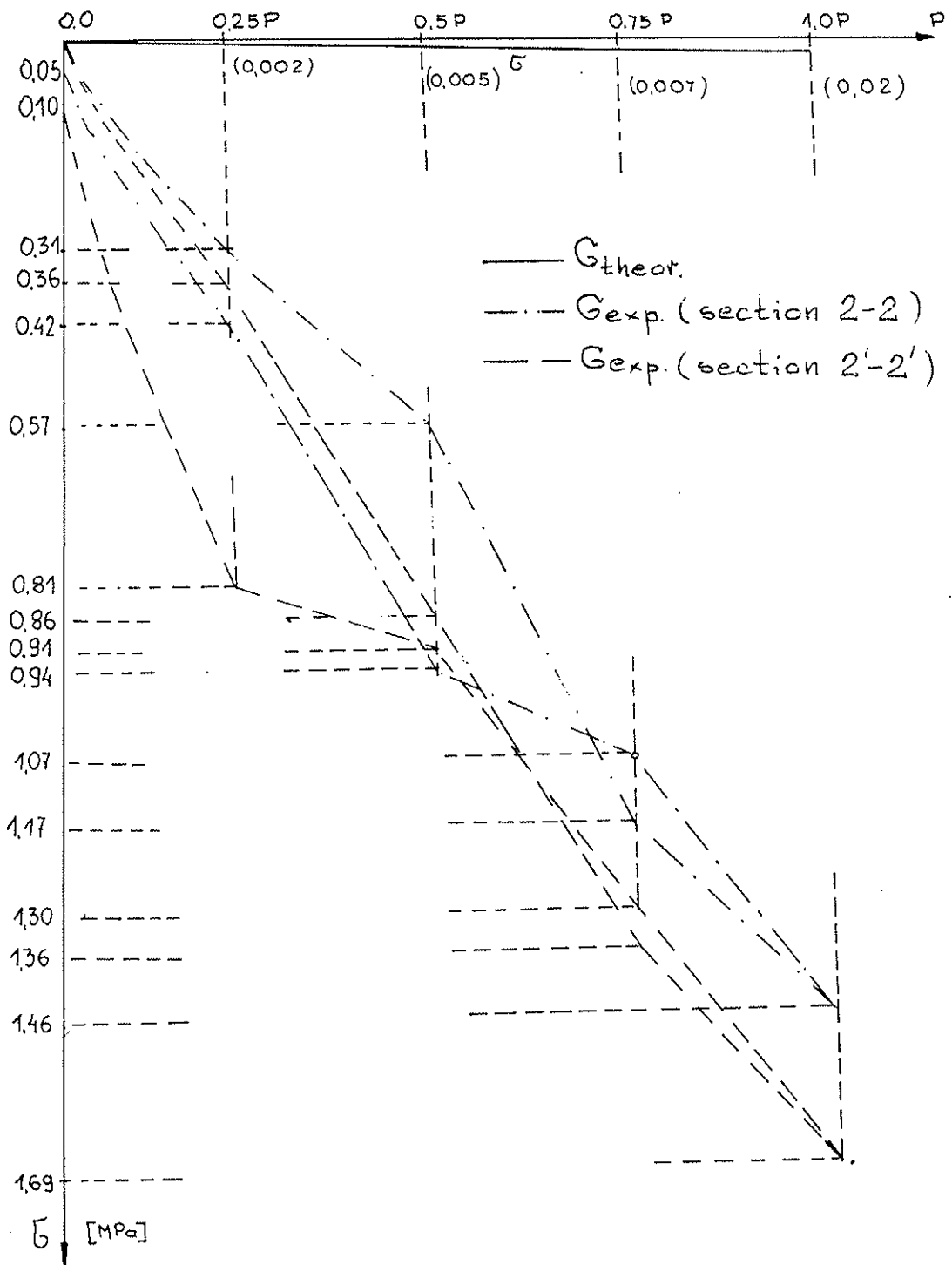


Fig.17. Graphs of interdependence between load "P" and stresses " σ " in 3 - 3 and 3' - 3' sections during the second cycle of the arch No. 4 loads.

P = 21 kN

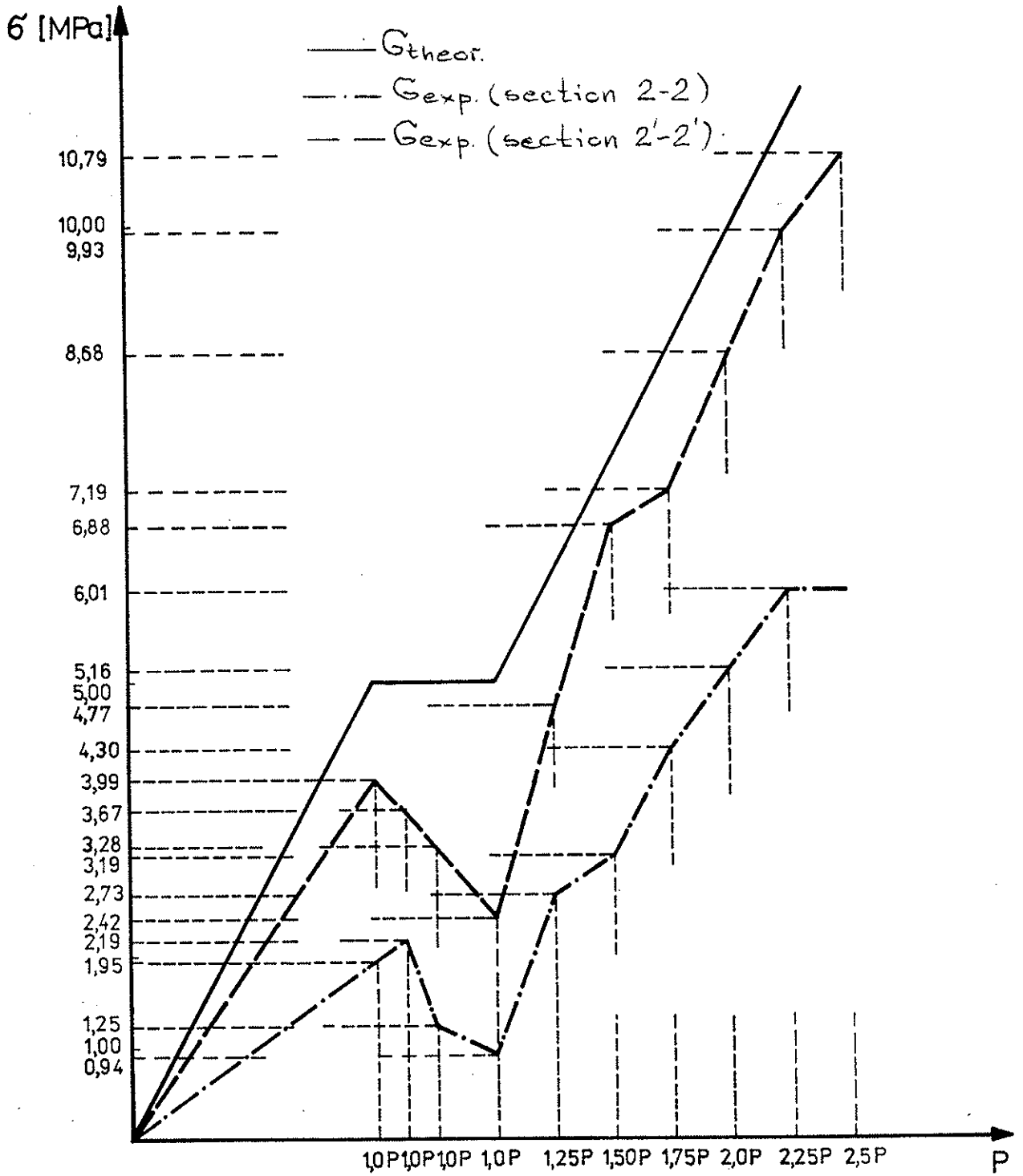


Fig.18. Graphs of interdependence between load "P" and stresses "σ" in lower fibres of 2 - 2 and 2' - 2' sections during the fifth cycle of the arch No. 4 loads.

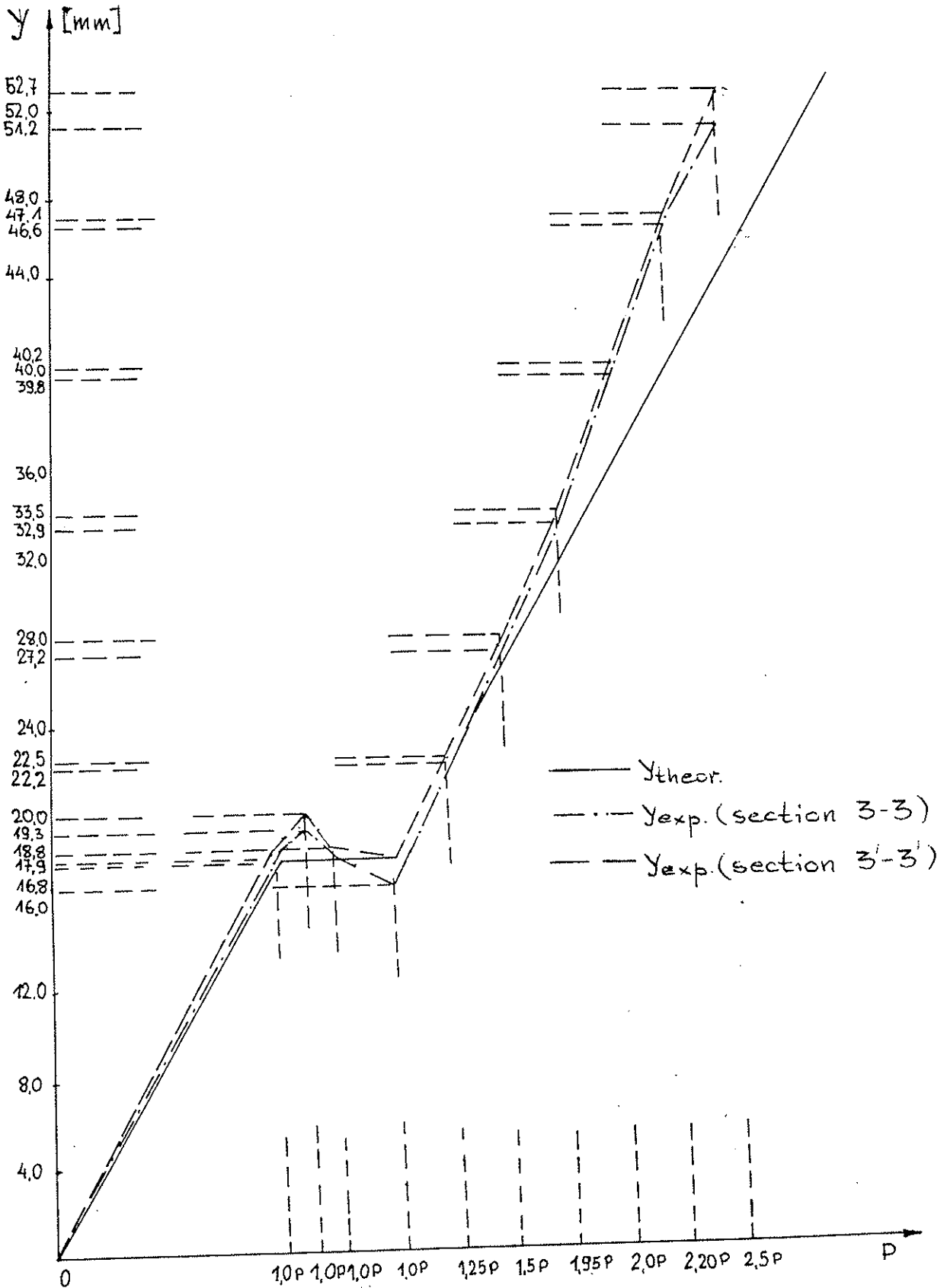


Fig.19. Graphs of interdependence between load "P" and deflection "y" in 3 - 3 and 3' - 3' sections during the fifth cycle of the arch No. 4 loads.

3. Analysis of testing results

3.1. Arch No. 1

Relationship of the average normal stresses defined experimentally during the cycles IIA, IIB and IIC to the theoretically calculated stresses in separate sections was as follows:

Section	1 - 1	- 1,198
Section	2 - 2	- 1,118
Section	3 - 3	- 1,130
Section	3' - 3'	- 1,200
Section	2' - 2'	- 1,069
Section	1' - 1'	- 1,324.

The deflection values are given summarilly for all the archs in table No 2.

The destruction power was defined under unsymmetrical load.

3.2. Arch No. 2

Relationship of the average normal stresses

$\bar{\sigma}_{exp}$: $\bar{\sigma}_t$ for the cycles IIA, IIB and IIC.

Section	1 - 1	- 1,007
Section	2 - 2	- 1,101
Section	3 - 3	- 0,899
Section	3' - 3'	- 1,104
Section	2' - 2'	- 1,067
Section	1' - 1'	- 1,092

The destruction power was defined under unsymmetrical load.

3.3. Arch No. 3

Relationship of the average normal stresses

$\bar{\sigma}_{exp}$: $\bar{\sigma}_t$ for the cycles IIA, IIB, and IIC.

Section	1 - 1	- 0,993
Section	2 - 2	- 1,117
Section	3 - 3	- 0,831
Section	3' - 3'	- 0,991
Section	2' - 2'	- 1,193
Section	1' - 1'	- 0,920

The destruction power was defined under unsymmetrical load.

3.4. Arch_No._4_

Relationship of the average normal stresses

exp : t for the cycles IIA, IIB, and IIC.

Section	1 - 1	- 0,959
Section	2 - 2	- 0,954
Section	3 - 3	- 0,890
Section	3'- 3'	- 0,937
Section	2'- 2'	- 1,094
Section	1'- 1'	- 1,156

The deflection values are given in table No.2.

According to the testing programme the arch No. 4 was destructed under symmetrical load.

The testing was carried on within the fifth /V/ cycle loading the arch with the dense boards distributed symmetrically to the ridge joint /Fig.No.1/. During the testing the arch was not physically destructed because with the load.

$P = 2,75$ $P_d = 2,75 \times 2100 = 577$ skg = 57,7 KN was so great bucking from the plane that the further load increasing threatened with falling down of the tested arch as well as the attendant arch. Taking into consideration the above mentioned fact as well as regarding safety of people employed during the testing the fifth /V/ cycle was completed at the load $P = 2,7$ P_d

3.5. Recapitulation of the test results in reference to all the archs.

a/ Normal stresses.

Relationship of the overage normal stresses experimentally during the second II cycle

$$/ \frac{IIA + IIB + IIC}{3} /$$

in the given section in relation to the theoretical stresses, is illustrated by the table No.1

The genaralized coefficient for the all tested arch expressing relationship of the all arch average experimental stresses to the theoretical stresses was found as below:

the arch No. 1	-	1.138
the arch No. 2	-	1.054
the arch No. 3	-	1.040
the arch No. 4	-	1.008

4. Conclusions

In virtue of the experimented test results analysis as well as theoretical calculations the following general conclusions, referring three joint archs with parabolic shape, made of glued timber, may be drowned out as bellow:

1/ Distributions of normal stresses in transverse sections situated close to support and ridge joints were quite different from the theoretical ones. It seems that it was caused by irregular or eccentric load transmission through the steel joint construction.

In the rest sections situated at $L/4$ length from the supports the difference are much smaller and the generalized coefficient for the all tested archs, expressing relationship of the all arch average experimental stresses to the theoretical stresses is equal 1.042. So the difference between results of calculations and experiments is within about 5% range.

2/ The limitary archs load capacity was found to be much bigger from the calculated load capacity.

In the archs Nos 1,2 and 3, which were put under unsymmetrical load, factor of safety defined as the relationship of the destructive load to the characteristic load is contained in the range 3 - 3.25.

Only in the arch No. 4 which was tried to be destructed under the symmetrical load it was impossible to define value of the factor because the stiffenings used in the arch under such great load were quite insufficient.

Testing was carried out at the moment when the said loads relation was 2.75. It is quite probable that in the case of using the proper stiffenings the loads relation will be the same as in the other archs tested under unsymmetrical load, that is not smaller then 3.

3/ The archs stiffness was not much different from the calculated value. The maximum arch deflection under symmetrical load appeared in the middle of the arch span. Value of those reflections measured during the tests was about 18.9 mm and the theoretically calculated value was 17.8 mm, so the experimentally defined deflections were bigger from the calculated ones of 6 %.

4/ The positive results of tests obtained under the casual load testify of the correct tested archs manufacture technology.

INTERNATIONAL COUNCIL FOR BUILDING RESEARCH STUDIES AND DOCUMENTATION
WORKING COMMISSION W18A - TIMBER STRUCTURES

ULTIMATE STRENGTH OF WOODEN BEAMS WITH TENSION REINFORCEMENT
AS A FUNCTION OF RANDOM MATERIAL PROPERTIES

by

R Candowicz and T Dziuba
Agricultural University Poznan
Poland

MEETING TWENTY - TWO
BERLIN
GERMAN DEMOCRATIC REPUBLIC
SEPTEMBER 1989

ULTIMATE STRENGTH OF WOODEN BEAMS WITH TENSION REINFORCEMENT
AS A FUNCTION OF RANDOM MATERIAL PROPERTIES

Ryszard Ganowicz, D. Sc.
Professor of Civil Engineering
Agricultural University
Poznań, Poland

Tadeusz Dziuba, D. Sc.
Agricultural University
Poznań, Poland

Introduction

Ultimate strength of wooden glue-laminated beams depends on many factors mostly being random variables. This phenomenon results in an important scatter of ultimate strength determined experimentally. This paper presents a further step in the analysis of the problem. Some earlier results of our investigations were presented formerly [1, 2, 3]. The digital simulation methods were continuously used in our analysis. The paper deals with the ultimate strength of rectangular cross-sections reinforced with rods made of comparatively strong material.

Model of failure

The experiments performed by T. Dziuba [1, 2] showed that there are three main failure mechanisms (see the fig. 1):

Type "0" - failure occurs as a result of outermost tension fibers break.

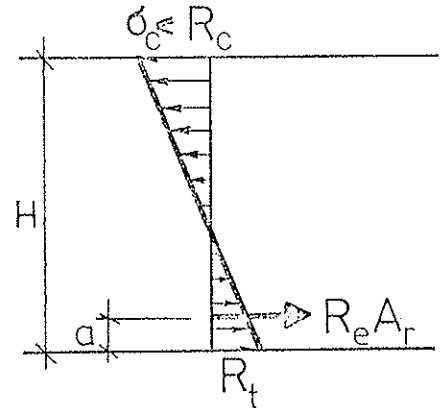
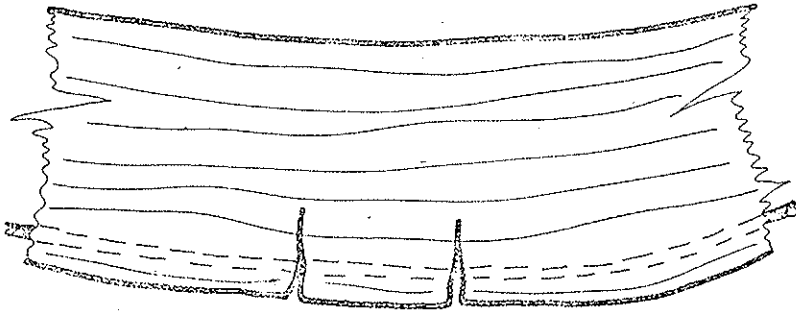
Type "1" - failure occurs due to the tension fibers break, while compression zone is partially yielding.

Type "2" - failure occurs due to the compression zone damage.

-2-

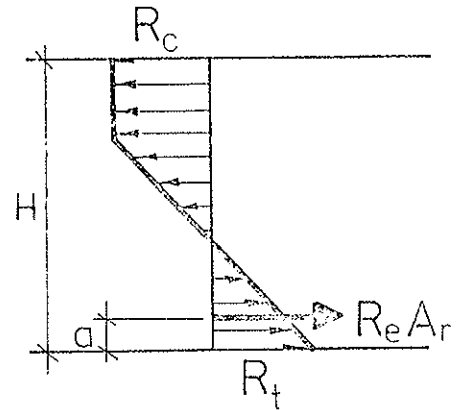
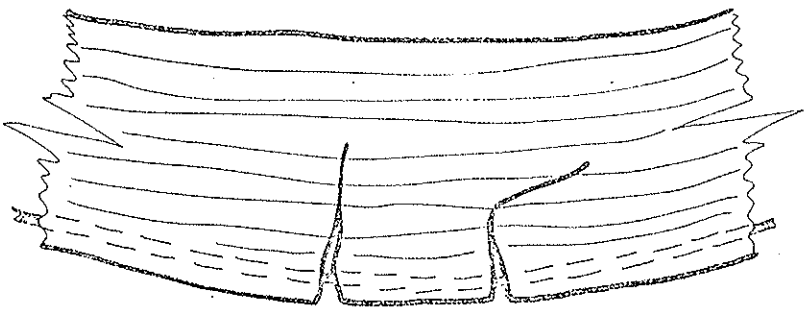
POSSIBLE TYPES OF FAILURE

TYPE "0"



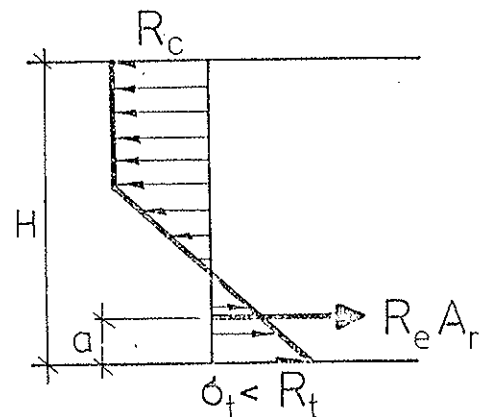
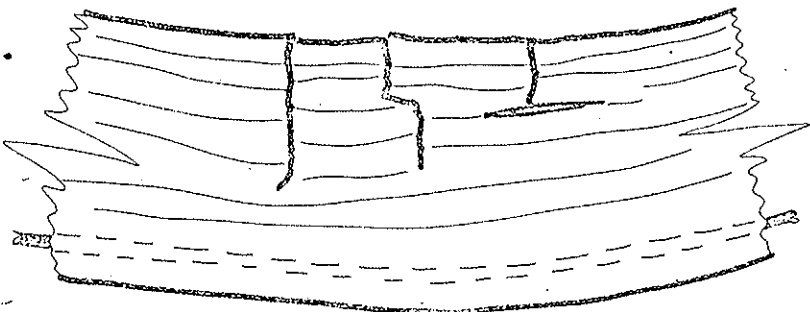
$$\frac{M_{ult}}{W_{x0}} = R_c \left\{ \frac{\omega^3 + (\omega + 2\omega_s)^3}{2(\omega + \mu\omega_s)^2} + 3\mu\omega_s \left(\frac{\omega}{\omega + \mu\omega_s} - \alpha \right) \right\}$$

TYPE "1"



$$\frac{M_{ult}}{W_{x0}} = R_c \left\{ 3(1 - \mu\omega_s\alpha) - 4 \frac{(1 - \mu\omega_s)^2}{1 + \omega} \right\}$$

TYPE "2"



$$\frac{M_{ult}}{W_{x0}} = R_c \left\{ \frac{3\psi^2 - 1 + 2[\sqrt{(\psi - \mu\omega_s)^2 - (\psi - 1)^2} - \mu\omega_s]^3}{\psi - \mu\omega_s + \sqrt{(\psi - \mu\omega_s)^2 - (\psi - 1)^2}} + 3\mu\omega_s \left[2 - \alpha - \frac{2\psi}{\psi - \mu\omega_s + \sqrt{(\psi - \mu\omega_s)^2 - (\psi - 1)^2}} \right] \right\}$$

Fig. 1

Theoretical assumptions of the model were presented in the paper [2]. The idealization of mechanical properties of wood is shown in the fig. 2. Moreover it was assumed that the stress in the reinforcement is equal to the yield point when beam failure occurs.

The three above described failure mechanisms lead to the three formulae for "ultimate strength" M_{ult}/W_{x0} presented in the fig. 1. The each type of failure possesses following limitations:

Type "0": $\epsilon_t = \epsilon_t^{ult}$ (fig. 1 and fig. 2), $\epsilon_c \leq \epsilon_{pl}$;

the above conditions result in the limit value

$$\mu \leq \mu_0 = \frac{1-\omega}{2\omega_s}$$

Type "1": $\epsilon_t = \epsilon_t^{ult}$, $\epsilon_{pl} < \epsilon_c \leq \epsilon_c^{ult}$ and

$$\mu_0 < \mu \leq \mu_1 = \left[\psi - 0.5(1 + \omega^2) \right] / \left[\omega_s (\psi + \omega) \right]$$

Type "2": $\epsilon_c = \epsilon_c^{ult}$, $\epsilon_t < \epsilon_t^{ult}$, and $\mu > \mu_1$.

In the above formulae the following abbreviations were applied:

$$\alpha = a/H, \quad \mu = A_r/B \cdot 2H, \quad W_{x0} = \frac{2}{3} B H^2, \quad \omega_s = R_e/R_c,$$

$$\omega = R_t/R_c, \quad \psi = \epsilon_c^{ult} / \epsilon_{pl},$$

B - width of the cross-section,

M_{ult} - ultimate bending moment,

Further symbols are presented in the fig. 1 and fig. 2.

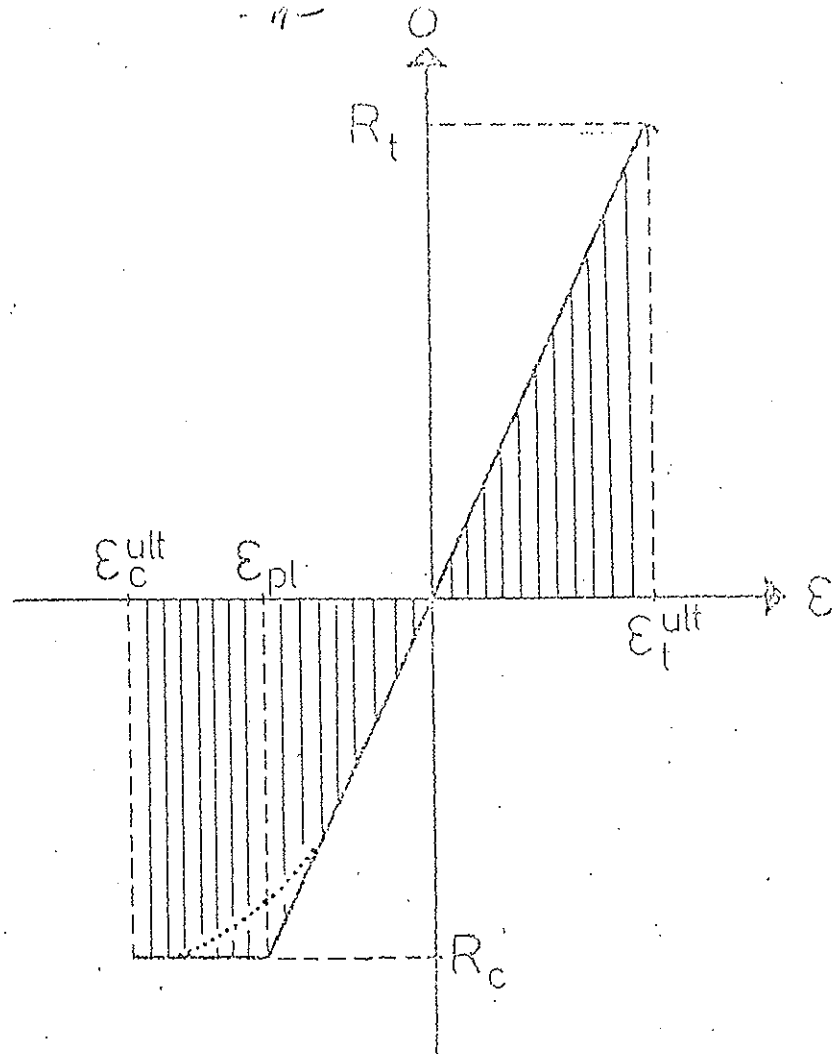


Fig. 2

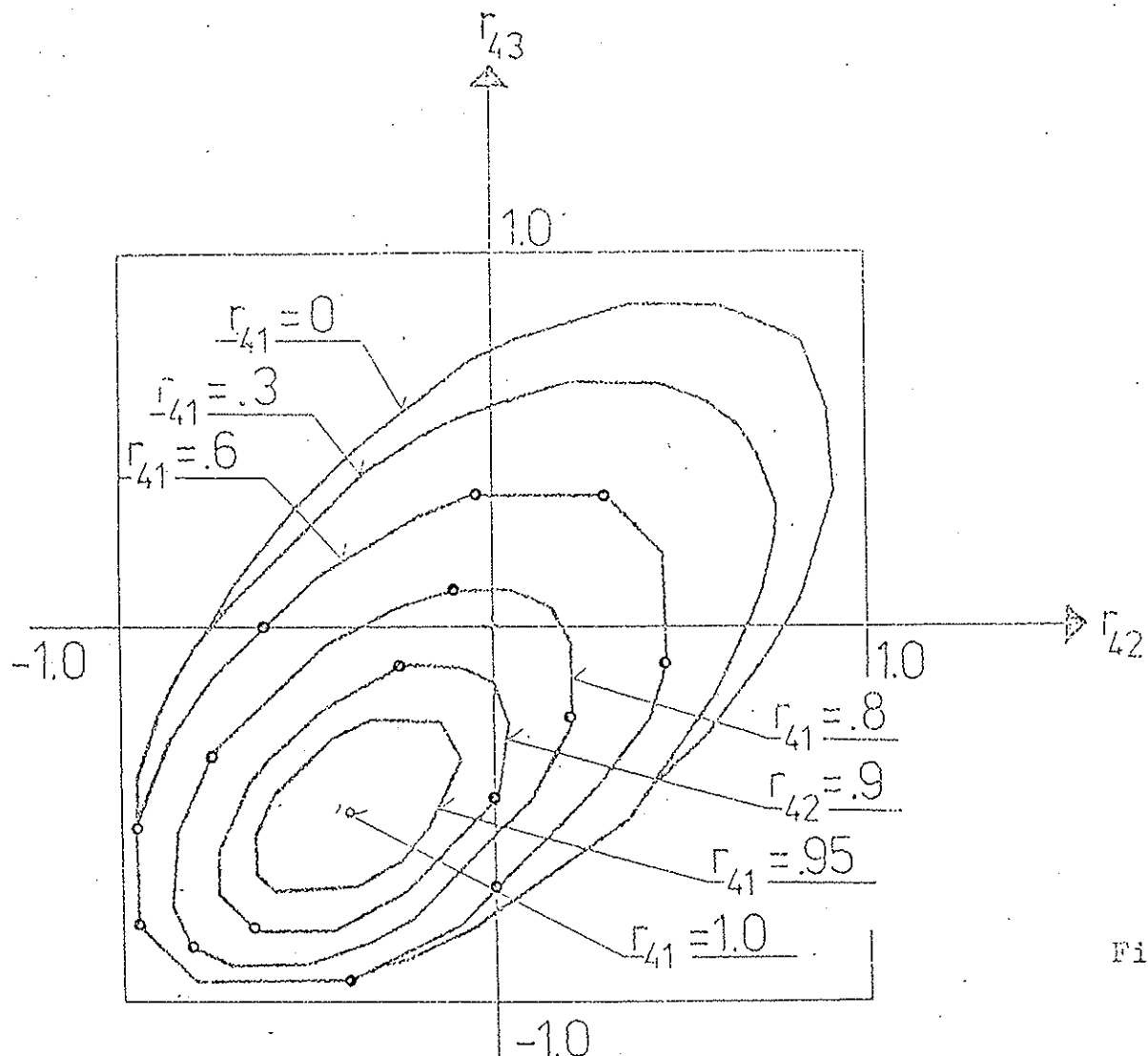


Fig. 3

Stochastic analysis

Almost all values appearing in the formulae presented in the fig. 1 and the fig. 2 are random variables. In the present paper we assume that the following five variables are random: R_c , ε_{pl} , ε_c^{ult} , R_t and R_e . This way ultimate strength of wooden cross-section ought to be treated as a function of five random variables. To start with the digital simulation it is necessary to built up the covariance matrix \underline{C} :

$$\underline{C} = \begin{pmatrix} s_{R_c}^2 & \cdot & \cdot & \cdot & \cdot \\ r_{12} s_{R_c} s_{\varepsilon_{pl}} & s_{\varepsilon_{pl}}^2 & \cdot & \cdot & \cdot \\ r_{13} s_{R_c} s_{\varepsilon_c^{ult}} & r_{23} s_{\varepsilon_{pl}} s_{\varepsilon_c^{ult}} & s_{\varepsilon_c^{ult}}^2 & \cdot & \cdot \\ r_{14} s_{R_c} s_{R_t} & r_{24} s_{\varepsilon_{pl}} s_{R_t} & r_{34} s_{\varepsilon_c^{ult}} s_{R_t} & s_{R_t}^2 & \cdot \\ \emptyset & \emptyset & \emptyset & \emptyset & s_{R_e}^2 \end{pmatrix}$$

Where: s - standard deviations, r_{ijk} - correlation coefficients. Each element of this matrix should be determined experimentally. However it is impossible to establish correlation coefficients r_{14} , r_{24} , r_{34} in a direct experiment. Some theoretical discussion [3, 4] enables to find a certain domain in which these coefficients should be situated. This domain is limited by the inequality (fig. 3):

$$1.3667 r_{14}^2 + 1.671 r_{24}^2 + 1.8785 r_{34}^2 + 0.3975 r_{14} r_{24} + 1.1345 r_{14} r_{34} - 1.8913 r_{24} r_{34} \leq 1$$

The remaining parameters of the matrix \underline{C} were established experimentally (see table 1).

Table 1.

	R_c	ϵ_{pl}	ϵ_c^{ult}	R_t	R_e
R_c	m= 62.3 s= 5.93 [MPa]
ϵ_{pl}	$r_{12}= .4044$	m= 5.15 s= 0.69 [%]	.	.	.
ϵ_c^{ult}	$r_{13}= .5056$	$r_{23}= .656$	m= 8.61 s= 2.44 [%]	.	.
R_t	?	?	?	m= 79.3 s= 20.2 [MPa]	.
R_e	\emptyset	\emptyset	\emptyset	\emptyset	m= 535 s= 27 [MPa]

Digital simulation procedure (fig. 4)

The random variables joint distribution was assumed to be normal (gaussian). The generation procedures were based on the proposals from the literature [5]. The numerical data presented in the table 1 are based on the experiments made by T.Dziuba [1]. One has to mention that the simulation procedure was conducted for arbitrary chosen coefficients r_{14} , r_{24} , r_{34} from the domain shown in the fig. 3, assuming that r_{14} is nonnegative.

Results and conclusions

The four levels of reinforcement were assumed, according to

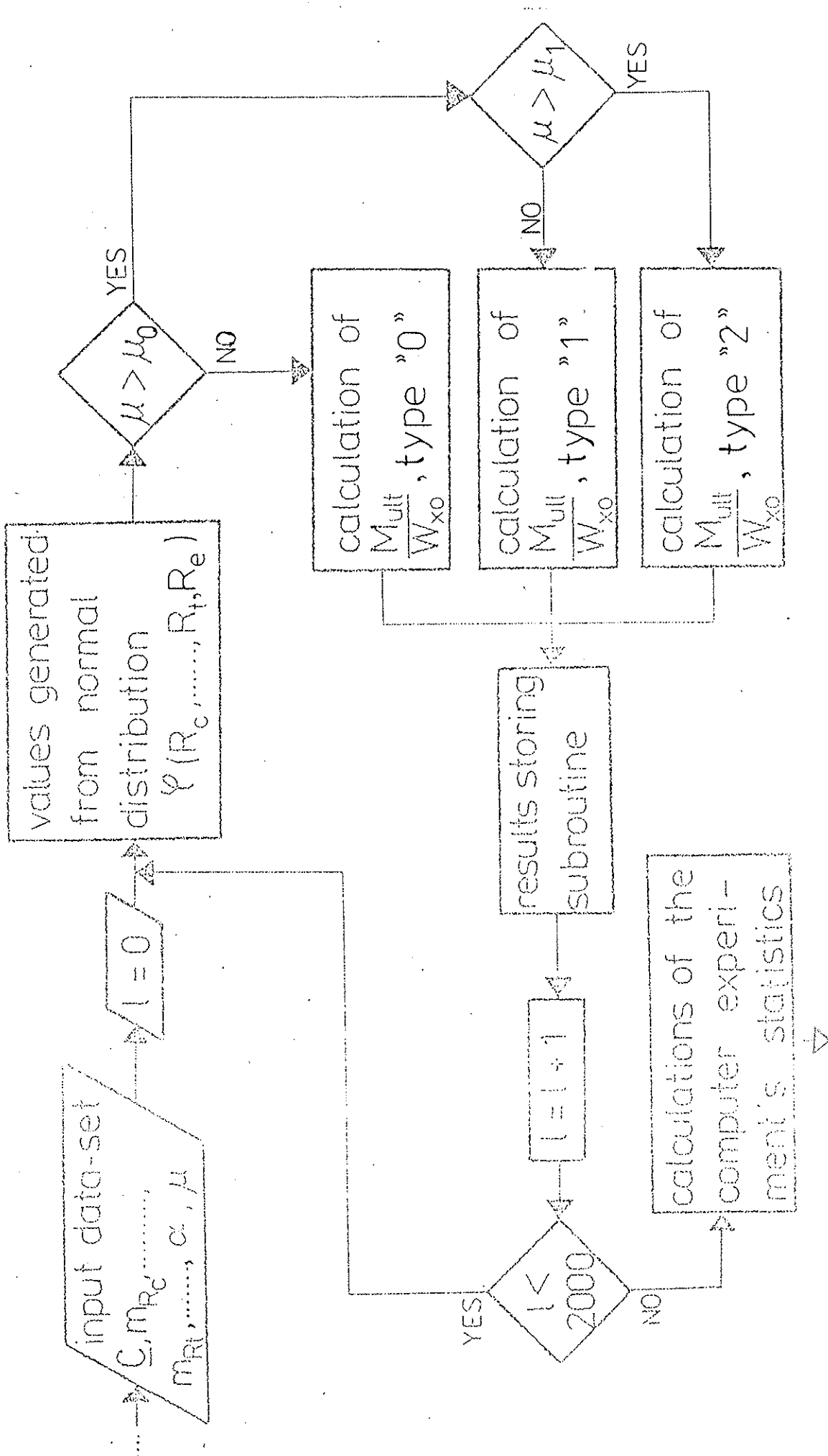


Fig. 4

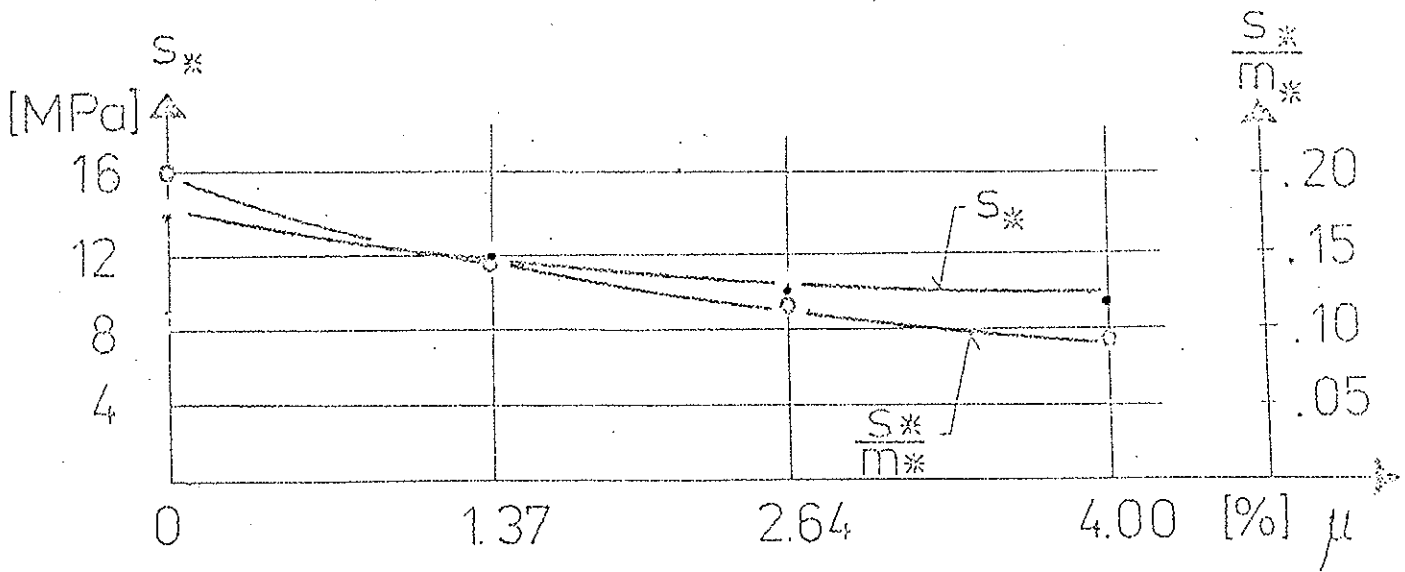
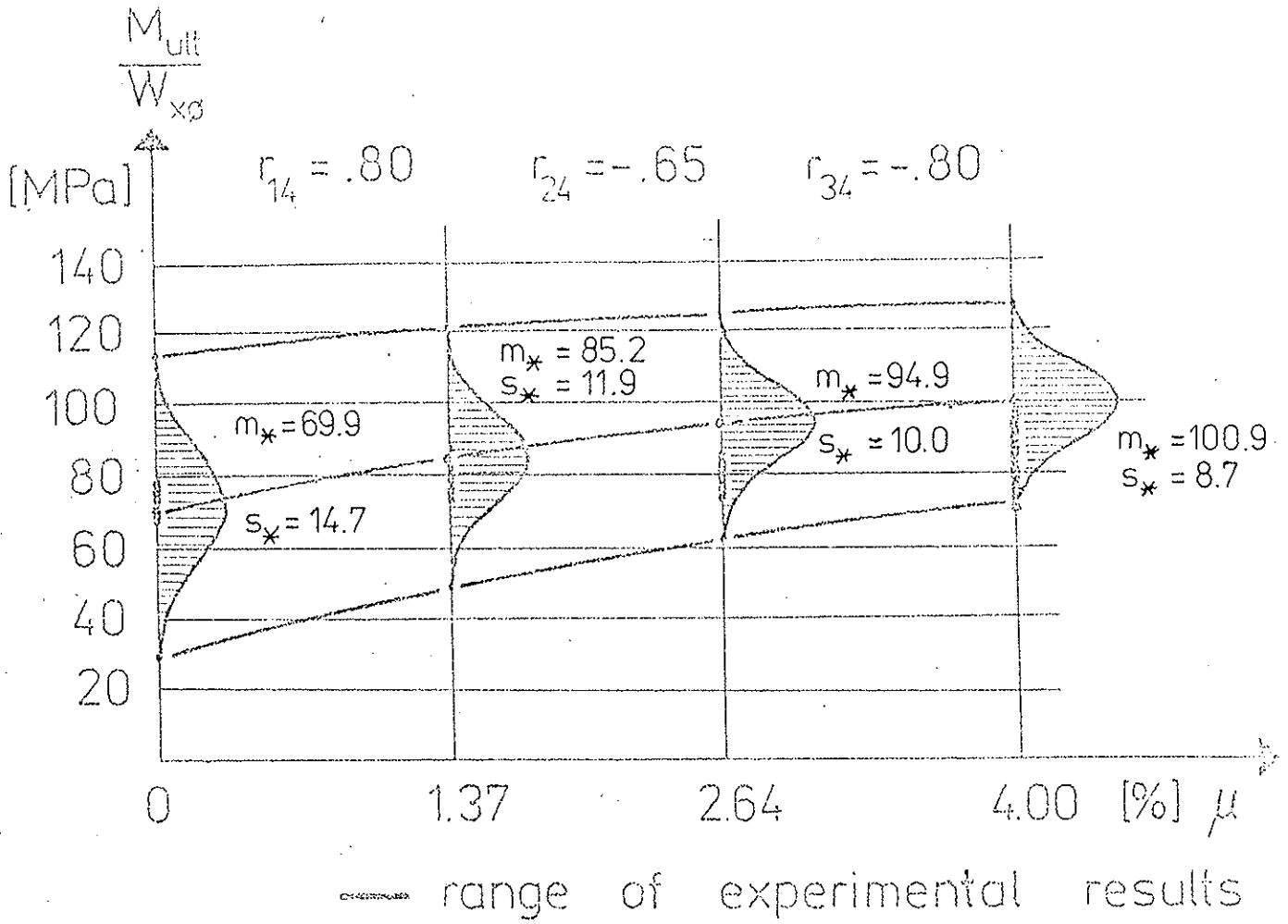
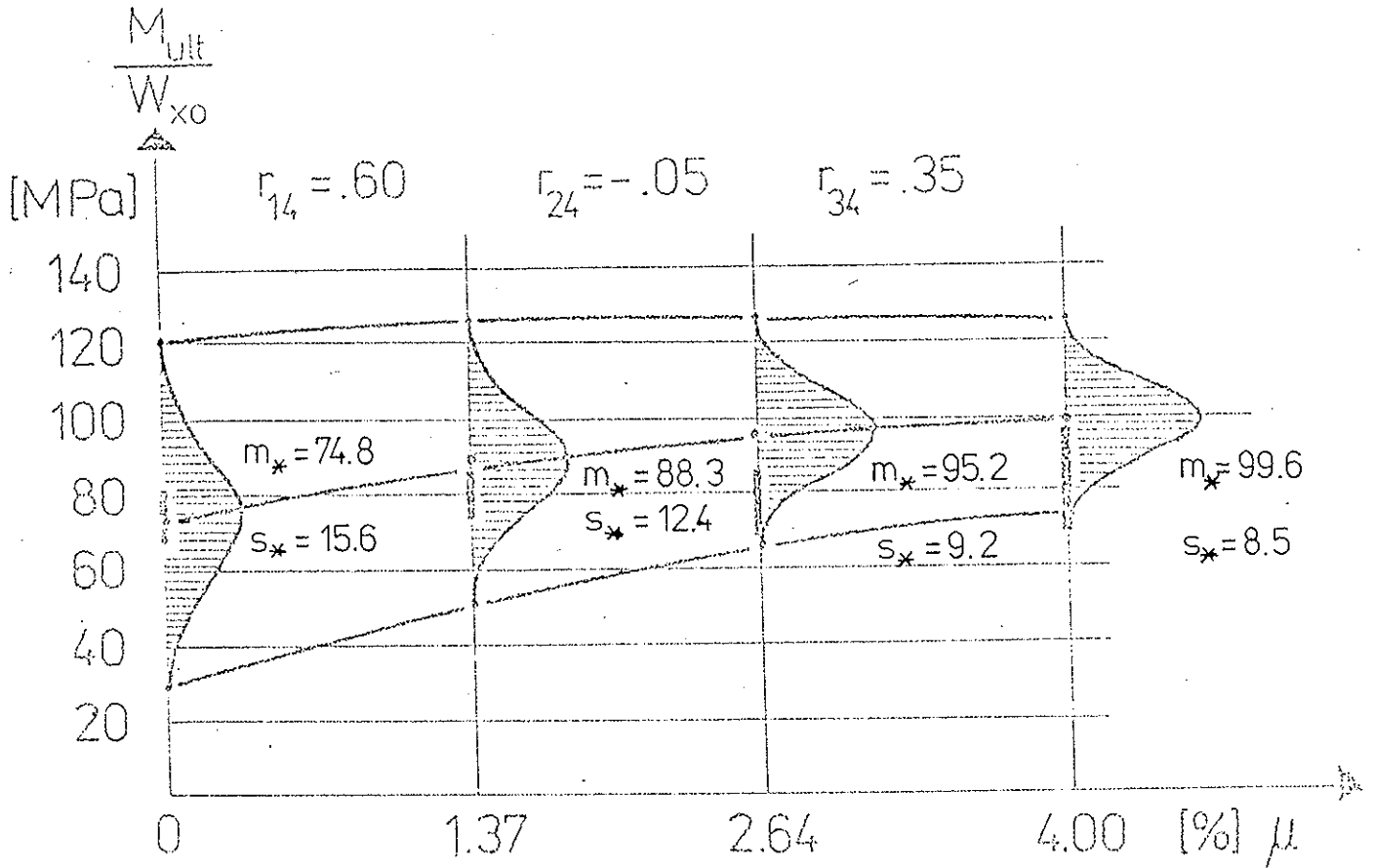


Fig. 5



range of experimental results

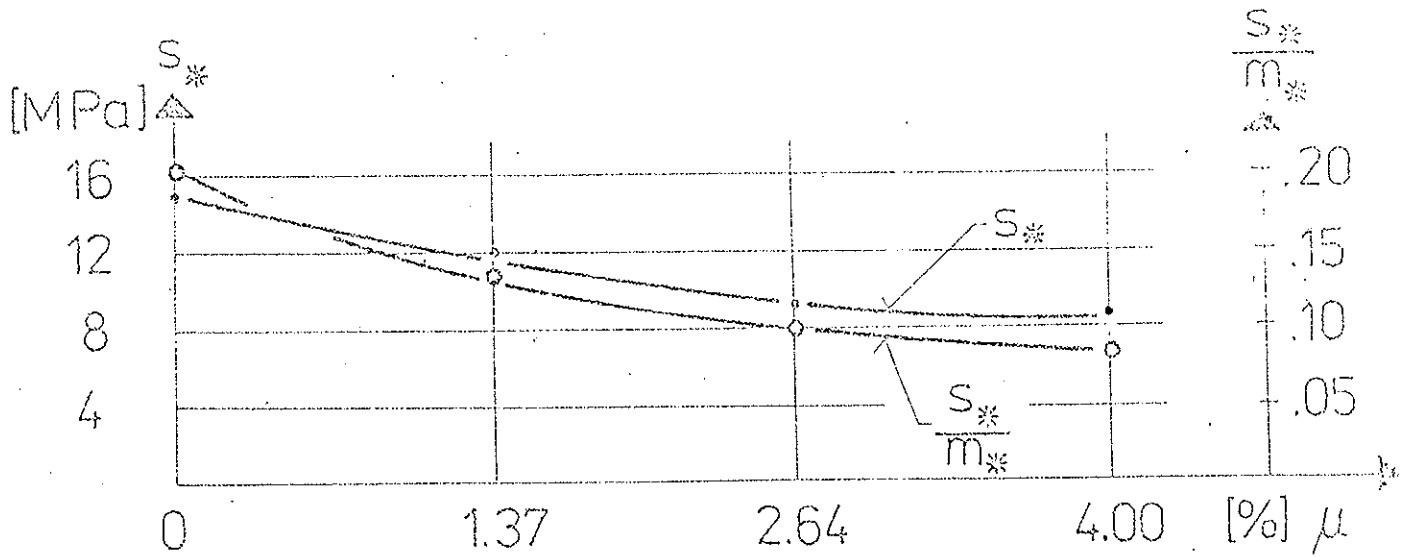


Fig. 6

the former experiments: 0%, 1.27%, 2.64%, 4.00% [1].

The 104 series of computer simulation with 2 000 sampling in each series were performed. In each series mean value " m_* " and standard deviation " s_* " were calculated.

The detailed results for a freely chosen values of the vector \underline{r} are illustrated in the fig. 5 and the fig. 6, where are also presented the results of laboratory experiments made earlier [1].

The results indicate that an increase of reinforcement amount causes an increase of ultimate strength mean value and - what is more important - a decrease of standard deviation.

It appears that the computer simulation method may be a very useful and costs saving substitution for real experiments. It seems to us that the ideas presented in the paper may be used in further studies on bearing capacity of wooden beams.

References

- [1] Dziuba T. 1980: Bearing capacity of reinforced wooden beams. Agricultural University of Poznań (doctoral thesis, in Polish).
- [2] Dziuba T. 1985: The ultimate strength of wooden beams with tension reinforcement. *Holzforschung und Holzverwertung* 37 (6) : 115 - 119.
- [3] Dziuba T., Ganowicz R. 1988: Random analysis of ultimate strength of wooden beams with tension reinforcement. *Int. Conference on Timber Engineering, Seattle USA, Proceedings Vol. 2: 848 - 854.*
- [4] Hauke J., Pomianowska J. 1987: Correlation relations from the point of view of nonnegative-definiteness of a block matrix, (in Polish). *Przegląd Statystyczny* 34, (3): 219 - 224.
- [5] Zieliński R. 1979: Random numbers generators. Generation and testing of random numbers on digital computers. WNT Warszawa.

INTERNATIONAL COUNCIL FOR BUILDING RESEARCH STUDIES AND DOCUMENTATION

WORKING COMMISSION W18A - TIMBER STRUCTURES

GUIDELINES FOR DESIGN OF TIMBER TRUSSED RAFTERS

by

H Riberholt
Department of Structural Engineering
Technical University of Denmark
Denmark

MEETING TWENTY - TWO

BERLIN

GERMAN DEMOCRATIC REPUBLIC

SEPTEMBER 1989

0. Preface

0.1 Scope

The intention of this paper is to describe some methods applicable for the design of plane timber trusses. The paper gives a proposal for a structure and setting for a standard for design methods. The content of the individual sections must be considered further.

Such methods may be divided into three operations, but these do not need to be independent and they will in general not just be carried out as one sequence from the top to the bottom.

1. Static analysis of a truss.
2. Strength verification of the timber.
3. Strength verification of the connections.

The paper concentrates on plane timber trusses with nail plate connections, and it proposes an analysis method which can be carried out with ordinary plane frame programs.

Meanwhile this does not imply that it only can be used for such a case. It can also be applied to trusses with other types of connectors, if the method is adapted to their static behaviour. Further some of the ideas can be employed in more general models, which for example take into account spatial behaviour, non-linearities in the material or in the geometry and so on.

At the past CIB-W18A meetings several papers have been presented and discussed. They have dealt with the following operations in the design of a truss.

1. Static analysis of a truss

/CIB W18 15-14-1 Guidelines for the static models of trussed rafters, 1982/. This paper proposes general static models, which to a large extent have been used in succeeding CIB-papers on trusses.

The CIB W18 papers /17-14-2, 17-14-3, 18-14-1, 19-14-1, 19-14-2/ deal with simpli-

fied analysis of trussed rafters, and they are based on models proposed in /15--14-1/. Since it recently was realized by CIB W18A that simplified methods are not required, the work in this area has stopped.

Presently a need is identified for guidelines for a plane frame analysis of trusses, so this paper will deal with this.

Further it has been assumed that loads on the trusses are specified by other authorities, so CIB W18 will not deal with it.

2. Strength verification of the timber

The main assumption is that this can be carried out as described in the timber codes, for example /CIB, 1983. Structural timber design code/. Some wellknown adaptation methods, such as effective column length, will be employed.

But besides this some effects special for timber trusses can be utilized. An example is pronounced moment peaks in the chords, which have been presented and discussed in /CIB—W18/17--14-2/. This present paper will deal with these special effects.

3. Strength verification of the connections.

The strength verification of the connections is described in /Noren, 1986. Design of joints with nail plates — Principles/ and in /Noren 1981/, which describes the methods in details.

It is suggested that these two papers shall define how the strength verification of a nail plate connection is carried out.

0.2 Available static analysis methods and their application.

The prevailing analysis methods in practice at present and in the near future are based on plane frame programs. Their assumptions are typical: Linear elasticity, first order method (geometric non-linearity is not considered), straight beam elements. Further some programs have the option that deformations in the joints can be modelled by a prescribed slip or a spring element. More refined assumptions are not common in practical programs according to a survey carried out recently, see /Smith 1989/.

It is a scope of this paper to set up guidelines so that analyses with such plane frame programs reflects the real static behaviour of the truss as well as possible.

One of the parameters in the static model of a truss is the principle modelling of the deformation in the connections. There exist the two possibilities: Prescribed slip and an Elastic spring element. A mixture of these two options could be favourable.

Prescribed slip

The prescribed slip method has as the basic idea, that the nail plate connections normally are dimensioned so that their strength capacity is fully utilized in the ultimate state. From tests the deformations (slips) are known at this state, and it is the impression that for a certain type of connection the slip close to failure has a fairly constant value independent of the size of the plate, see for example /Noren 1981/ section 2.6. So if this slip is prescribed in the connection the static model should reflect the actual static behaviour.

If the designer wish to reduce this slip he only has to give the plate an over-size. Therefore the guidelines should comprise a description of how the slip depend on the relative strength utilization of the nail plate connection.

The objections against this method are:

That the designer must for each load case know the size and direction of the forces and moments in the connections. This knowledge could arise from a previous analysis or pre-analysis in the iteration.

The slip is taken into account in a rather coarse manner.

Elastic spring element

Due to the non-linear behaviour of the connections the stiffness constant must be determined as a secant-modulus. Depending on whether the analysis is for the serviceability state or ultimate state the secant must be determined from a slip at a low or a high stress level.

The objections against this method are similar to those against the slip method:

The designer must for each load case know the relative strength utilization in order to determine the secant modulus. The stiffness matrix must thus be updated for each load case. Again this knowledge could arise from a pre-analysis.

The slip is taken into account in a rather coarse manner. For example the influence of the moment on the stiffness for a force will normally not be considered even though it is theoretically possible to set up such a relation.

Recommendation of methods taking into account the slip in the connections.

Since both methods have advantages and disadvantages it is recommended to let the user make his own choice. So the necessary information and values of slip and stiffness constants must be available. In /Noren 1981/ some values are given, but it seems necessary to have the values in the nail plate certificates too.

For some special or extreme cases it would be advantageous if the guidelines could state that slip can be disregarded. The degree of extremity is may be not so extreme, it could be sufficient to have a nail plate connection with a certain oversize (50%–100%).

1. GENERAL

1.1 Object

Static analysis of a truss.

The object of the guidelines is to constitute a basis for the static analysis of timber trussed rafters in the serviceability state or the ultimate state.

The guidelines concentrate on the analysis of plane timber trusses with nail plate connections by means of practical available plane frame programs. But the methods can too be applied to trusses with other types of connectors if the method is adapted to their static behaviour. Further they can be employed in more general models, which for example take into account spatial behaviour, non-linearities in the material or in the geometry.

Strength verification of the timber

Further, the paper describes how there can be dealt with some effects, which are special for timber trusses and which are not dealt with in the timber codes such as /CIB 1983/.

1.2 Definitions

Bay:

Structure (timber beam) between two neighbouring nodes.

Beam element:

An element, which models a timber part.

Connections:

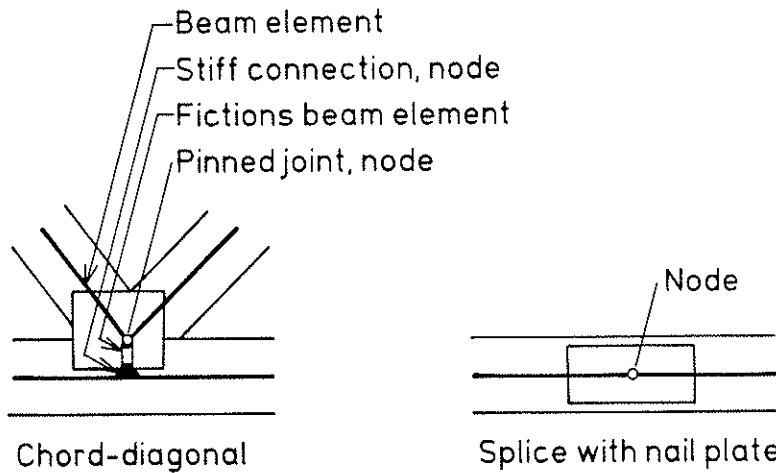
Domain where timber parts and/or nail plates are in contact in such a way that forces may be transferred between the parts.

Fictitious beam element:

Beam element, employed in connections in order to model their static behaviour.

Node:

Intersection point of system lines of beam elements.



Spring element:

An element, which can be used to model the mutual translation or rotation between timber parts in a connection.

2. THE FRAME MODEL

2.1 General description of the elements and the methods of the model

The frame model is build up by means of some elements. Straight beam elements model the timber parts, fictitious beam elements model some constraints (ties) in or static behaviour of the connections and also spring elements model the elastic behaviour of the connections.

All the elements can be linear elastic, but elements based on material non-linearity will with realistic material properties reflect reality better.

The deformation in the connections can also be considered by means of a prescribed slip or by means of a combination of prescribed slip and elastic spring elements.

Geometric non-linearity (column effect) can be disregarded by the frame analysis if it is taken into account in the strength verification of the members.

If a geometric non-linear frame program is used for the analysis then the stiffness parameters shall be given the design values for the actual conditions and imperfections shall be considered.

2.2 Description of the elements

2.2.1 Beam elements

The timber parts are modelled as straight beam elements. These shall allow for the deformations originating in axial strain plus curvature of the timber parts.

Geometry

As a principal rule the system lines of the beam elements shall coincide with the centre of gravity of the timber parts. For the chords this shall always be the case.

In the diagonals the system lines of the beam elements do not need to coincide with the centre of gravity of the timber parts. However, the system lines shall lie within the cross section of the timber. In the case that there is not coinciding this must be taken into account in the strength verification, for example by adding an eccentricity moment to that of the beam element.

Stiffness constants

The stiffness constants EA and EI are calculated based on the actual timber dimensions and qualities.

Degrees of freedom in the coupling to other elements

Connections between beam elements are modelled in the following ways depending on the static behaviour of the real connection if such one exists.

Pinned connections

Pinned connections and prescribed slip(s)

Completely stiff

Completely stiff and prescribed slip(s)

Fictitious beam elements

Spring elements

Spring elements and prescribed slip(s)

Pinned connections

A pinned connection can be used if the rotational stiffness S_{θ} of the connection between the two timber parts is essential smaller than that of the connected timber parts. That is

$$S_{\theta} \ll 3 EI/\ell$$

where EI Bending stiffness of the timber part
 ℓ Bay length for the timber part

The rotational stiffness of the connection must be evaluated at the actual stress level. This means that for a nail plate connection fully stressed by the internal forces there is no moment capacity and therefore no essential rotation stiffness.

In the model the position of the pinned connection shall reflect the load transfer in the connection. Annex 1 gives some examples of the position for different types of nail plate connections.

Further the deformations of a connection can be modelled by a prescribed slip between the beam elements connected to the node in the connection.

Completely stiff connections

Beam elements modelling the very same timber part are connected completely stiff.

A beam element can also be connected completely stiff to the node in the connection if the rotational stiffness S_{θ} of the connection between the two timber parts at the actual stress level is larger than that of the connected timber part. That is

$$S_{\theta} > 3 EI/\ell$$

where EI Bending stiffness of the timber part
 ℓ Bay length of the timber part.

Further, for certain connections the static behaviour tends to make them rotational stiff. For example where compression forces are transferred by contact. In such cases completely

stiff connections can be assumed if the nail plate connection is oversized by a factor k_{σ} , i.e. that the strength verification is carried out for forces and moments increased by the factor k_{σ} .

The rotational stiffness must be verified by tests or similar. In annex 1 the oversize factor k_{σ} is given for some examples.

Further, the deformation in the connection can be taken into account by means of a prescribed slip.

Fictitious beam elements and spring elements

Beam elements are normally connected to fictitious beam elements by means of a pinned connection.

The connection to a spring element shall be completely stiff since the total slip is modelled by that of the spring element.

The modelling of these elements and the consideration of slip in the connections is described in other sections.

2.2.2 Fictitious beam elements

A fictitious beam element can be employed to reflect the static behaviour of a connection. It can thus be used to model some constraints in the connections, for example originating in contact between timber parts or ties from nail plates. The use of fictitious beam elements is illustrated in Annex 1.

Geometry

The system line of a fictitious beam elements shall as well as possible coincide with the force transfer path

Stiffness Constants

The result of the analysis is normally not sensitive to the values of the stiffness constants EA and EI. The reason why is typical that the fictitious elements are short. So frequently

they can be assigned stiffnesses of approximately the same order as that of the adjacent beam elements.

The axial stiffness constant EA can be calculated from the stiffness of a may be block of wood subjected to compression or a may be nail plate subjected to tension.

The bending stiffness constant EI can be determined in a similar way. If the fictitious beam element is connected to both nodes by pinned joints the value of EI may be chosen arbitrarily.

Degrees of freedom in the coupling to other elements

Generally the coupling should be modelled by a pinned connection. But completely stiff connections can be used if justified by methods similar to those described in section 2.2.1.

2.2.3 Spring elements

A spring element can be employed to model elastic slip, either relative translation or rotation, in a connection.

Geometry

The spring element shall be placed in the middle of the connection. It shall in no case be placed outside the connection area.

Stiffness constants

The values of the stiffness constants shall be based on measurements. They shall be determined on secant moduli reflecting the actual stress level in the connection, and they shall consider creep of the connection.

In a fully stressed connection the secant modulus shall be based on the stress level defined in section 2.3.3. If the stress level is lower then this can be taken into account by an increase in the secant modulus.

Comment:

Section 2.6 of /Noren, 1981/ gives some guidelines for the values of the stiffness constants.

It is acceptable to assume, that the stiffness for the two relative displacements and the relative rotation are independent of each other. This means for example that the stiffness for a relative displacement in one direction can be assumed independent of partly the force in the other ortogonal direction, partly the moment.

Degrees of freedom in the coupling to other elements

The spring elements are normally coupled completely stiff to the nodes.

2.3 Description of the analysis methods.

A static model consists of the elements described in section 2.2, and they are connected in accordance with the given guidelines. In this section guidelines are given for the loading, the support and the consideration of the slip in the connections.

Since the purpose of the static analysis is different for the serviceability state and for the ultimate state there can be differences in the approximations and therefore different static models for the two states.

2.3.1 Loadings

The trusses must be analysed for the loads provided by the relevant codes. In principle, the truss must be subjected to the loads as they act in reality. For example, in a roof with purlins, the truss must in principle be loaded by concentrated forces.

A row of concentrated forces may be equated to a distributed line load if the difference between the moments from the two loading cases is less than 10%, or if it is on the safe side.

Note: For lattice trusses the concentrated loads from purlins with equidistant distances can be equated with a distributed load if the distance between the purlins is less than 40% of the bay length.

Larger concentrated forces, including reactions, must be applied where they act in reality.

For lattice trusses it is acceptable to undertake the strength dimensioning for the load case "dead load + man load F" in the following way.

$$\sigma = \frac{1}{4} \frac{F\ell}{W} \leq f_m$$

where ℓ is the horizontal bay length. (i.e. the small normal forces are neglected).

2.3.2 Supports

Unless the supports are designed specially they can be assumed to behave as pinned joints positioned in the middle of the support areas.

For trusses with both top and bottom chords, it can be assumed that vertical loads are taken by one firm simple support and the other supports being joints on rollers. For horizontal load all the supports can be assumed to behave as pinned joints on rollers but kept in position by springs, which are assigned stiffnesses, corresponding to that of the supporting structures.

2.3.3 Modelling the slip in the connections

The slip in the connections shall at least be considered in those connections, of which the slip is essential for the distribution of the internal forces and moments. Annex 2 contains examples, where it for some truss types is estimated necessary to consider the slip in some of the connections.

The slip in a connection can be considered by a prescribed slip, a spring element or a combination of these two methods.

The prescribed slip or the secant modulus of the spring element shall for each load case be determined from the stress level which actually occurs in the connection.

But if the static analysis is used for the strength verification it is acceptable to use values valid at a constant stress level equal to 60% of the characteristic strength of the connection.

Creep shall be considered by the determination of the slip or the secant modulus.

Guideline:

For stress levels deviating from 60% the relation between stress and slip can be determined from

$$\text{Stress level} = \frac{\tau}{f_k} = 0.37 \frac{u}{u_{60}} \left(2 - 0.37 \frac{u}{u_{60}} \right)$$

where

- τ Shear stress between nail plate and timber
- f_k Characteristic strength of τ
- u Slip at the stress level
- u_{60} Slip at a stress level of 60%

If there is used a combination of the two methods the employed prescribed slip and spring stiffness shall be determined so that the total slip in the model is equal to the real slip.

3. STRENGTH VERIFICATION

3.1 Strength verification of the timber parts

The strength verification of the timber parts shall be carried out as described in the Timber Codes, for example /CIB, 1983/.

If the frame analysis is geometric non-linear (internal forces and moments are determined in the deflected state) then the column effects in the rupture criteria of the Timber Codes can be disregarded. But the effects of initial imperfections shall be considered.

In the following sections there are given guidelines for how to deal with some effects, which are special for timber trusses, and which are normally not considered in the Timber Codes.

3.1.1 Reduced column lengths

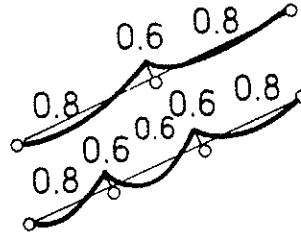
For bars or beams over one bay and without special stiff connection to the nodes the reduced column length is equal to the length between the nodes.

For continuous beams, i.e. chords, with a distributed lateral load of constant intensity along the total length, the following reduced column lengths are valid. A continuous beam is a beam either without splices over several bays or with splices positioned so that the compressed beam would be stable even if all the splices behaved as pinned joints. It is further assumed that the splices are designed to be completely stiff according to section 2.2.1.

For continuous beams with lateral load but without essential end moments the following reduced column lengths are valid.

- In an outer bay : $0.8 \cdot \text{bay length}$
- In an inner bay : $0.6 \cdot \text{bay length}$
- At a node : $0.6 \cdot \text{largest adjacent bay length}$

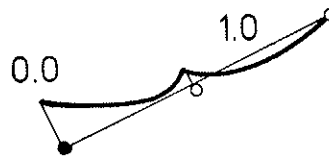
Reduced column lengths related to the bay lengths or the largest adjacent bay length.



For continuous beams with lateral load and an essential end moment the following reduced column lengths are valid.

- Beam end with moment : 0.0, i.e. no column
- In the bay second from the end : 1.0 bay length
- Remaining bays and nodes : As described above

Reduced column lengths related to the bay lengths.



For continuous beams without lateral load (centrally loaded columns) the reduced column lengths may be assumed equal to the bay length.

3.1.2 Strength verification of cross sections at a moment peak.

For the strength verification of normal stresses in a cross section at a distinct moment peak the bending strength can be increased by a factor k_m .

Continuous timber members

For timber members continuous over several bays and loaded laterally the bending strength

can be increased by a factor k_m which depends on the Coefficient of Variation, C.V., of the bending strength. (see Annex 3 for justification.)

$$k_{m,p} = \begin{cases} 1 + 0,4 \frac{C.V.}{30\%} & \text{for } C.V. \leq 30\% \\ 1.4 & \text{for } C.V. > 30\% \end{cases}$$

Timber members with an end moment

For a timber member with an end moment, for example originating in an eccentricity, the bending strength can be increased by a factor

$$k_{m,e} = \begin{cases} 1 + 0,4 \frac{C.V.}{20\%} & \text{for } C.V. \leq 20\% \\ 1.4 & \text{for } C.V. > 20\% \end{cases}$$

(For justification, see /Riberholt, 1980/).

3.2 Strength verification of the nail plate connections

The strength verification of the nail plate connections shall be carried out as described in /Noren, 1981/ and /Noren, 1986/ with the mechanical parameters given in the certificate of the nail plate type.

4. REQUIREMENTS TO THE PRODUCTION OF THE TRUSSES.

In order to secure that the static behaviour of the truss is as assumed and that it can stand normal handling the following requirements are set up.

The timber parts shall touch each other in at least one point. Under the nail plates the gap in the joint must not exceed 2 mm. For compressed connections, which are assumed completely stiff, this gap shall not exceed 1 mm.

*) The position of the nail plates must be within the tolerances ± 5 mm and the effective anchorage area must never be less than 90% of the necessary.

*) The nail plates must be pressed close to the timber in 75% of the plate area. The gap between nail plate and timber must never exceed 2 mm, or what is specified in the Certificate of the nail plates.

After the pressing of the nail plates there must in the timber not occur essential splitting or crushing marks.

The trusses must be marked with text showing:

Maximum truss distance c-c mm

Lateral bracing of lattice, if any

Support area of the bottom chord with a tolerance of ± 10 mm

The connections shall be capable of resisting the forces and moments during transportation, storage and erection. For example, when the truss lies down the splices in the chords and the ridge connection shall be capable to resist the moments or they must have a moment capacity equal to that of the chords.

5. REQUIREMENTS TO THE FINISHED STRUCTURE.

Note. This chapter is not completed, but it should contain requirements of the same type as those below.

It must be secured that in the finished structure the trusses have a behaviour equal to that assumed in the static model.

A proper lateral bracing must be established during the erection and in the finished structure (Requirements, proposals).

If there are partitions right below the bottom chord it must be secured that this do not break when the truss deflects. This may be assumed fulfilled when ...

*) Clauses may be omitted here if they are given elsewhere.

References

CIB, 1983. Structural timber design code.

Johnson, A.I. 1953. Strength, safety and economical dimensions of structures.

Madsen, B. & A.H. Buchanan, 1985. Size effects in timber explained by a modified weakest link theory. CIB-W18/18-6-4/.

Noren, B. 1981. Design of joints with nail plates, CIB-W18/14-7-1/.

Noren, B. 1986. Design of joints with nail plates – Principles, CIB-W18/19-7-7/.

Riberholt, H, 1980. Strength distribution of timber structures. IUFRO, Oxford.







Riberholt, H. 1982. Guidelines for static models of trussed rafters, CIB-W18/15-14-1/.

Smith, Peter, 1989. Capabilities of, and methods used in existing MiTek (Europe) software for the analysis and design of trussed rafters.

Annex I. Connection models.

The annex gives some examples of the modelling of connections. These can be modelled either as pinned joints or as completely stiff connections if some requirements are fulfilled. For some connections a sufficient requirement is that the nail plate connection is oversized so that it has a capacity to transfer the actual internal forces and moments increased by a factor k_{σ} . The values of k_{σ} are given for some connections, for which it may be relevant to employ completely stiff connections in the static model.

Symbols

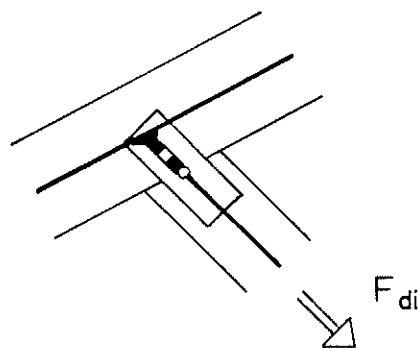
	Timber member
	Nail plate
	System line for beam elements modelling timber members
	Fictitious beam element
	Pinned joint
	Completely stiff connection

A1.1. Connections between 2 timber parts

Chord–diagonal

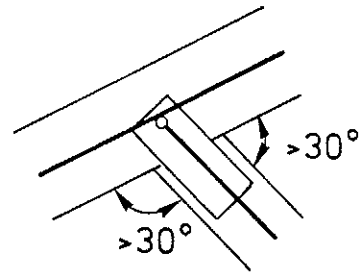
$$F_{di} > 0 \quad k_{\sigma} = 1.8$$

$$F_{di} \leq 0 \quad k_{\sigma} = 1.4$$



Chord–diagonal

No essential shear force in the diagonal

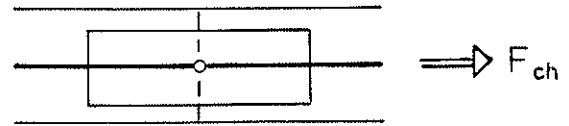


Splice

$$F_{ch} > 0 \quad k_{\sigma} = 1.8$$

$$F_{ch} \leq 0 \quad k_{\sigma} = 1.4$$

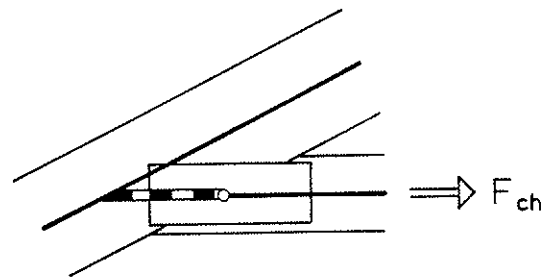
For a pinned joint in compression, $F_{ch} < 0$, the plate connection shall be capable to transfer at least 2/3 of the total force.



2 Chords

$$F_{ch} > 0 \quad k_{\sigma} = 1.8$$

$$F_{ch} \leq 0 \quad k_{\sigma} = 1.4$$

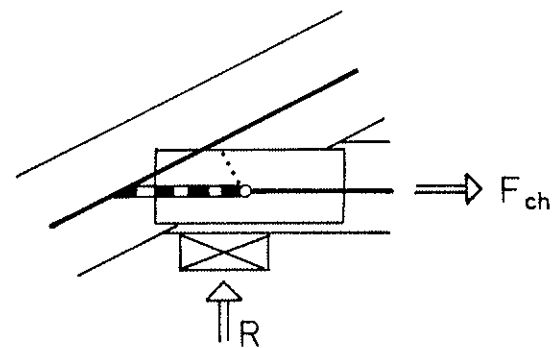


Heel joint, centric support

The values of k_{σ} are as given for 2 chords.

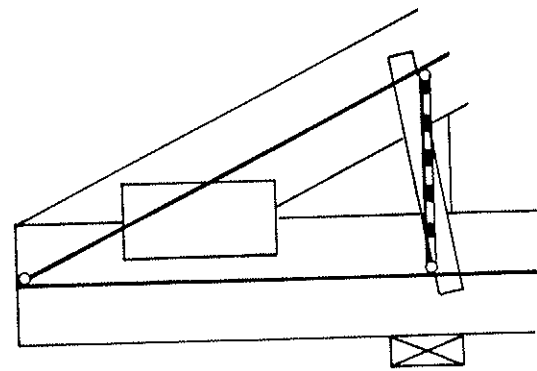
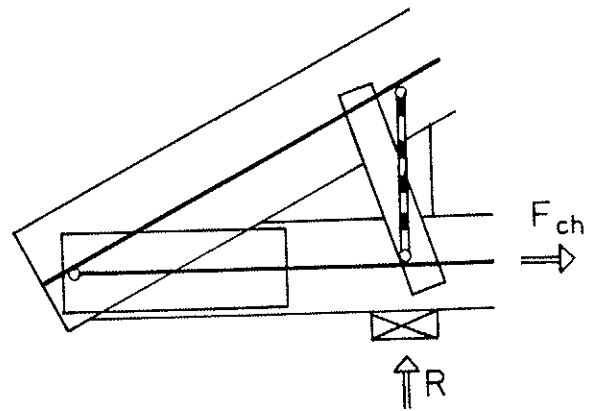
But if $F_{ch} > 0$ and $R > 0$ $k_{\sigma} = 1.4$

Further the fictitious beam member can be placed as the dotted line.



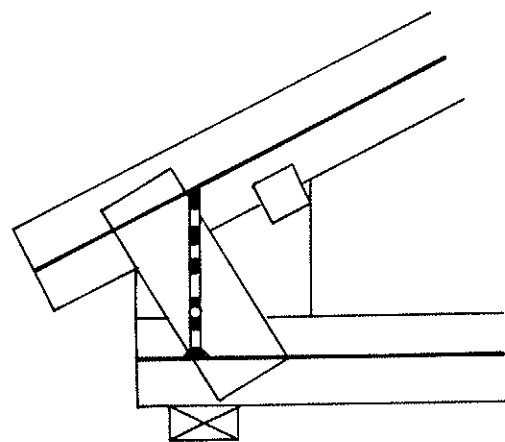
Heel joints, cantilevered

Above the support area there must always be contact between the top and bottom chord, for example by a wedge. If the height of the wedge h_w is larger than 200 mm, the grain direction in wedge should be perpendicular to the chord. The wedge must be kept in position by nail plats.



Heel joint with a high wedge

If the joint is designed to transfer the moment then the connection can be modelled as completely stiff.

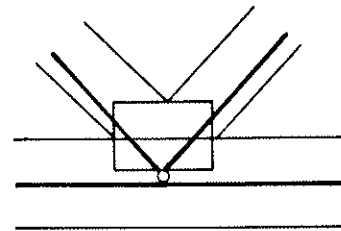
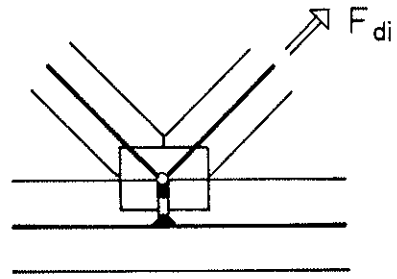


A1.2. Connections between 3 timber parts

Chord–diagonals

$$F_{di} > 0 \quad k_{\sigma} = 1.8$$

$$F_{di} \leq 0 \quad k_{\sigma} = 1.4$$



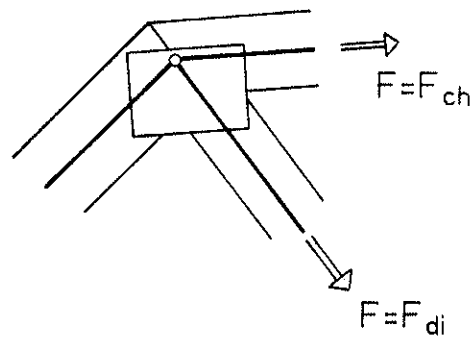
The nail plates must be capable to transfer the eccentric forces.

Inclined chords–diagonal

The connection between the node and the beam (timber) member can be modelled completely stiff. Depending on the direction of the force in the member:

$$F > 0 \quad k_{\sigma} = 1.8$$

$$F \leq 0 \quad k_{\sigma} = 1.4$$



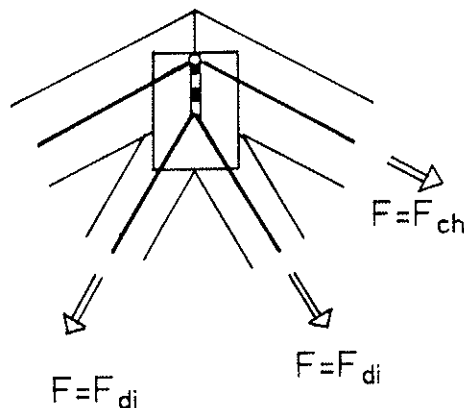
A1.3. Connections between several timber parts.

The connection between a node and a beam element can be modelled completely stiff. Depending on the direction of the force in the member: The required oversize factor k_{σ} is given in the following.

Ridge connection

$$F > 0 \quad k_{\sigma} = 1.8$$

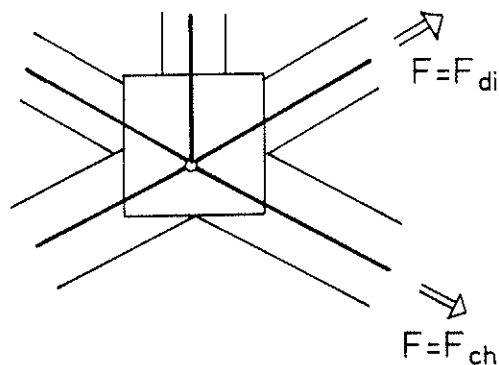
$$F \leq 0 \quad k_{\sigma} = 1.4$$



Connection in a scissor truss

$$F > 0 \quad k_{\sigma} = 1.8$$

$$F \leq 0 \quad k_{\sigma} = 1.4$$

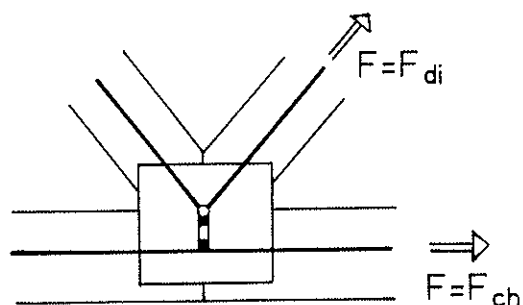


Chord splice – diagonals

The figure shows a model where the nail plate connection to the two chord parts has sufficient strength to transfer force and moment.

$$F > 0 \quad k_{\sigma} = 1.8$$

$$F \leq 0 \quad k_{\sigma} = 1.4$$



Annex 2. Connections where slip shall be considered.

The slip in the connections shall be considered when it is essential for the distribution of the internal forces and moments.

Some truss configurations are sensitive to slip in certain connections, so typical it is sufficient to model the slip in those connections. The connections in question are typical those in which a slip will cause large curvatures in timber parts.

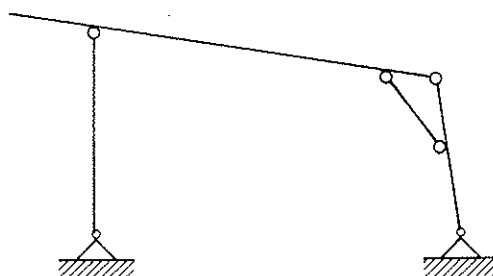
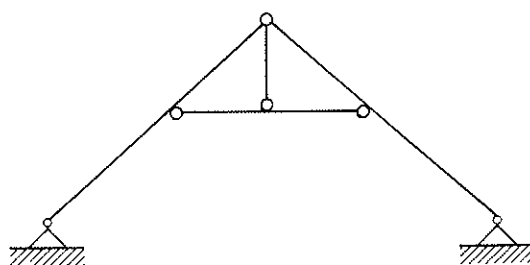
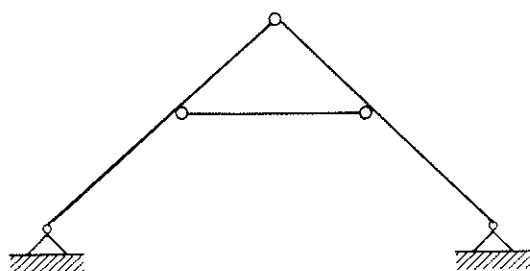
The following sections give examples of truss configurations and connections in which the slip shall be considered if nail plates are employed as connectors. It is typical that the connections in question are:

Hell joints: Slip in the chord direction.

Splices: Rotation and translation in the chord direction.

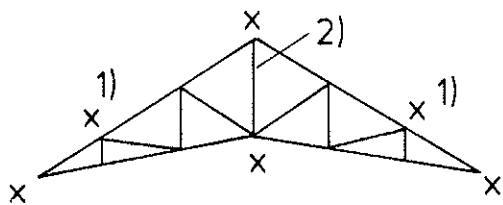
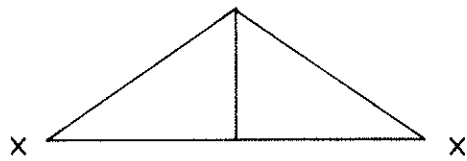
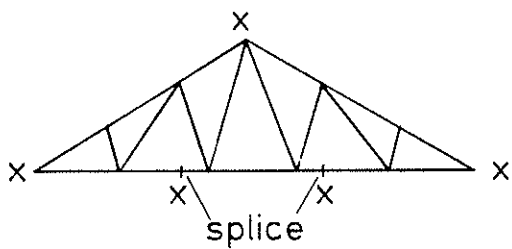
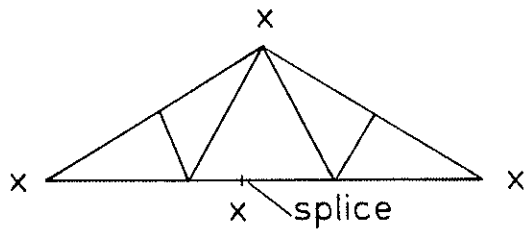
Ridge connections: Slip in the chord direction.

A.2.1. Truss configurations not sensitive to slip.

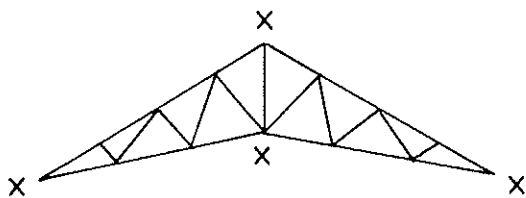


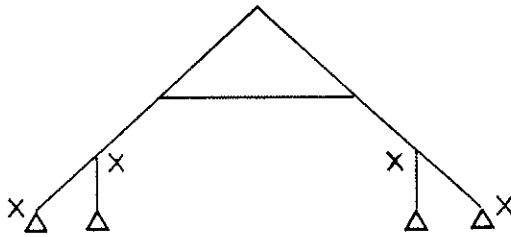
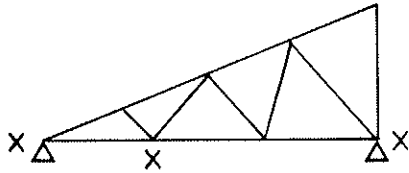
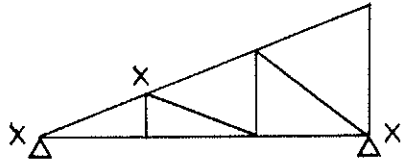
A.2.2. Truss configurations sensitive to slip.

The slip shall at least be considered in the connections marked with x.



Slip shall be considered:
1) Between chord and diagonal.
2) Vertical slip.





Annex 3. Derivation of:

Effects of the distribution of the internal forces and moments.

Since the normal force frequently is constant along the bay length it is suggested to disregard the distribution effect on the tensile strength and the compression strength.

Shear is normally not decisive for the design of trusses so it is suggested to employ strength values as prescribed by the actual Timber Code.

But for the moment stresses it is typical that they can vary along the length of the timber parts in other ways than assumed at the determination of the bending strength values given in the Timber Codes. Since the bending capacity of a timber part depends on the distribution along the length it is suggested to take this effect into account.

The research carried out in this area is scattered and how to deal with this effect has hardly found its final method of description. For example research is going on at Trätekt Stockholm.

Research carried out

The dependency between the bending strength and the distribution of the internal moment has been investigated by /Madsen & Buchanan, 1985/. The employed theoretical description was Weibull's Weakest Link. Unfortunately, the estimated values of the shape parameter k varied quite a lot, an estimation based on a slope analysis when the length was varied gave k -values in the range of 2.9 to 7.8, and another estimation based on different load configurations gave k -values in the range of 1.3 to 7.2. It is expectable to have a variation in k between different species and grades because k is related to the Coefficient of Variation. The authors suggest a k -value of 3.5, which should give sufficient precision for engineering purposes for the type of timber in question (Canadian). $k = 3.5$ correspond to a Coef. Var. = 0.32 in a 2-parameter Weibull distribution.

In /Riberholt, 1980/ this dependency between bending strength and M -distribution has been investigated too. Here it is chosen to describe the strength of timber by a probability distribution of cross sections with such defects. The figure below shows the probability distribution for 3 beams with different moment distributions.

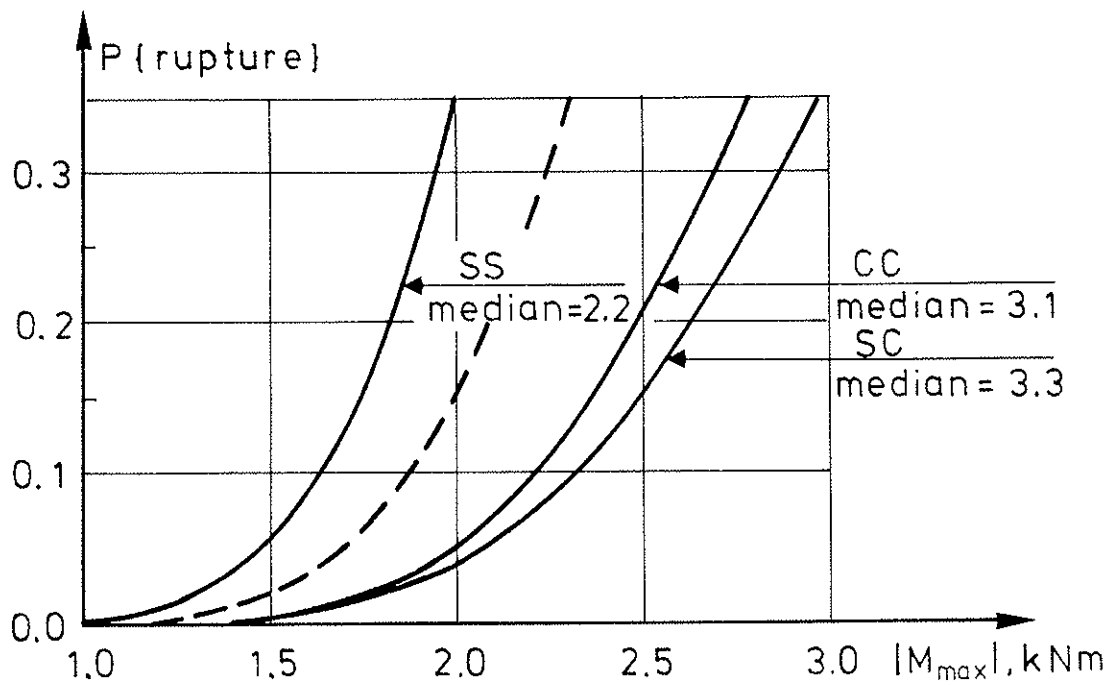
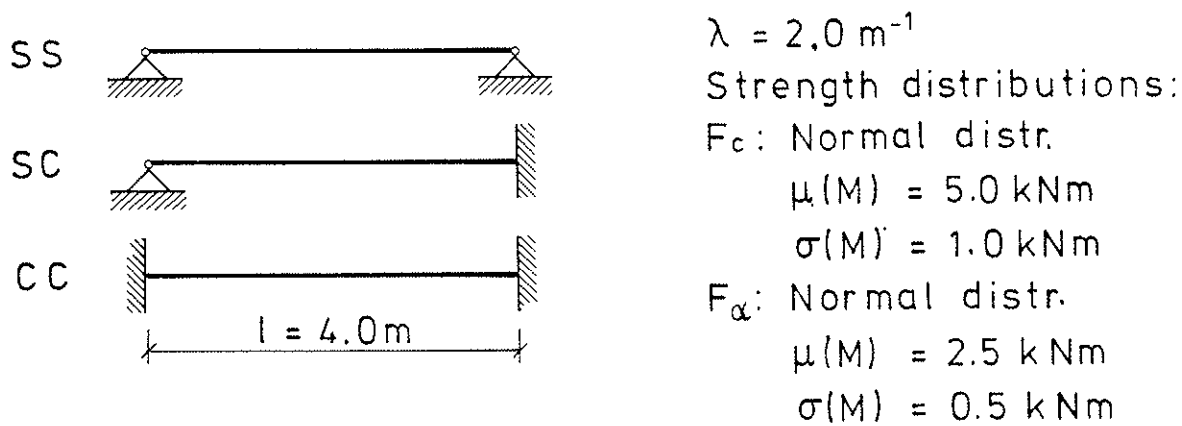


Figure 8.1 Timber beams with different supports, simple supported or clamped. The dotted lines represent F_α .

It should be noticed that the difference between the beams which are supported Simple-Clamped and Clamped-Clamped is relatively little, and for practical purposes it can be disregarded.

In /Johnsen, 1953/ there is in figure 13 given a visualization of how the relative mean bending strength varies with the Coef. Var. For a 2-parameter Weibull distribution the 5th-percentile will vary in the same manner.

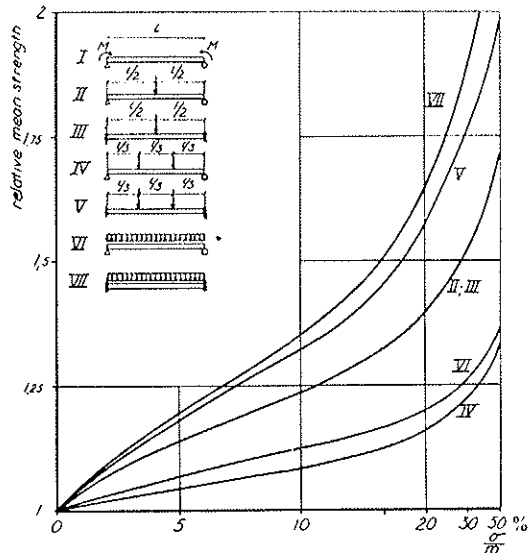


Fig. 13. Relation between the mean value of the strength (expressed in terms of the maximum stress) at loads of various types and the strength at a constant moment (type of load No. I). This relation has been determined in accordance with the distribution of extreme values of the type No. II ($x_1 = 0$). The comparison relates to beams of equal dimensions having the same value of $\frac{\sigma}{m}$. If the material is perfectly brittle, the term "strength" refers to the total strength. If the material is perfectly plastic, the term "strength" refers either to (a) that strength which corresponds to yielding

at the weakest point or to (b) that strength which corresponds to yielding in the first member. In statically determinate systems, the strength (b) corresponds to the total strength. [If the material is plastic, it is assumed in these cases that either (a) the strength in the elementary unit volumes or (b) the strength corresponding to yielding in a cross section is distributed in conformity with the distribution of extreme values of the type No. II ($x_1 = 0$).]

Comparisons and suggestions

In order to illustrate the effect of using different theoretical descriptions the ratios between the strength at max. moment of a simple-simple and clamped-clamped beam loaded with a distributed load has been calculated based partly on a Poisson Proces, figure 8.1, partly on a Weibull distribution, figure 13. The two ratios are 1.35 and 1.37 respectively for the 5-percentiles, so this difference is negligible for a coefficient of variation of 0.20.

By using the Weibull theory in /Johnson, 1953/ the ratio between the strength of a reference beam and any other beam can be calculated. As reference beam is chosen a simple supported beam with 2 concentrated forces in the third points. Table A3.1 gives the ratios.

Table A3.1

Ratios $f_m/f_{m,ref}$ for timber beams with different supports and load configurations.

Support: Simple or Clamped	Load type	Coefficient of variation:			
		0.10	0.15	0.20	0.30
SS	2 concentrated $a = 1/3\ell$	1	1	1	1
SS	Distributed	1.04	0.14	1.03	1.03
CC	2 concentrated $a = 1/3\ell$	1.23	1.30	1.35	1.44
CC	Distributed	1.25	1.35	1.14	1.53

It can be seen that the difference in the ratios for different load types are small as long as the moment distributions are similar. The large difference occurs when the max. moment occurs at a peak, here at the supports. So as a practical simplification it could be acceptable to allow that for strength verification of cross sections at a moment peak the bending strength could be increased by a factor depending on the Coef. Var.

In figure A3.1 the calculated strength ratios are shown for concentrated and distributed loads. Further there is shown a suggestion for a moment–strength factor, which is on the safe side.

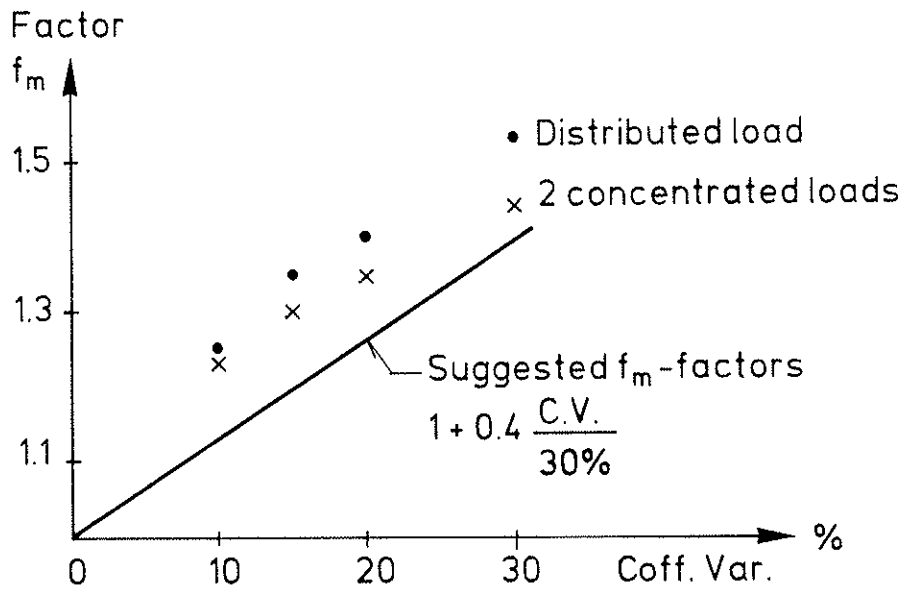


Figure A3.1.

Strength ratios for beams with clamped supports, and a suggestion for a moment–strength factor for strength verification of cross sections at a moment peak.

INTERNATIONAL COUNCIL FOR BUILDING RESEARCH STUDIES AND DOCUMENTATION
WORKING COMMISSION W18A - TIMBER STRUCTURES

SUGGESTED CHANGES IN CODE BRACING RECOMMENDATIONS
FOR BEAMS AND COLUMNS

by

H J Burgess
Timber Research and Development Association
United Kingdom

MEETING TWENTY - TWO
BERLIN
GERMAN DEMOCRATIC REPUBLIC
SEPTEMBER 1989

CONTENTS

page no

Introduction	1
DRAFT CLAUSE	1
BACKGROUND	3
1 - DISCRETE RESTRAINTS FOR IDEAL BEAMS	3
Combinations of R and S to prevent buckling	4
Special relationships between R and S	5
Tables	7
Application to beam-columns	8
2 - INITIALLY CURVED COLUMN	10
One restraint	11
Two restraints	11
Three restraints	12
3 - PRACTICAL IMPLICATIONS	14
Load in interbrace length	14
Limitation of deflection at restraint	15
Restraint stiffness for higher modes	16
General rule for r restraints	17
Brace strength	18
REFERENCES	20

SUGGESTED CHANGES IN CODE BRACING RECOMMENDATIONS
FOR BEAMS AND COLUMNS

Paper 21-15-4 considered an adaptation of the bracing requirements calculated by Brüninghoff (1983) to take account of column buckling in modes higher than the first. Further work has now been done to allow the following suggestions to be made for a Code section on bracing. As bracing recommendations are not given in the current version of the CIB Code, the wording of EC5 has been followed. Background notes are given to indicate the nature of the additional calculations; a detailed explanation will be published separately. The main conclusion agrees with the British code for steelwork, but is reached by an entirely new form of calculation with no influence from the British recommendation which is of unknown origin; it can be derived from calculations for the 'ideal' column as described in paper 21-15-4 but was in use before publication of the necessary data by Klemperer and Gibbons (1932,1933).

DRAFT CLAUSE

5.2.6 Bracing

Adequate bracing shall be provided to avoid lateral instability of individual members and the collapse of the whole structure due to external loading such as wind.

The stresses due to initial curvature and induced deflection shall be taken into account.

The theory of linear elasticity may be used.

The initial deviations from straightness at midspan shall as a minimum be taken as $l / 450$ for glued laminated beams and as $l / 300$ for other structures.

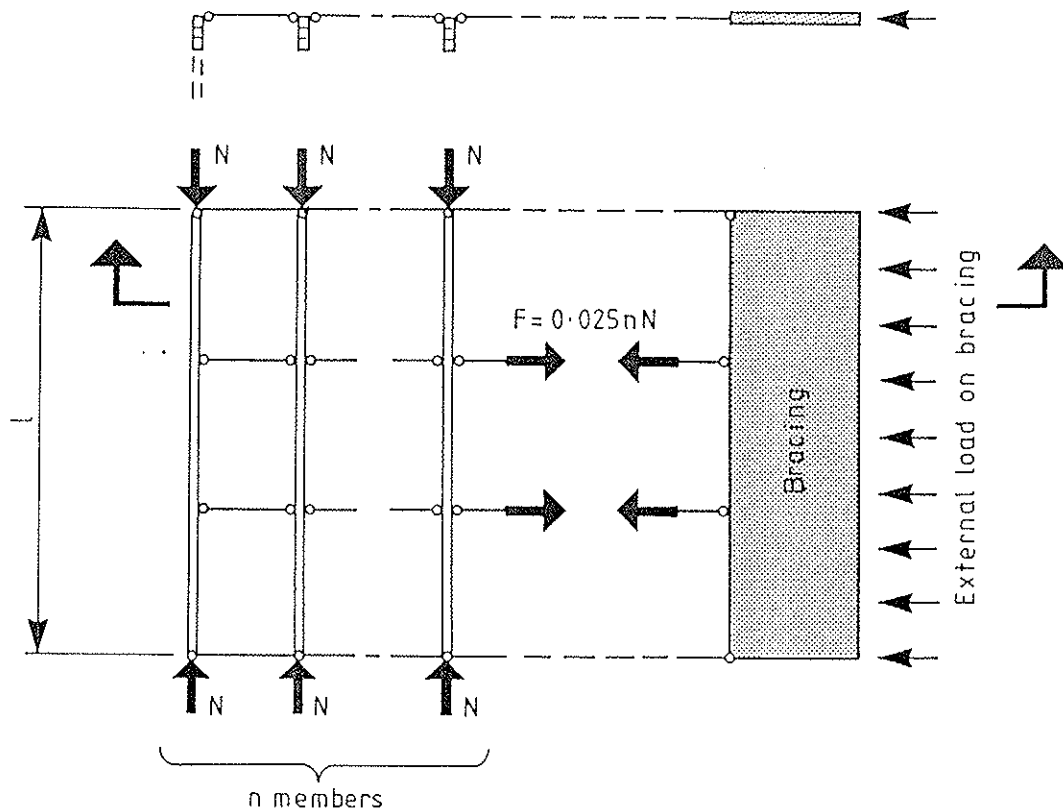


Figure 5.2.6a. Bracing system

With n equal members (eg beams or chords in a truss) of rectangular cross-section, the bracing should in addition to external loads (eg wind) be designed for a point load F at each line of bracing having the value

$$F = 0.025nN \quad (5.2.6a)$$

where N is the axial force in a member at the point of application of the brace.

Where the member is a beam with maximum moment M the value of N should be taken as $mM \frac{P_c}{M_c}$ where m is the number of spans ($m = 1 +$ number of restraints).

Where the member is a truss N is the maximum compressive force.

For a beam-column which is free to deflect vertically at the points of restraint, N should be taken as

$$N = mM \frac{P_c}{M_c} + P \quad (5.2.6b)$$

where P is the longitudinal compressive force.

P_c and M_c are critical values for the full length l .

BACKGROUND

1 - DISCRETE RESTRAINTS FOR IDEAL BEAMS

The brace stiffness required for the full bracing of ideal beams under equal end moments has been calculated for one, two and three restraints.

CALCULATION METHOD

The following example indicates the method of calculation for two restraints with anti-symmetric buckling as shown in Figure 1. The diagram on the left is a plan view of the deflected centre line of an ideal beam buckling laterally under the action of equal end moments applied in a plane perpendicular to the paper, this plane being the central longitudinal plane of the undistorted beam. At the third points of the beam, the lateral deflection of its centroidal line is resisted by an elastic lateral restraint with modulus S N/mm and rotation is resisted by an elastic torsional restraint of modulus R expressed in N-mm per radian of rotation. Assuming a deflection f and a rotation θ at each of the two points, the force applied to the beam by the linear lateral restraint is Sf and the moment resisting rotation is $R\theta$. The corresponding reactions at each end of the beam are $\frac{Sf}{3}$ and $\frac{R\theta}{3}$ as shown in Figure 1.

Outer portion

Using the subscript letter 'o' for the outer section of the beam in Figure 1, the differential equations are

$$EI \frac{d^2 u_o}{dz^2} + \gamma M \phi_o - \frac{Sf}{3} \gamma = 0 \quad (1)$$

$$C \frac{d\phi_o}{dz} - M \frac{du_o}{dz} + \frac{R\theta}{3} = 0 \quad (2)$$

Inner portion

The equations are

$$EI \frac{d^2 u_i}{dz^2} + \gamma M \phi_i - \frac{Sf}{3} z + Sf \left(z - \frac{L}{3} \right) = 0 \quad (3)$$

$$\text{and} \quad C \phi_i - M u_i + \frac{R\theta}{3} z - R\theta \left(z - \frac{L}{3} \right) = 0 \quad (4)$$

Applying the conditions at $z = \frac{L}{3}$, namely $u_0 = u_i = f$ and $u'_0 = u'_i$, the solution found is

$$u_i = \frac{f - \left(\frac{R\theta}{M} + \frac{CSf}{\gamma M^2} \right) \frac{L}{9}}{\sin \frac{kL}{3}} \sin kz + \left(\frac{R\theta}{3M} + \frac{C}{\gamma M^2} \frac{Sf}{3} \right) z \quad (5)$$

$$u_i = \frac{1}{k} \left(\frac{R\theta}{M} + \frac{CSf}{\gamma M^2} \right) \sin \left(kz - \frac{kL}{3} \right) + \frac{f - \left(\frac{R\theta}{M} + \frac{SfC}{\gamma M^2} \right) \frac{L}{9}}{\sin \frac{kL}{3}} \sin kz - \left(\frac{R\theta}{M} + \frac{SfC}{\gamma M^2} \right) \left(\frac{2}{3} z - \frac{L}{3} \right) \quad (6)$$

$$\phi_i = \frac{1}{k} \left(\frac{R\theta}{C} + \frac{Sf}{\gamma M} \right) \sin \left(kz - \frac{kL}{3} \right) + \frac{fM}{C} - \frac{\left(\frac{R\theta}{C} + \frac{Sf}{\gamma M} \right) \frac{L}{9}}{\sin \frac{kL}{3}} \sin kz - \frac{Sf}{\gamma M} \left(\frac{2}{3} z - \frac{L}{3} \right) \quad (7)$$

where $k = M \sqrt{\frac{\gamma}{CEI}}$.

Combinations of R and S to prevent buckling

In (6) when $z = \frac{2}{3}L$, $u_i = -f$, ie

$$-f = 2f \cos \frac{kL}{3} + \left(\frac{R\theta}{M} + \frac{CSf}{\gamma M^2} \right) \left(\frac{1}{k} \sin \frac{kL}{3} - \frac{2}{9}L \cos \frac{kL}{3} - \frac{L}{9} \right) \quad (8)$$

and from (7) when $z = \frac{2}{3}L$, $\phi_i = -\theta$ giving

$$-\theta = 2 \frac{fM}{C} \cos \frac{kL}{3} + \left(\frac{R\theta}{C} + \frac{Sf}{\gamma M} \right) \left(\frac{1}{k} \sin \frac{kL}{3} - \frac{2}{9}L \cos \frac{kL}{3} \right) - \frac{Sf}{\gamma M} \frac{L}{9} \quad (9)$$

$$\text{or} \quad \theta = - \frac{2 \frac{fM}{C} \cos \frac{kL}{3} + \frac{Sf}{\gamma M} \left(\frac{1}{k} \sin \frac{kL}{3} - \frac{2}{9}L \cos \frac{kL}{3} - \frac{L}{9} \right)}{1 + \frac{R}{C} \left(\frac{1}{k} \sin \frac{kL}{3} - \frac{2}{9}L \cos \frac{kL}{3} \right)} \quad (10)$$

Putting this in (8) and writing T for $\frac{1}{k} \sin \frac{kL}{3} - \frac{2}{9}L \cos \frac{kL}{3} - \frac{L}{9}$, f is eliminated giving

$$-1 = 2 \cos \frac{kL}{3} - \frac{\left(2 \frac{R}{C} \cos \frac{kL}{3} + \frac{RS}{\gamma M^2} T \right) T}{1 + \frac{R}{C} \left(T + \frac{L}{9} \right)} + \frac{CS}{\gamma M^2} T \quad (11)$$

(11) provides an expression giving the values of the stiffness moduli R and S that will resist lateral buckling when a moment $M > 2M_c$ is applied. An infinite set of combinations of S and R will achieve this. The case of chief interest is that for full bracing when $M = 3M_c$ where M_c is the critical moment for whole-length buckling, $\frac{\pi \sqrt{CEI}}{L}$. Then $k = M \sqrt{\frac{Y}{CEI}} = 3M_c \sqrt{\frac{Y}{CEI}} = \frac{3\pi}{L}$, the expression T becomes $\frac{L}{q}$ and (11) becomes

$$1 = \frac{SL}{81P_e} \left(\frac{RL}{qC} + 1 \right) \quad (12)$$

$$\frac{RL}{C} = 9 \left(\frac{81}{SL/P_e} - 1 \right) \quad (13)$$

where $P_e = \frac{\pi^2 EI}{L^2}$ is the full-length Euler load.

$\frac{RL}{C}$ is plotted against $\frac{SL}{P_e}$ in Figure 2. Any pair of values of R and S which satisfy (13) will be adequate to restrain the beam of Figure 1 against lateral buckling under the full end moment $M = 3M_c$.

Special relationships between R and S

A particular pair of values R and S satisfying (13) may be found by relating the two in such a way that the relation between f and θ when $M = 3M_c$ is the same as that between the central displacement and twist in the unrestrained ideal beam after buckling. The relationship is

$$\frac{f}{\theta} = \frac{L \sqrt{CY}}{\pi \sqrt{EI}} = \frac{C}{M_c} \quad (14)$$

as applied in papers 19-10-1 and 20-2-1. Inserting $k = \frac{3\pi}{L}$ in (10) for full bracing ($M = 3M_c$) and equating the result to (14) for a half-wave of length L:

$$\frac{f}{\theta} = \frac{1 + 2 \frac{RL}{C} \frac{L}{q}}{6 \frac{M_c}{C} - \frac{SL}{27M_c q}} = \frac{L \sqrt{CY}}{\pi \sqrt{EI}} = \frac{C}{M_c}$$

giving $\frac{RL}{qC} = \frac{5}{2} - \frac{SL}{2 \times 27 P_e} \quad (15)$

Putting this in (12)

$$1 = \frac{SL}{81P_e} \left(\frac{7}{2} - \frac{3}{2} \frac{SL}{81P_e} \right)$$

If $A = \frac{SL}{81P_e}$

$$3A^2 - 7A + 2 = 0$$

with solutions $\frac{S_L}{81P_e} = \frac{1}{3}$ or $\frac{S_L}{P_e} = 27$ accompanied by $\frac{R_L}{C} = 18$ from (12)
 or $\frac{S_L}{81P_e} = 2$ giving $\frac{R_L}{C} = -\frac{1}{2}$ which is invalid.

A second relationship may be found for a half-wave of length $\frac{L}{2}$

$$\frac{f}{\theta} = \frac{1 + 2\frac{R_L}{C}\frac{L}{q}}{6\frac{M_c}{C} - \frac{S_L}{27M_c\delta}} = \frac{C}{2M_c}$$

leading to $3A^2 - 8A + 4 = 0$

with solutions $\frac{S_L}{81P_e} = \frac{2}{3}$ or $\frac{S_L}{P_e} = 54$ with $\frac{R_L}{C} = 4\frac{1}{2}$
 or $\frac{S_L}{81P_e} = 2$ giving $\frac{R_L}{C} = -\frac{1}{2}$ as above.

To obtain a third relationship for a half-wave of length $\frac{L}{3}$

$$\frac{f}{\theta} = \frac{1 + 2\frac{R_L}{C}\frac{L}{q}}{6\frac{M_c}{C} - \frac{S_L}{27M_c\delta}} = \frac{C}{3M_c}$$

leading to $A^2 - 3A + 2 = 0$

with solutions $\frac{S_L}{81P_e} = 2$ giving $\frac{R_L}{qC} = -\frac{1}{2}$ or $\frac{S_L}{81P_e} = 1$ for which $\frac{R_L}{qC} = 0$
 from (12).

This last result gives the same restraint stiffness as that required for full bracing of an ideal column with two braces, $S = 81\frac{P_e}{L}$.

The results for the three relationships are shown in Table 2 of the following set of three, the other two showing the results obtained for one brace and three braces. The right-hand column of each table shows that a conservative solution for the necessary brace stiffness S may be obtained by assuming there is no torsional restraint ($R = 0$). The value of $\frac{S_L}{P_e}$ in each case is then the same as for braced ideal columns and if m is the number of spans the slope of the distorted beam at the restraint when $M = mM_c$ is equal to that of an unrestrained ideal beam of length L/m after buckling.

If provision is made for rotational as well as translational restraint, the necessary value of S is divided by m to obtain the figure in the left-hand column of each table and the associated value of R may be found from the tables.

Table 1 - ONE RESTRAINT

	$\frac{f}{\theta} = \frac{C}{M_c}$	$\frac{f}{\theta} = \frac{C}{2M_c}$
	one $\frac{1}{2}$ -wave	two $\frac{1}{2}$ -waves
$\frac{SL}{P_e} =$	8	16
$\frac{RL}{C} =$	4	0
$R =$	$\frac{S}{2P_e} C$	0

Table 2 - TWO RESTRAINTS

	$\frac{f}{\theta} = \frac{C}{M_c}$	$\frac{f}{\theta} = \frac{C}{2M_c}$	$\frac{f}{\theta} = \frac{C}{3M_c}$
	one $\frac{1}{2}$ -wave	two $\frac{1}{2}$ -waves	three $\frac{1}{2}$ -waves
$\frac{SL}{P_e} =$	27	54	81
$\frac{RL}{C} =$	18	$4\frac{1}{2}$	0
$R =$	$\frac{2}{3} \frac{S}{P_e} C$	$\frac{1}{12} \frac{S}{P_e} C$	0

Table 3 - THREE RESTRAINTS

	$\frac{f_0}{\theta_0} = \frac{C}{M_c}$	$\frac{f_0}{\theta_0} = \frac{C}{2M_c}$	$\frac{f_0}{\theta_0} = \frac{C}{3M_c}$	$\frac{f_0}{\theta_0} = \frac{C}{4M_c}$
	one $\frac{1}{2}$ -wave	two $\frac{1}{2}$ -waves	three $\frac{1}{2}$ -waves	four $\frac{1}{2}$ -waves
$\frac{SL}{P_e} =$	$64 \times \frac{1}{4} (2 + \sqrt{2})$ = 54.63	$64 \times \frac{1}{2} (2 + \sqrt{2})$ = 109.25	$64 \times \frac{3}{4} (2 + \sqrt{2})$ = 163.9	$64 \times (2 + \sqrt{2})$ = 218.5
$\frac{RL}{C} =$	$12 (2 + \sqrt{2})$ = 40.97	$4 (2 + \sqrt{2})$ = 13.66	$\frac{4}{3} (2 + \sqrt{2})$ = 4.552	0
$R =$	$\frac{3}{4} \frac{S}{P_e} C$	$\frac{1}{8} \frac{S}{P_e} C$	$\frac{1}{36} \frac{S}{P_e} C$	0

The bottom line of each table shows the relationships between R and S for the special cases considered. Continuing the notes for two restraints, graphs showing the restraint stiffness required for $\frac{M}{M_c}$ ranging from 2 to 3 may be obtained from (11) as follows:-

$R = \frac{2}{3} \frac{S}{P_e} C$ When k is written $\frac{\pi M}{L M_c}$, T in (11) becomes

$$T = L \left(\frac{1}{\pi} \frac{M_c}{M} \sin \frac{\pi M}{3 M_c} - \frac{2}{9} \cos \frac{\pi M}{3 M_c} - \frac{1}{9} \right)$$

Writing A for the term in brackets and inserting $R = \frac{2}{3} \frac{S}{P_e} C$ in (11) gives

$$\left(\frac{SL}{P_e} \right)^2 + \left\{ 9 \frac{M^2}{M_c^2} \left(1 + \frac{1}{9A} \right) + \frac{2 M^2}{A M_c^2} \cos \frac{\pi M}{3 M_c} + \frac{27}{2} \right\} \left(\frac{SL}{P_e} \right) + \frac{27 M^2}{A M_c^2} \left(\cos \frac{\pi M}{3 M_c} + \frac{1}{2} \right) \quad (16)$$

$R = \frac{1}{12} \frac{S}{P_e} C$ Similarly, this gives

$$\left(\frac{SL}{P_e} \right)^2 + \left\{ 9 \frac{M^2}{M_c^2} \left(1 + \frac{1}{9A} \right) + \frac{2 M^2}{A M_c^2} \cos \frac{\pi M}{3 M_c} + 108 \right\} \left(\frac{SL}{P_e} \right) + \frac{108 M^2}{A M_c^2} \left(2 \cos \frac{\pi M}{3 M_c} + 1 \right) \quad (17)$$

$R = 0$ (11) becomes

$$\frac{SL}{P_e} = - \frac{M^2}{M_c^2} \frac{1}{A} \left(1 + 2 \cos \frac{\pi M}{3 M_c} \right) \quad (18)$$

Lines plotting $\frac{M}{M_c}$ against $\frac{SL}{P_e}$ are drawn in Figure 3 for the three special relationships between R and S applied in connection with the antisymmetric case of Figure 1. The corresponding solutions for the symmetrical case are also shown for comparison with the graphs drawn by Klemperer and Gibbons for braced ideal columns. The figures in the bottom table for three braces are derived by a simplified method and graphs have not been drawn for this case.

Application to beam-columns

Although not yet proved in detail, it seems reasonable to expect that the results for a beam under equal end moments accompanied by longitudinal forces at the ends will be additive. Assuming conservatively that there is no rotational restraint, the full bracing requirement $\frac{SL}{P_e} = 81$ for two braces would provide either for end moments $3M_c$ or end forces $9P_e$. If both types of load are present, the limitation would be

$$\frac{M}{3M_c} + \frac{P}{9P_e} \leq 1$$

To enable the Klemperer and Gibbons graph to be used, the effective combination would be

$$\left(\frac{M}{3M_c} + \frac{P}{4P_e} \right) \times 9 = 3\frac{M}{M_c} + \frac{P}{P_e} \quad (19)$$

- this sum being treated as the effective end load for calculating bracing requirements. In the general case with m spans, the effective end load should be taken as

$$m \frac{M}{M_c} + \frac{P}{P_e} \quad (20)$$

where M_c and P_e are the values for the full length L . That is, $\frac{M}{M_c}$ is multiplied by the number of spans and added to $\frac{P}{P_e}$ to enable the column graph to be used.

If provision is made for the torsional restraint shown in the left-hand column of each table, $\frac{M}{M_c}$ may be added to $\frac{P}{P_e}$ without first multiplying by the number of spans, m .

The above background notes refer to ideal beams and columns. The following section considers columns with initial imperfections.

BACKGROUND

2 - INITIALLY CURVED COLUMN

A method for the design of columns with initial curvature has been proposed by Winter (1958) as described also by Trahair and Nethercot (1984) with reference to other literature on the topic. The method below was developed following a study of evocative work by Bache and Klemperer (1937) which provides experimental verification of both their formulae and the ones to be developed for one or two braces.

The results are expressed in a very simple form by using the expressions given by Klemperer and Gibbons for the bracing of ideal columns as follows, the subscript of S referring to the number of braces:

$$S_1 = \frac{2Pk}{\frac{kL}{2} - \tan \frac{kL}{2}} \quad (21)$$

$$S_2 = \frac{Pk}{\sin^2 \frac{kL}{3} \cot \frac{kL}{2} - \cos \frac{kL}{3} \sin \frac{kL}{3} + \frac{kL}{9}} \quad (22)$$

$$S_3 = \frac{P}{L} \frac{-\frac{1}{kL} \sin \frac{kL}{2} + \frac{1}{2} \cos \frac{kL}{2} - \frac{1}{\sqrt{2}} \left(\sin^2 \frac{kL}{4} + \frac{2}{kL} \sin \frac{kL}{4} - \frac{1}{2} \right)}{\left(\frac{1}{k^2 L^2} - \frac{1}{8} \right) \sin^2 \frac{kL}{4} + \frac{1}{kL} \left(\frac{1}{2} - \cos \frac{kL}{4} \right) \sin \frac{kL}{4} + \frac{1}{16}} \quad (23)$$

The last of these is not given in explicit form by Klemperer and Gibbons but may be deduced from their results by noting that the discriminant of the quadratic solution for S_3 is a perfect square.

The form of initial curvature chosen for each case is partly a mathematical convenience but is mainly suggested by the earlier work cited. It was felt important to obtain a result comparable with Winter's illustration for three restraints, and in all the cases studied the form of initial curvature corresponds to the deflected shape adopted by Klemperer and Gibbons for calculating the full bracing requirements of ideal columns.

One restraint

In figure 4 the initial curvature shown by the dotted line has the form $y_s = a \sin \frac{\pi}{L} x$, the subscript standing for sinusoidal. If the additional deflection is y_1 the differential equation for the left half of the column is

$$\frac{d^2 y_1}{dx^2} + \frac{P}{EI} y_1 = \frac{Sf}{2EI} x - \frac{P}{EI} a \sin \frac{\pi}{L} x \quad (24)$$

where f is the value of y_1 at the central restraint. Applying the conditions $y_1 = 0$ when $x = 0$, $y_1' = 0$ when $x = \frac{L}{2}$ and $y_1 = f$ when $x = \frac{L}{2}$ the solution can be brought to a form which gives at the centre

$$y_1 = \frac{\frac{P}{P_e} a}{1 - \frac{P}{P_e}} \left[\frac{1}{1 - \frac{S}{2PK} \left(\frac{KL}{2} - \tan \frac{KL}{2} \right)} \right] \quad (25)$$

or

$$\frac{y_1}{a} = \frac{\frac{P}{P_e}}{\left(1 - \frac{P}{P_e}\right) \left(1 - \frac{S}{S_1}\right)} \quad (26)$$

The resulting graph is plotted in Figure 5 where a special scale is used for overlaying on the corresponding graph by Bache and Klemperer, and the function plotted is total deflection divided by initial as in their diagram. The further graphs to be drawn for two and three restraints will use the same plotting method so that all are comparable.

Two restraints

In Figure 6 the antisymmetric shape precedes the symmetrical buckling into three half-waves that will take place when P is increased to $9P_e$, and the initial curvature is taken as $y_s = a \sin \frac{2\pi}{L} x$.

Using the subscript letter 'o' to refer to the outer section of the column, the additional deflections y_o and y_i are found from

$$\frac{d^2 y_o}{dx^2} + \frac{P}{EI} y_o = \frac{Sf}{3EI} x - \frac{P}{EI} a \sin \frac{2\pi}{L} x \quad (27)$$

$$\frac{d^2 y_i}{dx^2} + \frac{P}{EI} y_i = -\frac{2}{3} \frac{Sf}{EI} x + \frac{SfL}{EI} - \frac{P}{EI} a \sin \frac{2\pi}{L} x \quad (28)$$

The conditions $y_0 = 0$ when $x = 0$, $y_0 = y_1 = f$ when $x = \frac{L}{3}$, $y'_0 = y'_1$ when $x = \frac{L}{3}$ and finally $y_1 = 0$ when $x = \frac{L}{2}$ lead to the solution giving for the left-hand restraint

$$y_0 = \frac{\frac{P}{4P_e} a \sin \frac{2\pi}{3}}{1 - \frac{P}{4P_e} \left(1 - \frac{S}{PK} \left(\sin^2 \frac{kL}{3} \cot \frac{kL}{2} - \cos \frac{kL}{3} \sin \frac{kL}{3} + \frac{kL}{9} \right) \right)} \quad (29)$$

or $\frac{y_0}{a \sin \frac{2\pi}{3}} = \frac{\frac{P}{4P_e}}{\left(1 - \frac{P}{4P_e} \right) \left(1 - \frac{S}{S_2} \right)}$ (30)

$a \sin \frac{2\pi}{3} = 0.866a$ is the value of y_s at $x = \frac{L}{3}$ so the left-hand side of (30) gives the ratio of the additional deflection to the original deflection at the restraint.

The corresponding graph in the Bache and Klemperer style is shown in Figure 7.

Three restraints

Figure 8 shows the symmetrical shape preceding antisymmetric buckling in four half-waves. The initial curvature is taken as $y_s = a \sin \frac{3\pi}{L} x$. The case for a single half-wave of initial curvature has also been solved, giving much smaller deflections for a given restraint stiffness. For the more conservative case in Figure 8 the differential equations are

$$\frac{d^2 y_0}{dx^2} + \frac{P}{EI} y_0 = \left(f_0 - \frac{f_1}{2} \right) \frac{5x}{EI} - \frac{P}{EI} a \sin \frac{3\pi}{L} x \quad (31)$$

$$\frac{d^2 y_1}{dx^2} + \frac{P}{EI} y_1 = -\frac{5f_1}{2EI} x + \frac{5f_0 L}{EI 4} - \frac{P}{EI} a \sin \frac{3\pi}{L} x \quad (32)$$

Applying the conditions $y_0 = 0$ when $x = 0$, $y_0 = y_1 = f_0$ when $x = \frac{L}{4}$, $y'_0 = y'_1$ when $x = \frac{L}{4}$ gives solutions for y_0 and y_1 which both contain f_0 and f_1 . The further relation $y'_1 = 0$ when $x = \frac{L}{2}$ gives f_0 in terms of f_1 , and then the condition $y_1 = -f_1$ when $x = \frac{L}{2}$ leads to a complex result which may be written

$$\frac{y_1}{a} \left\{ 1 - \phi(s, P) \right\} = \frac{\frac{P}{9P_e}}{1 - \frac{P}{9P_e}} \quad (33)$$

The expressions involved are too complicated to show that $\phi(S,P) = \frac{S}{S_3}$ but computer plotting of (33) in the Bache and Klemperer style gives curves in Figure 9 which exactly coincide with those obtained from

$$\frac{y_i}{a} = \frac{\frac{P}{4P_e}}{\left(1 - \frac{P}{4P_e}\right)\left(1 - \frac{S}{S_3}\right)} \quad (34)$$

and this is taken as the solution. The same curves may also be obtained from

$$\frac{y_0}{a \sin \frac{3\pi}{4}} = \frac{y_0}{a\sqrt{2}} = \frac{\frac{P}{4P_e}}{\left(1 - \frac{P}{4P_e}\right)\left(1 - \frac{S}{S_3}\right)} \quad (35)$$

Equations (25) and (29) may be expressed in the same way as (33) and detailed study makes it evident that (33) provides the essence of a proof for the general case of r restraints. If 'a' is kept on the right-hand side and put equal to zero, the solution for an ideal column is obtained as

$$\phi(S,P) = 1$$

implying in each case above that $S = S_r$ so that $\phi(S,P) = \frac{S}{S_r} = 1$. The solution for r restraints will therefore be taken as

$$\frac{\delta_i}{c} = \frac{\frac{P}{r^2 P_e}}{\left(1 - \frac{P}{r^2 P_e}\right)\left(1 - \frac{S}{S_r}\right)} \quad (36)$$

in which δ_i = additional deflection at restraint

c = initial deflection at restraint

r = no of restraints = no of $\frac{1}{2}$ -waves in y_s

S_r = restraint stiffness to prevent buckling of ideal column under end load $P < m^2 P_e$, governed by design of a single span.

BACKGROUND

3 - PRACTICAL IMPLICATIONS

Paper 21-15-4 considered simple rules for the discrete bracing of ideal columns, but there are two deficiencies in the results when applied in practical cases:

- (1) In real columns, the load that may be applied to the interbrace length $\ell = L/m$ is less than the Euler load.
- (2) On the other hand, the bracing stiffness for a given load on an ideal column needs to be greatly increased for a real column with initial imperfections, to limit deflection at the restraints.

Load in interbrace length

The permissible load in a single span may be limited by stress or deflection, but deflection will often be the governing feature for a column or beam-column of deep cross-section which is loaded in the plane of the principal axis and discretely braced in the weak direction. For such cases, previous work on unbraced columns has determined the permissible end load by limiting the additional deflection u_1 to 0.003ℓ and assuming an initial deviation from straightness of $0.005\ell/i$ corresponding to an amplitude $u_0 = \frac{0.005\ell}{\sqrt{3}} = 0.002887\ell$ for a rectangular section. Then from

$$u_1 = \frac{\frac{P}{P'_e}}{1 - \frac{P}{P'_e}} u_0$$

$$\frac{P}{P'_e} = \frac{u_1}{u_0 + u_1} = \frac{0.003\ell}{(0.002887 + 0.003)\ell} = 0.5096 \quad (37)$$

where $P'_e = m^2 P_e$ is the Euler load for the interbrace length.

In the previous work, different values 0.003 and 0.002887 have been deliberately maintained to enable their effect to be seen more easily in the later stages of calculations where for example 0.5096 would be recognized while 0.5 or $\frac{1}{2}$ might arise for other reasons. An exception will be made in the following calculations to obtain very simple

results using a proposal by Winter (1958) that the additional deflection of a restraint might be limited to the same value as the initial deviation from straightness at the restraint.

Taking the example of two restraints, Figure 10 for ideal columns has been traced from the paper by Klemperer and Gibbons (1932) to show the required brace stiffness for values of $\frac{P}{P_e}$ ranging from 1 with no bracing to $m^2 = 9$ with full bracing ($\frac{5L}{P_e} = 81$) to force buckling in three half-waves ($m = 3$). The upper curve of shallower slope corresponds to equation (22) above for S_2 . The steeper curve is for symmetrical distortion of the column at lower brace stiffnesses and will not be needed in the following work.

Multiplying the full bracing value of $\frac{P}{P_e}$ by 0.5 instead of 0.5096 to give 4.5 reduces the required stiffness from the ideal value $81 \frac{P_e}{L}$ to about $6.5 \frac{P_e}{L}$ on the upper curve of Figure 10.

Limitation of deflection at restraint

If the figures 0.003 and 0.002887 were retained, equation (30) would yield

$$S = S_2 \left\{ 1 - \frac{\frac{P}{P_e} \times 0.002887 \frac{L}{2} \sin \frac{2\pi}{3}}{\left(4 - \frac{P}{P_e}\right) \times 0.003 \frac{L}{2}} \right\} \quad (38)$$

as the brace stiffness required to limit the additional deflection at the brace to 0.003 times the half-wave length in Figure 6 while the initial deviation at the same point is $a \sin \frac{2\pi}{3}$, a being the amplitude of the dotted line. Adopting Winter's proposal instead, (38) becomes

$$S = S_2 \left\{ 1 - \frac{\frac{P}{P_e}}{4 - \frac{P}{P_e}} \right\} \quad (39)$$

and since $\frac{P}{P_e}$ is taken as $0.5m^2$ to limit interbrace deflection this gives

$$S = 10S_2 = 10 \times 6.5 \frac{P_e}{L} = 65 \frac{P_e}{L}$$

- approaching the value $81 \frac{P_e}{L}$ for full bracing of the ideal column.

Restraint stiffness for higher modes

Curves like the upper curve of Figure 10 have only been plotted for up to three restraints. Their curvature is not great and a conservative estimate of the required bracing stiffness may be obtained by treating them as straight lines. If it is assumed that this also applies to larger numbers of restraints, the simple result found is that the restraint stiffness required for the halved end load with Winter's deflection limitation is exactly the same as the stiffness required for the ideal column with the same number of restraints.

Taking five restraints for a numerical example, the restraint stiffness $S_{f,id}$ for full bracing of an ideal column as given by Timoshenko and Gere (1961) and checked by Burgess (1989) using a simple method is

$$\begin{aligned} S_{f,id} &= \frac{6}{L} \times \frac{\pi^2 EI}{0.268} = \frac{6}{L} \times \frac{36}{0.268} \times \frac{\pi^2 EI}{L^2} = \frac{6}{L} \times \frac{36}{0.268} P_c \\ &= 806 \frac{P_c}{L} \end{aligned}$$

The horizontal axis of Figure 10 shows values of $\frac{S_{id}L}{P_c}$ which will be called Δ_5 in relation to Figure 11 for five restraints, showing the assumed straight-line variation corresponding to the upper curve in Figure 10 for two restraints.

In Figure 11 the equation of the sloping line is

$$\frac{P}{P_c} = \frac{36-25}{806} \Delta_5 + 25$$

$$\text{When } \frac{P}{P_c} = 0.5m^2 = 0.5 \times 36 = 18$$

$$18 = \frac{11}{806} \Delta_5 + 25$$

$$\text{giving } \Delta_5 = -512.9$$

From equation (36) if $\frac{\delta_1}{c} = 1$ as suggested by Winter,

$$S = S_5 \left(1 - \frac{\frac{P}{P_c}}{25 - \frac{P}{P_c}} \right) = S_5 \left(1 - \frac{18}{25 - 18} \right)$$

$$= -1.5714 S_5$$

$$= -1.5714 \times (-512.9 \frac{P_c}{L}) = 806 \frac{P_c}{L}$$

$$= S_{f,id} \text{ as averred.}$$

General rule for r restraints

To demonstrate the same rule for r restraints with $m = r + 1$ spans, the equation of the straight line is taken as

$$\frac{P}{P_e} = \frac{(r+1)^2 - r^2}{\Delta_{f,id}} \Delta_r + r^2$$

When $\frac{P}{P_e} = 0.5m^2 = 0.5 (r+1)^2$ (40)

$$\frac{(r+1)^2}{2} = \frac{(r+1)^2 - r^2}{\Delta_{f,id}} \Delta_r + r^2$$

$$\Delta_r = \left\{ \frac{(r+1)^2}{2} - r^2 \right\} \frac{\Delta_{f,id}}{(r+1)^2 - r^2} \quad (41)$$

- giving the brace stiffness required for an ideal column with the end load reduced from the full value $m^2 P_e$ to limit the single-span deflection.

Using equation (36) to limit deflection at the brace in the way suggested by Winter, ie $\frac{\delta_1}{c} = 1$, the 'ideal' value Δ_r must be increased to

$$\Delta = \Delta_r \left(1 - \frac{\frac{P}{P_e}}{r^2 - \frac{P}{P_e}} \right)$$

Substituting for $\frac{P}{P_e}$ from (40),

$$\Delta = \Delta_r \left\{ \frac{r^2 - (r+1)^2}{r^2 - \frac{(r+1)^2}{2}} \right\} \quad (42)$$

and inserting Δ_r from (41) gives

$$\Delta = \Delta_{f,id} \quad (43)$$

for all values of r when the variation of Δ_r with $\frac{P}{P_e}$ is approximated as a straight line and Winter's suggested limitation is adopted for deflection at the restraint, with the ideal maximum end load halved to limit deflection in a single span.

This approach is very convenient, avoiding the use of complex functions S_r such as those in equations (21) to (23) except for a single figure which has already been worked out for each value of r.

Brace strength

The work above shows how use may be made of figures already published for up to 11 restraints for an ideal column. It must be emphasised that this is only a convenient way of expressing the results obtained from differential equations such as those applied for Figure 8. Although found equal to $\Delta_{f,id}$ at the end of the previous section, these results do not relate to ideal columns but are derived for columns with initial curvature.

Kirby and Nethercot (1979) explain that studies for ideal columns produce requirements for the stiffness of restraints but not for their strength, going on to describe Winter's approximate method for obtaining a required strength by allowing for initial imperfections. The study above also enables the necessary strength of a brace to be found, by multiplying its stiffness by the deflection permitted.

Equation (38) derived from equation (30) for two restraints incorporated a deflection limitation of $0.003\frac{l}{2}$. Since $\frac{l}{2}$ cancels with the $\frac{l}{2}$ in the numerator, the limitation may equally be taken as $0.003\frac{l}{3}$ corresponding to an initial 'curvature' of $0.005\frac{l}{l}$ where $l = L/3$. For a conservative estimation of the brace strength needed, the value $0.003\frac{L}{m} = 0.003l$ will be adopted.

This allows a return to the section 'Brief derivation' (of a $2\frac{1}{2}\%$ rule) in paper 21-15-4, which finished with the words "Writing $\delta = 0.003l$ cannot be justified without a deeper study of the work'. Repeating the derivation in the light of the calculations above, the required brace stiffness which is equal to the stiffness required for the full bracing of an ideal column, ie $S_{f,id} = \Delta_{f,id} \frac{P_e}{L}$ from equation (43), may also be expressed

$$S_{f,id} = \frac{m^2 P_e}{\gamma l} \quad (44)$$

- from expression (v) of Art.2.6 in Timoshenko and Gere (1961).

If the force in the brace is Q for a deflection 0.003ℓ ,

$$Q = S_{f,id} \times 0.003\ell$$

Also $P = 0.5096m^2 P_e$, taken as $0.5m^2 P_e$ above, so substituting for P_e and $S_{f,id}$ in (44) gives

$$\frac{Q}{P} = \frac{0.003}{0.5\gamma}$$

and taking $\gamma = 0.25$ as the lowest value given by Timoshenko and Gere,

$$\frac{Q}{P} = \frac{0.003}{0.5 \times 0.25} = 0.024$$

The rule for Code application may then state that the required strength of each brace is equal to $2\frac{1}{2}$ percent of the force in the column when the deflection of the point braced is limited to 0.003 of the interbrace span, $\ell = L/m$.

REFERENCES

- Bache, R F and W B Klemperer (1937) - The behaviour of bowed columns with intermediate elastic supports. J1 Aer Sc, Vol 4, No 4, pp 149-153, Feb 1937
- Brüninghoff, H (1983) - Determination of bracing structures for compression members and beams. CIB-W18 paper no 16-15-1, Lillehammer, May/June 1983.
- Burgess, H J (1989) - Methods for calculating the stiffness of discrete restraints for the full bracing of ideal columns. Ninth report of lateral stability and bracing projects (TRADA internal report), April 1989.
- Kirby, P A and D A Nethercot (1979) - Design for Structural Stability, CONSTRADO Monograph. London, Collins, 1979. (Updated paperback, 1985).
- Klemperer, W B and H B Gibbons (1932) - On the buckling strength of beams under axial compression, bridging elastic intermediate supports. Paper No 35, unpublished papers presented at ASME meetings in 1932, June 1932.
- Klemperer, W B and H B Gibbons (1933) - Über die Knickfestigkeit eines auf elastischen Zwischenstützen gelagerten Balkens. Z. angew. Math. u. Mech, Vol 13, p 251, 1933.
- Timoshenko, S P and J M Gere (1961) - Theory of Elastic Stability. London, McGraw-Hill, 2nd ed 1961.
- Trahair, N S and D A Nethercot (1984) - Bracing requirements in thin-walled structures. Chapter 3 of Developments in Thin-walled Structures, Vol 2. London, Elsevier, 1984.
- Winter, G (1958) - Lateral bracing of columns and beams. J1 Struct Div, ASCE, Paper 1561, March 1958.

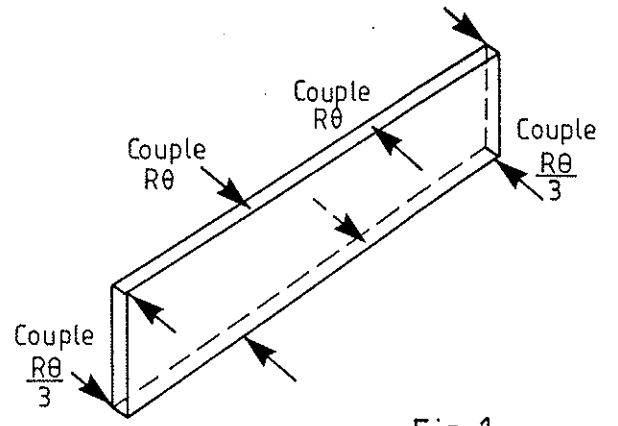
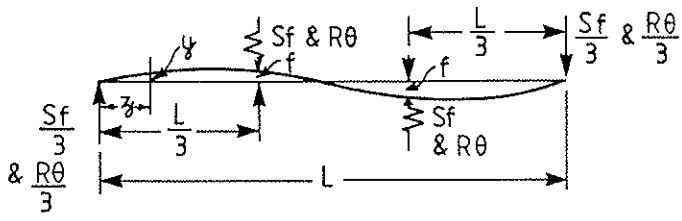


Fig. 1

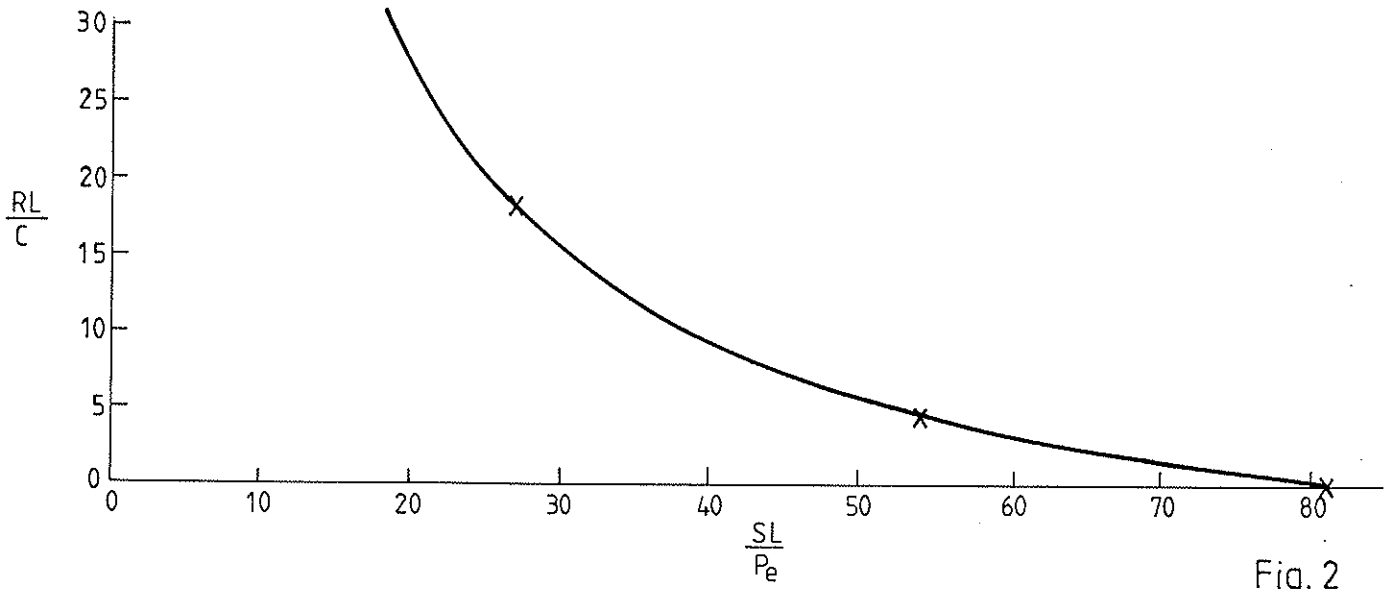


Fig. 2

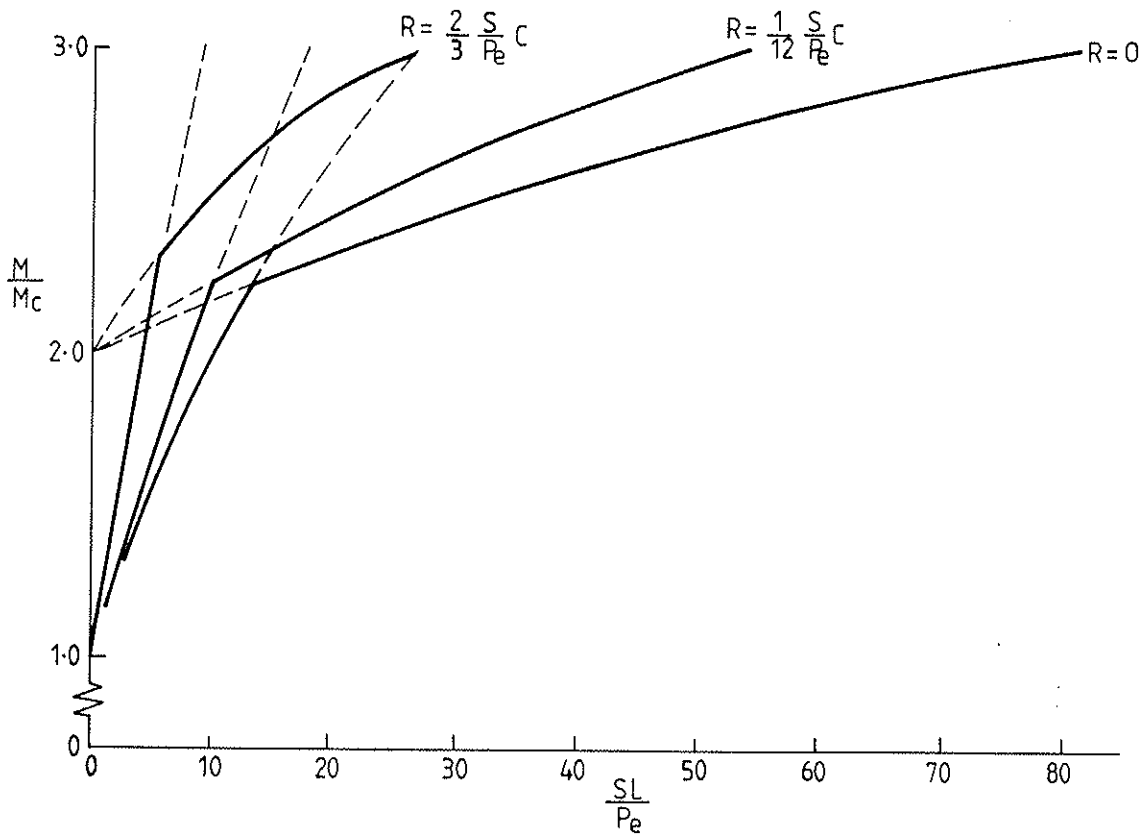


Fig. 3

Fig. 5

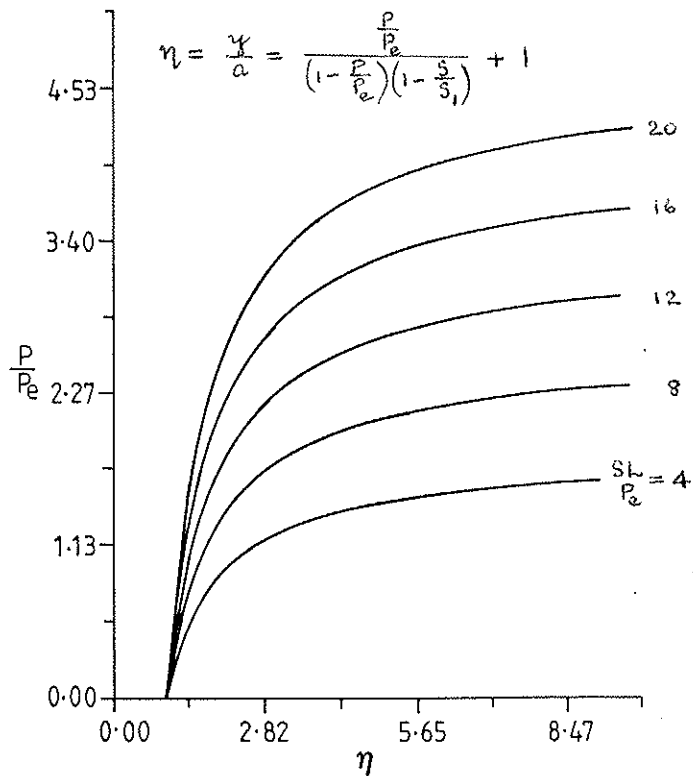


Fig. 4

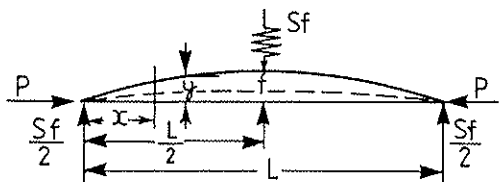


Fig. 7

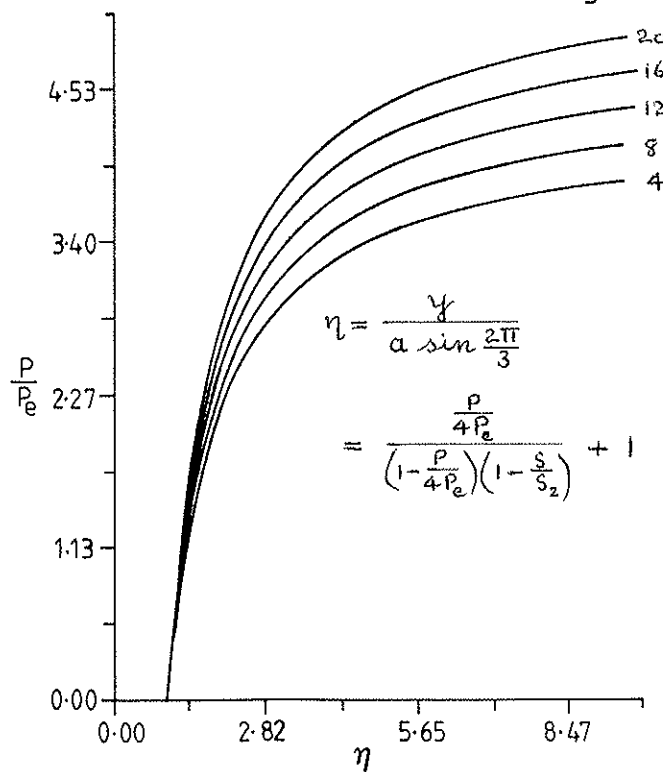
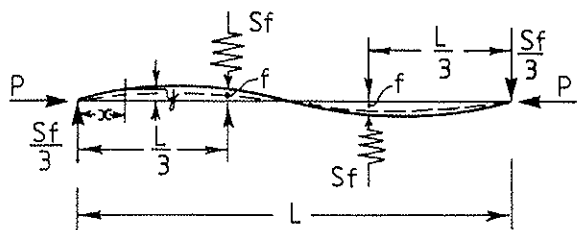


Fig. 6



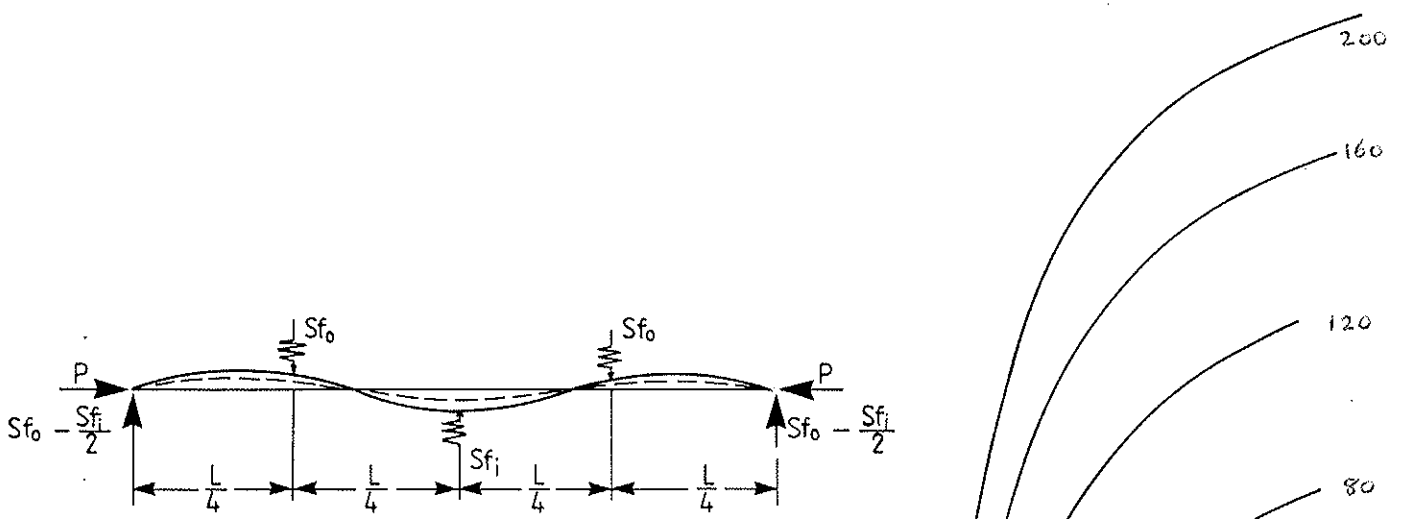


Fig. 8

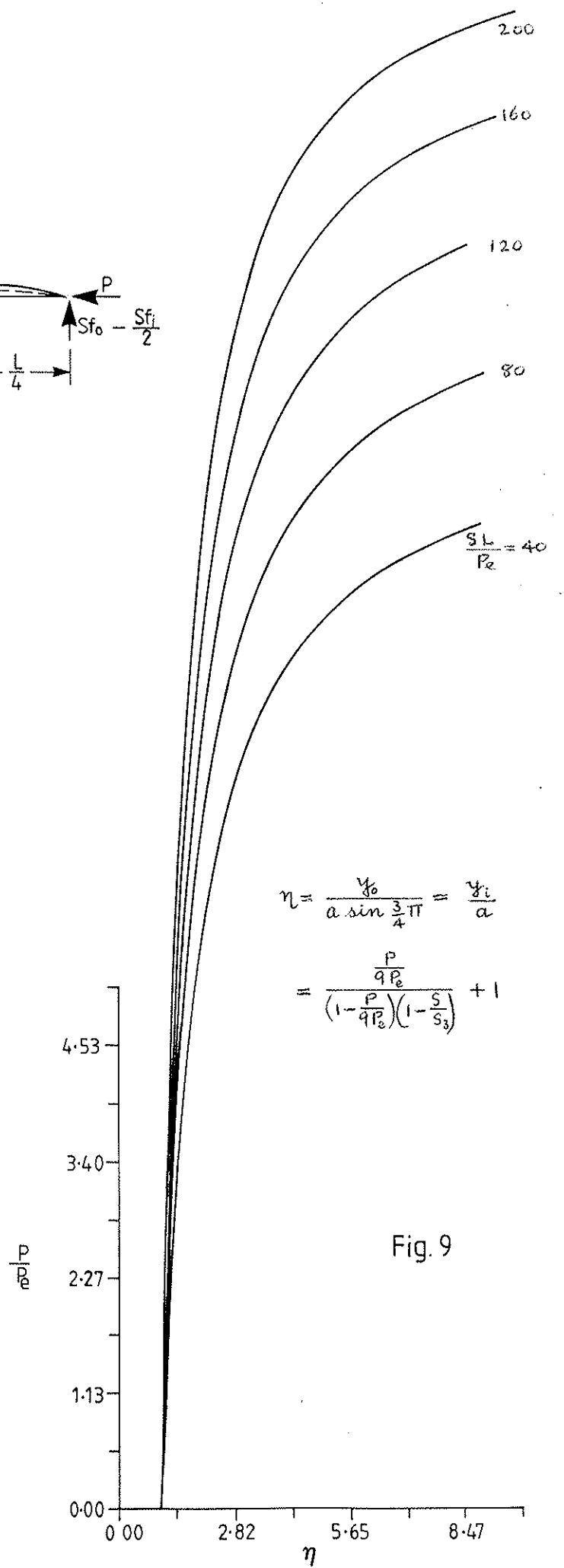


Fig. 9

Fig. 10

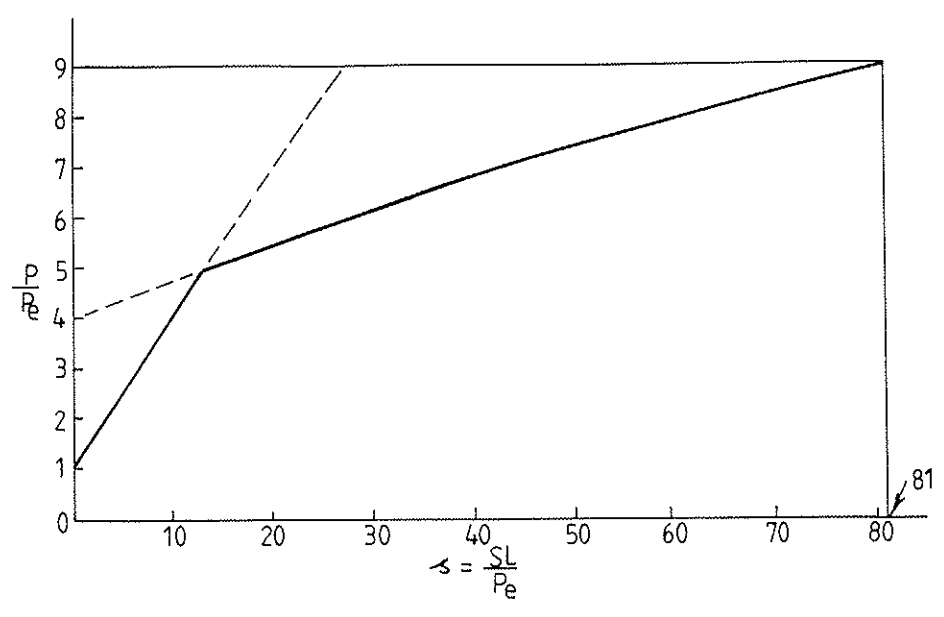
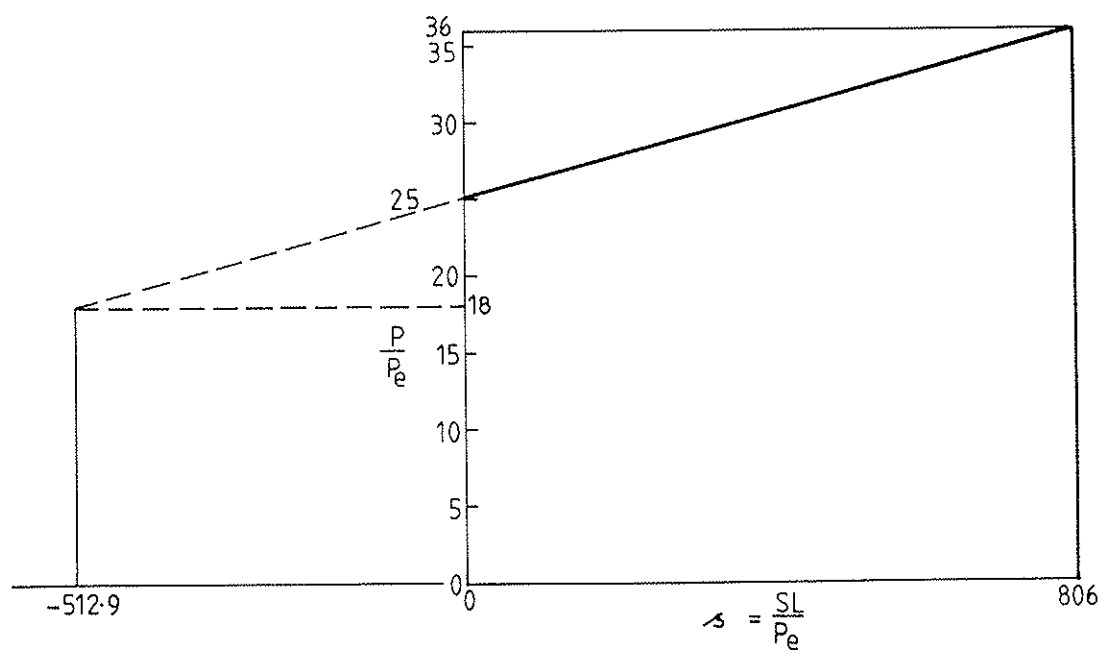


Fig. 11



INTERNATIONAL COUNCIL FOR BUILDING RESEARCH STUDIES AND DOCUMENTATION
WORKING COMMISSION W18A - TIMBER STRUCTURES

RESEARCH AND DEVELOPMENT OF TIMBER FRAME STRUCTURES
FOR AGRICULTURE IN POLAND

by

S Kus and J Kerste
Rzeszow University of Technology
Poland

MEETING TWENTY - TWO
BERLIN
GERMAN DEMOCRATIC REPUBLIC
SEPTEMBER 1989

Prof. Dr. Hab. Eng. Stanisław Kuś
Dr. Eng. Jerzy Kerste
Rzeszów University of Technology
Poland

RESEARCH AND DEVELOPMENT OF TIMBER FRAME STRUCTURES
FOR AGRICULTURE IN POLAND

After the Second World War over twenty years long break in the development of timber structures has been observed in Poland. The simple reason of it was the fascination with concrete and steel as universal and effective building materials. Up till 70 very few experimental research tests of full scale structures have been performed. As result the structural solutions were very wood consuming, and the former skilful timber artisans profession was vanishing.

The revision of this trend was forced by the demand of economy of energy consuming materials. The come back of timber structures was stimulated by the comparison of results of cattle breed in farm buildings of different materials, where the timber ones proved to create the most convenient microclimate. Research program sponsored by the central funds permitted to start in 1975 with the production of glued, laminated timber structures, a Research Steering Committee has been created and lot of new developments entered into the building market.

Actual experience proved the economy of timber use in sport building, in family housing, in ware storage, agricultural and church buildings. In social investments tendency to apply timber was stimulated because of fact that it was outside of official reglamentation, but in farm building the reason is that timber is the local material, easy to get near the building sites, resistant to aggressive environment easy to production and assem-

bling and because it creates very convenient healthy microclimate for breed.

1. Polish systems of timber farm buildings.

Relatively higher price of glued laminated timber structures is limiting their application to the biggest agricultural investments. For common use more traditional structural solutions have been used.

Most of them followed the static scheme of fixed in foundation column with triangular formwork as articulated beam spanning 6.0 ÷ 12.0 ÷ 18.0 ÷ 24.0 m. In this structure the net her tie was sometimes made of steel rod. The system distance was normally from 1.5 ÷ 3.0 m.

These systems were soon replaced by timber three hinge frames with the spans 9.0 ÷ 18.0 m. The development of these structures based on successive investigation and experimental testing is the item of this report.

First of them was the box section three pin frame BHD 3, designed in early seventies. The belts were rectangular timber sections joined together by inclined planks, thus forming the double web. The inclination of roof was 20°. The outer belt of column was vertical the inner inclined to the center. Some modification created the system "Bieszczady 75", with the span 16.5 m, distanced 3.0 m, where the inner belt of column was vertical and the outer inclined to outside. The web planks were fastened to the belts by nails. The skew planks primarily inclined to the center were soon replaced by structurally more correct inclined to outside, to take better the shear forces in "Rzeszów 77k" /fig.1 and fig.2/. Consumption of timber was rather high and reached 3.55m³/100 m², up to 4.3 m³/100 m². The main deficiencies of these systems, often used for sheep breeding in mountainous regions of Po-

land, were: big nails consumption, susceptibility to quality of execution and technologically demanded system of planking not permitting to carry correct all the internal forces. Some of these structures were obliged even to be strenghtened on site. After narrow cooperation of the Rzeszów Design Office for Agricultural Building with the Rzeszów University of Technology different improvements of the structure have been made. They were based on the full scale checking of the prototypes on special testing arrangement where the frames were horizontally loaded by hydraulic jacks. Thus the system "Małopolska 80" was created. The main idea was to replace the nailing by circular teeth steel fasteners "BISTYP", to apply formwork frame instead of planked web, and to force high quality of execution by correctly placed fasteners. "BISTYP" fasteners permit to carry the forces up to 30 kN, and have the formal state approval.

The three hinge frame structure "Małopolska 80" is presented on fig.3. The timber consumption index decreased to $2.7\text{m}^3/100\text{m}^2$. Main advantages of this system are:

- clear statical system causing small timber consumption,
- small number of units, repeated diagonals,
- axial net of struts,
- market available section of wood 50/140,
- possibility of use of the same frame for different combination of external actions /snow and wind zones/ by the variable distance of frames /3.0 ÷ 4.5 ÷ 6.0 m/.

2. Loading device for investigations.

Some interest may attend the special device to load the full scale frames in horizontal position. This arrangement gives different advantages. It permits to load separate structures /fig.3/ the access to different points of structure is very easy, as well

as all the measurements of strains and deformations, even with their diagrams. Simple steering of jacking process, different points of load apply and full safety up till the break of tested structure proved to be very convenient. The principle of internally equilibrated system was successfully applied /fig.4/. The tested units are supported on the load carrying steel beam similar as on site, and both structures laing on the distance blocks on the floor, are tacked together.

Hydraulic jacks of two side action 110 kN were applied in 10 + 18 points simulating the constant or local action. Precise pressure meters permitted to control the speed of loading. Strains were measured by digital tensometers, deformations by clock distancemeters, or by geodesial methods. Loads were applied according the rules of CIB Timber Standard up till the collapse of the structure /fig.5/. The humidity of timber just after the break was checked by drying and weighing method. This was done independently from the general humidity checking by elektro resistant instruments. Destruction followed usually in most strained tensioned rods; external belts of columns or top belt of beam near the corner. The average general safety factor of "Rzeszów 77" planked frames $\bar{S} = 3.79$ proved to be too high, and was forceing to make improvements. The "Rzeszów 77k" frame differed from the former by decrease of belts sections and planks depth, and replace of outer tensioned belt by steel flat section.

Testing of 5 these frames showed totally different pattern of collapse. The break was caused by buckling of compressed belt of column. Average safety factor was $\bar{S} = 2.3$, accepted as sufficient.

Last of solutions, the framework frame "Małopolska 80" collapsed by loss of compression strength in compressed column rods, and their consequent buckling from the plane of structure. The

resulting general safety factor reached $\bar{s} = 2.07$, being sufficient according the Polish Timber Code PN - 81/B - 03150.01.

Very interesting conclusion from these rich investigations is that the standard deviation of bearing capacity of total structure is much lower than this on samples, defined by unhomogeneity factor.

For all tested units the timber was mechanically identified by Youngs modul on 60 x 60 x 1300 mm samples defined according the W.T. Curry method. All tested structures and samples made of fir wood from Bieszczady Mountains, characterized by Youngs modul equal 8000 MPa at moisture content 15%.

Comparison of strength parameters and timber consumption factors is presented on the tables I ÷ 4.

This short survey of results received by sequent change of design and experimental testing of several times repeated timber structures proves how success full may be the mutual interdependence of both structural methods.

Literature

- [1]. CIB Timber Standard. Testing of Timber Structures. 1976.
- [2]. Curry W.T.: Standard Methods of Test for the Determination of some Physical and Mechanical Properties of Timber in Structural Sizes. CIB W18, Aalborg 1976.
- [3]. Several detailed reports in Polish.

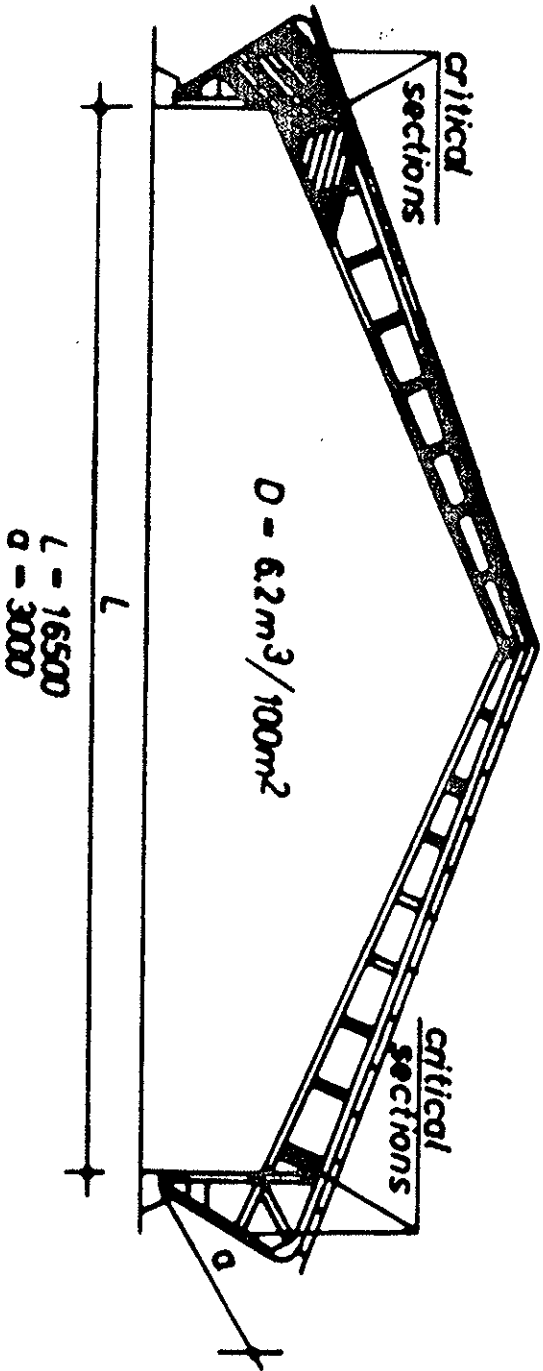


Fig. 1

Timber frame "Rzeszów 77"

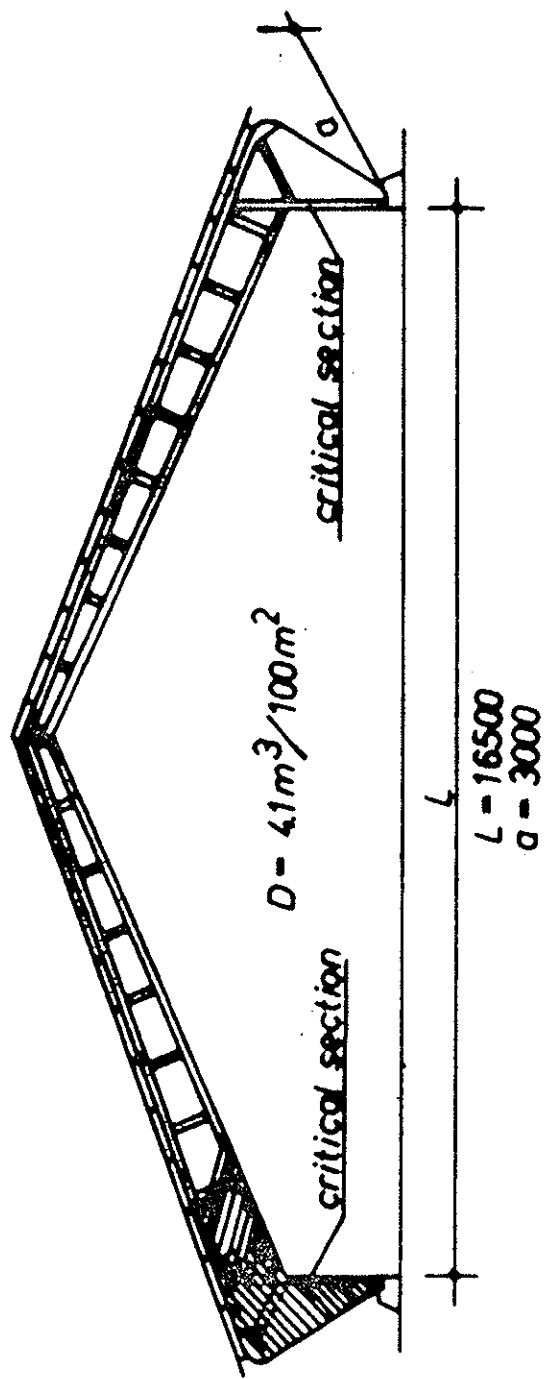


Fig. 2

Timber frame "Rzeszów 77k"

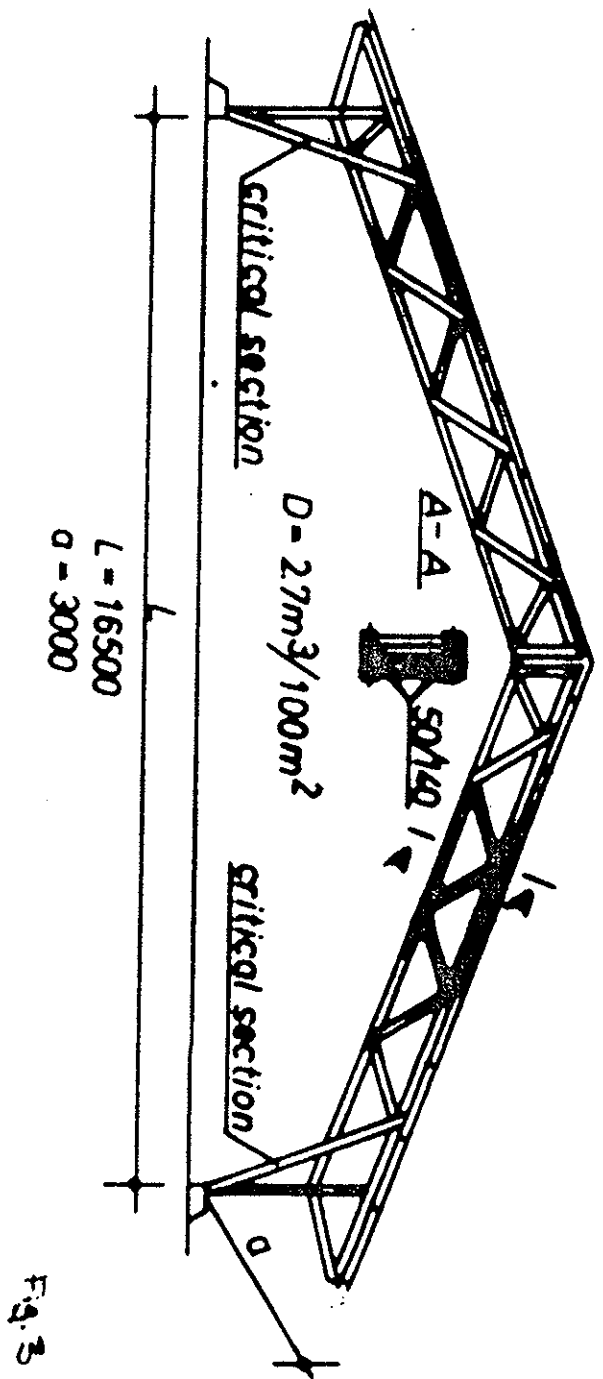


Fig. 3

Timber frame "Matopolska 80"

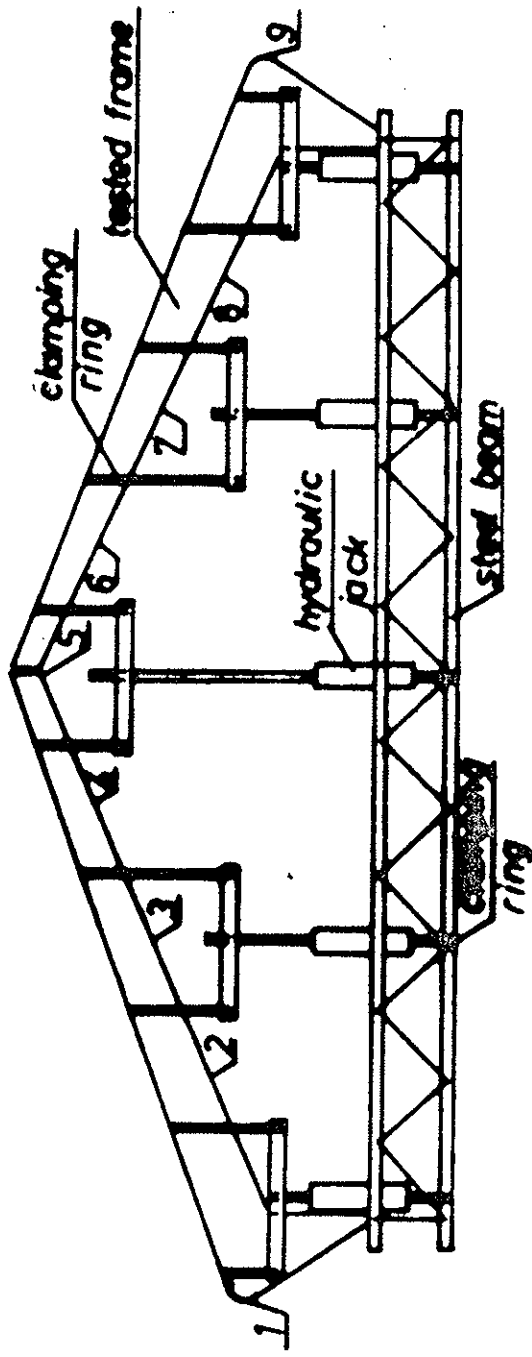


Fig.4

Full scale loading device for horizontal load testing of timber structures

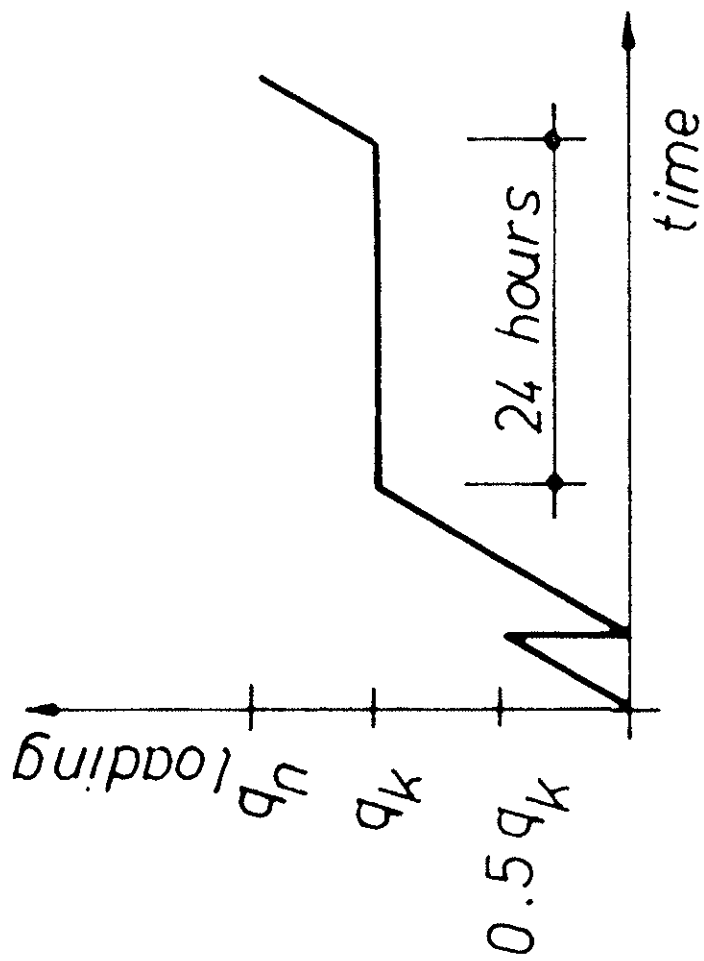


Fig. 5

Scheme of loading of structures

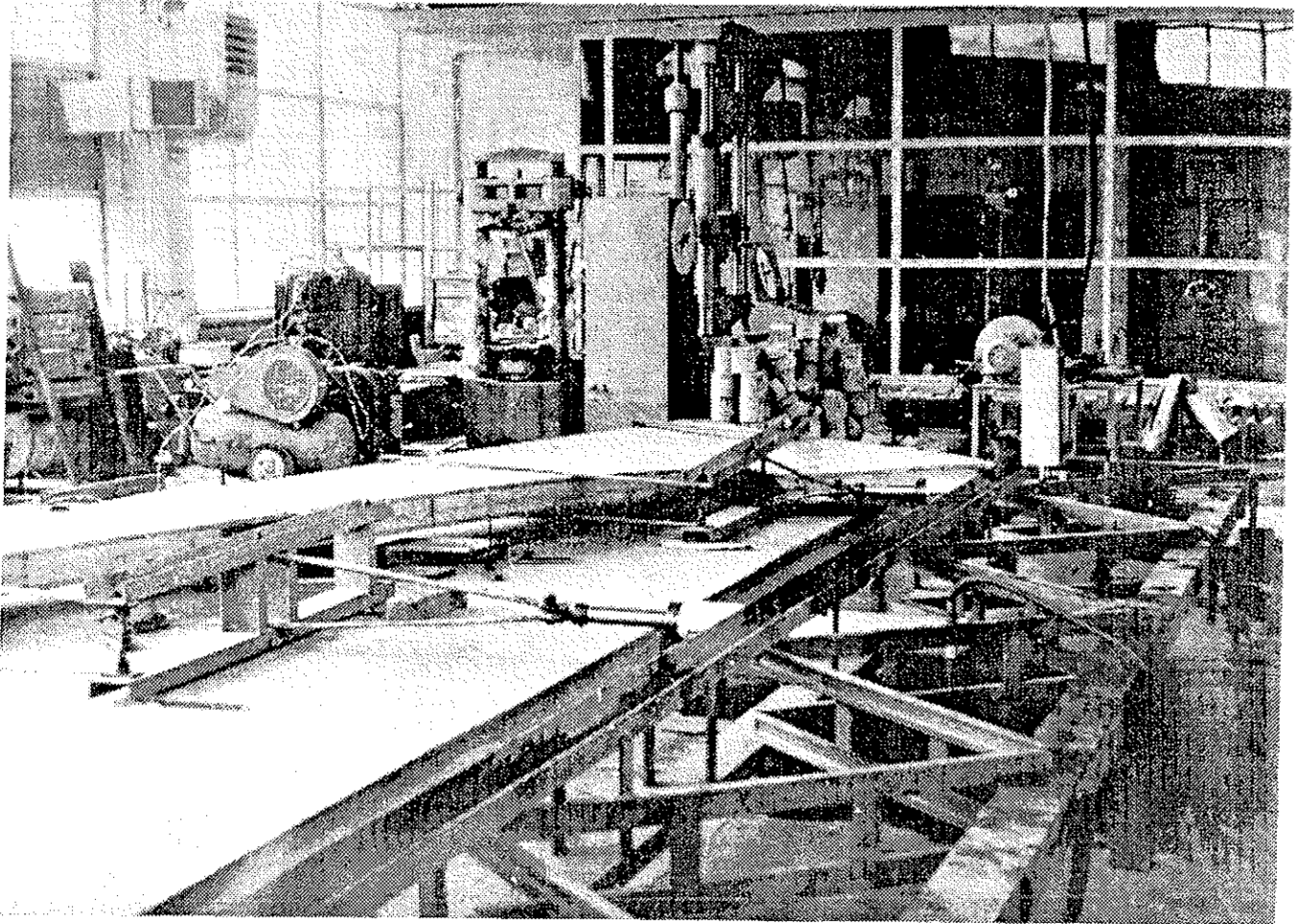


FIGURE 6

Frame type "Rzeszów 77" during testing

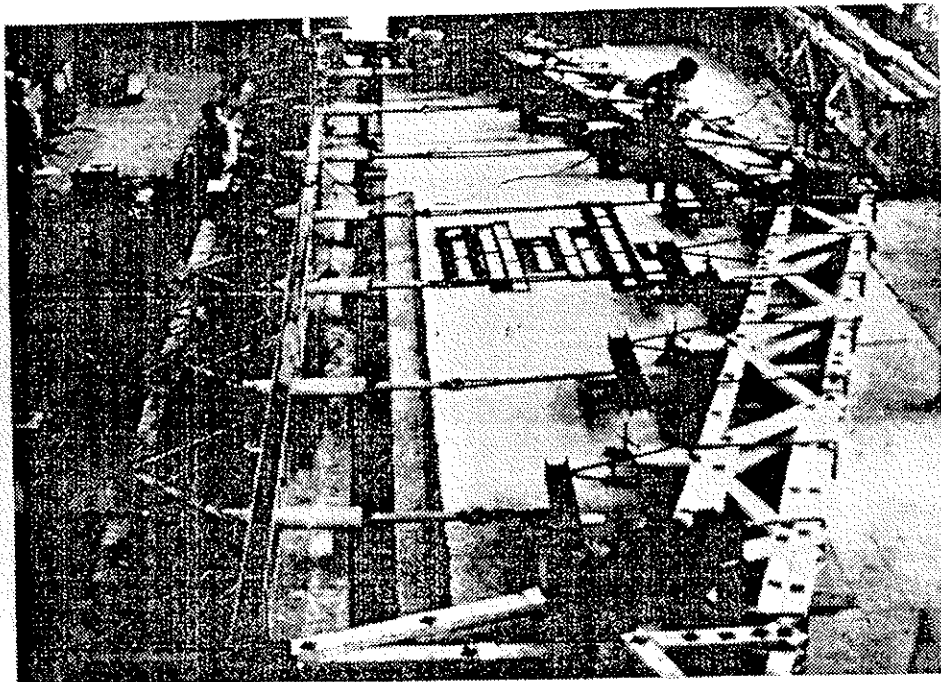


FIGURE 7

Frame type "Małopolska 80" during testing

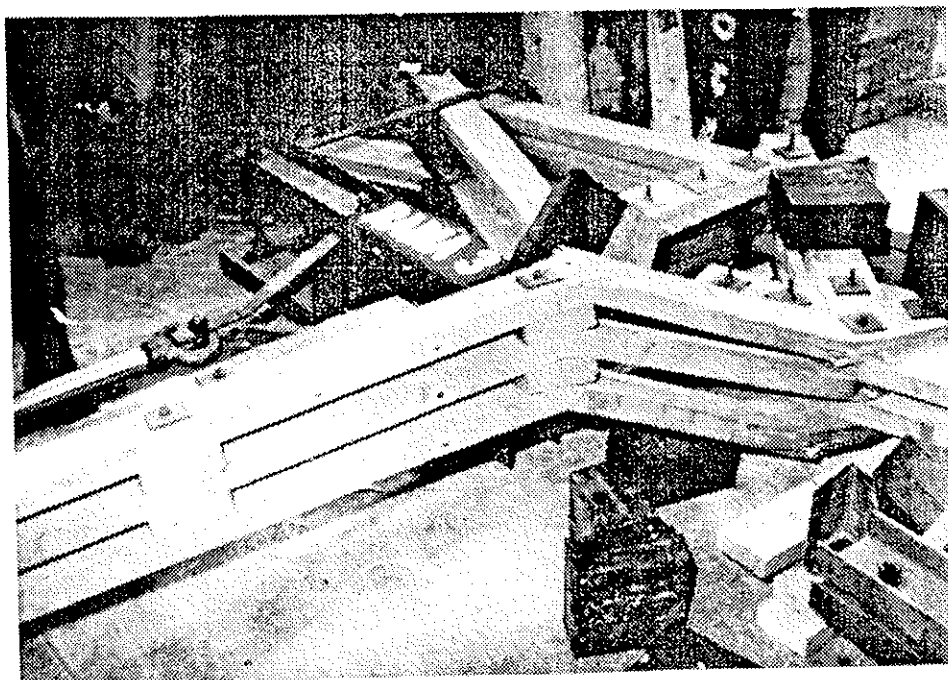


FIGURE 8

Destruction of compressed belt of frame column
"Małopolska 80"

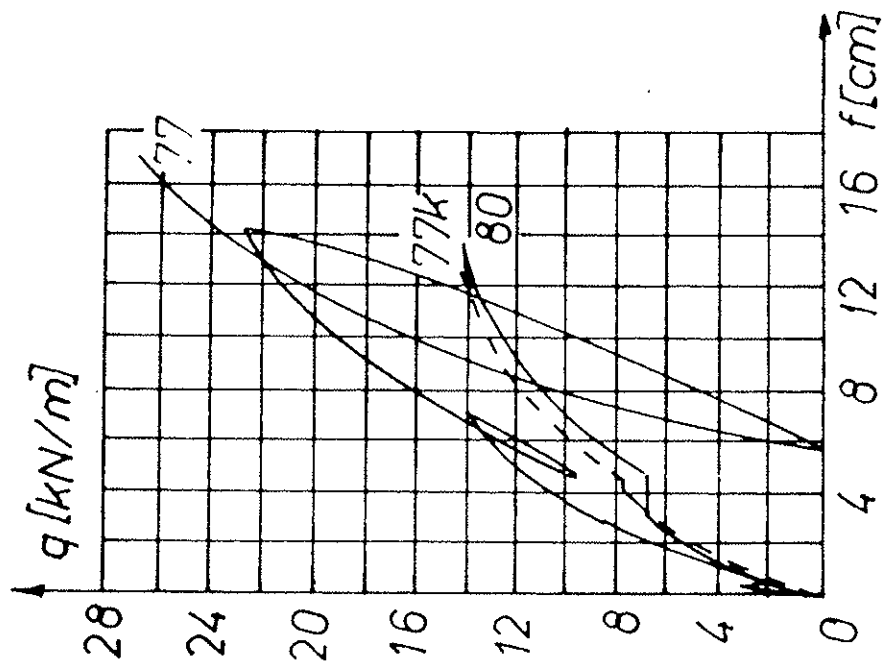


Fig. 9

Deflection of top nipple of frames "Rzeszów 77", "Rzeszów 77k" and "Małopolska 80" measured at testing

Table 1. Survey of collapse test of frames.

Type - No of frame	Characteristic load [kN/m]	Ultimate load [kN/m]	Safety factor	
			of frames s	mean value \bar{s}
Rzeszów 77	7.15	26.76 25.80 28.65	3.74 3.61 4.01	3.79
1				
2				
Rzeszów 77k	7.15	14.80 14.45 12.74 14.20 14.70	2.07 2.02 1.78 1.99 2.06	1.98 /2.31/ ^{1/}
1				
2				
3				
4				
5				
Małopolska 80	6.88	13.60 14.51 14.50	1.98 2.11 2.11	2.07
1				
2				
3				

1/

Humidity of "Rzeszów 77k" frames was ca w= 30 % while testing.

For comparison their safety factor recalculated to w= 22 %

equals s= 2.31.

Table 2. Stresses in timber measured at the breaking load.

Type of frame	Stress just before collapse	
	+ σ /MPa/	- σ /MPa/
Rzeszów 77	42.3	66.2
Rzeszów 77k	26.0	47.0
Małopolska 80	24.5	38.4

Table 3. Deformation of top nipple.

Type of frame	Point	Mean deflection at load	
		characteristic [cm]	ultimate [cm]
Rzeszów 77	1	--	5.2
	2	1.0	6.5
	3	1.9	11.6
	4	2.2	15.8
	5	2.4	17.2
	6	2.3	15.3
	7	2.0	11.4
	8	1.0	6.6
	9	--	5.3
Rzeszów 77k	1	--	3.4
	2	2.3	5.7
	3	3.3	9.1
	4	4.3	11.6
	5	4.3	12.5
	6	4.3	11.6
	7	3.4	9.0
	8	2.6	6.0
	9	--	4.2
Małopolska 80	1	1.7	4.3
	2	1.8	5.0
	3	2.9	8.6
	4	3.9	11.6
	5	4.8	14.6
	6	4.0	11.6
	7	2.6	8.3
	8	1.6	4.9
	9	1.2	3.8

Table 4. Timber consumption index.

Type of frame	Material consumption per 100 m ² of area			
	Timber m ³	%	Steel kg	%
Bieszczady 75	4.3	69	439	57
Rzeszów 77	6.2	100	765	100
Rzeszów 77k	4.1	66	607	79
Małopolska 80	2.7	44	472	62

INTERNATIONAL COUNCIL FOR BUILDING RESEARCH STUDIES AND DOCUMENTATION

WORKING COMMISSION W18A - TIMBER STRUCTURES

**ENSURING OF THREE-DIMENSIONAL STIFFNESS
OF BUILDINGS WITH WOOD STRUCTURES**

by

A K Shenghelia
ZNIISK Kutcherenko Moscow
USSR

MEETING TWENTY - TWO

BERLIN

GERMAN DEMOCRATIC REPUBLIC

SEPTEMBER 1989

A.K.Shenghelia, candidate of technical
sciences
(ZNIISK Kutcherenko, Moscow)

ENSURING OF THREE-DIMENSIONAL STIFFNESS OF BUILDINGS WITH WOOD STRUCTURES

One of the important aspects for wood structures as well as for any structures, is the ensuring of three-dimensional stiffness of buildings and structures as a whole, both by means of braces and by means of enclosure construction elements - such as girders, ribs of coating plates and wall panels framework.

Usually, girders and coating plate ribs are calculated for bending or unsymmetrical bending depending on roofing slope. When used as longitudinal elements of tie systems, they must also take normal force (compression or tension), which appears in tie truss posts. The same force must be taken by attachment of girders and plate ribs to load-carrying structures.

At present the aspect of ensuring of three-dimensional stiffness of buildings with load-carrying wood structures is approached intuitively, and in most cases groundless solutions are made, which lead to increased expenditure of lumber and steel.

In the present article the question of inclusion in work of tie systems of girders and plate ribs as longitudinal stiffness elements is being considered. For this purpose experimental and theoretical investigations of specimens of connection of girders to load-carrying elements were carried out.

During the work on technical solutions of assemblies propositions of calculation methods of tie systems stated in /1/, were accepted as theoretical preconditions. The example of tie systems design for craneless industrial building with coating of

wood glued beams, span 18 m, spacing 6 m, was assumed as a basis. Building height up to column top is 7,2 m. According to snow load it is the IV building region, and according to wind load it is the II building region.

According to this example, maximal forces in longitudinal elements of tie systems, which attachments of girders or plate ribs to load-carrying elements should be calculated for, make up the following values: compression - $N_c = 3,99$ kN, tension - $N_t = 2,67$ kN.

Additional theoretical researches on influence of various factors upon calculation forces value were carried out: kind and spacing of load-carrying structures; span and height of building.

For example, in case of trusses as load-carrying structures N_c increases by 6,8% and N_t increases by 10%; with spacing 3 m N_c decreases by 73% and N_t is 2,58 times as little; with span 24 m N_c increases by 1% and N_t decreases by 0,6%; with building height 4,8 m N_c decreases by 5% and N_t increases by 7%. As is obvious, all these factors, spacing excluding, have insignificant influence upon horizontal force value, therefore attachment assemblies of girders and plates to load-carrying structures were designed for force $N = 4$ kN. Since in the example under consideration roofing slope $i = 0,05$ is not great, pitch component of horizontal load was not considered, but with slopes $i \geq 0,25$ (especially in lancet arches) its influence can be significant and should be considered in concrete design.

When working out variants of technical solutions for as-

semblies, two basic preconditions dominated: minimal metal expenditure and simplicity of work at building site. Therefore, nail connections were chosen without use of metal and with use of minimal quantity of metal in shape of strips and angle pieces.

Girder fragments with cross section 120x160 mm, length 500 mm in cut variant and 1 000 mm in uncut variant and load-carrying structure fragments with dimensions 140x400x400 mm were cut out from glued beams (dimensions: 140x400x3000 mm). manufactured at Volokolamsky experimental building structures factory in 1986 and tested for lateral bending. Beams were manufactured of second rate deals (pine boards), thickness 32-33 mm. Up to the moment of testing average specimen wood humidity made up 10,5-11,7%. It was tested all together ten specimens - two "twins" of each of five design modifications.

Specimens were tested for normal force action, applied to central line of girder fragments attached to load-carrying structure fragment. Fig. 1 shows full-scale photos of test rig on force floor. Under the action of force girder fragments have the possibility of free vertical travel with respect to load-carrying structure fragment which is pinched between two stock rests. Metal plate, fastened at two branches of stock post (see Fig. 1. *b*) in direction of specimen horizontal axis, serves for preventing of joint specimen bulging. To minimize friction influence between specimen and metal plate, its inner surface was oiled with special oil.

Specimens of assemblies were tested in plastic stage by means of jack *ДГ*-5. Loading was made stage by stage with periodic load relief after each stage to estimate residual defor-

mations. Value of the first loading stage made up 4,89 kN or 1,22 N . Then increment in each stage made up about 1,6 kN. For example, 4,89; 6,5; 8,11; 9,75 kN etc. Loading of specimens and load relief was made with constant speed. Test duration up to failure of individual specimens made up from 25 to 50 min. Deformations were measured by means of dial indicators (two on each specimen), and as for last three specimens - by means of Maksimov deflectometers. Scale factor of both instruments is 0,001 mm.

Specimen I-1 was tested without instruments. First, vertical load was applied without horizontal plate, therefore the joint found itself in complicated stressed state: it was subject to bending besides shearing forces. Specimen's centre bulged from vertical plane, and lower fragment of girder twisted around fragment of load-carrying structure. A crack appeared across the grain in load-carrying element along the lower line of nails (Fig. 2).

Then specimen I-1 was turned and tested, excluding bulging in centre, that is for vertical load, up to failure. This time these cracks found themselves along the upper line of nails, as specimen was turned during the test.

In the rest of the specimens deformations of attachment were measured. Dial indicators were placed on each side to the left and to the right in upper part of specimen and they registered the shift of upper girder fragment with respect to fixed bench mark in load-carrying element (see Fig. 1). Axis deformation graphs were constructed. Values of deformations were got as averaged ones, according to indications of two instruments. In all specimens tested deformations appeared to be lower by far than

normalized limit with calculated load-carrying capacity - 2 mm. For example, see specimen II-1 deformation graph (Fig. 3). With load 4,89 kN (1,22 N) deformation made up only 0,08 mm. With Load 129,5 kN (3,24 N) deformation made up 1,97 mm. This indicates high reliability of joint design. With load 18,71 kN full deformation was 10,14 mm and residual deformation was 9,61 mm.

When specimen I-2 was destructed, three nails were sheared (two ones from the left and a lower one from the right). These nails connected angle pieces with load carrying element. Upper right nail was almost completely pulled out from load-carrying element.

When specimens II-1 and II-2 were destructed stop bars shifted with respect to load-carrying element by 46 and 54 mm respectively (Fig. 4.a). Specimens III-1 and III-2 (Fig. 4.b) were destructed in analogical way. Bar shift made up 45 and 32 mm respectively.

Specimens IV-1 and IV-2 were destructed with the same load. Lining bar split across the grain, in place of four and two nails (Fig. 4.c); shift with respect to load-carrying element was 7-9 and 6-11 mm respectively for the first and the second specimen.

In specimens V-1 and V-2 the crack appeared in place of right (Fig. 4.d) and left lower nail, accompanied by lining plate shift with respect to load-carrying element by 5-7 and 9-11 mm, respectively for the first and the second specimen.

To estimate load-carrying capacity of tested joints, according to method of Y.M. Ivanov /2/, reliability factors K_p to breaking force value N_b were calculated by means of formula:

and actual reliability factors $K_p = 1,38(1,94 - 0,116 \lg t)$
 $K_f = \frac{N_B}{N_n}$

where $t = \frac{t_1'}{38,2}$;
 t_1' - is duration of reaching breaking force, in sec;
 $N_n = N$ - calculated load-carrying capacity of the joint.

Results are shown in the table.

Table

Specimen mark	N_B	t_1'	t	K_p	K_f
I-1	32,43	3000	78,5	2,37	8,1
I-2	26,83	3000	78,5	2,37	6,7
II-1	21,24	1800	47,12	2,41	5,3
II-2	21,24	1500	39,27	2,42	5,3
III-1	23,64	1800	47,12	2,41	5,9
III-2	22,84	1800	47,12	2,41	5,7
IV-1	13,75	2100	54,97	2,4	3,44
IV-2	13,75	1800	47,12	2,41	3,44
V-1	26,83	2400	62,82	2,4	6,7
V-2	26,04	3000	78,5	2,37	6,5

As the table indicates, all the joint specimens tested have sufficient load-carrying capacity and reliability and can be recommended to design organizations for introduction into working drawings of buildings for various purposes.

As a result of carried out experimental and theoretical investigations of attachment specimens of girders to load-carrying structures the following conclusion was drawn:

1. Testing method was maximal close to real work of construction joint elements and imitated their stressed state in building coating.

2. The possibility of use of wood girders and plate ribs as longitudinal elements of tie systems in building coatings was experimentally confirmed.

3. With roofing slope $i \geq 0,25$ attachment of girders and plate ribs to load-carrying structures should be tested for perception of slope component of vertical load on the coating.

4. When calculating girders and plate ribs the influence of horizontal force can be disregarded because of its insignificance in general balance of stressed state of these construction elements.

5. With the use of girders and plate ribs as longitudinal elements of tie systems appreciable economical effect can be achieved decrease of wood and steel expenditure by 30-40% in braces of the building.

Offers for inclusion into new version of SNiP 2.03.06 "Wood structures" were developed.

List of literature

1. Text-book for wood structures design (to SNiP II-25-80) -
M: Strojisdats, 1986. - p. 216.
2. Recommendations to testing of wood structure joints - M:
Strojisdats, 1981. - p. 40.

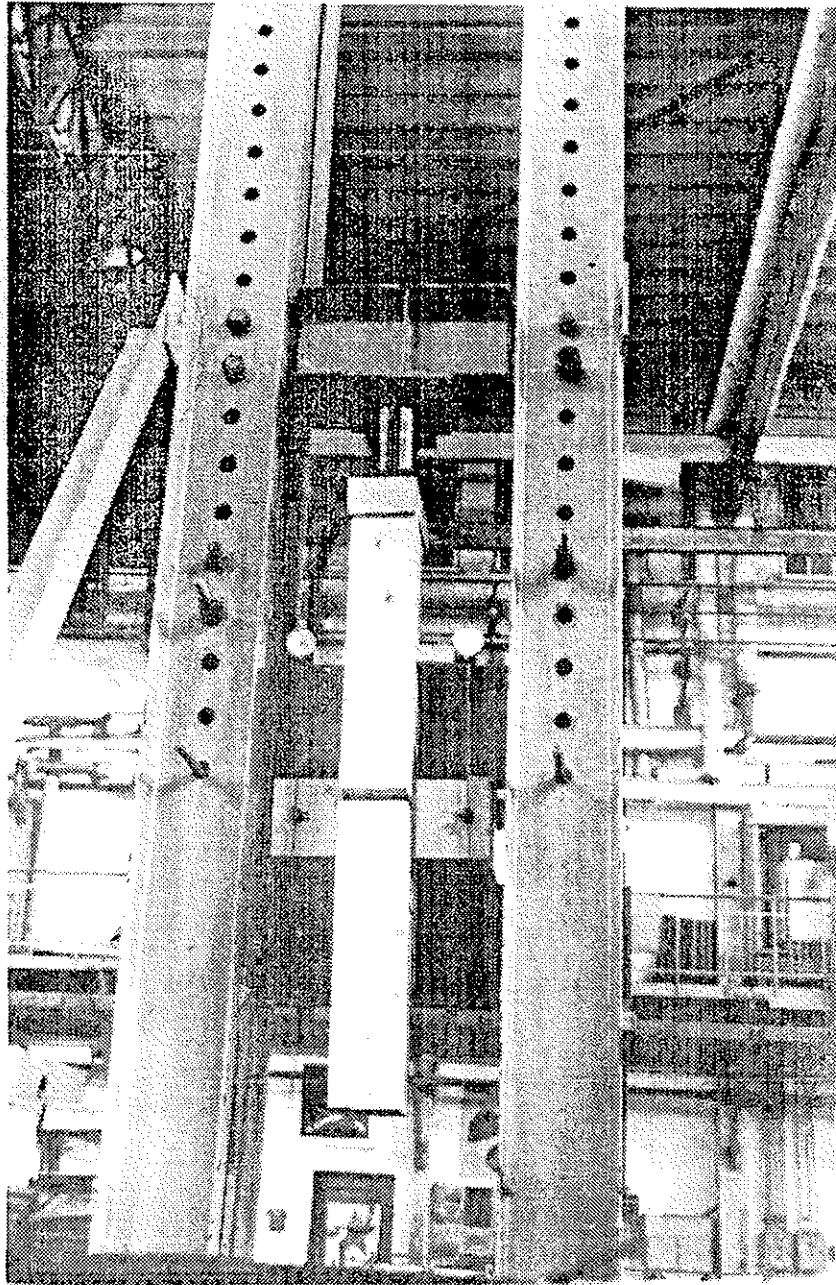


FIGURE 1(a)

Test rig with installed specimen; without metal plate

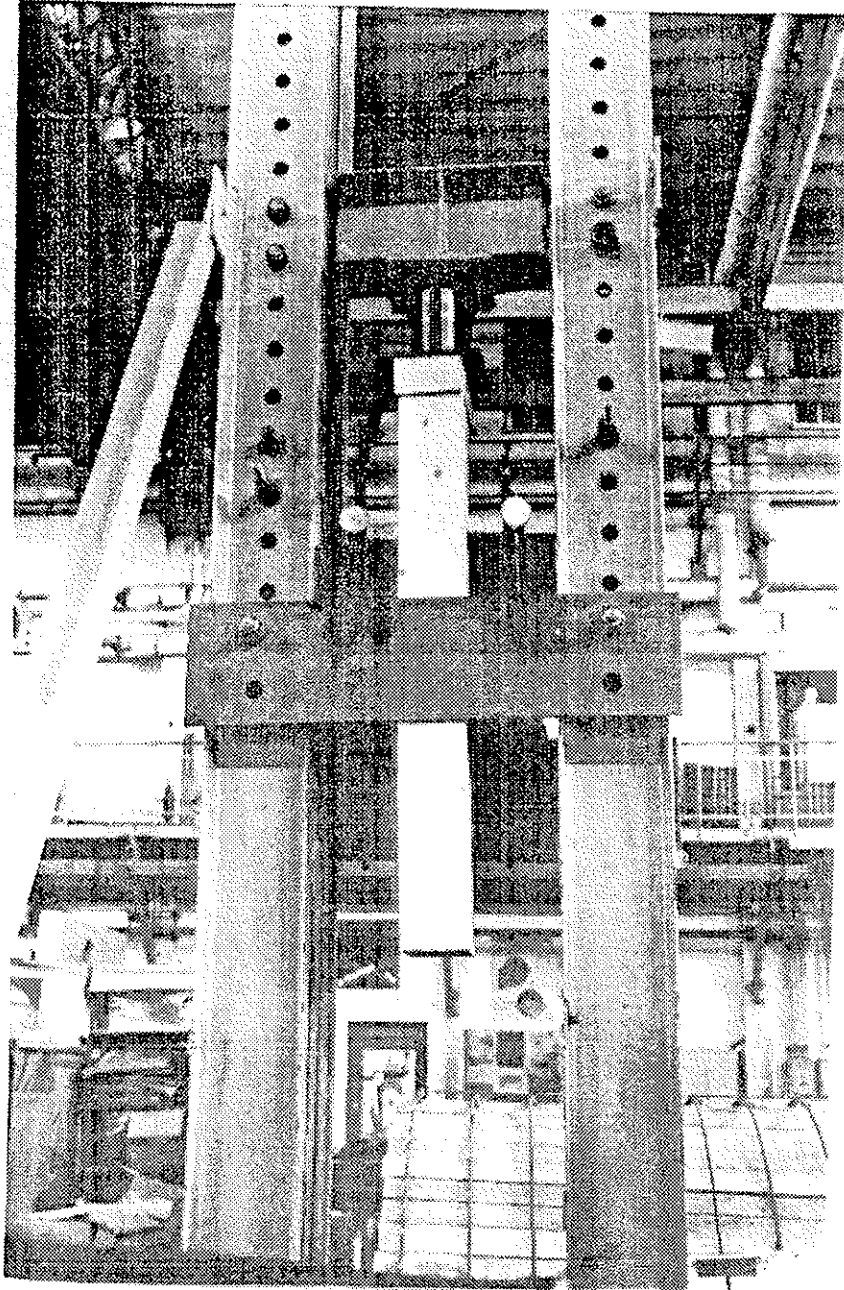


FIGURE 1(b)

Test rig with installed specimen: with metal plate

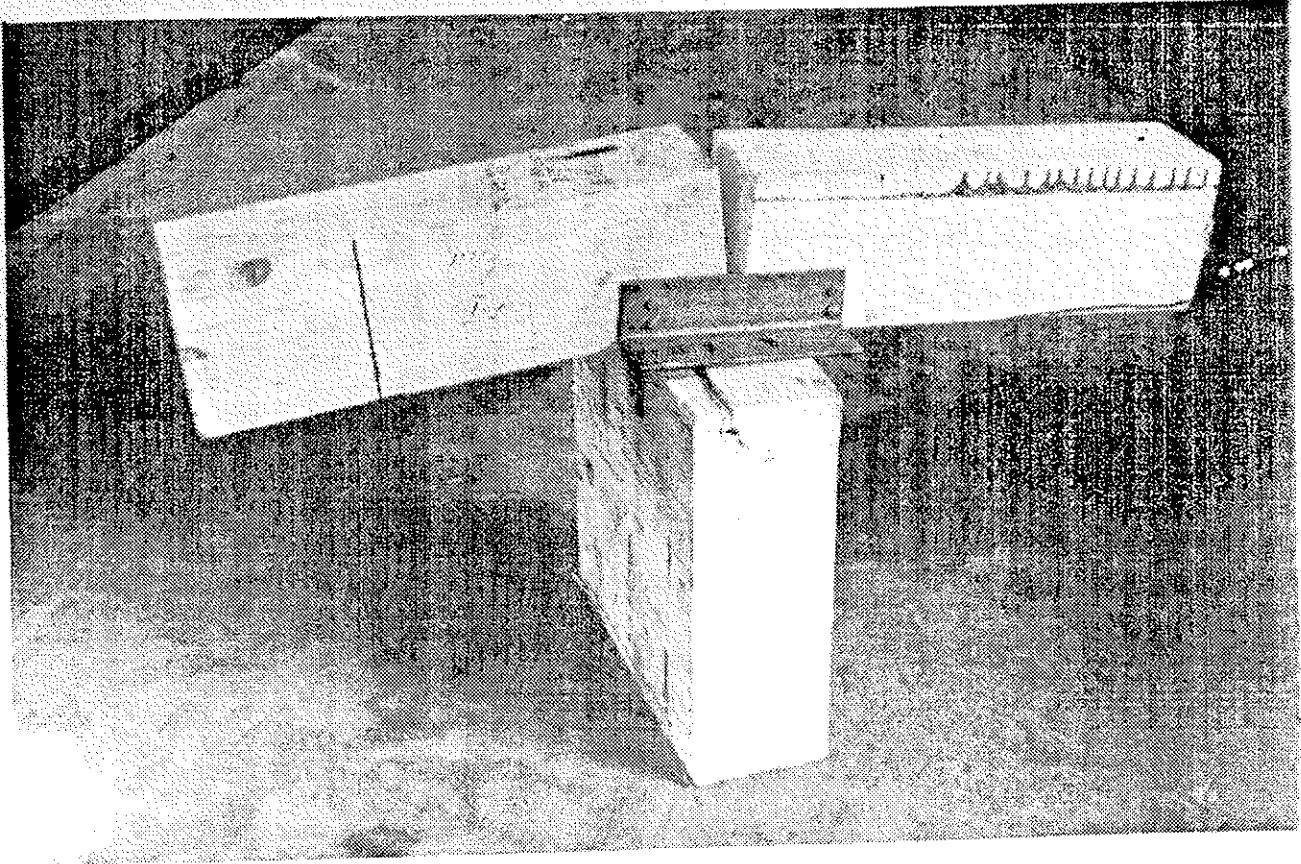


FIGURE 2

Specimen I-1 after failure

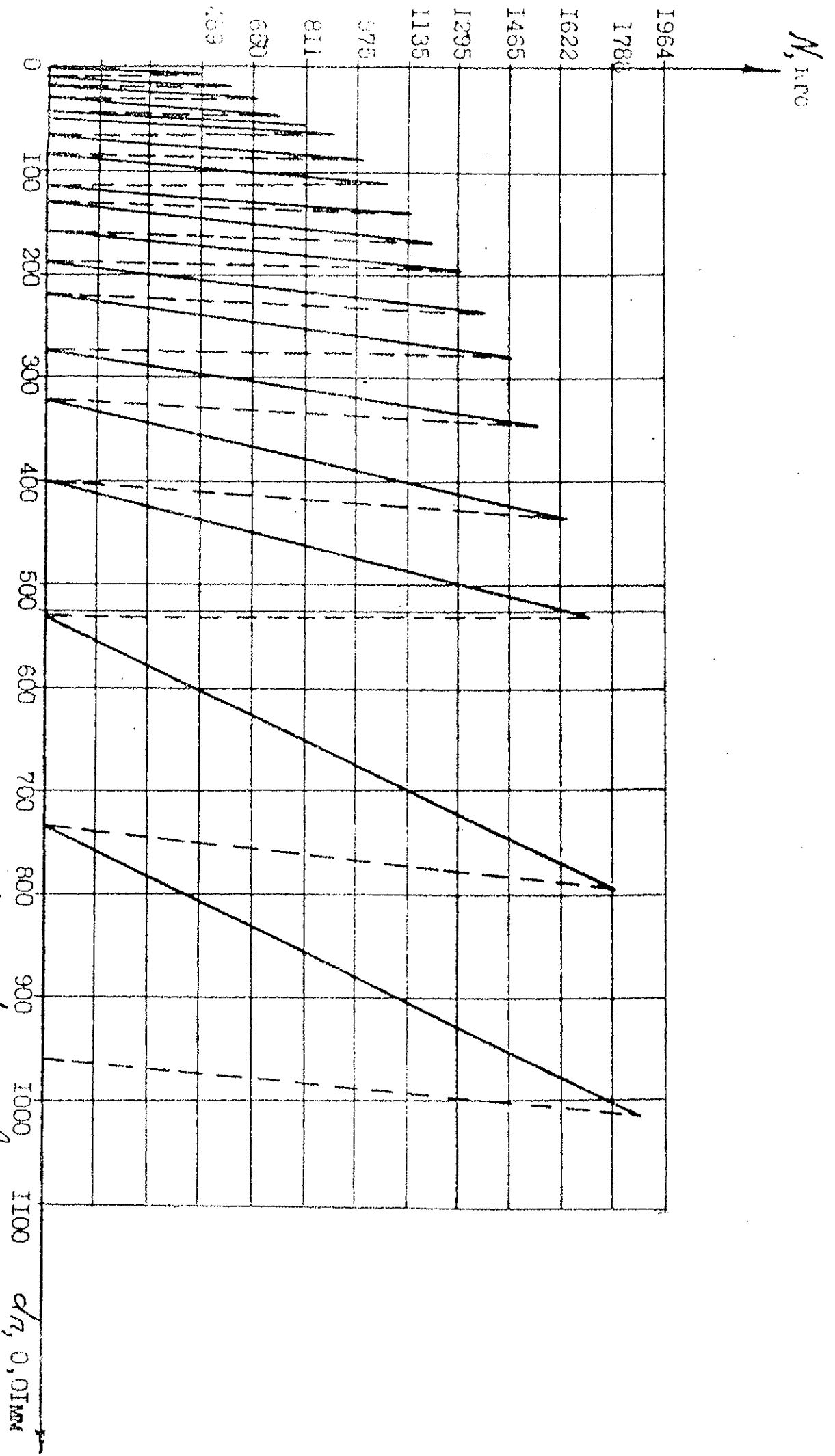


Fig. 3. Deformations of specimen II-1

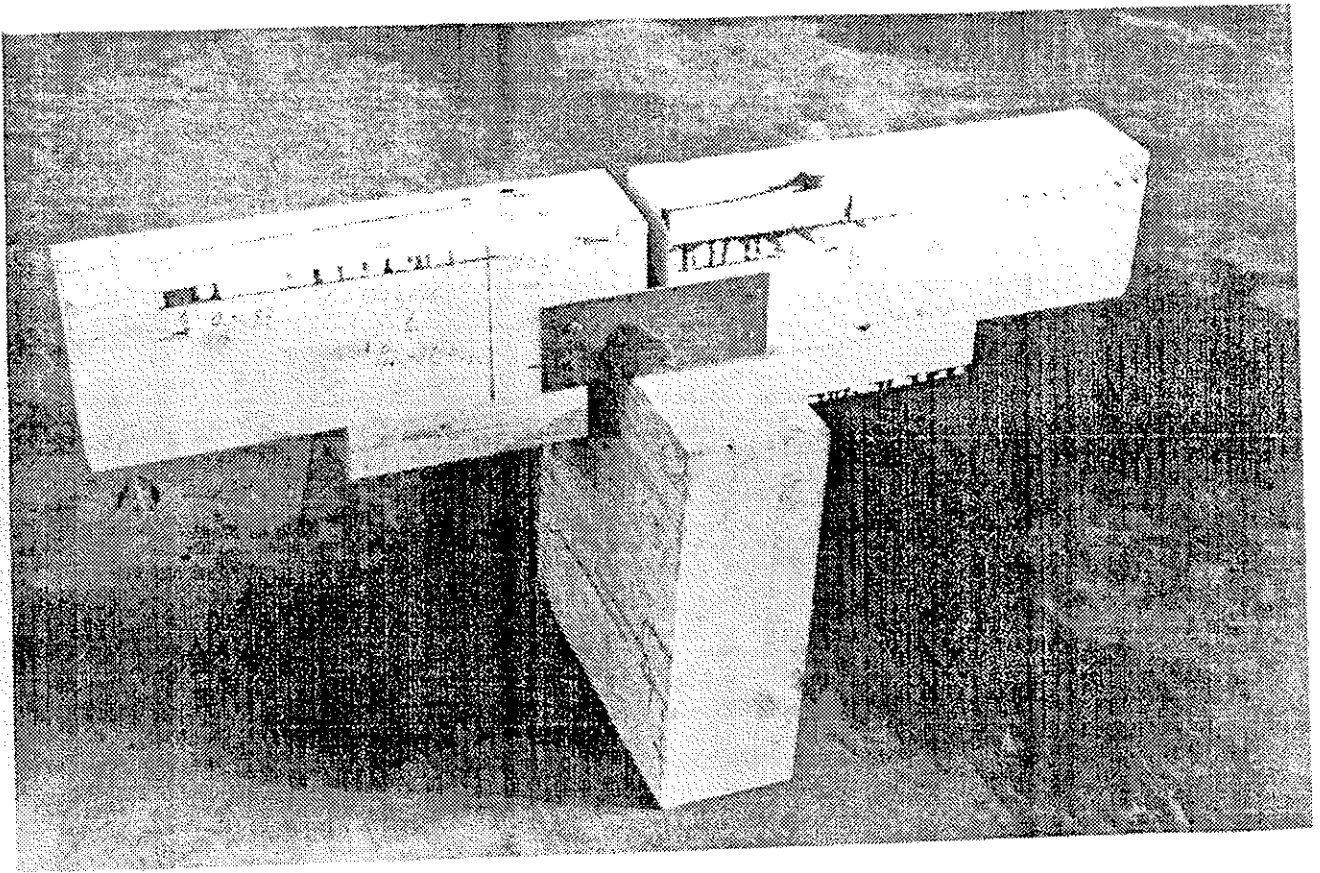


FIGURE 4(a)
Specimen after failure
II-1

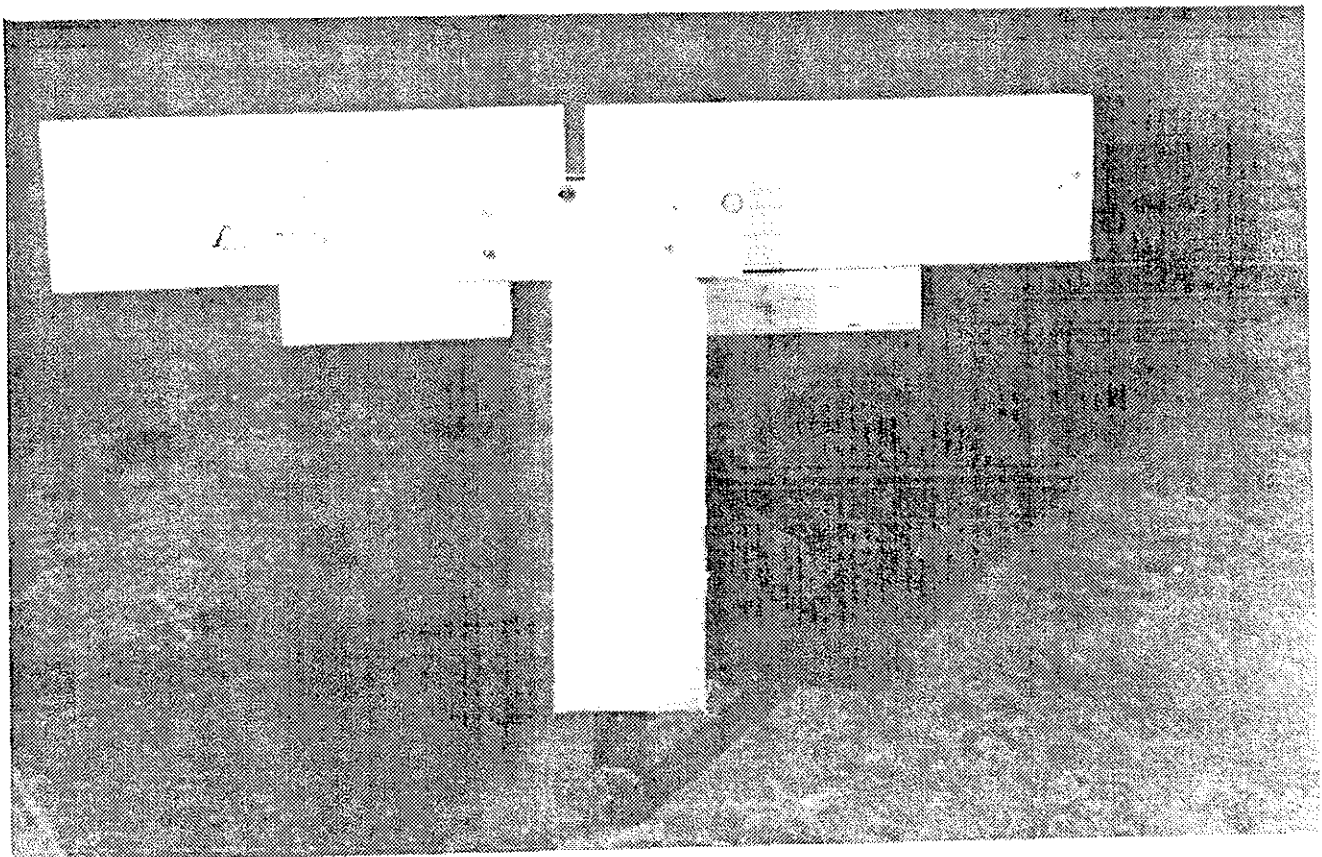


FIGURE 4(b)
Specimen after failure
III-1

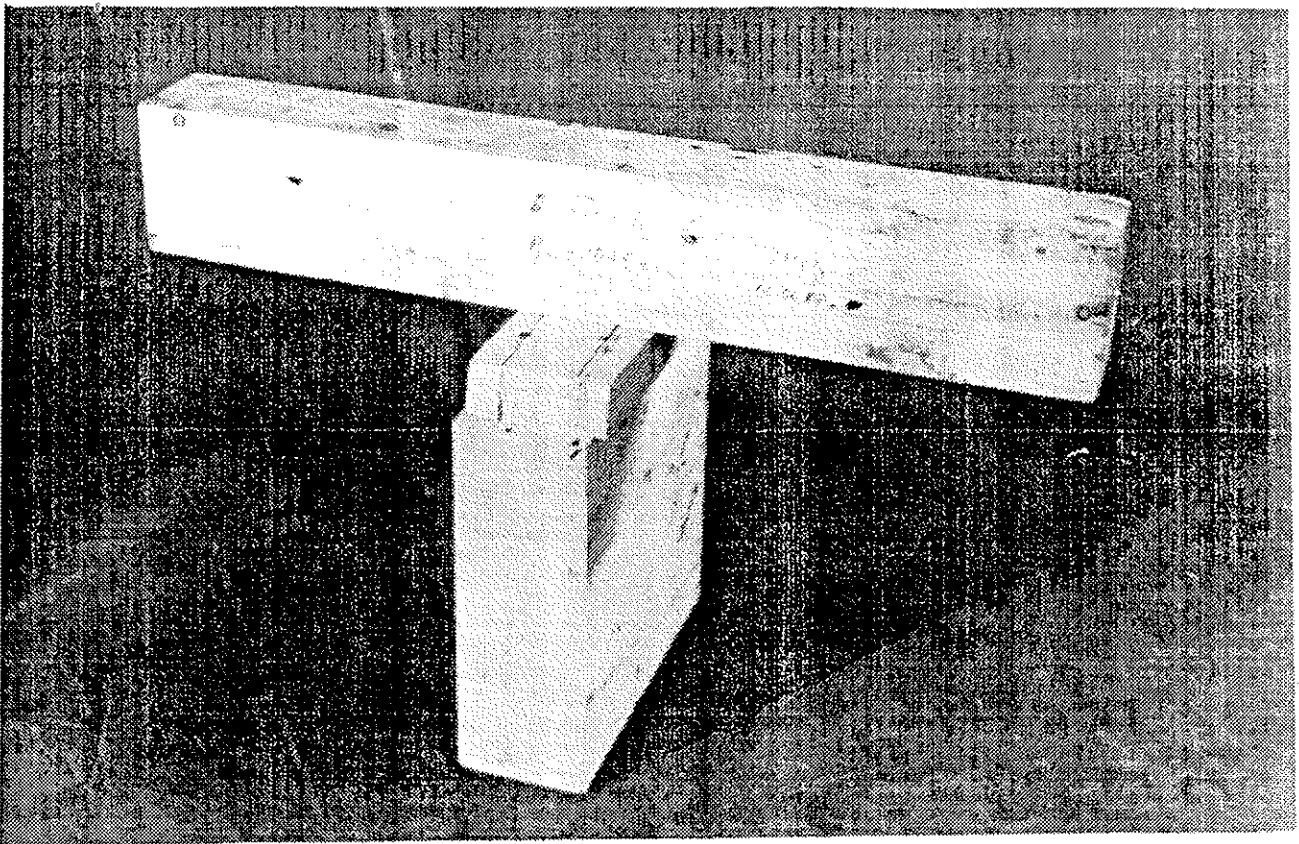


FIGURE 4(c)
Specimen after failure
IV-1

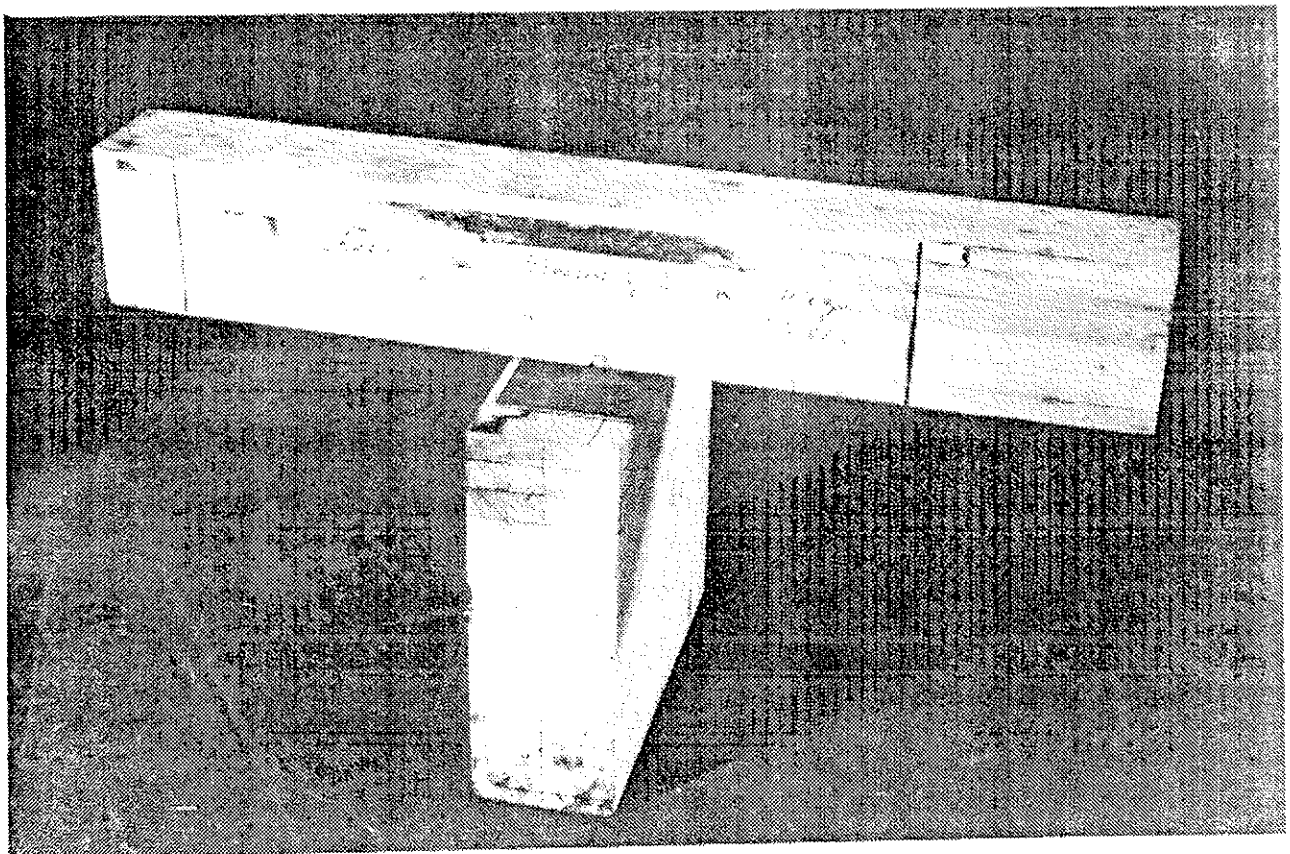


FIGURE 4(d)
Specimen after failure
V-2

INTERNATIONAL COUNCIL FOR BUILDING RESEARCH STUDIES AND DOCUMENTATION
WORKING COMMISSION W18A - TIMBER STRUCTURES

SEISMIC BEHAVIOR OF ARCHED FRAMES
IN TIMBER CONSTRUCTION

by

M Yasumura
Building Research Institute
Ministry of Construction
Japan

MEETING TWENTY - TWO
BERLIN
GERMAN DEMOCRATIC REPUBLIC
SEPTEMBER 1989

SEISMIC BEHAVIOR OF ARCHED FRAMES IN TIMBER CONSTRUCTION

MOTOI YASUMURA*

1. INTRODUCTION

Arched frames of glued-laminated timber have been used widely in large scale construction. As the vertical loads such as the dead load and the snow load are generally more critical than the lateral loads in the large span structure, few studies have been done on the seismic behavior of the arched frames. In the previous paper(1), the mechanical properties of the joints in glued-laminated beams subjected to the reversed cyclic loads were investigated. In this study, the arched frames of the glued-laminated timber having the joints in the principal rafters were subjected to the reversed cyclic lateral loads, and the mechanical properties of the frames were investigated.

Time-history earthquake response of the three-hinged frames was obtained from the linear model and the bi-linear elastic model, and the influence of joints of the principal rafters on the seismic behavior of the frame was also studied in this paper.

2. DESCRIPTION OF SPECIMEN

Four arched frames of glued-laminated timber were subjected to the vertical load and the reversed cyclic lateral loads. Specimens were reduced scale models and designed in consideration of the building of 30 meters in span. Specimens included a two-hinged frame and three-hinged frames as shown in Fig.1. One of the arched frames had no joints in the principal rafters, and in other specimens the principal rafters were connected with the mechanical joints as shown in Fig.2 so that they could transmit the moment and shear forces.

*Senior Research Officer, Dr.Agr.,Dpt. of Structural Engineering, Building Research Institute, Ministry of Construction, Tsukuba, Japan

The span of the specimen was 10 meters and the cross section of the members was 15-by 45 centimeters. The species of the glued-laminated timber was Ezomatsu (*P.jezoensis* Carr.) and Todomatsu (*A. sachalinensis* Fr.Schm.), and the thickness of the laminae was one centimeter. The outline of each specimen is described as follows;

Specimen-3HNJ: Three-hinged frame having no joints in the principal rafters.

Specimen-3HSP: Three-hinged frame of which principal rafters were connected with the steel plates and eight bolts per joint of 16 millimeters in diameter as shown in Fig.2(a).

Specimen-3HSI: Three-hinged frame of which principal rafters were connected with a steel plate inserted in the glued-laminated timber and six bolts per joint of 16 millimeters in diameter as shown in Fig.2(b).

Specimen-2HSP: Two-hinged frames of which principal rafters were connected with the steel plates and six bolts per joint of 16 millimeters in diameter as shown in Fig.2(c)

3. TEST METHOD

Fig.3 shows the outline of the test apparatus. The specimen was set on the reaction floor and the reversed cyclic lateral loads as shown in Fig.4 were applied at the top of the specimen together with the vertical constant load. The vertical constant load was fixed 22.5kN for a three-hinged frame and 32.3kN for a two-hinged frame by simulating the dead load of the building. The vertical and horizontal displacements of the specimen and the strain of the members were measured with the electronic transducers and strain gages.

4. EXPERIMENTAL RESULTS

4.1 DESCRIPTION OF FAILURE

Among the four specimens, three specimens failed with the radial stress at the curved part of the glued-laminated timber. This failure was not expected except for the specimen having no joints, and it was expected that the joints in the principal rafters had yielded before the glued-laminated wood was failed when the specimen was designed. However the curved part of the glued-laminated wood except for Specimen-3HSI failed with relatively low radial stress of 96.6kN/cm^2 . In Specimen-3HSI, a steel plate connecting the glued-laminated beams yielded and broke suddenly. These results indicate that the difference of the safety factors (strength-to-allowable stress ratio) among the steel, wood and mechanical joints should be considered in case of the design procedure.

4.2 HYSTERESIS LOOPS

Load-deflection curves of each specimen are shown in Fig.5. In three-hinged frames having the joints in the principal rafters, particular effect of the initial slips of the joints on the hysteresis loops was observed. This effect might be caused by the difference of moment distribution in the right and left joints. In two hinged frame this effect was small because the influence of the vertical load to the moment distribution was smaller than that in three-hinged frames.

4.3 EQUIVALENT VISCOUS DAMPING

The equivalent viscous damping was obtained from the hysteresis curves of each specimen, and the calculated values are shown in Fig.6, where the equivalent viscous damping is obtained from the ratio of the absorbed energy to the external work performed in each loop (See Fig.6).

The equivalent viscous damping of Specimens 3HSP and 3HSI was 2 to 3% when the deformation was small. These values coincided with the equivalent viscous damping obtained from the experiment of the mechanical joints in glued-laminated beams(1). The equivalent viscous damping of Specimen-2HSP was 4% when the deforma-

tion was very small, and it decreased to 2.5% and increased again to approximately 5%. This trend is exactly the same as that in the experiment of the joint, and this fact shows that the mechanical properties of the joint are reflected directly to those of two-hinged frames because the influence of the vertical load to the moment distribution is small in two-hinged frames, while the influence of mechanical properties on the frames is more complicated in the three-hinged frames. The equivalent viscous damping of three-hinged frames having no joints in the principal rafters was approximately 1%, and it was found that the arched frame having no joints showed very small damping capacity. The equivalent viscous damping after the glued-laminated wood had failed by the radial stress was approximately 4%.

4.4 STRENGTH AND DUCTILITY

Table 1 shows the maximum lateral load, horizontal displacement for the maximum load, and Fig.7 shows the relation between the lateral load and the horizontal displacement. The maximum load of each specimen was 74.6 to 78.0kN regardless of the types of the specimen. The maximum lateral load was not affected a lot by the types of joint because in most specimens the curved part failed with the radial stress. However, the horizontal displacement for the maximum load of the specimen having no joints in the principal rafters was the smallest, and that of the other specimens were 1.8 to 2.4 times as large as that of the specimen having no joints, and it was found that the joints of the principal rafters affected on the ductility of the frames.

Table 1 Maximum load and horizontal displacement for maximum load

SPECIMEN	MAX.LOAD (kN)	MAX.DEF (rad.)
3HNJ	75.5	0.0177
3HSP	74.6	0.0430
3HSI	77.1	0.0347
2HSP	78.0	0.0315

5. TIME-HISTORY EARTHQUAKE RESPONSE ANALYSIS

5.1 MODELING OF HYSTERESIS LOOPS

Time-history earthquake response analysis was performed on a three-hinged frame as shown in Fig. 8 of which span and height of the eaves were respectively 30 meters and 9 meters. Two hysteresis models as shown in Fig.9 was assumed. Linear model was assumed for a frame having no joints in the principal rafters (Model(1)), and Bi-linear elastic model was assumed for a frame having the mechanical joints in the principal rafters (Model(2)) from the experimental results of arched frames. In Model(2), the lateral stiffness of a frame was reduced to one third of the initial stiffness when the moment at one of the joints became zero. Although more accurate models depending on the hysteresis loops should be used in the frame having the joints, simple models were used to investigate the seismic behavior of the frame before the failure of the glued-laminated timber and the joints. The damping of the frame was assumed to be 0.01 and 0.02 for Models (1) and (2) respectively from the experimental results. Japanese construction code(2) requires that the drift of each story of the building caused by the seismic shear for moderate earthquake motions ($C_0=0.2$) should not exceed 1/200 (this value can be increased to 1/120 if the non structural members shall have no severe damage at the increased story drift limitation) of the story height. Three lateral stiffness of 3.29kN/cm, 5.49kN/cm and 8.23kN/cm were assumed which corresponded to the lateral displacement ratio of 1/120, 1/200 and 1/300 at the eaves in static design depending on the base shear of 0.2.

5.2 EARTHQUAKE ACCELEROGRAM

Following accelerograms were used for the dynamic analysis.

- (a) EL CENTRO May 1940 North-South.
- (b) TAFT July 1952 East-West.
- (c) HACHINOHE May 1968 North-South.

The maximum acceleration of these accelerograms was adjusted to 450gal so that the maximum acceleration response of a frame should be approximately 900 to 1000gal.

5.3 RESULTS

Fig.10 shows the maximum acceleration response in Models (1) and (2). The maximum acceleration response of the frame varied from 468 to 1021gal in Model(1) and 427 to 888gal in Model(2) according to the lateral stiffness of the frame. The maximum acceleration response was the largest when the natural period of a frame was 0.95 seconds ($K=5.5\text{kN/cm}$) in EL CENTRO NS and HACHINOHE NS accelerogram excitation and 0.78 seconds ($K=8.2\text{kN/cm}$) in TAFT EW accelerogram excitation. The maximum acceleration magnification factor was 2.27 in Model(1) and 1.97 in Model(2).

Fig.11 shows the maximum displacement response in Models (1) and (2). The maximum displacement response was 12.1 to 27.6cm in Model(1) and 11.5 to 24.4cm in Model (2). The maximum displacement response was the largest when the natural period was 1.23 seconds ($k=3.3\text{kN/cm}$) in HACHINOHE NS accelerogram excitation, and the maximum horizontal displacement ratio was approximately 1/37 in Model(1) and 1/33 in Model(2).

Fig.12 shows the lateral force corresponding to the maximum displacement response in Models (1) and (2). The maximum lateral force varied from 58.9 to 128kN in Model(1) and 38.6 to 58.0kN in Model(2). In any earthquake accelerogram excitation, the maximum lateral force in Model(2) was reduced to approximately a half of that in Model(1). This reduction of the lateral force in Model(2) might be caused mainly by the reduction of the lateral stiffness with the joint slips, and it seems that the seismic load can be reduced in the frame having certain types of mechanical joints. However, further study should be done regarding the energy absorption in the hysteresis loops.

6. CONCLUSIONS

Summarizing the results of this study, the following conclusions are lead.

(1) Three specimens among four failed with the radial stress at the curved part of the glued-laminated wood, and one failed with the yield of a steel plate connecting the principal rafters. Both kinds of failures were not expected when the specimens were

designed, and the difference of the safety factors among the steel, wood and mechanical joints should be considered in case of the design procedure.

(2) In three-hinged frames having the joints in the principal rafters, particular effect of the initial slips of the joint was observed. This effect might be caused by the difference of the moment distribution in the right and left joints, and this effect was small in two-hinged frame.

(3) The equivalent viscous damping of the three-hinged frames having the joints in the principal rafters was 2 to 3% when the deformation was small, and it coincided with the equivalent viscous damping obtained from the experimental results of the joints.

(4) The equivalent viscous damping of the three-hinged frame having no joints in the principal rafters was approximately 1%, and showed low damping capacity.

(5) The equivalent viscous damping of the frame after the failure of the glued-laminated timber by the radial stress at the curved part increased to approximately 4%.

(6) The maximum load of each frame was 74.6 to 78.0kN regardless of the types of joint. The maximum radial stress calculated from the maximum load was approximately 96.6kN/cm².

(7) The horizontal displacement for the maximum load in three-hinged frames and a two-hinged frame having the joints in the principal rafters were 1.8 to 2.4 times as large as that of the frame having no joints.

(8) The maximum acceleration response of the three-hinged frame excited by the earthquake accelerogram of which maximum acceleration was adjusted to 450gal varied from 468 to 1021gal in the frame having no joints and 427 to 888gal in the frame having the joints in the principal rafters.

(9) The maximum displacement response was the largest when the natural period was 1.23 seconds ($k=3.3\text{kN/cm}$) in Hachinohe NS accelerogram excitation, and the maximum drift was 1/37 in the frame having no joints and 1/33 in the frame having the joints in the principal rafters of the height of eaves.

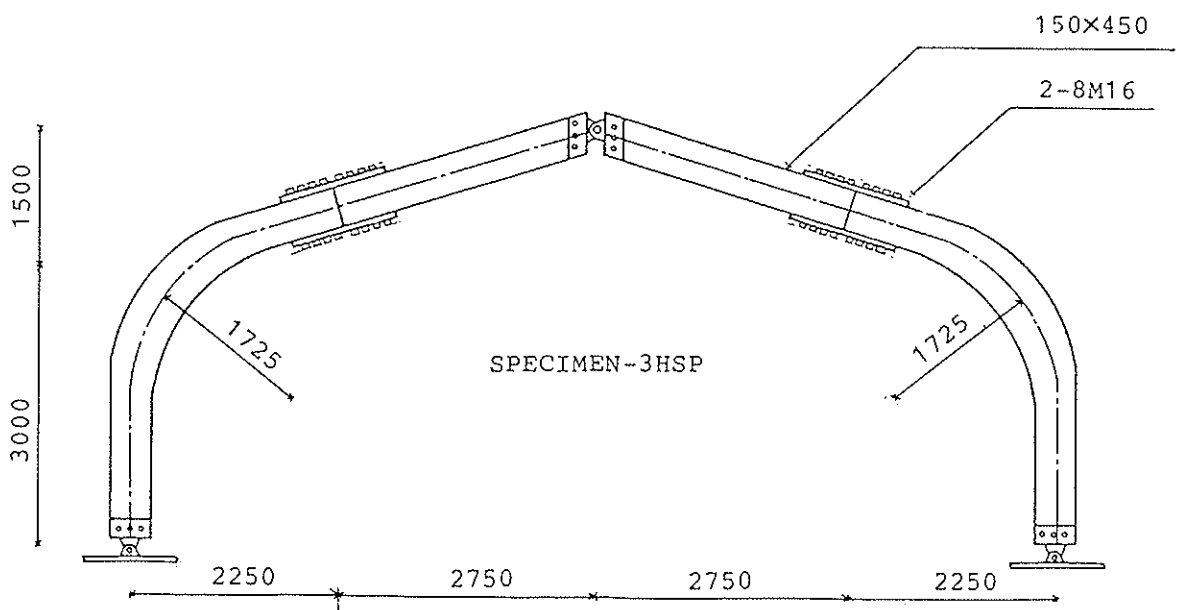
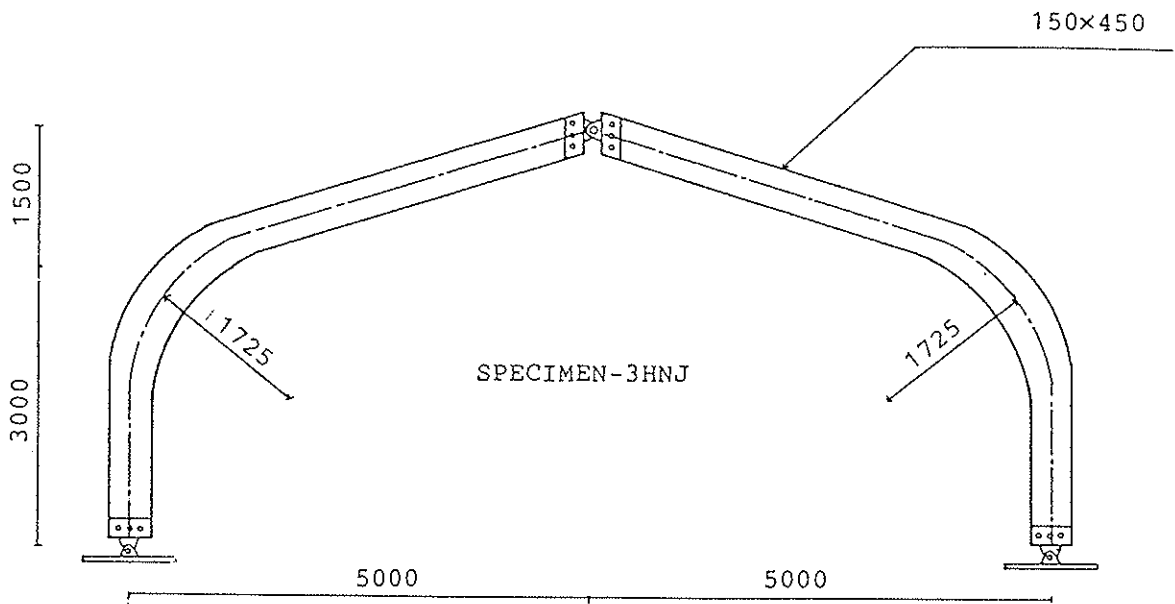
(10) The maximum shear response of the frame having the joints was reduced to about a half of that of the frame having no

joints. This fact concludes that the seismic load can be reduced in a three-hinged frame having certain types of joint in the principal rafters. However, further study should be done regarding the energy absorption in the hysteresis loops.

7. LITERATURE

(1) YASUMURA, M., "MECHANICAL PROPERTIES OF JOINTS IN GLUED-LAMINATED BEAMS UNDER REVERSED CYCLIC LADING", CIB-W18A, September 1989.

(2) " Building Standard Law, Enforcement Order Art.82", Ministry of Construction.



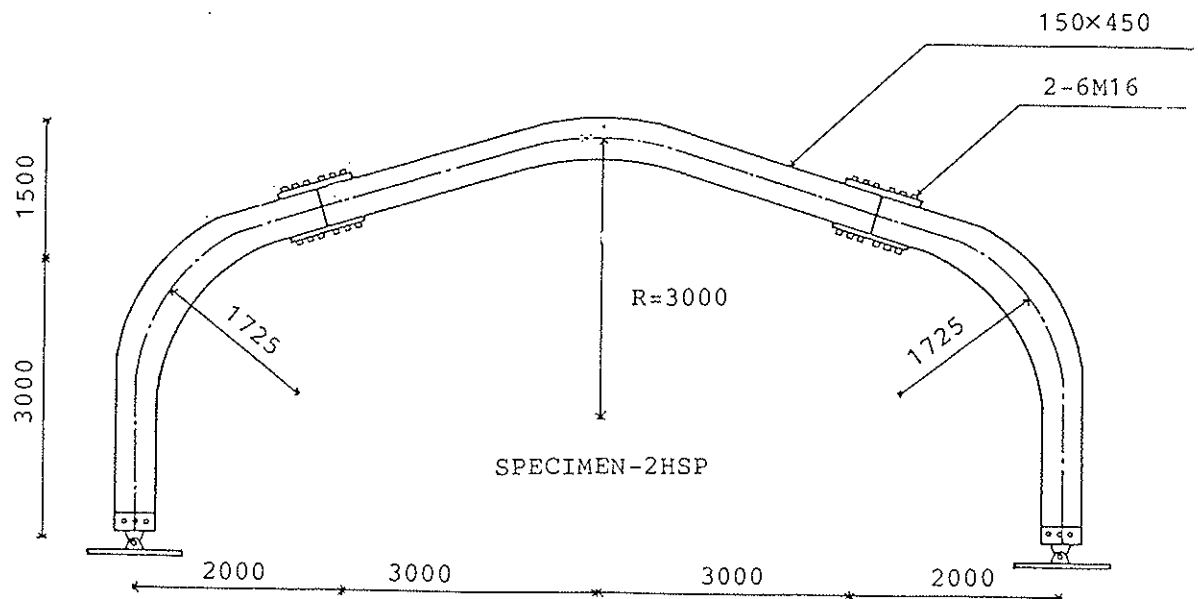
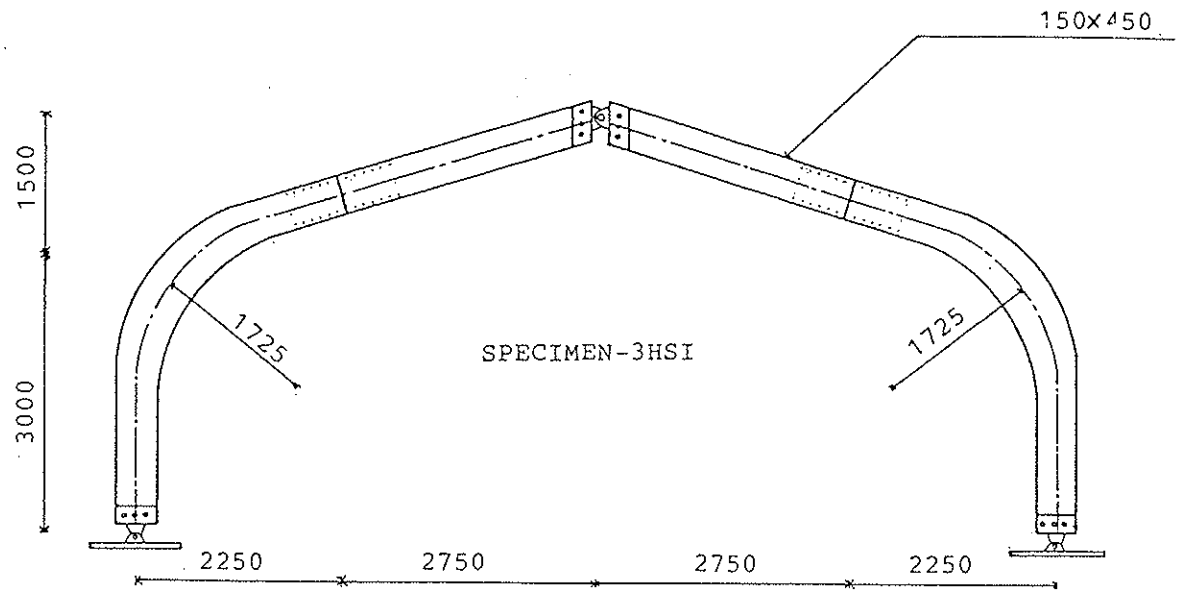


Fig.1 Shapes and kinds of specimens

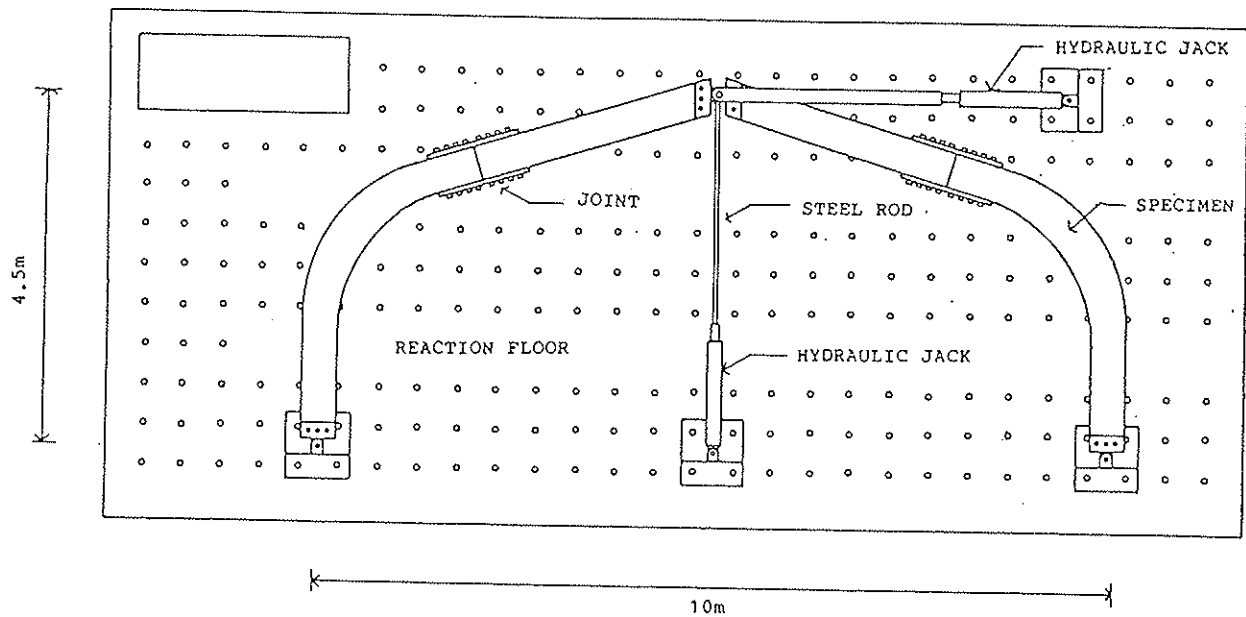


Fig.3 TEST APPARATUS

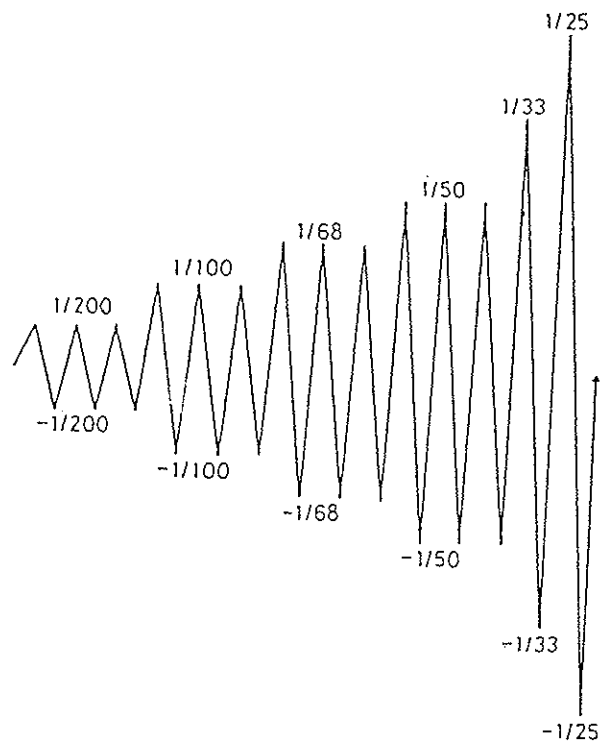
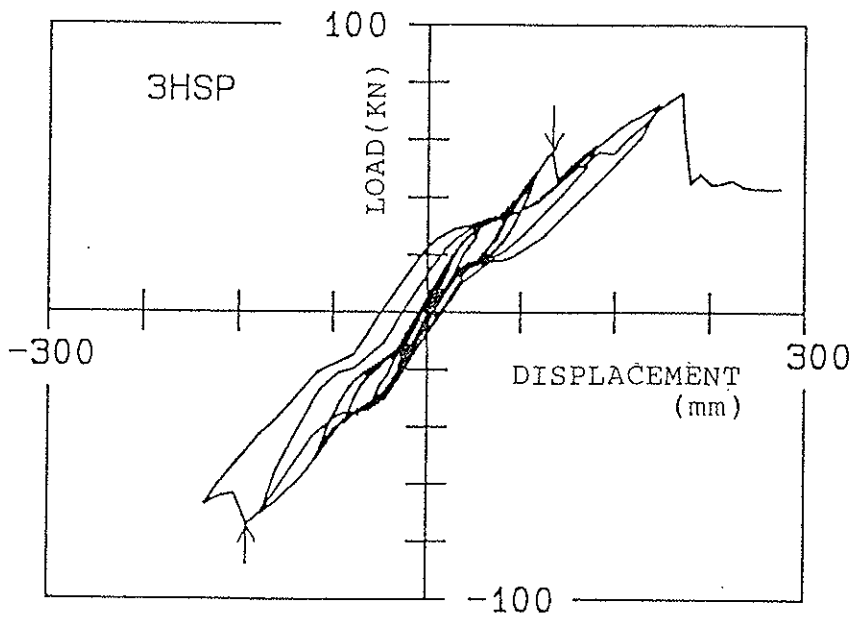
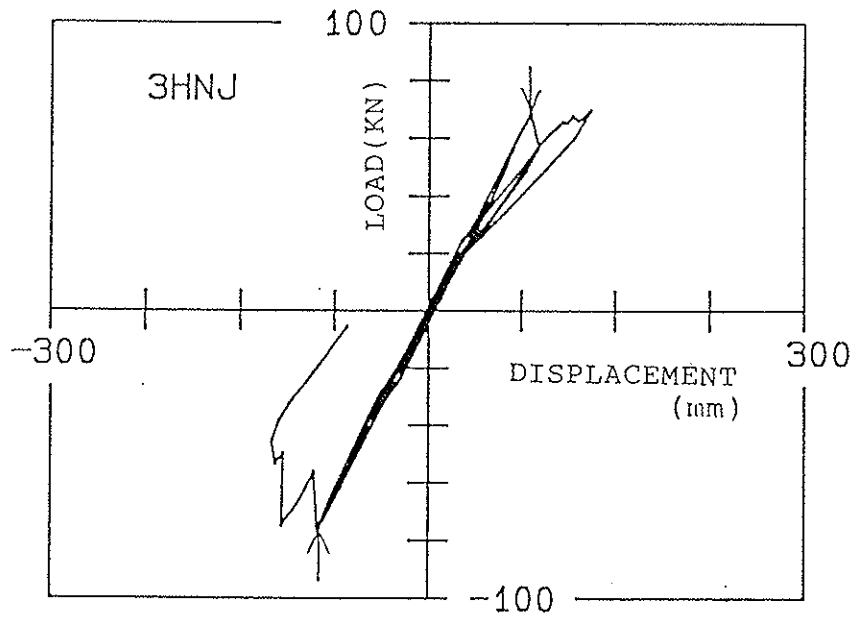


Fig.4 History of lateral load
 (The values represent the ratio of the horizontal displacement to the height of specimen)



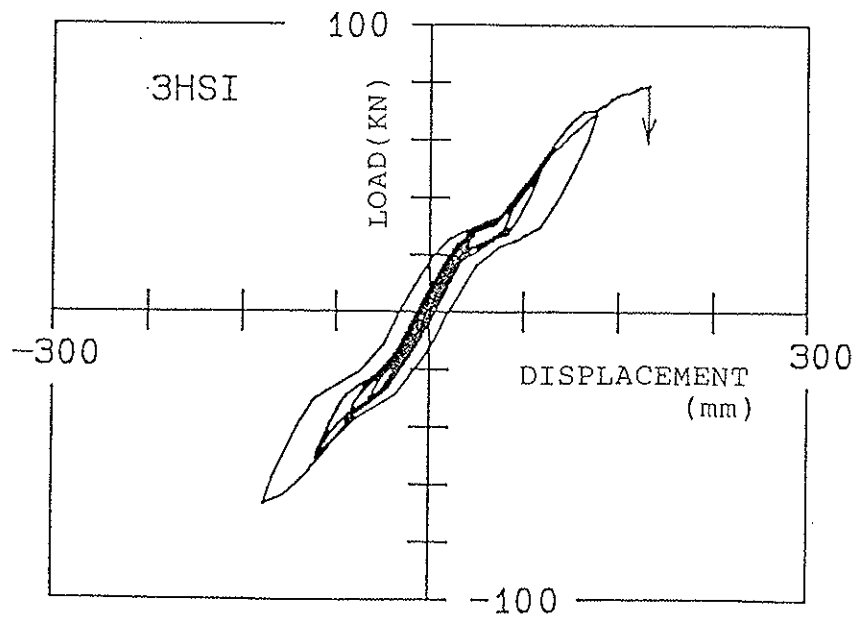
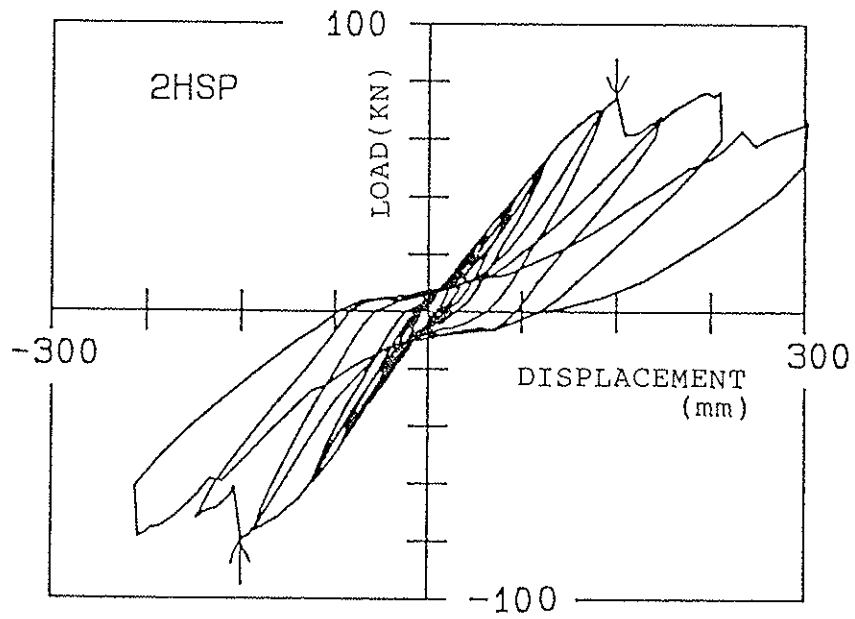


Fig.5 Relation between the lateral load and the horizontal displacement at the top

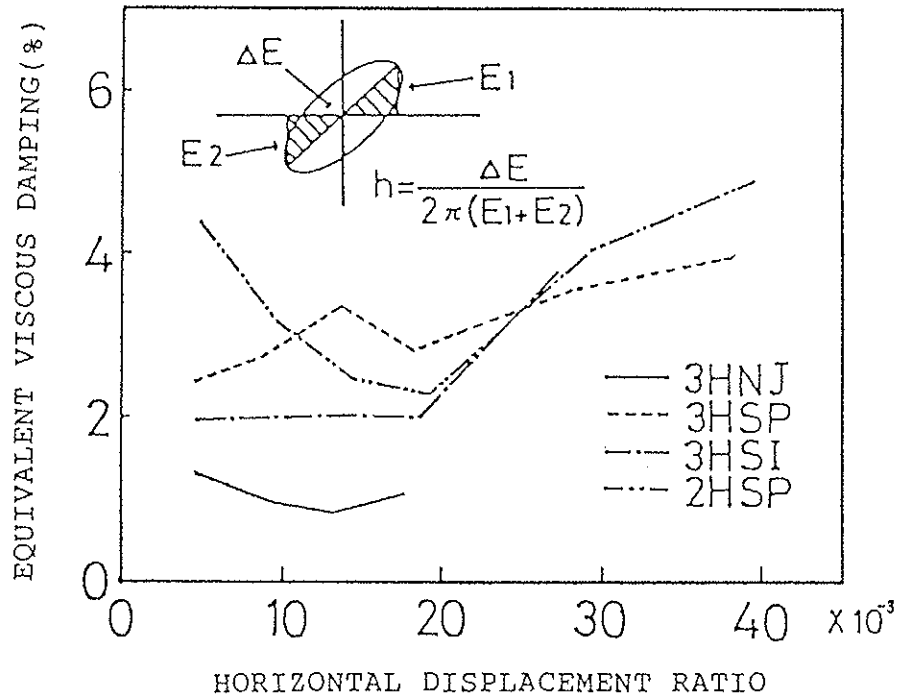


Fig.6 Equivalent viscous damping of each specimen

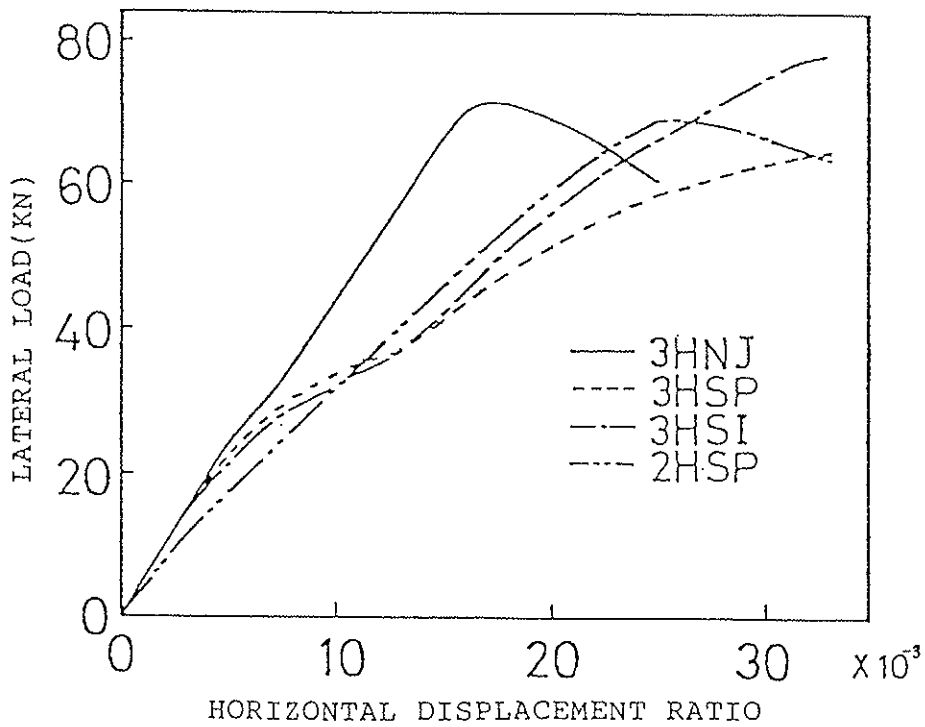


Fig.7 Relation between the lateral load and the horizontal displacement ratio

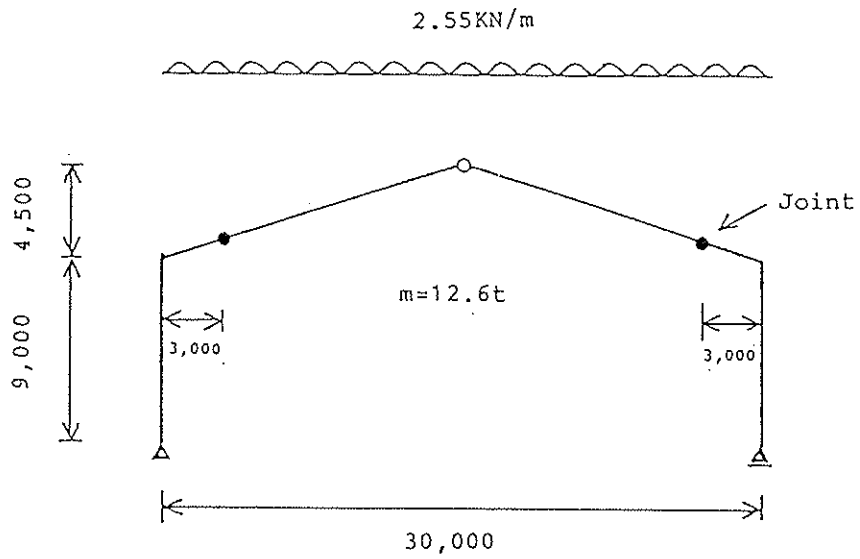
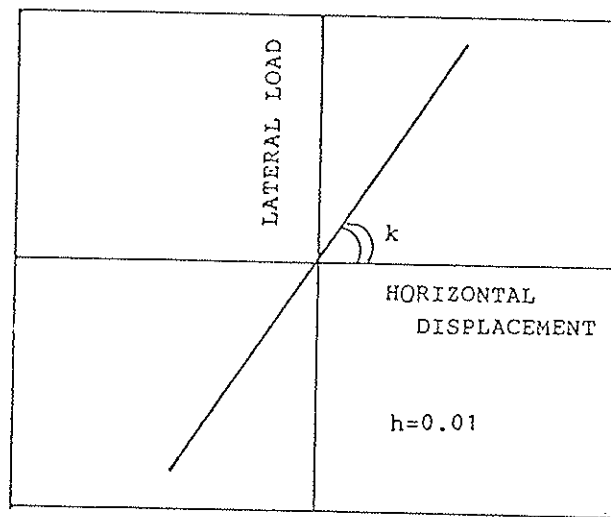
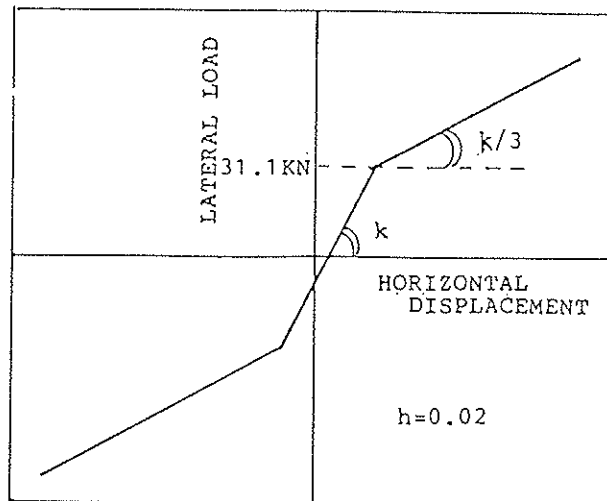


Fig.8 Three-hinged frame for dynamic analysis



(a) Model(1): Linear Model



(b) Model(2): Bi-linear Elastic Model

Fig.9 Hysteresis models for dynamic analysis

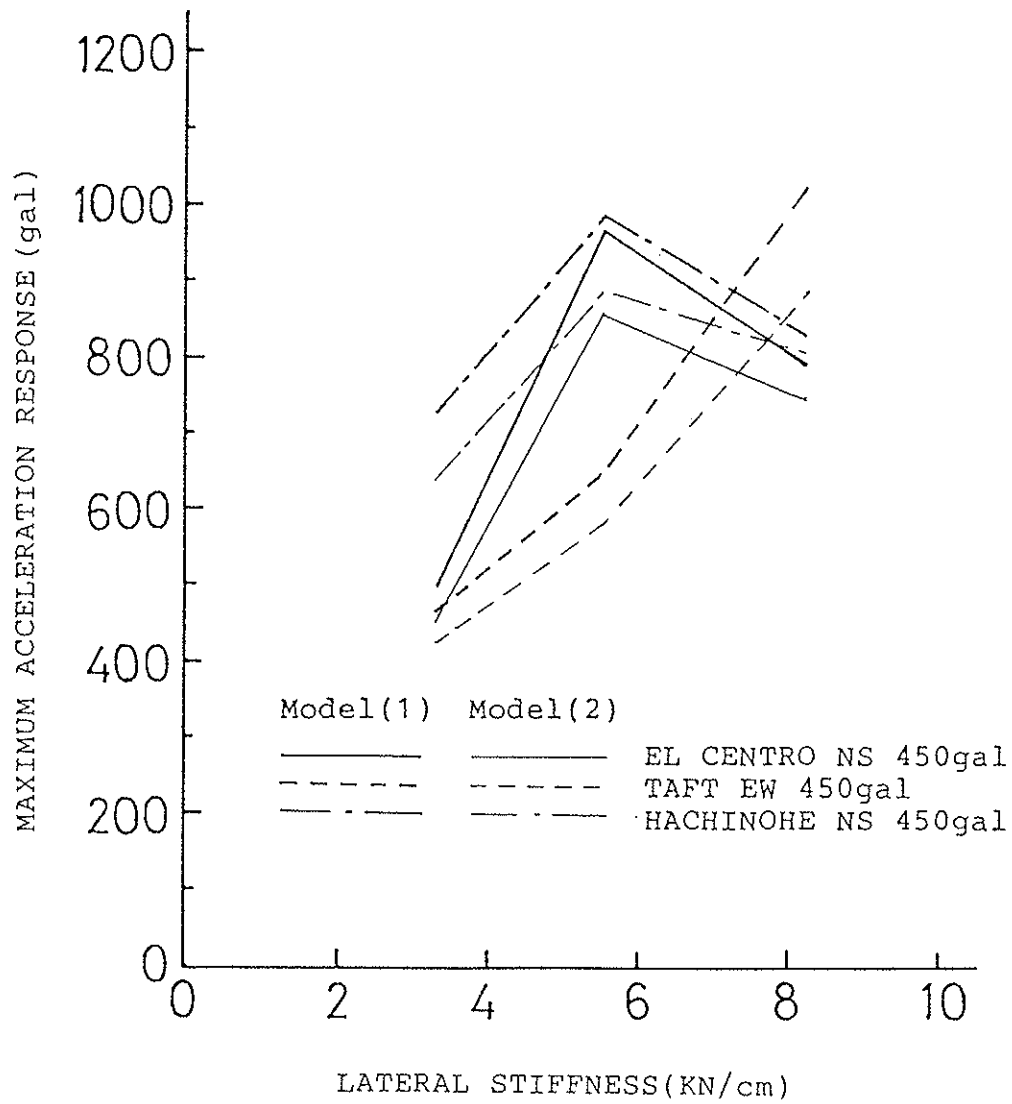


Fig.10 Calculated maximum acceleration response of a three-hinged frame(m=12.6t)

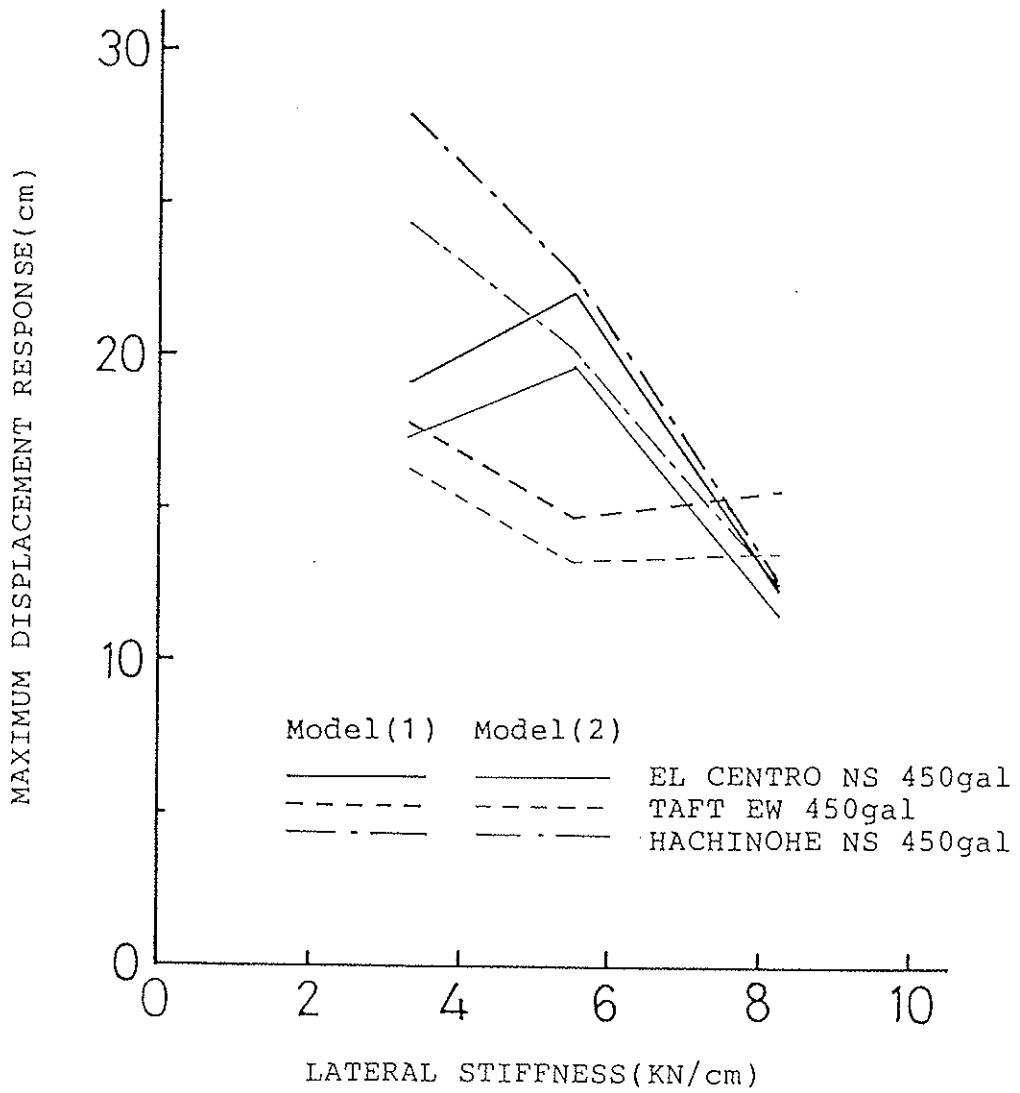


Fig.11 Calculated maximum displacement response of a three-hinged frame(m=12.6t)

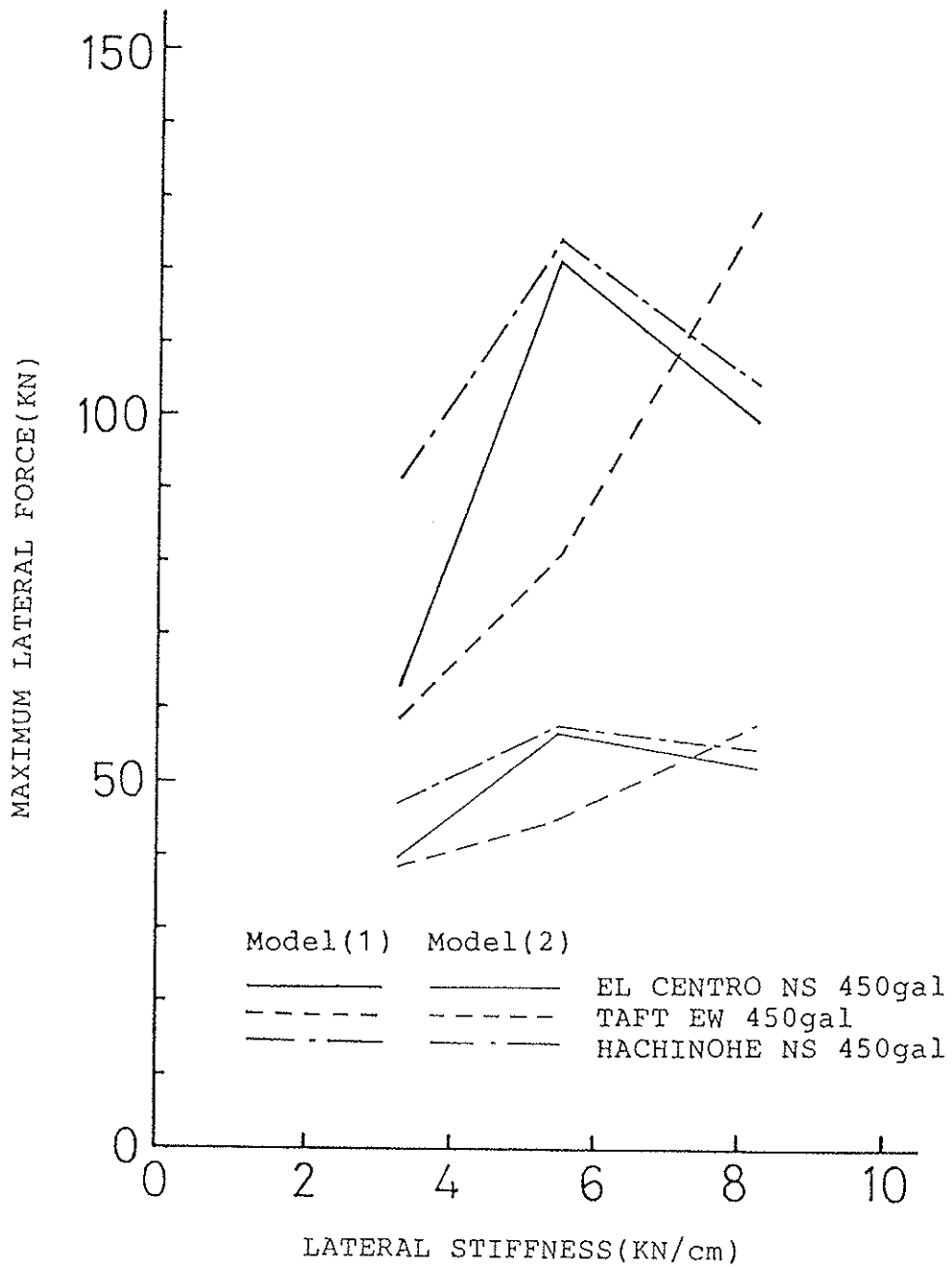


Fig.12 Calculated maximum lateral force of a three-hinged frame(m=12.6t)

INTERNATIONAL COUNCIL FOR BUILDING RESEARCH STUDIES AND DOCUMENTATION

WORKING COMMISSION W18A - TIMBER STRUCTURES

THE ROBUSTNESS OF TIMBER STRUCTURES

by

C J Mettem and J P Marcroft

Timber Research and Development Association

United Kingdom

MEETING TWENTY - TWO

BERLIN

GERMAN DEMOCRATIC REPUBLIC

SEPTEMBER 1989

THE ROBUSTNESS OF TIMBER STRUCTURES

INTRODUCTION

Structural timber is frequently used for clear spans in excess of nine metres in public buildings in Britain. Such applications are being actively promoted. For example, recreational activities and competitive sports are increasingly being enclosed by means of timber structures. This represents an ideal category of end-use for glulam. Also, with the trussed rafter market for domestic applications being largely saturated, that sector of the industry is increasingly offering solutions for roofs for non-residential groups of building. In these, clear spans of up to twenty metres are not uncommon. Glulam has far greater spanning potential, of course. Public buildings using glulam in excess of forty metres span do exist in Britain, although they are not at present commonplace.

On the continent of Europe, in Scandinavia and in North America, timber structures in excess of sixty metres span are relatively frequently found. The structural advantages, including lightness during erection and in foundation design, and good fire resistance, are well known to specialists. These features of structural timber can readily be supported with ample documentation. The ability of a timber structure to resist misuse however, and to remain stable after an accident which has affected its fabric, is less generally appreciated. In addition, the robustness of timber structures is a subject which is extremely sparsely documented. Yet it could probably be claimed that the majority of timber structures do possess an inherently high degree of robustness; or that robustness could be added with little extra detailing costs. The excellent performance of timber structures in seismic regions is almost legendary.

In Britain, there is a perceived disadvantage for timber in the way that the particular Building Regulations requirements for robustness might be achieved. There is also a lack of clarity, or even a complete gap in information, as regards provisions for meeting the specific current requirements for avoidance of disproportionate collapse in public buildings with clear spans exceeding nine metres.

Furthermore, TRADA became aware that the concept of structural robustness and the general principle of avoidance of damage disproportionate to the original cause, was to be incorporated in Eurocode No 1 and in the individual material codes for Europe.

As a consequence, a three year research project was proposed to collate and to supplement information on the response of timber structures to forces leading to collapse. During the project, the ability of selected structural timber forms to resist damage would be investigated. Finally, and as quite a major apportionment of the effort, improved design guidance on the subject would be drawn up. The proposal for such a project was approved, and the work was commenced, with UK Government (DoE) partial sponsorship, in March 1989.

The purpose of this paper is to make CIB W-18 members aware of the initial studies which have been undertaken on structural robustness, with special reference to timber. In addition, the consultations and assessments being undertaken will be described, with a view to inviting further comment and suggestions. Information on the requirements and solutions, if any, in other countries which W18 members represent, would be particularly valued.

CURRENT AND PREDICTED REQUIREMENTS FOR ROBUSTNESS

As this paper will show, there is a European context to the requirements for robustness. First, however, the British background will be examined. The notorious accidental event in Britain which made structural engineers aware of the risks of progressive collapse was of course the Ronan Point gas explosion. Regulations leading to the current Building Regulation A3 were developed as a consequence of the Government and the Institution of Structural Engineers enquiries and reports upon this incident.

Annex 1 reproduces the current Building Regulations and the Approved Document provisions with respect to 'Disproportionate Collapse'. These are the regulations for England and Wales, but in this respect, similar principles apply in other parts of the UK. It can be seen that for buildings having five or more storeys, the regulation is accepted as being satisfied through the use of certain parts of the codes and standards for concrete, steel and masonry.

For buildings of fewer storeys, however, but which are in public use and are of clear span exceeding nine metres, the requirement to avoid disproportionate collapse is equally valid. This is a point sometimes misunderstood in the interpretation of the regulations.

In the British codes for all three of the materials mentioned above, BS 8110, concrete; BS 5950, steel, and BS 5628, masonry, there are at least general considerations for the robustness of 'all buildings', 'four storey and below' or 'every building frame'. BS 5268: Part 2; 1988 on the other hand, is not referenced in the provisions meeting the requirement, presumably because it was thought that it would be unlikely to be used for buildings exceeding four storeys.

The inclusion of a requirement for all public buildings in excess of nine metres span, irrespective of storey height, renders this an anomaly, however. It might be advisable that in future the timber code which will be used in Britain should be thoroughly overhauled in respect of this and related accidental action requirements. The current clauses relating to accidental damage contain a mixture of topics, including an attempt to avert the worst consequences of exceptional snow drift loads arising from a relatively new loading code; an attempt to claim that 'no specific design requirements are normally necessary for buildings up to four storeys' (why?) and a mention of special occupancies such as flour mills and chemical plants.

The specific guidance given by British codes for concrete, steel and masonry always involves the incorporation of ties, in order to, as BS 5950 puts it, ensure that 'every building frame should be effectively tied together at each principal floor and roof level'. BS 8110 comes close to a reasonable definition of structural robustness, where, under the title of this single word, it requires that:

Structures should be planned and designed so that they are not unreasonably susceptible to the effects of accidents. In particular, situations should be avoided where damage to small areas of a structure or failure of single elements may lead to collapse of major parts of the structure.

For the foreseeable future in Britain, DoE have been giving consideration to the possibility of covering the performance requirements of Regulation A3 by a general guidance document on robustness. Consultation on the topic is currently in hand with the Institution of Structural Engineers. It is possible that these revisions may remove some of the artificial regulatory distinctions between 'Ronan Point' type buildings and others. For example, at present one is faced with the stark choice of deciding whether or not in certain instances an accidental loading pressure of 34 kN/m² applies. In addition, the regulations may be revised to acknowledge the general principle of the desirability of robustness, reflecting perhaps the common unified rules of EC1.

The term 'long span' has come into use in discussing the requirements for structures incorporating a 'clear span exceeding nine metres between supports'. It has even been proposed that this limit might be lowered to seven metres. Neither of these values are of course truly 'long spans'. For example, BS 6100 'Glossary of building and civil engineering terms' regards a span in excess of fifty metres as a 'large span structure'. This is more in accordance with the authors' understanding of the term.

THE EUROPEAN CONTEXT

The avoidance of disproportionate damage to construction works through accidental effects has been incorporated in the essential requirements of the Construction Products Directive. The requirement under 'Mechanical resistance and stability' is extracted as Annex 2 of this paper.

The early chapters of EC1 contain valuable guidance on the relevant principles to be followed, particularly if the clauses are considered carefully and reflected upon in the light of the accompanying commentary. The clauses felt to be relevant are incorporated in Annex 3 of this paper. It should be noted that the code assumes that: adequate supervision is always provided in factories and on site; construction is carried out by personnel having the required skill and experience, and the specified use of the structure will not be changed for the worse during its intended life, unless recalculation is carried out. Thus it might be inferred that in carrying out design checks against particular limit states in accidental situations, such as explosion or impact, the designer is not at the same time expected to consider that the structure might have deteriorated or might be overloaded.

The avoidance of disproportionate damage is a fundamental requirement of all of the commonly-formatted bases of design of the materials Eurocodes. EC1 requires that the main structure should normally be designed to be robust in such a way that it should not be damaged to an extent disproportionate to any original cause. The commentary suggests that this may be achieved by designing in such a way that if any single load bearing member becomes incapable of carrying loads, then this will not cause collapse of the whole structure. When necessary, it may be ensured by design or protection such that no essential member can be made ineffective as the result of an accident.

Accidental actions are those for which the occurrence in a given structure and at a significant value is improbable. The commentary to EC1 suggests that accidental actions may include mainly the forces resulting from:

- . impact
- . explosion
- . ground subsidence
- . earth or snow avalanches
- . tornados in regions not normally exposed

The very fact that accidents are defined here as having a low probability of occurrence highlights a major difficulty for those concerned with quantifying recommendations for design against accidental effects. Data are difficult to come by, and even more difficult to assess. Accidents involving runaway lorries, small parts falling off aircraft, and explosions are generally recorded, for example in press reports. However, only specialized organizations collate the information in a systematic way, and these bodies may not be willing to release sensitive information.

It should be noted that EC1 infers that the effects of earthquakes should only be treated as accidental actions if local geotechnical data show that they have a low probability of occurrence. The authors concur with this view, and intend that seismic loadings shall not be included within the project.

EC1 also appears to acknowledge that extremely rare and catastrophically large events, such as the falling of the fuselage of a Boeing 747 on part of the village of Lockerbie, simply cannot be provided for. The commentary mentions the situation 'when the estimated value of the force is so important that it would be unreasonable to wish to assess the integrity of the structure with regard to it'.

Although EC1 uses the word 'robust' in its 'fundamental requirement' text, the drafts of EC2, EC5 and EC6 appear to avoid the term in their preliminary stages. In the 'basis of design' chapter, from the clauses on fundamental requirements, through to those dealing with material properties, EC5 and EC6 contain virtually identical wording. They call for reliability with an acceptable probability and having due regard to costs. They suggest that this may be achieved by, amongst other measures, appropriate detailing. They also indicate that the safety of people is an uppermost consideration in the avoidance of ultimate limit states.

EC1 is more explicit on the choice of an acceptable degree of reliability, since it is intended to give the general principles concerning safety. It calls for the choice to be made taking into account:

- . risk to human life
- . the number of human lives endangered
- . economic losses resulting from failure
- . the amount of expense and effort required to reduce the risk of failure

This contrasts with the English Building Regulations, where the emphasis is entirely upon the risk to human life.

Accidental actions are defined qualitatively in all of the material Eurocodes, and are allocated their separate symbols:

A - accidental action

A_k - characteristic or specified value

$$A_d = \gamma_A A_k$$

A_d may also be directly specified

Currently there are no specified British national values that could be substituted for trial Eurocode design purposes, so far as timber structures are concerned. The value of 34 kN/m² referenced in relation to certain situations for steel structures in the Building Regulations would seldom if ever be capable of being withstood by timber construction. For timber, venting would be likely to be a better strategy in extreme blast loading situations.

Under 'design requirements', EC5 and EC6 state the verification conditions for ultimate limit states. In certain cases, design values of actions are directly compared with the corresponding design values of the resistance capacity. Accidental design situations are explicitly provided for as 'accidental combinations' of action. This will presumably give scope for the application of combination factors (ψ values) which take into account and alleviate improbable combinations (maximum snow and wind at the time of the accident!).

Both codes state that combinations for accidental design involve either an explicit accidental action A or the situation after an accidental event ($A = 0$). EC6 states explicitly that the latter case is not covered, whereas EC5 does not mention this, whether intentionally or not.

Design requirements for the short-term safety and stability of a structure which has been damaged by an accident, where the remaining parts of the structure are considered after a significant area has collapsed, must be especially problematical. This would require separate consideration from the case where one is designing ensure that in the first instance collapse is not progressive. Reliability acceptance would possibly be more akin to that for a structure under fire, during action by the fire services.

In its chapter on design, the Eurocode for masonry structures, EC6, contains guidance on how robustness may be achieved. No such information is to be found in EC5, however. EC6 calls for the general arrangement of the structure and the connexion of its various elements to be such as to give robustness. Buildings should be capable of resisting a notional horizontal load, applied at each floor or roof level simultaneously, equal to 1.5 per cent of the characteristic permanent load of the structure, considered in fundamental combination. Many timber structures could probably be shown to be capable of withstanding with little extra detailing such a horizontal load as 1.5 per cent of the characteristic permanent value, were it to be deemed appropriate.

The design clauses for masonry in accidental situations other than earthquakes echo the desirability of avoidance of catastrophic collapse, under reasonable circumstances. The connexions of walls to floors and roofs are emphasized. Tying systems are also given prominence in detailing clauses on limitation of accidental damage in a preliminary draft of EC2. EC6 even goes as far as to suggest that a boarded timber joist floor may be shown to develop sufficient diaphragm action to transmit lateral loads. It is not known to the authors whether any calculations have ever been performed to demonstrate this. It would certainly seem likely that at least a plywood diaphragm could perform well.

Concluding an overview of the developing proposals in the Eurocodes for avoidance of disproportionate damage, it has been shown that this is stated as a fundamental principle. It is required in the CPD, and stated in general terms in EC1 and in all of the materials codes. The requirement in principle is independent of building size, number of storeys, etc. All codes have agreed upon a definition of accidental actions.

Values of actions are a different matter of course, and these will presumably be a matter for the EC9 drafting experts to decide. There is a fair amount of guidance on acceptable degrees of reliability that might be used to place limits upon the cost of additional precautions, if any, for very small structures such as single occupancy dwellings. The Eurocodes for concrete and masonry will probably place considerable emphasis upon tying the structure together, as well as selecting forms having low sensitivity and providing for redundancy paths in load transfer. EC5 does not appear to have addressed these matters at all.

ASPECTS OF RESEARCH IN HAND

A literature review has been extended to robustness and the avoidance of disproportionate collapse in all structural materials, not merely timber. A list of the codes and standards referenced in the text of this paper is included as Annex 4, whilst some bibliographical items already collected are given in Annex 5. To date, the following organizations in Britain have provided useful information: the structural code committee concerned with the steel code BS 5950 and the Steel Construction Institute; the Structural Integrity Division of the Building Research Establishment; the Brick Development Association. Information is still scarce on certain questions. In particular the authors would like to know the reasoning which led to certain structural code committee decisions on apparently ad hoc detailing requirements and exemptions. Data relating areas or volumes of presumed localized failure due to the intensity and diffusion of

pressure from explosions are also required. Actual materials data for timber and mechanical fasteners for wood under extremely short duration loadings may also be found wanting.

In an assessment of the types of timber structure for which accidental damage design may be required, several aspects of work have been initiated.

Fire constraints and the designation of purpose groups of building for fire engineering considerations, may be indirectly helpful. It is realized, of course, that fire spread and resistance are completely separate topics from 'accidental damage design'. However, the size, plan and layout of a timber structure, according to its occupancy purpose, will be dictated to some extent by the spatial considerations relating to such requirements. Thus the assessment of the sensitivity of categories of timber structure to accidental damage may be assisted if maximum areas, volumes and room heights in terms of fire requirements can be stated. To this end, a schedule of such constraints has been drawn up and is being assessed.

In order to categorize 'long-span' public buildings in timber, in current regulations terms those having clear spans exceeding nine metres, a number of British firms involved in the manufacture of such buildings have been contacted, with a request for assistance. The types of timber structure presently being constructed in the UK, to which 'large numbers of people' could resort, have been reviewed. A good response was obtained from manufacturers, permitting a tabular categorization by form and by type of element (solid timber, glulam, trussed rafter, plywood components).

An important forthcoming step will be to commence to assess the categories of timber structure mentioned above in terms of their current robustness using typical details presently applied, and in terms of predicted new requirements. Hybrid structures (timber-masonry, etc) are also economically important, of course, and these will require inclusion in the exercise.

Preliminary calculations have been made, relating to the robustness of a typical long-span timber structure. This incorporated parallel, non load sharing frameworks. In attempting such practical calculations, difficulties have to be faced up to in deciding at what point collapse is considered to have become 'disproportionate' and under what conditions the remainder of the structure must survive. Analytical assessments of typical structures are likely to continue to play a part in the project, but at present it is felt that for these to continue, at least preliminary judgements must be made on reliability criteria, as well as the seeking of statistics on probability of accidental events related to building purpose groups.

ACCIDENTAL ACTIONS

Independently of the definitions and statements of causes of accidental action given in the Eurocodes (particularly EC1) which were reviewed above, the Steering Committee of the TRADA research project has considered various causes and their relevance to the robustness of timber structures. Clearly, it is not an economical approach to ignore the causes and simply explore the behaviour of the damaged timber structure independently of this. Indeed, in following limit state design procedures, it becomes virtually impossible to do so, because partial coefficients for actions and combination factors are probabilistically based and must be statistically assessed. Special statistical techniques, developed to deal with sparse, 'loose tolerated' data, may be required.

Explosions, especially those arising from various types of gas combustion, are clearly one of the main causes of accident which should be taken into account. Data on gas explosions frequently relate to incidents within confined spaces, especially in masonry buildings. For 'long-span' structures, including those incorporating service and ancillary rooms and chambers, such data are not easy to interpret. Further information is required on volume and ventilation effects, as well as pulse profiles for various gaseous mixtures. The Explosives Safety Branch of the Property Services Agency, Health and Safety Executive and similar bodies are to be approached.

Impact is another frequently-cited source of accidental damage to buildings. Views are commonly expressed on the effectiveness or otherwise of bollards and other protective devices in preventing vehicle impact. In general, it has to be concluded that adequate robustness should be provided against reasonably probable damage from impact, both from vehicles and from other normally rarer events, without placing reliance upon such dubious protective means.

In the view of those consulted, few other accidental situations which were relevant in Britain could be envisaged. Moderate sabotage damage might be more limited in its effect, if a reasonably robust structure were to be provided. It would presumably fall into the category of an uncertainty that could be qualitatively identified, but that would remain unquantifiable.

It was felt that any recommendations developed by the project should not attempt to cater for the effects of poor quality in manufacture or erection, nor for lack of quality control or inspection in the factory or on site. The assumptions in the preliminary sections of the Eurocodes support this view. Abuse of floor loading limits and similar misuse of buildings must also be eliminated from the scope.

Sudden localized foundation failures or subsidence of parts of a building are undoubtedly a possibility that must be admitted. However, it is likely to be a problem limited to known geographical regions, and one which must be dealt with both by taking special precautions and also by taking advantage of any robustness already added for more general reasons.

A strong contributory cause of the eventual complete collapse of already unsatisfactory buildings has often been noted to be the ponding of flat roofs which have deflected excessively. This has been observed in certain types of timber structure which have performed poorly. However, the remedy is clearly avoidance of exceeding the serviceability limit state in the first instance. The Eurocodes recognize that states which immediately precede structural collapse and which are considered in place of the collapse itself, are also treated as ultimate limit states. Hence a badly ponded flat roof would be deemed already to have failed, although in some instances the occupants might have wished to have been informed that this was the case, in order to leave in time!

It is also the view that exceptional drift snow loads do not constitute a genuine form of accidental loading, if their occurrence has been predicted by a probabilistic loading code. The BS 5268 code committee would be well advised to reconsider certain clauses recently inserted in the British structural timber code and to avoid further confusing the accidental damage provisions with this separate topic.

As already indicated, a review was made of the British code requirements for robustness. The British codes of practice for the major construction materials (timber, masonry, reinforced concrete and steel) have differing requirements for the provision of a robust and stable structure. However, the codes for all four materials have the following somewhat general requirements:

- . arrange the layout of the structure to ensure the required interaction between structural elements
- . ensure that the structure is insensitive to the effects of misuse or accident

These are the sole requirements of the timber code in respect of the provision of a robust and stable structure. The codes for the three other materials, on the other hand, also have a requirement that at any level, the structure shall be able to resist a notional horizontal load, given as a fraction, usually one and a half per cent, of the vertical load. This was estimated to take account of factors such as lack of verticality.

PROPOSALS

It seems reasonable to assume that the robustness of timber structures and their ability to withstand accidents should be equal to that for other materials. However, the comparison should be made in relation to building size and building occupancy class. Without major cost implications, code writers and designers in steel and reinforced concrete can at least adopt ad hoc precautions which will provide some required additional degree of resistance. In timber, however, it is important not simply to mimic such measures, but to consider the requirements from first principles.

The imposition of new and unacceptable requirements upon timber structures arising merely for the sake of harmonization across materials would be most unfortunate.

A consequence of the project might be a conscious decision that for certain classes of structure, including small buildings for example, the risk to life from accidental effects upon the building fabric are 'acceptably improbable'. Taking due account of the expense and effort in further reducing the risk of failure, it might be that design rules and details for such structures are unaltered. Nevertheless, it is important to demonstrate that this is so, rather than dismissing robustness as being of no consequence to timber structures.

In public buildings of some as yet undefined size or type, it seems unlikely that timber code writers and designers will be able to continue to evade the topic. The following steps are proposed, therefore:

- . categorize buildings in terms of purpose and end use. The purpose groups included in the 'English' Building Regulations for fire regulations may provide a starting point;
- . carry out a study of the availability of data and of the suitability of statistical techniques which may be employed in taking into account the criteria for reliability laid down in EC1 (risk to life; economic losses; expense to reduce risk).

In the end, it seems likely that it will be necessary to take best estimates and 'state of art' guidance upon effects of accidental actions, and to apply these analytically to the common features of the forms of construction concerned.

Finally, it is felt that because of the frequently inherently robust nature of timber construction, the effects of a number of forms of accidental action can be provided for, without greatly adding to costs. This will entail acceptance of the fact that a degree of localized damage is inevitable. However, methods can be developed which should enable measures to be described to limit that damage in its extent and to ensure that there are not risks of progressive collapse.

chriscib.rep

INTERNATIONAL COUNCIL FOR BUILDING RESEARCH STUDIES AND DOCUMENTATION
WORKING COMMISSION W18A - TIMBER STRUCTURES

INFLUENCE OF GEOMETRICAL AND STRUCTURAL IMPERFECTIONS
ON THE LIMIT LOAD OF WOOD COLUMNS

by

P Dutko
Technical University of Bratislava
Czechoslovakia

MEETING TWENTY - TWO
BERLIN
GERMAN DEMOCRATIC REPUBLIC
SEPTEMBER 1989

INFLUENCE OF GEOMETRICAL AND STRUCTURAL IMPERFECTIONS
ON THE LIMIT LOAD OF WOOD COLUMNS

Pavel DUTKO*

1. THEORETICAL ASSUMPTIONS

Real columns in wood structures are not ideally straight but have unavoidable imperfections, of shape which develop during the production process, transport, erection or exploitation of the structure.

Because of anisotropic structure of wood there is also an uneven distribution of matter over the cross section of the column so the geometric centre of the cross section does not coincide with the centre of gravity. The influence of these both imperfections - geometric and structural - which determining the limit load of the column can be taken into account considering an initially crooked column in the form of a half sine curve with a maximum initial out-of-straightness at mid-height e_0 . We will call e_0 an equivalent out-of-straightness.

The differential equation of an initially crooked column has the form /Fig.1/

$$EI \gamma'' = - M_z \quad /1/$$

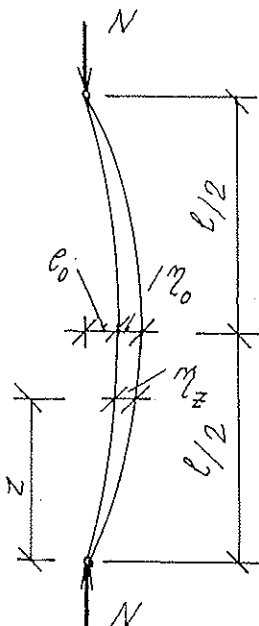
$$EI \gamma'' = - N. (e_z + \eta_z) \quad /2/$$

* Assoc. Prof., Dipl. Ing., Cand. Techn. Sci., Slovak Technical University, Civil Engineering Faculty, Chair for Steel and Timber Structures, Bratislava, Czechoslovakia

From Eq.2 we obtain the ordinate η_z in an arbitrary place of the column as

$$\eta_z = \eta_0 \cdot \sin \frac{\pi \cdot z}{\ell} \quad /3/$$

$$\eta_z'' = -\eta_0 \cdot \frac{\pi^2}{\ell^2} \cdot \sin \frac{\pi \cdot z}{\ell}$$



For $z = \frac{\ell}{2}$ is

$$\eta_0'' = \eta_0 \cdot \frac{\pi^2}{\ell^2} \quad /4/$$

Substituting η_0'' /Eq.4/ into Eq.2

$$-N \cdot (e_0 + \eta_0) = EI \cdot \eta_0 \cdot \frac{\pi^2}{\ell^2}$$

Fig. 1

we obtain an expression for the de-

flection of the column

$$\eta_0 = e_0 \cdot \frac{N}{N_E - N} \quad /5/$$

The ultimate stress of the column results from the strength condition

$$\frac{N}{A} + \frac{N \cdot e_0}{W} + \frac{N \cdot \eta_0}{W} = \sigma_f \quad /6/$$

which states that the normal stress at the most severely stressed fiber at midheight of the column can reach maximum the yield stress of the wood material.

Substituting the ultimate stress $\sigma_m = \frac{N_m}{A}$, Eq.5 for η_0 and relative eccentricity $m_0 = \frac{e_0}{j}$ / where j is defining the core radius/ into Eq.6 we obtain a quadratic equation for the ultimate stress in the form

$$\sigma_m^2 - \sigma_m [\sigma_E (1+m_0) + \sigma_f] + \sigma_f \cdot \sigma_E = 0 \quad /7/$$

from which we have

$$\sigma_{m_{1,2}} = \frac{\sigma_E (1+m_0) + \sigma_f}{2} \pm \sqrt{\frac{[\sigma_E (1+m_0) + \sigma_f]^2}{4} - \sigma_f \cdot \sigma_E} \quad /8/$$

According to the Czechoslovak standard ČSN 73 1701 "Design of wood building structures" the reliability of centrally loaded columns with compact cross section by

$$\sigma = \frac{N_d}{A \cdot \varphi} \leq \gamma_{rc} R_{cd} \quad /9/$$

where φ is the buckling coefficient, which can be evaluated from

$$\sigma_m = \sigma_f \cdot \varphi \longrightarrow \varphi = \frac{\sigma_m}{\sigma_f} \quad /10/$$

where σ_f is the compression strength of the wood.

The values of the buckling coefficient φ can be thus for columns of varying slenderness λ evaluated from the ratio of the ultimate stress σ_m and the compression strength of wood

$$\varphi_{1,2} = \frac{1}{2} \left[\frac{\sigma_m}{\sigma_f} \cdot (1+m_0) + 1 \right] \pm \sqrt{\frac{1}{4} \left[\frac{\sigma_m}{\sigma_f} \cdot (1+m_0) + 1 \right]^2 - \frac{\sigma_m}{\sigma_f}} \quad /11/$$

2. EXPERIMENTAL DETERMINATION OF PARAMETERS e_0 , m_0 , N_m , N_E

To be able to take into account the influence of geometrical and structural imperfections when assessing the reliability of compressed wood columns using Eq.9, it was necessary to determine the basic parameters for the ultimate stress calculation and the appropriate values of the buckling coefficient φ experimentally. The experiments were carried out

at the Department of Steel and Wood Structures at the Slovak Technical University in Bratislava.

Four types of columns were investigated /Fig. 2/:

- Type A - two-part column /without a distant piece/,
- Type B - built-up column of two basic parts,
- Type C - compact column,
- Type D - built-up column of one basic part and two continuous distant pieces.

Thirty specimens were fabricated and tested of every type with the slenderness $\lambda = 10; 20; 40; 60; 80; 100; 120$ - i.e. 840 columns in all. Their shape and dimensions are also in Fig. 2.

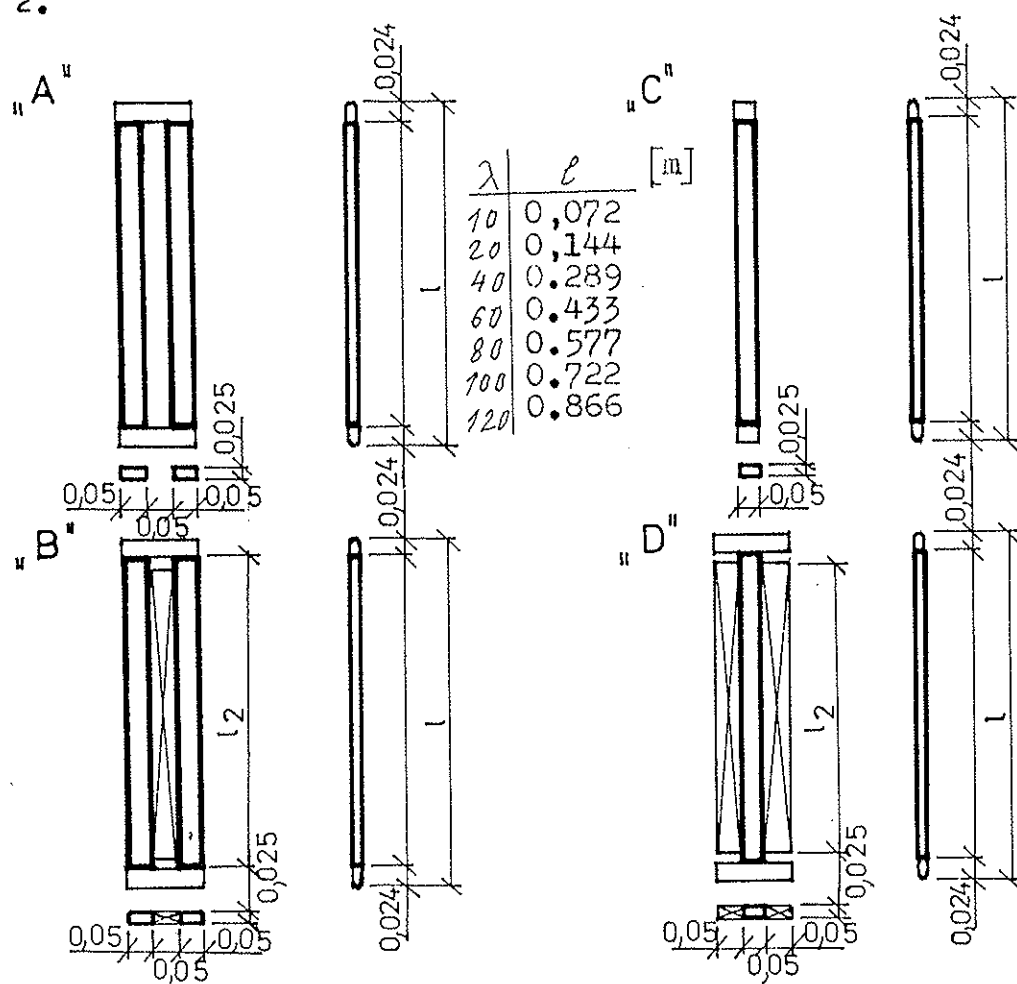


Fig. 2

The columns were fabricated from spruce timber 60 mm thick which was second seasoned for 6 months by 18°C temperature and 60 % abs. humidity. Under stabilized climatic conditions the humidity of wood specimen fluctuated in the range $w = 12$ to 13 % abs.

The experiments were carried out on a 1000 kN jack /Fig.3/.

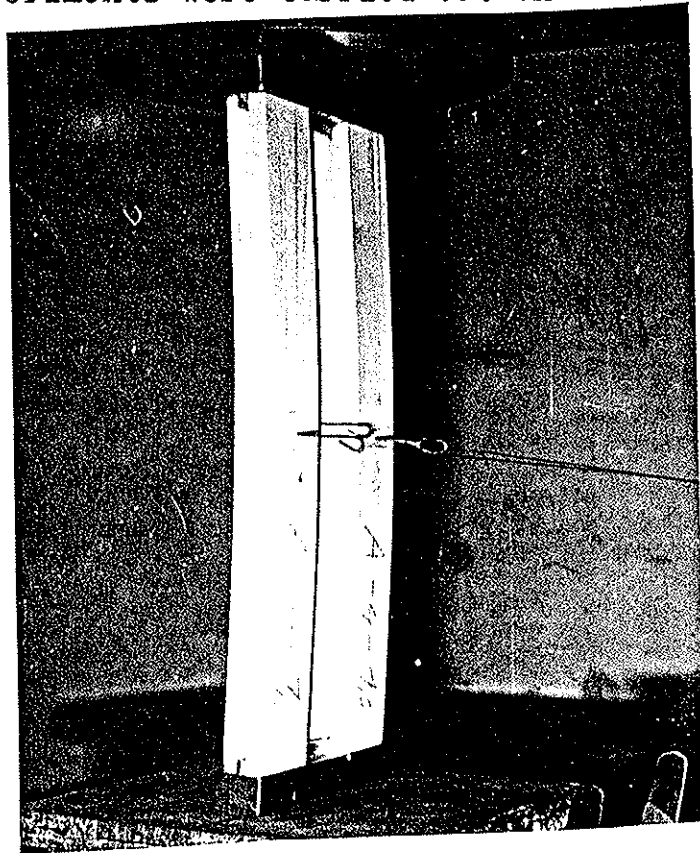


Fig. 3

The pinned support of the columns was in the plane of the assumed deflection assured by means of a steel fixture. The step of loading - 10 to 15 kN/min. At the end of the experiment - before reaching the collapse of the column - the rate of loading had showed down.

During the experiment was determined:

- a/ the transversal deformation at the midheight of the column η_0 of the basic parts of specimens under every load step

- of 1.0 kN with the accuracy 0.001 mm /Fig. 3/;
- b/ the ultimate load of the columns N_m /when the transversal deformations began quickly to rise without further raising of the load and the column failed under compression and bending/.

3. METHOD OF EVALUATION OF EXPERIMENTAL RESULTS

The values of parameter N_m were determined on the basis of direct measurements. The parameter e_o and N_E were determined by the method which was first published by R.S. Sauthwel [4]. The value of η_o in the middle of column height is

$$\eta_o = \frac{N \cdot e_o}{N_E - N} = \frac{e_o}{N_E/N - 1} \quad /12/$$

After rearrangement we obtain the equation of a line

$$e_o = \eta_o \frac{N}{N_E} - \eta_o \quad /13/$$

So, when we plot the values $\frac{\eta_o}{N}$ as a function of η_o , the points must lie on a line.

N - normal force in the column during load steps,

η_o - transversal deformation of the column at the midheight under the load N .

Practical use of the function in the determination of equivalent deformation e_o is shown in Fig. 4.

Equation /12/ can be rearranged into

$$\frac{\eta_o}{N} = \frac{e_o + \eta_o}{N_E} \quad /14/$$

from which we can determine the value of critical force

$$N_E = \frac{e_o + \eta_o}{\frac{\eta_o}{N}} = \cotg \alpha \quad /15/$$

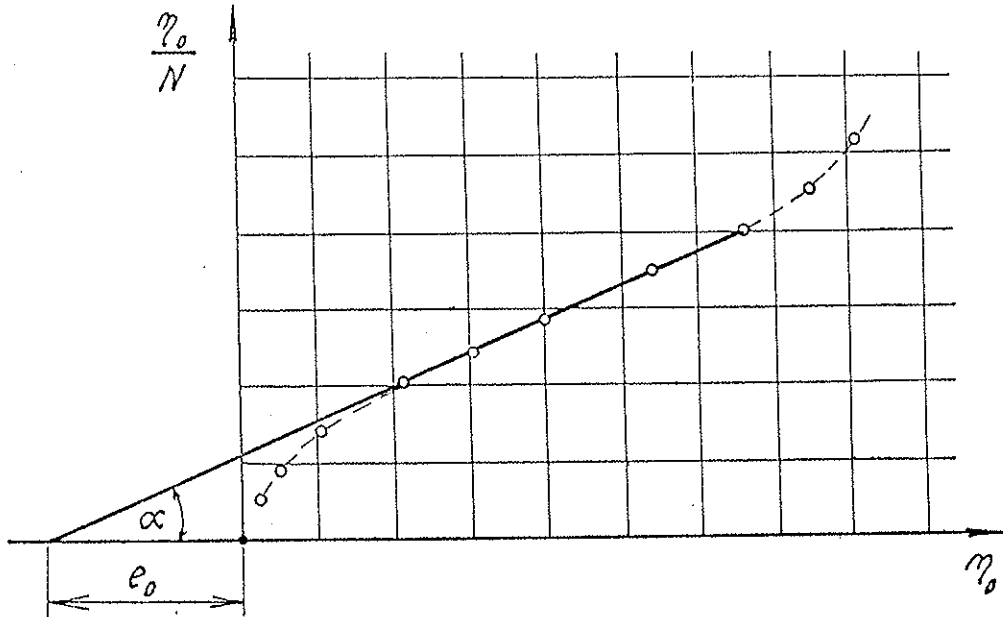


Fig. 4

where the value $\frac{e_0 + m_0}{\frac{N_c}{N}}$ is deduced from the diagram in Fig. 4.

The values of parameters N_m , N_E , e_0 and m_0 are stored in the author's archive.

The relationship of maximum probability values of equivalent deformation e_0 and relative eccentricity m_0 and also the relationship of minimum probability values of Euler's critical load N_E and the limit load N_m on the slenderness λ of the column was determined by regression analysis with the probability of occurrence of higher /in determining of e_0 and m_0 / or lower values /in determining N_E and N_m / $\rightarrow 0.001$.

The relationship of parameters $y = /e_0; m_0; N_E; N_m/$ on the slenderness of the column $x = / \lambda /$ was expressed by a polynomial whose degree k was chosen on the basis of esti-

mation of the functional relationship as follows:

- if the estimated curve is linear

$$k = 1 \quad y = A_0 + A_1 \cdot x^1$$

- if the estimated curve is non-linear

$$k = 2 \quad y = A_0 + A_1 \cdot x^1 + A_2 \cdot x^2$$

/16/

- if the estimated curve is non-linear with a point of inflection

$$k = 3 \quad y = A_0 + A_1 \cdot x^1 + A_2 \cdot x^2 + A_3 \cdot x^3$$

in which y - examined parameter / e_0 ; m_0 ; N_E ; N_m /,

A_i - coefficients of the regression curve.

4. RESULTS OF REGRESSION ANALYSIS OF PARAMETERS EXAMINED EXPERIMENTALLY

The results of regression analysis* of the examined parameters are shown in tables 1 to 16 for all types of columns.

The tables show:

- type of the column /A, B, C, D/;
 - examined parameter / e_0 ; N_E ; N_m ; m_0 /;
 - coefficients of the appropriate regression curve / A_0 ; A_1 ; ... A_i /;
- and numerical values and graphical representations of the examined parameter in the relationship to the slenderness of the column.

In the table 17 there are values of the ratio of minimal probability limit load to Euler's critical load N_m/N_E as a function of the slenderness $\lambda = 20$ to 120 for all examined types of columns. The graphical representation of the relationship /Fig.5/ allows us to observe the negative influence of geometric and structural imperfections on the limit load of wood columns.

* Computer code for regression analysis solution is from Vl. Mackuliak

Tab. 1

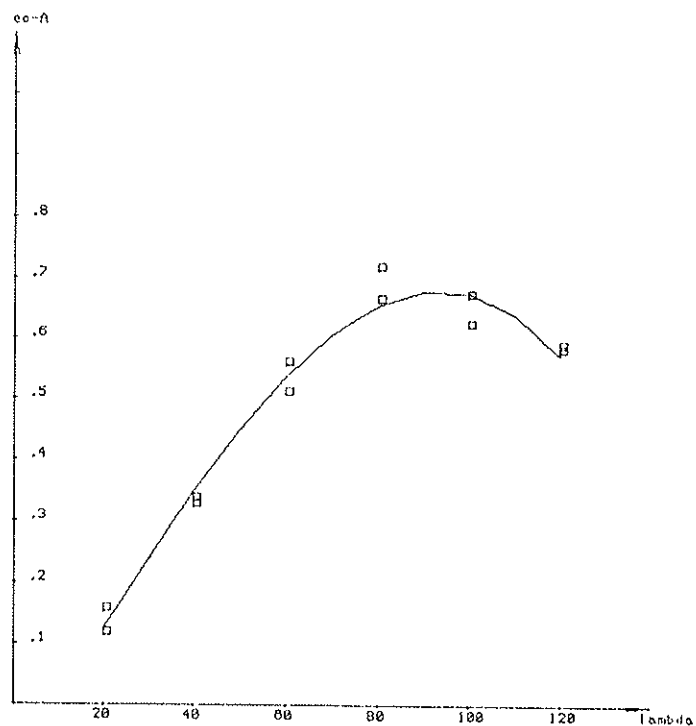
Subor-eo-A

$A_0 = -.100602195$
 $A_1 = .0109455612$
 $A_2 = 3.27419584e-05$
 $A_3 = -6.43389784e-07$

Index korelacie = .986999999

X= 20	Y= .156	Yt = .126
X= 20	Y= .117	Yt = .126
X= 40	Y= .327	Yt = .348
X= 40	Y= .336	Yt = .348
X= 60	Y= .559	Yt = .535
X= 60	Y= .509	Yt = .535
X= 80	Y= .664	Yt = .655
X= 80	Y= .716	Yt = .655
X= 100	Y= .621	Yt = .678
X= 100	Y= .672	Yt = .678
X= 120	Y= .587	Yt = .573
X= 120	Y= .578	Yt = .573

N= 327



Tab. 2

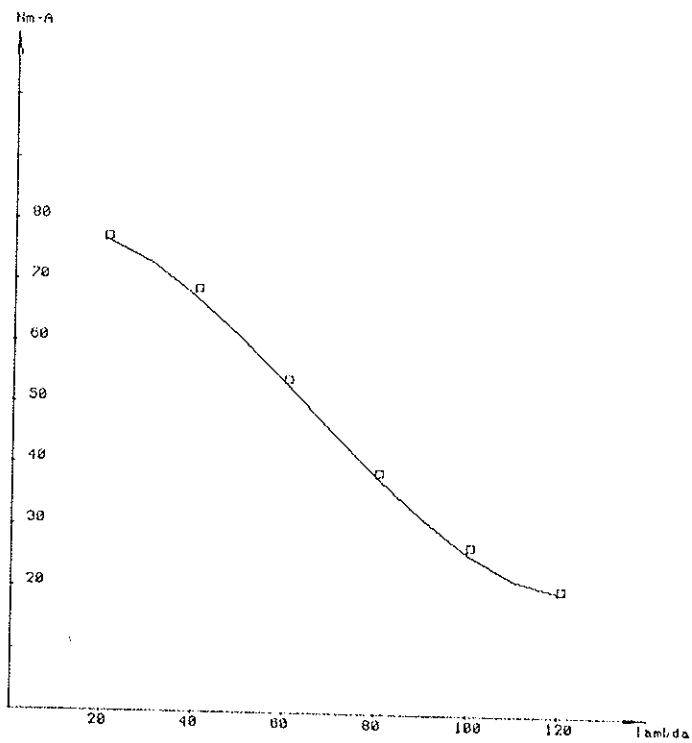
Subor-Nm-A

$A_0 = 77.4222419$
 $A_1 = .261104219$
 $A_2 = -.015605314$
 $A_3 = 7.86902485e-05$

Index korelacie = 1

X= 20	Y= 76.857	Yt = 77.032
X= 40	Y= 68.465	Yt = 67.934
X= 60	Y= 53.53	Yt = 53.906
X= 80	Y= 38.417	Yt = 38.726
X= 100	Y= 26.667	Yt = 26.17
X= 120	Y= 19.847	Yt = 20.015

N= 180



Tab. 3

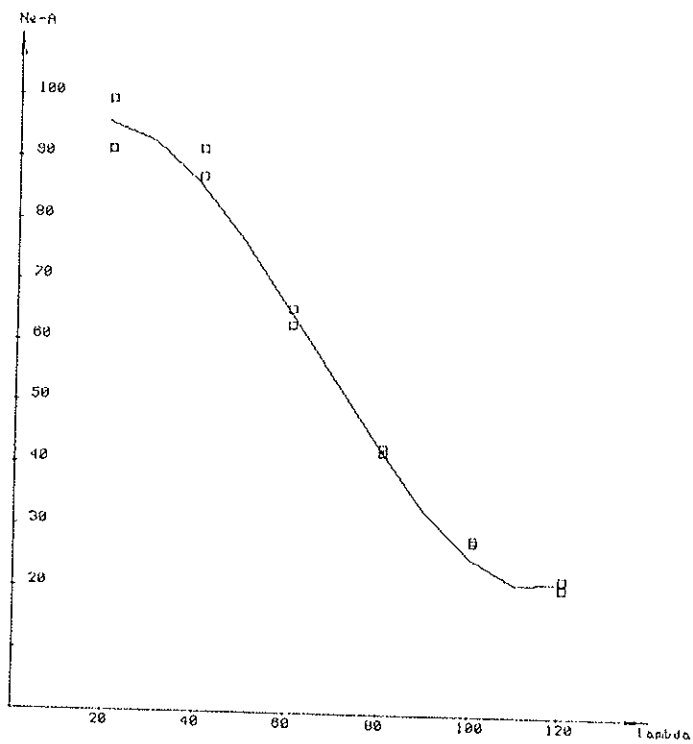
Subor-Ne-A

$A_0 = 87.4136554$
 $A_1 = 1.03501985$
 $A_2 = -.0331623096$
 $A_3 = 1.66599319e-04$

index korelacie = .995999999

X= 20	Y= 99.135	Yt = 96.182
X= 20	Y= 90.798	Yt = 96.182
X= 40	Y= 86.745	Yt = 86.417
X= 40	Y= 91.214	Yt = 86.417
X= 60	Y= 62.679	Yt = 66.116
X= 60	Y= 65.391	Yt = 66.116
X= 80	Y= 42.733	Yt = 43.275
X= 80	Y= 41.912	Yt = 43.275
X= 100	Y= 28.031	Yt = 25.892
X= 100	Y= 27.694	Yt = 25.892
X= 120	Y= 20.489	Yt = 21.962
X= 120	Y= 21.946	Yt = 21.962

N= 332



Tab. 4

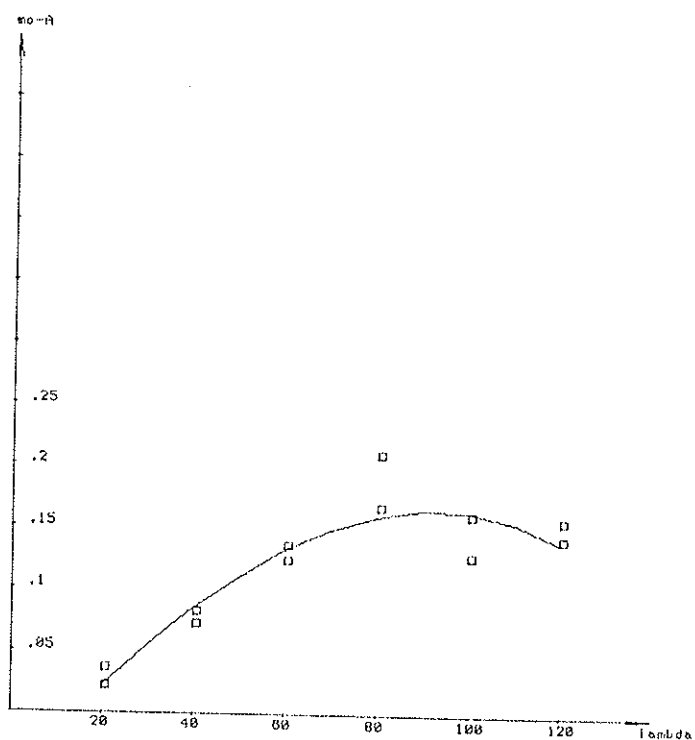
Subor-mo-A

$A_0 = -.0482288909$
 $A_1 = 3.72346993e-03$
 $A_2 = -5.73396483e-06$
 $A_3 = -1.0125436e-07$

index korelacie = .917999999

X= 20	Y= .036	Yt = .023
X= 20	Y= .021	Yt = .023
X= 40	Y= .071	Yt = .084999999
X= 40	Y= .081	Yt = .084999999
X= 60	Y= .134	Yt = .133
X= 60	Y= .122	Yt = .133
X= 80	Y= .165	Yt = .161
X= 80	Y= .208	Yt = .161
X= 100	Y= .126	Yt = .166
X= 100	Y= .159	Yt = .166
X= 120	Y= .141	Yt = .141
X= 120	Y= .155	Yt = .141

N= 328



Tab. 5

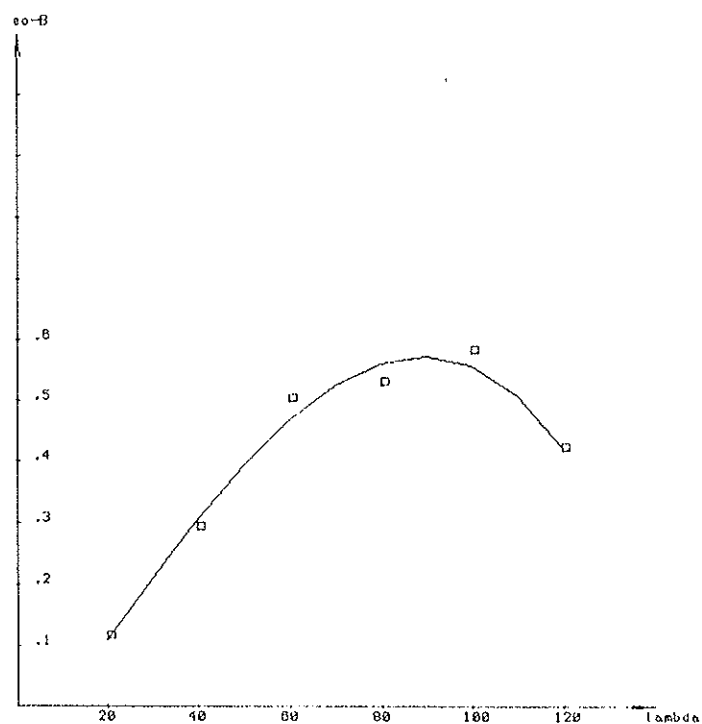
Subor-eo-B

$A_0 = -.0807171569$
 $A_1 = 9.01992583e-03$
 $A_2 = 4.45403441e-05$
 $A_3 = -7.06193348e-07$

index korelacie = .99

X= 20	Y= .114	Yt = .112
X= 40	Y= .292	Yt = .306
X= 60	Y= .501	Yt = .468
X= 80	Y= .529	Yt = .564
X= 100	Y= .58	Yt = .56
X= 120	Y= .418	Yt = .423

N= 149



Tab. 6

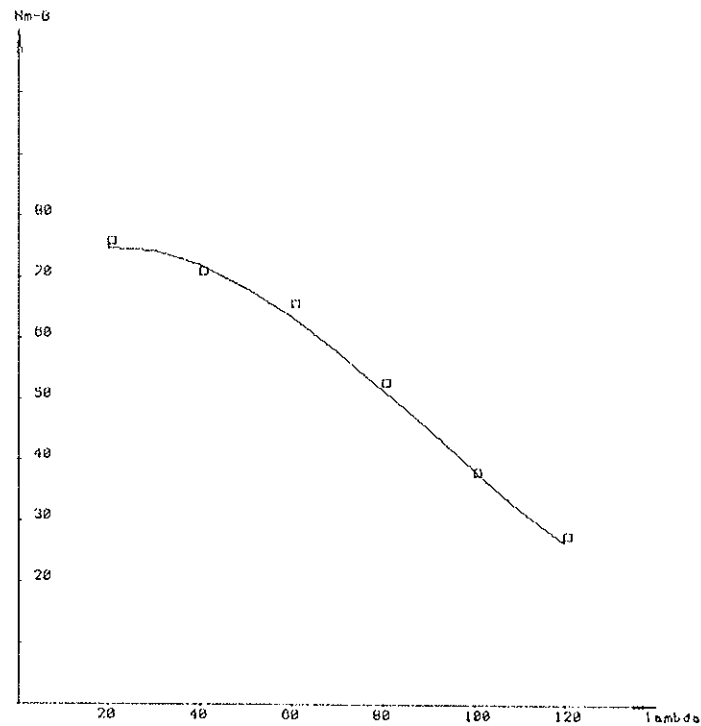
Subor-Nm-B

A 0 = 69.7358527
 A 1 = .502015429
 A 2 = -.0128445563
 A 3 = 4.72056774e-05

index korelacie = .997999999

X= 20	Y= 75.547	Yt = 75.016
X= 40	Y= 70.524	Yt = 72.286
X= 60	Y= 65.317	Yt = 63.813
X= 80	Y= 52.26	Yt = 51.861
X= 100	Y= 37.507	Yt = 38.698
X= 120	Y= 27.008	Yt = 26.588

N= 178



Tab. 7

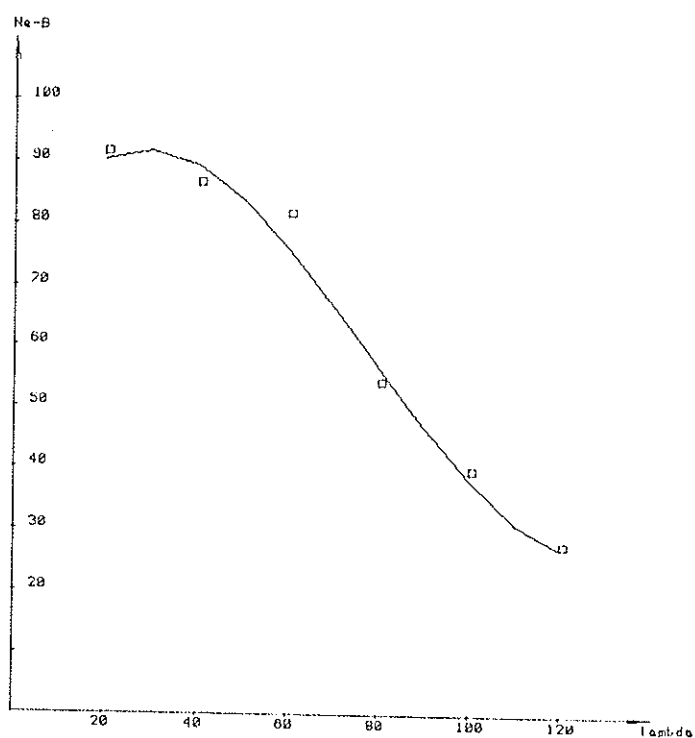
Subor-Ne-B

A 0 = 71.8869503
A 1 = 1.52580226
A 2 = -.0324826133
A 3 = 1.38933536e-04

Index korelacie = .992999999

X= 20	Y= 91.374	Yt = 90.521
X= 40	Y= 86.378	Yt = 89.839
X= 60	Y= 81.274	Yt = 76.507
X= 80	Y= 53.979	Yt = 57.196
X= 100	Y= 39.488	Yt = 38.575
X= 120	Y= 27.267	Yt = 27.311

N= 171



Tab. 8

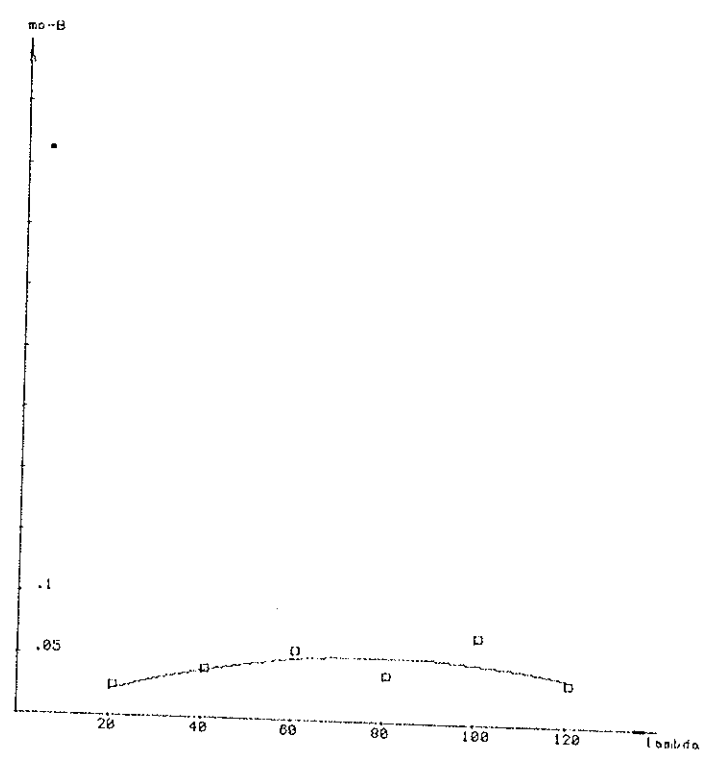
Subor-mo-B

A 0 = -3.5003738e-03
A 1 = 1.43280383e-03
A 2 = -8.98727502e-06

index korelacie = .68

X= 20	Y= .023	Yt = .022
X= 40	Y= .038	Yt = .039
X= 60	Y= .054	Yt = .05
X= 80	Y= .035	Yt = .054
X= 100	Y= .068	Yt = .05
X= 120	Y= .032	Yt = .039

N= 153



Tab. 9

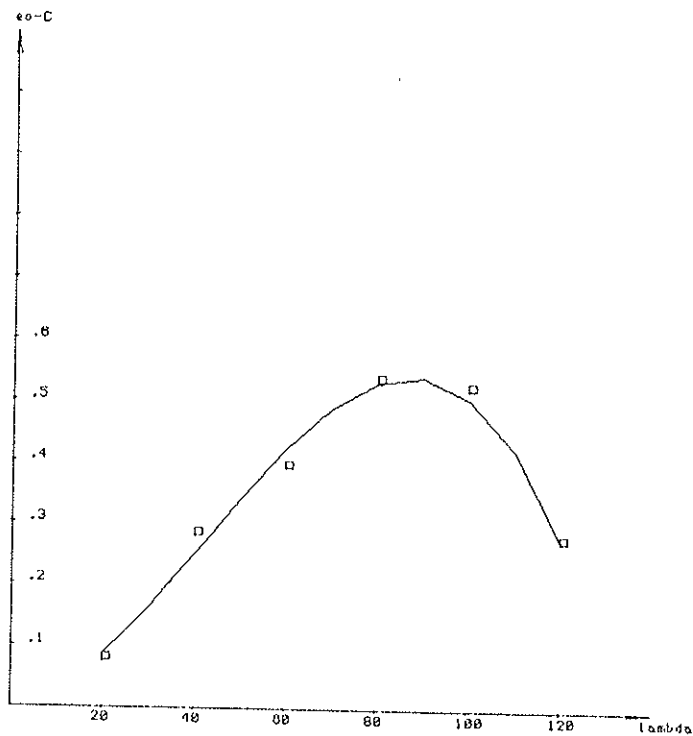
Subor-eo-C

$A_0 = .0100149319$
 $A_1 = 7.05664454e-04$
 $A_2 = 1.92994997e-04$
 $A_3 = -1.49983721e-06$

Index korelacie = .992

X= 20	Y= .078	Yt = .088999999
X= 40	Y= .283	Yt = .251
X= 60	Y= .394	Yt = .423
X= 80	Y= .535	Yt = .534
X= 100	Y= .524	Yt = .511
X= 120	Y= .276	Yt = .282

N= 155



Tab. 10

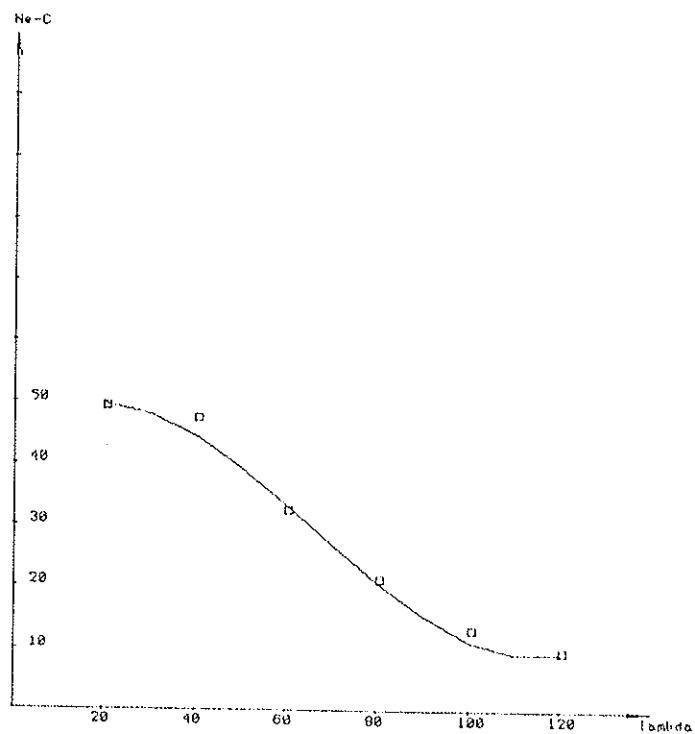
Subor-Ne-C

$A_0 = 44.7197328$
 $A_1 = .600265607$
 $A_2 = -.0186666685$
 $A_3 = 9.36294856e-05$

Index korelacie = .995999999

X= 20	Y= 49.167	Yt = 50.007
X= 40	Y= 47.047	Yt = 44.856
X= 60	Y= 32.047	Yt = 33.76
X= 80	Y= 20.84	Yt = 21.213
X= 100	Y= 12.938	Yt = 11.709
X= 120	Y= 9.289	Yt = 9.743

N= 167



: Tab. 11

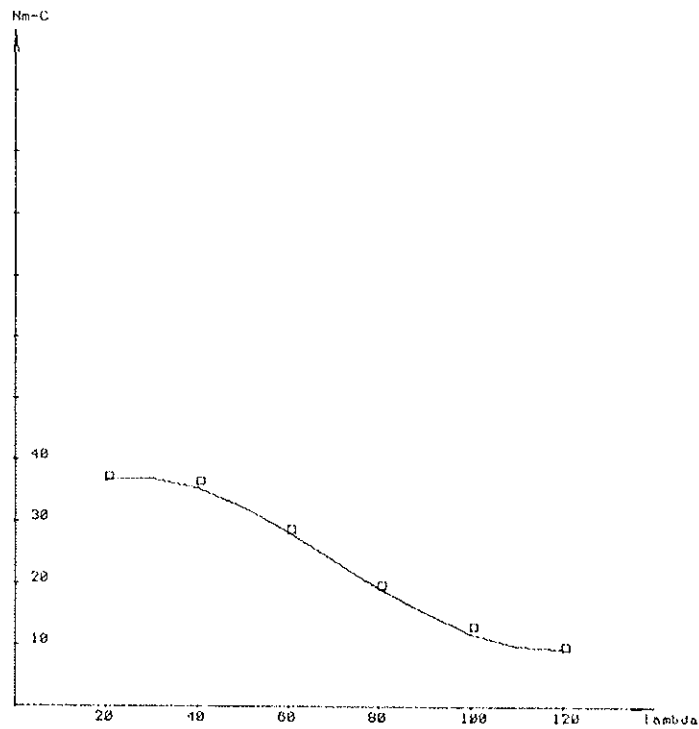
Subor-Nm-C

$A_0 = 29.4539009$
 $A_1 = .663497217$
 $A_2 = -.0156516169$
 $A_3 = 7.28754599e-05$

Index korelacie = .998999999

X= 20	Y= 36.88	Yt = 37.046
X= 40	Y= 36.113	Yt = 35.615
X= 60	Y= 28.33	Yt = 28.659
X= 80	Y= 19.338	Yt = 19.676
X= 100	Y= 12.665	Yt = 12.163
X= 120	Y= 9.452	Yt = 9.619

N= 180



Tab. 12

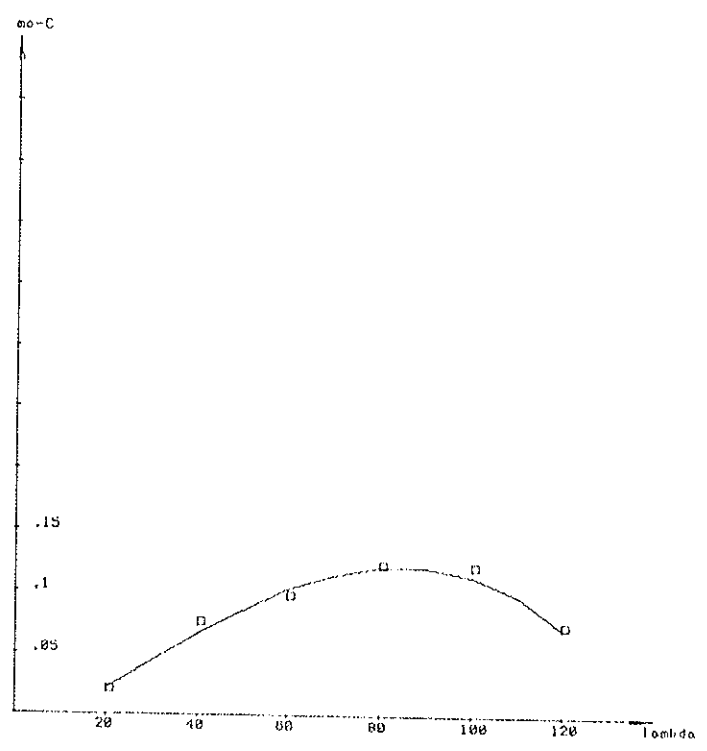
Subor-mo-C

A 0 = -.0218391523
A 1 = 2.03034462e-03
A 2 = 1.17117917e-05
A 3 = -1.83359195e-07

index korelacie = .99

X= 20	Y= .019	Yt = .022
X= 40	Y= .074	Yt = .066
X= 60	Y= .096	Yt = .103
X= 80	Y= .121	Yt = .122
X= 100	Y= .119	Yt = .115
X= 120	Y= .072	Yt = .074

N= 164



Tab. 13

Subor-eo-D

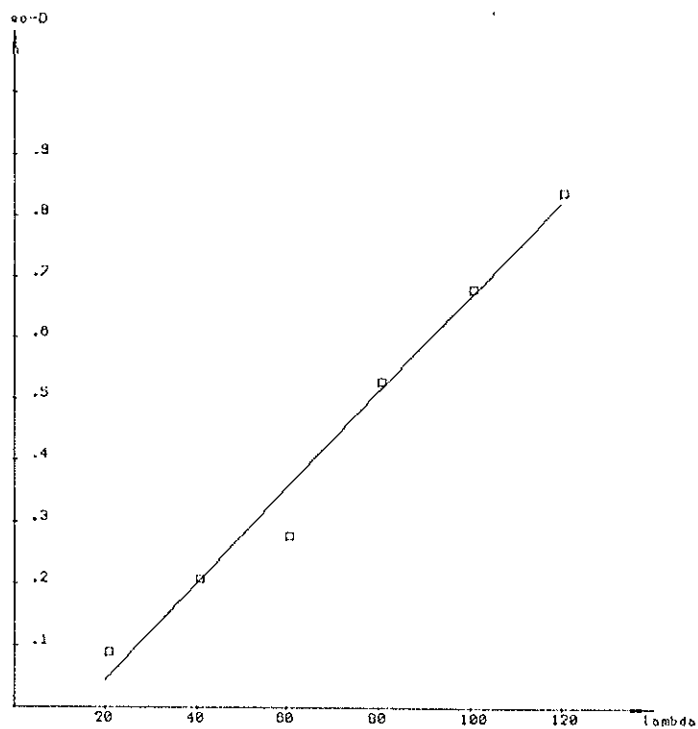
A 0 = -.110779238

A 1 = 7.79670994e-03

index korelacie = .99

X= 20	Y= .085	Yt = .045
X= 40	Y= .204	Yt = .201
X= 60	Y= .274	Yt = .357
X= 80	Y= .527	Yt = .513
X= 100	Y= .679	Yt = .669
X= 120	Y= .837	Yt = .825

N= 142



Tab. 14

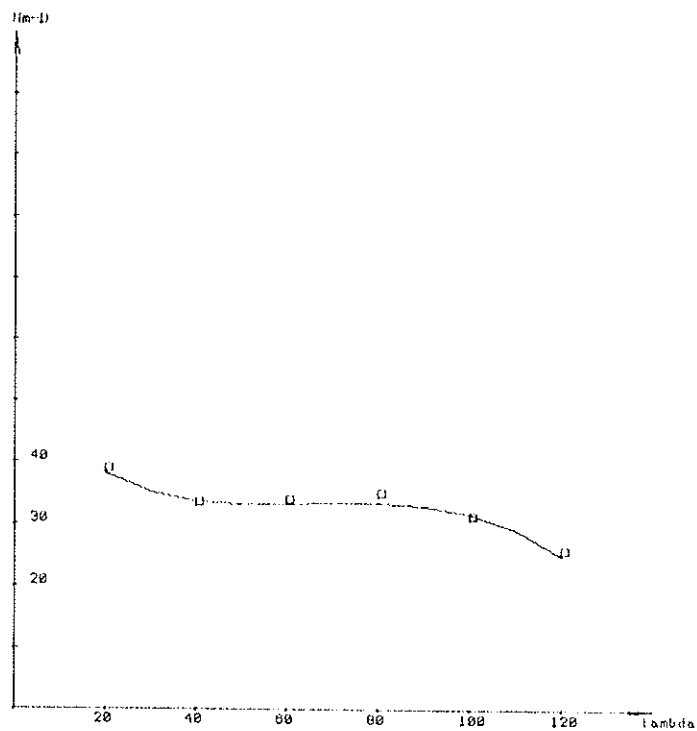
Subor-Nm-D

$A_0 = 49.8384221$
 $A_1 = -.800461776$
 $A_2 = .0125427529$
 $A_3 = -6.32966944e-05$

index korelacie = .982999999

X= 20	Y= 38.637	Yt = 38.34
X= 40	Y= 33.007	Yt = 33.837
X= 60	Y= 33.643	Yt = 33.293
X= 80	Y= 34.627	Yt = 33.667
X= 100	Y= 30.788	Yt = 31.923
X= 120	Y= 25.38	Yt = 25.022

N= 180



Tab. 15

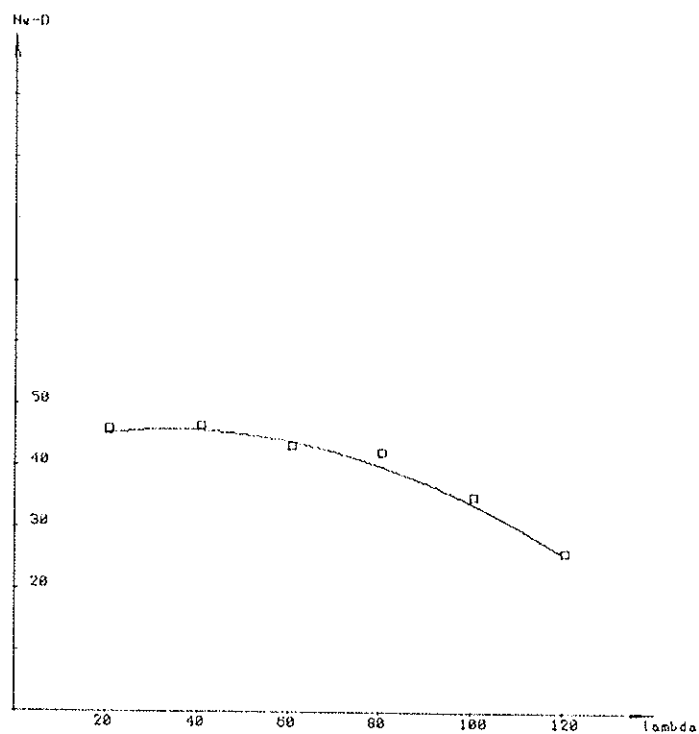
Subor-Ne-D

$\hat{A} 0 = 42.6523715$
 $\hat{A} 1 = .195351698$
 $\hat{A} 2 = -2.77997958e-03$

index korelacie = .992999999

X= 20	Y= 45.726	Yt = 45.447
X= 40	Y= 46.144	Yt = 46.018
X= 60	Y= 42.795	Yt = 44.366
X= 80	Y= 41.987	Yt = 40.489
X= 100	Y= 34.544	Yt = 34.388
X= 120	Y= 25.739	Yt = 26.063

N= 160



Tab. 16

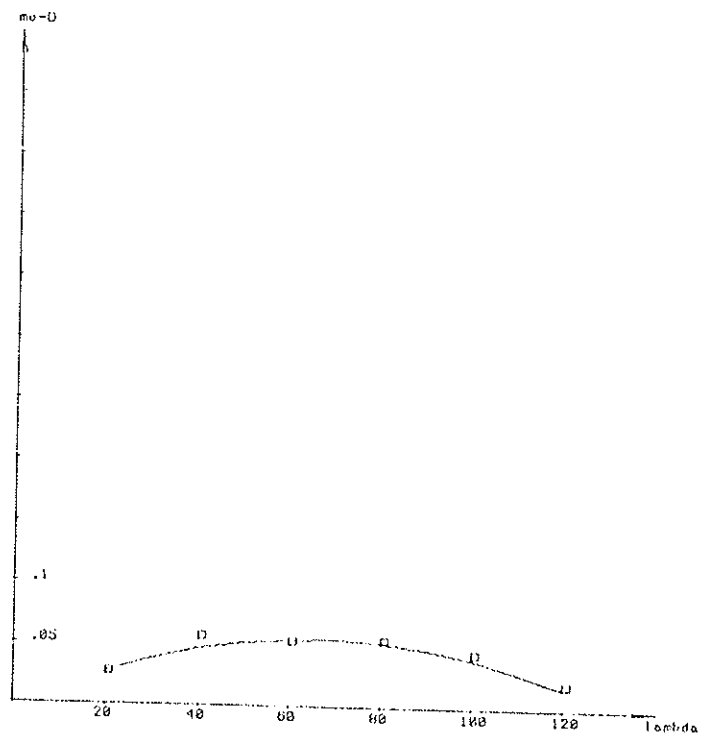
Subor-mo-D

$A_0 = -1.22028104e-03$
 $A_1 = 1.74834107e-03$
 $A_2 = -1.32167976e-05$

Index korelacie = .970999999

X= 20	Y= .026	YI= .028
X= 40	Y= .055	YI= .048
X= 60	Y= .052	YI= .056
X= 80	Y= .053	YI= .054
X= 100	Y= .043	YI= .041
X= 120	Y= .018	YI= .018

N= 153



Tab. 17

λ	Ratio N_m/N_E of a column of type			
	A	B	C	D
10	1	1	1	1
20	0.8009	0.8287	0.7408	0.8358
40	0.7861	0.8046	0.7939	0.7556
60	0.8153	0.8341	0.8494	0.7569
80	0.8949	0.9067	0.9275	0.8248
100	1.0100	1.0031	1.0387	0.9121
120	0.9113	0.9735	0.9873	0.9751

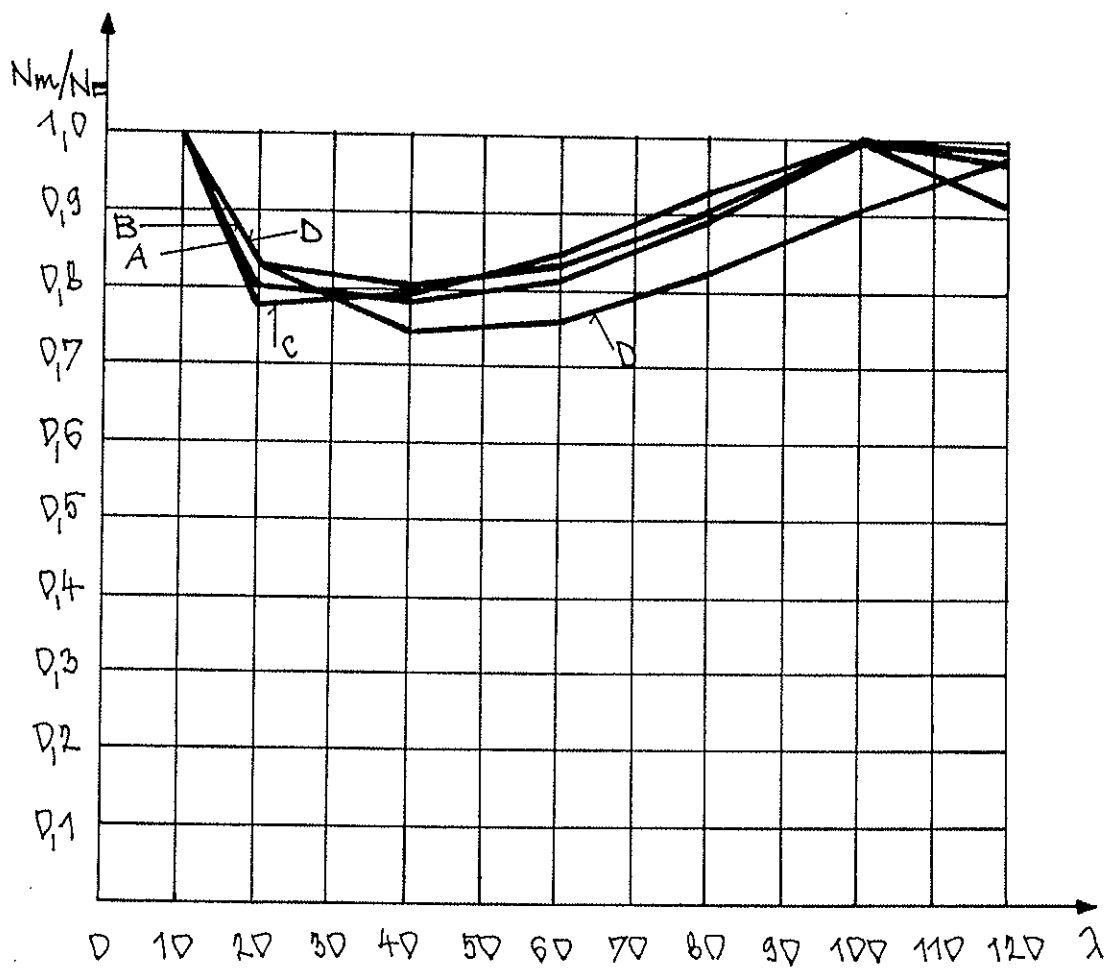


Fig. 5

5. CONCLUSION

Results of the mathematic-statistical evaluation of a large set of experiments for the determination of the limit load of wood columns have shown that the influence of geometrical and structural imperfections was mostly expressed in columns of slenderness $\lambda = 40$ /types A; B; D/ and $\lambda = 20$ /type D/. As can be seen from Fig. 5 the influence of imperfections is not neglective in columns of slenderness $\lambda = 40$ to 100.

Informations obtained from the theoretical and experimental analyses of the limit load of wood columns will serve as a basis for the work of the standard committee for ČSN 73 1701 "Design of wood building structures".

REFERENCES

- [1] Dutko, P.: Vzperná únosnosť prvkov drevených konštrukcií, Zborník-Stabilita dielcov a sústav, Dom techniky SVTS, Bratislava, 1974
- [2] Dutko, P. and col.: Drevené konštrukcie, ALFA, Bratislava 1976
- [3] Dutko, P.: Pevnostné riešenie vzperu drevených prútov a stanovenie ekvivalentnej odchýlky drevených tlačných prútov, Research report III-3-4/11, Stavebná fakulta SVŠT Bratislava, 1985 and Research Report III-3-1/8, Stavebná fakulta SVŠT Bratislava 1988
- [4] Southwel, R.V.: Proc.Roy.Soc. London, series A, Vol. 135, 1932
- [5] Dutko, P.: Únosnosť tlačných drevených prútov s geometrickými a štrukturálnymi imperfekciami, Zborník referátov IV. medzinárodného sympózia Drevo v stavebných konštrukciách, Bratislava-Kočovce, 1989.

INTERNATIONAL COUNCIL FOR BUILDING RESEARCH STUDIES AND DOCUMENTATION
WORKING COMMISSION W18A - TIMBER STRUCTURES

COMMENT ON THE STRENGTH CLASSES IN EUROCODE 5
BY AN ANALYSIS OF A STOCHASTIC MODEL OF GRADING

A proposal for a supplement of the design concept

by

M Kiesel
TH Wismar
German Democratic Republic

MEETING TWENTY - TWO
BERLIN
GERMAN DEMOCRATIC REPUBLIC
SEPTEMBER 1989

Comment to the strength classes in Eurocode 5 by an analysis of a stochastic model of grading

by

Michael Kiesel, TH Wismar, GDR

1. Introduction

In this comment an analysis of distribution functions of strength and elastic properties of timber subjectet to continuous classification is undertaken. Furthermore relations to Eurocode 5 /1/ will be shown.

In /1/ strength classes of timber are expressed by characteristic values X_k . These values are estimated by a fixed fractile of a statistical distribution. The type of distribution is determined by the 3-parameter Weibull distribution, the fractile by the 5-percentile value. Testing conditions ($20^{\circ} \pm 2^{\circ}\text{C}$; $65 \pm 5\%$) and load duration (3...5 mins.) by the investigation of test data of specimen in structural sizes are unified. Eurocode 5 likewise contains information about methods of classification for timber (visual assessment, non-destructiv measurment of one or more properties, combination of the two methods) and derives from this specific demands about the composition of the random sample.

2. Stochastic model

The stochastic model of continuous classification by Pöhlmann and Rackwitz /2/ is based on the bivariate normal distribution between the strength property Y and the grading criterion X

$$X \in N(\mu_x; \sigma_x^2) \quad Y \in N(\mu_y; \sigma_y^2).$$

The stochastic connection between the two properties is described through the coefficient of correlation ρ_{xy} .

From this distribution the linear regression analysis is derivated. The regression equation $E(Y|X) = \alpha + \beta x$ and the normal distributed error with the residual variance connect the dependent variate Y with the cause variable X .

The following connection exists between the variance of the strength property and the residual variance

$$\sigma_{\varepsilon}^2 = \sigma_y^2 \cdot (1 - \rho_{xy}^2) \quad (1)$$

The grading criterion X can only be determined with a measurement error τ . In the stochastic model this value τ is considered by a normal distribution $\tau \in N(0; \sigma_{\tau}^2)$. Under these assumptions the density function of the strength property of a grade is

$$f(y) = \frac{1}{\kappa \cdot \beta \cdot \sigma_1} \cdot \varphi\left(\frac{\frac{y-\alpha}{\beta} - \mu_x}{\sigma_1}\right) \cdot \left[\Phi\left(\frac{g_0 - \mu}{\sigma_2}\right) - \Phi\left(\frac{g_u - \mu}{\sigma_2}\right) \right] \quad (2)$$

where

$$\begin{aligned} \kappa &= \Phi\left(\frac{g_0 - \mu_x}{\sigma_4}\right) - \Phi\left(\frac{g_u - \mu_x}{\sigma_4}\right) & \sigma_4^2 &= \sigma_x^2 + \sigma_{\tau}^2 \\ \sigma_1^2 &= \frac{\sigma_{\varepsilon}^2}{\beta^2} + \sigma_x^2 & \sigma_2^2 &= \sigma_3^2 + \sigma_{\tau}^2 & \sigma_3^2 &= \frac{\sigma_x^2}{1 + \frac{\sigma_x^2 \beta^2}{\sigma_{\varepsilon}^2}} \\ \mu &= \left(\frac{y - \alpha}{\sigma_{\varepsilon}^2 \beta} + \frac{\mu_x}{\sigma_x^2} \right) \cdot \left(\frac{\beta^2}{\sigma_{\varepsilon}^2} + \frac{1}{\sigma_x^2} \right)^{-1} \end{aligned}$$

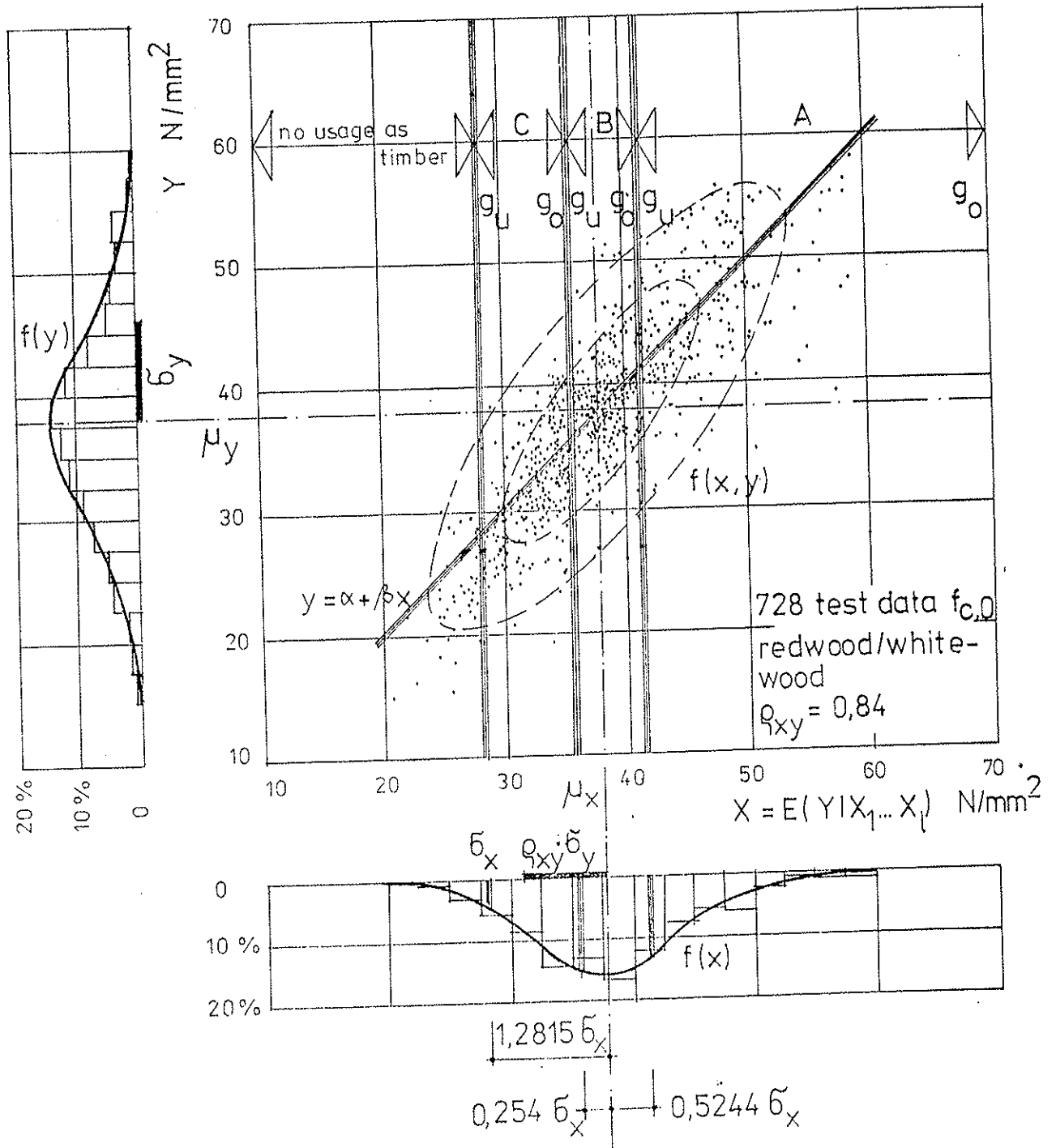
$\varphi, \Phi \dots$ density function, distribution function of the standardized normal distribution

The distribution function can be found by numerical integration

$$F(y) = \int^y f(y) \cdot dy \quad (3)$$

A generalization of the stochastic model results under consideration of the expected value $E(Y|X)$ of the regression equation as the grading criterion X . Then it is also possible to expand the analysis to the multiple regression model. This is shown in Fig. 1, where test data of compression parallel to grain and expected values of a multiple regression equation are contrasted.

Fig. 1 estimates test data of a random sample. For the bivariate normal distribution follows



grade	no usage as timber	C	B	A
output	10 %	30 %	30%	30 %

Figure 1 Stochastic model of grading for timber

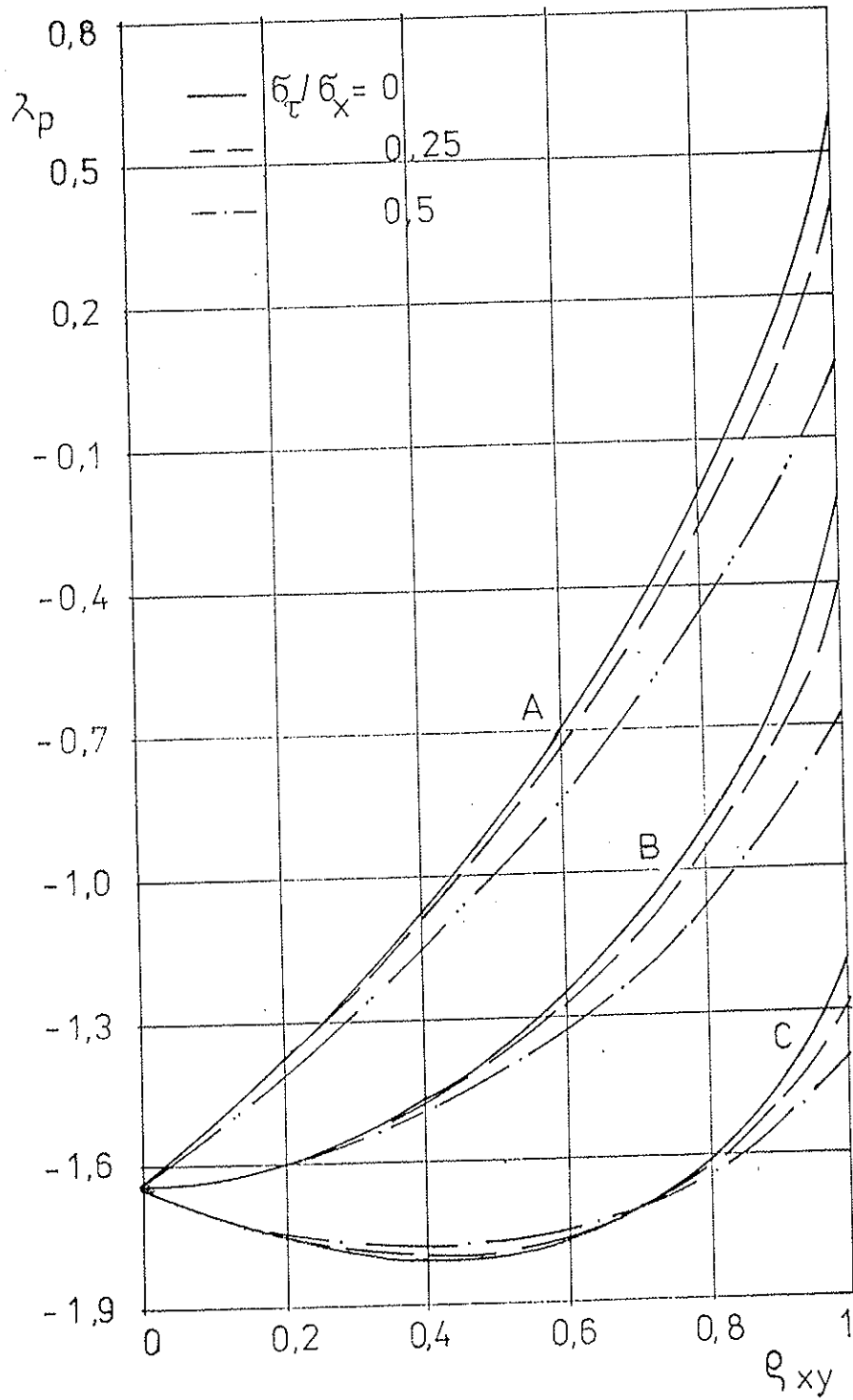


Figure 2 Values λ_p for the 0,05-fractile

$$\alpha = 0 ; \beta = 1 ; \mu_x = \mu_y ; \sigma_x = \rho_{xy} \cdot \sigma_y$$

Then it is possible to ascertain the characteristic fractiles of order p by

$$f_p = \mu_y + \lambda_p \cdot \sigma_y \quad (4)$$

The values λ_p for the 0,05-fractile under supposition of theoretical grades A, B and C according to Fig. 1 are described in Fig. 2.

3. Analysis of the stochastic model

For strength and elastic properties of non-classified European redwood and whitewood the characteristic parameter mean μ_y and coefficient of variation can be supposed by Table 1.

Table 1 Parameter of the normal distribution for non-classified European redwood and whitewood (moisture content 12 %) (N/mm ²)				
Parameter	Bending	Tension	Compression	Modulus of elasticity
	f_m	$f_{t,0}$	$f_{c,0}$	E_0
mean μ_y	45	30	35	11 000
coefficient of variation v_y	0,30	0,35	0,20	0,225

Following multiple coefficients of correlation (/3/, /4/ and own results) exist between strength and elastic properties and grading criterions.

Table 2 Multiple coefficients of correlation between grading criterions and strength and elastic properties of European redwood and whitewood

method of grading	correlation to			
	f_m	$f_{t,0}$	$f_{c,0}$	E_0
visual assesment(f.i./5/)	0,5	0,6	0,5	0,4
mechanical grading (criterion: modulus of elasticity)	0,7	0,7	0,7	1
mechanical grading (criterion: E_0 and knot area ratio)	0,75	0,8	0,75	1

Under these assumptions the characteristic 0,05-fractiles at Table 3 are resulting. These values apply for a classification into theoretical grades (signified A, B and C) described in Fig. 1. Furthermore the ratios

$$\delta = 0,05\text{-fractile} / 0,01\text{-fractile}$$

are ascertained to characterize the scatter of strength and elastic properties below the 0,05-fractile.

The results of this analysis are then used to assigne the grades to standard strength classes of Eurocode 5.

4. Conclusion for Eurocode 5

The theoretical analysis of the distribution functions for strength and elastic properties of timber grades shows, that the characteristic values X_k and the ratios δ depend to a high degree on the coefficients of correlation.

Table 4 Analysis of characteristic fractiles of theoretical grades
(European redwood and whiteoak - moisture content 12%)

	Grade A			Grade B			Grade C					
	$f_{0,05}$	\bar{f}	$C_x / 1/1$	$X_k / 1/1$	$f_{0,05}$	\bar{f}	$C_x / 1/1$	$X_k / 1/1$	$f_{0,05}$	\bar{f}	$C_x / 1/1$	$X_k / 1/1$
1. visual assessment												
	$\sigma_x / \sigma_x = 0,25$											
$f_{m,k}$	N/mm ²	32,4	1,34	28,5	26,2	1,44	25,0	20,8	1,63	19,0		
$f_{t,k}$	N/mm ²	22,2	1,38	17,0	16,6	1,55	14,5	11,5	2,02	11,5		
$f_{c,0,k}$	N/mm ²	28,5	1,18	26,0	25,3	1,21	21,5	22,4	1,24	17,5		
$E_{0,mean}$	N/mm ²	12100	1,24	12000	11120	1,27	11000	10350	1,31	9000		
$E_{0,k} / f_{c,0,k}$	-	290		320	291		340	293		370		
$E_{0,k} / f_{m,k}$	-	255		300	281		310	315		350		
2. mechanical grading (criterion: E_0)												
	$\sigma_x / \sigma_x = 0,25$											
$f_{m,k}$	N/mm ²	37,8	1,23	34,0	29,5	1,30	21,5	21,8	1,46	17,0		
$f_{t,k}$	N/mm ²	24,4	1,30	24,0	18,0	1,42	14,5	12,0	1,82	11,5		
$f_{c,0,k}$	N/mm ²	31,2	1,13	30,0	27,0	1,15	21,5	23,0	1,19	17,5		
$E_{0,mean}$	N/mm ²	13500	1,05	13500	11300	1,05	11000	9400	1,08	9000		
$E_{0,k} / f_{c,0,k}$	-	381		320	370		340	340		370		
$E_{0,k} / f_{m,k}$	-	315		250	340		310	360		350		

Table 4 Analysis of characteristic fractiles of theoretical grades
(European redwood and whitewood - moisture content 12%)

	Grade A			Grade B			Grade C					
	$f_{0,05}$	γ	$c_x / \lambda /$	$\lambda_k / \lambda /$	$f_{0,05}$	γ	$c_x / \lambda /$	$\lambda_k / \lambda /$	$f_{0,05}$	γ	$c_x / \lambda /$	$\lambda_k / \lambda /$
3. mechanical grading (criterion: E_0 and knot area ratio) $b_g / b_x = 0,25$												
$f_{m,k}$	39,2	1,20		34,0	20,7	1,27		21,5	22,4	1,39		17,0
$f_{t,k}$	25,0	1,27		24,0	18,5	1,37		14,5	12,7	1,69		11,5
$f_{c,0,k}$	32,0	1,12		30,0	27,6	1,14		21,5	23,3	1,16		17,5
$E_{0,mean}$	13500	1,05	C7	13500	11300	1,05	C5	11000	9400	1,08	C3	9000
$E_{0,k} / f_{c,0,k}$	372			320	363			340	337			370
$E_{0,k} / f_{m,k}$	304			250	326			310	350			350

In order to reach a higher coefficient of correlation higher efforts are necessary for the technological process of grading, too.

a) The understandable separation of standard strength classes from specific grading rules in Eurocode 5, the great differences between the characteristic values of standard strength classes C6 to C8 and the for all strength properties unitary partial coefficient γ_m involve losses for the usage of the material properties, which would be possible through the principles of the code.

With regard to the accomplished analysis a widening of the classification rules as follows would be useful:

classification rules

$f_{m,k}$	$f_{c,0,k}$	$f_{t,0,k}$	$E_{0,mean}$	strength class
C_x	C_x	C_x	C_{x-1}	C_x

Then it would be possible to assigne the theoretical grade B for machine stress grading into the strength class C6.

b) A great scatter of strength properties for tension below the 0,05-fractile is characteristic for the theoretical grade C (corresponding standard strength class C3). In agreement with the available praxis in the GDR by the standards /5/ and /6/ it should be discussed if the usage of materials of this standard strength class for tension stresses had to be excluded.

c) In analysis of the stochastic model different ratios $E_{0,k}/f_{m,k}$ and $E_{0,k}/f_{c,0,k}$ from the values in /1/ are resulting. The effects of these deviations have to be proofed. An example therefore gives Fig.3 .

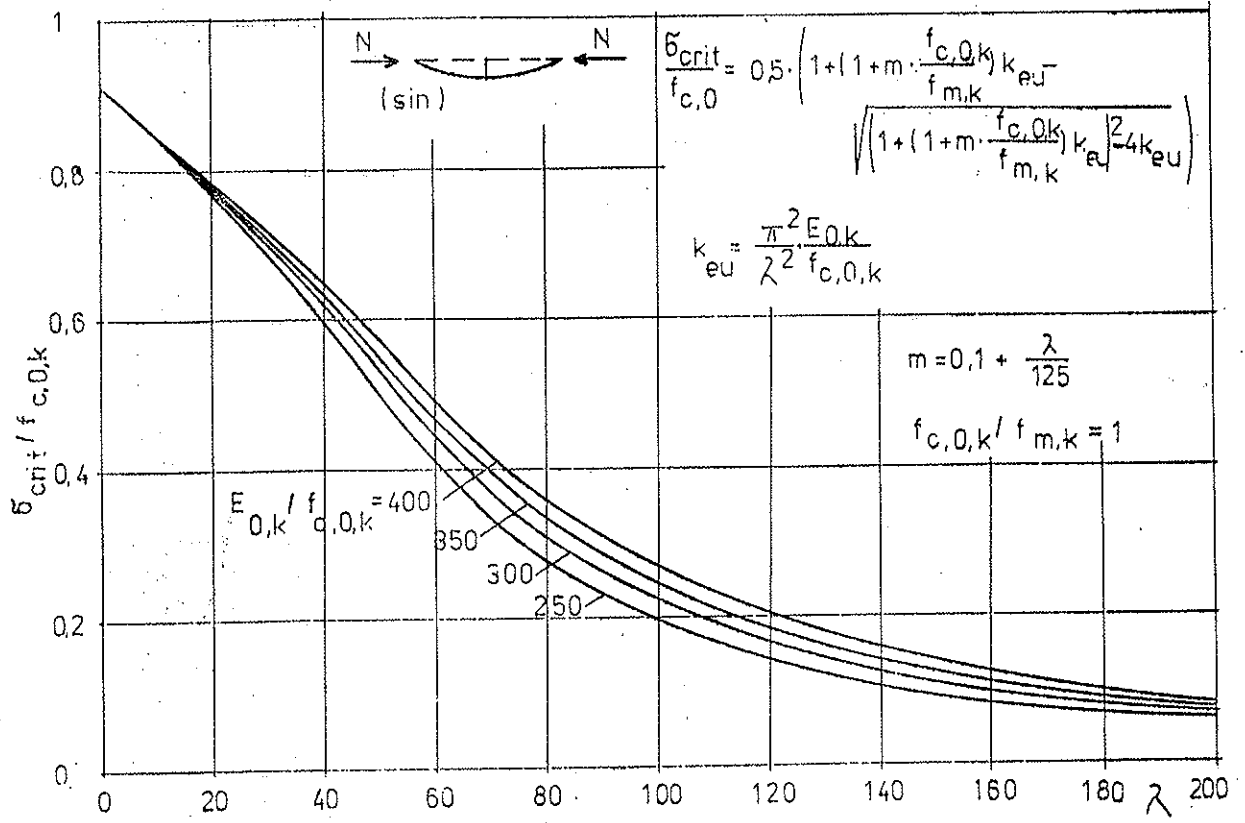


Figure 3 Critical stresses of columns

5. Literature

- /1/ Eurocode 5: Gemeinsame einheitliche Regeln für Holzbauwerke.- Deutsche Entwurfsfassung, 87-10
- /2/ Pöhlmann, S.; Rackwitz, R.: Zur Verteilungsfunktion der Festigkeitseigenschaften bei kontinuierlich durchgeführten Sortierungen. - In: Materialprüfung 23. (1981), S. 277-278
- /3/ Glos, P.: Die maschinelle Sortierung von Schnittholz.- In: Holz-Zentralblatt (1982) 13.- S.153-155
- /4/ Apitz, R.: Beitrag zur Bestimmung der Festigkeitseigenschaften von Bauholz bei Biegebeanspruchung für eine Bemessung nach Grenzzuständen.- IH Wismar, Diss. ,1985
- /5/ TGL 117-0767: Bauschnittholz , Gütebedingungen.- Berlin, 1963
- /6/ TGL 33 135/ 01: Holzbau, Tragwerke.- Leipzig, 84-01

INTERNATIONAL COUNCIL FOR BUILDING RESEARCH STUDIES AND DOCUMENTATION

WORKING COMMISSION W18A - TIMBER STRUCTURES

**PERSPECTIVE ADHESIVES AND PROTECTIVE COATINGS
FOR WOOD STRUCTURES**

by

A S Freidin

Timber Structure Department of Ts NIISK, Moscow

USSR

MEETING TWENTY - TWO

BERLIN

GERMAN DEMOCRATIC REPUBLIC

SEPTEMBER 1989

PERSPECTIVE ADHESIVES AND PROTECTIVE COATINGS
FOR WOOD STRUCTURES

Principal requirement, which traditionally refers to adhesives and protective coatings for wood structures, including low-rise house-buildings, is atmospheric and temporal durability. Atmospheric durability has connection with water resistance which serves as preliminary express-test for estimation of properties of coatings and adhesives.

Development of industrialized manufacture of new wood board materials, perfection of new wood structures design solutions, and especially increased ecological requirements to environment protection and to ensuring of sanitary and hygienic purity of industrial production and usage of structures (including wooden houses), led to necessity of revision of adhesive and protective paintwork material assortment, used during wood structure manufacture. Intensive development of chemical industry in the field of manufacture of new polymer adhesives and protective materials, as well as success of estimation of process mechanisms which take place in wood structures when using them under different temperature and humidity conditions, favours this.

Research of glued and protected wood under different temperature-humidity conditions, carried out during many years, including the influence of static and dynamic cyclic load, allowed to draw conclusion that in most cases non-chemical destruction processes is the reason of failure of glued joints or protective coatings; and physical fatigue processes appear because of the action of internal stresses caused by the difference between deformation processes of wood or wood materials on the one hand, and of polymer glu-

ed joints or coatings on the other hand.

A d h e s i v e s. Resorcinol resin adhesives and phenolic-elastomer adhesives are the most high-quality adhesives, which are used everywhere for manufacture of main wood structures. Attempts to substitute them for epoxy adhesives, which have better physical-mechanical characteristics and high adhesion towards various materials, proved a failure. It depends upon specific nature of wood and of materials on its basis. It is known that adhesion towards wood materials is determined not only by chemical processes but by mechanical forces also, because of adhesive flow-in into cut wood grain and impregnation of boundary wood layer with adhesive. Due to good wetting power and not very high viscosity these processes are effective when using resorcinol resin, phenolic and similar adhesives.

Nowadays great attention is paid to improving traditional adhesives of resorcinol resin type. The question is to improve economic and sanitary-hygienic characteristics of adhesives and to carry out modification of adhesive properties.

As for the first task, perspective adhesives are those demanding possibly lesser resorcin expenditure without deterioration of service properties of adhesives. At the same time it is required that final product should emit less noxious substances, and besides that when synthesizing adhesives it should be less toxic waste polluting environment. Furthermore, it is impossible to forget about power-intensity. With other equal conditions, less power-intensive adhesive during synthesis and processing will have advantages.

Phenolic-resorcinol adhesives with their properties differ very little from resorcinol adhesives ones but they are more eco-

nomic and require less resorcin which is expensive and scarce, it made for their wide use. However, there are not very many adhesive sorts among them with small content of free phenol. As one can judge by the following data, the least content of free phenol is registered for Soviet adhesives $\Phi P\Phi-50$ and $\Phi P\Phi-50K$ and for Finnish one $P\Phi-30$:

$\Phi P\Phi-50K$ (USSR)	- 4,0%
$\Phi P\Phi-50$ (USSR)	- 5,3%
$\Pi\Phi K-I4P$ (USSR)	- 4,0%
$P\Phi-30$ (Finland)	- 3,0%
Cauresin 440 (GFR)	-14,0%
Racoll $\Phi P-I00$ (GFR)	-15,3%
Sofra $P\Phi-I85$ (France)	- 8,7%
Casco I7I0 (Sweden)	- 7,0
Aerodux I85 (Switzerland)	-18%

Besides, adhesives $\Phi P\Phi-50$ and $\Phi P\Phi-50K$ have the following advantage: during synthesis they are obtained by no-waste technology without sewage, drying and so on. As for technological properties, storage terms and so on, they don't yield to usual adhesives.

Furthermore, adhesive $\Phi P\Phi-50K$ is one of the most economic adhesives of such type, as it requires a little resorcin. Ratio phenol: resorcin during synthesis makes up 100:300. Adhesives $\Phi P\Phi-50$ and $\Phi P\Phi-50K$ are widely used for manufacture of the most main wood structures in the USSR.

As it is known, Estonian oil shales are the source of unique raw material - alkyl resorcins, which substitute resorcin successfully during adhesive synthesis. This caused purchase of licence for manufacture of adhesives from alkyl resorcins by Japan and Finland. Alkyl resorcin-phenolic adhesive $\Pi\Phi K-I4P$ is widely used

in the USSR for manufacture of mass agricultural, industrial and cultural-public buildings. Improved adhesives of this type are developed in order to reduce expenditure coefficients of raw material and to improve sanitary-hygienic and technological characteristics of final product.

As for the second task, the most effective adhesive modification is that for the purpose of regulation of deformation characteristics and for the purpose of creation of adhesives with preset properties (tailor-made adhesives). It is required not only for glueing traditional wood structures but for manufacture of structures from materials, which differ by mechanical characteristics, as in this case the most considerable temperature-humidity and other internal stresses appear, which reduce durability. For example, connection of wood structure elements with the help of glued-in wood metal bars can be mentioned, as well as structure manufacture from new wood base material - cement-chip boards and so on. Adhesives of resorcin type yield to modification in most effective way.

Modification principles and industrial compounding are developed for adhesives, modified with liquid rubbers and synthetic rubber latexes. Modification of adhesive $\Phi P\Phi-50$ with liquid polysulphide rubber gives up adhesive $\Phi P\Phi-50T$; modification of adhesive $\Phi P\Phi-50$ with butadiene-styrene-acryl-nitril latex gives up adhesive $\Phi P\Phi-50J$. Modulus of elasticity of these adhesives can fluctuate within considerable range. It ensures essential decrease of internal stresses without considerable change of load-carrying capacity.

Thus, when pinewood joints, shear strength of adhesive $\Phi P\Phi-50J$ makes up not less than 6,5 MPa with destruction of wood, and

in oak-, beech- and hornbeamwood it makes 13,5 MPa.

Modulus of elasticity of adhesive $\Phi P\Phi-50T$ decreases from 1160 to 370 MPa in comparison with adhesive $\Phi P\Phi-50$, when 35 mass. p, polysulphide rubber are used for 100 mass.p. of resin, and internal stresses make up from 5,5 to 1,2 MPa, respectively. For similar change of properties of adhesive $\Phi P\Phi-50H$ considerably greater quantity of latex is used. This fact reduces essentially adhesive cost. The second advantage of resorcin-latex adhesives is the possibility to use liquid hardener instead of powdery paraformaldehyde. Adhesives $\Phi P\Phi-50T$ and $\Phi P\Phi-50H$ are recommended for joints of wood with steel bars instead of epoxy ones, as they have higher heat stability, what is important in case of fire. When temperature increases from 20°C up to 150°C, breaking load of such joints with epoxy adhesive decreases by 89% and with adhesive $\Phi P\Phi-50T$ - by 27%.

Adhesive $\Phi P\Phi-50H$ is recommended for manufacture of panel structures from box-like elements of Folding type on the basis of cement-chipboards. Such structures are used in block-containers and in few-storey house-building.

Experimental check has shown that such modified adhesives successfully resist to accelerate cyclic temperature-humidity ageing.

From adhesives of other types in some countries polyurethane water-dispersive adhesives are widely spread. They are two-component ones and consist of water dispersion of polymer and hardner. By changing ratio of dispersion and hardener technological and physical-mechanical characteristics of glued joint can be easily regulated. In this respect polyurethane adhesives differ essentially from epoxy, resorcin and other adhesives.

The greatest experience is accumulated in Japan and the the USA in the field of use of waterdispersive polyurethane adhesives for plywood manufacture, for production of panels for few-storey house-building and for wood particle boards manufacture. Glued wood with polyurethane adhesive Isoset doesn't yield to wood glued with phenol-resorcin adhesive.

According to literature basis, Japan has about 15 years of practical experience in the field of mass application of standard houses with wall, roof and floor panels made with such polyurethane adhesives. In the USA these adhesives are used for manufacture of doors and other millwork working under atmospheric conditions, as well as for manufacture of fire-resistant structures.

However, one should admit that polyurethane adhesives have not yet won firm position in wood structure industry. Future will show if hopes are justified for this adhesive class, which is widely used for glueing other structural materials.

P r o t e c t i v e c o a t i n g s. Perfection of protective treatment of wood structures and wood materials goes in various directions. On the one hand, there is a task of development of compound with complex action: fire-, bio-, moisture-proof. They are required for limited class of conditions but their absence causes great trouble for spreading of application of such structures.

When developing preparations of complex action, various modifications are created, which ensure presence of prevailing effect (bio-, fire- or moisture-protection). This allows to choose protective means considering structure purpose and conditions of exploitation. On the other hand, it is required to make a proposal about improvement to technical-economic indices of protection process, on the basis of long-term exploitation of protected wood materials,

as well as on the basis of laboratory research of polymer and other materials.

The problem of improvement of constructive measures for wood structure protection can be also singled out.

As an example of complex action compound one can mention compound on the basis of trichlorethylphosphate (TCEP), mass product of chemical industry. Mentioned compound doesn't conceal texture of wood, doesn't wet it in the process of protective treatment, doesn't reduce glueing strength. It ensures even by surface application (expenditure 600 g/m^2) high fire-resistance level of wood and of wood board materials. At the same time compound is characterized by high level of bioprotective ability with expenditure 200 g/m^2 .

Nowadays, it is studied the following problem: how to give hydrophobic properties to wood or wood board materials treated with TCEP.

As the basic component of the compound (TCEP) is effective plasticizer, this problem cannot be solved by traditional way, by means of application of paintwork materials.

Among the compounds, characterized by complex of protective properties, composition BK can be singled out on the basis of brown coal wax, cheap material in wide supply. High moisture- and bioprotective effect of composition mentioned combines with certain fire-protective ability, caused by insignificant bloating by fire influence.

Nowadays, great attention is paid to development of fire- and explosion-proof, ecologically pure water-dispersive compounds, intended for protection of structures against humidification by exploitation. Level of compound protective properties should be commensurable with analogous index of organosoluble paintwork materi-

als on the basis of alkyd and perchlorvinyl resins, which were earlier used for these purposes.

Among studied compounds the most effective ones are water compounds on the basis of latexes of some synthetic rubbers, including rubbers combined with various active admixture.

In particular, latex-phosphate composition "Fankor" is developed for protection of cement-chipboards. This composition is characterized by high atmospheric durability, adhesive strength, long-term protective effect.

INTERNATIONAL COUNCIL FOR BUILDING RESEARCH STUDIES AND DOCUMENTATION
WORKING COMMISSION W18A - TIMBER STRUCTURES

**PROPOSAL FOR INCLUDING AN UPDATED DESIGN METHOD
FOR BEARING STRESSES IN
CIB W18 - STRUCTURAL TIMBER DESIGN CODE**

by

B Madsen
Department of Civil Engineering
University of British Columbia
Vancouver, B.C.
Canada

MEETING TWENTY - TWO
BERLIN
GERMAN DEMOCRATIC REPUBLIC
SEPTEMBER 1989

PROPOSAL FOR INCLUDING
an
UPDATED DESIGN METHOD FOR BEARING STRESSES
in
CIB W18 - STRUCTURAL TIMBER DESIGN CODE

The present method of dealing with bearing stresses in CIB W18 - Structural Timber Design Code is not logical because it neglects the geometry of the member involved in the design. Furthermore the strength values in compression perpendicular to the grain are based upon a test method containing stress concentrations at the end of the bearing plate. The apparent bearing stress may therefore not be correctly reflected for other geometries than that used in the particular test.

The development of a more rational method is presented in the appended paper.

The recommended design method is described in the following and a graphical illustration of its use is also enclosed.

An approximate method for estimating the deformations associated with the bearing stresses is contained in the proposal.

PROPOSED LIMIT STATES DESIGN METHOD

If the bearing plate covers the full length of the member then the plate length l is given by:

$$l = P_y / \sigma_y b$$

If the plate does not cover the full length so that there are end distances L_1 and L_2 , the length l may be reduced by $L_1/4$ (but not more than $D/4$). This reduced length, l_r , shall not be less than $l/4$.

The deformation, Δ_y , of the plate with respect to the other side of the member at factored loads will be

$$\Delta_y = \frac{P_y D}{E_{\perp} b (l_r + l_c)} + 0.002 D$$

where:

$$l_c = L_1/2 \text{ (but not more than } D/2) \text{ plus} \\ L_2/2 \text{ (but not more than } D/2).$$

The deformation at service load P will be

$$\Delta = \frac{PD}{E_{\perp} b (l_r + l_c)}$$

In the above

P_y = factored load

P = service load

σ_y = yield stress at 0.2% strain from tests with 100% of the area loaded

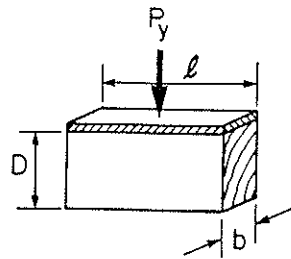
E_y = modulus of elasticity from tests with 100% of area loaded

b = breadth

D = depth

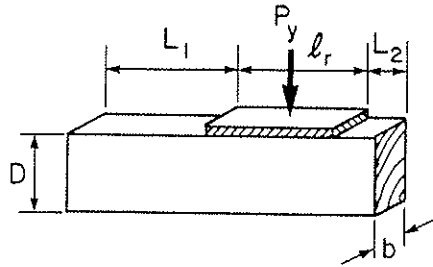
DESIGN METHOD FOR BEARING

CASE 1 : NO OVERHANGING ENDS



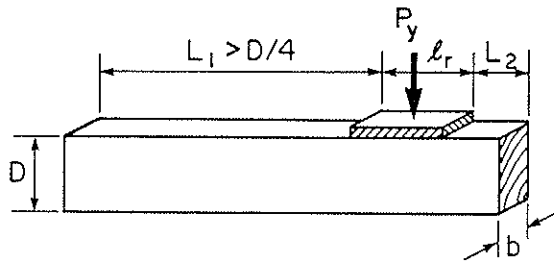
$$l = \frac{P_y}{\sigma_y b}$$

CASE 2 : L_1 and L_2 both $< D/4$



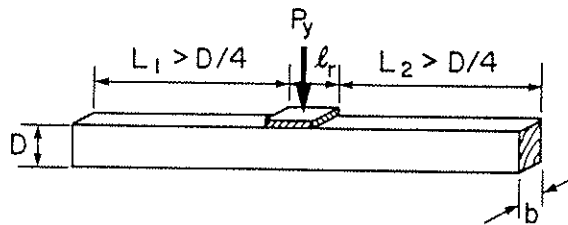
$$l_r = l - \frac{L_1}{4} - \frac{L_2}{4} > \frac{l}{3}$$

CASE 3 : $L_1 > D/4$ and $L_2 < D/4$



$$l_r = l - \frac{D}{4} - \frac{L_2}{4} > \frac{l}{3}$$

CASE 4 : L_1 and L_2 bigger than $D/4$



$$l_r = l - \frac{D}{4} - \frac{D}{4} > \frac{l}{3}$$

DEFORMATION Δ_y FOR FACTORED LOADS

$$\Delta_y = \frac{P_y D}{E_{\perp} b (l_r + l_c)} + 0.002D$$

where

$$l_c = \frac{L_1}{2} (< D/2) + \frac{L_2}{2} (< D/2)$$

DEFORMATION Δ AT SERVICE LOADS

$$\Delta = \frac{P D}{E_{\perp} b (l_r + l_c)}$$

Reprinted from

**Canadian
Journal of
Civil Engineering**

Réimpression du

**Revue
canadienne de
génie civil**

A design method for bearing stresses in wood

B. MADSEN, R. F. HOOLEY, AND C. P. HALL

Volume 9 • Number 2 • 1982

Pages 338–349



National Research Council Canada
Conseil national de recherches Canada

A design method for bearing stresses in wood

BORG MADSEN, R. F. HOOLEY, AND C. P. HALL¹

Department of Civil Engineering, University of British Columbia, Vancouver, B.C., Canada V6T 1W5

Received September 30, 1981

Revised manuscript accepted February 18, 1982

The paper points out that the present method used to design bearing plates for wood subjected to stresses perpendicular to the grain is inadequate because it neglects the effect of the specific geometry. A design method that more correctly reflects the actual conditions is presented together with test data that represent the material properties in a more realistic way.

The design method is discussed and compared with limit states design and design examples are presented. The method includes a conservative estimate of the deflections.

Can. J. Civ. Eng., 9, 338-349 (1982)

Introduction

Wood is a complicated anisotropic material exhibiting many different modes of failure. Design procedures for lumber or timber must take this fact into consideration. The failure mode for wood subjected to compression perpendicular to the grain is very different from the failure mode in either tension or compression parallel to the grain. As a very simplified model of the structure of clear wood, one can visualize the individual cells as drinking straws and the piece of wood as a bundle of these straws held together by a weak rubber glue representing the lignin in which the cells are embedded, as shown in Fig. 1. The cells, or straws, are very strong in their lengthwise direction. When subjected to tension, failure often takes place by tearing of the cell walls in a brittle fracture mode. When the material is subjected to compression parallel to the grain the cells act as hollow columns with some lateral support provided from cell to cell. The failure mode is more ductile and often caused by local buckling failure of the cells, which is manifested by the typical compression wrinkles. Tension forces occurring perpendicularly to the grain will have to be transmitted through the lignin (or rubber glue in the model) and, as mentioned, the lignin does not have much structural strength. This strength is about two orders of magnitude weaker than the tension strength parallel to the grain. Compression forces perpendicular to the grain are transmitted through the thin cylinder walls, which act as arches, so that the failure mode can be visualized as a stability failure in the cell walls, as indicated in Fig. 2.

The above applies to clear wood. For timber or lumber, where knots and other growth characteristics occur, the failure mechanism is much more complicated. However, for compression perpendicular to the grain, the above model is nevertheless representative of

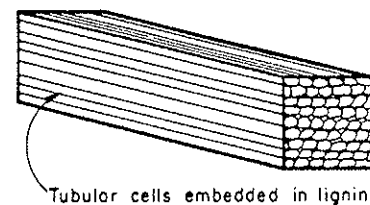


FIG. 1. Model of clear wood structure.

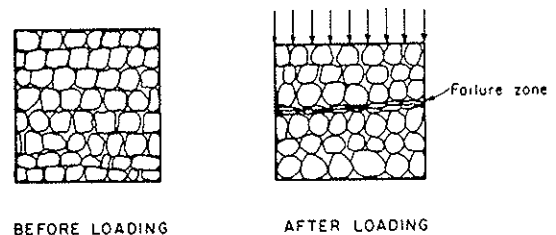


FIG. 2. Failure mode in compression perpendicular to grain.

the weakest material since grain distortions and knots tend to prevent the buckling of the cell walls.

Applications

When timber or lumber is used for structural members, compression forces perpendicular to the grain often occur. Figure 3 shows some examples of loading conditions where the compression stresses perpendicular to the grain should be checked. In most cases the designer will find that the stresses are lower than the allowable stresses and no further considerations have to be given to them. However, the cost of connections can be governed by the compression perpendicular to the grain and it thus becomes important. Compression perpendicular to the grain has also taken on added importance in the design of prefabricated trusses. The loads can be quite high and it is sometimes necessary to provide increased bearing areas by using steel plates

¹Present address: Swan Wooster Engineering Co., Vancouver, B.C., Canada.

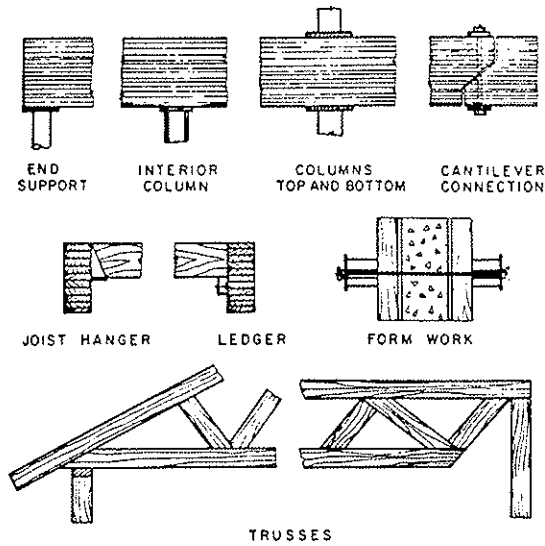


FIG. 3. Examples of bearing.

where the truss rests on walls. It has, therefore, become important to have a realistic design method for compression loadings perpendicular to the grain.

Present design method

The present design method as laid out in CSA 086 (Canadian Standards Association 1980) simply consists of making sure that the stress on the bearing area does not exceed the allowable stress set out in the code for the appropriate species groups. Thus the designer has to ascertain that:

$$\frac{P}{bl} \leq \sigma_{\perp all}$$

where P = working load, b = width of the bearing area, l = length of the bearing area, and $\sigma_{\perp all}$ = allowable bearing stress (C_{\perp} in the Canadian Standard).

Typical values of $\sigma_{\perp all}$ are given in Table 1 for dry and wet service conditions; the values for wet conditions are two thirds of those for dry conditions.

It is assumed that σ_{\perp} is influenced by the duration of load in the same manner as, for instance, bending, and the allowable stress $\sigma_{\perp all}$ can be increased by 15% for snow loads (2 months) and 33% for wind loads.

In addition to the above modification, the code allows for increases in $\sigma_{\perp all}$ if the bearing length is less than 150 mm. To quote Clause 3.3.2.5 of CSA 086:

When lengths of bearing or diameters of washers are less than 150 mm and no part of the bearing area is closer to the end of the member than 75 mm, the allowable bearing stress may be multiplied by the appropriate modification factor as set forth in Table 4 provided that such bearing areas do not occur in positions of high flexural stress.

TABLE 1. $\sigma_{\perp all}$ (MPa) by CSA 086

	Dry	Wet
Lumber		
Douglas fir-larch	3.17	2.12
Hemlock-fir	1.61	1.08
Hemlock-tamarack	2.78	1.86
Coast species	1.61	1.08
Spruce-pine-fir	1.67	1.12
Western cedar	1.92	1.29
Northern species	1.61	1.08
Northern aspen	1.23	0.82
Glulam		
Douglas fir-larch	3.17	2.10
Hemlock-fir	2.86	1.90
Lodgepole pine or spruce	2.86	1.90

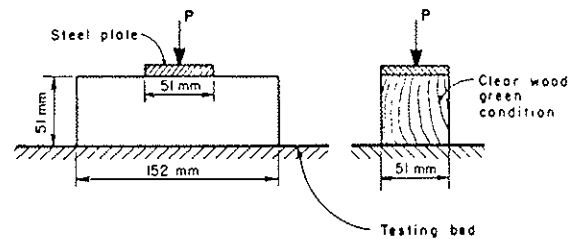


FIG. 4. ASTM D143 test specimen.

Table 4 of CSA 086, Clause 3.3.2.5. Modification factors for various lengths of bearing

Length of bearing (mm)	Modification factor
25.0	1.40
50.0	1.20
75.0	1.13
100.0	1.10
150.0 or more	1.00

Substantial increases (up to 40%) in the allowable stresses can thus be permitted. However, it is relatively rare that the bearing plate is removed by 75 mm from the end of the beam so the increases are, in fact, very limited in their application. This increase was intended primarily for washers, where the stress can be very high indeed.

It should be noted that the code does not provide guidance on the permitted deformations or how they are to be calculated. This is left to the designer to judge.

The test used to obtain information on the material property $\sigma_{\perp all}$ is described in the *Annual book of ASTM Standards* (American Society for Testing and Materials 1976).

The specimen used is a block 51 mm × 51 mm × 152 mm long, as shown in Fig. 4. The load is applied through a rigid steel plate 51 × 51 mm on the surface

that is radial to the annual rings. Thus only one third of the 152 mm long surface is loaded. A load-deformation curve is obtained from the test at a rate of loading of 0.3 mm/min.

The proportional limit is read from the curve and the average value from several tests is used as a base for the allowable stress for a particular species. The specimens are tested in the green condition and the test results multiplied by 1.5 to convert to dry values. This number is then divided by a factor of 1.5 to allow for duration of load and safety factor to obtain the allowable stress $\sigma_{\perp all}$ for dry material.

The American Society for Testing and Materials (ASTM) method described is also used as the base for the Canadian Code, CSA 086. In essence, then, the average green strength at the proportional limit is used as the dry $\sigma_{\perp all}$ or, expressed differently, the difference in strength between the wet and dry material is the allowance for duration of load, accidental overload, and variation in material properties.

Comments on present design method

Canadian Standard CSA 086 allows an increase in bearing stress only if the plate is less than 150 mm long and the end distance is greater than 75 mm. It appears logical to the authors that some end distance is necessary before allowing an increase. It is not logical, however that if a 75 mm end distance is sufficient on, say, a 75 mm deep beam it is also sufficient on a 1500 mm deep beam. As well, an increase may be in order for a 100 mm long plate on a 1500 mm deep beam, but is the same increase in order for a 100 mm long plate on a 40 mm deep beam? It is common in stress analysis for such increases to be functions of dimensionless ratios instead of numerical values.

The material property obtained from the ASTM test is undoubtedly correct for a beam with its middle third loaded over a length equal to its depth. However, the behaviour of the specimen would be quite different if loaded over 100% of its length from that if loaded over 10% of the length. This test is of use in determining the relative behavior of various species but is of little use in designs with different geometries.

In summary, the design and test systems must interact so as to reflect the shape or geometry of the component under analysis. Because of this, a research program was undertaken at the University of British Columbia to investigate the response of various geometries to compression perpendicular to the grain.

Research on effect of geometry

The simplest shape to deal with is the block $l \times D \times b$ of Fig. 5a symmetrically loaded by a force P on a rigid bearing plate covering 100% of the area $l \times b$. If

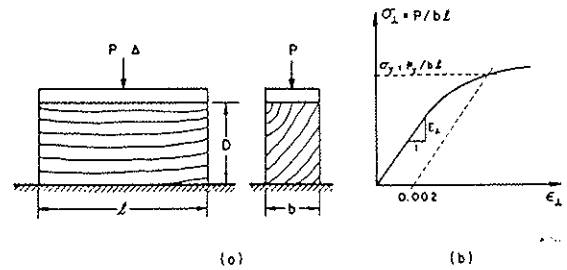


FIG. 5. Basic compression test.

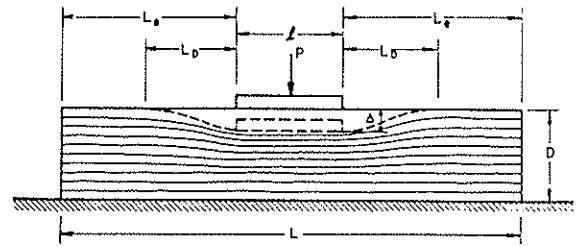


FIG. 6. Central beam test.

the plate is stiff enough then all portions of the wood have the same stress ($\sigma_{\perp} = P/bl$) and strain ($\epsilon_{\perp} = \Delta/D$) perpendicular to grain. It is assumed here that D/b is small enough that lateral buckling will not occur. The stress-strain plot for this block (Fig. 5b) shows a linear portion at the start that defines E_{\perp} and a gradual yielding to indicate a ductile, not brittle, behavior. The yield stress σ_y is defined on this plot as the stress at a 0.2% offset strain. Test results on this block, which establish the basic material properties E_{\perp} and σ_y needed for design, are presented later in this paper.

The question of the behavior of more complex geometries was investigated by Hall (1980). The central beam test of Fig. 6 shows one of these geometries; a beam of length L is loaded through a rigid plate of length l and width b . It is assumed that the beam rests on a rigid base. In this case stress and strain vary continuously over the beam with a large stress riser at the end of the plate where it bites into the wood.

Finite element analyses in the elastic range for various values of l/L and l/D showed the following.

(1) For long beams there was a definite length L_D from the edge of the plate beyond which stress and strain were essentially zero.

(2) The length L_D , called the decay length, was approximately $1.5D$.

(3) As L decreased from $l + 2L_D$ to l there was a gradual transition to the basic compression test of Fig. 5.

(4) The stress was fairly uniform across the central portion of the plate but approached infinity near the sharp corner, as shown in Fig. 7. A rounded corner

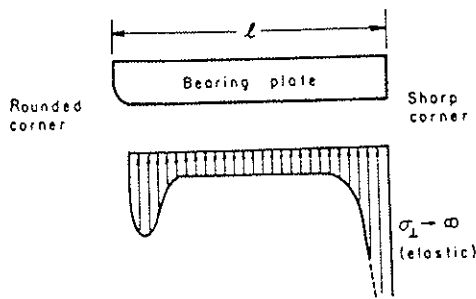


FIG. 7. Distribution of σ_{\perp} under plate.

would remove this singularity but still leave a large stress near the edge.

An inspection of Fig. 6 shows that the top deformed fibres of the beam have relatively large double curvature and, therefore, carry moment and shear. It is this action that spreads the load laterally. Such a system can be modelled as a beam on elastic foundations where the foundation modulus is $k = E_{\perp} b/D$ and the EI of the beam is $E_{\perp} bd^3/12$. A beam depth $d = 0.17D$ was found to duplicate finite element results to within 5%. The decay length (Hetenyi 1946) for the beam of Fig. 8 is given by.

$$[1] \quad L_D \cong 3(4EI/k)^{1/4} = 0.6D(E_{11}/E_{\perp})^{1/4}$$

It is shown later in this paper that E_{11}/E_{\perp} is approximately 50; the decay length therefore becomes $1.6D$ which confirms observations from the finite element calculations. Since the shaded area under the deflected shape of Fig. 8 is $\Delta L_D/3$, the end shear of the beam will be $k\Delta L_D/3$ or, by substitution, $0.53\sigma_{\perp}bD$. Vertical equilibrium of the plate then gives.

$$[2] \quad \sigma_{\perp} = \frac{P}{b(l + 1.06D)}$$

if the end distance L_e is greater than $1.6D$.

If the end distance is less than $1.6D$, then curve-fitting to the finite element results gives.

$$[3] \quad \sigma_{\perp} = \frac{P}{b(l + 0.84\sqrt{DL_e})}$$

With σ_{\perp} known from [2] or [3] the deflection of the plate becomes

$$[4] \quad \Delta = \frac{\sigma_{\perp} D}{E_{\perp}}$$

Equations [2] and [3] show that the load is spread over a length greater than l . The concentrated end shears V of the elastic foundation model correspond to the stress risers at the ends of the plate in the continuous model. Since these local stress risers cause yielding of the wood at loads well below the proportional limit, it is suggested that they be ignored in design and that σ_{\perp}

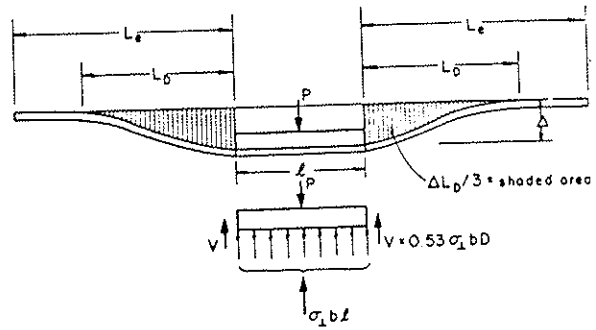


FIG. 8. Beam on elastic foundation.

be calculated from [2] or [3]. Such a procedure is acceptable with a ductile material such as wood loaded perpendicular to the grain.

The ASTM specimen has $l/D = 1$, $L/D = 3$, and $L_e = D$. Equation [3] will show $\sigma_{\perp} = 0.54 P/(bl)$ to give $\Delta = 0.54 PD/(bIE_{\perp})$. If this factor 0.54 is not taken into account when calculating E_{\perp} from the ASTM test, the value will be too large by a factor of 1.85. Instead of $E_{\perp} = E_{11}/20$ a more reasonable value should be $E_{11}/37$. Tests presented later herein show that $E_{\perp} \cong E_{11}/50$, a long way from $E_{11}/20$.

The beam on an elastic foundation will have its maximum bending stress at the edge of the plate. Since integration shows that the center of gravity of the shaded area of Fig. 8 is $L_D/6$ from the edge of the plate, the maximum moment M becomes

$$[5] \quad M = (0.53\sigma_{\perp} bD) \frac{L_D}{6} = 0.14\sigma_{\perp} bD^2$$

and the maximum bending stress becomes

$$[6] \quad \sigma_{11} = 6M/bd^2 = 30\sigma_{\perp}$$

Now, a plate designed by CSA 086 for a $\sigma_{\perp} = P/bl$ of 3.1 MPa would have a real σ_{\perp} , according to the theory presented here, of approximately 2.1 MPa and a flexural stress of 30×2.1 or 63 MPa at the edge of the plate. It was not possible to check this large stress by finite element analysis due to the stress riser at the edge of the plate and it is undoubtedly pushing the elastic foundation model too far to predict such a stress with accuracy. It does, however, show that a large compressive stress parallel to the grain exists at the edge of the plate, and this may be the reason why CSA 086 does not allow any increase in bearing stress in regions of high bending stress. The authors would like to point out, however, that most tests for establishing an allowable bending stress are carried out with point loads on the compressive edge of the beam. Although these point loads induce a large additional stress σ_{11} at the end of the bearing plates, this effect is automatically considered when establishing allowable bending stresses. In

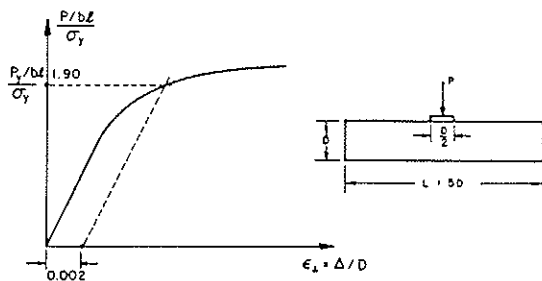


FIG. 9. Inelastic analysis ($l/D = 0.5$; $L/D = 5.0$; $L_c/D = 2.25$).

addition, most test beams fail in the tension region that is not loaded by bearing plates. In summary, then, it is suggested that increases in σ_{\perp} be allowed in regions of high bending compressive, but not tensile, stress.

The elastic model just presented duplicates numerical and test results and gives a good insight into the behavior of the system. It was extended (Hall 1980) to other geometries but the results will not be given here because the authors feel that the practical solution lies with an inelastic analysis, especially when limit states design is used.

Inelastic analyses were obtained by altering the finite element program to follow the σ_{\perp} versus ϵ_{\perp} curve of Fig. 5b in piecewise linear steps for each element. The σ_{11} versus ϵ_{11} curve was assumed to be elastic-perfectly plastic with $E_{11} = 12\,400$ MPa and yielding at 55 MPa. The shear stress-strain curve was also elasto-perfectly plastic with $G = 690$ MPa and yielding at 9.7 MPa. Figure 9 shows the results of such an analysis for $l/D = 0.5$ and $L/D = 5.0$. The ordinate of Fig. 9 is the average applied stress, $P/(bf)$, under the plate divided by σ_y , the yield stress of the material, and the abscissa is the average strain Δ/D . The yield load P_y is defined as the load required to cause an offset strain of 0.2%, as for the basic compression test. It is important to note that the system begins to yield at an apparent yield stress $P_y/(bf)$ of $1.9\sigma_y$ for this geometry because some of the load is spread laterally by beam action of the top fibres.

The slope of the straight portion of Fig. 9 will be more than E_{\perp}/σ_y , again because of lateral load transfer. Deflections in this linear region will be given by [4] with σ_{\perp} from [2] or [3]. The deflection Δ_y at yield will be the elastic deflection evaluated at P_y plus $0.002D$ or:

$$[7] \quad \Delta_y = \sigma_{\perp} D / E_{\perp} + 0.002D$$

where

$$[8] \quad \sigma_{\perp} = \frac{P_y}{b(l + 1.06D)}; \quad L_c > 1.6D$$

$$[9] \quad \sigma_{\perp} = \frac{P_y}{b(l + 0.84\sqrt{DL_c})}; \quad L_c < 1.6D$$

Figure 10 shows the results of numerous inelastic

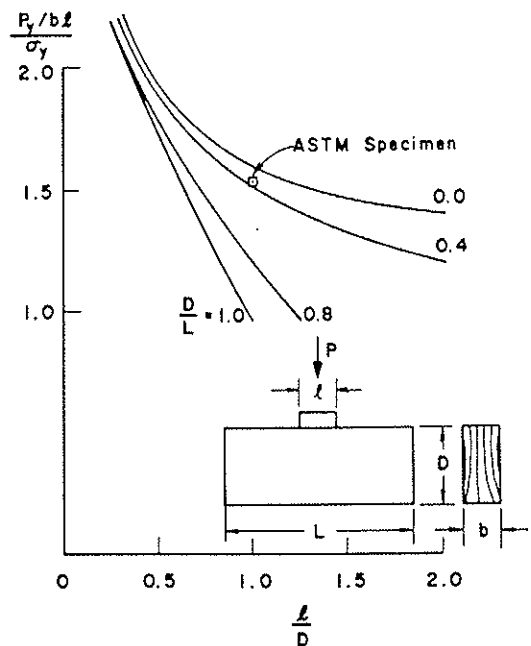


FIG. 10. Inelastic results.

finite element runs for various values of l/D and D/L . Yielding occurs in all cases at a mean stress under the plate that is greater than (or equal to) the yield stress of the material. The increases shown in Fig. 10 are based upon a rational approach and should replace the limited increase allowed in the present Code (CSA 086) for compression perpendicular to the grain.

The ASTM test block ($l/D = 1$, $D/L = 1/3$) is plotted in Fig. 10 to show that yielding occurs at $1.55\sigma_y$. In other words, if the ASTM test gives an apparent yield stress, $P_y/(bf)$, of 3.1 MPa the real yield stress for the material will be only $3.1/1.55 = 2.0$ MPa. Tests (Hall 1980) covering the inelastic range confirm the curves of Fig. 10.

The curves shown in Fig. 10 could be used for limit states design but they need to be converted to simple formulas by curve-fitting. The elastic foundation model provides an insight into the behavior at yield, if it is assumed that a hinge develops in the beam of depth d at the edge of the plate at $P = P_y$. The high bending stresses found at these points using an elastic analysis confirm this assumption. With a hinge the shaded area of Fig. 8 is halved, to $\Delta L_D/6$, showing that less load is transferred from under the plate. Vertical equilibrium of the plate then gives:

$$[10] \quad \sigma_y = \frac{P_y}{b(l + 0.53D)}; \quad L_c > 1.6D$$

or

$$[11] \quad \sigma_y = \frac{P_y}{b(l + 0.42\sqrt{DL_c})}; \quad L_c < 1.6D$$

Although these expressions fit the numerical results

fairly well, and indicate the behavior at yield, actual curve fitting of the symmetrical case and of geometries with unequal end distances gives the simple overall rules presented in the next section.

Proposed limit states design method

If the bearing plate covers the full length of the member then the plate length l is given by

$$[12] \quad l = P_y / \sigma_y b$$

If the plate does not cover the full length so that there are end distances L_1 and L_2 , the length l may be reduced by $L_1/4$ (but not more than $D/4$) plus $L_2/4$ (but not more than $D/4$). This reduced length, l_r , shall not be less than $l/3$.

The deflection Δ_y of the plate with respect to the other side of the member at factored loads will be,

$$[13] \quad \Delta_y = \frac{P_y D}{E_{\perp} b (l_r + l_c)} + 0.002D$$

where $l_c = L_1/2$ (but not more than $D/2$) plus $L_2/2$ (but not more than $D/2$).

The deflection at service load P will be,

$$[14] \quad \Delta = \frac{PD}{E_{\perp} b (l_r + l_c)}$$

In the above $P_y =$ factored load, $P =$ unfactored load, $\sigma_y =$ yield stress at 0.2% offset strain from a test with 100% of the area loaded, and $E_{\perp} =$ modulus from a test with 100% of the area loaded.

The restriction that l_r not be less than $l/3$ not only eliminates negative plate lengths but also limits the apparent stress to $3\sigma_y$. Although CSA 086 limits a stress increase to 1.4, this is on top of a stress based on the ASTM specimen. Since this specimen shows a stress increase of 1.55 to start with, the total is 1.55×1.4 or 2.17. This increase was arbitrarily changed to 3.0 because the proposal herein is more rational.

Research on material properties

It was beyond the scope of the previously mentioned thesis (Hall 1980) to obtain values of σ_y and E_{\perp} for design purposes, but without these the method cannot, of course, be implemented. Estimates of σ_y could be obtained by back-figuring the deflection curves from the ASTM test data but it was thought more appropriate to collect new data using a specimen of a greater height to improve the accuracy in the deformation measurements.

A testing program was therefore undertaken to establish values for three groups of wood, Douglas fir-larch, hemlock-fir, and spruce-pine-fir. Two hundred specimens from each species group were tested. Half of these were tested in the dry condition, the other half in the wet condition. The specimens were from

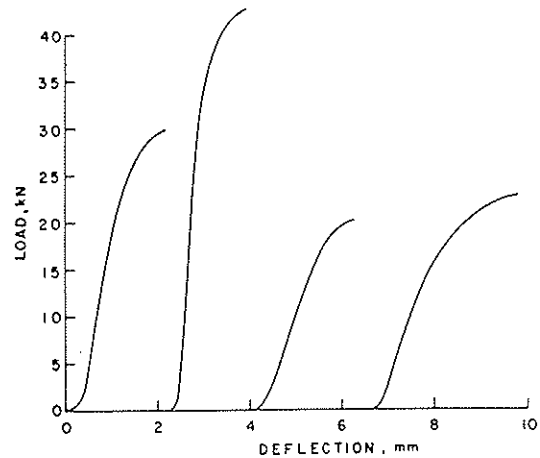


FIG. 11. Typical load-deflection curves (spruce-pine-fir).

commercially graded boards but were, in general, free from defects. The size was $38 \times 90 \times 145$ mm. A rigid plate 38×145 mm covered 100% of the loaded area. The rate of loading was 4 mm/min. A load-deformation curve was obtained for each specimen.

The specimens were weighed and moisture meter readings and dimensions were recorded for each. The grain orientation was noted as well as the presence of any visual defects. The material to be tested in the wet condition was placed in a moisture room to absorb moisture and weighed just before testing; the moisture content was determined by the change in weight.

The spread in the data was found to be large. To find out if this was caused by the fact that two or more species were contained in the species groups, species identification was carried out. The hemlock-fir group was split into hemlock and Amabilis fir by microscopic observation; a chemical method was used for the spruce-pine-fir group to identify the individual species.

Test results

The data collected resulted in a large data bank which was analyzed, grouped both by commercial species as well as by individual species. In addition the information was broken down into wet and dry material properties. Several graphs were prepared for each subgroup but they are too numerous to be included in this paper and are possibly only of interest to a few readers. All graphs are assembled in a separate volume and available from the authors upon request. The Appendix gives a list of the contents.

(a) Load-deformation curves

As mentioned, a load-deformation curve was obtained from each specimen. The load at 17 preselected deformations was read from the curves (Fig. 11) and the stresses at different strains were calculated. From this,

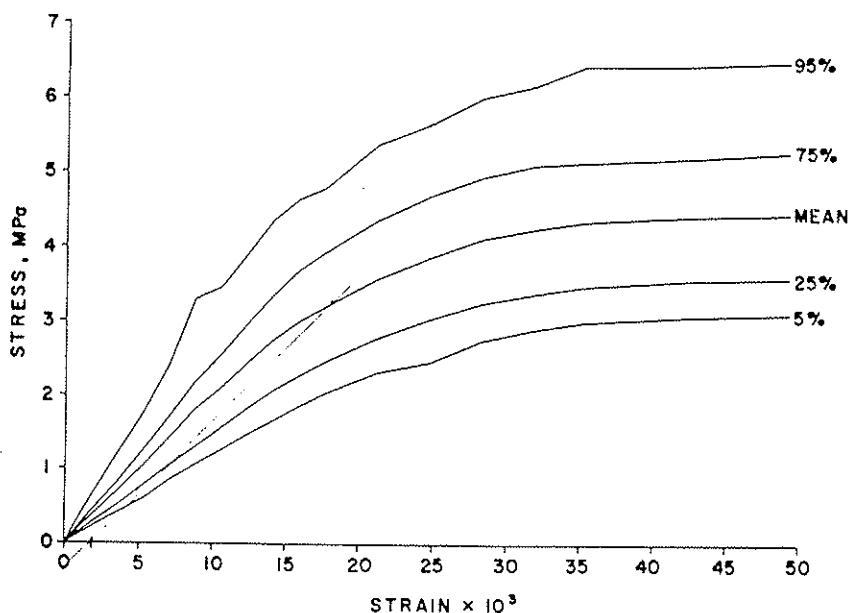


FIG. 12. Stress versus strain (composite of spruce-pine-fir specimens).

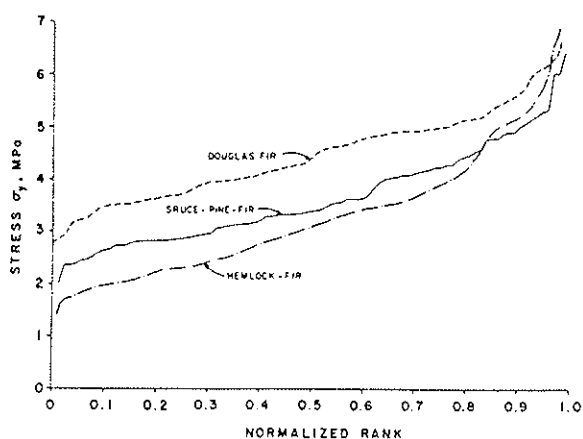


FIG. 13. Strength distribution of species groups - dry.

a composite stress-strain curve was constructed, as shown in Fig. 12, that depicts the spruce-pine-fir species group. The mean value is shown, together with lines for other percentiles, which gives an impression of the spread in the data (the lines do not represent the stress-strain curve for the individual specimens but represent the behaviour of the species group).

(b) *Strength and stiffness*

The stress σ_y at the 0.2% offset strain was determined from the individual stress-strain curves; Fig. 13 shows the distributions in the form of stress vs. normalized rank for the commercial species groups in the dry condition and the results for the wet condition are shown in Fig. 14.

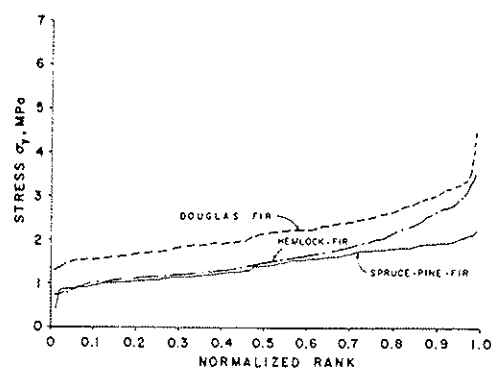


FIG. 14. Strength distribution of species groups - wet.

The mean values and the standard deviations are given in Table 2 for the many subgroups, together with the estimate of the 5th percentile value. Table 2a shows values for the dry condition, Table 2b for the wet condition.

The modulus of elasticity is treated in the same way and the results are shown in Table 2; Fig. 15 shows them in graphical form.

(c) *Density*

Scattergrams were prepared of stress vs. density and Fig. 16 shows the results for the spruce-pine-fir group.

(d) *Others*

As mentioned, the presence and kind of knots was recorded. The average value for the stress σ_y and the average modulus of elasticity is shown in Table 3 for

TABLE 2. Test results
(a) Dry

	N*	0.2% offset strength σ_y			Elasticity		Density (g/cm ³)	5 percentile		$\frac{\bar{\sigma}}{\bar{\sigma}_{D-F}}$	$\frac{E}{E_{D-F}}$
		$\bar{\sigma}$	s†	5 percentile	E	s†		$\bar{\sigma}$	$\bar{\sigma}_{D-F}$		
Douglas-fir	87	4.52	0.9	3.21	283	109	0.46	0.71	1.00	1.00	1.00
Hemlock-fir	110	3.32	1.31	1.74	204	135	0.43	0.52	0.73	0.73	0.72
Hemlock	54	3.83	1.31	1.88	252	160	0.46	0.49	0.85	0.85	0.89
Amabilis fir	56	2.86	1.11	1.64	159	82	0.40	0.57	0.63	0.63	0.56
Spruce-pine-fir	91	3.66	0.94	2.42	248	80	0.41	0.66	0.81	0.81	0.88
Spruce	49	3.17	0.67	2.27	220	76	0.38	0.72	0.70	0.70	0.78
Pine	42	4.22	0.90	2.87	280	72	0.44	0.68	0.93	0.93	0.99

(b) Wet

	N*	0.2% offset strength σ_y			Elasticity		Density (g/cm ³)	5 percentile		$\frac{E}{E_{D-F}}$	$\frac{\bar{\sigma}_{wet}}{\bar{\sigma}_{dry}}$
		$\bar{\sigma}$	s†	5 percentile	E	s†		$\bar{\sigma}$	$\bar{\sigma}_{D-F}$		
Douglas-fir	90	2.17	0.61	1.43	191	74	0.43	0.65	0.48	1.00	0.48
Hemlock-fir	95	1.62	0.73	0.75	103	67	0.41	0.46	0.49	0.54	0.49
Hemlock	57	1.81	0.64	0.93	116	64	0.44	0.51	0.47	0.61	0.47
Amabilis fir	38	1.33	0.78	0.68	85	66	0.37	0.59	0.47	0.45	0.47
Spruce-pine-fir	98	1.42	0.38	0.89	90	36	0.39	0.63	0.39	0.47	0.39
Spruce	61	1.28	0.35	0.77	81	36	0.38	0.60	0.40	0.42	0.40
Pine	36	1.65	0.31	0.99	105	31	0.42	0.60	0.39	0.55	0.39

*N = number of tests.
 †s = standard deviation.
 ‡D-F refers to Douglas fir.

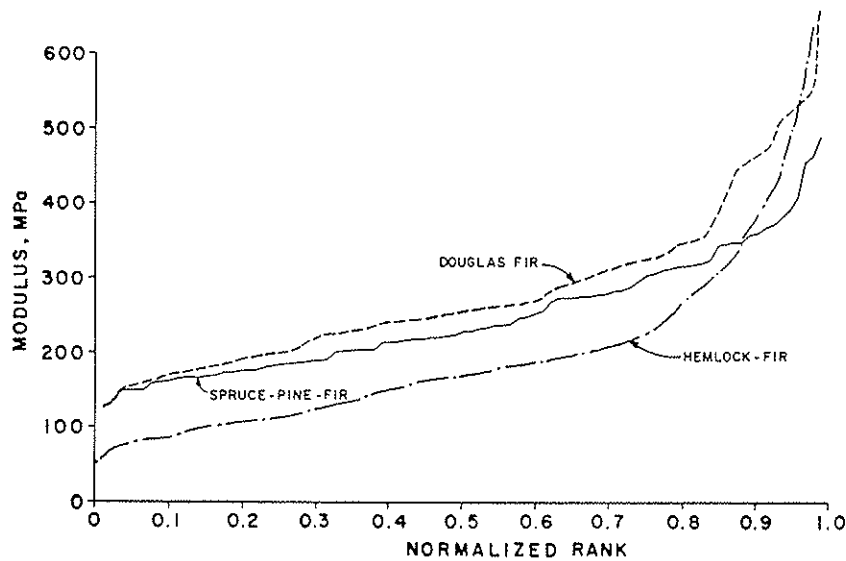


FIG. 15. Distribution of modulus of elasticity for species groups ($r = 0.83$).

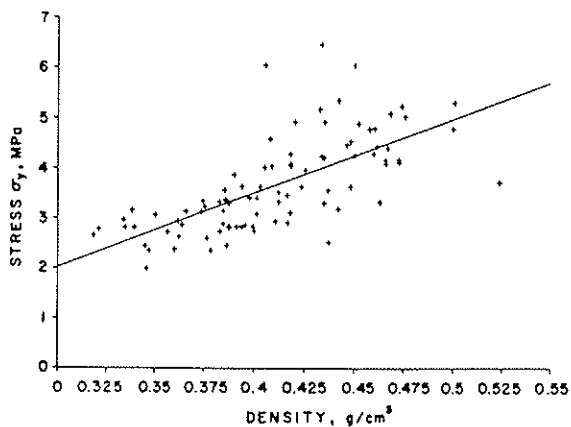


FIG. 16. Scattergram of σ_y versus density.

the three commercial species groups.

The ring orientation was classified into one of six groups as shown in Table 4 and Fig. 17 where average values of σ_y and the modulus of elasticity are presented.

Discussion of results

The differences between the load deflection curves were found to be very great indeed. This applies not only to all the species groups but also to the individual species. However, it is characteristic of all of them that they exhibit some ductility and that no definite breaking point exists.

Table 2a contains the information on dry material. Differences between the species groups are evident in all the properties listed. Douglas fir is the strongest species group followed by the spruce-pine-fir group

(SPF) with the hemlock-fir group being the weakest. Hemlock is substantially stronger than Amabilis fir and pine is stronger than spruce. The ratio of 5th percentiles to average strength also varies between the species groups. Correlation between density and strength does not seem to be very strong.

Table 2b shows statistics for wet material. Here it can be seen that compression perpendicular to the grain is a property very sensitive to moisture content. The wet strength is less than one half of the dry strength. It would also seem that the influence of moisture content depends on the species group, the SPF group being more sensitive to moisture than the other species groups. The observed loss in strength due to change in moisture content is much larger than that presently recognized by North American codes (0.67). The research presented here is unfortunately not sufficient to establish at what moisture content the change in strength takes place. More work in that area is desirable.

Table 3 shows that the inclusion of knots increases strength and Table 4 indicates that ring orientation does not affect strength or stiffness in a consistent manner.

Design criteria

The establishment of the design criteria for compression perpendicular to the grain does require some careful consideration. The serviceability limit state is not hard to visualize. It could be determined by deformations that would cause annoyance in line with the usual serviceability concept. However, the ultimate limit state is more difficult to define since loss of strength or collapse is not involved. The suggested

TABLE 3. Properties of woods of different knot classes*

	Dry			Wet		
	1	2	3	1	2	3
Douglas fir σ_y (MPa)	4.33	4.71	4.81	2.09	2.25	2.37
Mean E_{\perp} (MPa)	272	288	322	180	199	228
N^{\dagger}	46	35	6	52	31	7
Hemlock-fir σ_y (MPa)	3.20	3.59	4.39	1.56	1.99	1.46
Mean E_{\perp} (MPa)	191	233	301	98	137	87
N^{\dagger}	80	28	2	78	13	4
Spruce-pine-fir σ_y (MPa)	3.56	3.70	3.75	1.42	1.39	1.59
Mean E_{\perp}	241	246	275	87	88	119
N^{\dagger}	44	34	13	72	20	6

* Knot class: 1 = clear; 2 = wide face knot; 3 = spike knot.

 $^{\dagger}N$ = number of tests.

TABLE 4. Effect of ring orientation

	Dry*						Wet*					
	1	2	3	4	5	6	1	2	3	4	5	6
Douglas fir, mean σ_y (MPa)	5.4	4.7	4.3	4.5	5.0	5.1	2.7	2.4	2.0	2.0	2.9	2.3
N	3	9	46	17	8	4	2	13	30	27	7	11
Hemlock-fir, mean σ_y (MPa)	3.8	3.5	2.9	3.0	5.4	5.4	1.8	1.8	1.4	1.4	2.2	2.3
N	13	19	52	17	7	2	14	19	38	16	7	1
Spruce-pine-fir, mean σ_y (MPa)	3.3	3.8	3.5	4.4	4.9	4.0	1.4	1.3	1.3	1.4	2.0	1.7
N	33	23	15	3	1	16	12	30	21	15	1	19

	Dry*						Wet*					
	1	2	3	4	5	6	1	2	3	4	5	6
Douglas fir, mean E (MPa)	265	279	240	307	466	310	230	184	170	174	337	199
N	3	9	46	17	8	4	2	13	30	27	7	11
Hemlock-fir, mean E (MPa)	235	204	148	186	545	401	110	122	78	86	200	198
N	13	19	52	17	7	2	14	19	38	16	7	1
Spruce-pine-fir, mean E (MPa)	219	245	211	375	464	309	86	76	77	82	194	130
N	33	23	15	3	1	16	12	30	21	15	1	19

* The numbers 1-6 refer to ring type (see Fig. 17).

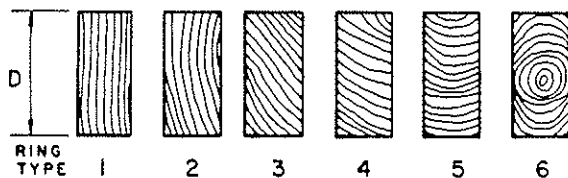


FIG. 17. Ring types.

0.2% offset value for a strength criterion represents an arbitrary point where the strains become larger for a given load increment, but it does not represent failure as such. In some way the strength criterion therefore becomes more akin to a serviceability limit state. Since the failure mode and the consequence of failure is different for compression perpendicular to the grain from,

for instance, bending, special consideration has to be given to this property. Should factored loads be used? Should the property be characterized by the mean value or should a near-minimum value be used? It is common to use unfactored loads in conjunction with average properties (E_{avg} for deflection), whereas for ultimate limit states a 5th percentile value is used in conjunction with factored loads.

Since the compression perpendicular to the grain is a hybrid case, the Committee on CSA 086 could consider use of the following options:

- 5th percentiles with factored loads;
- 5th percentiles with unfactored loads;
- average values with factored loads; or
- average values with unfactored loads.

TABLE 5. Material properties for design examples

	R (MPa)	$\sigma_y = \phi R$ (MPa)	E_t (MPa)	Lumber C_t (MPa)*	Glulam C_t (MPa)*
Douglas fir	4.52	3.4	283	3.17	3.17
Hemlock-fir	3.32	2.5	204	1.61	2.86
Spruce-pine-fir	3.66	2.75	248	1.67	2.86

* From Canadian Standards Association (1980).

Option (a) would be ultra-conservative and option (d) would be too liberal. Thus options (b) and (c) are the most realistic ones. The ratio of 5th percentile to mean value ranges from 0.52 to 0.72 for the dry condition. A load factor of 1.25 is used for dead loads and 1.5 is used for live loads. The practical range for dead loads on timber structures is 0.35–0.7 kN/m² whereas most live loads lie in the range of 1.8–4.8 kN/m² (1 kN/m² = 1 kPa). Thus the ratio of unfactored loads to factored loads lies in the range of 0.67–0.75.

The designer would have calculated the reactions or bearing forces using factored loads, so from his point of view it would probably be more convenient to provide stresses to be used with factored loads rather than with unfactored loads.

Option (b) is slightly more conservative than option (c) and the Code Committee would have to decide what policy is to be followed. For calculation of the example to follow, option (c) was chosen.

The selection of an appropriate value of the performance factor ϕ is also subject to some judgement in this case. As mentioned, the variability of both σ_y and E_t is large and for that reason ϕ should be low (0.7–0.8). However, it is not possible to perform a rigorous calibration to existing practice since the basis for previous designs neglected the important influence of geometry. To the knowledge of the authors, compression perpendicular to the grain has not caused structural failures in the sense of collapse, but it is known that serviceability failures, caused by neglect of bearing stresses during design, have occurred. The selection of a value for ϕ will thus have to be a Committee decision. For the purpose of the following design examples, a value of $\phi = 0.75$ was chosen.

It should be pointed out that information about the effect of the duration of load is not available. Experimental work may be difficult to conduct since rupture failure is not involved, but it would nevertheless be useful to have good information on creep.

Design examples

The proposed design method is illustrated by two examples, one of support at the end of a truss, the other of interior support of a glulam beam. It is assumed that dry service conditions prevail. The design is done for each of the three species groups and compared with the

present CSA 086 design method. The material properties used are given in Table 5.

The truss with a 20 m span and a 38 × 140 mm lumber bottom chord is loaded with a 0.3 kN/m dead and a 0.7 kN/m snow load. The end reaction is then given by

$$[15] \quad P_y = (1.25 \times 0.3 + 1.5 \times 0.7)10 = 14.5 \text{ kN}$$

$$[16] \quad P = (0.3 + 0.7)10 = 10.0 \text{ kN}$$

Table 6 shows calculations, bearing plate lengths, and deflections.

The 130 × 760 mm continuous glulam beam example considers an interior column with 24 kN dead and 96 kN snow loads to give

$$[17] \quad P_y = 1.25(24) + 1.5(96) = 174 \text{ kN}$$

$$[18] \quad P = 24 + 96 = 120 \text{ kN}$$

Table 7 shows calculations, bearing plate lengths, and deflections.

Discussion and conclusions

This paper deals specifically with the case of wood subject to compression perpendicular to the grain in conjunction with a rigid steel plate. A reasonable model to describe the behavior of such a system is for the longitudinal fibres next to the plate to act as a beam on an elastic foundation. This beam, with a depth approximately 17% of the full depth of the member, serves to spread the load away from the plate if there is sufficient end distance. Thus, the deeper the main beam, the deeper the beam on the elastic foundation and the more load is spread away from the plate. From the above, it is concluded that:

(1) the present ASTM method of establishing properties perpendicular to the grain applies only to that specific geometry;

(2) basic properties should be established from test specimens with 100% of their area loaded;

(3) load carrying capacity is greatly influenced by geometry and this must be considered in any design system;

(4) present CSA 086 specifications that use numerical limits on lengths are not sound and should be replaced by dimensionless ratios; and

TABLE 6. Truss design example

	Douglas fir	Hemlock-fir	Spruce-pine-fir
$l = P_y/b\sigma_s$	$\frac{14\ 250}{38(3.40)}$	$\frac{14\ 250}{38(2.50)}$	$\frac{14\ 250}{38(2.75)}$
l (mm)	110	150	136
Reduction = $D/4^*$ (mm)	35	35	35
$l_c = l - D/4$ (mm)	75	115	101
$l(CSA) = P/bC_s$	$\frac{10\ 000}{38(3.17)}$	$\frac{10\ 000}{38(1.61)}$	$\frac{10\ 000}{38(1.67)}$
$l(CSA)$ (mm)	83	163	158
$l_r + l_c^\dagger$ (mm)	145	185	171
$\Delta = \frac{PD}{E_s b(l_r + l_c)}$	$\frac{10\ 000(140)}{283(38)145}$	$\frac{10\ 000(140)}{204(38)185}$	$\frac{10\ 000(140)}{284(38)171}$
Δ (service) (mm)	0.90	0.98	0.87

* $L_1 > D$, $L_2 = 0$.† $l_c = D/2$.

TABLE 7. Glulam beam example

	Douglas fir	Hemlock-fir	Spruce-pine-fir
$l = P_y/b\sigma_s$	$\frac{174\ 000}{130(3.4)}$	$\frac{174\ 000}{130(2.5)}$	$\frac{174\ 000}{130(2.75)}$
l (mm)	394	535	487
Reduction = $D/4 + D/4$ (mm)	380	380	380
l_c^* (mm)	131	178	162
$l(CSA) = P/bC_s$	$\frac{120\ 000}{130(3.17)}$	$\frac{120\ 000}{130(2.86)}$	$\frac{120\ 000}{130(2.86)}$
$l(CSA)$ (mm)	291	323	323
$l_r + l_c$ (mm)	891	938	922
$\Delta = \frac{PD}{E_s b(l_r + l_c)}$	$\frac{120\ 000(760)}{283(130)891}$	$\frac{120\ 000(760)}{204(130)938}$	$\frac{120\ 000(760)}{248(130)922}$
Δ (service) (mm)	2.8	3.7	3.1

* $l_c > l/3$ governs.

(5) numerous test results presented here can form the basis for choosing more realistic material properties.

Acknowledgements

The theoretical work contained in this paper was financed by the Canadian Forestry Service and the material tests were conducted using a grant from the Natural Sciences and Engineering Research Council. The authors wish to express their appreciation for this financial support.

- AMERICAN SOCIETY FOR TESTING AND MATERIALS. 1976. Annual book of ASTM Standards. Part 22, D 143-52. Easton, MD.
- CANADIAN STANDARDS ASSOCIATION. 1980. Code for engineering design in wood. National Standard of Canada CAN3-086-M80, Rexdale, Ont.
- HALL, C. P. 1980. Behaviour of compression perpendicular to grain loading in wood. M.A.Sc. thesis, University of British Columbia, Vancouver, B.C.
- HETENYI, M. 1946. Beams on elastic foundations. University of Michigan Press, Ann Arbor, MI.

Appendix — Contents of back-up information on test data

Dry material diagrams

- Composite stress-strain relationship
- 0.2% offset stress vs. rank
- Modulus of elasticity vs. rank
- Scattergram of 0.2% offset stress vs. density
- Density vs. rank

For: Douglas fir, hemlock-fir, hemlock, Amabilis fir, spruce-pine-fir, spruce, pine.

Wet material diagrams

- Composite stress-strain relationship
- 0.2% offset stress vs. rank
- Modulus of elasticity vs. rank
- Scattergram of 0.2% offset stress vs. density
- Density vs. rank
- 0.2% offset stress vs. moisture content
- Modulus of elasticity vs. moisture content

For: Douglas fir, hemlock-fir, Amabilis fir, spruce-pine-fir, spruce, and pine.

INTERNATIONAL COUNCIL FOR BUILDING RESEARCH STUDIES AND DOCUMENTATION

WORKING COMMISSION W18A - TIMBER STRUCTURES

**PROPOSAL FOR INCLUDING SIZE EFFECTS IN
CIB W18A TIMBER DESIGN CODE**

by

B Madsen
Department of Civil Engineering
University of British Columbia
Vancouver, B.C.
Canada

MEETING TWENTY - TWO

BERLIN

GERMAN DEMOCRATIC REPUBLIC

SEPTEMBER 1989

PREFACE

The main purpose of this paper is to make specific recommendations for the inclusion of size effects as they apply to the primary strength properties for commercial timber (Tension, Bending and Compression) into the CIB W18 Timber Design Code. A secondary purpose is to comment on the proposal and provide references where additional information on this topic can be found.

BENDING

1. The characteristic bending strength has to be converted to reflect a specific size (depth, breadth and length) and a specified load configuration.

Suggestion:

That the bending strength to be quoted be that of a 38x184 mm cross section and that the length be for a 3.00 m long pieces subjected to two concentrated loads applied in the third points.

2. The general design requirement is that:

Factored Action < Factored Resistance

(In the following the terminology from the Canadian code has been used to present the general idea; it can easily be converted to the format adopted in the Eurocode or the CIB W18 code.)

In detail the design formula becomes:

$$(1.25 \text{ DL} + 1.5 \text{ LL})_{\text{MOMENT}} < \sigma R_o S \left(\frac{l}{l_o}\right)^{g_1} \left(\frac{d}{d_o}\right)^{g_2} \left(\frac{b}{b_o}\right)^{g_3} K_{LC} K_D K_T K_H K_L K_{Sb}$$

DL = Dead load

b = Breadth of Beam

LL = Live load

K_{LC} = Load configuration factor

σ = Resistance factor

K_D = Duration of Load factor

R_o = Characteristic strength

K_T = Treatment factor

S = Section Modulus

K_H = Systems factor

l = Length of Span

K_L = Lateral stability factor

d = Depth of Beam

K_{Sb} = Moisture content factor

o = subscripts indicate the chosen standard size for reporting the strength

This complicated design formula can be greatly simplified by dividing it into two steps. Step 1 is the establishment of a design stress applicable to the specific design at hand using the known information pertaining to the beam. Step 2 is the establishment of a suitable cross section fulfilling the design requirements. We get:

Step 1	Step 2
$< R_o \left(\frac{l}{l_o}\right)^{g_1} \left(\frac{b}{b_o}\right)^{g_3} K_{LC}$	$\sigma \frac{1}{6} b d^2 \left(\frac{d}{d_o}\right)^{g_2}$
$K_D K_T K_H K_L K_{Sb}$	
size effect adjustments	ordinary adjustments

The ratio $\frac{b_o}{b}$ can, based upon test, be set to unity and therefore neglected.

$\left(\frac{d_o}{d}\right)^{g_1}$ and K_{LC} can be combined into a single factor and a table produced which will cover most design cases. A suggested set of values for K_{LC} is shown in Table 1 where the size effect parameter g_1 has been chosen as 0.25.

The ordinary adjustment factors are the same as found in the usual tables.

We can now define and calculate R_D as:

$$R_D = R_o K_{LC} (K_D K_T K_H K_L K_{Sb})$$

The design equation can then be written as:

$$(1.25 \text{ DL} + 1.5 \text{ LL})_{\text{MOMENT}} < \sigma R_D \frac{1}{6} b d^2 \left(\frac{d_o}{d}\right)^{g_1}$$

with $d_o = 184 \text{ mm}$ and $g_1 = 0.25$ we find:

$$< \sigma R_D \underbrace{184^{0.25} \frac{1}{6} b d^{1.75}}_{S'}$$

By defining a modified section modulus as $S' = 0.6 bd^{1.75}$, it is possible to get back to the familiar design equation:

$$(1.25 \text{ DL} + 1.5 \text{ LL})_{\text{MOMENT}} < \sigma R_D S'$$

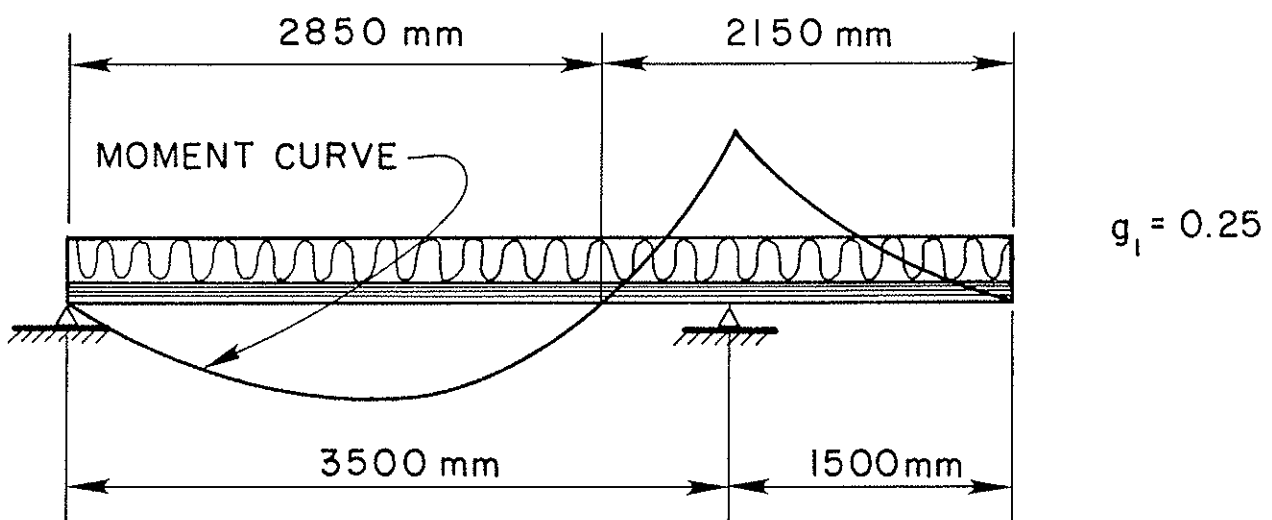
where

$$R_D = R_o K_{LC} (K_D K_T K_H K_L K_{Sb})$$

$$S' = 0.6 bd^{1.75}$$

Tables of S' can be produced and published together with the ordinary cross-sectional information.

The length to be used for conversion of the published strength should be the distance from zero moment to zero moment. This is illustrated in the following example:



The positive moment acts over a length of 2850 mm so the length effect is:

$$\left(\frac{3000}{2150}\right)^{0.25} = 1.01$$

The negative moment acts over a length of 2150 mm so the length effect is:

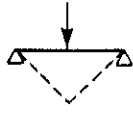
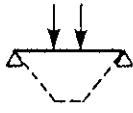
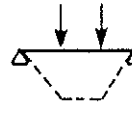

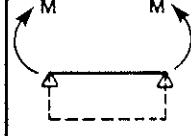
$$\left(\frac{3000}{2150}\right)^{0.25} = 1.09$$

However, the shape of the negative portion of the moment curve is not parabolic, as it is for the positive moment, but akin to the triangular moment curve caused by a single concentrated force, so the load configuration of 1.23 should be used. The factor K_{LC} then becomes

$$1.23 \times 1.09 = 1.34$$

which should be used for the negative moment.

TABLE 1: LENGTH AND LOAD CONFIGURATION FACTOR K_{LC}

LENGTH m	U. D. L.					M
						
1.0	1.62	1.37	1.32	1.24	1.08	
1.5	1.46	1.23	1.19	1.12	0.98	
2.0	1.36	1.15	1.11	1.04	0.91	
3.0	1.23	1.04	1.00	0.94	0.82	
4.0	1.14	0.97	0.93	0.87	0.76	
5.0	1.08	0.92	0.88	0.83	0.72	
6.0	1.03	0.87	0.84	0.79	0.69	
7.0	1.00	0.84	0.81	0.76	0.66	

$$g = 0.25$$

TENSION MEMBERS

1. The characteristic tension strength has to be converted to a specific size and a defined load configuration.

Suggestion:

The standard becomes a 38x184 mm cross section and a 3000 mm length with a constant tension force along the length.

2. Both a length effect and a depth effect exist in tension but those can be combined into a single factor, K_{LT} , as shown in Table 2.
3. The designer can avoid the use of the table by using the basic formula for K_{LT}

$$K_{LT} = \left(\frac{3000}{l}\right)^{0.3} \times \left(\frac{184}{d}\right)^{0.2}$$

4. In case the tension force varies along the length of the member, a load configuration factor can be applied.

TABLE 2
ADJUSTMENT FACTORS K_{LT} FOR LENGTH AND WIDTH

LENGTH m	38x89	38x140	38x184	38x235	38x286
1.0	1.61	1.47	1.39	1.32	1.28
1.5	1.43	1.30	1.23	1.17	1.13
2.0	1.31	1.20	1.13	1.07	1.04
2.5	1.23	1.12	1.06	1.01	0.98
3.0	1.16	1.06	1.000	0.95	0.92
4.0	1.07	0.98	0.92	0.87	0.85
5.0	1.00	0.91	0.86	0.82	0.79
6.0	0.94	0.86	0.81	0.77	0.75
8.0	0.87	0.80	0.75	0.71	0.69
10.0	0.81	0.74	0.70	0.67	0.64
15.0	0.72	0.66	0.62	0.59	0.57
30.0	0.58	0.53	0.50	0.48	0.46

$g = 0.3$

$g = 0.2$

$$K_{LT} = \left(\frac{3000}{\text{SPAN}}\right)^{0.30} \times \left(\frac{184}{\text{DEPTH}}\right)^{0.20}$$

COMPRESSION MEMBERS

Both a length effect and a depth effect exist in compression (restrained in both in weak and strong direction) but this size effect can best be introduced in conjunction with a change to a rational column formula that fully recognizes that columns often are subject to combined stresses.

SOME QUESTIONS AND ANSWERS ABOUT SIZE EFFECTSa) Why are there size effects in Timber?

Size effects exist in any material where the strength varies throughout the volume of the structural members and where failure in the cross section causes failure of the member.

In wood (in the sense of clear "defect-free" wood) imperfections exist on the microscopic level (weaknesses in the connections between fibres).

In timber (commercial timber) additional defects exist on the macroscopic level (knots, splits, etc.). The number of defects generally decrease with increasing quality [20].

Because of the variation in strength throughout the structural member, failure stress becomes associated with the probability of a weak spot ending up in a high stressed zone (tension zone).

Because the distribution of the defects might be different along the length, depth and breadth of the member, it is necessary to talk about length effect, depth effect and breadth effect. In addition to this, we must also recognize the load configuration effect caused by the fact that the external forces on the member may stress a greater or smaller portion of the member [14].

Numbers in square brackets refer to the test of references. Copies of references can be obtained from the author upon request.

b) How are size effects quantified?

The size effects can be described by the weakest link theory which, loosely put, says that the logarithm of strength is linearly related to the logarithm of length (or depth, or breadth). It is suggested that the slope of this log-log relationship is to be used as a measure of the size effect and that it be signified by g . Using g as the measure, the size effect is increasing with increasing values of g and the two are almost linear in relationship [18].

A series of convenient formulae have been collected in Appendix A and a description of their derivation is found in Reference [14].

The effect of the size effect can also be expressed with a size effect factor, K_{LC} , and it is proposed to be used K_{LC} in the code presentation [18].

c) How accurate should g be determined?

In the practical range for lumber the factor K_{LC} is not very sensitive to value of g . Therefore it will suffice to determine and report g as 0.05, 0.10, ..., 0.45, 0.50 [19].

d) Is g different for the different strength properties?

Unfortunately, yes! The value of g does vary between tension, compression, and bending. It is necessary to establish the value for g for each of the three properties separately.

The table below gives values for the length effect and depth effect for the Spruce, Pine, Fir species group. The values for the length effect is well established while the depth effect must be considered tentative because the test were not extensive for that

effect. A comprehensive testing programme dealing specifically with width effect is presently being conducted [18].

SPECIES GROUP S-P-F	$g_{0.05}$		STRENGTH REMAINING	
	LENGTH	DEPTH	LENGTH	DEPTH
Tension	0.22	0.05	0.85	0.96
Compression	0.10	(0.35)	0.93	(0.80)
Bending	0.20	0.23	0.87	0.84

e) Is g constant throughout the strength distribution?

No, it has been observed that $g_{0.05}$ and for instance $g_{0.50}$ can be quite different but for structural purposes we are mostly interested in $g_{0.05}$.

This difference is in part caused by different failure modes in the weaker portion of the distribution than those predominating in the strong portion of the strength distribution [19,20].

f) Must the strength testing be done using the standard size selected?

Not necessarily. It is quite acceptable to use the test method presently used as long as information is available so the test data can be converted to the standard size chosen for reporting the strength.

The size selected has been chosen because it lies roughly in the "middle" of the range of sizes and lengths being used in practice. This was done in order to minimize the necessary adjustments. The loading with the loads in the third points was chosen because the conditions are very close to a uniformly distributed load which will then not need an adjustment.

It is important that the test specimen is placed in testing machine in the same manner as the material will be used in the final application. Preselecting the worst defect will bias the test results relative to those for a random placemat which is what normally happens in practice.

LIST OF REFERENCES PERTAINING TO

SIZE EFFECTS IN LUMBER

- [1] Barrett, J.D., 1974. Effect of Size on Tension Perpendicular-to-Grain Strength of Douglas-Fir. Wood and Fiber Science 6(2): 126-143
- [2] Bechtel, S.C. and Norris, C.B., 1952. Strength of Wood Beams and Rectangular Cross Section as Affected by Span-depth Ratio. USDA Forest Service. Forest Products Laboratory Report M. R1910 42 p.
- [3] Bohannon, B., 1966. Effect of Size on Bending Strength of Wood Members. U.S. F.P.L. Research Paper FPL 56. Madison, Wisconsin 31 p.
- [4] Buchanan, A.H., 1983. Effect of Member Size on Bending and Tension Strength of Wood. Presented at IUFRO Wood Eng. meeting Madison, Wisconsin 31 p.
- [5] Camben, A.J., 1957. The Effect of Depth on the Strength Properties of Timber Beams with an Analysis of the Stresses and Strains Developed. Forest Products Research Special Report. No. 12, DSIR London
- [6] Dietz, A.G.H., 1942. Stress-strain Relations in Timber Beams. Bulletin American Society Testing Materials No. 118 p.19.
- [7] Leicester, R.H., 1973. Effect of Size on the Strength of Structures. CSIRO Australian Forest Products Laboratory, Division of Building Research Technology, Paper No. 71 p.1.
- [8] Leicester, R.H., 1985. Configuration Factors for the Bending Strength of Timber. Technical Paper, CIB Conference, Beit Oren, Israel.
- [9] Liu, J.Y., 1980. Shear Strength of Wood Beams : A Weibull Analysis. ASCE Journal of the Structural Division 106 (ST10) pp 2035-2052.
- [10] Liu, J.Y., 1981. A Weibull Analysis of Wood Member-bending Strength in: F.T.C. Loo (ed) Failure Prevention and Reliability. Society of Mechanical Engineers pp 57-64.
- [11] Madsen, B. and Nielsen, P.C., 1976. In-grade Testing: Size Investigations on Lumber Subjected to Bending, Structural Research Series No. 15. Dept. of Civil Engineering, University of British Columbia, Vancouver.
- [12] Madsen, B., 1978. Size Effects in Lumber for Bending. Proceedings First International Conference on Wood Fracture. WFPL Forintek Canada Corp., Vancouver. p. 101
- [13] Madsen, B. and Stinson, T., 1982. In-Grade Testing of Timber Four or More Inches in Thickness (1982). 34 pages.
- [14] Madsen, B. and Buchanan, A.H., 1985. Size Effects in Timber Explained by a Modified Weakest Link Theory. Technical Paper, CIB Conference, Beit Oren, Israel.
- [15] Madsen, Borg, 1985. Design of Single Members with Special Reference to Length Effects. Proceedings of Symposium of Forest Products Research International Achievements and the Future, Pretoria April 22-26, 1985.

- [16] Madsen, Borg, 1987. Characteristic Strength and Length Effects for Lumber. Submitted to Canadian Standards Association Committee 086 in charge of: "Engineering Design in Wood", May 1987, 71 pages.
- [17] Madsen, Borg, 1988. Length Effects in Timber. 1988 International Conference on Timber Engineering, Seattle, Wash. August, 1988.
- [18] Madsen, Borg, 1989. Length Effects in Timber. Submitted for publication to the Canadian Journal of Civil Engineering, March, 1989.
- [19] Madsen, Borg, 1989. Size Effects in Defect-Free Wood. Submitted for publication to the Canadian Journal of Civil Engineering, March, 1989.
- [20] Madsen, Borg, 1989. Size Effects in Lumber. Are they important? Second Pacific Timber Engineering Conference, Auckland, New Zealand, August 28-31, 1989.
- [21] Madsen, Borg, 1989. Proposal for Including Size Effects in CIB-W18A Timber Design Code. 22nd Meeting, CIB Working Group W18A Timber Structures, East Berlin, G.D.R., September 25-28, 1989.
- [22] Moe, J., 1961. 'The Mechanisms of Failure of Wood in Bending'. Publication International Assn. for Bridge and Structural Engineering, Vol.12, p.163.
- [23] Newlin, J.A. and Trayer, G.W., 1941. Form Factors of Beams Subjected to Transverse Loading Only. USDA F.P.L. Report No. 1310.
- [24] Nwokoye, 1975. Strength Variability of Structural Timber. The Structural Engineer, 53(3) p. 139.
- [25] Orosz, I., 1976. Relationship between Apparent Modulus of Elasticity, Gage Length and Tensile Strength of Lumber. Wood Science and Technology, 10, p.275-291.
- [26] Riberholt, H. and Madsen, H.P., 1979. Strength Distribution of Timber Structures - Measured Variation of the Cross Sectional Strength of Structural Lumber. Structural Research Laboratory, Technical University of Denmark, Rapport No. R114.
- [27] Showalter, K.L., 1985. Effect of Length on Tensile Strength Parallel-to-Grain in Structural Lumber. Thesis submitted in partial requirement for MSc Virginia Polytechnic, Blacksburg, VA.
- [28] Sumiya and Sugihara, 1957. Size Effects in the Tensile and Bending Strength of Wood. Mokuzai Gakkaishi,, 3(5) p.168.
- [29] Williamsen, J.A., 1982. Bending Strength of Pinus Radiata, M.E. Thesis Dept. of Civil Engineering, University of Auckland, New Zealand.

APPENDIX A

Length Effect:
$$\frac{X_1}{X_2} = \left(\frac{L_2}{L_1}\right) g_1$$

Depth Effect:
$$\frac{X_1}{X_2} = \left(\frac{d_2}{d_1}\right) g_1$$

Stress Distribution Effect:
$$f_m = \left(\frac{1+1/g_3}{C}\right) g_3 f_t$$

Or for $C = 0.5$:
$$f_m = 2 (1 + 1/g_3)^{g_3} f_t$$

Breadth Effect:
$$\frac{X_1}{X_2} = \left(\frac{b_2}{b_1}\right) g_4$$

Load Configuration:
$$L_e = \frac{g_1 + a/L}{g_1 + 1} L$$

INTERNATIONAL COUNCIL FOR BUILDING RESEARCH STUDIES AND DOCUMENTATION

WORKING COMMISSION W18A - TIMBER STRUCTURES

**CIB STRUCTURAL TIMBER DESIGN CODE
PROPOSED CHANGES OF SECTION ON THIN-FLANGED BEAMS**

by

J König
Swedish Institute for Wood Technology Research
Sweden

**MEETING TWENTY - TWO
BERLIN
GERMAN DEMOCRATIC REPUBLIC
SEPTEMBER 1989**

In the following is given a proposal of changes of the section on thin-flanged beams in CIB Structural Timber Design Code (CIB Report, Publication 66, 1983). The background material is given in CIB-paper "Thin-walled wood-based flanges in composite beams" by J. König (Berlin 1989).

7.1.2 Thin-flanged beams (stiffened plates)

Assuming a linear variation of strain over depth the stresses shall satisfy the conditions given in section 5.1.

The influence of non-uniform distribution of stresses over the flange width due to shear lag and buckling and the influence of flange curling shall be taken into consideration.

If $b_w < 8h_f$, the shear stresses may be assumed uniformly distributed over the width of the section 1-1 shown in fig. 7.1.2.

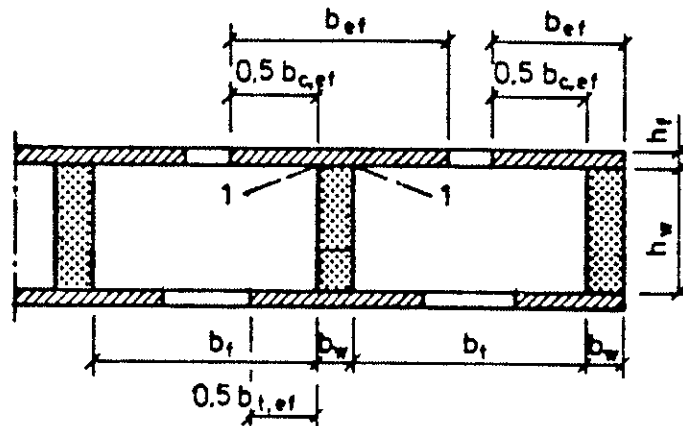


Figure 7.1.2_a. Thin-flanged beam

Unless otherwise proved the member should be considered as a number of I-beams (taking the load on a width of $b_f + b_w$) or U-beams (taking the load on a width of $0.5 b_f + b_w$) with an effective flange width, b_{ef} , see fig. 7.1.2 a, where

$$b_{ef} = b_{c,ef} + b_w \text{ (or } b_{t,ef} + b_w \text{)} \quad (7.1.2 \text{ a})$$

or

$$b_{ef} = 0.5 b_{c,ef} + b_w \text{ (or } 0.5 b_{t,ef} + b_w \text{)} \quad (7.1.2 \text{ b})$$

respectively.

The effective width $b_{c,ef}$ and $b_{t,ef}$ respectively due to the effect of shear lag is given in table 7.1.2. The effective width with respect to buckling is given by

$$b_{ef} = b \quad \text{for } \alpha \leq 0,67 \quad (7.1.2 c)$$

$$b_{ef} = b_f \sqrt{\frac{\sigma_{crit}}{\sigma_e}} (1 - 0,22 \sqrt{\frac{\sigma_{crit}}{\sigma_e}}) \quad \text{for } \alpha > 0,67 \quad (7.1.2 d)$$

where

$$\alpha = \sqrt{\sigma_e / \sigma_{crit}}$$

σ_e = axial stress at the web at the mid-plane of the flange under the assumption that the flange is homogenous.

σ_{crit} = critical stress.

σ_{crit} should be determined as

$$\sigma_{crit} = k_{crit,0} \frac{\pi^2 \sqrt{(EI)_x (EI)_y}}{ta^2}$$

where $k_{krit,0}$ is given in Figure 7.1.2 b.

$(EI)_x$ is the bending stiffness of the panel per unit width in bending about the X-axis. For a homogeneous orthotropic panel with the main directions x and y ,
 $(EI)_x = \frac{1}{12} Et^3 / (1 - \nu_{xy} \nu_{yx})$, where ν_{xy} and ν_{yx} are Poisson's ratios. For wood-based panels $\nu_{xy} \nu_{yx} \approx 0$ can be assumed.

$(EI)_y$ as $(EI)_x$, but in bending about the Y-axis.

$(GI)_{tor}$ is the torsional stiffness per unit width of the panel. For a homogeneous orthotropic panel, $(GI)_{tor} = Gt^3/3 + [\nu_{xy} (EI)_x + \nu_{yx} (EI)_y] \approx Gt^3/3$.

$$\beta_1 = \frac{\ell}{a} \sqrt[4]{(EI)_x / (EI)_y}. \quad \text{For an isotropic panel, } \beta_1 = \ell/a.$$

$$\beta_2 = 0.5 (GI)_{tor} / \sqrt{(EI)_x (EI)_y}. \quad \text{For an isotropic panel, } \beta_2 = 2G/E.$$

a, ℓ, t See Figure 7.1.2 b.

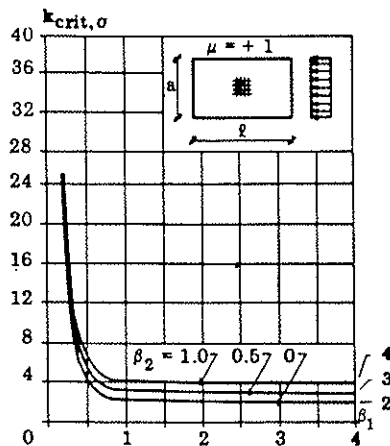


Figure 7.1.2_b.

The values of table 7.1.2 and Equations (7.1.2 c,d) may be used for calculations both in ultimate and serviceability limit state.

Table 7.1.2 Effective width with respect to shear lag

Flange	$b_{c,ef}$ or $b_{t,ef}$
Plywood with the fibre direction in extreme plies	
parallel to the web	0.1 l
perpendicular to the web	0.1 l
Particle fibre board with random fibre orientation	0.2 l

l is the span, however, for continuous beams l is the distance between the points with zero moment

The effect of flange curling must be considered when $u > 0,05 (h_w + h_f)$

where

u = maximum deflection of the flange towards neutral axis of the composite beam.

The calculation of the second moment of area of the composite beam may be carried out assuming that the distance of the flange from the neutral axis of the composite beam is reduced by $\frac{2}{3} u$.

The maximum deflection of the flange towards the neutral axis of the beam may be calculated as

$$u = \frac{5}{384} \frac{\sigma_f^2 t b_f^4}{E_b (EI)_f z} \quad (7.1.2 e)$$

when the flange is assumed to be simply supported at its edges at the webs, and

$$u = \frac{1}{384} \frac{\sigma_f^2 t b_f^4}{E_b (EI)_f z} \quad (7.1.2 f)$$

when clamped edges can be assumed.

The following notations are used in the equations:

σ_f = uniformly distributed axial stress at the midplan
of the flange under the assumption that the flange is
homogenous

E_b = the modulus of elasticity of the web material

$(EI)_f$ = bending stiffness per unit width of flange in transverse
direction

z = distance from the flange to the neutral axis of the composite beam

If the load-bearing capacity of the flange is reduced due to buckling or shear lag a reduced value of σ_f may be used in equations (7.1.2 e,f):

$$\sigma_f = \sigma_e \frac{b_{ef}}{b}$$

INTERNATIONAL COUNCIL FOR BUILDING RESEARCH STUDIES AND DOCUMENTATION
WORKING COMMISSION W18A - TIMBER STRUCTURES

MODIFICATION FACTOR FOR "AGGRESSIVE MEDIA"

A proposal for a supplement to the CIB model code

by

K Erler

Wismar College of Technology
German Democratic Republic

and

W Rug

Academy of Building of the GDR
Institute for Industrial Buildings
German Democratic Republic

MEETING TWENTY - TWO

BERLIN

GERMAN DEMOCRATIC REPUBLIC

SEPTEMBER 1989

1. Introduction

Timber has a high resistivity to chemically aggressive agents. This is one of the reasons why timber structures are frequently being used in the construction of storage halls for chemical materials or of industrial buildings with an aggressive environment.

Also with agricultural systems and plants, at certain buildings (storage halls and production buildings) a high chemical stress and strain (loading) is occurring as well.

Failures and damages done to timber structures in these fields of application are showing, however, that the corrosive action of said materials and substances on the timber and the connections (fasteners) is often being underestimated. In the GDR, frequently nailed roof frames and trusses with thin boards are being used for agricultural buildings which have been optimized exclusively in terms of the material consumption. The chemical agents are easily and promptly penetrating the thin boards which will result in a corrosion of the nails.

The CIB Code /1/ is hitherto not yet including any recommendations with a view to considering the attack of chemically aggressive substances on timber structures.

This report shall present a proposal for a supplement to the CIB Code.

The degree of aggressiveness (corrosivity) of the chemical action (e.g. of salts, acids or bases) in a solid, liquid or gaseous state of aggregation, the period of time of the action concerned, the location of the structure concerned as related to the environmental conditions, the kind of timber used and the structural design are altogether resulting in the formation of a corrosion system. These individual factors are deciding the rate of destruction of the timber.

The proposal concerning the provision of a factor for considering the chemical action is based on both investigations and studies using removed timber components and laboratory tests.

2. Proposal for a Supplement to the CIB Code

Timber is resistant to weak acids with a normal indoor temperature and to alkaline solutions with a low concentration. A corrosive action is occurring only due to strongly acid and strongly alkaline solutions. In general, the timber corrosion is insignificant within the pH-value range of $2 > \text{pH} < 11$.

With the majority of chemicals in a solid, liquid or gaseous state of aggregation, the corrosive action is decreasing in the course of time and a destruction is occurring only in zones located near the surface (see also Erler /2/).

The factor for considering the chemical action is being determined subject to the degree of stressing (exposure), i.e. the degree of aggressiveness.

The cross-sectional dimensions are influencing the effect of the corrosive action on the loadbearing capacity. Therefore, the factor has been fixed subject to the timber cross section. The corrosive action is also being influenced by applied protective systems which will be taken into consideration as well.

The aggressive action of gases is resulting from the concentration of the gas concerned. Based on the concentration of the gases, the degree of stressing of the chemical action is being determined subject to the moisture grade.

A dependence of the degree of stressing on the moisture grade is being verified for solids as well.

3. Examples

(a) Timber components of storage halls

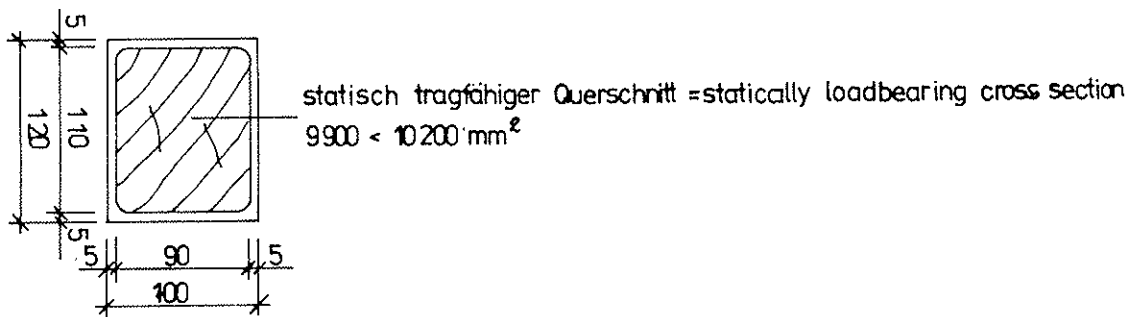
At a hall for the storage of potash, square timber components sized 100 by 120 mm are being used. The storage hall is not being heated.

Classification: moisture grade 2;
the degree of stressing according to Table 4
is BG II.

The modification factor subject to the cross-sectional dimension and to the degree of stressing is 0.85 according to Table 5 (see /2/).

The statically loadbearing cross section is to be reduced by this value as follows:

$$\text{avail. } A = 0.85 \cdot 12,000 \text{ mm}^2 = 10,200 \text{ mm}^2.$$



Thus, a protective layer of timber amounting to 5 mm is remaining as a structural corrosion protection.

By means of square timber components removed from existing potash storage halls with a service life of 50 to 70 years, the strength over the cross section has been determined (see Figure 1). One can see that just in the boundary zone of < 5 mm a considerable reduction in strength may be verified.

(b) Nailed roof frames of storage halls

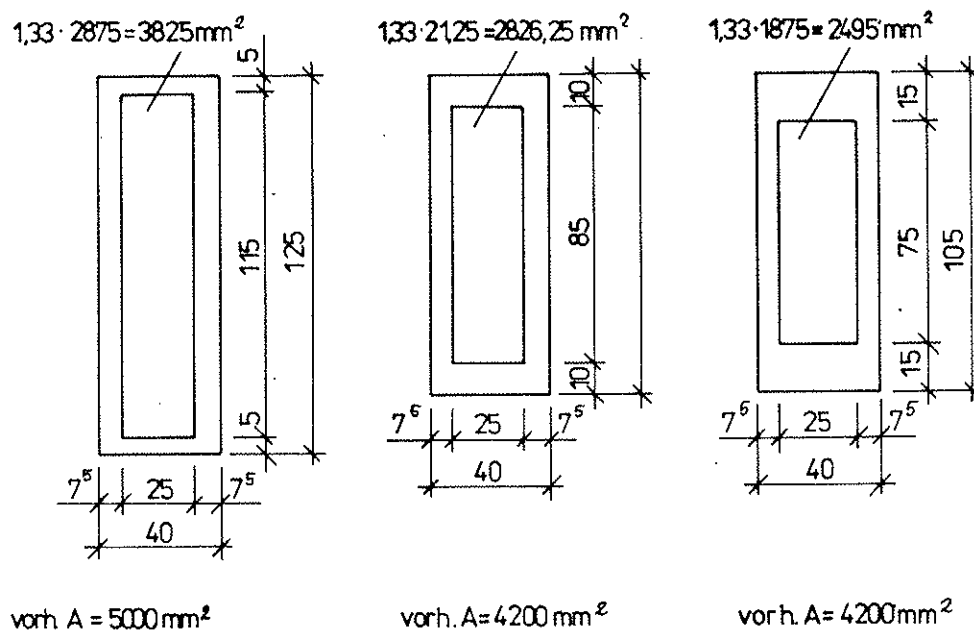
For roofing over an unheated hall for the storage of fertilizers, a nailed roof frame is being used. The members are made up of timber boards sized 25/115, 25/85 and 25/75 mm.

Classification: moisture grade 2;

the degree of stressing according to Table 4 is BG II.

Modification factor = 0.75, $A \leq 9,000 \text{ mm}^2$ (acc. to Table 5).

The cross sections being statically fully utilized must be increased by the factor of $1/0.75 = 1.33$.



Small-size cross sections are being penetrated almost completely whereas with large-size cross sections the aggressive substances are incorporating only in the boundary zones (see the Figures 1 and 2).

Therefore, minimum cross sections and minimum thicknesses have been fixed for the degrees of stressing BG II and BG III.

From structural failures and damages done to nailed roof frames with the above-mentioned cross sections of the timber boards (i.e. 25 x 115, 25 x 85 and 25 x 75 mm), a maximum service life of 25 years only can be verified as compared with 60 years in the case of a normal environment.

There are only the following two approaches to increase the service life:

- (1) increase of the cross sections, taking into consideration the required minimum values, and
- (2) application of a suitable and efficient corrosion protection system.

References

- /1/ CIB
Structural Timber Design Code
1983

- /2/ Erler, K.:
Korrosion und Anpassungsfaktoren für chemisch aggressive
Medien bei Holzkonstruktionen
(Corrosion and Modification Factors for Chemically
Aggressive Media with Timber Structures)

Modification factor $\gamma_{d,4}$ as to "Aggressive Media" at the limit state of the loadbearing capacity (GZT) and limit state of the usability (GZN) of structural timber (BH) and glued laminated timber (BSH)

The kinds of medium are being divided into gases, solutions and solids. By means of the criteria as to concentration of the medium and moisture grade, the degrees of stressing (BG) I, II and III are being determined.

Table 1:

Degree of stressing (BG)	Explanation
BG I	not or slightly aggressive
BG II	moderately aggressive
BG III	highly aggressive

Thus, after the classification of the media into ranges of aggressiveness the degree of stressing (BG) is to be determined by means of the tables following hereinafter. With the BG, the modification factor $\gamma_{d,4}$ for aggressive media can be drawn from Table 5 subject to the cross-sectional size of the timber components.

Table 2: Ranges of aggressiveness (A) and degrees of stressing (BG) for gases

Table 2a: Ranges of aggressiveness (A) for gases

Gas, increasing aggressiveness	Group of gas, with a concentration of ... (mg/m ³)		
	A 1	A 2	A 3
1. CH ₂ O (formaldehyde)	1...200	-	-
2. NH ₃ (ammonia)	0.5...20	-	-
3. SO ₂ (sulphur dioxide)	0.2...10	10...200	-
4. NO ₂ (nitrogen dioxide)	0.1...5	5...25	above 25
5. HCl (hydrogen chloride)	0.05...1	1...10	above 10
6. Cl ₂ (chlorine)	0.02...1	1...5	above 5

Table 2b: Degrees of stressing (BG) for gases

Degree of aggressiveness (A)	Moisture grade (FK)		
	FK 1	FK 2	FK 3
A 1	I	I	I
A 2	I	II	II
A 3	II	II	II

Table 3: Degree of stressing for solutions

Group	Solution	pH-value	Concentration of the solution	Degree of dissociation (with 1-normal solution)	Degree of stressing		
acids	nitric acid HNO_3	below 2	up to 5	high	III		
			above 5		III		
	hydrochloric acid HCl	4	up to 5	high	III		
			above 5		III		
	sulphuric acid H_2SO_4	4	up to 5	medium	I		
			above 5/ above 15		II/III		
	acetic acid CH_3COOH	4	above 15	low	I		
bases	soda lye NaOH	above 13	up to 2	high	II		
			above 2		III		
	potash lye KOH			up to 2	high	II	
		above 2	III				
	ammonium hydroxide NH_4OH		up to 5	low	I		
			above 5		II		
salt solutions	chloride solutions: KCl, NaCl	7	up to 10/ above 10	medium	I/II		
	sulphate solutions: Na_2SO_4 (Glauber's salt)		up to 10/ above 10			medium	I
	$(\text{NH}_4)_2\text{SO}_4$ (ammonium sulphate)		5				
(organic compound)	urea $\text{CO}(\text{NH}_2)_2$	2	up to 40		II		

Table 4: Degrees of stressing for solid media

Solid medium	pH-value	Solubility in water	Hygrosco-picity	Degree of stressing (BG) with moisture grade		
				FK 1	FK 2	FK 3
potash fertilizer	8	good (up to 20 %)	good	I	II	II
urea	9	good (up to 40 %)	high	I	II	II
superphosphate	3	(up to 5 %)	good	I	I	II
sodium chloride	7	good	good	I	I	II
ammonium sulphate	5	good (up to 40 %)	low	I	I	I

Table 5:

Modification factors $\gamma_{d,4}$ for aggressive media subject to the timber cross-sectional size

Degree of stressing (BG)	Cross-sectional size (10^3 mm^2)	Factor $\gamma_{d,4}$
BG I		1.0
BG II	< 9	0.75
	< 30	0.85
	≥ 30	0.95
BG III	< 9	0.65
	< 30	0.75
	≥ 30	0.85

Note: Minimum dimension of the timber component concerned with BG II and BG III: 40 mm; minimum cross-sectional area: 4,000 mm^2 .

$\gamma_{d,4}$ is related to the area of the unimpaired cross section.

Permitted timber preservatives (protective agents) are not having any aggressive action on the timber. When using efficient linings (surfacing) or coatings, the value of $\gamma_{d,4}$ will be equal to 1.

INTERNATIONAL COUNCIL FOR BUILDING RESEARCH STUDIES AND DOCUMENTATION

WORKING COMMISSION W18A - TIMBER STRUCTURES

**TIMBER DESIGN CODE IN CZECHOSLOVAKIA
AND COMPARISON WITH CIB MODEL CODE**

by

P Dutko

Technical University of Bratislava

Czechoslovakia

and

B Kozelouh

Research Institute for Timber Engineering

Bratislava, Czechoslovakia

MEETING TWENTY - TWO

BERLIN

GERMAN DEMOCRATIC REPUBLIC

SEPTEMBER 1989

Ing. Bohumil Koželouh, CSc.

Staatliches Holzforschungsinstitut Bratislava /ČSSR/

STAND DER ENTWICKLUNG DER BEMESSUNGSMETHODEN VON HOLZKONSTRUKTIONEN IN DER ČSSR

1. Einführung

Die Entwicklung der Bemessungsmethoden von Tragkonstruktionen stellt die Bestrebung um die optimale Lösung des Gegensatzes zwischen den Sicherheitsforderungen und der Wirtschaftlichkeit der Konstruktionen dar. Im Grundsatz geht es um die Erreichung der höchsten Wirtschaftlichkeit bei der gleichzeitigen Erfüllung der Bedingung, dass die Konstruktion ihrem Zwecke während der ganzen Nutzungszeit zuverlässig dienen wird.

Die Zuverlässigkeit der Baukonstruktion bedeutet im breiteren Sinne die Eigenschaft dem projektmässigen Zwecke im geforderten Zeitabschnitt dienen zu können. In diesem breiteren Sinne hängt die Zuverlässigkeit zum Beispiel auch von der konstruktiven und bauphysikalischen Projektierung, von der Qualität der Ausführung, von dem Holzschutz und von dem Brandschutz, von der richtigen Nutzung und von der Bauerhaltung der Konstruktionen ab.

Aus dem engeren /theoretischen/ Standpunkt bezieht sich jedoch der Begriff der Zuverlässigkeit von Baukonstruktionen vorwiegend auf die Tragelemente und Tragsysteme und auf die Methoden der Beurteilung ihrer Sicherheit und Nutzungsfähigkeit. In diesem engeren Sinne wird die Zuverlässigkeit oft als die Wahrscheinlichkeit ausgedrückt, dass der in der Konstruktion in Betracht genommene Grenz Zustand /der Tragfähigkeit oder Nutzungsfähigkeit/ nicht zustande kommt.

Die Zuverlässigkeit von Holztragkonstruktionen kann nach den tschechoslovakischen Vorschriften durch die Berechnung /Grundverfahren/, durch die Belastungsprüfungen /in Spezialfällen/- oder durch die Kombination dieser zwei Methoden ermittelt werden.

2. Bemessungsmethoden

Für die Bemessung von Holzkonstruktionen auf Grund der Berechnung sind die zuständigen Berechnungsnormen massgebend - vor allem geht es um die Holzbaunorm und um die Belastungsnorm - durch

welche in der Regel auch die Bemessungsmethode bestimmt wird. Bei der praktischen Bemessung wird die Zuverlässigkeit der Konstruktion auf Grund der Sicherheitsbedingungen und der Nutzungsfähigkeitsbedingungen /das bedeutet auf Grund der mathematischen Beziehungen für den Nachweis der Tragfähigkeit der Querschnitte oder Verbindungen, bzw. der Verformung der Tragelemente/ beurteilt, durch welche die sogenannte allgemeine Zuverlässigkeitsbedingung in den Berechnungsnormen praktisch ausgedrückt wird. Die allgemeine Zuverlässigkeitsbedingung kann in folgender Form dargestellt werden [1]

$$A \leq B$$

wo das Symbol A die Aktion des Systems "Konstruktion - Belastung - Umwelt" /zum Beispiel Biegemoment oder Durchbiegung des Trägers/ repräsentiert und das Symbol B die Grenze /Barriere/ darstellt, welche die Grösse A im Laufe der Nutzungszeit der Konstruktion nicht überschreiten darf.

Die Holzbauvorschriften haben lange Zeit auf der Methode der zulässigen Spannungen beruht, von der noch bis jetzt in einer Reihe von Ländern Gebrauch gemacht wird. Diese Methode ist in ihrer ursprünglichen Konzeption deterministisch, das bedeutet, dass die Eingangsgrössen der Belastung sowie der Konstruktionseigenschaften als fest /nicht als zufällig/ betrachtet werden. In der ČSSR wurden die Holzkonstruktionen nach der Methode der zulässigen Spannungen bis zum Ende des Jahres 1970 berechnet, wann die Wirksamkeit der ČSN 73 2050 [2] ein Ende fand.

Die Bestrebungen um die genauere Erfassung der Beziehung zwischen der Belastung und Tragfähigkeit, Nutzungsfähigkeit bzw. Wirtschaftlichkeit der Baukonstruktionen, haben zur Entwicklung der probabilistischen Sicherheitsmethoden und zur Entwicklung des Verfahrens nach Grenzzuständen geführt.

In den probabilistischen Sicherheitsmethoden werden die Eigenschaften der Belastung, Konstruktion und der Umgebung im Einklang mit der Wirklichkeit als zufällige Variablen in Betracht genommen, die mit der Hilfe der mathematisch-statistischen Methoden und der Wahrscheinlichkeitstheorie untersucht werden. Das Ziel der probabilistischen Sicherheitsmethoden ist es sicherzustellen, dass die wirkliche Bruchwahrscheinlichkeit $p_f = p(R < S)$ /dargestellt

durch die schraffierte Fläche auf dem Bild 1/ die zuständige projektmäßige Wahrscheinlichkeit nicht überstiege. Die zugehörige Wahrscheinlichkeit des "Nichtbruches" $/1 - p_f/$ wird als Zuverlässigkeit bezeichnet.

Bei den Holzkonstruktionen im Gegensatz zu den Konstruktionen aus anderen Baustoffen wird die relativ hohe Variabilität und die rheologischen Eigenschaften des Materials sowie der Konstruktion in Geltung gebracht. Es wurde gezeigt [3], dass die Baustoffe mit der hohen Variabilität der mechanischen Eigenschaften /zu denen auch Holz gehört/ bei der Festsetzung der Versagenswahrscheinlichkeit auf eine andere Weise behandelt werden müssen, als die Baustoffe mit einer niedrigeren Variabilität.

In Abhängigkeit von der theoretischen Ebene werden die probabilistischen Sicherheitsmethoden gewöhnlich in drei Ebenen eingeteilt; in der tschechoslovakischen Literatur werden sie als die Methode der extremen Werte, als die Methode der funktionalen Extreme und als die exakte Methode bezeichnet [4], aus dem internationalen Standpunkt ist die Einteilung in drei Ebenen mit der englischen Bezeichnung Level 1 - 2 - 3 verbreitet. Die probabilistischen Sicherheitsmethoden ermöglichen theoretisch die höchstmögliche effektive Lösung des Problems der Zuverlässigkeit und der Wirtschaftlichkeit der Tragkonstruktionen; das grösste Hindernis auf dem Wege zur praktischen Anwendung der höheren Ebenen dieser Methoden sind die unzureichenden Erkenntnisse über die statistische Verteilung der Belastung und der Resistenz der Konstruktion. Es kann deshalb angenommen werden, dass in der absehbaren Zeit die tschechoslovakischen Holzbauvorschriften auf das weitere auf der Methode der extremen Werte gegründet sein werden, die auch als die halbprobabilistische Methode bezeichnet wird.

Das Bemessungsverfahren nach Grenzzuständen hat auch bei den Holzkonstruktionen in einer Reihe von Ländern das Verfahren nach zulässigen Spannungen ersetzt. Das Verfahren nach Grenzzuständen wurde in die Praxis schon am Anfang der fünfzigen Jahre in Ungarn und in der UdSSR eingeführt, später auch in anderen Ländern, gewöhnlich zuerst für die Betonkonstruktionen. Die Prinzipien dieser Konzeption wurden schon vor 60 Jahren formuliert [5].

Der Grenzzustand der Konstruktion ist erreicht, wenn die

Konstruktion nicht im Stande ist den projektmässigen Betriebsanforderungen zu entsprechen, für die sie projektiert wurde. Die Grenzzustände werden in zwei Gruppen eingeteilt:

- Grenzzustände der ersten Gruppe, bei denen es zum Versagen der Tragfähigkeit oder zur völligen Unbrauchbarkeit der Konstruktion kommt /z.B. durch das Versagen der Formstabilität, der Stabilität der Lage oder durch das Festigkeitsversagen jedweder Natur/
- Grenzzustände der II. Gruppe, die die normale Nutzung der Konstruktion erschweren und die die Grenzen des annehmbaren und des unannehmbaren Zustandes aus dem Standpunkt der konstruktiven, technologischen, psychologischen oder hygienischen Auswirkungen bei der normalen Nutzung der Konstruktion kennzeichnen. Bei den Holzkonstruktionen wird in der Praxis am häufigsten der Grenzzustand der unzulässigen Verformung /in der Regel wird die Durchbiegung nachgewiesen/ untersucht, die mit Hinsicht auf den relativ niedrigen E-Modul des Holzes bei der Bemessung oft entscheidend ist. Weitere Fälle der Grenzzustände der Nutzungsfähigkeit von Holzkonstruktionen sind unzulässige Schwingungen, lokale Beschädigung /einschliesslich Risse/, lokale Beulen von dünnen Stegen oder Beplankungen ohne Bruch u.a.

Es ist notwendig zu bemerken, dass das Versagen der Konstruktion /d.h. die Erreichung des Grenzzustandes/ kann von weiteren Ursachen beeinflusst werden, die mit Lasteinflüssen unmittelbar nicht zusammenhängen und mathematisch schwierig dargestellt werden. Diese Grenzzustände hängen gewöhnlich mit der Dauerhaftigkeit der Konstruktion zusammen und bei den Holzkonstruktionen gehört zu ihnen die biologische Beschädigung des Holzes /durch Fäulnispilze, Insekten/ und die Korrosion der aus Stahl verfertigten Verbindungsmittel.

Die Beziehung des Verfahrens nach Grenzzuständen zu den mathematisch-statistischen bzw. probabilistischen Methoden, die oft als eines der Grundattribute dieser Methode bezeichnet werden, wurde im Laufe der Entwicklung präzisiert. Das Verfahren nach Grenzzuständen macht von den mathematisch-statistischen und probabilistischen Methoden Gebrauch oder führt sie ein, diese hängen jedoch mit der Natur der Grenzzustände im Grunde nicht zusammen [1, 4].

Das Verfahren nach Grenzzuständen bringt die Unsicherheit der Belastung sowie der Resistenz der Konstruktion und auch die Nutzungsbedingungen und die Bedeutung der Konstruktion mit Hilfe der Teilsicherheitsfaktoren zum Ausdruck /nach der gegenwärtigen Methode, die in der ČSN 73 0031/ST. SEV 384-76 [6] ihre Definition findet, sind das der Lastfaktor γ_f , Kombinationsfaktor γ_c , Materialfaktor γ_m , Wertigkeitsfaktor γ_n und Anpassungsfaktoren γ_d /, was im Vergleich zu der Methode der zulässigen Spannungen eine genauere Ausdruckweise der Sicherheit und die Unifikation des Berechnungsvorganges ermöglicht.

Die Bemessungsmethode, die von den Teilsicherheitsfaktoren abhängig ist /die sogenannte Methode der Partialkoeffizienten/ hat jedoch eine breitere Bedeutung und wird auch als die Bemessungsmethode der 1. Ebene /Level 1/ bezeichnet. Zum Beispiel der Vorschlag der internationalen Holzbaunorm ISO/CIB [7] der auf dieser Methode basiert, kann auch für die deterministischen Bemessungsmethoden verwendet werden /der Lastfaktor γ_f wird durch den Einheitswert eingeführt/. Andererseits die Grenzzustände können auch mit den Methoden der höheren Ebenen /mit den probabilistischen Sicherheitsmethoden/ untersucht werden. Es wird deshalb empfohlen, den Begriff "Grenzzustände" nur dann zu benützen, wenn es sich um die Charakteristik der einzelnen Grenzbetriebsanforderungen handelt, d.h. der Grenzen auf der sogenannten Zustandcharakteristik der Konstruktion [4].

3. Stand und Entwicklung tschechoslovakischen Holzbauvorschriften

In der ČSSR wurde für die Berechnung von Baukonstruktionen nach Grenzzuständen die gesetzliche Voraussetzung durch die Ausgabe der Norm ČSN 73 0031 aus dem Jahre 1963 gebildet. Diese Norm hat die Grundsätze dieser Methode formuliert, die in den RGW Ländern angenommen wurden [8].

An diese Grundvorschrift hat sich die Belastungsnorm und die Berechnungsnormen für die Bemessung von Konstruktionen aus einzelnen Baustoffen angeknüpft. Für die Holzkonstruktionen war es die ČSN 73 1701 aus dem Jahre 1971 [9], die neben der sowjetischen Norm N i TU 122-55 als eine der ersten Normen für die Berechnung von Holzbaukonstruktionen nach Grenzzuständen zustande kam.

Für die Beurteilung der ökonomischen Wirksamkeit des neuen

Bemessungsverfahren ist ein wichtiges Kriterium der Vergleich mit dem bisherigen Verfahren, das für die Projektierung einer ganzen Menge von realisierten Bauwerken angewendet wurde. Dabei wird oft die Forderung hervorgehoben, dass die nach dem neuen Verfahren bemessenen Konstruktionen im Durchschnitt einen höheren Materialverbrauch nicht ausweisen, als es bei der Anwendung des alten Verfahrens war. Für die Holzkonstruktionen haben wir versucht eine womöglich allgemeine Vergleichsmethodik zu formulieren, wie es aus der Arbeit [10] hervorgeht.

Durch die neue Ausgabe der ČSN 73 0031/ST SEV 384-76 [6] wurde in der ČSSR eine einheitliche Konzeption der Grenzstände im Rahmen der PGW und auch im breiterem internationalen Masstab eingeführt. Revidiert wurde auch die tschechoslovakische Belastungsnorm für die Baukonstruktionen [11] und die Norm für die Bezeichnungen [12]. In diese Norm wurden die Angaben aus der ST SEV 1565-79 [13] eingearbeitet. Mit Hinsicht auf diese Grundvorschriften wurde die revidierte ČSN 73 1701-Ausgabe 1984 [14] ausgearbeitet, die gleichzeitig im Einklang mit der inländischen und ausländischen Entwicklung auf dem Gebiet der Holzbaukonstruktionen in der letzten Zeit ergänzt wurde.

Ausser der Grundnorm ČSN 73 1701-84 beziehen sich auf die Projektierung und Ausführung von Holzbaukonstruktionen unmittelbar vor allem diese weiteren tschechoslovakischen Normen:

- ČSN 49 1531-72 Holz für Baukonstruktionen
- ČSN 73 2052-66 Herstellung geleimter Holzelemente
- ČSN 73 2810-64 Ausführung von Holzbaukonstruktionen
- ON 73 6212-84 Projektierung von Holzbrücken.

Die gegenwärtige Berechnungsmethode von Baukonstruktionen nach ČSN 73 0031/ST SEV 384-76 [6] ist auf der sogenannten Methode der extremen Werte gegründet, die die erste /niedrigste/ Ebene der probabilistischen Sicherheitsmethoden darstellt. Die Zuverlässigkeitsbedingung kann nach [4] in allgemeiner Form

$$A(a_{id}) \leq B(b_{jd})$$

dargestellt werden, wo A der Ausdruck des gegenwärtigen Vorhandensein der Konstruktion und der Belastung ist, welche die Funktion der Rechenwerte der Eingangsgrössen /z.B. Belastung,

Querschnittabmessungen u.a./ ist. Die Grösse B ist die Funktion der Recheneigenschaften der Konstruktion, der Belastung u.a. und repräsentiert die Grenze, die von der Grösse A in der Nutzungszeit des Bauwerkes nicht überschritten werden darf. Mit Hinsicht darauf, dass der jetzige Stand der Erkenntnisse über das zufällige Verhalten der Grössen die in die Berechnung eingeführt werden /Belastung, Materialeigenschaften, geometrische Parameter u.a./ es nicht erlaubt, die deterministischen Methoden auszuschliessen, wird die benützte Methode auch als halbprobabilistisch bezeichnet.

Bei der Berechnung nach Grenzzuständen werden allgemein die Rechenwerte der Last in Betracht genommen

$$F_d = F_n \cdot \gamma_f$$

wo F_n die Normlast und γ_f der Lastfaktor ist, der für die Grenzzustände der I. und II. Gruppe differenziert wird /dem entspricht die sogenannte Extremlast und Betriebslast/. Für die Grenzzustände der II. Gruppe wird vorläufig $\gamma_f = 1,0$ eingeführt.

Die gesellschaftliche Bedeutung des Bauwerkes mit Hinsicht auf die Folgen der etwaigen Erreichung des Grenzzustandes wird mit dem Wertigkeitsfaktor γ_n in Betracht genommen. Mit dem Wertigkeitsfaktor wird /nach der in der ČSSR angenommenen Methodik/ der Lastfaktor adjustiert.

Mit der Frage der Einführung des Einflusses der zufällig variablen Abweichungen der geometrischen Parameter /querschnittabmessungen/ in die Berechnung hängt eng die Inbetrachtung eines weiteren variablen Faktors - Anwendung von Standardquerschnitten von Schnittholz /Bauelementen/ bei der Projektierung; diese zwei Einflüsse wirken gegeneinander. Bei der Festsetzung der in der ČSN 73 1701 angegebenen Rechenfestigkeiten wurden diese beiden Einflüsse berücksichtigt [15] und gewöhnlichen Fällen kann man deshalb aus den Nominalwerten der geometrischen Parameter ausgehen.

Grenzzustände der Tragfähigkeit

Für die Grenzzustände der I. Gruppe wird in der ČSN 73 1701-84 die Zuverlässigkeitsbedingung in der Form

$$S_{ud} \leq \gamma_u \cdot R_{ud}$$

ausgedrückt, wo

S_{ud} - Krafteinfluss der extremen Rechenlast

R_{ud} - Rechentragfähigkeit des Querschnittes oder der Verbindung unter den Grundnutzungsbedingungen

γ_u - Produkt der Anpassungsfaktoren bei der Berechnung nach Grenzzuständen der I. Gruppe.

Bei den Holzbaukonstruktionen ist es allgemein notwendig die Anpassungsfaktoren Holzfeuchte und Belastungsdauer immer zu berücksichtigen, mit Hinsicht auf die markante Einwirkung dieser Bedingungen auf die mechanischen Eigenschaften des Materials und der Konstruktion.

Die ČSN 73 1701-84 unterscheidet aus statischer Sicht nur zwei Holzfeuchteklassen - die sogenannte geschützte und ungeschützte Exposition. Die Lastklassifizierung nach der Belastungsdauer ist in der Übereinstimmung mit der Belastungsnorm [11] berücksichtigt; dabei werden die folgenden Belastungskategorien unterschiedet:

- ständige und/oder langzeitige Last
- kurzzeitige Last ausser der Windlast
- Windlast
- ausserordentliche Verkehrslast.

Ausser den Anpassungsfaktoren Holzfeuchte und Belastungsdauer werden für die einzelnen Konstruktionstypen, Bauelemente oder Verbindungen weitere Anpassungsfaktoren in Betracht genommen:

- Anpassungsfaktor "Holzkrümmung"
- Anpassungsfaktor "Querschnittshöhe" bzw. "Querschnittsform" für die Biegebeanspruchten Bauglieder
- Anpassungsfaktor, der den Einfluss von rechtwinkligen Ausklinkungen bei Biegeträgern berücksichtigt
- Anpassungsfaktor für die verleimten Knotenverbindungen mit Pressnagelung.

Der Rechenwert der Festigkeit ist durch die Beziehung

$$R_d = \frac{R_n}{\gamma_m}$$

gegeben. Dabei R_n ist der Normwert der Rechenfestigkeit, der mit

der statistischen 0,95 Garantie /5 % - Quantil/ unter definierten Bedingungen festgesetzt wird. Für die Holzbaukonstruktionen sind diese Bedingungen nach [7] die Kurzzeitbelastung /3 - 5 Min./, Temperatur 20 ± 2 °C und relative Luftfeuchtigkeit $0,65 \pm 0,05$.

Bei der Festsetzung der Normfestigkeiten des Holzes und der Holzwerkstoffe werden zwei verschiedene Vorgänge benützt:

a/ Standardprüfungen an kleinen fehlerfreien Proben, die durch die Anwendung von Beiwerten von Holzfehlern und Querschnittabmessungen ergänzt werden

b/ Prüfungen von Konstruktionselementen in der normalen Grösse und Qualität. Dieser Vorgang ermöglicht praxisnähere Resultate und setzt sich immer mehr durch, obwohl er grösseren Material- und Arbeitsansatz erfordert. Als eine fortschrittliche Variante dieses Vorganges kann man maschinelle Schnittholzsortierung betrachten.

Durch den Materialfaktor γ_m wird der Normwert der Festigkeit in die Rechenfestigkeit transformiert. Dadurch wird die Komponente der Festigkeitsstreuung ausgedrückt, die im Normwert nicht eingeschlossen ist, und auch weitere variable und unvariable Einflüsse werden in rücksicht genommen. Bei den Holzkonstruktionen sind das z.B. die Methode und die Stufe der Kontrolle der Schnittholzsortierung, Stufe der Fertigungskontrolle und Kontrolle der fertigen Bauelemente, Stufe der Kontrolle des Entwurfes /der Berechnung/ und weitere Faktoren.

Der Materialfaktor γ_m ist bei den Holzkonstruktionen mit Rücksicht auf die Anisotropie des Holzes von der Art der Beanspruchung, weiter auch von dem Typ /von den Dimensionen/ der Prüfkörper und von der Sortierung abhängig. Für die Festsetzung der Werte der Materialfaktoren und der Normwerte der Rechenfestigkeiten /bzw. der Tragfähigkeiten der Verbindungen/ stehen für die Holzbaukonstruktionen in der ČSSR bis jetzt nicht genug experimentelle Unterlagen zur Verfügung. In der ČSN 73 1701-84 sind daher bis auf weiteres nur die resultierende Rechenfestigkeiten der Materialien bzw. die Rechenbelastungen der Verbindungen festgesetzt.

Grenzzustände der Nutzungsfähigkeit

Die Zuverlässigkeitsbedingung für den durch den Verformungseffekt beschriebenen Grenzzustand der Nutzungsfähigkeit kann auf folgende Weise ausgedrückt werden: die Verformung von der Rechenbetriebslast /welche bei den Holzkonstruktionen mit dem Lastfaktor $\gamma_f = 1,0$ festgesetzt wird/ darf den Grenzwert der bemessenen Verformung nicht überschreiten. Bei den Holzkonstruktionen wird gewöhnlich die Durchbiegung nach der Formel

$$f \leq f_{lim}$$

nachgewiesen.

Die Sicherstellung der Zuverlässigkeit von Holzkonstruktionen aus dem Standpunkt der Grenzzustände der II. Gruppe wird vorläufig vor allem auf die genauere Berechnung der Verformung mit Hinsicht auf die Schubdurchsenkung, Nachgiebigkeit der Verbindungen und Berücksichtigung der Kriechverformungen bei der Langzeitlast beschränkt. Die Norm ČSN 73 1701-84 ermöglicht dabei zwei Vorgänge:

- a/ Nachweis der kurzzeitigen Durchbiegung, für welche die projektmäßige Grenzwerte f_{lim} festgelegt sind,
- b/ approximative Berechnung der wirklichen Durchbiegung bei der Langzeitbelastung, wenn es aus Betriebsgründen notwendig ist diese Durchbiegung nachzuweisen.

Materialgüte

Ein Schlüsselproblem der Zuverlässigkeit von Holzkonstruktionen mit Rücksicht auf ihre Projektierung, Ausführung und Gütesicherung ist die Garantie der technischen Parameter des Materials, d.h. die Sicherstellung der effektiven Auswahl /Sortierung/ des Bauholzes nach dem Verwendungszweck /nach den mechanischen Eigenschaften/.

Aussichten der Bemessungsmethoden

Es kann vorausgesetzt werden, dass die gegenwärtige Normmethodik für die Bemessung von Baukonstruktionen, die auf der sogenannten halbprobabilistischen Methode der extremen Werte gegründet ist, im Laufe der nächsten 15 - 20 Jahre im Prinzip unverändert bleiben wird. Das Programm der normbildenden Arbeiten und der Forschungsarbeiten kann im allgemeinen als fortschreitende Vervollkommenung und Präzisierung des Verfahrens "nach Grenzzuständen"

bei der gleichzeitigen Schaffung der Bedingungen für die Entwicklung der probabilistischen Sicherheitsmethoden und zwar sowohl aus dem Standpunkt der Theorie /der Bemessungsmethoden/ als auch aus dem Standpunkt des Materials, der Ausführung und der Gütesicherung. Die Gewinnung der normbildenden Unterlagen muss sich dabei auf die Resultate der wissenschaftlichen Arbeiten, der Forschungs- und Entwicklungsarbeiten stützen.

Auf dem Gebiet der Holzkonstruktionen zeigt es sich zweckmäßig, die Aufmerksamkeit vor allem auf folgende Fragen zu richten:

a/ Fortlaufende Ergänzung und Vertiefung der Erkenntnisse über das Verhalten der Materialien und Verbindungen von Holzkonstruktionen zwecks Ermittlung der Unterlagen für die Festsetzung der Normwerte der Rechenfestigkeit und der partialen Materialfaktoren der Holzbaustoffe und der Verbindungen. Es handelt sich vor allem um diese Probleme:

- Festlegung der Normwerte der Rechenfestigkeit und der Materialkennwerte von Holzbaustoffen und Verbindungen mit Hilfe der Proben in konstruktiven Dimensionen
- Festlegung der Wahrscheinlichkeitsverteilung und der statistischen Charakteristik der mechanischen Eigenschaften von Holzbaustoffen und Verbindungen
- Überprüfung des Einflusses der Nutzungsbedingungen auf die Wahrscheinlichkeitsverteilung der mechanischen Eigenschaften
- Ermittlung /Untersuchung/ der statistischen Modelle für die Tragfähigkeit von Holzbauelementen bzw. Holzkonstruktionen

b/ Vervollkommung der Berechnungsmodelle und der experimentalen Modelle mit Hinsicht auf die treueste Erfassung der konkreten Einwirkung der Konstruktion. Dabei soll unter anderem folgendes in Betracht genommen werden:

- Nutzungsbedingungen
- rheologische Eigenschaften des Materials und der Konstruktion
- Einfluss der Imperfektionen
- Sortierung von Schnittholz
- Entwicklung der Rechentechnik /man kann voraussetzen, dass die Berechnungsnormen ein Bestandteil der Computer-Databanken sein werden/.

c/ Ergänzung von Lastannahmen mit Hinsicht auf die rheologischen Eigenschaften der Materialien /Informationen über die Lastdauer und Lastgeschichte/.

Es muss hervorgehoben werden, dass für die Realisation des angedeuteten Programmes die internationale Kooperation und Zusammenarbeit vorausgesetzt werden muss.

LITERATUR

1. Tichý, M. - Vorlíček, M.: Spolehlivost stavebních konstrukcí /Zuverlässigkeit von Baukonstruktionen/. Skriptum, ČVUT Praha 1983.
2. ČSN 73 2050 Projektování dřevěných konstrukcí /Projektierung von Holzkonstruktionen/. Ausgabe 1956.
3. Foschi, R.O.: A discussion on the application of the safety index concept to wood structures. Canadian Journ. of Civ. Eng. 6, 1979, No 1, 51-58.
4. Tichý, M. - Dobr, J.: Možní stavy stavebních konstrukcí. Komentár k ČSN 73 0031 /Grenzzustände von Baukonstruktionen. Erläuterungen zu ČSN 73 0031/ Vydavatelství ÚNM, Praha 1980.
5. Tichý, M.: Šedesát let mezních stavů /Sechzig Jahre Grenzzustände/. Stavebnický časopis 34, 1986, No. 10, 713-721.
6. ČSN 73 0031/ST SEV 384-76. Stavební konstrukce a základy. Základní ustanovení pro výpočet. /Baukonstruktionen und Gründungen. Grundsätze für die Berechnung/.
7. CIB Structural Timber Design Code, sixth edition, 1983. CIB-W 18 Timber Structures.
8. Keldyš, W.M.: Berechnung von Baukonstruktionen nach den Grenzbeanspruchungen. Moskva 1951, VEB Verlag Tech. Berlin 1953
9. ČSN 73 1701 Navrhování dřevěných stavebních konstrukcí /Projektierung von Holzbaukonstruktionen/. Ausgabe 1971.
10. Koželouh, B.: Navrhování prvků dřevěných konstrukcí podle ČSN 73 1701 - předběžné zhodnocení spotřeby materiálu. /Entwurf der Elemente von Holzkonstruktionen nach der Norm ČSN 73 1701 - vorläufige Bewertung des Materialbedarfs/. Inženýrské stavby 1972, No. 2, 61-64.
11. ČSN 73 0035 Zatížení stavebních konstrukcí /Belastung von Baukonstruktionen/. Ausgabe 1978.
12. ČSN 73 0030 Písmenné značky veličin pro navrhování staveb /Bezeichnungen für Bauprojektierung/. Ausgabe 1984.
13. ST SEV 1565-79 Normativno-techničeskaja dokumentacija v strojitel'stve. Bukvennyje oboznačenija.
14. ČSN 73 1701 Navrhovanie drevených stavebných konštrukcií /Projektierung von Holzbaukonstruktionen/. Ausgabe 1984.
15. Koželouh, B.: Navrhování dřevěných stavebních konstrukcí. Komentár k ČSN 73 1701 /Projektierung von Holzbaukonstruktionen. Erläuterungen zur ČSN 73 1701, Ausgabe 1971/. Vydavatelství Úradu pro normalizaci a měření, Praha 1971.

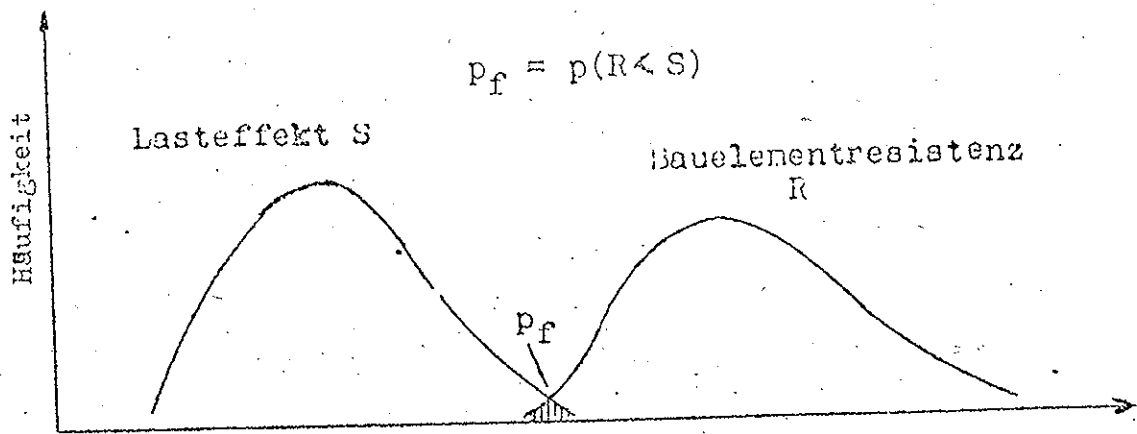


Abb. 1. Wahrscheinlichkeitsverteilung von Lasteffekt S und Bauelementresistenz R

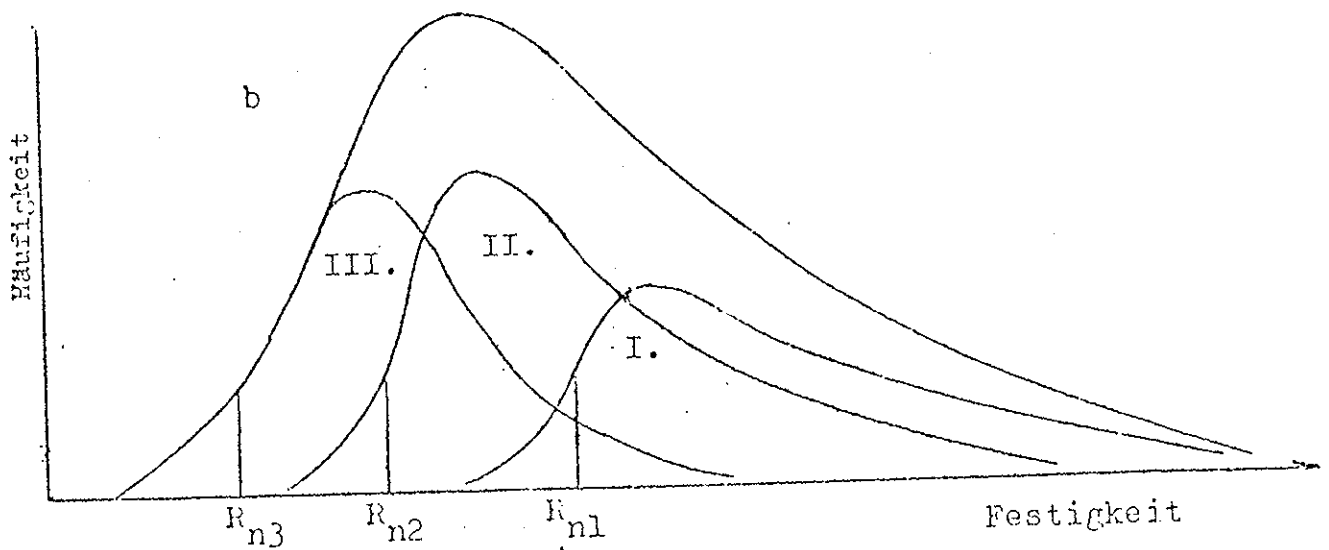
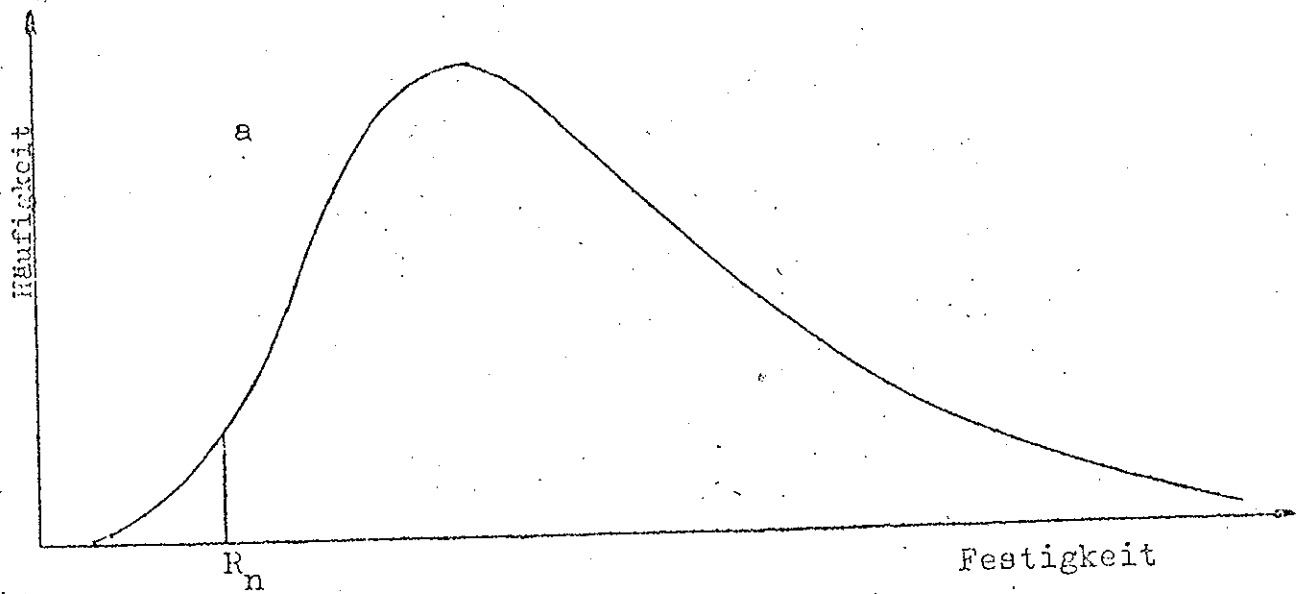


Abb. 2 Wahrscheinlichkeitsverteilung der Biegefestigkeit
 a - unsortiertes Bauholz; b - drei Güteklassen

INTERNATIONAL COUNCIL FOR BUILDING RESEARCH STUDIES AND DOCUMENTATION
WORKING COMMISSION W18A - TIMBER STRUCTURES

NEW GDR TIMBER DESIGN CODE
STATE AND DEVELOPMENT

by

W Rug, M Badstube and W Kofent
Academy of Building of the GDR
Institute for Industrial Buildings
German Democratic Republic

MEETING TWENTY - TWO
BERLIN
GERMAN DEMOCRATIC REPUBLIC
SEPTEMBER 1989

NEW G D R TIMBER DESIGN CODE - STATE AND DEVELOPMENT

Table of Contents

1. State of the Research Work
2. Draft Code (1989)
 - 2.1. Arrangement, Designations and Definitions
 - 2.2. Bases for Design and Calculation
 - 2.3. Building Materials Requirements
 - 2.3.1. Sorting of the Timber
 - 2.3.2. Quality Control for the Production of Glued Laminated Timber
 - 2.3.3. Investigations into the Strength of Structural Timber and Glued Laminated Timber
 - 2.3.4. Characteristic Strengths
 - 2.3.5. Factor for Considering the Moisture Content and the Load Action Period
 - 2.3.6. Factor for Considering the Action of Aggressive Media
 - 2.4. Limit States of the Serviceability
 - 2.5. Calculation and Dimensioning (Design)
 - 2.5.1. Individual Structural Components
 - 2.5.2. Composite Structural Components
 - 2.5.3. Connections
3. Summary
4. References (Publications)
5. Annexes (Tables and Figures)

NEW G D R TIMBER DESIGN CODE - STATE AND DEVELOPMENT

1. State of the Research Work

Since 1985, in the GDR a new timber design code is being prepared and elaborated which shall be based on the method of limit states. Reports concerning the accomplished basic activities and the content of the individual draft codes are included in the papers mentioned under references /1/, /2/ and /3/. The future design and calculation code shall mainly consist of three parts (see the Table 1).

Part 1 shall be assimilated to the CIB Model Code and the Eurocode. It will comprise the definitions, symbols, units and bases for the calculation, design and construction of timber structures (see para 2 hereinafter).

In connection with the project of the new code, other existing codes and standard specifications must be modernized since their rules and regulations will then no longer comply with the latest state (see Table 2).

Both the new code and the revised codes shall correspond to the international trend being represented by the CIB Model Code /4/ and the Eurocode 5 /5/ (see also Tables 1 and 2).

The research work concerning the bases (fundamentals) for all three parts of the code has been continued.

2. Draft Code (1989)

2.1. Arrangement, Designations and Definitions

The arrangement, the designations and the definitions have been revised anew as compared with the reports indicated under /1/, /2/ and /3/ and are now corresponding to the Eurocode 5 /5/ (see *Figure 1*).

Merely in the chapters 3 and 5, structural timber and glued laminated timber only are being dealt with. Timber engineering mate-

rials, glues and mechanical connecting means (fasteners) are being dealt with in a separate Part 3 of the Draft Code. Chapter 6 will be modified according to the specifications included in the TGL 33 135/01 Code of the GDR.

The great number of tests performed with a view to achieving a scientific consolidation of the new timber design code has been accomplished in compliance with and on the model of the RILEM/CIB recommendations as to the testing of structural timber and connections (fasteners). Within the next years, the test codes in the GDR will be revised in accordance with the ISO Codes.

2.2. Bases for Design and Calculation

Exceptions to the Eurocode are existing with regard to the load factors. The GDR Code dated 1978 for the design loads is fixing load factors for the calculation by limit states /6/.

In compliance with /6/, the load factors as summarized in Table 3 are applicable.

The design values of the load are being determined by means of the following equation:

$$S = \gamma_n \left(\sum_{i=1}^n F_i^n \cdot \gamma_{f,i} + \sum_{j=1}^m \psi_j \cdot F_j^n \cdot \gamma_{f,j} \right)$$

where $i = 1 \dots$ is the index for permanent and long-term actions

$j = 1 \dots$ is the index for short-term and instantaneous actions

γ_n = according to Table 4 as per /7/

ψ = according to Table 5 as per /6/

γ_f = according to Table 3 as per /6/

In compliance with /7/, a valency factor ranging - subject to the reliability grade - between $0.9 < \gamma_n \leq 1.1$ is applicable (see Table 4). Thus, the different degree of reliability of the structure concerned as to the level of the design specification is being taken into consideration.

The combination factor Ψ is considering the reduced probability of a simultaneous exceeding of several loads and is having - according to /6/ - the values as indicated in Table 5 .

In Table 6 , the partial safety coefficients for actions as applicable in the GDR are being compared with those values included in the Eurocode. In this connection, the valency factor has been taken into consideration.

The Eurocode 5 is fixing higher values for the partial safety coefficients concerning actions.

As between the previous proposal for the moisture grades indicated in /3/ and those values fixed in the Eurocode 5, there have been only slight differences which are now eliminated by an approximation to the Eurocode 5 (see Table 7).

Table 7 shows the allocation of different kinds of utilization to the modified moisture grades.

An analogous approach was adopted concerning the load action period grades. The GDR proposal from 1987 as compared with the Eurocode is illustrated in Figure 2 . Also the slight difference of the classification of the load action period as compared with the Eurocode 5 has been eliminated by means of the new GDR Draft Code of 1988 (see Figure 2).

The GDR Code for the design loads /6/ comprises a classification of the loads which are being allocated to the new grades of the load action period as shown in Table 8 .

Table 9 includes a comparison of different code proposals concerning the modification factor for considering the influence of the load action period.

A proposal for the grouping into a time grade is shown in Table 10b.

2.3. Building Materials Requirements

2.3.1. Sorting of the Timber

Hitherto, in the GDR structural timber has still exclusively been sorted according to visual criteria.

Said criteria were fixed by a code dated 1963 /8/. This code is corresponding in general to the DIN 4074 Code dated 1958 /10/.

The present sorting code specification has been revised in 1988 (see /9/) and is now considering also hardwood in addition to softwood. Moreover, now a mechanical sorting of the softwood and hardwood is possible as well.

The visual criteria have been revised in part. However, as before a grouping into quality grades is being accomplished.

The criteria for the mechanical sorting are based on the quality grades in combination with the modulus of elasticity in bending which mechanically can be determined in a fairly easy way (see Figure 3).

However, the sorting effects are different subject to defined grade limits for the moduli of elasticity which is being demonstrated by an initial investigation into the influence of different grade limits (see Figure 4).

With the variants 0 and 1, the values of the modulus of elasticity have been fixed so that they are within the range of the 5 % fractiles (quantiles) for strength grade III (variant 0) or of the minimum values for all strength grades, respectively. With variant 0, the quantity of structural timber of quality grade II according to strength grade II is slightly increasing whereas with variant 1 the sorting effect is identical with a visual sorting by quality grades (see Figure 4). The quantity of structural timber of quality grade 1 according to strength grade I is decreasing with a simultaneous considerable increase in strength. The small percentage of sorted-out timber due to the low modulus of elasticity for the strength grade III must be purchased with a loss in strength as compared with the visual sorting. By means of the variants 2 and 3, the strength of the strength grades II and III can be improved as compared with the variant 0; however, this results in considerably increasing the percentage of sorted-out timber.

The connections and interdependencies must be taken into account with future economic studies and investigations. With a view to achieving a percentage of sorted-out timber being as small as possible, for the Draft Code the grade limits of the variant 0_b) have been fixed (see Figure 3).

2.3.2. Quality Control for the Production of Glued Laminated Timber

The technical conditions and specifications and the safeguarding of a constant quality for the production of glued laminated timber are being arranged in the GDR by means of separate codes (see /12/ and /13/). In compliance with said codes, regular checks of the tensile shear strength of the glued joint, the tensile strength of the key-dovetail connection and the flexural strength of glued laminated timber beams in structural timber dimensions must be performed.

Said codes will be revised within the next years, and in future they shall correspond to the testing specifications of the ISO Codes and to the international standard specifications for the production of glued laminated timber.

2.3.3. Investigations into the Strength of Structural Timber and Glued Laminated Timber

With a view to determining the characteristic material strengths, experimental studies and investigations have been accomplished. In this connection, issues of focal interest were investigations into the flexural and compressive strength of structural timber and glued laminated timber which has been sorted mechanically and visually.

Flexural strength of structural timber:

The studies and investigations have been performed by Apitz /20/ by using test specimens in structural timber dimensions. An interpretation (evaluation) of the tests is illustrated in Figure 5. The characteristic values were determined as a result of the three-parametric Weibull distribution according to the GDR Code No. 38791/03. The characteristic values of the visually and mechanically sorted quality grades of timber can be allocated to the strength grades of the Eurocode as indicated hereinafter (see also Figure 5).

	Quality grade acc. to GDR Code	Strength grade acc. to Eurocode grade	stress
Visually sorted timber	G I	C 6	28.5 N/mm ²
	G II	C 5	24.0 N/mm ²
	G III	C 3	19.0 N/mm ²
Mechanically sorted timber	F 1	C 7	38.0 N/mm ²
	F 2	C 6	28.5 N/mm ²
	F 3	C 3	19.0 N/mm ²

A remarkable feature is the insignificant scattering as to the strength with mechanically sorted timber (see Figure 6) which, however, is also dependent on the selection of the sorting criteria. The sorting criteria used in the revised sorting standard specification have been selected so that with the strength grade 3 the yield is as high as possible (no rejects, if possible). Thus, the strength and the scattering for the strength grade 3 are within the range of the visually sorted timber (see Figure 5).

Compression strength of structural timber:

The compression strength in parallel with the grain of visually sorted timber has been studied and investigated by Kiesel (see /26/). An interpretation of the authors reveals small differences between spruce and pine timber. The values were combined for the two kinds of timber in order to obtain data concerning softwood. The allocation to the grades according to the Eurocode 5 results in a conformance with the characteristic values for the compression strength in parallel with the grain (see Figure 7).

Quality grade (GK1) acc. to GDR Code	Failure strength N/mm ²	Number of specimens n	Strength grade acc. to Eurocode compression strength
GK1 I	26.22	542	C 6
GK1 II	24.03	124	C 5
GK1 III	17.23	41	C 3

Bulk density of structural timber:

When performing the tests with regard to the compression strength in parallel with the grain, the bulk density was recorded as well. The values resulting from an interpretation (evaluation) are as follows:

pine timber	580 ... 577 ... 557 kg/m ³	(quality grade GK1 I to III)
spruce timber *	433 ... 464 ... 481 kg/m ³	(quality grade GK1 I to III)

In the case of spruce timber, the bulk density is increasing with a diminishing quality grade. This is not in contradiction with the practice of the visual sorting since the bulk density is not being measured.

The bulk density is being taken into consideration directly or indirectly only with the mechanical sorting. (*Figure 8a, 8b*)

Visually sorted pine timber and spruce timber can be allocated to the bulk density grade D 500 and D 400, respectively. Consequently, softwood is corresponding to grade 400 with the strengths squarely to the grain when allocated to said grade. The values are as follows:

tension 0.4 N/mm^2 ; compression 7.0 N/mm^2 .

Tension strength of layers of boards for the production of glued laminated timber:

The tension strength of layers of boards with and without key-dovetail connection which previously have been sorted visually or mechanically is being illustrated in Figure 9. Figure 9 reveals a distinct influence of the method of sorting on the strength of layers of boards without key-dovetail connection.

In the case of layers of boards with key-dovetail connection, an influence can be found as well which, however, is not as distinct as that in the aforesaid instance. The characteristic values are within the range of those values indicated by Ehlbeck in /23/ for laminae with and without key-dovetail connection only with quality grade I and strength grade I.

The experimental values for the flexural and tensile strength are being classified in compliance with characteristic values according to Annex 2 of the Eurocode 5.

Key-dovetail connections are in part reducing the strength considerably.

As a rule, key-dovetailed timber must therefore be grouped into a category being inferior by one grade (see Figure 9).

Flexural strength of glued laminated timber:

Hitherto, 3 sorts of glued laminated timber are existing. The individual layers of boards are being sorted visually (see BSH 1 to BSH 3 in Table 11, with BSH meaning glued laminated timber). For the future, in the GDR there will be 3 additional sorts of glued laminated timber with which the layers of boards will be sorted mechanically.

The flexural strength of glued laminated timber is illustrated in Figure 10.

The increased characteristic strengths for mechanically sorted glued laminated timber must be attributed to the fairly insignificant scatterings with small quantities of test specimens. A distinct difference in strength can also be found as between glued laminated timber beams without key-dovetail connection in the external zone and those with key-dovetail connection in the external zone.

An allocation to the strength grades indicated in Table A 2.1 of the Eurocode is being accomplished in Figure 10 as well.

Flexural strength of glued laminated timber subject to the girder depth:

(a) mechanically sorted glued laminated timber girders

With regard to the still somewhat obscure connection between cross-sectional height and flexural strength with mechanically sorted glued laminated timber girders, experimental studies and investigations were carried out. For this purpose, 12 girders each of "M 3"-type glued laminated timber with a cross-sectional height of 192, 288 and 608 mm have been produced and tested.

All test specimens were provided with key-dovetail connections in the test zone since during the production glued laminated timber girders without key-dovetail connections in the outside layer are hardly being manufactured.

From the values according to Figure 11 one can see that up to a height (depth) of 608 mm the characteristic strength is not decreasing. Also the mean values for the modulus of elasticity which are required for the limit state of the usability are not decreasing up to depths of 608 mm.

(b) visually sorted glued laminated timber girders

In addition to the studies and investigations as mentioned in para (a) hereinbefore, previous investigations performed with visually sorted glued laminated timber girders have been evaluated. Up to a depth of 800 mm the characteristic value is not decreasing. Only at a depth of 992 mm the characteristic value will be diminished by 6 %. The mean value of the modulus of elasticity is not decreasing over the girder depth.

Schöne /21/ has accomplished investigations into the influence of the girder depth on the flexural strength of glued laminated timber beams. As a result of the tests using beams without key-dovetail connection, the power function which is taken as a basis in the Swiss Code SIA 164 was being verified as a tendency.

However, with key-dovetail connections existing in the test zone no influence can be determined. In the case of such girders, the strength of the key-dovetail connection is of a decisive significance for the maximum carrying capacity (bending strength) of the beam. The mean bending failure strength is only slightly larger than the mean value of the tensile strength of the key-dovetail connection which is statistically covered by a great number of tests /21/. From the point of view of the actual production with average board lengths of about 2 m, the application of a depth-dependent factors seems to be unjustified /21/.

Flexural strength of glued laminated timber subject to the moisture of timber:

The influence of the moisture on the flexural strength should be studied for a timber moisture of $\omega \geq 15$ %. The tests have been carried out by using mechanically sorted "M 3"-type glued laminated timber with key-dovetail connections in the test zone (cross section: $h = 192$ mm; $b = 97$ mm).

The investigations and tests covered the influence for $w \leq 15 \%$, $w = 18 \%$ and $w = 24 \%$. The timber moisture of $w \geq 18 \%$ has been achieved by storing the glued laminated timber girders in the humid room. A typical moisture distribution is illustrated in Figure 12. It can be seen that after 146 days of storage with a climate of $T = 20^\circ \text{C}$. and $\varphi = 95 \%$ only the boundary zones are containing the required timber moisture of $u = 24 \%$. As for the timber moisture of both 18% and 24% , 12 beams each have been tested.

However, in the heart the timber moisture is about 18% . Figure illustrates that up to a timber moisture of $w \leq 18 \%$ no decrease of the characteristic strengths is occurring. Only with $w \geq 24 \%$, the strength is being reduced by 7% .

The mean values of the modulus of elasticity in bending are decreasing with an increasing timber moisture (see Figure 13).

2.3.4. Characteristic Strengths

Table 12 shows the characteristic strengths as well as the mean moduli of elasticity and shear moduli G for visually and mechanically sorted structural timber and glued laminated timber. The values are largely corresponding to the strength grades of the Eurocode 5.

2.3.5. Factor for Considering the Moisture Content and the Load Action Period

The factor being applied to take the moisture content and the load action period into consideration corresponds to the value included in the Eurocode 5 /5/ (see Table 13).

2.3.6. Factor for Considering the Action of Aggressive Media

Studies and investigations carried out in the GDR concerning the influence of aggressive media have demonstrated that many chemical agents and substances are exercising a strength-reducing influence and action only in the boundary zone of the timber cross sections (see also /24/). Timber structures are being used in the chemical industry and in agriculture due to their high resistance to che-

mical attacks.

It is recommended to take the action of aggressive substances on timber into consideration by applying a special factor. Said factor is being explained in /25/.

It is being indicated subject to 3 stress degrees and the cross-sectional size. The stress degrees are resulting from the classification or integration of available media (gases, solutions and solids) into ranges of aggressiveness.

With gases and solids, the moisture grade must be taken into consideration when performing the above-mentioned classification (see Tables 74a to 74j').

2.4. Limit States of the Serviceability

Timber has a distinct creep behaviour which must be considered with the calculation of the downward deflections. The magnitude of creep is mainly dependent on the kind of timber, the type of loading, the degree of loading and the environmental influences.

An evaluation of the creep tests and investigations from the publications and of our own test findings resulted in preparing initial proposals as to coefficients of creep of beams subjected to bending (see Table 15). The differences as compared with the Eurocode are insignificant, In the future code, the values of the Eurocode will be taken as a basis.

2.5. Calculation and Dimensioning (Design)

2.5.1. Individual Structural Components

The calculation and dimensioning (design) of individual components is largely corresponding to the proper chapter of the Eurocode 5 /5/. Since no specifications concerning biaxial bending are included in the Eurocode 5 and the CIB Code /4/, this part will be dealt with anew taking into account the applicable TGL 33 135/01 standard specification of the GDR.

(a) tension in the direction of grain, see Figure 74

(b) tension rectangularly to the direction of grain, see Figure 74

- (c) compression in the direction of grain, see Figure 15
- (d) compression at an angle to the direction of grain, see Figure 15
- (e) bending, uniaxial, see Figure 16
- (f) bending, biaxial, see Figure 16
- (g) shear / solid timber girder, see Figure 17
- (h) shear / glued laminated timber girder, see Figure 17
- (i) combined stresses, see Figure 18
- (j) compressed members, see Figure 19a, 19b, 19c

Since hitherto the creep influence of the timber has been left out of consideration in the stability check calculation for compression members (see Figure 19a), special tests and investigations were carried out at the Wismar College of Technology and a proposal for the calculation of compression members was elaborated.

The procedure (approach) comprises the stress calculation according to the second-order theory at the pre-deformed member with an increase in buckling due to flexural creep for a period of 50 years (see Figure 20).

Different stability checks have been compared with one another by plotting the stresses from the characteristic standard values of the loads $\sigma_{c,0,k}$ subject to the coefficient of slenderness λ (see Figure 21).

Results:

- Curve 1 comprises the ω -approach according to the GDR Code TGL 33 135/01 /19/
- Curve 2 comprises the second-order theory according to the Eurocode 5 /5/ or Figure 19a, respectively
- Curve 3 comprises the second-order theory according to the SNiP Code /16/
- Curve 4 comprises the second-order theory considering the creep influence according to the Wismar College of Technology /14/.

The investigations are being accomplished for sawn structural timber of the quality grade II or the strength grade C 5, respectively. The ratio of loading selected concerning the permanent load to the total load is 85 %. The mean load factor $\gamma_{G,Q}$ for this is 1.145. For the sawn structural timber, the related eccentricity of $\eta = 0.006$ and the material factor of $\gamma_m = 1.4$

have been selected.

For the load action period grade "long", the modification factor is $K_{mod} = 0.8$ /5/.

When looking at the developments as plotted in Figure 21, one will see that above $\lambda = 100$ the curves according to the Eurocode (curve 2) and according to the SNI Code (curve 3) are almost coinciding with the ω -approach (curve 1).

Below $\lambda = 100$, the curves 2 and 3 are more considerably deviating or shifting towards the top which thus means that they are comprising a higher loadbearing capacity (stress acceptance) than the ω -approach according to curve 1.

Due to taking the creep influence into consideration, above $\lambda = 30$ the curve 4 is located below the ω -approach curve 1 and is consequently comprising a lower loadbearing capacity.

As compared with all other approaches, the design method with the creep influence (curve 4) is the most real one; however, it involves an increased material consumption as compared with the ω -approach (curve 1).

Since no failure cases have transpired from the construction practice in connection with the application of the ω -approach over longer periods of time, the exact method (curve 4) is being dispensed with and the stability check according to the Eurocode 5 (curve 2) is being accepted.

2.5.2. Composite Structural Components

(Figure 23 to 28)

Glued thin-webbed girders and stiffened sheets (plates) are being dealt with separately in Part 3 of the Draft Code.

Composite (i.e. built-up) compression members with a T, I or box section as well as frame and lattice members are being calculated and dimensioned according to the CIB Code /4/, pp. 55-65, taking into consideration the TGL 33 135/01 Code, pp. 14-18.

In the case of composite components with mechanical connecting means (fasteners), the calculation of the effective moment of inertia I_{ef} is being accomplished according to the CIB Code /4/, p. 57, whereas the proper modulus of displacement (translation) K is being calculated according to the Eurocode 5 /5/, p. 77 (see Figure 23).

The calculation of bracings and plane frames according to the Eurocode 5 /5/ is being prepared for the practical utilization. With regard to "bracings", see the Figure 28.

2.5.3. Connections

The check calculation of connecting means (fasteners) according to the Eurocode 5 is being improved taking into account the TGL 33 135/01 Code.

Figures 29 to 37 comprises an indication of the check for nails. Bolts, dowels, wood screws, hexagonal bolts, special dowels etc. are being dealt with analogously (see Figure 32 to 36).

3. Summary

To sum up, it can be stated that the calculation and design of structures made of structural timber and glued laminated timber are being accomplished to a great extent according to the Eurocode 5 taking into account the national particularities as included in the TGL 33 135/01 Code. With a view to facilitating the practical application of the check conditions and specifications, the formulae and factors extracted from the Eurocode 5 must still be handled and prepared to render them favourable for the application.

4. References (Publications)

- /1/ Rug, W.; Badstube, M.:
New Developments of Limit State Design for the New GDR Timber Design Code; Academy of Building of the GDR; W 18 Paper 19-102-4; Florence, 1986.
- /2/ Rug, W.; Badstube, M.:
Developments of a GDR Limit States Design Code for Timber Structures; Academy of Building of the GDR, Institute for Industrial Buildings; CIB W 18 Paper 20-102-1; Dublin, 1987.
- /3/ Rug, W.; Badstube, M.:
Research Towards a New GDR Timber Design Code Based on Limit States Design; Academy of Building of the GDR, Institute for Industrial Buildings; CIB W 18 Paper 21-102-1; Vancouver, 1988

- /4/ CIB Structural Timber Design Code, CIB Report 1983, Publication of Working Group W 18, Timber Structures, Sixth Edition, January 1983.
- /5/ Crubile, P.; Ehlbeck, J.; Brünninghoff, H.; Larsen, H.J.; Sunley, J.: 1987
Eurocode 5, Gemeinsame einheitliche Regeln für Holzbauwerke (Entwurf), Bericht für die EG
(Eurocode 5, Common Uniform Rules for Timber Structures (Draft), Report for the European Community)
- /6/ GDR Code:
TGL 32274; Lastannahmen für Bauwerke; Ausgabe Mai 1979
(TGL...; Design Loads for Structures; Edition of May 1979) - Publishers: Verlag für Standardisierung, Leipzig/GDR.
- /7/ GDR Specification No. 207/88 of the State Construction Supervision Authority: Wertigkeitsfaktoren bei der Berechnung nach Grenzzuständen (Valency Factors in the Calculation by Limit States) - Bulletin of the State Construction Supervision Authority 12 (1988) No. 7, pp. 53-56.
- /8/ GDR Code:
TGL 117-0767, 1963; Bauschnittholz, Gütebedingungen (TGL...; Sawn Structural Timber, Quality Specifications)
- /9/ GDR Code:
TGL 33 135/03, Entwurf 1988; Holzbau, Tragwerke, Gütebedingungen für Bauschnittholz (TGL..., Draft of 1988; Timber Construction, Loadbearing Systems, Quality Specifications for Sawn Structural Timber)
- /10/ FRG Code:
DIN 4074, 1958: Bauholz für Holzbauteile
(DIN...: Structural Timber for Timber Components)
- /11/ FRG Code:
DIN 4074, Entwurf September 1988: Gütebedingungen für Nadel-schnittholz, Sortierung nach der Tragfähigkeit
(DIN..., Draft of September 1988: Quality Specifications for Sawn Coniferous Timber, Sorting acc. to the Loadbearing Capacity) - Published in: Bauen mit Holz (1988) 11, pp. 767-772.
- /12/ GDR Code:
TGL 33 136/01, Januar 1987: Holzbau, Bauteile aus Brettschichten geklebt; Technische Bedingungen
(TGL...dated Jan. 1987: Timber Construction, Components Made of Glued Laminated Timber; Technical Specifications)
- /13/ GDR Code:
TGL 33 136/02, November 1978: Holzbau, Bauteile aus Brettschichten geklebt; Qualitätssicherung bei der Herstellung
(TGL...dated Nov. 1978: Timber Construction, Components Made of Glued Laminated Timber; Quality Control in the Production)

- /14/ Kaiser, K.:
Beitrag zur Bemessung von knickgefährdeten Holzbauteilen nach der Methode der Grenzzustände
(Paper on the Design of Timber Components Exposed to the Risk of Buckling by the Limit States Method)
Research Report G 4 of the Wismar College of Technology; Wismar, 1988.
- /15/ GDR Code:
TGL 33 135/01: Holzbau, Tragwerke, Berechnung, Bauliche Durchbildung
(TGL...: Timber Construction; Loadbearing Systems, Calculation, Structural Design) - January, 1984.
- /16/ USSR Code:
SNiP II-25-80: Baunormen und Bauvorschriften; Projektierungsnormen, Holzkonstruktionen
(SNiP...: Construction Standards and Building Regulations; Planning and Design Standards, Timber Structures) - Moscow, 1982.
- /17/ Lisner, K.:
Zum Nachweis der Tragfähigkeit von Verbindungsmitteln nach Grenzzuständen im Holzbau
(On the Check of the Loadbearing Capacity of Connecting Means by Limit States in Timber Construction)
Research Report G 4 of the Dresden University of Technology; Dresden, 1988.
- /18/ Larsen, H.J.:
Eurocode 5, Timber Structures; CIB W 18/18-1-2, Meeting Eighteen; Oren, June 1985.
- /19/ GDR Code:
TGL 33 135/01 and /02: Holzbau, Tragwerke, Berechnung, Bauliche Durchbildung
(TGL...: Timber Construction; Loadbearing Systems, Calculation, Structural Design) - Leipzig, 1984.
- /20/ Aplitz, R.:
Beitrag zur Bestimmung der Festigkeitskennwerte von Bauholz bei Biegebeanspruchung für die Bemessung nach der Methode der Grenzzustände
(Paper on the Determination of the Strength Characteristics of Structural Timber with Flexural Load for the Design by Adopting the Limit States Method) - Wismar College of Technology, Type A Thesis; Wismar, 1985.
- /21/ Schöne, W.:
Der Einfluß der Trägerhöhe auf die Biegefestigkeit von Brett-schichtholz
(The Influence of the Girder Depth on the Flexural Strength of Glued Laminated Timber)
Scientific Journal of the Leipzig College of Technology; Leipzig, 1989 - under preparation --.

- /22/ Larsen, H.J.:
Proposed Changes of Sections on Lateral Instability,
Columns and Nails;
CIB-W 18/21-100-1, Meeting Twenty-One; Vancouver/Canada,
September 1988.
- /23/ Ehlbeck, J.; Colling, F:
The Strength of Glued Laminated Timber - Influences of La-
mination Qualities and Strength of Timber Joints;
CIB-W 18 Paper 21-12-3; Meeting Twenty-One; Vancouver, 1988.
- /24/ Erler, K.; Rug, W.:
Modification Factor "Aggressive Media" - A Proposal for a
Supplement of CIB-Model-Code;
CIB-W 18, Meeting Twenty-Two; Berlin (GDR), 1989.
- /25/ Erler, K.:
Corrosion and Modification Factor "Aggressive Media" in
Timber Structures;
CIB-W 18, Meeting Twenty-Two; Berlin (GDR), 1989.
- /26/ Kiesel, :
Beitrag zur Ermittlung der Verteilungsfunktion der Festig-
keitseigenschaften des Bauholzes unter besonderer Berücksich-
tigung des Festigkeitsverhaltens bei der Druckbeanspruchung
für eine Bemessung nach Grenzzuständen
(Paper on the Determination of the Distribution Function of
the Strength Properties of Structural Timber with Particular
Consideration of the Strength Behaviour under Compressive
Stress for a Limit States Design)
Wismar College of Technology; Research Report; Wismar, 1988.

Compression in the direction of grain
(without buckling risk)

$$\sigma_{c,o,d} \leq f_{c,o,d}$$

Compression at an angle to the direction of grain

- $\alpha = 90^\circ$: $\sigma_{c,90,d} \leq K_{c,90} \cdot f_{c,90,d}$

- $\alpha =$ at random:

$$\sigma_{c,\alpha,d} \leq f_{c,o,d} - (f_{c,o,d} - f_{c,90,d}) \sin \alpha$$

- deformation:

$$u = K_{u,90} \cdot \frac{\sigma_{c,90,d}}{E_{90,mean}} \cdot h$$

Meanings:

$K_{c,90}$ factor taking into account the influence of the amount of loading l on the strength, acc. to /5/, table 5.1.5.

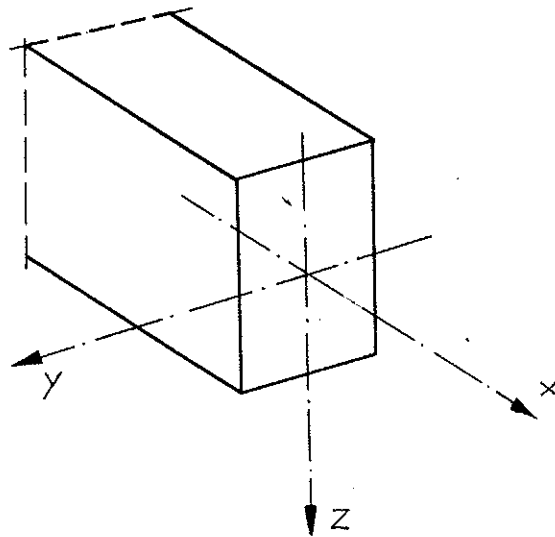
$K_{u,90}$ deformation coefficient acc. to /5/, (5.1.5. c and d)

Figure 15: Calculation of individual components, compression

Bending

- uniaxial: $\sigma_{m,d} \leq K_{inst} \cdot f_{m,d}$

- biaxial: $\sigma_{m,d,y} + \sigma_{m,d,z} \leq K_{inst} \cdot f_{m,d}$



Meanings:

K_{inst} factor taking into account the influence of the lateral deflection (tilting) on the loadbearing capacity, acc. to /5/, (5.1.6. c to e)

λ_m tilting slenderness degree acc. to /5/, (5.1.6. b and f)

Figure 16: Calculation of individual components; bending

Shear due to transverse force

- for solid timber girders and glued laminated timber girders with a volume of $V \leq 0.1 \text{ m}^3$:

$$\tau_d \leq K_V \cdot f_{V,d}$$

- for glued laminated timber girders with $V > 0.1 \text{ m}^3$:

$$Q_d \leq K_V \cdot K_{vd,V} \cdot K_{dis,V} \cdot K_l \frac{4}{3} \cdot b \cdot h \cdot f_{V,d}$$

Meanings:

K_V factor taking into account the influence of the stress concentration due to disengaging (notching) on the strength, acc. to /5/, (5.1.7.1 c to e)

$K_{vd,V}$ factor taking into account the size of the stressed volume V on the strength, acc. to /5/, (5.1.7.2 c)

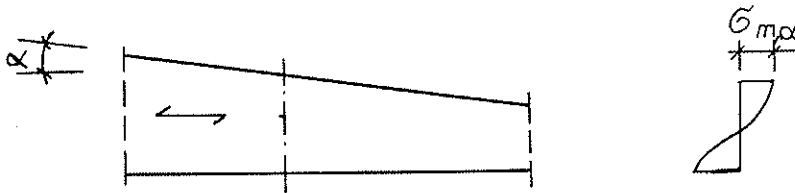
$K_{dis,V}$ factor taking into account the influence of the transverse force distribution on the strength, acc. to /5/, (5.1.7.2 d)

K_l factor taking into account the influence of the girder length l on the strength, acc. to /5/, (5.1.7.2 b)

Shear due to torsion

$$\tau_{tor,d} \leq 1.2 \cdot f_{V,d}$$

Figure 17: Calculation of individual components; shear

Girder with a variable depth

- tension at the angle α to the direction of grain:

$$\sigma_{m,\alpha,d} \leq k_{t,\alpha} \cdot f_{m,d}$$

- compression at the angle α to the direction of grain:

$$\sigma_{m,\alpha,d} = k_{c,\alpha} \cdot f_{m,d}$$

Meanings:

$k_{t,\alpha}$ conversion factor in the case of a rectangular cross section, acc. to /5/, (5.1.9 a)

$k_{c,\alpha}$ conversion factor in the case of a rectangular cross section, acc. to /5/, (5.1.9 b)

Tension and bending

$$\frac{\sigma_{t,o,d}}{f_{t,o,d}} + \frac{\sigma_{m,d}}{f_{m,d}} \leq 1$$

Compression and bending

(without buckling risk)

$$\frac{\sigma_{c,o,d}}{f_{c,o,d}} + \frac{\sigma_{m,d}}{f_{m,d}} = 1$$

Shear due to torsion and transverse force

$$\left(\frac{\tau_d}{f_{v,d}}\right)^2 + \frac{\tau_{tor,d}}{1.2 f_{v,d}} = 1$$

Figure 18: Calculation of individual components;
combined stresses

Stability check calculation

$$\frac{1}{K_c} \cdot \frac{\sigma_{c,o,d}}{f_{c,o,d}} + \frac{1}{K_m} \cdot \frac{\sigma_{m,d}}{f_{m,d}} \leq 1$$

Meanings:

K_c buckling coefficient acc. to /5/, (5.1.10 g)

K_m buckling coefficient acc. to /5/, (5.1.10 d)

Explanation concerning K_c , K_m

K_c and K_m are being calculated only for the strength class C 5!

In compliance with and by means of /5/, tables A 2.1 a and A 2.3 b it results as follows:

$$f_{m,k} = 24 \frac{N}{mm^2} \quad \frac{E_{o,k}}{f_{c,o,k}} = 340$$

$$f_{c,o,k} = 21.5 \frac{N}{mm^2} \quad \eta = 0.006$$

The following applies to the limit slenderness λ_G :

$$\sigma_{eu,k} = f_{c,o,k} = \frac{\pi^2 \cdot E_{o,k}}{\lambda_G^2}$$

$$\text{thus resulting therefrom: } \lambda_G = \pi \cdot \sqrt{\frac{E_{o,k}}{f_{c,o,k}}} = 57.9 \sim 58.$$

The following applies to the slenderness :

$$\sigma_{eu,k} = \frac{\pi^2 \cdot E_{o,k}}{\lambda^2}$$

$$K_{eu} = \frac{\sigma_{eu,k}}{f_{c,o,k}} = \left(\frac{\lambda_G}{\lambda} \right)^2 = \left(\frac{58}{\lambda} \right)^2$$

$$K_m = 1 - \frac{K_c}{K_{eu}} \cdot \frac{\sigma_{c,o,d}}{f_{c,o,d}} = 1 - K_c \left(\frac{\lambda}{58} \right)^2 \cdot \frac{\sigma_{c,o,d}}{f_{c,o,d}}$$

Figure 19a: Calculation of individual components;
compressed members

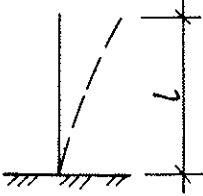
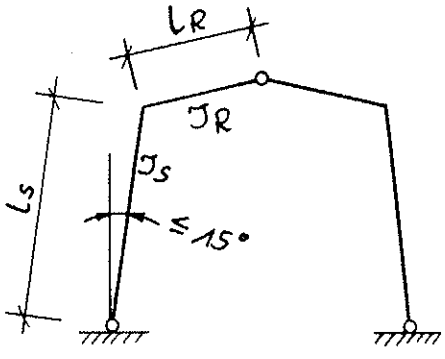
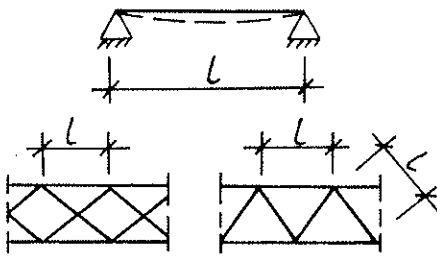
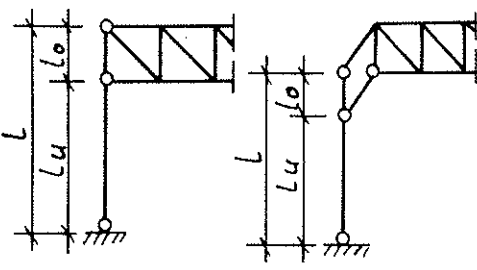
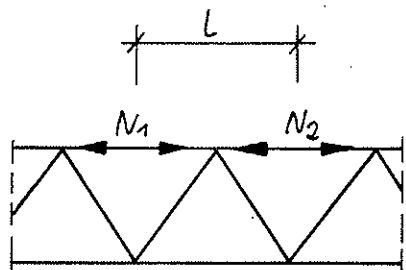
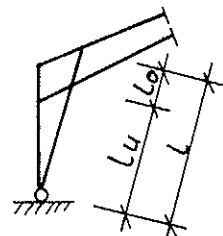
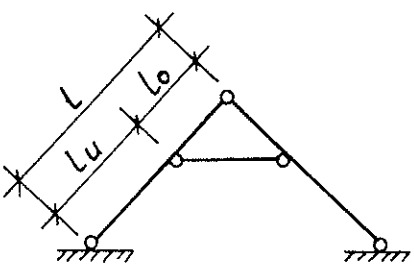
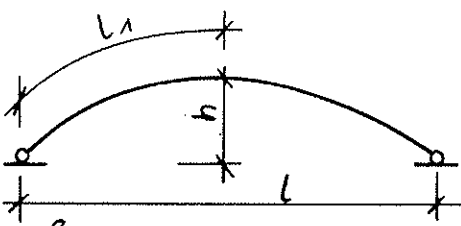
static (stability) system	β	static (stability) system	β
	2		$\sqrt{4 + 3,2 \frac{J_s}{J_R} \cdot \frac{L_R}{L_S}}$
	1	 <p>for $l_0 \leq l_u$</p>	$2 - 1,3 \frac{l_0}{l}$
	$0,75 + 0,25 \cdot \frac{N_2}{N_1}$	 <p>Inner frame corner - laterally supported $l_{crit} = l_u, l_0$ - not laterally supported $l_{crit} = l$</p>	
 <p> $l_u < 0,7L: 0,8$ $l_u \geq 0,7L: 1$ </p>		 <p>for $0,15L \leq h \leq 0,5L$</p>	1,25

Figure 19b: Calculation of individual components; buckling length coefficients β acc. to 1/13/

Compression

$$\sigma_{c,o,d} \leq K_{c,1} \cdot f_{c,o,d}$$

Compression with bending

$$\frac{\sigma_{c,o,d}}{K_{c,1} \cdot f_{c,o,d}} + \frac{\sigma_{m,d}}{f_{m,d}} \leq 1$$

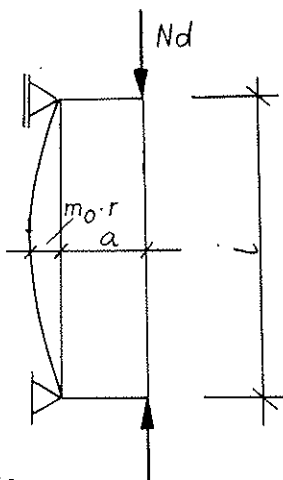
Meanings:

$K_{c,1}$ compression factor acc. to /22/ (5.1.7 b-c)

Figure 19c: Calculation of individual components; columns

Stability check calculation:

$$(1 + m \cdot \eta_{crit} \cdot K_{\varphi}) \cdot \frac{N}{A} \leq f_{c,o,d}$$



Meanings:

m amount of eccentricity $m = m_0 + \frac{M \cdot A}{N \cdot W}$

m_0 random eccentricity $m_0 = 0.1 + \frac{\lambda}{K_0}$

K_0 factor, $K_0 = 140$ for structural timber of the strength class C 5 with a rectangular or square cross section

M moment increasing the random eccentricity
 $M = N \cdot a$

η_{crit} enlargement factor $\eta_{crit} = \eta_{crit} \left(\frac{\sigma_{eu,d} \cdot A}{N_d} \right)$

$\sigma_{eu,d}$ Euler's stress $\sigma_{eu,d} = \frac{\pi^2 \cdot E_{o,d}}{\lambda^2}$

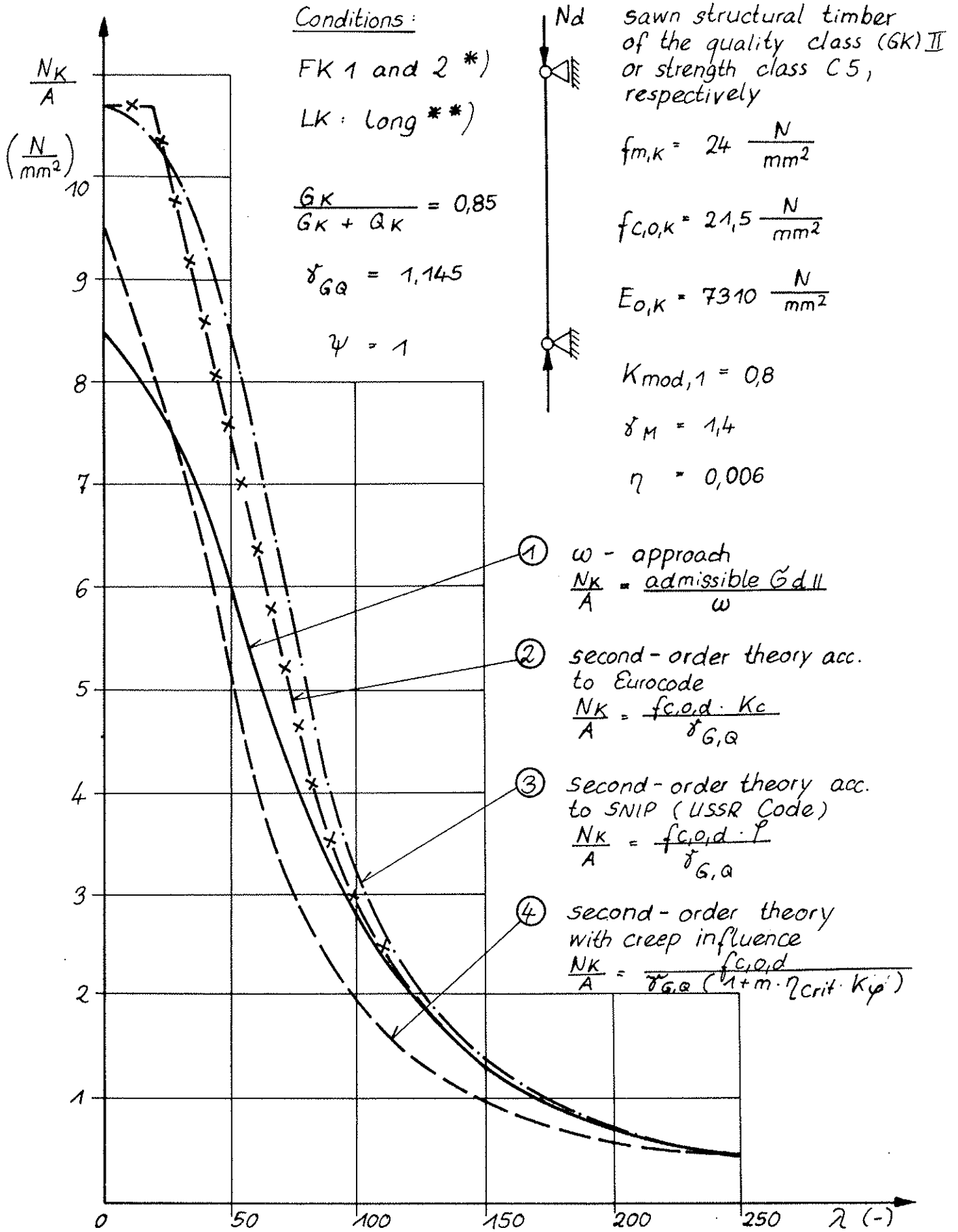
K_{φ} long-term factor $K_{\varphi} = K_{\varphi} \left(\frac{\sigma_{eu,d} \cdot A}{N_{G,d}} \right)$

$N_{G,d}$ permanent compressive force (stress)

r heart (core) dimension

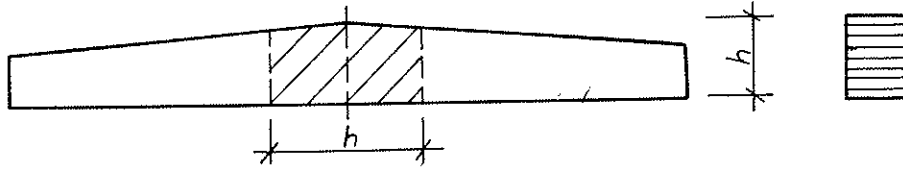
$E_{o,d}$ design value $E_{o,d} = \frac{E_{o,k} \cdot K_{mod,1}}{\gamma_M}$

Figure 20 : Method for the design of compressed members being exposed to a buckling risk by adopting the second-order theory with creep influence acc. to / 13 /



*) FK = moisture class **) LK = Load action period class

Figure 21: Comparison of different stability check calculations



Bending: $\sigma_{m,d} \leq f_{m,d}$

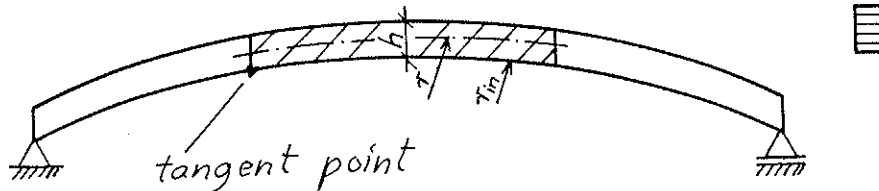
Tension perpendicular to the grain:

$$\sigma_{t,90,d} \leq K_{vol} \cdot K_{dis} \cdot f_{t,90,d}$$

Meanings:

- K_{vol} volume factor acc. to /5/, (5.1.11 g)
- K_{dis} distribution factor acc. to /5/, (5.1.11 h and i)
- $\sigma_m, \sigma_{t,90}$ stresses acc. to /5/, (5.1.11 e and f)

Arched girder



Bending: $\sigma_{m,in,d} \leq K_r \cdot f_{m,d}$

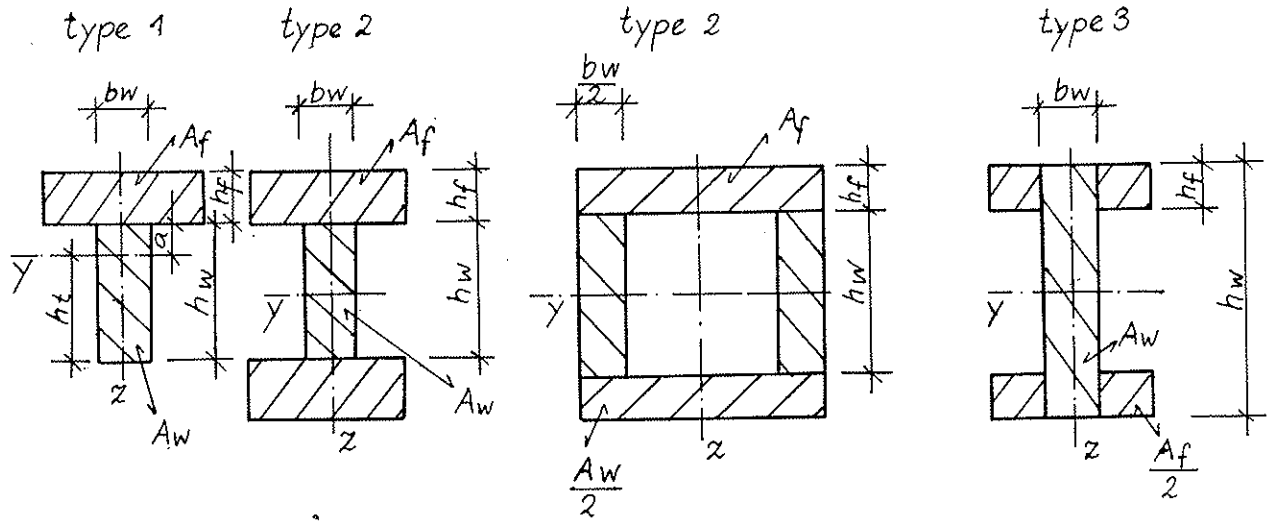
Tension perpendicular to the grain:

$$\sigma_{t,90,d} \leq K_{vol} \cdot K_{dis} \cdot f_{t,90,d}$$

Meanings:

- K_r factor of curvature acc. to /5/, (5.1.12 b and e)
- K_{vol} volume factor acc. to /5/, (5.1.12 i)
- K_{dis} distribution factor acc. to /5/, (5.1.12 j and k)
- $\left. \begin{matrix} \sigma_{m,in,d} \\ \sigma_{t,90,d} \end{matrix} \right\}$ stresses acc. to /5/, (5.1.12 d and h)

Figure 22: Calculation of individual components; saddle roof girder and arched girder



$$I_{ef} = I_0 + \gamma (I_{tot} - I_0)$$

Meanings:

- I_{ef} effective moment of inertia about the Y-axis
- I_0 sum of the inherent moments of inertia
- I_{tot} total moment of inertia
- γ efficiency factor

$$\gamma = \frac{1}{1 + \frac{\pi^2 A_f \cdot E}{l^2 \cdot K} \cdot s}$$

- A_f flange cross-sectional area
- E modulus of elasticity
- l effective span
- s spacing of the timber fasteners pushed into one row
- K modulus of displacement acc. to /5/, page 77

Figure 23 : Calculation of built-up (composite) components; cross sections with mechanical timber fasteners

Bending:

In this connection,

- the check calculation conditions acc. to Figure 16, and
 - the cross section values acc. to Figure 23
- are applicable.

Meanings:

$\sigma_{m,d}$ design value of the stress
For cross sections of the types 1 to 3 acc. to /4/,
(71.5 - 13)

For type 1:
$$\sigma_{m,d} = |\sigma_{w,ult,d}| = \frac{M_d}{J_{ef}} \cdot h_t$$

For types 2 and 3:
$$\sigma_{m,d} = |\sigma_{w,ult,d}| = \frac{M_d}{J_{ef}} \cdot \frac{h_w}{2}$$

$f_{m,d}$ design value of the strength

$$f_{m,d} = \frac{f_{m,K} \cdot K_{mod,i}}{\gamma_M}; \quad i = 1, 2$$

$f_{m,K}$ characteristic value of the strength acc. to /5/,
table A 2.1 a

$K_{mod,1}$ modification factor acc. to /5/, table 3.1.3.

γ_M material factor acc. to /5/, table 2.3.3.

Figure 24 : Calculation of built-up components; bending

Maximum shear

In this connection,

- the check calculation conditions acc. to Figure 17, and
- the cross section values acc. to Figure 23 are applicable.

Meanings:

τ_d design value of the stress

For type 1 cross section:

$$\tau_d = \max \tau_d = \frac{V_d h_t^2}{2 \cdot J_{ef}}$$

For type 2 cross section:

$$\tau_d = \max \tau_d = \frac{V_d}{J_{ef} \cdot bw} \left(\gamma \cdot A_f \frac{(h_w + h_f)}{2} + \frac{1}{8} A_w h_w \right)$$

For type 3 cross section:

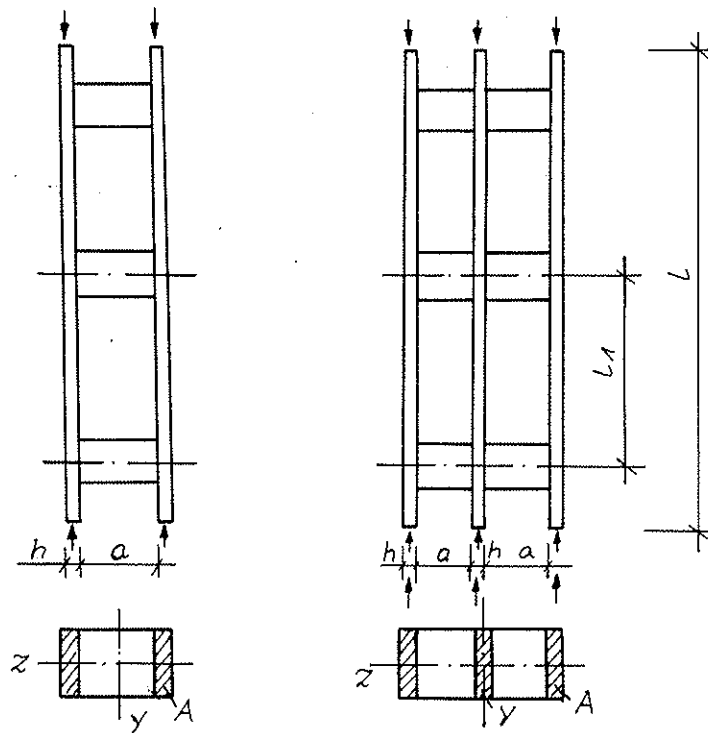
$$\tau_d = \max \tau_d = \frac{V_d}{J_{ef} \cdot bw} \left(\gamma \cdot A_f \frac{(h_w - h_f)}{2} + \frac{1}{8} A_w h_w \right)$$

acc. to /4/ (71.14 - 16)

Figure 25: Calculation of built-up components; shear

$$\text{type 1: } 2 \times \frac{F}{2}$$

$$\text{type 2: } 3 \times \frac{F}{3}$$



$$F_d \leq F_{crit,d}$$

Meanings:

F_d design value of the total compressive load at the spread compressed member

$F_{crit,d}$ design value of the buckling load of the spread compressed member

$$F_{crit,d} = \frac{F_{crit,K}}{\gamma_M} \cdot K_{mod,1}$$

$F_{crit,K}$ characteristic buckling load

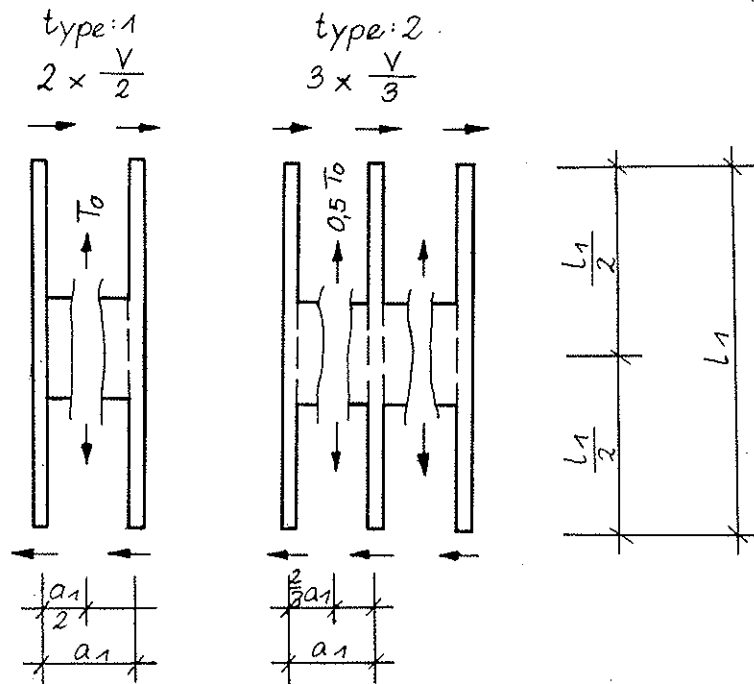
$$F_{crit,K} = K_c \cdot f_{c,0,k} \cdot A_{tot}$$

$$A_{tot} = n \cdot A$$

K_c buckling coefficient acc. to /5/, (5.1.10 g) for λ_{ef}

λ_{ef} effective degree of slenderness acc. to /4/ (72.3)

Figure 26: Calculation of built-up components; spread compressed members



The shear braces must be checked for the following shear forces T according to Figure 16 and Figure 17:

- type 1: $T_d = T_{o,d}$
- type 2: $T_d = 0.5 T_{o,d}$

Meanings:

$T_{o,d}$ design value of the shear force

$$T_{o,d} = \frac{V_d \cdot l_1}{a_1}$$

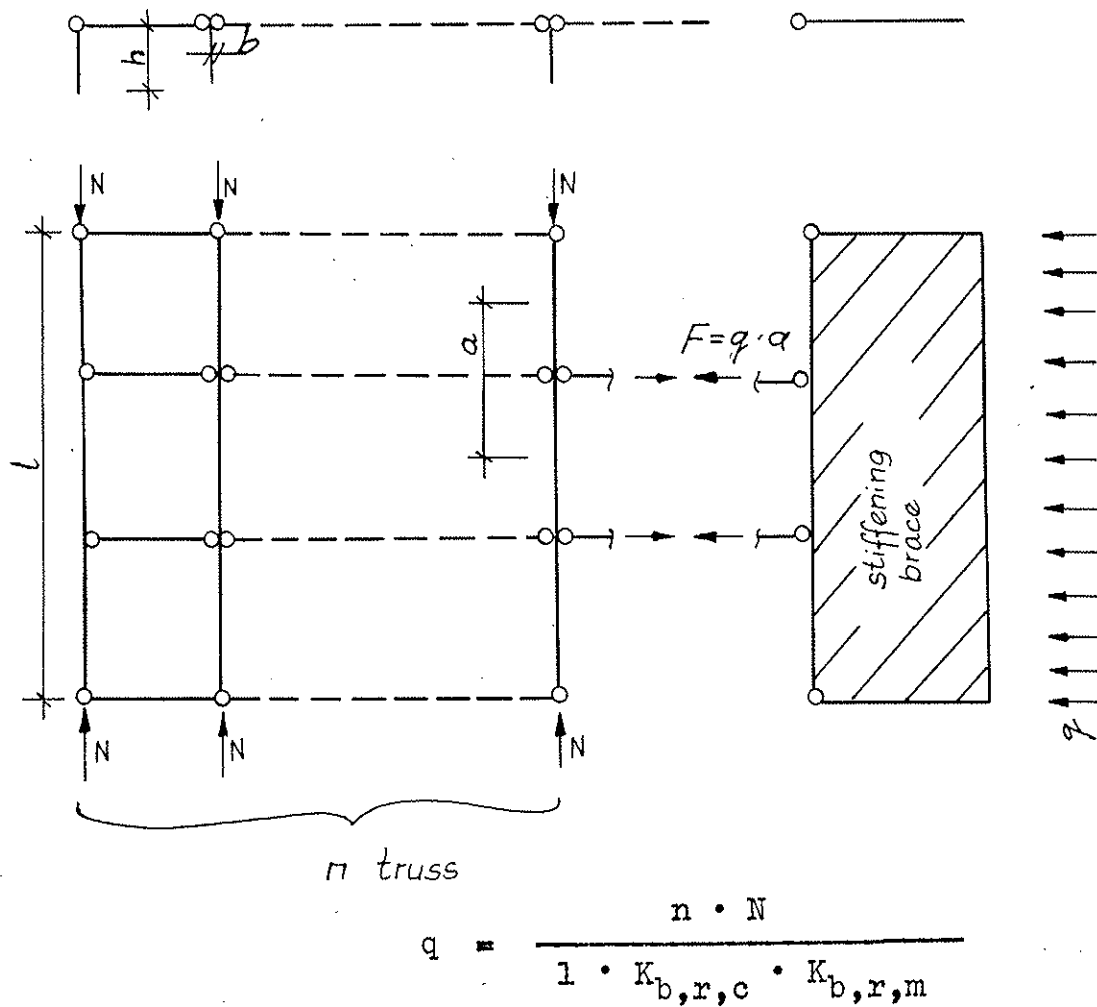
V_d design value of the transverse force

$$V_d = \frac{V_K \cdot K_{mod,1}}{\gamma_M}$$

V_K characteristic value of the transverse force acc. to / 4/ (72.5)

Figure 27:

Calculation of built-up components; spread compressed members



Meanings:

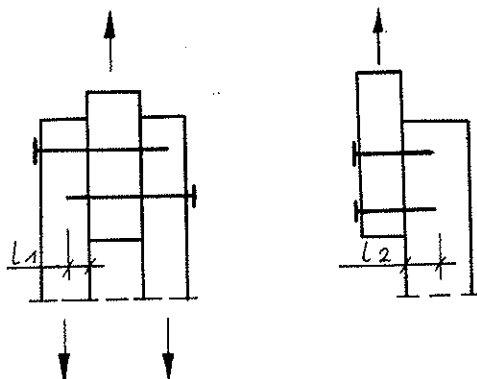
q distributed lateral load per unit of length due to stabilization;
it is acting in addition to the external loads (e.g. wind)

$K_{b,r,c}$ acc. to /5/, (5.2.6 b)

$K_{b,r,m}$ acc. to /5/, (5.2.6 g)

Figure 28: Calculation of built-up components; stiffening braces

Nails being stressed perpendicularly to their axis



For each nail:

$$F_{1a,d} \cong R_{1a,d} \quad \text{for connections of timber with timber}$$

$$F_{1a,d} \cong 1.25 R_{1a,d} \quad \text{for connections of sheet steel with timber}$$

Meanings:

$F_{1a,d}$ design value of the loading perpendicular to the nail axis

$R_{1a,d}$ design value of the loadbearing capacity perpendicular to the nail axis

$$R_{1a,d} = \frac{l_i}{\min l_1} \cdot \frac{R_{1a,K}}{\gamma_M} \cdot K_{\text{mod},1}$$

γ_M material factor acc. to /17/

l_i depth of penetration

$\min l_1$ minimum depth of penetration

- for round nails: $\min l_2 = 6 d$

- for grooved and threaded nails: $\min l_2 = 4 d$

$K_{\text{mod},1}$ modification factor acc. to /5/, table 3.1.3.

$R_{1a,K}$ characteristic loadbearing capacity perpendicular to the nail axis

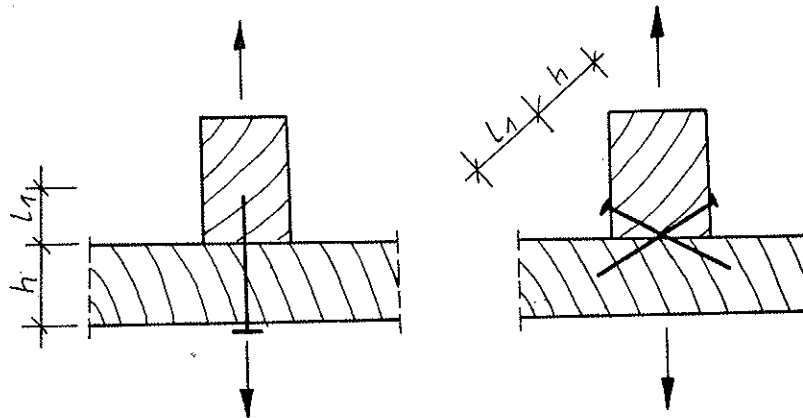
$$R_{1a,K} = K \cdot d^\beta$$

d nail diameter

K, β parameters acc. to /5/, (5.3.2. b and c)

Figure 29: Calculation of timber fasteners; nails

Nails being stressed in the direction of their shank



For each nail: $F_{ax,d} \leq R_{ax,d}$

Meanings:

$F_{ax,d}$ design value of the loading in the direction of shank

$R_{ax,d}$ design value of the loadbearing capacity in the direction of shank

$R_{ax,d} = R_{ax,K}$ for round nails.

Round nails must not be subjected to a long-term loading!

$R_{ax,d} = \frac{R_{ax,K}}{\gamma_M} \cdot K_{mod,1}$ for nails being not round, grooved and threaded nails.

$R_{ax,K}$ characteristic loadbearing capacity in the direction of shank

$R_{ax,K} = 18 \cdot 10^{-6} \cdot \rho^2 \cdot d \cdot h + 300 \cdot 10^{-6} \cdot \rho^2 \cdot d^2$

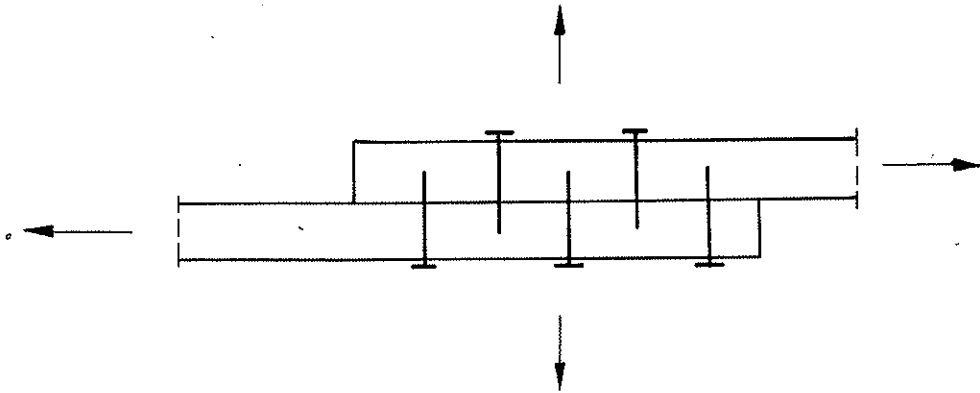
for round nails;

otherwise acc. to /5/, (5.3.3. a,c)

ρ characteristic bulk density (5 %-quantile); kg/m^3

Figure 30: Calculation of timber fasteners; nails

Combined stressing



For round nails:

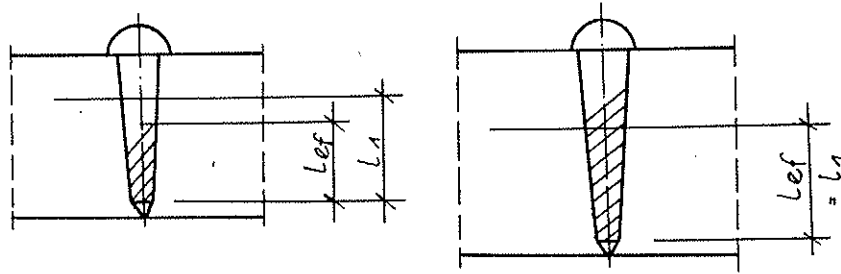
$$\frac{F_{ax,d}}{R_{ax,d}} + \frac{F_{la,d}}{R_{la,d}} \leq 1$$

For grooved and threaded nails:

$$\left(\frac{F_{ax,d}}{R_{ax,d}} \right)^2 + \left(\frac{F_{la,d}}{R_{la,d}} \right)^2 \leq 1$$

Figure 37 : Calculation of timber fasteners; nails

Wood screws being stressed perpendicularly to their axis



For each wood screw: $F_{1a,d} \leq R_{1a,d}$

Meanings:

$F_{1a,d}$ design value of the loading perpendicular to the wood screw axis

$R_{1a,d}$ design value of the loadbearing capacity perpendicular to the wood screw axis

$$R_{1a,d} = \frac{l_1}{\min l_1} \cdot \frac{R_{1a,K}}{\gamma_M} \cdot K_{mod,1}$$

$R_{1a,K}$ characteristic loadbearing capacity perpendicular to the wood screw axis

- acc. to /5/ (5.3.7. a,b) for connections of timber with timber

- acc. to /5/ (5.3.7. d) for connections of sheet steel to timber

l_1 depth of penetration

$\min l_1$ minimum depth of penetration; $\min l_1 = 4 d_1$

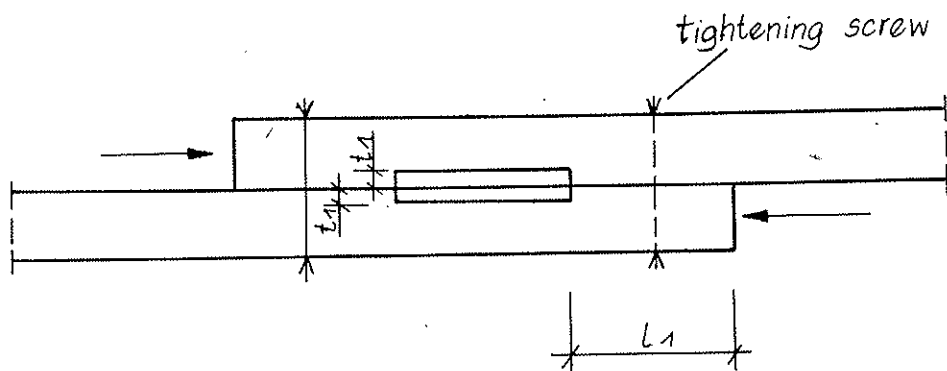
d_1 external thread diameter of the wood screw

γ_M material factor acc. to /17/

$K_{mod,1}$ modification factor acc. to /5/, table 3.1.3.

Figure 32 : Calculation of timber fasteners; wood screws

Stressing in parallel with the flat connector (dowel)



For each flat connector: $F_d \leq R_d$

Meanings:

F_d design value of the loading in parallel with the flat connector

R_d design value of the loadbearing capacity in parallel with the flat connector

$$R_{c,o,d} = \frac{R_{c,o,K}}{\gamma_M} \cdot K_{mod,1} \cdot t_1 \cdot b \quad (1)$$

$$R_{v,o,d} = \frac{R_{v,o,K}}{\gamma_M} \cdot K_{mod,1} \cdot l_1 \cdot b \quad (2)$$

$R_{c,o,K}$ characteristic compression strength of the timber acc. to /17/

$R_{v,o,K}$ characteristic shear strength of the timber acc. to /17/

t_1 depth of penetration of the connector; $t_1 = 15$ mm

l_1 fore-timber length; $l_1 = 8 t_1$

γ_M material factor acc. to /5/

$K_{mod,1}$ modification factor acc. to /5/, table 3.1.3.

Figure 33 : Calculation of timber fasteners; flat connectors

Bolts (studs) and connectors (dowels) being stressed perpen-
dicularly to their axis

(continued)

ρ_K characteristic bulk density (5 %-quantile), kg/m^3
 $t_1 ; t_2$ timber thicknesses, mm
 d bolt (stud) diameter, mm
 $K_{\alpha,1} ; K_{\alpha,2}$ factors taking into account the influence of the
 angle as between force and direction of timber
 grain

$$K_{\alpha,1} ; K_{\alpha,2} = \frac{K_{90}}{K_{90} \cos^2 \alpha + \sin^2 \alpha}$$

$$K_{90} = 0.32 + 10 \cdot d^{-1.5}$$

γ_M material factor acc. to /17/
 $K_{\text{mod},1}$ modification factor acc. to /5/, table 3.1.3.

(b) Connections of sheet steel with timber

Lateral steel butt straps:

R_K is to be calculated with $t_1 = t_2 =$ timber thickness

Central steel butt strap:

R_K is to be calculated acc. to /5/ (5.3.5. d-f), (5.3.5. f)
 to be multiplied by 1.4

Figure 34 : Calculation of timber fasteners;
 bolts (studs) and connectors (dowels)

Wood screws being stressed in the direction of their shank

For each wood screw:

$$F_{ax,d} \leq R_{ax,d}$$

Meanings:

$F_{ax,d}$ design value of the loading in the direction of shank

$R_{ax,d}$ design value of the loadbearing capacity in the direction of shank

$$R_{ax,d} = \frac{R_{ax,K}}{\gamma_M} \cdot K_{mod,1}$$

$R_{ax,K}$ characteristic loadbearing capacity in the direction of shank

$$R_{ax,K} = (1.5 + 0.6 d) \sqrt{\rho_K} (l_{ef} - d)$$

l_{ef} effective length of thread (within the timber component to be attached)

d screw shank diameter, mm

ρ_K characteristic bulk density (5 %-quantile), kg/m^3

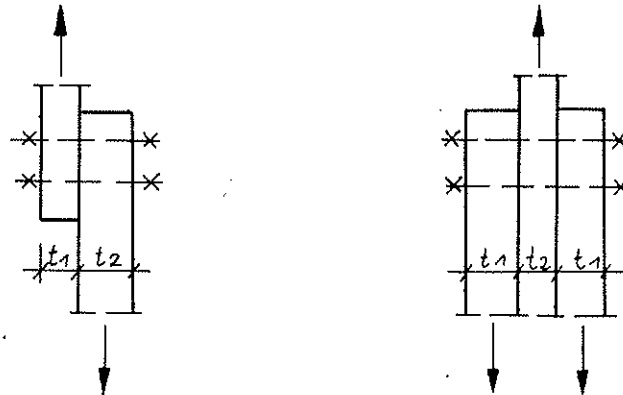
γ_M material factor acc. to /17/

$K_{mod,1}$ modification factor acc. to /5/, table 3.1.3.

Figure 35 : Calculation of timber fasteners; wood screws

Bolts (studs) and connectors (dowels) being stressed perpendicularly to their axis

(a) Connections of timber with timber



For each bolt and/or connector: $F_d \leq R_d$

Meanings:

F_d design value of the loading perpendicular to the bolt (stud) axis

R_d design value of the loadbearing capacity perpendicular to the bolt (stud) axis

$$R_d = \frac{R_K}{\gamma_M} \cdot K_{mod,1}$$

R_K characteristic loadbearing capacity perpendicular to the bolt (stud) axis acc. to /5/, (5.3.5. b-f)

For single-shear timber fasteners:

$$R_K = 0.2 \cdot f_{b,K} (K_{\alpha,1} t_1 + K_{\alpha,2} t_2) d$$

$f_{b,K}$ bolt-bearing property (pressure):

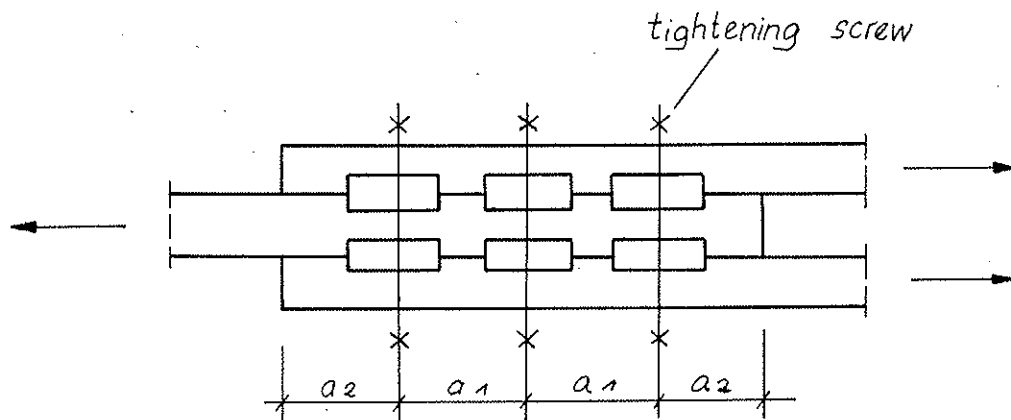
$$f_{b,K} = 0.075 \rho_K \text{ (MPa)}$$

connector-bearing property (pressure):

$$f_{b,K} = 0.09 \rho_K \text{ (MPa)}$$

(to be cont'd.)

Special connectors being stressed perpendicularly to their axis



For each special connector:

$$F_d \leq R_d$$

in connection with structural requirements concerning the amount of \min^A, d, a_1, a_2

Meanings:

F_d design value of the loading perpendicular to the axis of the special connector

R_d design value of the loadbearing capacity perpendicular to the axis of the special connector

$$R_d = \frac{R_K}{\gamma_M} \cdot K_{\text{mod},1}$$

R_K characteristic loadbearing capacity perpendicular to the axis of the special connector, acc. to /5/

γ_M material factor acc. to /17/

$K_{\text{mod},1}$ modification factor acc. to /5/, table 3.1.

\min^A minimum cross section of the timber components to be connected, acc. to /15/

d tightening screw diameter acc. to /15/

$a_1 ; a_2$ spacings of the special connectors acc. to /15/

Figure 36 : Calculation of timber fasteners; special connectors (lay-in connectors, bolted connectors)

Table 1: Parts of the Future GDR Timber Design Code			
Part	Title	Objective	Date of completion (year)
1	Timber construction; Loadbearing systems; Calculation and structural design	Establishment of wide conformity with the CIB Model Code and the Eurocode	1990
2	Timber construction; Analysis of the structural state of repair and reconstruction of existing (historic) timber structures	Generalization of the experience prevailing in this field for many years	1991
3	Timber construction; Wood-based engineering materials and constructions consisting of these materials	Establishment of wide conformity with the CIB Model Code and the Eurocode	1992

T a b l e 2 : GDR Standard Specifications related to the new GDR Timber Design Code which must be revised within the next years

GDR Standard Specification (TGL)	Draft dated (year)	Title	Completion of the planned revision(year)	Objective of the revision
33136/01	1987	Timber construction; Building components of glued laminated timber; Technical specifications	1992	Approach to the international trend in the testing of finger joints and beams
33136/02	1978	Timber construction; Building components of glued laminated timber; Quality control in the production	1993	Approach to the international trend
42704	1986	Bridges in traffic construction; Timber bridges; Calculation and structural design	1995	Design based on limit states
117-0767	1963	Structural timber; Sorting by quality grades and strength classes	1992	Establishment of a wide conformity with the ECE Code

T a b l e 3 : Load factors acc. to /6/	
Kind of load	Load factors ¹⁾
Dead load	0.8 ... 0.9 ²⁾ 1.1 ... 1.3 0.82 ... 0.935 ²⁾ 1.065 ... 1.18
Live loads in residential and public/community buildings and structures ³⁾	1.2 ... 1.4
Live loads in industrial and agricultural buildings and structures ³⁾	1.2 ... 1.4
Loads of liquids in pipings	1.0 ... 1.1
Wind loads ³⁾	1.2 ... 1.3
Snow loads	1.4
<p>1) They apply only to the limit state of the loadbearing capacity (GZT); as for the limit state of the usability (GZN), $\gamma_f = 1.0$ is applicable if no particular specifications are fixed.</p> <p>2) To be applied if the reduction of the loading should have an unfavourable effect.</p> <p>3) Additional values are indicated in /6/.</p>	

Table 4 : Reliability classes and valency factors for the limit state of the load-bearing capacity (GZF) acc. to /7/

Reliability class	Consequences in the case of failure	Kind of utilization of the building/structure	Valency factor
1	2	3	4
I	- very high risks for the population	<ul style="list-style-type: none"> - safety-relevant structures of nuclear plants and systems - embankment-type dams and barrages of hydro dams with a capacity of $\geq 10^7 \text{ m}^3$ - industrial and storage buildings and structures with a very high risk potential - buildings and structures in which crowds totalling as from 3,000 people may gather 	1.1 ¹⁾
II	<ul style="list-style-type: none"> - high risks for crowds of people - high economic losses - high cultural losses 	<ul style="list-style-type: none"> - buildings and structures with frequent crowds totalling ≥ 500 people - sports stadiums as far as they do not fall under the reliability class I - theatres, cinemas, concert halls, churches - schools, auditoriums - passenger terminal buildings of railway stations, airports - high-rise buildings of hotels and ward blocks as well as of boarding-schools - hospitals - department stores and indoor markets with a sales floor area of $\geq 10,000 \text{ m}^2$ - bridges in the construction of traffic facilities - buildings and structures with a considerable national-economic importance - main buildings of power plants - selected stacks with a height of $\geq 50 \text{ m}$ - dams/barrages of hydro dams with a capacity of $\geq 10^5$ and $< 10^7 \text{ m}^3$ 	1.05

Table 4 (cont'd.), page 2

1	2	3	4
<p>(reliab. class II, cont'd.)</p>		<ul style="list-style-type: none"> - buildings and structures of a great public importance and with a particular representative character <ul style="list-style-type: none"> . buildings/structures of central state organs, parties and mass organizations . museums containing irretrievable treasures - buildings and structures for disaster control and civil defence purposes 	4
<p>III</p>	<ul style="list-style-type: none"> - risks for groups of people - considerable economic consequences 	<ul style="list-style-type: none"> - residential buildings - office buildings as far as they do not fall under the reliability class II - industrial, public/social and agricultural buildings and structures as far as they do not fall under other reliability classes - central storage buildings and structures for the population's supply and provision; storage facilities for technical equipment of great value - building constructions in the erection state and in case of fire - loadbearing structures of systems for the transmission and distribution of electrical energy 	1.0
<p>IV</p>	<ul style="list-style-type: none"> - insignificant risks for people - insignificant economic consequences 	<ul style="list-style-type: none"> - smaller, single-storey production (service) buildings and workshops of the locally controlled industry and of agriculture - greenhouses with roof frame spans of ≥ 12 m - buildings/structures for the storage of agricultural products, fertilizers and innocuous chemicals - objects of the site facilities with service periods of ≥ 8 years - bungalows and arbours 	

Table 4 (cont'd.), page 3

1	2	3	4
V	<ul style="list-style-type: none"> - very insignificant risks for people - very insignificant economic consequences 	<ul style="list-style-type: none"> - smaller, single-storey buildings of an insignificant economic importance in which people are not staying permanently <ul style="list-style-type: none"> • greenhouses with roof frame spans of <12 m • barns, sheds • individual garages • smaller storage buildings of a secondary importance 	0.90

1) To be fixed by agreement with the State Building Supervision Authority.

T a b l e 5 : Combination factor acc. to /6/		
Load combination	Number of the short-term loads	Ψ
Basic combination ¹⁾	1	1.0
	2 or 3	0.9
	> 3	0.8
Special combination ²⁾	≥ 1	0.8

1) maximum load, without instantaneous load

2) maximum load, including instantaneous load

T a b l e 6 : Comparison of the partial safety values for actions as applicable in the GDR and acc. to Eurocode 5 /5/

Permanent actions γ_G	Partial safety values in the GDR by reliability classes acc. to /6/					Partial safety values in the Eurocode 5 acc. to /5/	
	I	II	III	IV	V	+))	++))
- smallest effect	1.0	1.0	1.0	1.0	1.0	1.0	1.0
- unfavourable effect	>1.20	1.16	1.10	1.05	1.0	1.35	1.2
Variable actions γ_Q							
- one with its characteristic value	>1.54	1.47	1.40	1.33	1.26	1.5	1.35
- one with its accompanying value						1.5	1.35

+) normal partial safety values

++) reduced partial safety values 1)

1) For single-storey structures with a medium span and only occasional utilization. This corresponds to the reliability class V in the GDR.

T a b l e 7 : Proposal as to moisture classes and allocated climatic conditions

Moisture class	Classification of the category of building/structure and climatic conditions	Timber moisture	Relative air humidity at 20°C	Remarks
1	2	3	4	5
1	<ul style="list-style-type: none"> - Enclosed buildings/structures with heating (well ventilated; no rooms with moisture sources) - Enclosed buildings/structures, slightly heated (well ventilated; no rooms with moisture sources) 	$\omega \leq 12 \%$	$\varphi \leq 65 \%$	
2	<ul style="list-style-type: none"> - Enclosed buildings/structures without heating (well ventilated; with rooms having weak moisture sources) - Glued laminated timber and square timber components being exposed to the utilization conditions of the moisture class 3 which, however, are provided with a hydrophobic protective coat 	$12 < \omega \leq 18 \%$	$65 \leq \varphi \leq 85 \%$	1) Grain storage facilities, works halls and assembly halls of the metalworking industry

(cont'd.)

Table 7 (cont'd.), page 2

1	2	3	4	5
<p>1</p> <ul style="list-style-type: none"> - Enclosed buildings/structures with²) rooms having moisture sources - Free-standing building/structures made of medium- to large-sized timber cross sections such as square timber members and glued laminated timber components - Components made of boards and laths being exposed to a utilization according to moisture class 2 - Roofed buildings/structures being open on all sides, with unprotected components - Small-sized components of free-standing buildings/structures such as laths, boards, planks - Glued laminated timber and square timber components being exposed to utilization conditions of moisture class 2 which, however, serve for roofing over halls for the storage of fertilizers, in particular of urea - Buildings/structures with wet rooms which have a permanent air humidity of $\varphi \geq 95\%$ - Building components being located in water 	<p>3</p> <p style="text-align: center;">$18 < \omega \leq 26\%$</p> <p style="text-align: right;">$\omega > 30\%$</p>	<p>4</p> <p style="text-align: center;">$\varphi \geq 85\%$</p>	<p>2)</p> <p>e.g. baths, swimming pool halls, weaving mills, foodstuffs enterprises, industrial and water-supply wet rooms such as tanneries, laundries etc.</p> <p>In case of doubt, the allocation will be accomplished according to the magnitude of the permanently acting air humidity by agreement with the State Building Supervision Authority.</p>	

Table 8 : Classes 1) of the load action period acc. to Eurocode and allocation, load classes acc. to GDR Code /6/

Load action period		Classification of the loads acc. to GDR Code
class/permanent load	magnitude as to time	
1	2	3
A long	10 years	Permanent loads such as the dead load of the building/structure, the actions due to soil (earth) and/or water permanently surrounding the building/structure concerned, as well as the tensioning forces at the time $t = \infty$ long-term loads such as dead loads of dismountable partitions, loads from stationary equipment including its filling or surcharges such as the material to be conveyed on conveyor belts, internal pressure, e.g. of tanks, silos, loads in rooms serving for storage purposes, e.g. warehouses (stores), libraries, technologically conditioned temperature actions lasting for a long period, actions resulting from surrounding soil (earth) or water as far as they do not fall under the permanent loads, load resulting from deposits, e.g. dust, actions resulting from the shrinkage of the building materials, actions resulting from the rheological behaviour, actions resulting from movable conveying and lifting equipment as far as they fall under the long-term loads, such as foundry cranes etc.

(cont'd.)

1	2	3
<p>B medium</p>	<p>6 months</p>	<p>Short-term loads, such as loads in zones located near stationary equipment, e.g. service, handling and attendance zones, acting at the stage of erection, assembly and/or dismantling, loads occurring at switch-in and switch-off (i.e. starting and stopping) stages and with the trial operation, loads resulting from movable conveying and lifting equipment, including material to be conveyed, live loads in residential and public/community buildings as far as they are not resulting from technological equipment, snow loads, ice loads</p>
<p>C short</p>	<p>1 week</p>	<p>Short-term loads, such as wind climatically conditioned temperature actions</p>
<p>D impulsive</p>		<p>Instantaneous loads, such as forces due to operating troubles (breakdowns), e.g. short circuit, rupture (failure), impact, explosion pressures, forces due to inertia ("mass forces") as a result of earthquake, actions due to mining subsidence and other special loads squalls (gusts)</p>
<p>1) They are characterized by the effect of a constant load.</p>		

K mod. acc. to standard code or proposal, respectively

No.	kind of loading	3 sec	3..5min	< 10h	100h (1week)	1 month	1000h (1year)	< 10 years	50 years	US, Canada (evaluated by Swiss Speck)		GDR (1985)	GDR proposal (1996)	Eurocode 5 acc. to / 91	DN 1052 (84)	TGL 53435 (84)	Eurocode 5 for moisture classes 1 and 2	GDR proposal (1988)	USSR SNiP (1984)	USSR Code (1984)	
										for all quality classes + glued laminated timber	for all quality classes + glued laminated timber										
		fm, f0	f0, fv	high-quality timber	low-quality timber	for all quality classes + glued laminated timber	for all quality classes + glued laminated timber	for all quality classes + glued laminated timber													
1.	impulsive	1,1	1,1	1,1	1,1	1,1	1,1	1,1	1,1	1,2	-	1,2		fm f00 fc, 90 ft, 90			fm f00 fc, 90 ft, 90	1,3	1,2	1,4	
2.	short-term test	(1,0)	(1,0)	(1,0)	(1,0)	(1,0)	(1,0)	(1,0)	(1,0)	1,0	1,0	1,0									
3.	very short-term	0,95	0,90	1,0	0,95	1,0	0,95	1,0	0,95	0,85	-	1,0									
4.	short-term									0,80											
5.	short-term	0,80	0,70	1,0	0,80	0,85	0,80	0,70	1,0	0,75	0,85	0,85		0,95			1,0				
6.	short-term (long-term)									0,80	0,85										
7.	medium-term	0,70	0,50	1,0	0,70	0,90	0,50	0,80	0,85	0,65	0,75	0,70		0,90			0,90	1,0			
8.	long-term (normal)	0,55	0,35	0,70	0,55	0,85	0,55	0,85	0,60	0,65	0,75			0,85			0,80				
9.	long-term (permanent)									0,55	0,60	0,60						0,85	0,80		0,8

1) related to 1 hour
 2) related to 10 seconds
 3) horizontal mass loads and earthquake loads
 4) conditions of transport and assembly

Table 10a: Time classes

Time class	Duration of the load action
A	Permanently and/or for a long period (e.g. dead load, live load)
B	For a short period (e.g. live load, snow)
C	For a very short period (e.g. wind)
D	Suddenly (e.g. impact, earthquake)

Table 10b: Load combinations; grouping into time classes

Load combination	Time class			
	A	B	C	D
A + B	IA \geq 85 %	IA < 85 %	-	-
A + C	IA \geq 85 %	-	IA < 85 %	-
A + B + C	IA \geq 85 %	IC \leq 15 %	IC < 15 %	-
A + B + C + D	IA \geq 85 %	LD \leq 15 % IA \geq 85 %	-	LD > 15 % -

IA (etc.) means load component (percentage) of time class A (etc.) of the total load

e.g. $IA = \frac{A}{A+B}$

Table 11: Design of the new grades of glued laminated timber						
Sort	BSH 1	BSH 2	BSH 3	BSH M1	BSH M2	BSH M3
Sorting of the layers of boards	visually	visually	visually	mechanically	mechanically	mechanically
kind of timber	NSH GK I,II	NSH GK II	NSH GK I,II	NSH F I	NSH F II	NSH F II
KZV (mm)	≥ 250	≥ 250	≥ 0	≥ 250	≥ 250	≥ 250
kind of timber	NSH GK I,II	NSH GK III	NSH GK I,II	NSH F III	NSH F III	NSH F II
KZV (mm)	≥ 250	≥ 0	≥ 0	≥ 0	≥ 0	≥ 0
<p>Meaning of the abbreviations: BSH = glued laminated timber NSH = sawn coniferous timber (pine, spruce or larch) GK = quality class (grade); F = strength class KZV = staggering of key-dovetail connections ("finger joints")</p>						

Table 12: Strength classes, characteristic values and mean moduli of elasticity and shear moduli

	sawn structural timber			glued laminated timber			round timber	GK II hard wood							
	quality class (GK)			grade											
	I	II	III	I	2	3			M1	M2	M3				
strength class acc. to Eurocode 5 10/87	C6	C5	C3	C7	C6	C3	C6	C6	C5	C5	C5/6	C5			
bending	R_m^n	28,5	24	19	38	28,5	19	28,5	24	21,5	33,3	28,5	24	26,5	24
tension	$R_{t,0}^n$	17	14,5	7,1	24	17	11,5	14,4	4,8	14,4	14,6	15,7	13,6	15,8	17
	$R_{t,90}^n$	0,5	0,45	0,35	0,6	0,5	0,35	0,45	0,35	0,45	0,35	0,5	0,35	0,5	0,5
compression	$R_{c,0}^n$	26	21,5	17,5	30	26	17,5	26	21,5	19	21,7	26	21,5	26	26
	$R_{c,90}^n$	8	7,5	6,8	11	8	6,8	7,5	6,8	7,5	6,8	8	6,8	7,8	11,3
shearing off // to grain	$R_{a,0}^n$	2,0	1,7	1,5	2,9	2,0	1,5	1,7	1,5	1,7	1,5	2,0	1,5	1,5	3
shear from transverse force	R_{t}^n	2,7	2,3	2,0	3,8	2,7	2,0	2,7	2,0	2,1	2,0	2,7	2,3	2,7	2,7
moduli	E_0^n	12000	11000	9000	13500	12000	9000	12000	11000	10000	12500	12000	11000	12000	12500
	E_{90}^n	400	350	300	450	400	300	400	350	300	400	400	350	400	600
	G^n	750	700	550	850	750	550	750	700	600	800	750	700	750	1000
	$E_{0,5\%}$	8500	7500	6500	9500	8500	6500	8500	7500	8500	9000	8500	7500	8000	9000
	$G_{5\%}$	550	500	400	600	550	400	500	500	500	600	550	500	550	600

Table 13: Modification factor $\gamma_{d,1}$ as to "long-term behaviour" for the limit state of the loadbearing capacity (GZT)

Time class	Moisture class (FK)			
	FK 1 BH	FK 2 BSH	FK 3 BH	FK 3 BSH
A	0.85	0.8	0.65	0.4
B	1.0	1.0	0.75	0.5
C	1.2	1.2	0.9	0.6
D	1.3	1.3	1.0	0.65

Meaning of the abbreviations:
 BH = structural timber
 BSH = glued laminated timber

For air temperatures of $35^{\circ}\text{C} \leq T \leq 50^{\circ}\text{C}$ and moisture class FK 1, $\gamma_{d,1}$ shall be multiplied by 0.85.

T a b l e 14a: Modification factor $\gamma_{d,4}$ as to aggressive media" for the GZT and GZN limit states for structural timber (BH) and glued laminated timber (BSH)

The kinds of the media are grouped into gases, solutions and solids. By considering the criteria as to concentration of the medium concerned and the moisture class, the stress degrees (BG) I, II, III are obtained:

Stress degree (BG)	Explanation
BG I	Not or slightly aggressive
BG II	Moderately aggressive
BG III	Highly aggressive

T a b l e 14f: Modification factors $\gamma_{d,4}$ for aggressive media subject to the timber cross-sectional size

Note: Minimum dimension of the timber component with stress degrees BG II and BG III: 40 mm
Minimum cross-sectional area: 4,000 mm²

Approved timber preservatives do not exercise any aggressive influence (action) on the timber. The value of the modification factor is equal to $\gamma_{d,4} = 1$ when using efficient linings or coatings.

Stress degree (BG)	Cross-sectional size (10 ³ mm ²)	Factor $\gamma_{d,4}$
BG I		1.0
BG II	< 9	0.75
	< 30	0.85
	≧ 30	0.95
BG III	< 9	0.65
	< 30	0.75
	≧ 30	0.85

Ranges of aggressivity and stress degrees for gases

Table 74b: Ranges of aggressivity for gases			
Gas, increasing aggressivity	Gas group with a concentration (mg/m ³) amounting to:		
	A 1	A 2	A 3
1. CH ₂ O (formaldehyde)	1 ... 200	-	-
2. NH ₃ (ammonia)	0.5 ... 20	-	-
3. SO ₂ (sulphur dioxide)	0.2 ... 10	10 ... 200	-
4. NO ₂ (nitric oxide)	0.1 ... 5	5 ... 25	above 25
5. HCl (hydrogen chloride)	0.05 ... 1	1 ... 10	above 10
6. Cl ₂ (chlorine)	0.02 ... 1	1 ... 5	above 5

Table 74c: Stress degrees for gases			
Range of aggressivity	Moisture class		
	FK 1	FK 2	FK 3
A 1	I	I	I
A 2	I	II	II
A 3	II	II	II

T a b l e 74d: Stress degrees for solutions					
Group	Solution	pH-value	Concentration of the solution	Degree of dissociation	Stress degree
Acids	nitric acid HNO_3	below 2	up to 5 above 5	high	III III
	hydrochloric acid HCl		up to 5 above 5	high	III III
	sulphuric acid H_2SO_4		up to 5 above 5 / above 15	medium	I II / III
	acetic acid $\text{C}_2\text{H}_4\text{O}_2$	4	above 15	low	I
Bases	soda lye NaOH	above 13	up to 2 above 2	high	II III
	potash lye KOH		up to 2 above 2	high	II III
	ammonium hydroxide NH_4OH		up to 5 above 5	low	I II
Salt solutions	chloride solutions: KCl , NaCl	7	up to 10 above 10	medium	I II
	sulphate solutions: Na_2SO_4 (Glauber's salt)		up to 10 above 10	medium	I II
	$(\text{NH}_4)_2\text{SO}_4$ (ammonium sulphate)	5	up to 40		I
(Organic compound)	urea $\text{CO}(\text{NH}_2)_2$	2	up to 40		II

T a b l e 14e Stress degrees for solid media

Solid medium	pH-value	Solubility in water	Hygros- copicity	Stress degree (BG) with FK 1 FK 2 FK 3
Potash fertilizer	8	good (up to 20 %)	good	I II II
Urea	9	good (up to 40 %)	high	I II II
Superphosphate	3	(up to 5%)	good	I I II
Sodium chloride	7	good	good	I I II
Ammonium sulphate	5	good (up to 40 %)	low	I I I

Table 15: Creep factor K_{Creep}

No.	Kind of loading	Time (period)	Eurocode 5 1987 moisture class			Eurocode 5 1985 acc. to moisture class			GDR proposal (1987) moisture class acc. to Eurocode					
			1	2	3	1	2	3	1	2	3			
1	impulsive	< 3sec	-	-	-	1	2	3	-	-	-	-	-	-
2	short-term test	3-5 min	-	-	-	1,0	1,25	1,5	-	-	-	-	-	-
3	very short-term	< 10h	1,0	1,1	1,5				-	-	-	-	-	-
4	short-term	1 day												
5	short-term	100 h (1 week)	1,2	1,3	2,0	1,2	1,5	2,0	1,0	< 1,65	1,6	< 1,3	[3,3]	
6	short-term (long-term)	1 month												
7	medium-term	10000 h (1 year)												
8	long-term (normal)	< 10 years	1,5	1,8	3,0	1,5	2,0	3,0						
9	long-term	50 years							1,5	[2,5]	2,5	< 2,0	[5,0]	

() applies to glued laminated timber

< > applies when using timber which is too wet and was dried back; e.g. $w_a \geq 30\%$ $w_e \leq 10\%$

[] w_a = initial moisture
 w_e = final moisture

Figure 1a: Moisture classes (proposal of 1987) in comparison with Eurocode 5

Moisture class (FK)	Relative air humidity φ (%) (T = 20 ± 2°C)	Moisture of timber ω (%)	Moisture class acc. to Eurocode 5	Relative air humidity φ (%) ¹⁾	Moisture content ω (%)
FK 1	< 80	≤ 18	1	< 65	≤ 12
FK 2	80 ≤ φ ≤ 95	> 18 to 24	2	65 ≤ φ ≤ 80	≤ 18
FK 3	> 95	> 24	3	> 80	≥ 18

1) Value is being exceeded only for some weeks a year.

Industrial Code Specification

December,
1989

G D R	Timber Construction Loadbearing Structures Calculation	Structural Design	TGL 33 135/04 E89
-------	--	-------------------	----------------------

Table of Contents

1. Introduction
(Purpose and scope, assumptions, units, symbols, definitions, reference documents)
2. Fundamentals for draft and design
(Basic demands and requirements, definitions and classifications, design requirements, durability, particular regulations for timber structures)
3. Building materials
(Structural timber, glued laminated timber)
4. Limit state of the usability
(Deflections, vibrations)
5. Calculation and design
(Individual components, built-up components, fasteners)
6. Execution and supervision
(General assembly, transport and erection)

Figure 1 : Arrangement of the Code

① Wood's curve

② Eurocode 5, draft 1987
(moisture classes 1+2, $w \leq 18\%$
New GDR Code, draft 1989

③ New GDR Code, draft 1987,
for structural timber / moisture
class 1, $w \leq 18\%$
(moisture content factor at
 $w \geq 18\% = 0,8$ acc. to Eurocode
and $0,85$ acc. to GDR Code)

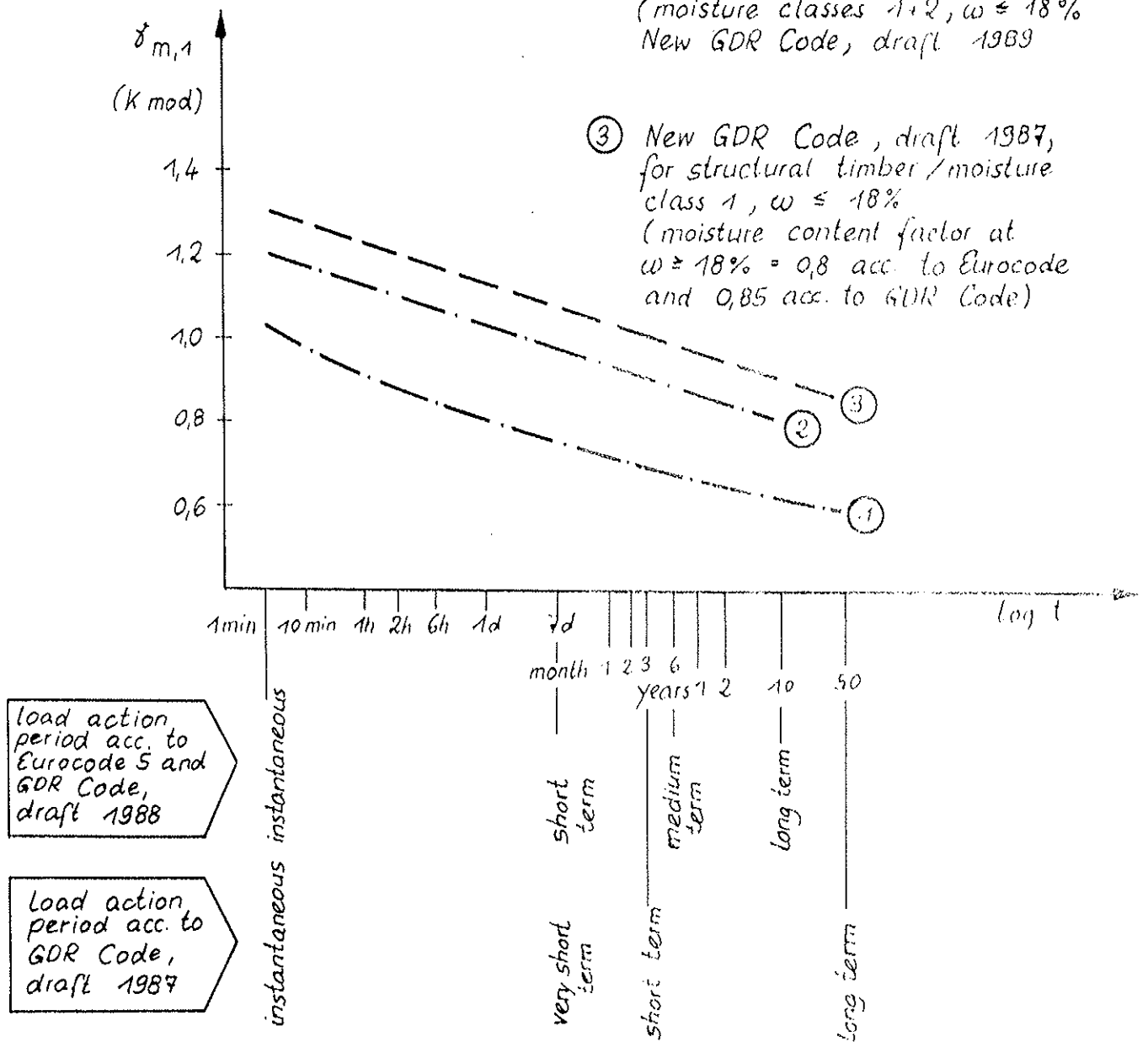


Figure 2: Factor $k_{d,1}$ - Long term behaviour for limit states of the loadbearing capacity (GZT) (with the exception of tensile strength perpendicular to the grain acc. to Eurocode 5)

Figure 3: Strength classes (F) of sawn structural timber or layers of glued laminated timber

quality classes (GK)

Not suitable for loadbearing components

GK III		F III		
GK II			F II	
GK I				F I
	softwood	7000	9500	12000
	hardwood	8000	11000	14000

$f_m \left(\frac{N}{mm^2} \right)$

structural timber
100% (310 specimens)

$R_{m,5\%} = 26,8 \text{ N/mm}^2$ (all non-classified specimens)
visuell sorting (knottiness etc)

quality class I
31,0%

$R_{m,5\%} = 29,6 \text{ N/mm}^2$

quality class II
46%

$26,4 \text{ N/mm}^2$

quality class III
23%

$23,9 \text{ N/mm}^2$

variant 0 a) and b)

mechanical sorting acc. to knottness + modulus of elasticity

strength class I
17,0%

$R_{m,5\%} = 46,3 \text{ N/mm}^2 (1,56)$
non-loadbearing range: 1%

strength class II
50%

$27,8 \text{ N/mm}^2 (1,05)$

strength class III
32%

$20,1 \text{ N/mm}^2 (0,84)$

variant 2

variant 2

strength class I
17,4%

$R_{m,5\%} = 46,34 \text{ N/mm}^2 (1,56)$

strength class II
27,7%

$37,12 \text{ N/mm}^2 (1,4)$

strength class III
26,45%

$25,01 \text{ N/mm}^2 (1,46)$

non-loadbearing range: 28,4% [$R_{m,5\%} = 19,89 \text{ N/mm}^2$]

variant 3

variant 3

strength class I
21,3%

$R_{m,5\%} = 46,42 \text{ N/mm}^2 (1,56)$

strength class II
37,7%

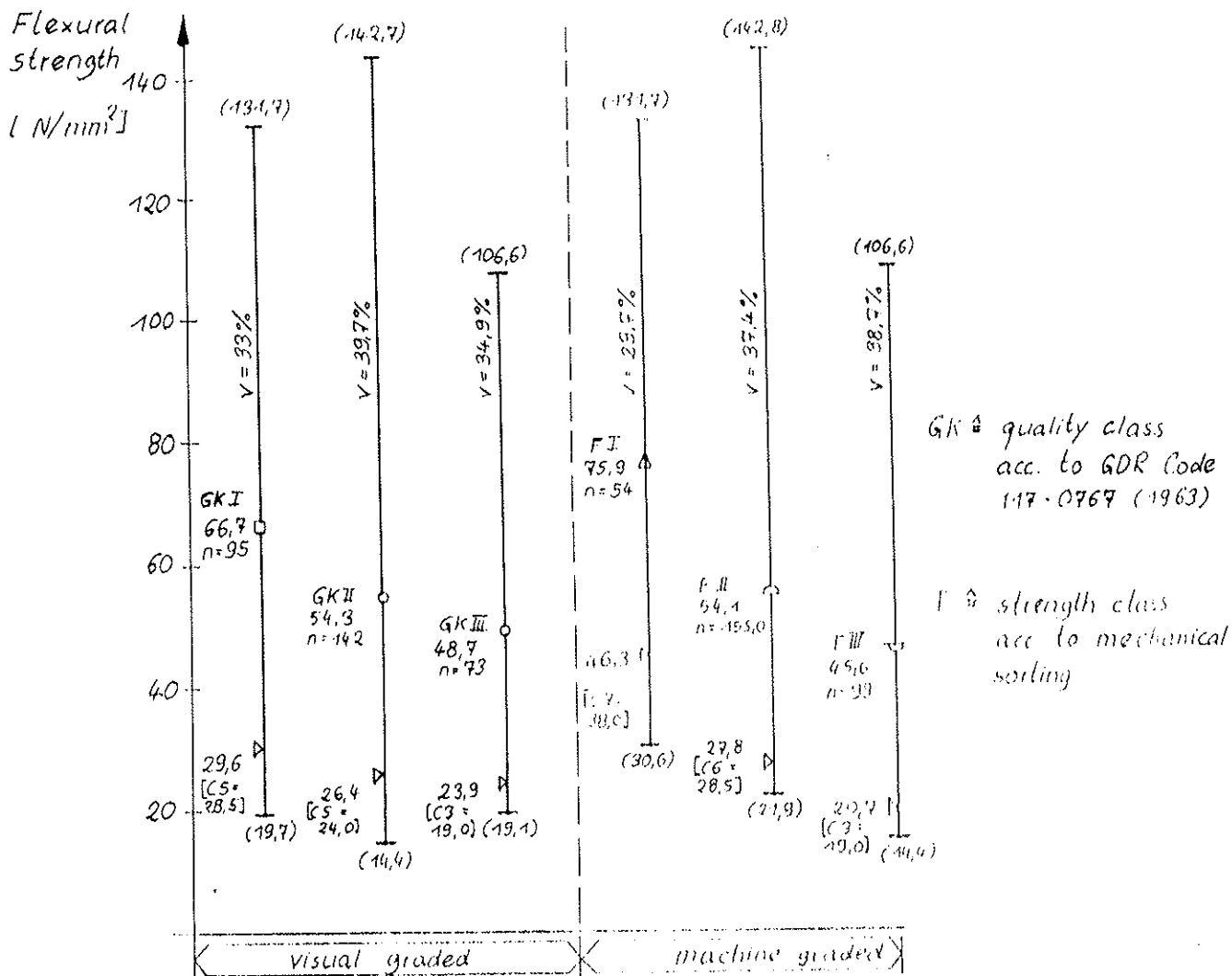
$35,55 \text{ N/mm}^2 (1,35)$

strength class III
34,8%

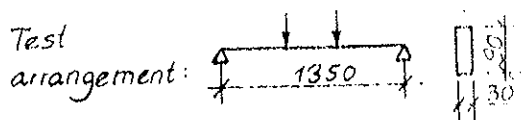
$24,37 \text{ N/mm}^2 (1,02)$

non-loadbearing range: 6,2% [$R_{m,5\%} = 15,71 \text{ N/mm}^2$]

Figure 4: Sorting effect with structural timber (bending stress) depending on the selected class limits
() - value · ratio to the $R_{m,5\%}$ -value of the quality class



- n - number of girders
- ▷ - 5% - quantiles of the 3 - parametric Weibull distribution acc. to GDR Code TGL 3893.1/03
- v - variation coefficient, %
- () - maximum / minimum value
- [] - strength class acc. to Eurocode 5, draft 1987, annex 2



Test conditions:

- temperature of 20°C
- moisture content 8...13%
- test duration from 3...5 minutes

Figure 5: Bending strength of structural timber sorted acc. to various sorting procedures

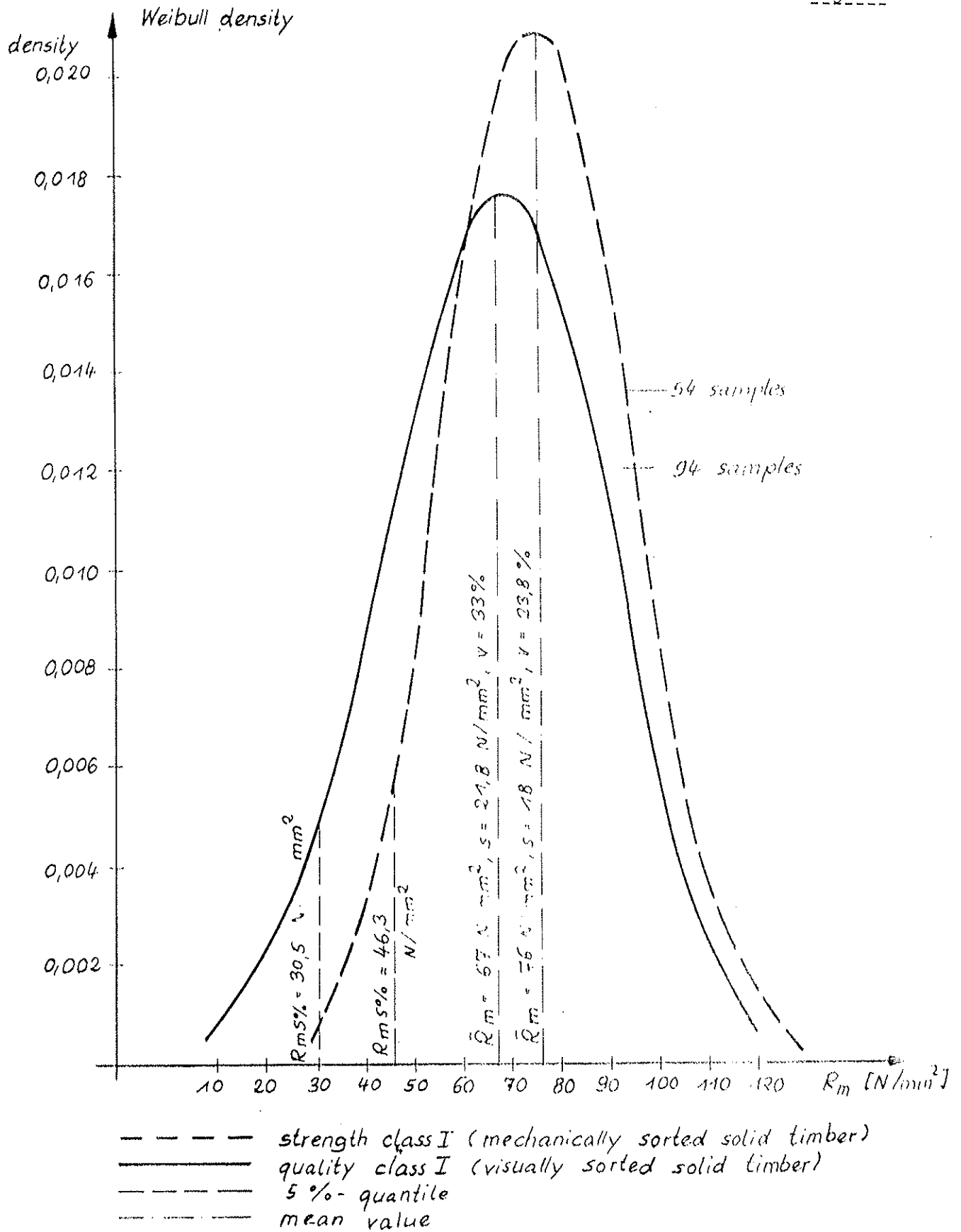
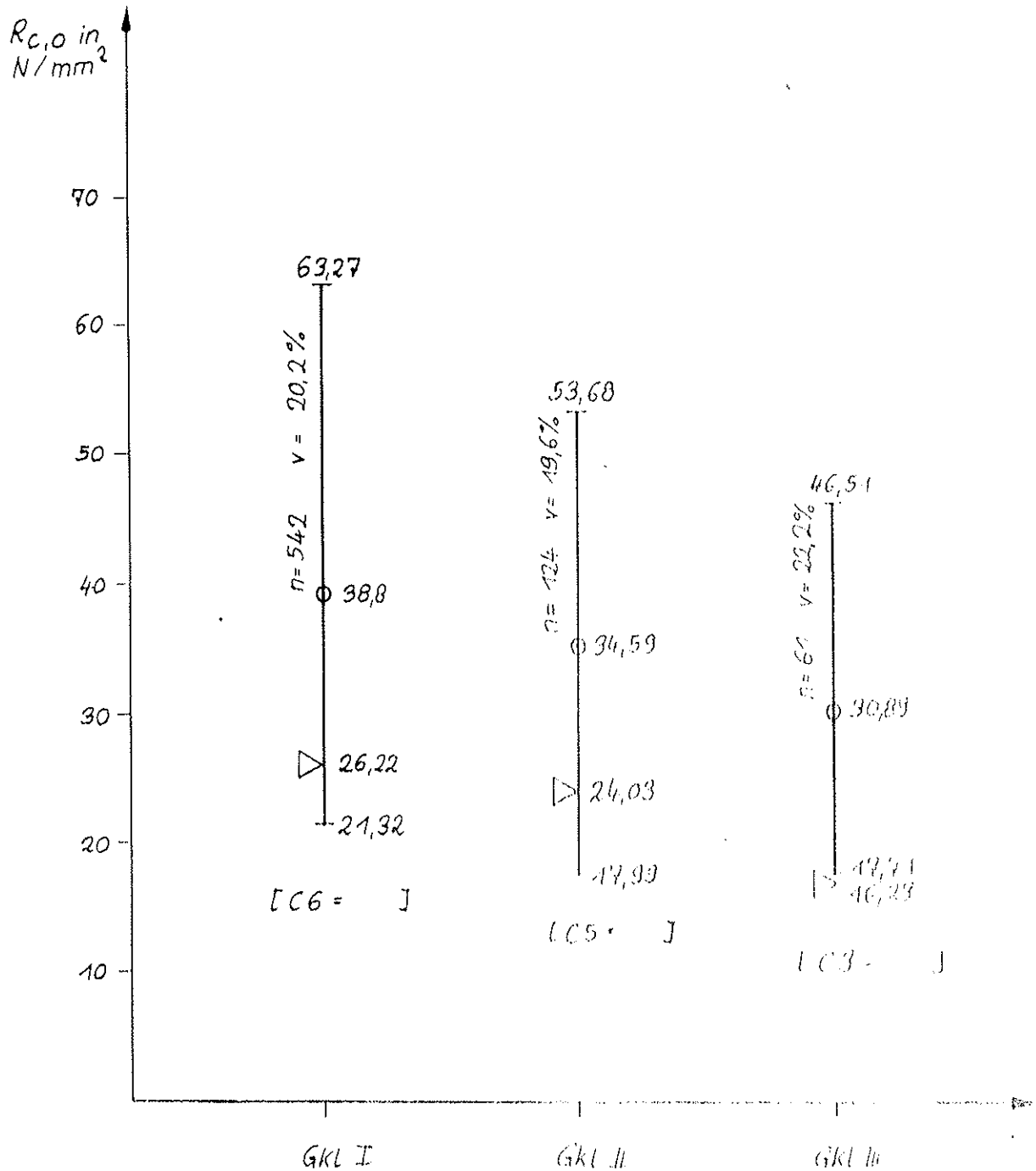


Figure 6: Comparison of mechanically and visually sorted structural timber of the strength class I and/or quality class I (bending failure strength)

Figure 7: Compression strength of sawn coniferous timber in parallel with the grain



□ mean value

▷ 5% - quantile of the 3 parametric Weibull distribution acc. to the GDR Code TGL 13879:1/03

n number of specimens

v variation coefficient

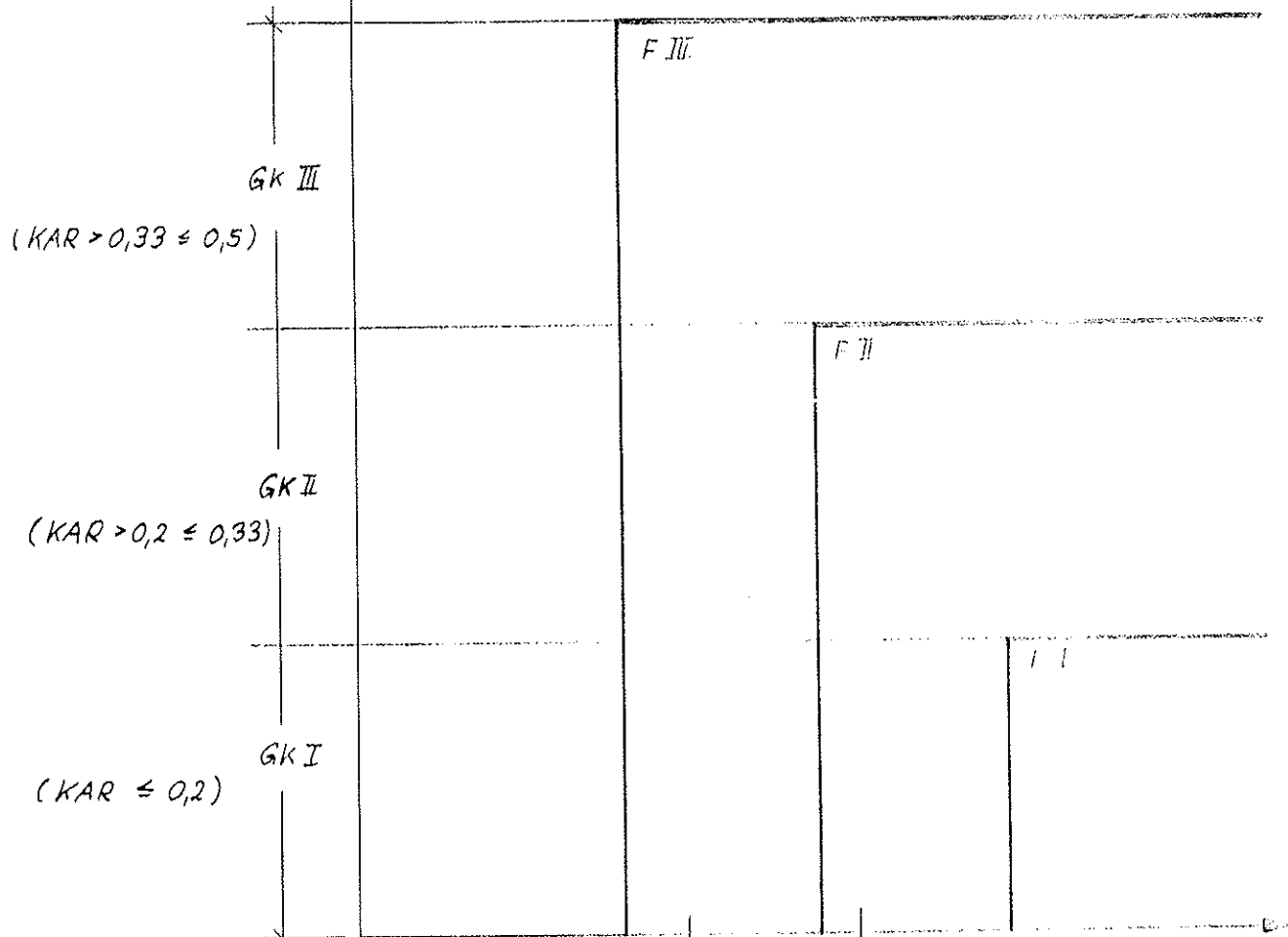
[] strength class acc. to Eurocode 5; draft 1987, annex 2

Meanings:

- GK quality class
- F strength class
- E_m modulus of elasticity in bending
- NSH sawn coniferous timber
- KAR knot area ratio acc. to DIN 4074

quality class
acc. to GDR
Code
TGL 117- 0767

Not suitable for loadbearing
components!



variant 0	a) old :	6000	9000	12000	$E_m \left(\frac{N}{mm^2} \right)$
	b) new :	7000	9500	1200	
variant 1	a) min E	4000	5000	6500	
variant 2	b) E_{mean}	10000	11000	12000	
variant 3	c) E_{mean}	8000	10000	11000	

Figure 8: Strength classes of structural timber (sawn coniferous timber) or layers of glued laminated timber

Figure 8a: Bulk density of sawn coniferous timber (structural timber) sorted visually by quality classes (GK)
 Specimens: Wismar, 1987

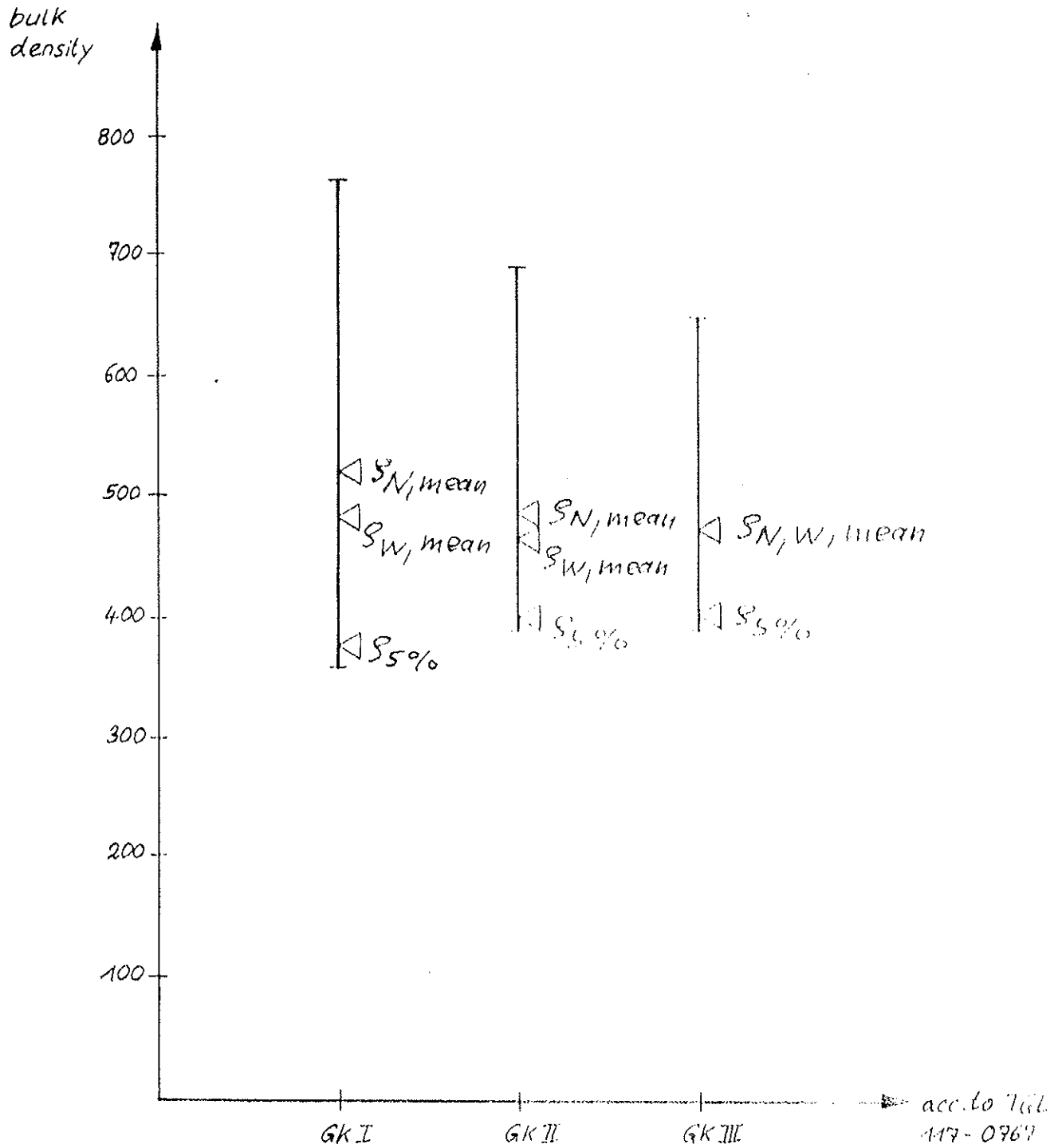
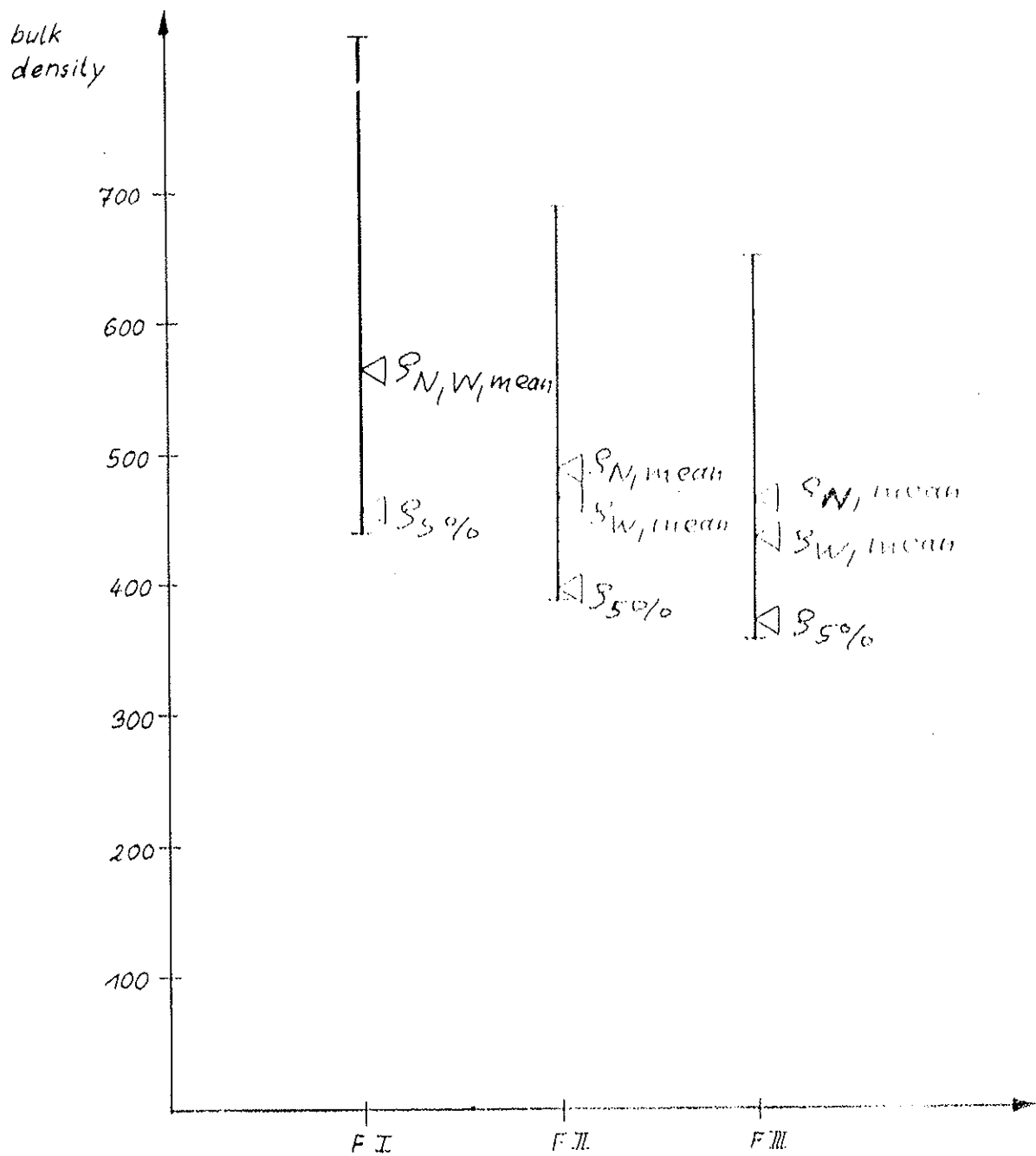
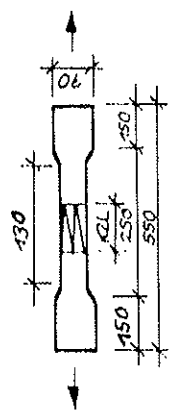


Figure 8 b: Bulk density of sawn coniferous timber
(structural timber) sorted mechanically
by strength classes (F)
Specimens : Wismar, 1987





— without finger joints
 - - - KZL = 50 mm
 - - - = 20 mm

Test conditions:

Temperature 20°C
 Moisture 8... 13%
 test duration from 3... 5 minutes

n = number of specimens
 Δ = 5% - quantiles of 3- parametric Weibull distribution acc. to GDR Code T4L 38794/03
 v = variation coefficient, %
 ◊ = 1% - quantiles of the Weibull distribution

() = maximum / minimum value
 GK = quality class acc. to GDR Code T4L 147-0767 (1983)
 F = strength class acc. to mechanical sorting
 // = strength class acc. to Eurocode draft 14/2, annex

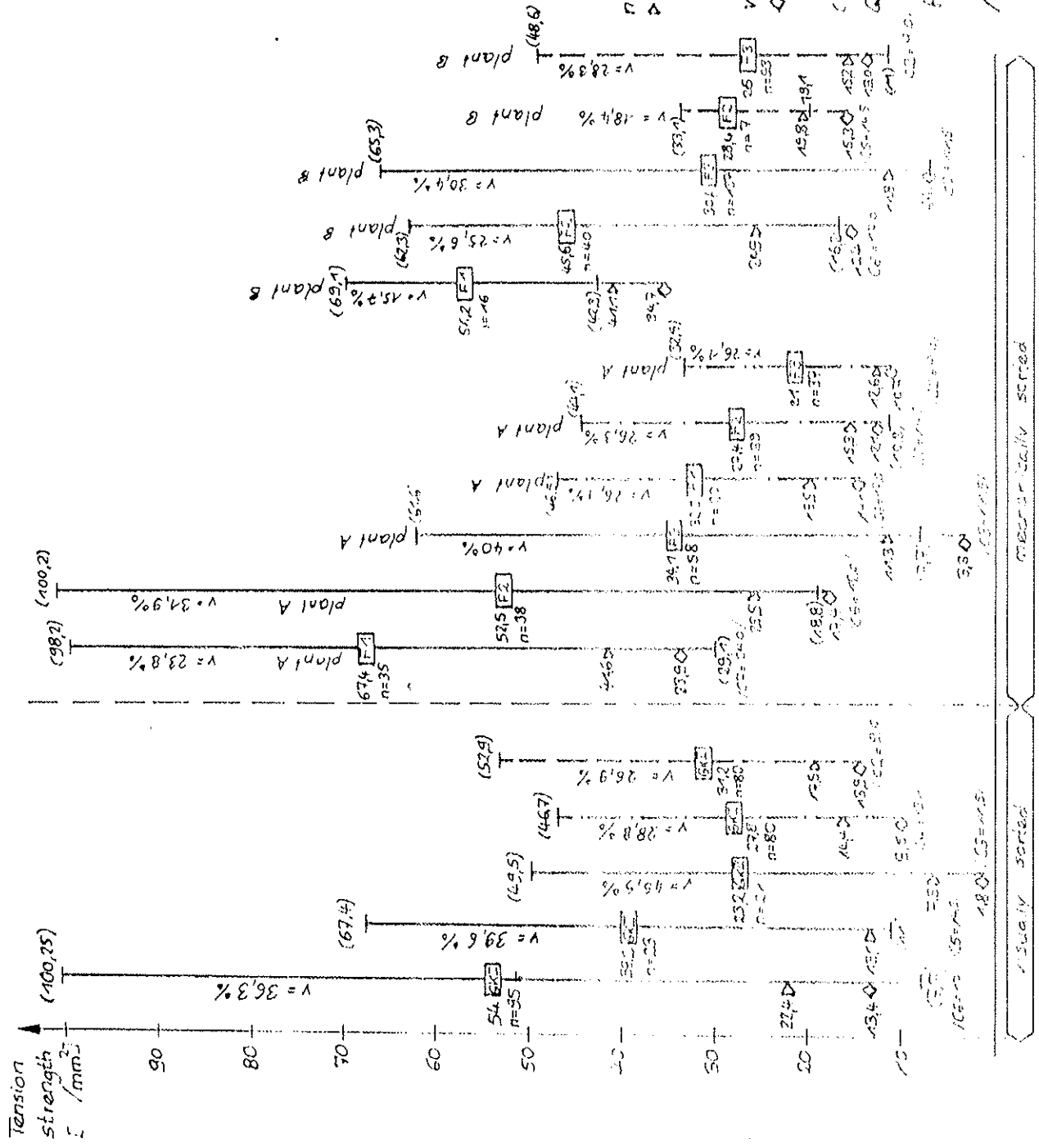
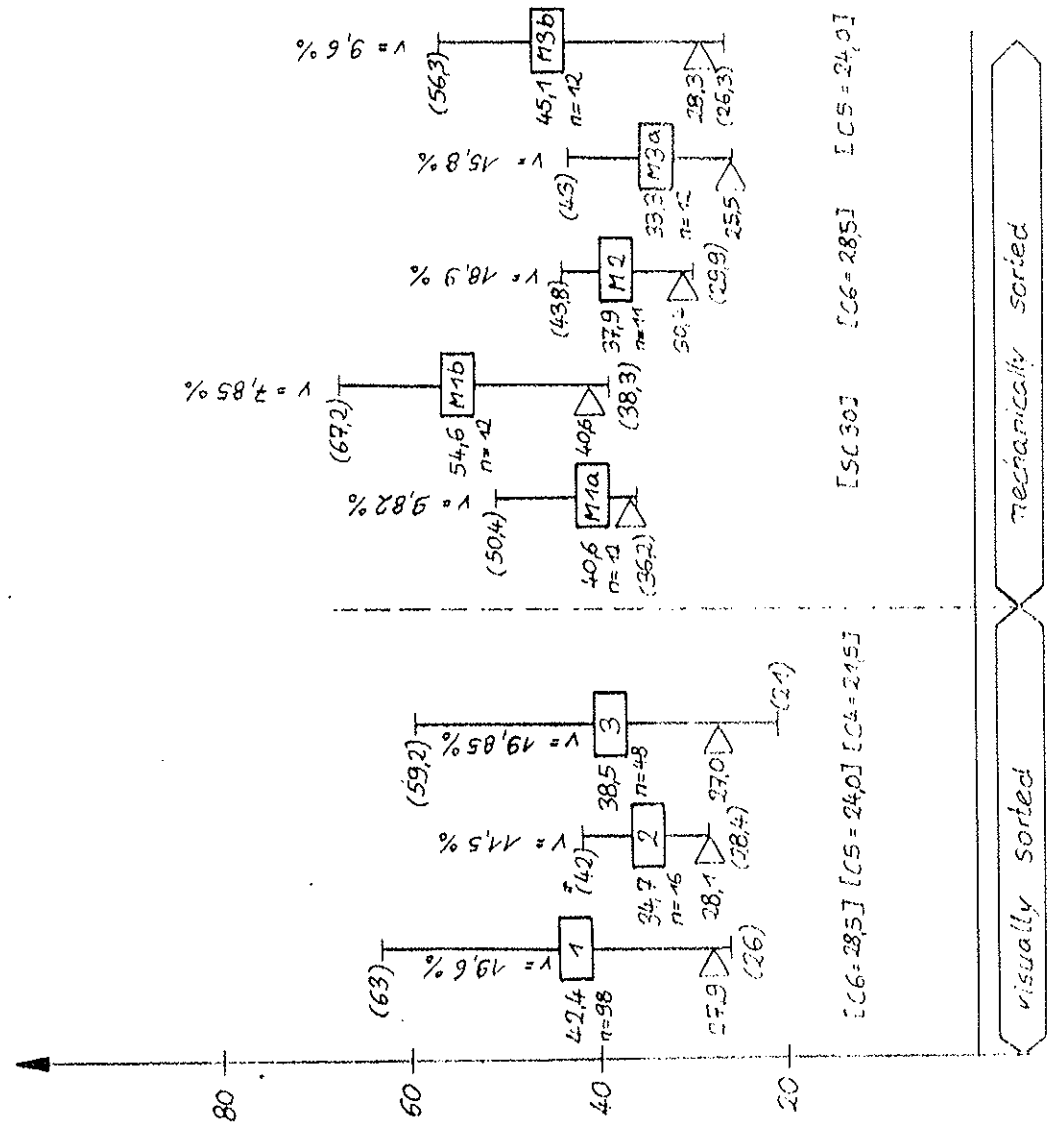


Figure 9: Tension strength of boards 3- glued laminated timber

Bending strength [N/mm²]



- 1 Sort 1, production 85/86 h = 288 mm
- 2 Sort 2, production 84 h = 288 mm
- 3 Sort 3, production 85/86 h = 288 mm

- M1a Sort M1 1.) h = 192 mm with key-dovetailing ("finger joints") in the outermost layer
- M1b Sort M1 2.) h = 192 mm without key-dovetailing ("finger joints") in the outermost layer

- M2 1.)
- M3a 1.)
- M3b 2.)

Test conditions:

- Temperature of 20 ± 2°C
- moisture content ≤ 10%
- test duration from 3...5 minutes

- n = number of beams
- D = 5% - quantiles of 3-Parameter Weibull distribution according to GDR-Code 53791/03
- v = variation coefficient, %
- () = maximum / minimum value
- Δ = strength class for structural timber according to Eurocode 5, Annex 2

Test arrangement:

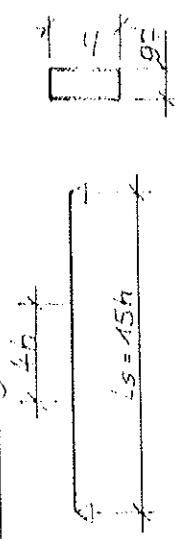
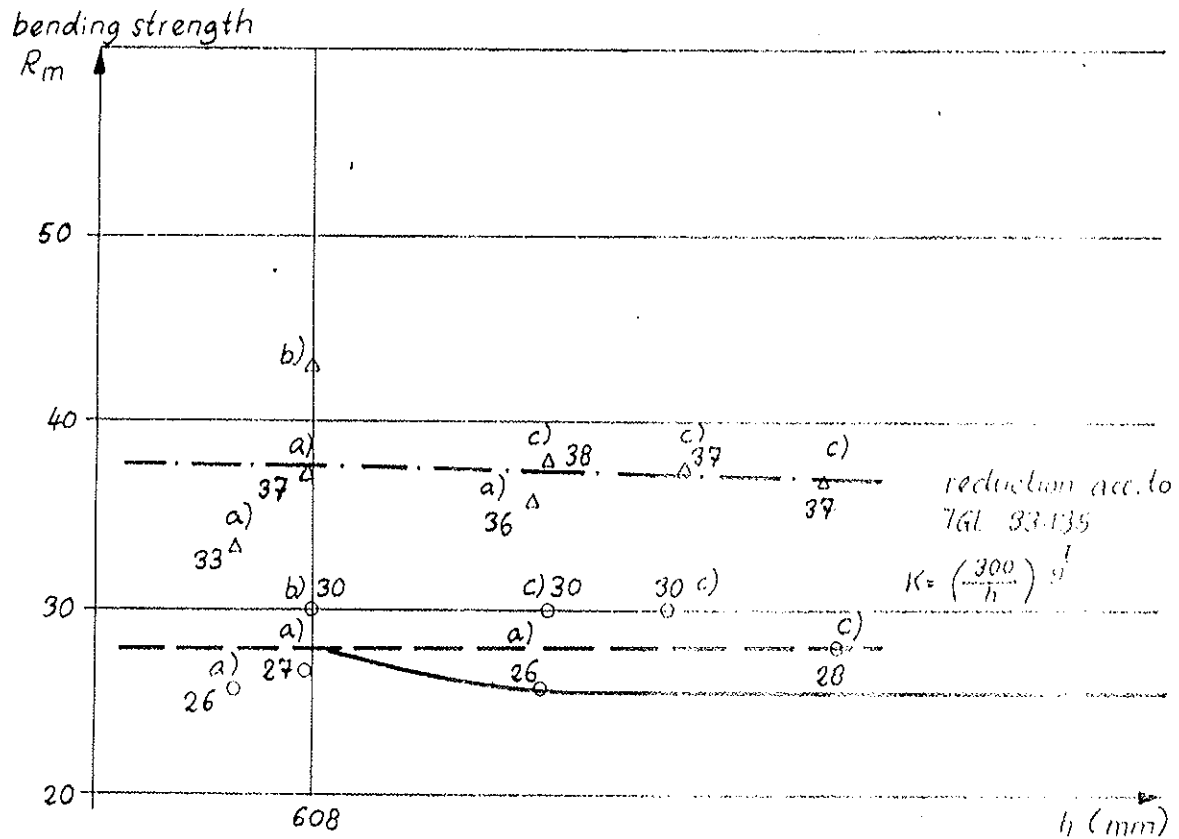


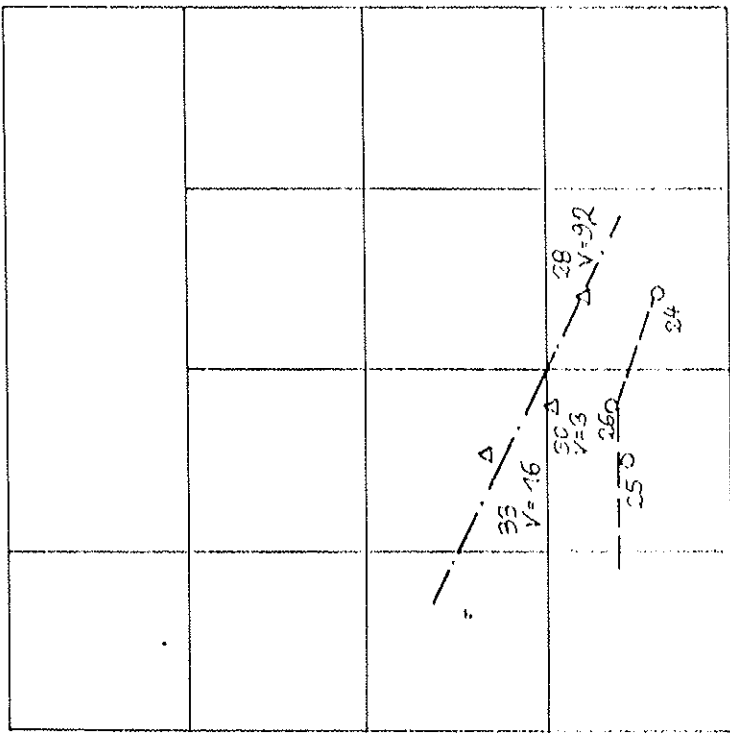
Figure 10: Bending strength of glued laminated timber; layers sorted acc. to various sorting procedures



- 5% - quantile acc. to GDR Code 16L 33791/03
- △ mean values
- a) test values of 1986/87, mechanical sorting (n=12)
- b) test values of 1985/86, visual sorting
- c) test values (1974), visual sorting

Figure 11: Bending strength of glued laminated timber subject of the girder depth acc. to tests performed in the GDR

Bending strength [N/mm]



timber moisture %

- o 5% - evaluate acc. to TGI 33751/02
 - Δ mean value (n=12)
- All beams with key-closetail ("finger joints") staggered in the test zone

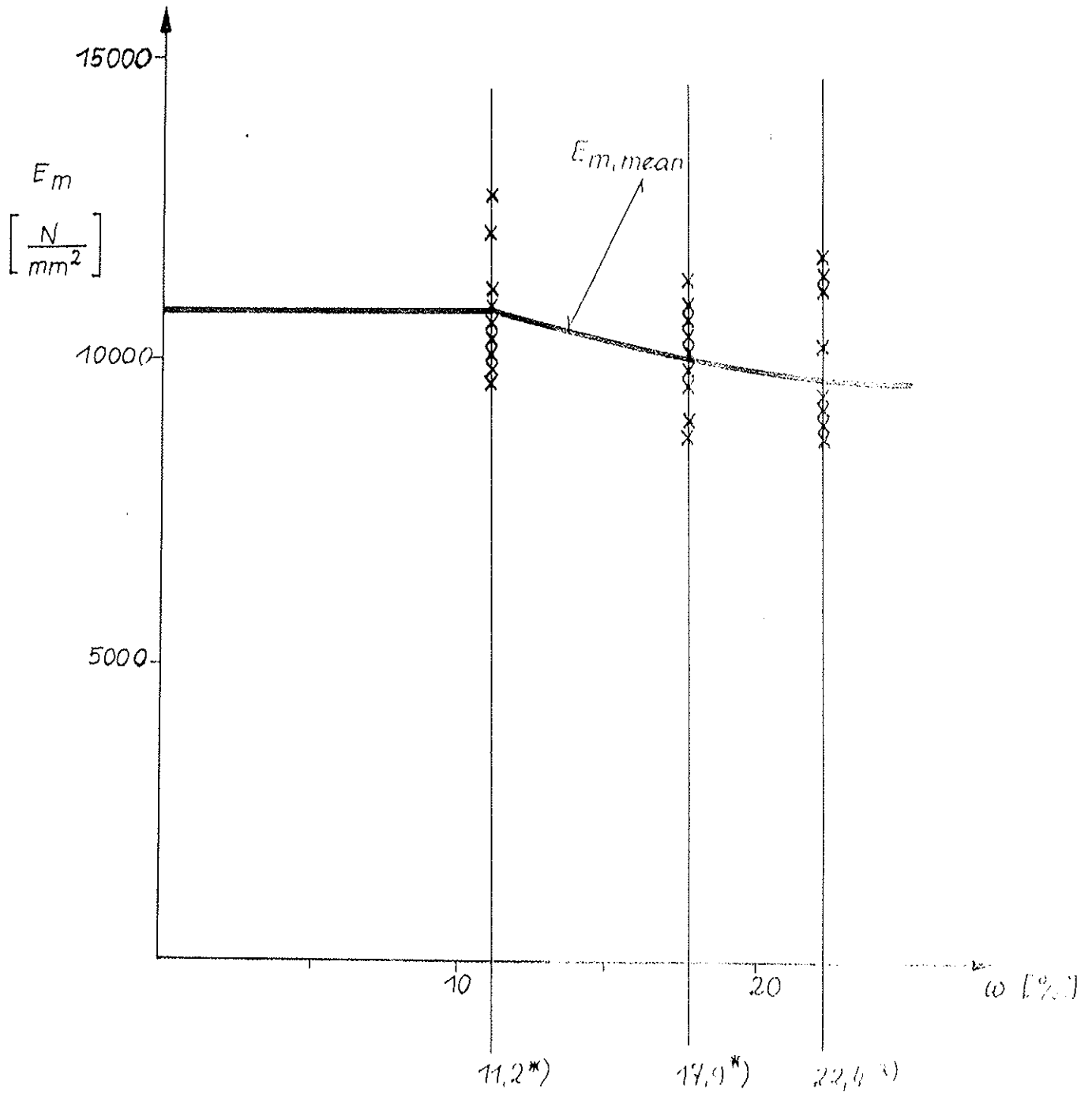
Figure 12: Bending strength of glued laminated timber subject to the timber moisture

24,7	22,3	21,0	22,1	25,4	25,0
23,5	20,5	20,1	20,9	22,2	26,4
21,6	20,3	18,0	17,4	19,1	21,2
21,1	19,0	17,8	18,1	19,0	21,2
22,1	19,9	18,1	18,4	20,3	22,2
22,0	21,9	20,8	21,3	23,1	25,1
97					192

heart
 $w_{mean} \sim 18\%$

layer 1 (tension)
 $w_{mean} = 22,4\%$

Moisture distribution, w (%), over the cross section of GLT after 146 days of storage with a climate of $T = 20^\circ C$, $\varphi = 95\%$ (mean values from kiln-drying tests acc. to 1 of 12 girders)



*) in the tension boundary layer

Figure 13: The modulus of elasticity in bending E_m subject to the timber moisture ω with glued laminated timber (BSH M3) girders.

Tension in the direction of grain

$$\sigma_{t,o,d} \leq f_{t,o,d}$$

Meanings:

$\sigma_{t,o,d}$ design value of the stress

$f_{t,o,d}$ design value of the strength

$$f_{t,o,d} = \frac{f_{t,o,K} \cdot K_{mod,i}}{\gamma_M}, \quad i = 1 \text{ to } 4$$

where

$f_{t,o,K}$ characteristic value of the strength acc. to /5/, table A 2.1a

$K_{mod,i}$ modification factor acc. to /5/, table 3.1.3.

γ_M material factor acc. to /5/, table 2.3.3.2.

Tension perpendicular to the direction of grain

$$\sigma_{t,90,d} \leq K_{vol} \cdot K_{dis} \cdot f_{t,90,d}$$

Meanings:

K_{vol} factor taking into account the influence of the size of the stressed volume V on the strength, acc. to /5/, (5.1.3.b)

K_{dis} factor taking into account the influence of the stress distribution on the strength, acc. to /5/, (5.1.3.c)

Figure 14 : Calculation of individual components; tension

INTERNATIONAL COUNCIL FOR BUILDING RESEARCH STUDIES AND DOCUMENTATION
WORKING COMMISSION W18A - TIMBER STRUCTURES

TIMBER STRENGTH PARAMETERS FOR THE NEW USSR DESIGN CODE
AND ITS COMPARISON WITH INTERNATIONAL CODE

by

Y Y Slavik, N D Denesh and E B Ryumina
Central Research Institute of Building Structures Moscow
USSR

MEETING TWENTY - TWO
BERLIN
GERMAN DEMOCRATIC REPUBLIC
SEPTEMBER 1989

the accepted specification of international code, particularly in the document ISO TK/165 DIS 8972 "Solid timber-structural grouping".

For this purpose the timber tests databank of the CRIMT (Central Research Institute of Mechanical Treatment of wood of the USSR Forest Product Ministry) was used. The databank contained tests data for bending, tension and compression of more than 12 thousand specimen of timber of different quality. For tested specimens the timber from 9 forest regions were used.

Generalized probabilistic models of lumber strength distribution were defined by computer analysis of the tests data. These models were fit to normal distribution functions. On this basis the following probabilistic parameters of short-term strength in MPa were determined for different stressed state types (\bar{R} - mean value, S_R - standard deviation):

	\bar{R}	S_R
bending on the edge	33,63	11,83
bending on the flat	43,97	13,69
tension	21,9	8,99
compression	26,3	6,98

In order to create an advisable specification of structural timber by strength classes, the probabilistic method of measuring control of strength was used, which considered the error of measurement. The standard error δ was calculated as the ratio of error of evaluation of strength parameter R by control parameter Z (S_{RZ}) to the standard deviation of strength parameter (S_R):

$$\delta = S_{RZ} / S_R \quad (1)$$

Calculations based on the probabilistic model gave the following values of R_n :

Standard strength class according to ISO TK/165	Characteristic strength in MPa					
	bending on the edge according to		tension according to		compression according to	
	our model	ISO	our model	ISO	our model	ISO
T-38	49	-	25	24	29	30
T-30	40	-	19	19	24	24
T-24	33	-	15	15	21	19
T-19	27	-	11	12	18	15
T-15	22	-	7,8	9,5	15	15

It is seen from the table, that the strength values of timber in this specification are close enough to each other and that the specification of DIS 8972 ISO TK/165 may be taken as a basis for suitable specification for a USSR code.

Numerous tests of glued laminated timber in bending showed, that according to its strength it may be related to strength classes T-30 and T-38 depending on the perfection of the manufacture technology.

Existing statistical data on timber strength distributions allow to base the value of partial coefficient γ_m .

Since the value of this coefficient expresses transition from the lower 5-percentile value to the lower 0,5 percentile value, the determining factors here are: the probability density function of strength and the value of coefficient of variation of strength (V_R).

Practice shows, that the Gauss distribution at high levels of

reliability leads to acceptance of unsubstantiated excessive reserve of strength since the left tail of this distribution stretches to $-\infty$. Numerous verifications of the test data of timber of different quality showed that the strength distribution may most accurately be described by lognormal function. According to this function γ_m can be determined using the following expression:

$$\gamma_m = \exp(\beta_R - \beta_n) v_R, \quad (2)$$

where β_R and β_n - safety indexes at reliability 0,995 and 0,95 (2,58 and 1,65) respectively.

Thus, for the determination of γ_m it was necessary to define the values of v_R .

Statistical analysis of timber tests data showed, that v_R depended on the type stressed state, on the method of grading and the strength class. For average values of v_R at machine stress grading one may take: in bending - 0,2, tension - 0,25, compression - 0,12. At visual assessment for higher strength classes (T-24 and higher) - 0,25, 0,30 and 0,15, respectively; for lower strength classes (T-19 and lower) - 0,3, 0,35 and 0,15 respectively. For glued laminated members the values of v_R are, respectively 0,15, 0,2 and 0,1.

With account for these values of v_R the magnitudes of γ_m will be as follows:

Method of grading	Strength class	Values γ_m		
		bending	tension	compression
1	2	3	4	5
Machine stress grading	any	1,2	1,26	1,12

	1	2	3	4	5
Visual		T-24 and higher	1,26	1,32	
		T-19 and lower	1,32	1,38	1,15
		T-30 and T-38 for glued la- minated mem- bers	1,15	1,20	1,10

The calibration of modification factor γ_d we carried out with a second moment structural reliability approach, which uses means and variances of loads or stress in structure (Q) and load-carrying capacity or strength (R).

If the random values R and Q are described with a lognormal function of distribution, probability of faultless service of structure is evaluated by safety index β :

$$\beta = \ln(\bar{R}/\bar{Q}) / \sqrt{v_R^2 + v_Q^2}, \quad (3)$$

where \bar{R} , \bar{Q} - mean values of R and Q respectively;

v_R and v_Q - coefficients of variation for strength and load parameters, lower than 0,35.

If the distribution function of \bar{R} and \bar{S} are unknown, the safety index β is considered as formal measure of risk and can be used only for evaluation in comparative analysis.

On the basis of this method the modification function γ_d was determined in order to take into account combined effect of the temperature-humidity conditions of service of structure and real loads. γ_d defined from (4) ensures the given level of reliability of iniform structural members in different climate classes.

$$\gamma_d = (\bar{R}_i/\bar{R}_0) \exp[\beta_0(\sqrt{v_{R_0}^2 + v_Q^2} - \sqrt{v_{R_i}^2 + v_Q^2})], \quad (4)$$

where \bar{R}_0, ν_{R_0} - mean value and coefficient of variation of timber strength parameter at a temperature of 20°C and moisture 12%;

\bar{R}_i, ν_{R_i} - mean values and coefficient of variation of timber strength parameter in any climate class;

β_0 - given safety index.

For calculations statistical data of temperature, moisture of timber in structure and load (snow and permanent) changes as well as their combinations in different climate zones of USSR were studied. The dependence of strength on temperature and moisture for solid timber members (60x120 mm) of different quality were determined experimentally.

At the first stage of research this allowed to determine the values of γ_d for the roof structure of non-heated buildings where the maximum of snow load coincides with lowered temperature of wood (approximately 0°C), resulting in an increase of its strength. For this service conditions a value of 1,1-1,2 is recommended for γ_d depending on the type of stressed state of structure.

The suitability of the use of the second moment approach for practical calculations of γ_d was confirmed by comparison of the results to those determined by Monte-Karlo statistical simulation method. The results of calculations by these two methods gave close values for γ_d .

In our subsequent research we intend to extend the problem of determination of γ_d involving long-term strength changes by probabilistic methods.

**INTERNATIONAL COUNCIL FOR BUILDING RESEARCH STUDIES AND DOCUMENTATION
WORKING COMMISSION W18A - TIMBER STRUCTURES**

**NORWEGIAN TIMBER DESIGN CODE
EXTRACT FROM A NEW VERSION**

by

**E Aasheim and K H Solli
The Norwegian Institute of Wood Technology
Norway**

**MEETING TWENTY - TWO
BERLIN
GERMAN DEMOCRATIC REPUBLIC
SEPTEMBER 1989**

NORWEGIAN TIMBER DESIGN CODE - EXTRACT FROM A NEW VERSION

by Erik Aasheim and Kjell H. Solli

The Norwegian Institute of Wood Technology

September 1989

INTRODUCTION

The Norwegian timber design code "NS 3470 Timber structures Design rules" was published in 1973 as a limit state design method. After minor revisions in 1976 and 1979, a committee has been working for four years with a new edition that will be published this year.

The basic documents used in this work are, in addition to the old Norwegian code, CIB Structural Timber Design Code (CIB-report, publication 66, 1983) and Eurocode No 5: Common unified rules for timber structures.

CHARACTERISTIC VALUES FOR TIMBER

There are given values for 5 grades of timber, according to the Norwegian grading rules "NS 3080 Quality specifications for solid timber for structural use" (2. edition 1988). Characteristic strength and stiffness values are given in Table 1 for short-term loads and moisture class 1:

		T12	T18	T24	T30	T40
bending	f_{mk}	12.0	18.0	24.0	30.0	40.0
tension						
- par. to grain	f_{t0k}	7.0	11.0	14.5	18.0	25.0
- perp. to grain	f_{t90k}	0.3	0.4	0.4	0.4	0.4
compression						
- par. to grain	f_{c0k}	13.0	17.0	21.5	27.0	32.0
- perp. to grain	f_{c90k}	6.0	7.0	7.0	7.0	7.0
shear	f_{vk}	2.0	2.8	2.8	2.8	2.8
calculation of stability (5 %)						
modulus of						
- elasticity	E_{0k}	5000	6250	7500	8750	10000
- shear	G_k	310	390	470	550	620
calculation of deformations (50 %)						
modulus of						
- elasticity, par.	E_0	7000	8700	11000	12300	13500
- elasticity, perp.	E_{90}	230	290	370	410	450
- shear	G	440	540	690	770	840

Table 1. Characteristic strenght and stiffness.

MODIFICATION FACTOR FOR DURATION OF LOAD AND MOISTURE CONTENT

The load-duration classes are defined in Table 2:

Load-duration class	Order of duration
A. Long-term	$T > 6$ months
B. Medium-term	$1 \text{ week} \leq T \leq 6$ months
C. Short-term	$T < 1$ week

Table 2. Load-duration classes.

The moisture classes are defined in Table 3:

Moisture class	Relative humidity	Average quillibr. moisture content
1.	$RH < 0.65$	$f < 0.12$
2.	$0.65 \leq RH \leq 0.80$	$0.12 \leq f \leq 0.18$
3.	$RH > 0.80$	$f > 0.18$

Table 3. Moisture classes.

Characteristic strength and stiffness values are given in Table 1 for short-term loads and moisture class 1. For other load-duration classes or combinations thereof, and other climate classes, the strength values are multiplied by the modification factor k_r given in Table 4:

	Modification factor k_r			
	$f_m, f_{t0}, f_{c0},$ $f_v, f_{c90}, E_0 k$		f_{t90}	
Load-duration class	Moisture class			
	1 - 2	3	1 - 2	3
A	0.80	0.65	0.55	0.45
B	0.90	0.70	0.70	0.55
C	1.00	0.80	0.85	0.70

Table 4. Modification factor for strength values, k_r .

For deformation calculations the modification factor k_{cr} is given in Table 5. It is important to notice that the deformation based on the characteristic stiffness is multiplied by the factor k_{cr} .

	Modification factor k_{cr} for deformations calculated by E_0, E_{90}, G		
Load-duration class	Moisture class		
	1	2	3
A	1.50	1.80	3.00
B	1.20	1.30	2.00
C	1.00	1.10	1.50

Table 5. Modification factor for deformations, k_{cr} .

If a load combination consists of actions belonging to different load-duration classes, the deformation should be calculated separately for the different actions with the appropriate creep factors.

GLUED LAMINATED MEMBERS

For design of glulam members the tables 1, 2, 3, 4 and 5 apply. In addition the characteristic values should be multiplied by the lamination factor k_{lam} given in Table 6.

Strength class of lamella	T12	T18	T24	T30	T40
f_m, f_{t0}, f_{c0}	1.4			1.3	1.2
f_{t90}, f_{c90}	1.0				
f_v	1.2				
$E_0 k, E_0, G$	1.2				

Table 6. Lamination factor, k_{lam} .

LOAD SHEARING FACTOR

If four or more similar structural elements act together to support a common load, the values for the characteristic strength can be multiplied by the load shearing factor k_{lf} .

The load shearing factor can be calculated from the following:

$$n \geq 4 \quad \begin{aligned} k_{lf} &= 1 + 0.06 \cdot V \cdot \sqrt{\beta} \\ k_{lf} &\leq 1 + 0.6 \cdot V \end{aligned}$$

$$n \geq 6 \quad \begin{aligned} k_{lf} &= 1 + 0.07 \cdot V \cdot \sqrt{\beta} \\ k_{lf} &\leq 1 + 0.7 \cdot V \end{aligned}$$

Where

$$\beta = \frac{l_h^4 \cdot (EI)_f}{l_f^3 \cdot a \cdot (EI)_h}$$

- n = Number of similar and parallel main elements
- V = Coefficient of variation for the strength of the main elements (0.15 for graded timber, 0.10 for glulam)
- l_h = Span of the main elements
- l_f = Span of the load shearing elements (= the distance between the main elements)
- a = The distance between the load shearing elements
- (EI)_h = Stiffness of the main elements
- (EI)_f = Stiffness of the load shearing elements

For steel parts $k_{lf} = 1.0$ should be used.

PARTIAL COEFFICIENTS FOR MATERIALS AND ACTIONS.

For the ultimate limit state the material partial coefficients consist of two factors. The product will be from 1.1 up to 1.32 depending on the type of structure, material, quality control, consequence of failure etc.

The action partial coefficients are taken from another Norwegian code "NS 3479 Design loads for structures". For the ultimate limit state, the coefficient is 1.2 for permanent actions (dead load) and 1.6 for variable actions (snow loads etc.). The mean value for the action partial coefficient will in Norway be in the order of 1.5.

For serviceability limit state both the material partial coefficient and the action partial coefficients should be 1.0.

DESIGN VALUES

The design values should be given as:

$$f_d = \frac{f_k \cdot k_r \cdot k_{lf}}{\gamma_m} \quad \text{for solid timber}$$

$$f_d = \frac{f_k \cdot k_r \cdot k_{lf} \cdot k_{lam}}{\gamma_m} \quad \text{for glulam.}$$

Where

- f_d = design strength
 f_k = characteristic strength
 k_r = modification factor for load duration and moisture classes
 k_{lf} = load shearing factor
 k_{lam} = lamination factor for glulam
 γ_m = material partial coefficient

DEPTH FACTOR

Bending strength is related to a depth of 200 mm and tension strength to a width (i.e. greatest cross-section dimension) of 200 mm. If depth or width respectively is h , the bending strength or tension strength should be multiplied by k_h :

$$k_h = \left(\frac{200}{h} \right)^{0.2}$$

For $h \geq 198$ mm and for glulam: $k_h = 1.0$

For $h \leq 98$ mm: $k_h = 1.15$

LATERAL INSTABILITY

In bending the design strength should be multiplied by a lateral buckling factor $k_{vipp} \leq 1.0$ depending on the slenderness ratio λ_m . For local timber λ_m is determined by:

$$\lambda_m = \frac{0.065}{b} \cdot \sqrt{l_{ef} \cdot h}$$

l_{ef} = Effective length of the beam. For a number of support conditions and load combinations l_{ef} is given in the code.

k_{vipp} is determined from:

$$k_{vipp} = 1.0 \quad \text{for} \quad \lambda_m \leq 0.75$$

$$k_{vipp} = 1.56 - 0.75 \lambda_m \quad \text{for} \quad 0.75 < \lambda_m < 1.40$$

$$k_{vipp} = 1/(\lambda_m)^2 \quad \text{for} \quad 1.40 \leq \lambda_m$$

COLUMNS

For columns the design compression strength should be multiplied by a buckling factor k_λ dependent on the material parameters and the slenderness ratio. A table and formulas for the buckling factor are given in the code. Figure 1 shows the buckling curve compared to the curve given in the CIB-code:

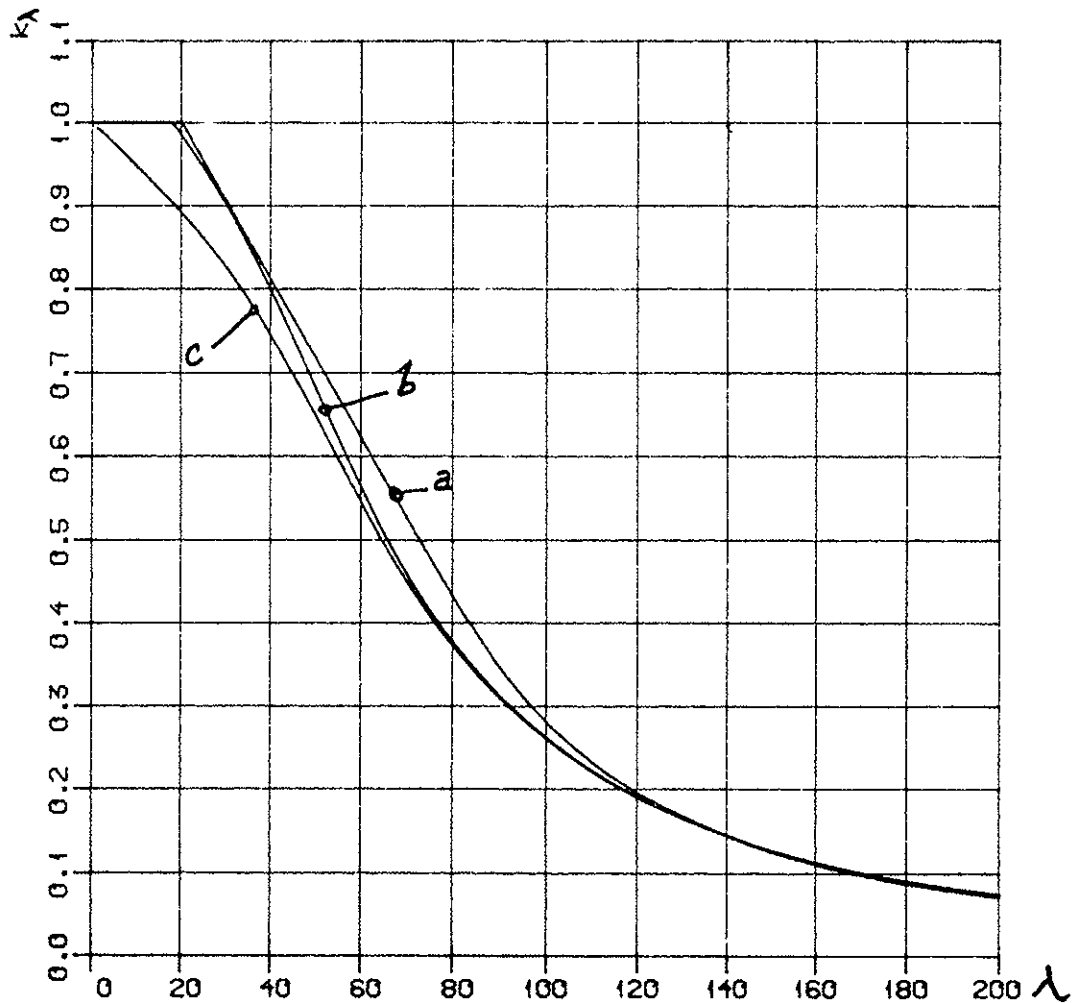


Figure 1. Buckling factor k_λ dependent on the slenderness ratio λ (T30).

- Curve a) from the old norwegian code
- " b) from the new norwegian code
- " c) from the CIB-code

COMMENTS NS 3470 - CIB STRUCTURAL TIMBER DESIGN CODE

The new Norwegian timber design code is in principle rather close to the CIB Report, publication 66, 1983. In the following some of the differences will be discussed:

Strength classes and characteristic values

From our national experience we have chosen 5 strength classes from annex 42 in the CIB-code. Some of our values are higher, specially the modulus of elasticity. The shear strength is according to our test results independent of the strength class.

Load-duration classes

We have introduced 3 classes where the CIB-code defines 5 classes. In our climate the snow load is very important and this load has a duration of up to 6 months. Our classes correspond to the classes in Eurocode 5.

Moisture classes

Our classes are identical to the classes defined in the CIB-code.

Modification factor for load-duration and moisture

We have chosen the same factors as Eurocode 5. The arguments for this are described in the commentary to Eurocode 5.

Glued laminated timber

Our code differs from the CIB-code. Instead of giving special values for glulam members, we use the basic values for solid timber multiplied with a lamination factor.

Load shearing factor

The formulas are based on a Norwegian theoretical work. The result is a load shearing factor between 1.0 and 1.1. In our old code we had a factor 1.2 which was adopted from a previous British Standard.

Partial coefficient for material

For the ultimate limit state the coefficient is prescribed by the relevant public authority, as stated in the CIB-code.

Depth factor

The CIB-code has not introduced a depth factor. We have used the same factor as given in Eurocode 5. This factor corresponds well to Norwegian test results.

Lateral instability

The method is the same as described in the CIB-code. Some simplifications have been done in some of the formulas.

Columns

Figure 1 shows the buckling curves. It can be seen that the CIB-code gives larger strength reduction for slenderness ratios less than approximately 60. Our curve is taken from Eurocode 5.

REFERENCES

1. CIB Structural Timber Design Code.
CIB Report Publication 66, 1983.
2. Eurocode No 5: Common unified rules for timber structures.
Report EUR 9887 EN, 1987.
3. NS 3470 Timber structures. Design rules. Third edition.
Norwegian Standards Association, November 1979.
4. NS 3470 Timber structures. Design rules. Fourth edition.
Norwegian Standards Association, June 1989 (not printed).
5. NS 3080 Quality specifications for solid timber for
structural use. Second edition. Norwegian Standards
Association, May 1988.
6. NS 3479 Design loads for structures. Second edition.
Norwegian Standards Association, February 1981.

(AAS) CIB-PAPER:T